

University of Alberta

**Turbulence Structure in Hydraulic Jumps
and Vertical Slot Fishways**

by

Minnan Liu ©

A thesis submitted to the

Faculty of Graduate Studies and Research

in partial fulfillment of the requirements for the degree of

Doctor of Philosophy

in

Water Resources Engineering

Department of Civil and Environmental Engineering

Edmonton, Alberta

Fall 2004



Library and
Archives Canada

Bibliothèque et
Archives Canada

Published Heritage
Branch

Direction du
Patrimoine de l'édition

395 Wellington Street
Ottawa ON K1A 0N4
Canada

395, rue Wellington
Ottawa ON K1A 0N4
Canada

Your file *Votre référence*

ISBN: 0-612-95973-2

Our file *Notre référence*

ISBN: 0-612-95973-2

The author has granted a non-exclusive license allowing the Library and Archives Canada to reproduce, loan, distribute or sell copies of this thesis in microform, paper or electronic formats.

L'auteur a accordé une licence non exclusive permettant à la Bibliothèque et Archives Canada de reproduire, prêter, distribuer ou vendre des copies de cette thèse sous la forme de microfiche/film, de reproduction sur papier ou sur format électronique.

The author retains ownership of the copyright in this thesis. Neither the thesis nor substantial extracts from it may be printed or otherwise reproduced without the author's permission.

L'auteur conserve la propriété du droit d'auteur qui protège cette thèse. Ni la thèse ni des extraits substantiels de celle-ci ne doivent être imprimés ou autrement reproduits sans son autorisation.

In compliance with the Canadian Privacy Act some supporting forms may have been removed from this thesis.

Conformément à la loi canadienne sur la protection de la vie privée, quelques formulaires secondaires ont été enlevés de cette thèse.

While these forms may be included in the document page count, their removal does not represent any loss of content from the thesis.

Bien que ces formulaires aient inclus dans la pagination, il n'y aura aucun contenu manquant.

Canada

To My Husband
&
My Parents

ACKNOWLEDGMENTS

I would like to express my sincere gratitude to my supervisors Dr. D. Z. Zhu and Dr. N. Rajaratnam for their patience, guidance, encouragement, understanding and support throughout the course of this study. Dr. Zhu and Dr. Rajaratnam devoted their time and effort to make this study a success. I consider it a matter of great privilege and a rare opportunity to work under their supervision.

I am also thankful to all my committee members for their time and efforts in reading this thesis thoroughly and making helpful comments and suggestions.

I wish to extend my thanks to Dr. M. R. Loewen and Dr. D. J. Wilson for their support and willingness to help.

I wish to thank Mr. Sheldon Lovell for his great help in the construction and maintenance of the experimental arrangements. The assistance of Mr. Perry Fedun is also acknowledged.

Also, my sincere gratitude and appreciation go to my husband, Jianmin Pang, for his patience, support, understanding and sacrifices during this study.

Finally, special thanks to Falun Dafa, also known as Falun Gong which is a practice that has brought better health and inner peace to millions around the world based on the universal principles of Truthfulness, Benevolence and Forbearance. It is Falun Dafa that helps me to get rid of illnesses and keep me healthy and energetic during this study.

TABLE OF CONTENTS

Chapter 1

Introduction.....	1
1.1 General.....	1
1.2 Organization of the thesis.....	3
1.3 References.....	5

Chapter 2

Evaluation of ADV Measurements in Bubbly Two-Phase Flows.....	7
2.1 Introduction.....	7
2.2 Principles of Measurement Techniques.....	8
2.2.1 MicroADV.....	8
2.2.2 Electrical probe.....	9
2.2.3 Fiber optic probe.....	11
2.3 Experimental Set-up and Experiments.....	14
2.4 Results and Discussions	16
2.4.1 Air concentration.....	16
2.4.2 Effects of air concentration and boundary on velocity measurements.....	18
2.5 Conclusions.....	21
2.6 References.....	22

Chapter 3

Turbulence Structure of Hydraulic Jumps of Low Froude Numbers.....	36
3.1 Introduction.....	36
3.2 Experimental Arrangement and Program.....	37
3.3 Experimental Results and Analysis.....	39
3.4 Conclusions.....	49

3.5	Appendix: Correction to MicroADV's Mean Velocity Measurement.....	50
3.6	References.....	51
Chapter 4		
Turbulence Structure of Flow in Vertical Slot Fishways.....		75
4.1	Introduction.....	75
4.2	Experimental Arrangement and Experiments.....	79
4.3	Processing Technique.....	83
4.4	Experimental Results and Discussions.....	84
	4.4.1 Overall structure of flow in pools.....	84
	4.4.2 Structure of jet flow formed at the slot.....	93
4.5	Conclusions.....	100
4.6	References.....	103
Chapter 5		
Conclusions and Recommendation for Further Research.....		199
Appendix		
A1	Experimental Study on Turbulence Structure in Hydraulic Jumps	206
	A1.1 Water surface profile for $F_1 = 2.0, 2.5, 3.32$	206
	A1.2 Mean velocity for $F_1 = 2.0, Q = 54.9 \text{ L/s}, y_1 = 7.1 \text{ cm}$	207
	A1.3 Mean velocity for $F_1 = 2.5, Q = 68.6 \text{ L/s}, y_1 = 7.1 \text{ cm}$	211
	A1.4 Mean velocity for $F_1 = 3.32, Q = 40 \text{ L/s}, y_1 = 4.1 \text{ cm}$	216
	A1.5 Processed turbulence data for $F_1 = 2.0, Q = 54.9 \text{ L/s},$ $y_1 = 7.1 \text{ cm}$	219
	A1.6 Processed turbulence data for $F_1 = 2.5, Q = 68.6 \text{ L/s},$ $y_1 = 7.1 \text{ cm}$	223
	A1.7 Processed turbulence data for $F_1 = 3.32, Q = 40 \text{ L/s},$ $y_1 = 4.1 \text{ cm}$	228

A1.8	Air concentration for $F_1 = 2.0$, $Q = 54.9$ L/s, $y_1 = 7.1$ cm	231
A1.9	Air concentration for $F_1 = 2.5$, $Q = 68.6$ L/s, $y_1 = 7.1$ cm	234
A1.10	Air concentration for $F_1 = 3.32$, $Q = 40$ L/s, $y_1 = 4.1$ cm	238
A2	Experimental Study on Turbulence Structure in Vertical Slot Fishways.....	241
A2.1	Overall structure of flow in the pool with coordinates (x, y, z).....	241
A2.1.1	Mean velocity for $S = 5.06\%$, $Q = 31.2$ L/s, $z = 10$ mm.....	241
A2.1.2	Mean velocity for $S = 5.06\%$, $Q = 31.2$ L/s, $z = 100$ mm.....	243
A2.1.3	Mean velocity for $S = 5.06\%$, $Q = 31.2$ L/s, $z = 150$ mm.....	245
A2.1.4	Mean velocity for $S = 5.06\%$, $Q = 52$ L/s, $z = 10$ mm.....	247
A2.1.5	Mean velocity for $S = 5.06\%$, $Q = 52$ L/s, $z = 150$ mm.....	249
A2.1.6	Mean velocity for $S = 5.06\%$, $Q = 52$ L/s, $z = 300$ mm.....	251
A2.1.7	Mean velocity for $S = 10.52\%$, $Q = 31.2$ L/s, $z = 10$ mm.....	253
A2.1.8	Mean velocity for $S = 10.52\%$, $Q = 31.2$ L/s, $z = 70$ mm.....	255
A2.1.9	Mean velocity for $S = 10.52\%$, $Q = 52$ L/s, $z = 100$ mm.....	257
A2.1.10	Processed turbulence data for $S = 5.06\%$, $Q = 31.2$ L/s, $z = 10$ mm.....	259
A2.1.11	Processed turbulence data for $S = 5.06\%$, $Q = 31.2$ L/s, $z = 100$ mm.....	263
A2.1.12	Processed turbulence data for $S = 5.06\%$,	

	$Q = 31.2$ L/s, $z = 150$ mm.....	267
A2.1.13	Processed turbulence data for $S = 5.06\%$, $Q = 52$ L/s, $z = 10$ mm.....	271
A2.1.14	Processed turbulence data for $S = 5.06\%$, $Q = 52$ L/s, $z = 150$ mm.....	275
A2.1.15	Processed turbulence data for $S = 5.06\%$, $Q = 52$ L/s, $z = 300$ mm.....	279
A2.1.16	Processed turbulence data for $S = 10.52\%$, $Q = 31.2$ L/s, $z = 10$ mm.....	283
A2.1.17	Processed turbulence data for $S = 10.52\%$, $Q = 31.2$ L/s, $z = 70$ mm.....	287
A2.1.18	Processed turbulence data for $S = 10.52\%$, $Q = 52$ L/s, $z = 100$ mm.....	291
A2.2	Structure of jet flow in the pool with coordinates (x_j, y_j, z)	295
A2.2.1	Maximum plane velocity locus.....	295
A2.2.2	Measurement points in (x_j, y_j) and its corresponding points in (x, y) for $S = 5.06\%$, $Q = 31.2$ L/s, $z = 10$ mm.....	296
A2.2.3	Measurement points in (x_j, y_j) and its corresponding points in (x, y) for $S = 5.06\%$, $Q = 31.2$ L/s, $z = 100$ mm.....	397
A2.2.4	Measurement points in (x_j, y_j) and its corresponding points in (x, y) for $S = 5.06\%$, $Q = 31.2$ L/s, $z = 150$ mm.....	398
A2.2.5	Measurement points in (x_j, y_j) and its corresponding points in (x, y) for $S = 10.52\%$, $Q = 31.2$ L/s, $z = 10$ mm.....	399
A2.2.6	Measurement points in (x_j, y_j) and its corresponding points in (x, y) for $S = 10.52\%$, $Q = 31.2$ L/s, $z = 70$ mm.....	300

A2.2.7	Processed mean velocity and turbulence data in jet flow for $S = 5.06\%$, $Q = 31.2$ L/s, $z = 10$ mm	301
A2.2.8	Processed mean velocity and turbulence data in jet flow for $S = 5.06\%$, $Q = 31.2$ L/s, $z = 100$ mm	304
A2.2.9	Processed mean velocity and turbulence data in jet flow for $S = 5.06\%$, $Q = 31.2$ L/s, $z = 150$ mm	306
A2.2.10	Processed mean velocity in jet flow for $S = 10.52\%$, $Q = 31.2$ L/s, $z = 10$ mm.....	308
A2.2.11	Processed mean velocity in jet flow for $S = 10.52\%$, $Q = 31.2$ L/s, $z = 70$ mm.....	309
A2.2.12	Processed turbulence data in jet flow for $S = 10.52\%$, $Q = 31.2$ L/s, $z = 10$ mm.....	310
A2.2.13	Processed turbulence data in jet flow for $S = 10.52\%$, $Q = 31.2$ L/s, $z = 70$ mm.....	312

LIST OF TABLES

Table		Page
2.1	List of Experiments.....	25
3.1	Details of Experiments.....	56
3.2	Order of Energy Dissipation Rate (m^2/s^3) in Different Regions of the Flow.....	56
4.1	Primary Details of the Experiments Undertaken in the Coordinate System (x, y, z).....	106
4.2	Primary Details of the Experiments Undertaken in the Coordinate System (x_j, y_j, z).....	106

LIST OF FIGURES

Figure		Page
2.1	SonTek 16-MHz down-looking 3D MicroADV.....	26
2.2	The electrical probe.....	27
2.3	Equivalent circuit of the electrical probe.....	27
2.4	The fiber optic probe.....	28
2.5	A well developed bubble signature.....	29
2.6	Definition sketch of free hydraulic jump.....	29
2.7	Time-averaged air concentration by fiber optic probe with sampling frequency of 100 kHz and sampling time of 2 minutes...	30
2.8	Air concentration by electrical probe for $F_1 = 2.0$	31
2.9	Accuracy of fiber optic probe compared with electrical probe.....	31
2.10	Section-averaged air concentration.....	32
2.11	Variation of \bar{C}_{\max} with F_1	32
2.12	Bubble size distribution at various x/y_2 locations for $F_1 = 2.0, 2.5$ and 3.32.....	32
2.13	Examples of MicroADV data: (a) clean record; (b) contaminated Record; and (c) contaminated record of (b) after cleaning using PSTM.....	33
2.14	Mean longitudinal velocity profile by MicroADV and Prandtl tube	34
2.15	Effect of air concentration on MicroADV data.....	35
2.16	Boundary effect on MicroADV data (without air-bubbles).....	35
3.1	(a) Definition sketch of free hydraulic jump; (b) experimental set-up in T. Blench Hydraulics Laboratory at the University of Alberta.....	57
3.2(a-c)	(a) Experiment 1 for $F_1 = 2.0$	58
	(b) Experiment 2 for $F_1 = 2.5$	59
	(c) Experiment 3 for $F_1 = 3.32$	60

3.3	Velocity distribution in central vertical plane.....	61
3.4	Variation of normalized maximum velocity u_m/U_1 with x/L	62
3.5	Variation of normalized length scale L/y_2 with F_1	62
3.6	Variation of normalized length scale b/y_1 with x/y_1	62
3.7	Distribution of Reynolds shear stress in central vertical plane.....	63
3.8(a-b)	(a) Distribution of longitudinal turbulence intensity in central vertical plane.....	64
	(b) Distribution of vertical turbulence intensity in central vertical plane.....	65
3.9	Variation of normalized maximum turbulence intensities and Reynolds stress in central vertical plane with x/y_2	66
3.10	Similarity profile of Reynolds stress.....	67
3.11	Similarity profile of vertical turbulence intensity.....	67
3.12	Similarity profile of longitudinal turbulence intensity.....	68
3.13	Similarity profile of turbulence kinetic energy.....	69
3.14	Variation of maximum turbulence kinetic energy in central vertical plane with x/y_2	69
3.15	Power spectrum of velocity: —, $G_u(f)/\overline{u'^2}$; —, $G_v(f)/\overline{v'^2}$; -----, $G_w(f)/\overline{w'^2}$; (a) without air bubbles and using raw data; (b) within air bubble region and using raw data; (c) within air bubble region and data processed using PSTM.....	70
3.16	Correlation-coefficient spectrum R_{uv} as a function of frequency f ..	71
3.17	Distribution of energy dissipation rate.....	71
3.18	Distribution of normalized energy dissipation rate in hydraulic jump.....	72
3.19	Distribution of Kolmogorov's length scale (in mm).....	73
3.20	Power spectrum: G_u for horizontal velocity and G_v for vertical velocity.....	74

4.1	Flow patterns in pools: (a) pattern 1 and (b) pattern 2 (Wu et al. 1999).....	107
4.2	Experimental set-up of vertical slot fishway: (a) side view; (b) plan view; (c) details of slot and pool (dimensions shown are in mm)...	108
4.3	Experiment for $S = 10.52\%$ and $Q = 31.2$ L/s in T. Blench Hydraulics Laboratory at the University of Alberta.....	109
4.4	Change of mean velocity and turbulence intensity with time: (a) $S = 10.52\%$, $Q = 31.2$ L/s, $x = 300$ mm, $y = 500$ mm, $z = 70$ mm; (b) $S = 5.06\%$, $Q = 52$ L/s, $x = 600$ mm, $y = 600$ mm, $z = 150$ mm; (c) $S = 5.06\%$, $Q = 31.2$ L/s, $x = 600$ mm, $y = 600$ mm, $z = 100$ mm	110
4.5	Sample of velocity time series for $S = 5.06\%$ and $Q = 31.2$ L/s at coordinate system (x_j, y_j, z)	111
4.6	Air concentration (%) for $S = 10.52\%$, $Q = 31.2$ L/s, $z = 70$ mm, ——, maximum plane velocity filament.....	111
4.7(a-f)	Plane velocity field in the pool for $S = 5.06\%$: ———→, this study; -----→, Wu et al. (1999); ———, V/V_{sm} contour (a) $Q = 31.2$ L/s, $z = 10$ mm..... (b) $Q = 31.2$ L/s, $z = 100$ mm..... (c) $Q = 31.2$ L/s, $z = 150$ mm..... (d) $Q = 52$ L/s, $z = 10$ mm..... (e) $Q = 52$ L/s, $z = 150$ mm..... (f) $Q = 52$ L/s, $z = 300$ mm.....	112 112 113 113 114 114
4.8(a-c)	Plane velocity field in the pool for $S = 10.52\%$: ———→, this study; -----→, Wu et al. (1999); ———, V/V_{sm} contour (a) $Q = 31.2$ L/s, $z = 10$ mm..... (b) $Q = 31.2$ L/s, $z = 70$ mm..... (c) $Q = 52$ L/s, $z = 100$ mm.....	115 115 116
4.9(a-f)	Vertical velocity distribution in the pool for $S = 5.06\%$, — — —, maximum plane velocity filament (a) $Q = 31.2$ L/s, $z = 10$ mm.....	117

	(b) $Q = 31.2$ L/s, $z = 100$ mm.....	118
	(c) $Q = 31.2$ L/s, $z = 150$ mm.....	119
	(d) $Q = 52$ L/s, $z = 10$ mm.....	120
	(e) $Q = 52$ L/s, $z = 150$ mm.....	121
	(f) $Q = 52$ L/s, $z = 300$ mm.....	122
4.10(a-c)	Vertical velocity distribution in the pool for $S = 10.52\%$, — — —, maximum plane velocity filament	
	(a) $Q = 31.2$ L/s, $z = 10$ mm.....	123
	(b) $Q = 31.2$ L/s, $z = 70$ mm.....	124
	(c) $Q = 52$ L/s, $z = 100$ mm.....	125
4.11(a-f)	Contours of normalized mean flow kinetic energy $K^{0.5}/V_{sm}$ for $S = 5.06\%$, — — —, maximum plane velocity filament	
	(a) $Q = 31.2$ L/s, $z = 10$ mm.....	126
	(b) $Q = 31.2$ L/s, $z = 100$ mm.....	126
	(c) $Q = 31.2$ L/s, $z = 150$ mm.....	127
	(d) $Q = 52$ L/s, $z = 10$ mm.....	127
	(e) $Q = 52$ L/s, $z = 150$ mm.....	128
	(f) $Q = 52$ L/s, $z = 300$ mm.....	128
4.12(a-c)	Contours of normalized mean flow kinetic energy $K^{0.5}/V_{sm}$ for $S = 10.52\%$, — — —, maximum plane velocity filament	
	(a) $Q = 31.2$ L/s, $z = 10$ mm.....	129
	(b) $Q = 31.2$ L/s, $z = 70$ mm.....	129
	(c) $Q = 52$ L/s, $z = 100$ mm.....	130
4.13(a-f)	Distribution of normalized Reynolds shear stress for $S = 5.06\%$, — — —, maximum plane velocity filament	
	(a) $Q = 31.2$ L/s, $z = 10$ mm.....	131
	(b) $Q = 31.2$ L/s, $z = 100$ mm.....	131
	(c) $Q = 31.2$ L/s, $z = 150$ mm.....	132
	(d) $Q = 52$ L/s, $z = 10$ mm.....	132
	(e) $Q = 52$ L/s, $z = 150$ mm.....	133

	(f) $Q = 52 \text{ L/s}, z = 300 \text{ mm}$	133
4.14(a-c)	Distribution of normalized Reynolds shear stress for $S = 10.52\%$, — — —, maximum plane velocity filament	
	(a) $Q = 31.2 \text{ L/s}, z = 10 \text{ mm}$	134
	(b) $Q = 31.2 \text{ L/s}, z = 70 \text{ mm}$	134
	(c) $Q = 52 \text{ L/s}, z = 100 \text{ mm}$	135
4.15(a-f)	Distribution of normalized longitudinal turbulence intensity for $S = 5.06\%$, — — —, maximum plane velocity filament	
	(a) $Q = 31.2 \text{ L/s}, z = 10 \text{ mm}$	136
	(b) $Q = 31.2 \text{ L/s}, z = 100 \text{ mm}$	136
	(c) $Q = 31.2 \text{ L/s}, z = 150 \text{ mm}$	137
	(d) $Q = 52 \text{ L/s}, z = 10 \text{ mm}$	137
	(e) $Q = 52 \text{ L/s}, z = 150 \text{ mm}$	138
	(f) $Q = 52 \text{ L/s}, z = 300 \text{ mm}$	138
4.16(a-c)	Distribution of normalized longitudinal turbulence intensity for $S = 10.52\%$, — — —, maximum plane velocity filament	
	(a) $Q = 31.2 \text{ L/s}, z = 10 \text{ mm}$	139
	(b) $Q = 31.2 \text{ L/s}, z = 70 \text{ mm}$	139
	(c) $Q = 52 \text{ L/s}, z = 100 \text{ mm}$	140
4.17(a-f)	Distribution of normalized transverse turbulence intensity for $S = 5.06\%$, — — —, maximum plane velocity filament	
	(a) $Q = 31.2 \text{ L/s}, z = 10 \text{ mm}$	141
	(b) $Q = 31.2 \text{ L/s}, z = 100 \text{ mm}$	141
	(c) $Q = 31.2 \text{ L/s}, z = 150 \text{ mm}$	142
	(d) $Q = 52 \text{ L/s}, z = 10 \text{ mm}$	142
	(e) $Q = 52 \text{ L/s}, z = 150 \text{ mm}$	143
	(f) $Q = 52 \text{ L/s}, z = 300 \text{ mm}$	143
4.18(a-c)	Distribution of normalized transverse turbulence intensity for $S = 10.52\%$, — — —, maximum plane velocity filament	
	(a) $Q = 31.2 \text{ L/s}, z = 10 \text{ mm}$	144

	(b) $Q = 31.2$ L/s, $z = 70$ mm.....	144
	(c) $Q = 52$ L/s, $z = 100$ mm.....	145
4.19(a-f)	Distribution of normalized vertical turbulence intensity for $S = 5.06\%$, — — —, maximum plane velocity filament	
	(a) $Q = 31.2$ L/s, $z = 10$ mm.....	146
	(b) $Q = 31.2$ L/s, $z = 100$ mm.....	146
	(c) $Q = 31.2$ L/s, $z = 150$ mm.....	147
	(d) $Q = 52$ L/s, $z = 10$ mm.....	147
	(e) $Q = 52$ L/s, $z = 150$ mm.....	148
	(f) $Q = 52$ L/s, $z = 300$ mm.....	148
4.20(a-c)	Distribution of normalized vertical turbulence intensity for $S = 10.52\%$, — — —, maximum plane velocity filament	
	(a) $Q = 31.2$ L/s, $z = 10$ mm.....	149
	(b) $Q = 31.2$ L/s, $z = 70$ mm.....	149
	(c) $Q = 52$ L/s, $z = 100$ mm.....	150
4.21(a-f)	Contours of normalized turbulence kinetic energy $K'^{0.5} / V_{sm}$ for $S = 5.06\%$, — — —, maximum plane velocity filament	
	(a) $Q = 31.2$ L/s, $z = 10$ mm.....	151
	(b) $Q = 31.2$ L/s, $z = 100$ mm.....	151
	(c) $Q = 31.2$ L/s, $z = 150$ mm.....	152
	(d) $Q = 52$ L/s, $z = 10$ mm.....	152
	(e) $Q = 52$ L/s, $z = 150$ mm.....	153
	(f) $Q = 52$ L/s, $z = 300$ mm.....	153
4.22(a-c)	Contours of normalized turbulence kinetic energy $K'^{0.5} / V_{sm}$ for $S = 10.52\%$, — — —, maximum plane velocity filament	
	(a) $Q = 31.2$ L/s, $z = 10$ mm.....	154
	(b) $Q = 31.2$ L/s, $z = 70$ mm.....	154
	(c) $Q = 52$ L/s, $z = 100$ mm.....	155
4.23	Power spectrum of velocity: ———, $G_u(f) / \overline{u'^2}$; - - -, $G_v(f) / \overline{v'^2}$;	

	——, $G_w(f)/\overline{w'^2}$	155
4.24	(a-b) Energy dissipation rate ε (m^2/s^3) for $S = 10.52\%$, $z = 10$ mm: (a) measured along x ; (b) measured along x_j	156
	(c-d) Energy dissipation rate ε (m^2/s^3) for $S = 10.52\%$, $z = 70$ mm: (c) measured along x ; (d) measured along x_j	157
4.25(a-f)	Contours of turbulence energy dissipation rate ε (m^2/s^3) for $S = 5.06\%$, — — —, maximum plane velocity filament	
	(a) $Q = 31.2$ L/s, $z = 10$ mm.....	158
	(b) $Q = 31.2$ L/s, $z = 100$ mm.....	158
	(c) $Q = 31.2$ L/s, $z = 150$ mm.....	159
	(d) $Q = 52$ L/s, $z = 10$ mm.....	159
	(e) $Q = 52$ L/s, $z = 150$ mm.....	160
	(f) $Q = 52$ L/s, $z = 300$ mm.....	160
4.26(a-c)	Contours of turbulence energy dissipation rate ε (m^2/s^3) for $S = 10.52\%$, — — —, maximum plane velocity filament	
	(a) $Q = 31.2$ L/s, $z = 10$ mm.....	161
	(b) $Q = 31.2$ L/s, $z = 70$ mm.....	161
	(c) $Q = 52$ L/s, $z = 100$ mm.....	162
4.27(a-f)	Contours of microscale λ_g (mm) for $S = 5.06\%$, — — —, maximum plane velocity filament	
	(a) $Q = 31.2$ L/s, $z = 10$ mm.....	163
	(b) $Q = 31.2$ L/s, $z = 100$ mm.....	163
	(c) $Q = 31.2$ L/s, $z = 150$ mm.....	164
	(d) $Q = 52$ L/s, $z = 10$ mm.....	164
	(e) $Q = 52$ L/s, $z = 150$ mm.....	165
	(f) $Q = 52$ L/s, $z = 300$ mm.....	165
4.28(a-c)	Contours of microscale λ_g (mm) for $S = 10.52\%$, — — —, maximum plane velocity filament	
	(a) $Q = 31.2$ L/s, $z = 10$ mm.....	166

	(b) $Q = 31.2$ L/s, $z = 70$ mm.....	166
	(c) $Q = 52$ L/s, $z = 100$ mm.....	167
4.29(a-f)	Contours of Kolmogorov length scale η (mm) for $S = 5.06\%$, — — —, maximum plane velocity filament	
	(a) $Q = 31.2$ L/s, $z = 10$ mm.....	168
	(b) $Q = 31.2$ L/s, $z = 100$ mm.....	168
	(c) $Q = 31.2$ L/s, $z = 150$ mm.....	169
	(d) $Q = 52$ L/s, $z = 10$ mm.....	169
	(e) $Q = 52$ L/s, $z = 150$ mm.....	170
	(f) $Q = 52$ L/s, $z = 300$ mm.....	170
4.30(a-c)	Contours of Kolmogorov length scale η (mm) for $S = 10.52\%$, — — —, maximum plane velocity filament	
	(a) $Q = 31.2$ L/s, $z = 10$ mm.....	171
	(b) $Q = 31.2$ L/s, $z = 70$ mm.....	171
	(c) $Q = 52$ L/s, $z = 100$ mm.....	172
4.31	(a-c) Distribution of longitudinal mean velocity in jet for $S = 5.06\%$ and $Q = 31.2$ L/s: (a) $z = 10$ mm; (b) $z = 100$ mm; (c) $z = 150$ mm.....	173
	(d-e) Distribution of longitudinal mean velocity in jet for $S = 10.52\%$ and $Q = 31.2$ L/s: (d) $z = 10$ mm; (e) $z = 70$ mm.....	174
4.32	Non-dimensional velocity profile.....	175
4.33	Variation of normalized maximum velocity u_{jm}/V_{sm} with $x_j/0.5b_0$	175
4.34	(a-c) Growth of jet half width in pool for $S = 5.06\%$ and $Q = 31.2$ L/s.....	176
	(d-e) Growth of jet half width in pool for $S = 10.52\%$ and $Q = 31.2$ L/s.....	177
	(f-h) Growth of jet half width in pool for $S = 5.06, 10.52\%$ and $Q = 31.2$ L/s.....	178
4.35	(a-c) Distribution of Reynolds shear stress in jet for $S = 5.06\%$ and $Q = 31.2$ L/s: (a) $z = 10$ mm; (b) $z = 100$ mm; (c) $z = 150$ mm	179

	(d-e) Distribution of Reynolds shear stress in jet for $S = 10.52\%$ and $Q = 31.2$ L/s: (d) $z = 10$ mm; (e) $z = 70$ mm.....	180
4.36	(a-c) Distribution of longitudinal turbulence intensity in jet for $S = 5.06\%$ and $Q = 31.2$ L/s: (a) $z = 10$ mm; (b) $z = 100$ mm, (c) $z = 150$ mm.....	181
	(d-e) Distribution of longitudinal turbulence intensity in jet for $S = 10.52\%$ and $Q = 31.2$ L/s: (d) $z = 10$ mm; (e) $z = 70$ mm.....	182
4.37	(a-c) Distribution of transverse turbulence intensity in jet for $S = 5.06\%$ and $Q = 31.2$ L/s: (a) $z = 10$ mm; (b) $z = 100$ mm, (c) $z = 150$ mm.....	183
	(d-e) Distribution of transverse turbulence intensity in jet for $S = 10.52\%$ and $Q = 31.2$ L/s: (d) $z = 10$ mm; (e) $z = 70$ mm.....	184
4.38	(a-c) Distribution of vertical turbulence intensity in jet for $S = 5.06\%$ and $Q = 31.2$ L/s: (a) $z = 10$ mm; (b) $z = 100$ mm, (c) $z = 150$ mm.....	185
	(d-e) Distribution of vertical turbulence intensity in jet for $S = 10.52\%$ and $Q = 31.2$ L/s: (d) $z = 10$ mm; (e) $z = 70$ mm.....	186
4.39	Variation of normalized maximum Reynolds stress in jet flow with $x_j/0.5b_0$: (a) $S = 5.06\%$, $Q = 31.2$ L/s; (b) $S = 10.52\%$, $Q = 31.2$ L/s.....	187
4.40	Variation of normalized maximum longitudinal turbulence intensity in jet flow with $x_j/0.5b_0$: (a) $S = 5.06\%$, $Q = 31.2$ L/s; (b) $S = 10.52\%$, $Q = 31.2$ L/s.....	188
4.41	Variation of normalized maximum transverse turbulence intensity in jet flow with $x_j/0.5b_0$: (a) $S = 5.06\%$, $Q = 31.2$ L/s; (b) $S = 10.52\%$, $Q = 31.2$ L/s.....	189
4.42	Variation of normalized maximum vertical turbulence intensity in jet flow with $x_j/0.5b_0$: (a) $S = 5.06\%$, $Q = 31.2$ L/s; (b) $S = 10.52\%$, $Q = 31.2$ L/s.....	190
4.43	Variation of longitudinal turbulence intensity along the jet	

	center-line for $S = 5.06, 10.52\%$ and $Q = 31.2 \text{ L/s}$	191
4.44	Distribution of normalized Reynolds shear stress in jet flow: (a) $S = 5.06\%$, $Q = 31.2 \text{ L/s}$; (b) $S = 10.52\%$, $Q = 31.2 \text{ L/s}$; ---, Gutmark & Wygnanski (1976); ----, Heskestad (1965); -·-·-, Bradbury (1965); -·-·-, Ramaprian & Chandrasekhara (1985)...	192
4.45	Distribution of normalized longitudinal turbulence intensity in jet flow: (a) $S = 5.06\%$, $Q = 31.2 \text{ L/s}$; (b) $S = 10.52\%$, $Q = 31.2 \text{ L/s}$; ---, Gutmark & Wygnanski (1976); ----, Heskestad (1965); -·-·-, Bradbury (1965); -·-·-, Ramaprian & Chandrasekhara (1985).....	193
4.46	Distribution of normalized transverse turbulence intensity in jet flow: (a) $S = 5.06\%$, $Q = 31.2 \text{ L/s}$; (b) $S = 10.52\%$, $Q = 31.2 \text{ L/s}$; ---, Gutmark & Wygnanski (1976); ----, Heskestad (1965); -·-·-, Bradbury (1965); -·-·-, Ramaprian & Chandrasekhara (1985).....	194
4.47	Distribution of normalized vertical turbulence intensity in jet flow: (a) $S = 5.06\%$, $Q = 31.2 \text{ L/s}$; (b) $S = 10.52\%$, $Q = 31.2 \text{ L/s}$; ---, Gutmark & Wygnanski (1976); ----, Heskestad (1965); -·-·-, Bradbury (1965); -·-·-, Ramaprian & Chandrasekhara (1985)...	195
4.48	Distribution of normalized longitudinal turbulence intensity in jet flow.....	196
4.49	Distribution of normalized transverse turbulence intensity in jet flow: (a) $S = 5.06\%$, $Q = 31.2 \text{ L/s}$; (b) $S = 10.52\%$, $Q = 31.2 \text{ L/s}$...	197
4.50	Distribution of normalized vertical turbulence intensity in jet flow: (a) $S = 5.06\%$, $Q = 31.2 \text{ L/s}$; (b) $S = 10.52\%$, $Q = 31.2 \text{ L/s}$	198

NOTATIONS*

Symbol	Description
a	constants [2];
A, B	constants [4];
b	length scale equal to y where $u = 0.5u_m$ and $\partial u/\partial y < 0$ [3] or length scale equal to y_j where $u_j = 0.5u_{jm}$ and $\partial u_j/\partial y_j < 0$ for plane turbulent jets [4];
b_+	length scale equal to y_j where $u_j = 0.5u_{jm}$ and $\partial u_j/\partial y_j < 0$ at the left half of the jet when looking downstream [4];
b_-	length scale equal to $ y_j $ where $u_j = 0.5u_{jm}$ and $\partial u_j/\partial y_j < 0$ at the right half of the jet when looking downstream [4];
b_0	width of the slot [4];
c	local void fraction [2];
C	mean volume air concentration by fiber optic probe [2];
C_e	mean volume air concentration by electrical probe [2];
\bar{C}	section-averaged air concentration [2];
\bar{C}_{\max}	maximum section-averaged air concentration [2];
E_0	supply voltage [2];
E_s	voltage across the R_s [2];
E_p	voltage across the electrical probe [2];

* The number in the square brackets [] denotes relevant chapter number.

F_1	supercritical Froude number equal to $U_1/\sqrt{gy_1}$ [2, 3];
f	frequency [3, 4];
g	gravitational acceleration [2, 3, 4];
G_u, G_v, G_w	power spectra of the corresponding velocity components, u' , v' and w' [3, 4];
G_{uv}	co-spectrum of the turbulence velocity components u' and v' [3];
Δh	energy loss in the jump [3] or water level difference between two adjacent pools [4];
I	current in the circuit [2];
K	mean flow kinetic energy per unit mass equal to $(u^2 + v^2 + w^2)/2$ [4];
K'	turbulence kinetic energy per unit mass equal to $(\overline{u'^2} + \overline{v'^2} + \overline{w'^2})/2$ [3, 4];
K'_m	maximum turbulence kinetic energy per unit mass [3];
k	wave number equal to $2\pi f/u$ [3, 4];
k_n	wave number corresponding to the Nyquist frequency [3];
k_d	wave number corresponding to the Kolmogorov length scale [3];
L	length scale equal to the value of x where $u_m = 0.5U_1$ [3] or length of the pool [4];
L_j	length of the jump [3];
m	constants [2];
M	total number of bubbles [2];
n	number of samples [2, 4];

N	percentage of the total number of bubbles at a point [2];
Q	discharge [2, 3, 4];
Q^*	dimensionless discharge equal to $Q/\sqrt{gSb_0^5}$ [4];
$\overline{q^2}$	total velocity variance equal to $\overline{u'^2} + \overline{v'^2} + \overline{w'^2}$ [4];
r^2	correlation coefficient [3, 4];
R_1	electrical resistance of a fluid [2] or Reynolds number equal to $U_1 \nu_1 / \nu$ [3];
R_{uv}	correlation-coefficient spectrum [3];
r	specific resistivity of a suspension [2];
r_1	specific resistivity of a fluid [2];
r_2	specific resistivity of suspended spheres [2];
R_s	arbitrary series electrical resistance [2];
R_p	electrical resistance of the electrical probe [2];
s	chord length [2];
S	slope of the vertical slot fishway [4];
t	time [3, 4];
T	total sampling time [2];
T_r	rise time in (ms) [2];
T_g	gas resident time [2];
U_1	depth-average velocity at the section where the jump starts (i.e. at $x = 0$) [2, 3];
u	time-averaged longitudinal velocity at any point [2, 3, 4];

u_m	maximum value of u at any x -station [3];
u_{prandtl}	mean velocity obtained by Prandtl tube [2];
u_{pstm}	mean velocity processed from MicroADV data using PSTM [2];
u_j	time-averaged longitudinal velocity in the x_j direction [4];
u_{jm}	maximum value of u_j at any x_j -station [4];
V_b	bubble velocity in (cm/s) [2];
V_{sm}	maximum velocity at the slot [4];
V	plane velocity vector at any point [4];
v	time-averaged velocity in the y direction at any point [4];
w	time-averaged velocity in the z direction at any point [4];
W	width of the flume [3] or width of the pool [4];
u', v', w'	fluctuating velocities in the x, y and z directions [3, 4];
u'_j, v'_j, w'_j	fluctuating velocities in the x_j, y_j and z directions for the jet flow [4];
x	longitudinal distance measured from the section where the jump starts [2, 3] or longitudinal distance measured from the upstream long baffle in the pool [4];
x_j	distance along the curved jet center-line measured from the point where the maximum plane velocity locus intersects with the slot [4];
y_j	distance measured from the jet center-line in the transverse direction orthogonal to x_j [4];
y	vertical distance from the bottom of the flume [2, 3] or transverse distance measured from the sidewall between the long baffles [4];

y_1	supercritical initial depth of the free jump [2, 3];
y_2	subcritical sequent depth of the free jump [2, 3];
y_0	average depth of flow in the pool [4];
z	transverse distance from the center of the flume [3] or a distance perpendicular to the flume bottom and measured from it [4];
ρ	mass density of fluid [3, 4];
ν	kinematic viscosity of fluid [3, 4];
ε	energy dissipation rate [3, 4];
$\bar{\varepsilon}$	average energy dissipation rate per unit mass [3, 4];
η	Kolmogorov length scale [3, 4];
σ	standard deviation of a random variable [2];
λ_g	Taylor microscale [4];
Subscript	
m	maximum value in a vertical profile [3] or in a transverse profile [4].

Chapter 1

Introduction

1.1 General

Hydraulic jump is one of the most interesting phenomena in the field of hydraulic engineering. Due to its importance in energy dissipation in hydraulic structures it has been studied extensively. The first recorded investigation was made by Bidone in 1818 (Rajaratnam 1967). Since then a large number of investigations have been undertaken on this subject. Major contributions have been reviewed by Rajaratnam (1967), McCorquodale (1986) and more recently by Hager (1992). However, most of the studies have been directed to the mean velocity field and global features like the relationship of sequent depths and length characteristics. The turbulence characteristics have received much less attention.

The air model study of free hydraulic jumps by Rouse et al. (1959) was the first attempt to make measurements of turbulence structure of hydraulic jumps. Their work was a significant contribution to the understanding of hydraulic jumps, but the air model may not have simulated all aspects of a real hydraulic jump due to lack of a continuously moving free surface. Resch and Leutheusser (1972a, b) obtained some limited turbulence measurements in hydraulic jumps with a hot-film anemometer. Overall, our knowledge of the turbulence in hydraulic jumps is very limited.

Another interesting topic is the study of fishways which are hydraulic

structures which enable fish overcome obstructions in their migration upstream. Fishways received considerable attention in recent years, given their importance in fish protection. Vertical slot fishways are one of the four main types of fishways and are commonly used in North America. Rajaratnam et al. (1986) were the first to perform a systematic study of vertical slot fishways. Further contributions to vertical slot fishways have been made by Rajaratnam et al. (1992), Wu et al. (1999) and more recently by Puertas et al. (2004). These investigations were concerned mainly with study on the mean flow structure. Little is known about the turbulence structure of flow in vertical slot fishways, which is important for assessing fish behavior in the vertical slot fishways.

The aforementioned two flows – hydraulic jumps and flow in vertical slot fishways are both bubbly two-phase flows. Although a study of the turbulence structure is necessary for a good understanding of the flows, it has been a problem to measure the turbulence due to the difficulty encountered in bubbly flows. By using the new technique of micro acoustics Doppler velocimeter (MicroADV), we have been able to measure the turbulence structure in hydraulic jumps and vertical slot fishways.

ADV is useful for the measurement of 3D instantaneous velocity field in water flows. However, ADV manufactures warn their users on the limitations in measuring in bubbly flows (SonTek 1997). Problems have been encountered when ADV was used in bubbly flows. These problems include increased noise energy and further the true turbulence characteristics were changed and velocities were

underestimated due to air bubbles present in the flows (Anderson and Lohrmann 1995; Nikora and Goring 1998; and Robinson et al. 2000). Therefore, the MicroADV was first examined in bubbly flows before being used to make turbulence measurements in the hydraulic jumps and vertical slot fishways.

1.2 Organization of the thesis

This thesis presents the evaluation of measurements by MicroADV in bubbly flows and results on the turbulence structure of both free hydraulic jumps and flows in vertical slot fishways. Each of the three investigations is presented in a separate chapter. Following is a brief introduction to each chapter.

In chapter 2, the use of MicroADV in bubbly two-phase flows is evaluated for use in free hydraulic jumps. This chapter starts with an introduction describing the difficulties encountered in measuring bubbly two-phase flows by ADV and other related instruments. Then it introduces the measurement techniques including the MicroADV for velocity measurements, and both fiber optic probe and electrical probe for air concentration measurements. Section 2.3 describes the experimental arrangement and experiments. The experimental results and discussions are presented in section 2.4 on the effects of air concentration and boundary on the measurements of MicroADV. Conclusions are given in section 2.5.

Chapter 3 presents the results of the experimental study on the turbulence structure of free hydraulic jumps. The main objective of this study is to obtain generalized turbulence characteristics of free hydraulic jumps which will be useful

for further study of the turbulence in other types of jumps and in the design of stilling basins. In the brief introductory section, the previous studies are reviewed and the necessity of the present study is described. Section 3.2 shows the experimental setup. The experimental results and analysis are presented in section 3.3. This section discusses the mean flow structure and especially the turbulence characteristics of free hydraulic jumps including the turbulence intensities, Reynolds shear stress, velocity spectra, dissipation, and length scale. Conclusions are formulated in section 3.4.

The objective of chapter 4 is to study the turbulence structure of flow in vertical slot fishways. The literature review and necessity of this study are given in the introduction section 4.1. Section 4.2 presents the experimental setup and experiments. Preliminary experiments were conducted and the results are also given in this section. The air concentration was measured which will give the accuracy of the MicroADV measurements based on the results presented in chapter 2, and the sampling time of the MicroADV was decided from the preliminary experiments. In section 4.3 of the processing technique, the processing method of MicroADV data is introduced. In section 4.4, the overall mean and turbulence structures of the flow in the pools are shown. The structure of the jet flow in the pools is specially discussed and compared with that of a plane turbulent jet. Conclusions are stated in section 4.5.

Chapter 5 presents a general discussion on the three contributions presented in chapters 2 to 4. For each of these contributions, a brief summary and suggestions for further study are provided.

1.3 References

- Anderson, S., and Lohrmann, A. (1995). "Open water test of the SonTek acoustic Doppler velocimeter." *Proceedings of IEEE 5th Working Conference on Current Measurements*, 188–192.
- Hager, W. H. (1992). *Energy dissipators and hydraulic jump*, Kluwer Academic, Dordrecht.
- McCorquodale, J. A. (1986). "Hydraulic jumps and internal flows," *Encyclopedia of fluid mechanics*, N. P. Chermisinoff, ed., Gulf Publishing, Houston, Vol. 2, Chap. 6, 120–173.
- Nikora, V. I., and Goring, D. G. (1998). "ADV measurements of turbulence: Can we improve their interpretation?" *J. Hydraul. Eng.*, 124(6), 630–634.
- Puertas, J., Pena, L. and Teijeiro, T. (2004). "Experimental approach to the hydraulics of vertical slot fishways." *J. Hydraul. Eng.*, 130(1), 10–23.
- Rajaratnam, N. (1967). "Hydraulic jumps." *Adv. Hydrosci.*, 4, 197–280, Ed. By V. T. Chow, Academic Press, N.Y.
- Rajaratnam, N., Van der Vinne, G. and Katopodis, C. (1986). "Hydraulics of vertical slot fishways." *J. Hydraul. Eng.*, 112(10), 909–927.
- Rajaratnam, N., Katopodis, C. and Solanki, S. (1992). "New designs for vertical slot fishways." *Can. J. Civ. Engrg.*, 19 (3), 402–414.
- Resch, F. J., and Leutheusser, H. J. (1972a). "Reynolds stress measurements in hydraulic jumps." *J. Hydraul. Res.*, 10(4), 409–429.
- Resch, F. J., and Leutheusser, H. J. (1972b). "Le ressaut hydraulique: mesures de

- turbulence dans la région diphasique.” *La Houille Blanche*, 4, 279–293.
- Robinson, K. M., Cook, K. R., and Hanson, G. J. (2000). “Velocity field measurements at an overfall.” *Transactions of ASAE*, 43(3), 665–670.
- Rouse, H., Siao, T. T., and Nagaratnam, S. (1959). “Turbulence characteristics of the hydraulic jump.” *Transactions, ASCE*, 124, 926–950.
- SonTek. (1997). *Acoustic Doppler Velocimeter Technical Documentation, Version 4.0*, San Diego, Calif.
- Wu, S., Rajaratnam, N. and Katopodis, C. (1999). “Structure of flow in vertical slot fishway.” *J. Hydraul. Eng.*, 125(4), 351–360.

Chapter 2

Evaluation of ADV Measurements in Bubbly Two-Phase Flows*

2.1 Introduction

Bubbly two-phase flows are often encountered in hydraulic engineering, but little information is available on the turbulent structure of these flows, although such knowledge is necessary for a thorough understanding of these flows. The main reason for this is the limitation of the currently available instrumentation for use in bubbly two-phase flows. Laser Doppler Anemometers are used for measuring turbulence of non-bubbly flows (e.g., Nezu and Rodi 1986; George and Lumley 1973). Resch et al. (1972, 1974) tried to use a hot-film anemometer to measure turbulence in bubbly two-phase flows by developing a digital method to separate the signals caused by water phase and gas phase.

Acoustic Doppler Velocimeter (ADV) is a common tool to measure 3D velocity field in laboratory and field environments (Lohrmann et al. 1994; Kraus et al. 1994; SonTek ADV specifications). A new version of ADV, MicroADV was introduced by SonTek in late 1997 with the goal of providing better accuracy and resolution than the standard ADV. However, problems arise when ADV is used in bubbly two-phase flows. Anderson and Lohrmann (1995) found that the energy of noise increased when ADV was placed in bubbly two-phase flows. Nielsen et al.

* The main content of this chapter has been published as a paper in the Proceedings of the Conference of Hydraulic Measurements & Experimental Methods, ASCE, Estes Park, Colorado, USA, 2002. (CD Rom)

(1998) examined the performance of ADV in a controlled air-water mixture. They found that the signal strength or the signal-to-noise ratio (SNR) of the signal echoed by tracing particles or air bubbles in the flow can be used as a criterion for separating the ADV output velocities for water and air. Nikora and Goring (1998) developed a simple technique to reduce the Doppler noise influence on turbulence characteristics measured by ADV. They found that the Doppler noise can change the true turbulence characteristics significantly and the air bubbles caused the noise energy up to 4–5 times that of the seeding materials, and 2–3 times that of fine silt particles. Robinson et al. (2000) attempted to use an ADV probe to measure the velocity at an overfall. They found that the ADV typically measured unrealistically low values of velocity in the region of high velocity with highly turbulent and highly air entrained flow. In this study we examine the effects of air bubbles and boundary on the measurements of MicroADV by performing experiments in hydraulic jumps.

2.2 Principles of Measurement Techniques

2.2.1 MicroADV

A MicroADV measures velocity of water by recording the Doppler shift produced by suspended particulate matters in the flow (e.g., sediment, small organisms and bubbles, etc.). In reality, the ADV technique is based on the pulse-coherent processing method in which the instrument sends two pulses of sound separated by a time lag, and then the phase difference of the return signal from each pulse divided by the time lag is proportional to the velocity of particles in the water

(SonTek 1997).

Fig. 2.1 shows a 16 MHz down-looking MicroADV made by SonTek which consists of three elements: the measuring probe, the signal conditioning module and the processor. The probe is attached to the conditioning module. The acoustic sensor is mounted on a rigid stem 40 cm long and is composed of one transmitter and three receivers. The receivers are aligned to intersect with the transmit beam at a small sampling volume located about 5 cm from the probe tip. This enables measurements to be taken without interfering with the flow. SonTek MicroADV specifications state that the shape of the sampling volume is a cylinder of 4.5 mm in diameter and 5.6 mm in height.

The velocity range, which determines the maximum velocity to be measured by the instrument, can be set to be ± 3 , ± 10 , ± 30 , ± 100 , or ± 250 cm/s. According to SonTek (1997), the Doppler noise is proportional to the velocity range setting. It is recommended that the minimum velocity range should be set to cover the maximum velocity expected in a given flow. The velocity measurement can reach an accuracy of $\pm 1\%$ of the velocity range. Data can be acquired at sampling rates up to 50 Hz and no recalibration is needed. The leading edge of the sampling volume can be placed as close as 0.5 mm to a boundary and the random noise is approximately 1% of the velocity range at 50 Hz.

2.2.2 Electrical probe

The electrical probe uses the electrical method to measure air concentration

in an air-water mixture, based on the difference in the electrical conductivity of a mixture of air and water and of water alone. Maxwell's equation for the conductivity of suspended homogeneous, non-polarizable spheres is described as

$$\frac{r - r_1}{2r + r_1} = C_e \frac{r_2 - r_1}{2r_2 + r_1} \quad (2.1)$$

in which C_e is the volume concentration of the suspended spheres, and r , r_1 and r_2 are the specific resistivities of the suspension, fluid and suspended spheres, respectively. For non-conducting spheres, Eq. (2.1) reduces to

$$C_e = \frac{r - r_1}{r + \frac{r_1}{2}} \quad (2.2)$$

Based on this principle, a simple air concentration probe developed by Lamb and Killen (1950) was remade in the T. Blench Hydraulics Laboratory at the University of Alberta, shown in Fig. 2.2. The equivalent circuit of the probe is shown in Fig. 2.3 where R_s is the resistance in series with the probe, R_p is the resistance of the probe, E_0 is the supplied voltage, and E_s and E_p are the voltages across the R_s and the probe, respectively.

If the specific resistivities are taken over the same volume, the ratio between them may be replaced by the electrical resistances. Assuming air bubbles in an air-water flow are spherical and non-conducting, then Eq. (2.2) can be rewritten as

$$C_e = \frac{E_0 - I(R_s + R_1)}{E_0 - I(R_s - \frac{R_1}{2})} \quad (2.3)$$

where C_e is the volume concentration of air and I is the current in the circuit.

It is noticed that R_1 is the resistance of pure water. If R_s is adjusted, when the probe is calibrated in pure water, to $R_s = R_1/2$, then Eq. (2.3) is converted into

$$C_e = 1 - 3 \frac{E_s}{E_0} \quad (2.4)$$

The probe, shown in Fig. 2.2, was made of two 10 mm by 100 mm long galvanized steel plates supported by a Teflon rod. The steel plates were insulated all round except for a 10 × 10 mm area on the inside and end. This area functions as the electrode for measuring the air concentration. The supply voltage was provided by a constant sine wave generator which gives a frequency of 5000 Hz and an output of 3 volts. The potential difference across R_s was recorded by a time integrated alternate current dial gauge.

Lamb and Killen (1950) obtained good accuracy from their electrical probe at concentration levels from 2 to over 90%, by comparing the data with those obtained in a mechanical sampler. Rajaratnam (1962) also used this kind of probe in his study to measure air concentrations up to 20%. Kwan (1991) and Chamani (1997) reported that the probe could measure air concentrations from 0.5 to 95%.

2.2.3 Fiber optic probe

A fiber optic probe (by Photonetics, Inc) was used to be as a detector of air bubbles based on the different reflection of light between air and water, shown in Fig. 2.4. Its sensor consists of a Model F32-10-1 probe and Optoflow 2210 Signal Conditioning Module. The probe has two optical fibers, one for transmitting light and the other for receiving it. The tip of the probe is a 1-mm-diameter conical

sapphire. Light is produced by the module and transmitted through a fiber optic cable to the probe tip. If the probe tip is surrounded by liquid, there is little light reflected back whereas in an air bubble the light is almost totally reflected back to the module for detection and processing. The module produces an analog output signal of approximately 0 volt when the probe tip is in liquid and a voltage of 10 volt when it is in an air bubble. The lower detection limit quoted by the manufacturer for this type of probe is a 0.5-mm-diameter bubble (Serdula and Loewen 1998). The advantage of a fiber optic probe is that it measures bubble size, bubble number and bubble velocity in addition to the void fraction.

Cartellier (1992) showed that a velocity estimate is accessible from a single optical probe. For a well developed signature generated by the bubbles impacting the probe shown in Fig. 2.5, he defined four points namely *A*, *B*, *D*, and *E*, where *A* is the starting point of the ascending slope, *B* is the starting point of the descending slope, and points *D* and *E* are, respectively, at 10 and 90% of the voltage difference (*DV*) between the liquid and gas levels. Cartellier (1992) found that the bubble velocity is correlated with its rise time which is defined as the duration between points *D* and *E*, and this correlation has to be obtained for each probe for the specific gas-liquid to be used by calibration.

In a previous study, Serdula and Loewen (1998) calibrated a fiber optic probe when it was oriented facing upstream with its axis parallel to the flow direction. They found that a power law relation exists between the bubble velocity V_b (cm/s) and the rise time T_r (ms) as

$$V_b = 10^a T_r^m \quad (2.5)$$

where m and a are constants defined by the calibration data. For the probe used in this study, $m = -1.03$ and $a = 1.55$.

The chord length, s , which is the distance across the bubble by the probe, is given by

$$s = V_b T_g \quad (2.6)$$

where T_g is the gas resident time defined by points A and B in Fig. 2.5. Because it is unlikely that a bubble will cross the probe tip along exactly its diameter, a probe can only measure the chord length of a crossing bubble instead of its diameter. Saberi et al. (1995) found from probability considerations that an average correction factor $3/2$ has to be used to multiply the chord length to get an estimate of its diameter.

The local void fraction is defined as (Herringe and Davis 1976)

$$c = \frac{\sum_{i=1}^M (T_g)_i}{T} \quad (2.7)$$

where c is the local void fraction, M is the total number of bubbles for which T_g was measured, and T is the total sampling time.

Cartellier and Achard (1991) reviewed the performance of various techniques (optical, impedance, thermal and electrochemical techniques) for measuring void fraction. They found that for the void fraction greater than 10%, fiber optic probes produced a relative error ranging from -19 to +11%. For the void fraction between 2 and 10%, only two tests were performed; for one test, the relative error ranged from -

21 to -7% and for the other, the range was from -56 to +2%. Cartellier (1990) claimed that a dispersed regime at low void fractions is not favorable for the use of optical probes because of large errors. But by placing the probe perpendicular to the flow Serdula and Loewen (1998) found that the relative error varied from -43 to +50% for the void fraction from 0.07 to 0.44%. Compared to the results above reviewed by Cartellier and Achard (1991), Serdula and Loewen (1998) have stated that the fiber optic probes can be used to make reasonably accurate measurements of the void fraction even in dispersed regime. Cartellier (1990) recommended that at low void fractions another measuring technique should be used to control the validity of the results obtained with fiber optic probes.

2.3 Experimental Set-up and Experiments

Free hydraulic jumps were produced in a horizontal rectangular flume with aluminum bottom and Plexiglas sidewalls, 0.46 m wide, 0.60 m deep and 7.6 m long. Two pumps were used to supply the head-tank from the laboratory sump and the discharges were measured by online magnetic flowmeters. Water entered the flume under a vertical sluice gate, provided with a streamlined lip so that a uniform supercritical stream with a thickness equal to the gate opening was produced (see Fig. 2.6). The tailwater depth was controlled by a vertical tailgate located at the downstream end of the flume.

Three experiments were carried out and Table 2.1 gives the details of these experiments. All the jumps were formed just downstream of the gate and hence the

depth of supercritical flow y_1 was equal to the gate opening. The velocity at the gate U_1 , was varied so that the flow had a Froude number, $F_1 = U_1 / \sqrt{gy_1}$, of 2.0, 2.5, and 3.32 where g is the gravitational acceleration. In Table 2.1 y_2 is the subcritical sequent depth and Q is discharge.

A point gauge with an accuracy of ± 0.5 mm was used to measure the depth of flow along the flume. A MicroADV was used to measure the instantaneous velocity field in the central vertical plane within the jump and several sections further downstream until the profiles became approximately invariant. The sampling frequency and sampling time were set to 50 Hz and 5 minutes, respectively. A Prandtl tube of external diameter of 3 mm was used to measure the corresponding mean velocity field. Air concentrations were measured by a fiber optic probe, which was calibrated by Serdula and Loewen (1998) when it was oriented facing upstream with its axis parallel to the flow direction. They observed that the local void fraction obtained by this probe was the same as the volume air concentration obtained from the video image data. Therefore, the local void fraction measured by this probe is used as the volume air concentration in this study. The sampling frequency of the fiber optic probe was 100 kHz and the sampling time was 2 minutes. The results of the fiber optic probe were compared with those from an electrical probe. The electrical probe used in this study was made in the T. Blench Hydraulics Laboratory at the University of Alberta. Detailed design and calibration information are available in Kwan (1991) and Chamani (1997).

2.4 Results and Discussions

In this section we first present the experimental measurements of air concentration and the comparison between the results using fiber optic probe and electrical probe. Then the velocity field obtained by the MicroADV and Prandtl tube is compared along with a discussion on the effects of air bubbles and boundary on the measurements of MicroADV.

2.4.1 Air concentration

Air concentration was measured at different sections from the toe of the jump to a downstream distance of about 6.6 ~ 9.0 times the subcritical depth. At every section, the concentration was measured at 1 cm intervals in the central vertical plane. The profiles of time-averaged air concentration, C , for free hydraulic jumps of $F_1 = 2.0, 2.5,$ and 3.32 are shown in Fig. 2.7, respectively, where x is the longitudinal distance from the gate and y is the vertical distance from the bed. These measurements were obtained using the fiber optic probe. Measurements of air concentration were not obtained in the top several centimeters due to the fluctuation of the free surface. It can be seen from Fig. 2.7 that most of the air is in the surface roller region, and the air concentration in this region increased with the Froude number at the same value of x/y_2 .

In order to check the accuracy of the fiber optic probe, an electrical probe was used to measure the air concentration profiles for Exp.1 ($F_1 = 2.0$). The results are shown in Fig. 2.8. Fig. 2.9 gives the comparison of the air concentration

measurements, where C and C_e are the concentrations by the fiber optic probe and electrical probe, respectively. It can be seen that for $C > 1\%$, the relative error between the two probes is within $\pm 20\%$, and for $C = 0.5 \sim 1.0\%$, the relative error is from -34 to $+20\%$. Note for $C < 0.5\%$, the measurements of the electrical probe are not accurate due to the observed zero drift.

Fig. 2.10 shows the variation of the section-averaged air concentration, \bar{C} , with x/y_2 for the three experiments. The profiles are similar to the observations of Rajaratnam (1962), i.e. \bar{C} increases rapidly up to a certain section, and then falls gradually to zero at some finite value of x/y_2 . The maximum section-averaged air concentration, \bar{C}_{\max} , for each case was plotted against the Froude number in Fig. 2.11 with the data and the equation $\bar{C}_{\max} = F_1^{1.35}$ obtained by Rajaratnam (1962). It indicates that the results obtained by the fiber optic probe agree well with Rajaratnam's data. Thus, the accuracy of the fiber optic probe in measuring air concentration larger than 0.5% is acceptable.

Typical bubble size distributions for the studied hydraulic jumps are plotted in Fig. 2.12 where N is the percentage of the total number of bubbles at a point. At the selected section, only the distribution at the point that has maximum number of bubbles is shown. The peak of these distributions varied between 2 and 3 mm, and the shape of bubble size distributions does not vary significantly with sections and Froude numbers. The time-averaged bubble diameter at each point for the three jumps was observed to be about $2.5 \sim 4.0$ mm.

2.4.2 Effects of air concentration and boundary on velocity measurements

Velocity measurements were obtained using a down-looking MicroADV. However, a special problem arises when the MicroADV was used in bubbly two-phase flows, i.e. spikes were detected when air bubble clouds pass through the sampling volume as shown in Fig. 2.13. Goring and Nikora (2002) suggested a phase-space thresholding method to despiking the contaminated ADV data caused by the flow velocity beyond the preset measurement velocity range or the contamination from previous pulses reflected from the boundaries. The idea of their method was based on that the differentiation enhances the high frequency part of a signal and good data cluster in a dense cloud. The variable and its derivations were plotted against each other in a three-dimensional phase-space plot. An ellipsoid defined by the expected maximum of a random series, $\sqrt{2 \ln n_1} \sigma$ where n_1 is the number of samples and σ is the standard deviation of the random variable, was used to screen out the spikes whose points were outside the ellipsoid. After a spike has been detected, they found that the most satisfactory method to replace it for ADV data is to use a third-order polynomial of best fit through 12 points on either side of the spike, then interpolated across the spike with this polynomial. The method iterates until the number of good data becomes constant. In this study, Goring and Nikora's method, called PSTM thereafter, was used to process the contaminated MicroADV data. The processed time series data (Fig. 2.13c) look satisfactory.

The mean velocity profiles measured by the MicroADV are compared with those obtained from the Prandtl tube in Fig. 2.14 where the MicroADV data were

processed by PSTM. Because the sampling volume of MicroADV is about 5 cm below the probe tip and the water surface fluctuates, there are zones where no measurement is available. It is shown in Fig. 2.14 that the mean velocities from MicroADV are smaller than those from Prandtl tube within the jump region with air bubbles, which is consistent for the three experiments. This is due to the effect of air concentration on MicroADV measurements which is given in Fig. 2.15 where u_{prandtl} is the mean velocity obtained by the Prandtl tube, and u_{pstm} is the mean velocity processed from MicroADV data using PSTM. The MicroADV was placed at least 4 cm above the bed in order to avoid the influence by the bed (bed effect discussed below). The linear relationship between the relative error and air concentration is described by the following equation:

$$(u_{\text{prandtl}} - u_{\text{pstm}}) / u_{\text{prandtl}} = 0.145C + 0.036 \quad (2.8)$$

with a squared correlation coefficient of 0.65 and the maximum air concentration of about 2.2%.

Matos et al. (2002) reported that ADV can provide reasonably accurate velocity measurements for air concentration up to 8% which is significantly larger compared to this study. One may note that in their experiments the air flow was produced by a linear porous diffuser installed at the bottom of the flume and the ADV used was down-looking. Therefore, the probe itself was in a place where the air concentration was less than that at the measurement point. However, in hydraulic jumps the situation is different. The probe itself was in a dense air bubble cloud which has a much higher value of air concentration. The air-water mixture in

between the probe and the sampling volume may change the sonic velocity and disperse the sound pulse transmitted and returned, which probably caused the significant underestimates of the velocity at high air concentrations.

In the transition region from the end of hydraulic jump to open channel flow where the air concentration is zero, the boundary effect on the measurements of MicroADV starts when the distance from the measurement point to the boundary is equal to or less than 3 cm (see Figs. 2.14 and 2.16). It is shown in Fig. 2.16 that the relative error of MicroADV measurements is about 3 ~ 15% for the distance ranging from 1 to 3 cm, and 11 ~ 23% for a distance of 0.5 cm. Without the effect of the bed, the relative error varies from -3 to +5.6%.

SonTek (1997) states that the leading edge of the sampling volume can be placed as close as 0.5 mm above the bed with the accuracy of $\pm 1\%$ of the velocity range. The height of the sampling volume is 5.6 mm for MicroADV. Therefore, the point of measurement limitation should be 3.3 mm above the bed. Unfortunately, it was not the case in this study. Finelli et al. (1999) showed that the height of the sampling volume might be larger than that given by the SonTek software. A large sampling volume could cause the bed being considered as part of the sampling volume when the MicroADV is positioned close to the bed. In such case, the MicroADV will underestimate the flow velocity because the velocity reading is averaged from the sampling volume (Finelli et al. 1999).

The relationship of the average relative error of u_{pstm} at each water depth with the water depth is given by the equation

$$\left(u_{\text{prandtl}} - u_{\text{pstm}} \right) / u_{\text{prandtl}} = 0.0784 y^{-0.83} \quad (2.9)$$

with a squared correlation coefficient of 0.74. This equation describes the average relative error well except at $y = 2.5$ and 3 cm, where the average relative errors are 10.4 and 11.7% respectively, much larger than the values given by the above equation. The reason for this is perhaps that with the two pulses sending by the MicroADV for each velocity measurement there is interference between the reflections of the first pulse from the bed and the second pulse from the sample volume, i.e. the two reflections reach the receivers at the same time (SonTek 1997).

2.5. Conclusions

We present the results of a laboratory study on the effects of boundary and air concentration on the measurements of MicroADV. Experiments were performed in hydraulic jumps with Froude number of 2.0, 2.5, and 3.32. For the flow without air bubbles, it was found that the boundary effect on the measurements of MicroADV starts when the distance from the measurement point to the boundary is equal to or less than 3 cm. The relative error of MicroADV measurements is about 3 ~ 15% for a distance ranging from 1 to 3 cm, and 11 ~ 23% for a distance of 0.5 cm. Away from the bed, the relative error varies from -3 to +5.6%. In situations with the average bubble size of about 2.5 ~ 4 mm and air concentration up to about 2.2% in the MicroADV measurement area, it was found that the relative error of MicroADV measurements is a linear function of air concentration.

2.6 References

- Anderson, S., and Lohrmann, A. (1995). "Open water test of the SonTek acoustic Doppler velocimeter." *Proceedings of IEEE 5th Working Conference on Current Measurements*, 188–192.
- Cartellier, A. (1990). "Optical probes for local void fraction measurements: Characterization of performance." *Rev. Sci. Instrum.*, 61(2), 874–886.
- Cartellier, A., and Achard, J. L. (1991). "Local phase detection probes in fluid/fluid two-phase flows." *Rev. Sci. Instrum.*, 62(2), 279–303.
- Cartellier, A. (1992). "Simultaneous void fraction measurement, bubble velocity, and size estimate using a single optical probe in gas-liquid two-phase flows." *Rev. Sci. Instrum.*, 63(11), 5442–5453.
- Chamani, M. R. (1997). "Skimming flow in a large model of a stepped spillway." Ph.D. thesis, University of Alberta, Canada.
- Finelli, C. M., Hart, D. D., and Fonseca, D. M. (1999). "Evaluating the spatial resolution of an acoustic Doppler velocimeter and the consequence for measuring near-bed flows." *Limnol. Oceanogr.*, 44(7), 1793–1801.
- George, W. K., and Lumley, J. L. (1973). "The laser-Doppler velocimeter and its application to the measurement of turbulence." *J. Fluid Mech.*, 60(2), 321–362.
- Goring, D. G., and Nikora, V. I. (2002). "Despiking acoustic Doppler velocimeter data." *J. Hydraul. Eng.*, 128(1), 117–126.
- Herringe, R. A., and Davis, M. R. (1976). "Structural development of gas-liquid

- mixture flows.” *J. Fluid Mech.*, 73(1), 97–123.
- Kraus, N. C., Lohrmann, R. A., and Cabrera, R. (1994). “New acoustic meter for measuring 3D laboratory flows.” *J. Hydraul. Eng.*, 120(3), 406–412.
- Kwan, A. P. (1991). “Air entrainment at free overfalls.” MSc thesis, University of Alberta, Canada.
- Lamb, O. P., and Killen, J. M. (1950). “An electrical method for measuring air concentration in flowing air-water mixtures.” *Technical Paper No. 2, Series B*, St. Anthony Falls Hydraulic Laboratory, University of Minnesota, U. S.
- Lohrmann, R. A., Cabrera, R., and Kraus, N. C. (1994). “Acoustic-Doppler velocimeter (ADV) for laboratory use.” *Proc., Symp. on Fundamentals and Advancements in Hydraul. Measurements and Experimentation*, C. A. Pugh, ed., ASCE, 351–365.
- Lohrmann, R. A., Cabrera, R., Gelfenbaum, G., and Haines, J. (1995). “Direct measurements of Reynolds stress with an acoustic Doppler velocimeter.” *Proceedings of IEEE 5th Working Conference on Current Measurements*, 205–210.
- Matos, Jorge, Frizell, Kathleen. H., André, Stéphanie., and Frizell, K. Warren. (2002). “On the performance of velocity measurement techniques in air-water flows.” *Proceedings of the Conference of Hydraulic Measurements & Experimental Methods 2002*, Estes Park, Colorado, USA. (CD Rom)
- Nezu, I., and Rodi, W. (1986). “Open channel flow measurements with a laser Doppler anemometer.” *J. Hydraul. Eng.*, 112(5), 335–355.

- Nielsen, K. D., Muste, M., and Weber, L. J. (1998). "Plunging jet measurement improvements using ADV." *Proceedings of the 1998 International Water Resources Engineering Conference*, ASCE, Reston, VA, USA, 1, 833–837.
- Nikora, V. I., and Goring, D. G. (1998). "ADV measurements of turbulence: Can we improve their interpretation?" *J. Hydraul. Eng.*, 124(6), 630–634.
- Resch, F. J., and Leutheusser, H. J. (1972). "Reynolds stress measurements in hydraulic jumps." *J. Hydraul. Res.*, 10(4), 409–429.
- Resch, F. J., Leutheusser, H. J., and Alemu, S. (1974). "Bubbly two-phase flow in hydraulic jump." *J. Hydraul. Div.*, 100(HY1), 137–149.
- Rajaratnam, N. (1962). "An experimental study of the air entrainment characteristics of hydraulic jump." *J. of Institution of Engineers, India*, 42, 247–273.
- Robinson, K. M., Cook, K. R., and Hanson, G. J. (2000). "Velocity field measurements at an overfall." *Transactions of ASAE*, 43(3), 665–670.
- Saberi, S., Shakouzadeh, K., Bastoul, D., and Militzer, J. (1995). "Bubble size and velocity measurement in gas-liquid systems: Application of fiber optic technique to pilot plant scale." *Can. J. Chem. Eng.*, 73(4), 253–257.
- Serdula, C. D., and Loewen, M. R. (1998). "Experiments investigating the use of fiber-optic probes for measuring bubble-size distributions." *J. Oceanic Engrg.*, 23, 385–399.
- SonTek. (1997). "Acoustic Doppler Velocimeter Technical Documentation." Version 4.0, San Diego, Calif.

Table 2.1 List of Experiments

Experiment	y_1 (mm)	U_1 (m/s)	F_1	y_2 (mm)	Q (L/s)
1	71	1.67	2.0	172	54.9
2	71	2.08	2.5	216	68.6
3	41	2.10	3.32	165	40.0

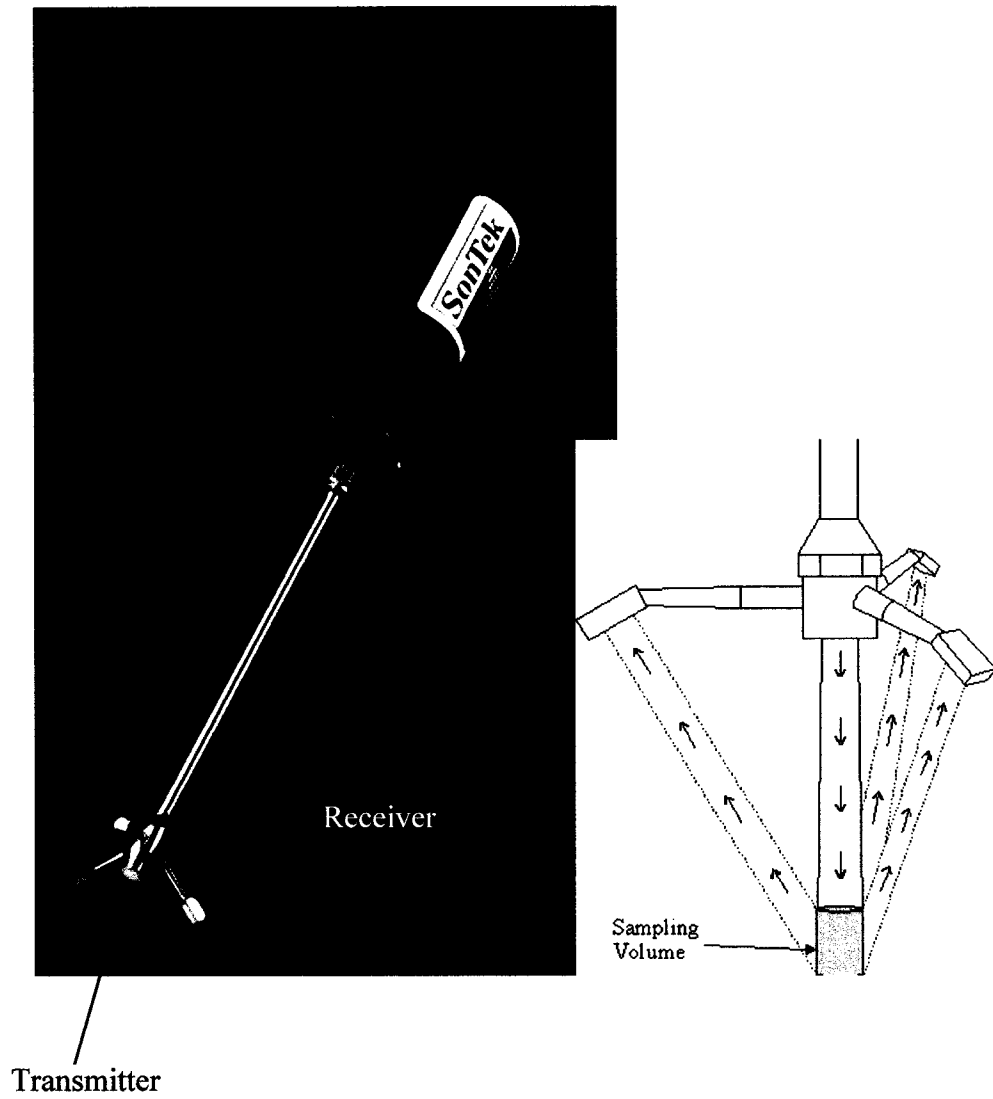


Fig. 2.1 SonTek 16-MHz down-looking 3D MicroADV



Fig. 2.2 The electrical probe

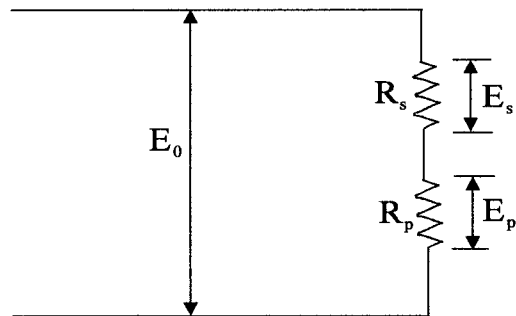


Fig. 2.3 Equivalent circuit of the electrical probe

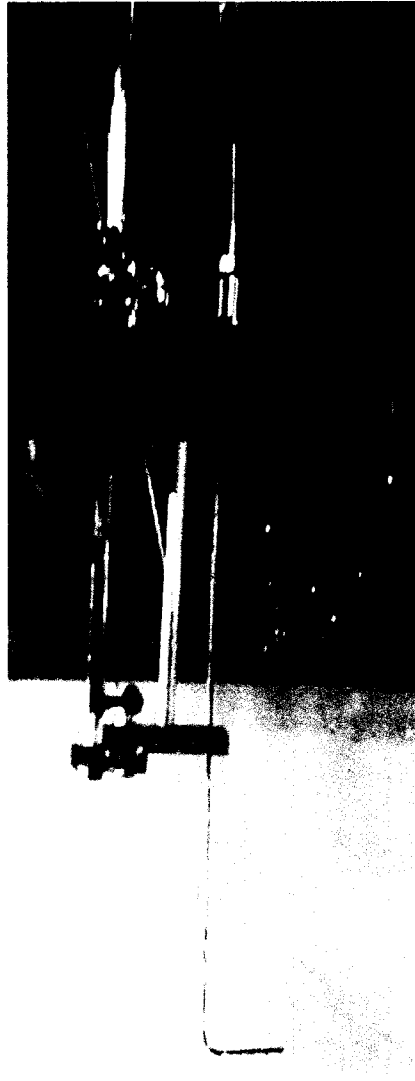


Fig. 2.4 The fiber optic probe

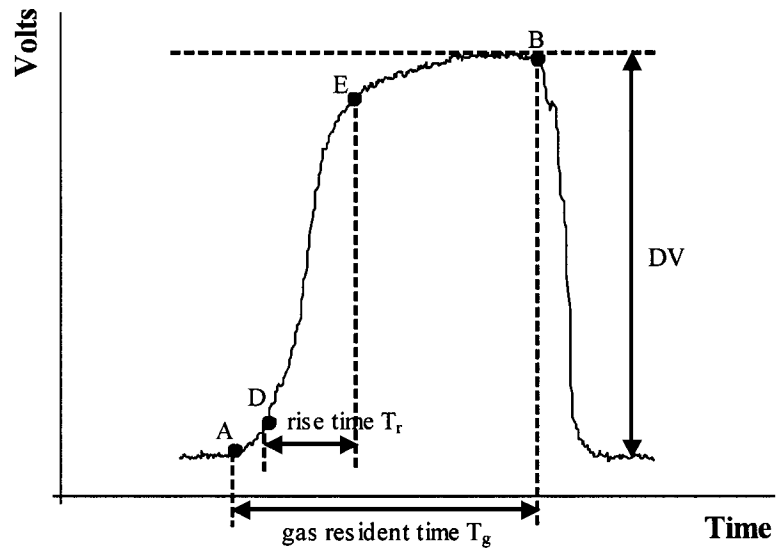


Fig. 2.5 A well developed bubble signature

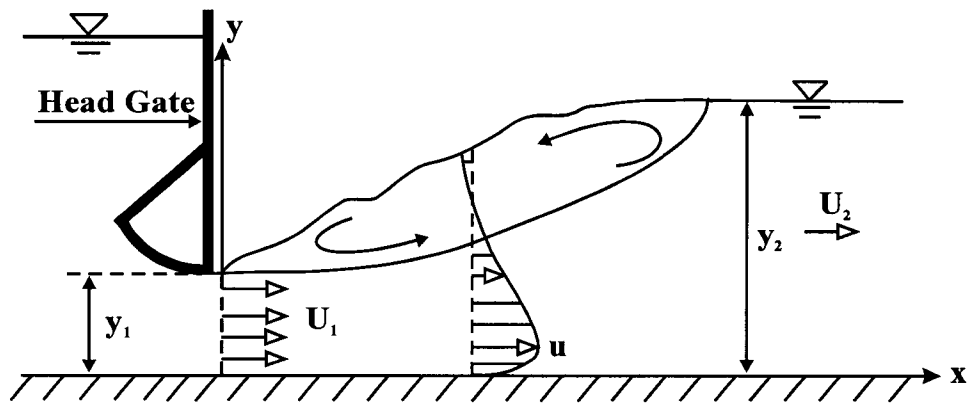


Fig. 2.6 Definition sketch of free hydraulic jump

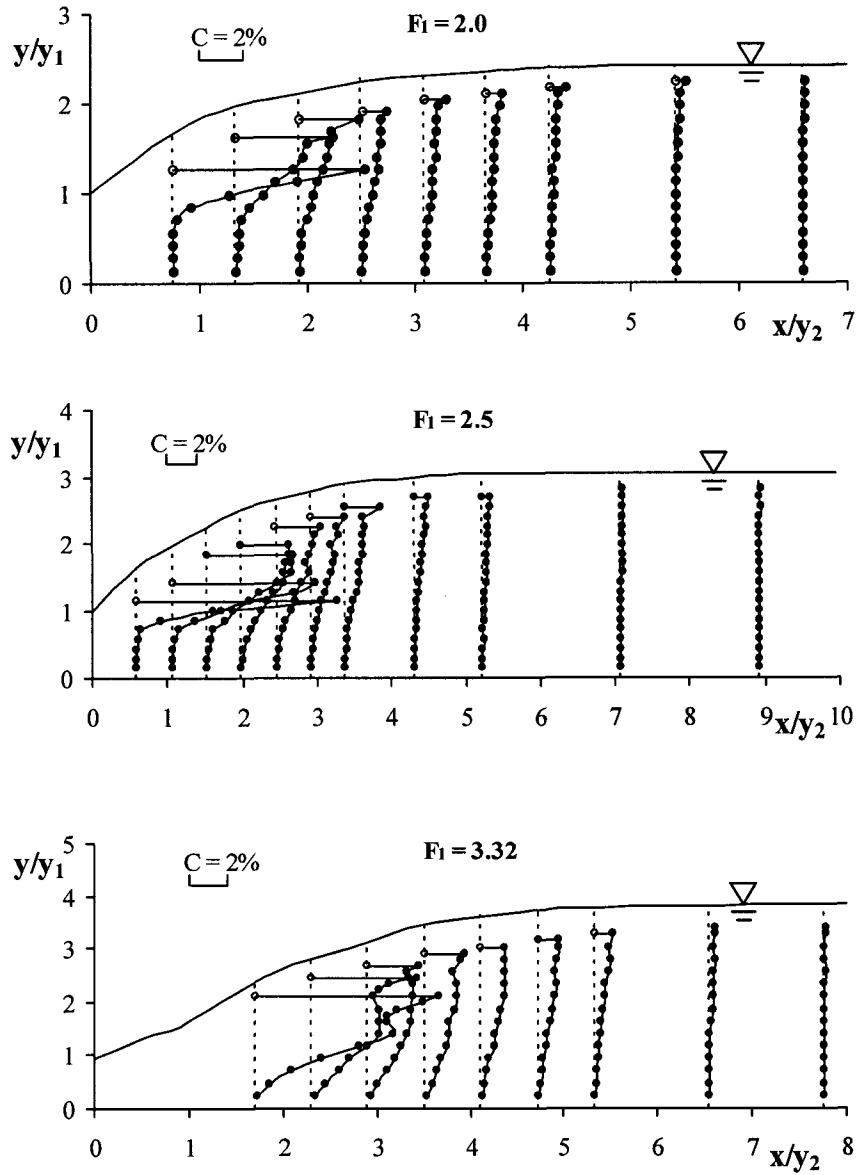


Fig. 2.7 Time-averaged air concentration by fiber optic probe with sampling frequency of 100 kHz and sampling time of 2 minutes

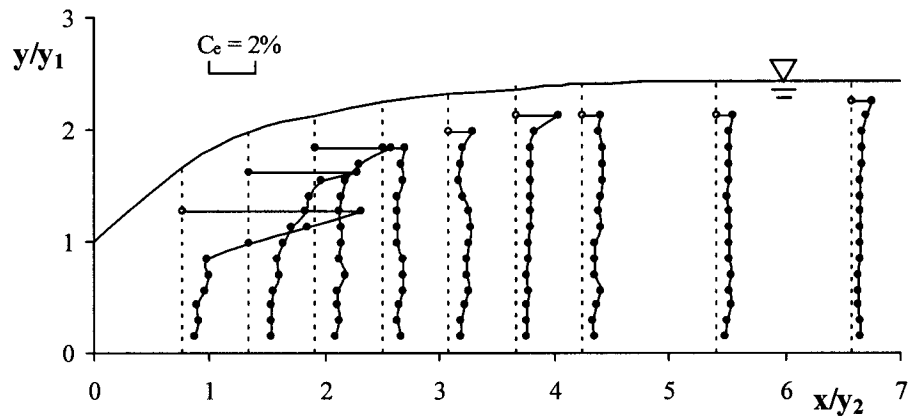


Fig. 2.8 Air concentration by electrical probe for $F_1 = 2.0$

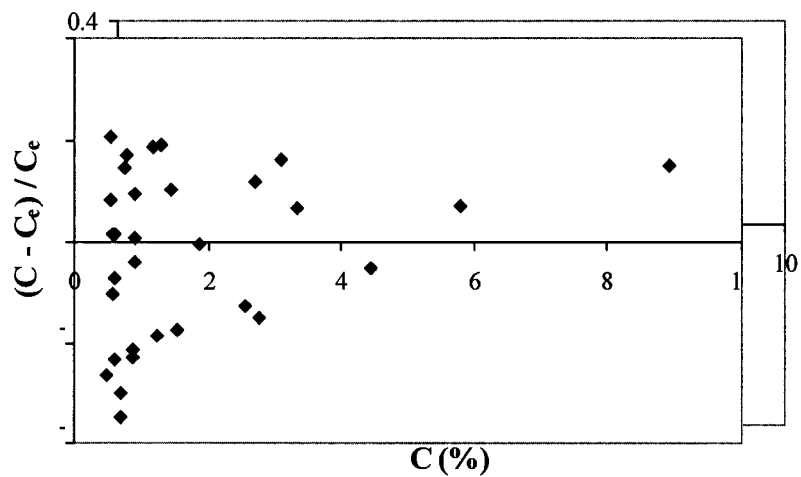


Fig. 2.9 Accuracy of fiber optic probe compared with electrical probe

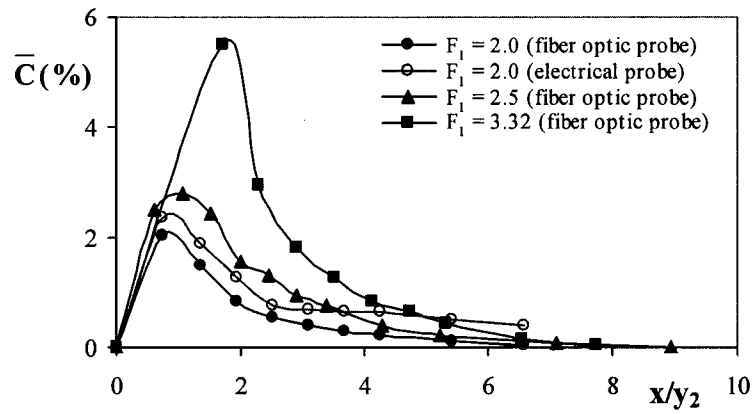


Fig. 2.10 Section-averaged air concentration

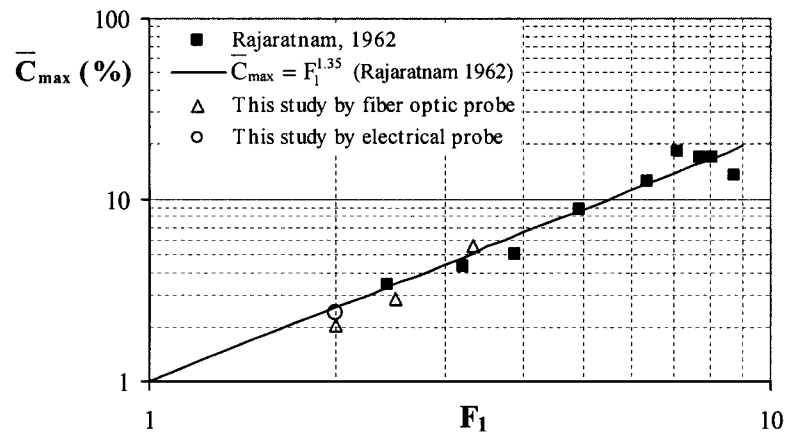


Fig. 2.11 Variation of \bar{C}_{max} with F_1

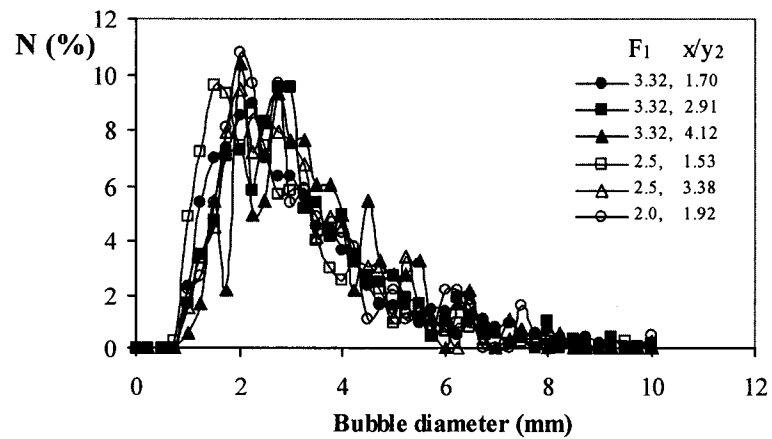


Fig. 2.12 Bubble size distribution at various x/y_2 locations for $F_1 = 2.0, 2.5$ and 3.32

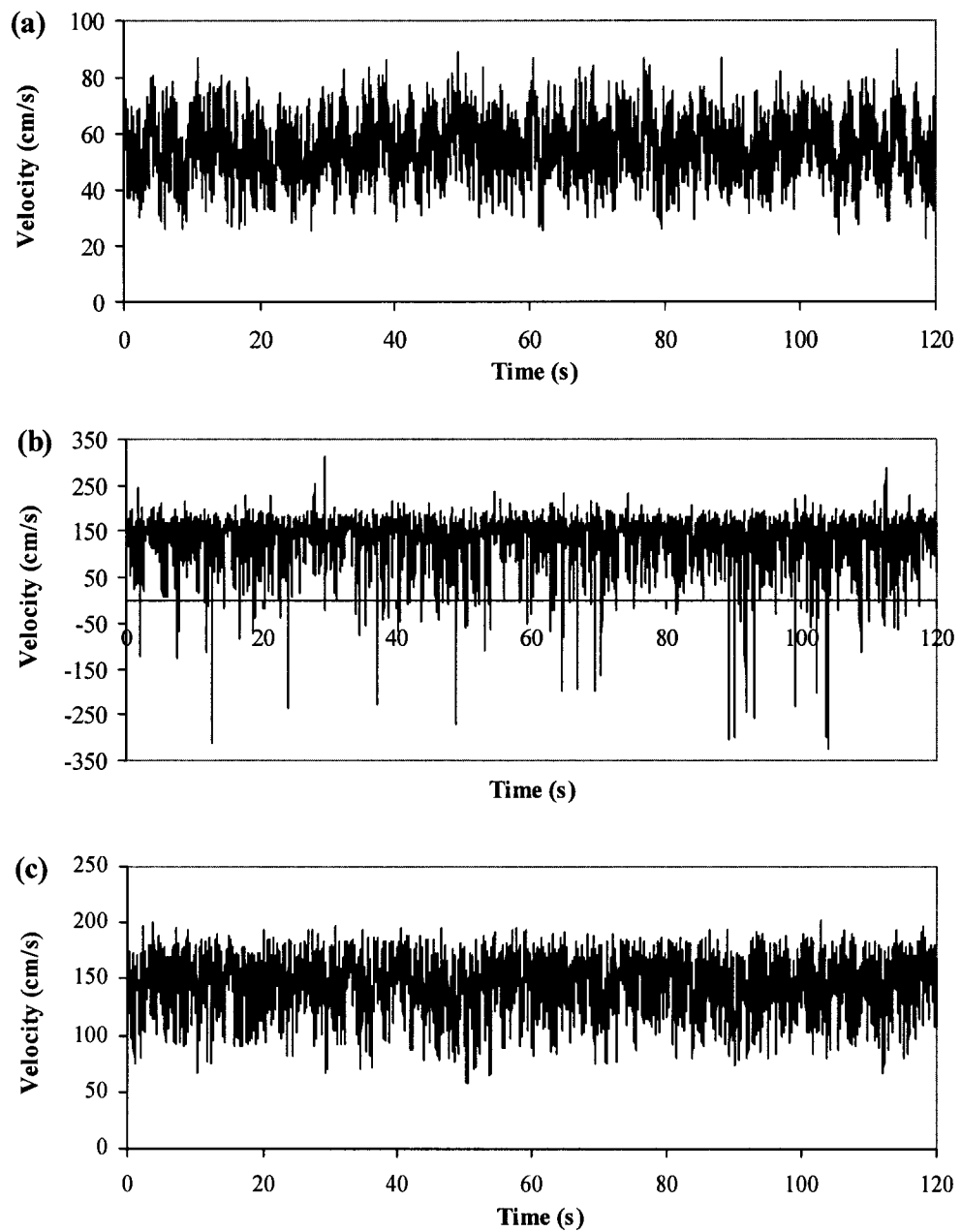


Fig. 2.13 Examples of MicroADV data: (a) clean record; (b) contaminated record; and (c) contaminated record of (b) after cleaning using PSTM

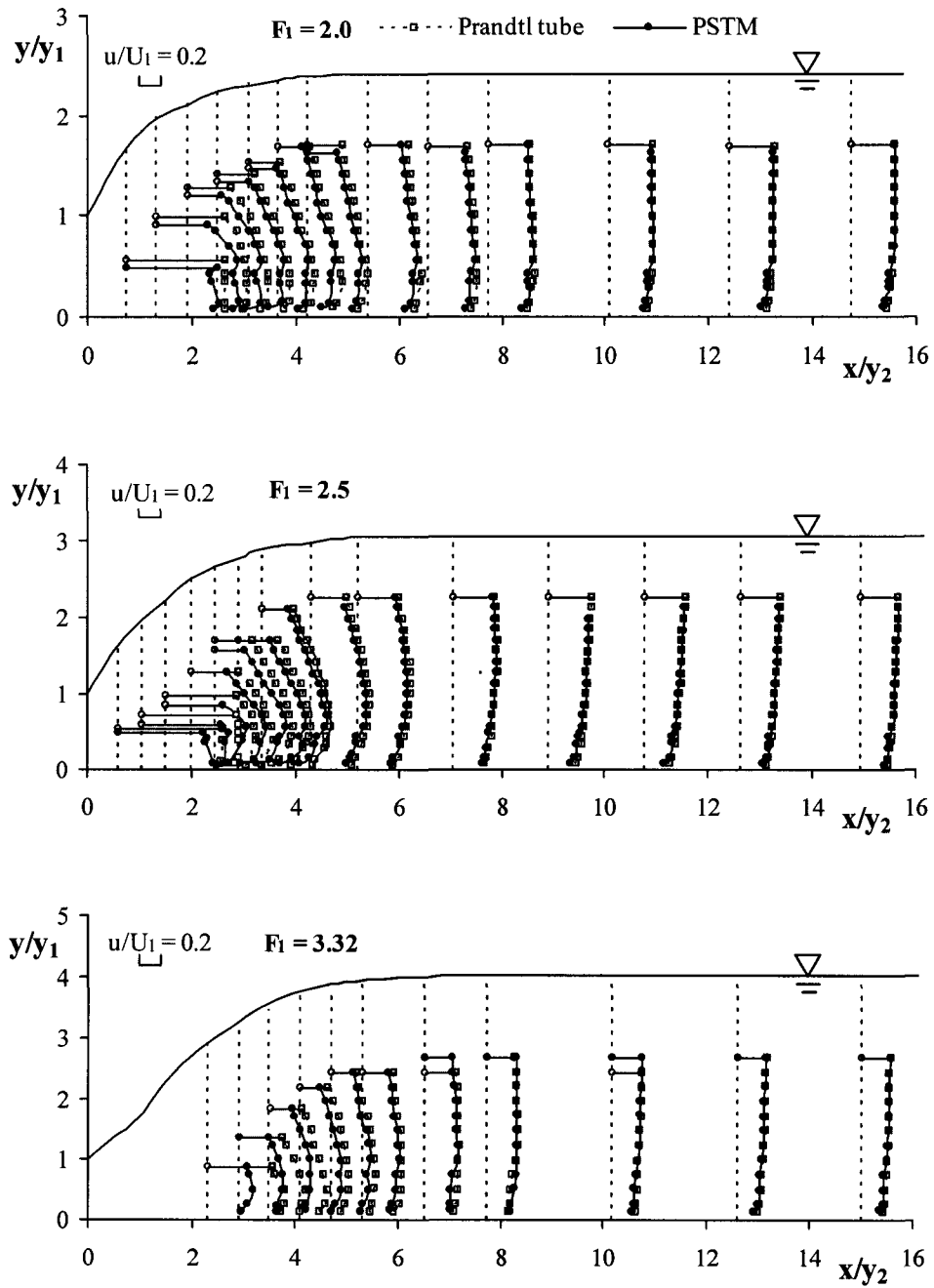


Fig. 2.14 Mean longitudinal velocity profile by MicroADV and Prandtl tube

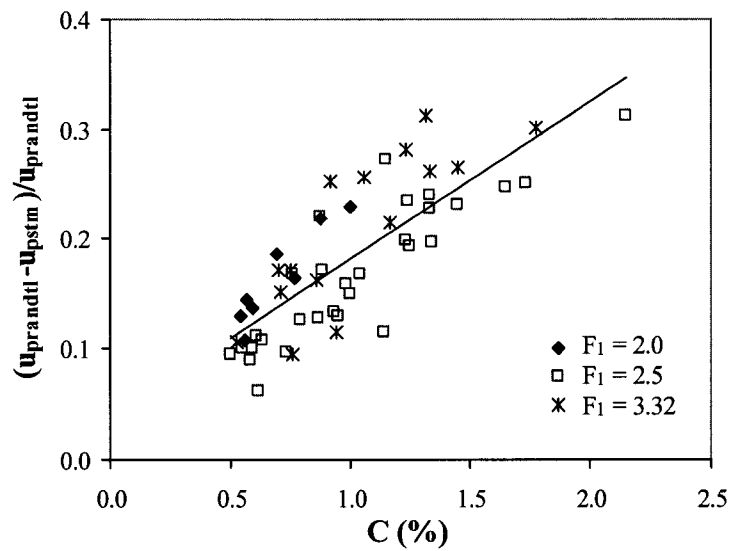


Fig. 2.15 Effect of air concentration on MicroADV data

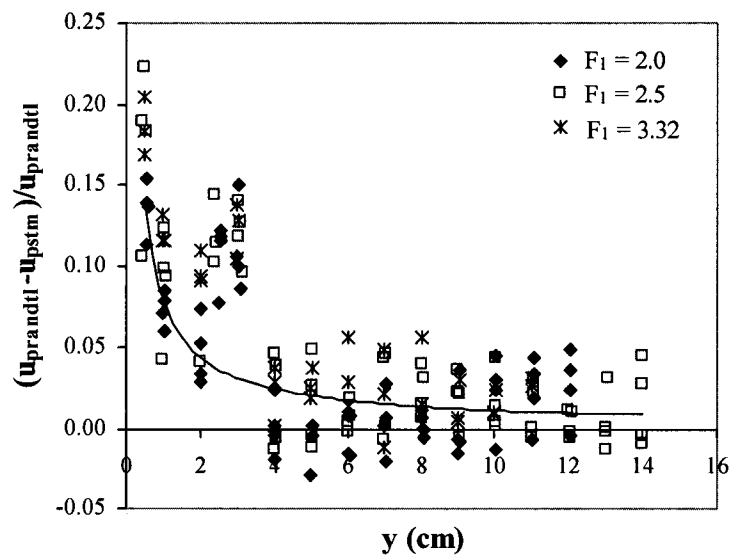


Fig. 2.16 Boundary effect on MicroADV data (without air-bubbles)

Chapter 3

Turbulence Structure of Hydraulic Jumps of Low Froude Numbers*

3.1 Introduction

Hydraulic jumps have been studied extensively because of their importance in energy dissipation below hydraulic structures (Peterka 1958; Rajaratnam 1967; McCorquodale 1986; and Hager 1992). A free hydraulic jump constitutes a rapid transition from supercritical to subcritical flow. Mainly due to the oscillating breaking front at the toe of the jump, air is entrained into the jump as bubbles making the hydraulic jump a bubbly two-phase flow. This air entrainment increases with the Froude number of the supercritical flow, F_1 , just upstream of the jump (Rajaratnam 1962; Liu et al. 2002). Due to measurement difficulty in bubbly two-phase flows, little is known about the turbulence structure of free hydraulic jumps, although such knowledge is necessary for understanding the jump.

Rouse et al. (1959) made the first attempt to measure turbulence characteristics in free hydraulic jumps in an air model using a hot-wire anemometer. The flow pattern of the jump was simulated in an air duct with a curved rigid boundary at the top to model the shape of the jump free surface. Jumps of three Froude numbers of 2, 4, and 6 were studied. Basic data of mean velocity, turbulence intensities and Reynolds shear stress were obtained, along with turbulence production and dissipation calculations. Their study was a significant contribution to

* The main content of this chapter will appear in a paper in the June 2004 issue of the Journal of Hydraulic Engineering, ASCE.

the understanding of the turbulence structure of hydraulic jumps. However, it appears that the air model may not have reproduced correctly all the main characteristics of water jumps (Peterka and Bradley 1959; Rajaratnam 1965; Wu and Rajaratnam 1995). The presence of a curved rigid boundary rather than the fluctuating upper free surface of the jump with gravity dominated roll-back and abundant air entrainment possibly caused some modification of the flow. Resch and Leutheusser (1972a, b) used a hot-film anemometer to make some limited measurements on the turbulence in free hydraulic jumps with Froude numbers F_1 of 2.85 and 6 in a water channel and presented the experimental results including mean velocity, turbulence intensities and Reynolds shear stress without general analysis.

To the authors' knowledge, no further measurements have been made on the turbulence in free hydraulic jumps. Hence, a laboratory investigation was conducted on free hydraulic jumps using a SonTek 16 MHz Micro acoustic Doppler velocimeter (MicroADV). Due to the limitation of ADV in measuring bubbly two-phase flow (Liu et al. 2002), the experiments were confined to relatively low Froude numbers. Detailed measurements of mean velocities, turbulence intensities and shear stresses were performed and these results with general analysis are presented herein.

3.2 Experimental Arrangement and Program

Free hydraulic jumps were produced in a horizontal rectangular flume of aluminum bottom and Plexiglas sidewalls, 0.46 m wide, 0.60 m deep and 7.6 m long. Two pumps were used to supply the head-tank from the laboratory sump and the discharges were measured by online magnetic flowmeters. Water entered the flume

under a vertical sluice gate, provided with a streamlined lip so that a uniform supercritical stream with a thickness equal to the gate opening was produced (Fig. 3.1). The tailwater depth was controlled by a vertical tailgate located at the downstream end of the flume.

A down-looking MicroADV was used to measure instantaneous velocity field in the central vertical plane within the jump and several sections further downstream until the end of the transition region from the jump to open channel flow was reached. The length of this transition region has been found to be approximately equal to 10 times the tailwater depth (Wu and Rajaratnam 1996). At every section, the velocity was measured at 1 cm interval. The sampling frequency and sampling time were set to 50 Hz and 5 minutes respectively.

MicroADV is a new version of ADV with better accuracy and resolution. ADV has become a useful instrument in measuring 3D velocity fields in laboratory and field environments by recording the Doppler shift produced by acoustic targets in the flow (Lohrmann et al. 1994; Kraus et al. 1994; SonTek 1997). The sampling volume of a MicroADV is located about 5 cm from the probe. According to SonTek, the sampling volume is cylindrical with a diameter of 4.5 mm and length of 5.6 mm. It can measure flow velocities from about 1 mm/s to 2.5 m/s with an accuracy of $\pm 1\%$ of the measurement range. Data can be acquired at sampling rates up to 50 Hz. The leading edge of the sampling volume can be placed as close as 0.5 mm to a boundary.

However, problems arise when ADV is used in bubbly two-phase flows. It

was found that the energy level of noise increased when ADV was placed in bubbly two-phase flow and the true turbulence characteristics were changed significantly (Anderson and Lohrmann 1995; Nikora and Goring 1998). Robinson et al. (2000) found that the ADV typically measured unrealistically low values of velocity in the region of high velocity with highly turbulent and highly air-entrained flow. Liu et al. (2002) found that spikes were detected when air bubbles pass through the sampling volume. Therefore, the MicroADV data were processed in this study by the phase-space thresholding method (PSTM) suggested by Goring and Nikora (2002) to get rid of the spikes. The idea of PSTM was based on that the differentiation enhances the high frequency part of a signal and good data cluster in a dense cloud in the phase space plotted using the variable and its derivatives against each other.

Three experiments were carried out and Table 3.1 summarizes the details. All jumps were formed just downstream of the gate and hence the depth of supercritical flow y_1 is equal to the gate opening (see Fig. 3.1). The velocity at the gate, U_1 , was varied so that Froude number, $F_1 = U_1 / \sqrt{gy_1}$, where g is the gravitational acceleration, was equal to 2.0, 2.5 and 3.32 for experiments 1, 2 and 3, respectively. The Reynolds number, $R_1 = U_1 y_1 / \nu$ where ν is the kinematic viscosity of water, was in the range of 86,100 – 147,680. In Table 3.1 y_2 is the subcritical sequent depth of the jump and Q is discharge. Fig. 3.2(a–c) show the hydraulic jumps produced with F_1 equal to 2.0, 2.5, and 3.32.

3.3 Experimental Results and Analysis

Figure 3.3 shows mean velocity distributions in the central vertical plane for

the three experiments, as measured by the MicroADV. It should be pointed out that all the MicroADV data were processed by PSTM in order to get rid of the spikes. Because the sampling volume of MicroADV is about 5 cm below the probe tip and the water surface fluctuates, there are zones where no results are available. It can be seen that the shape of the mean velocity distribution changes gradually from a plane wall jet-like profile within the jump to that of open channel flow far downstream. The mean vertical velocities are much smaller than the mean longitudinal velocities and are positive in the jump region studied, then almost reduce to zero in the transition region from the end of the jump to the section where the velocity profiles resemble those of fully developed turbulent open channel flow.

It was found that air bubbles and proximity to the boundary cause the MicroADV to underestimate the mean velocity (Robinson et al. 2000; Liu et al. 2002). The longitudinal mean velocity could be corrected for these errors as stated in the Appendix. Fig. 3.4 shows the variation of u_m/U_1 with x/L where u_m is the maximum value of the longitudinal mean velocity u at any station x , and L is the longitudinal distance at which $u_m = 0.5U_1$. In Fig. 3.4 the corrected values of u_m agree very well with those obtained by Prandtl tube for $F_1 = 2.0$ and 2.5 , but not for $F_1 = 3.32$. The experimental points for $F_1 = 2.0$ and 2.5 fall closer to the plane wall jet curve instead of the free jump curve (Wu and Rajaratnam 1995). This is possibly because the free jump curve was obtained from jumps with larger Froude numbers ($F_1 > 4$) whereas for smaller Froude numbers in this study, flow is more like a plane wall jet. Fig. 3.4 also shows the results of Resch and Leutheusser (1972b) for $F_1 =$

2.85 and 6.0, Schröder (1963) for $F_1 = 3.85$ and Rajaratnam (1965) for $F_1 = 3.9$ for comparison. Fig. 3.5 shows the variation of L/y_2 against F_1 for the experimental results of this present study as well as other related studies of free jumps. Most of the results are clustered together except perhaps the results of Rouse et al. (1959).

The variation of b/y_1 with x/y_1 is shown in Fig. 3.6 along with the curve of Rajaratnam (1965) where b is the length scale for the mean velocity, which is the normal distance from the boundary at which $u = 0.5u_m$ (see Fig. 3.1). It can be seen that the data in the current study agree well with the results of Rajaratnam (1965).

Figures 3.7 and 3.8 show the distributions of Reynolds stress $(-\overline{u'v'})$, and longitudinal and vertical turbulence intensities $\sqrt{\overline{u'^2}}$ and $\sqrt{\overline{v'^2}}$, respectively, for $F_1 = 2.0, 2.5$ and 3.32 . The turbulence intensities were corrected for the Doppler noise which will be discussed later. The variation of $(\sqrt{\overline{u'^2}})_m / U_1$, $(\sqrt{\overline{v'^2}})_m / U_1$ and $(\overline{u'v'})_m / U_1^2$ with x/y_2 is shown in Fig. 3.9 along with the mean line of current data. It was found that the maximum turbulence intensities and Reynolds stress decrease rapidly with x/y_2 within the jump and gradually level off in the transition region from the jump to usual open channel flow. The maximum vertical turbulence intensity is about one half of the maximum longitudinal turbulence intensity with a value of about 3% of U_1 when approaching the end of transition region, whereas $(\sqrt{\overline{u'^2}})_m$ has a value of about 5% of U_1 . $(\overline{u'v'})_m$ is about 0.04% of U_1^2 when approaching the end of the transition region. The results of Rouse et al. (1959) in the air model of the jump, Resch and Leutheusser (1972a) using a hot-film anemometer, and Liu and

Drewes (1994) using LDA are compared with the authors' results in Fig. 3.9. It can be seen that the data of Resch et al. for $F_1 = 2.85$ agree well with the authors' data except for $x/y_2 \leq 2$ for the maximum vertical turbulence intensity and maximum Reynolds stress, and the data with $F_1 = 6$ agree well with the authors' observations for $x/y_2 > 2$ except for the maximum longitudinal turbulence intensity. The longitudinal turbulence intensity measurements of Liu and Drewes (1994) are somewhat smaller compared to the present results, and the reason for the difference is not immediately clear. The results of Rouse et al. (1959) are noticeably different from this study and this is possibly because their air model did not reproduce all the characteristics of jumps with a free surface.

The similarity of Reynolds stress profiles within the jump region is checked for the three experiments shown in Fig. 3.10. The subscript m always refers to the maximum in a vertical profile. In Fig. 3.10 the experimental results show that the profiles in the jump for all the three Froude numbers are approximately similar. The maximum value of Reynolds stress occurs at $y/b \approx 0.9$. Profiles of the vertical turbulence intensity $\sqrt{v'^2}$ within the jump region were also found to be similar as shown in Fig. 3.11. Due to the limitation of ADV, the value of $(\sqrt{v'^2})_m$ was obtained only at few sections. The results of an attempt to discover as to whether the longitudinal turbulence intensity within the jump region is similar are shown in Fig. 3.12. The distribution of the normalized turbulence intensity $\sqrt{u'^2}$ is approximately similar for $F_1 = 3.32$, and $F_1 = 2.5$ for $y/b > 0.6$. It demonstrates some degree of

scatter for $F_1 = 2.0$, and for $F_1 = 2.5$ for smaller values of y/b . It appears that the turbulence penetrates into the bottom of the flow as the Froude number increases. All the results for the three experiments are shown in Fig. 3.12(d) and these results show similarity for $y/b > 0.7$, while the degree of scatter for $y/b < 0.7$ increases with the decrease of y/b .

The turbulence kinetic energy per unit mass K' is defined as

$$K' = (\overline{u'^2} + \overline{v'^2} + \overline{w'^2}) / 2 \quad (3.1)$$

where u' , v' , w' are the longitudinal, vertical and transverse velocity fluctuations, respectively. The similarity of the turbulence kinetic energy shown in Fig. 3.13 is very similar to that of the longitudinal turbulence intensity. The maximum value of K' occurs at $y/b = 0.8-0.9$ which is at about the same place of maximum Reynolds shear stress. Fig. 3.14 shows the variation of normalized maximum value K'_m with x/y_2 for the three experiments. It was found that K'_m decreases linearly with x/y_2 within the jump and this variation is described by the equation:

$$K'_m{}^{0.5} / U_1 = -0.016x / y_2 + 0.196 \quad (r^2 = 0.97) \quad (3.2)$$

In the transition region, K'_m gradually levels off reaching a constant value of $K'_m{}^{0.5} / U_1 = 0.04$.

Figure 3.15 shows typical power spectra $G_u(f)$, $G_v(f)$, $G_w(f)$ for the corresponding velocity components u' , v' , w' , where f is the frequency and the spectral density is divided by the corresponding turbulence intensity. The level off of the spectral density at high frequency is due to the Doppler noise which is an

inherent part of all Doppler-based back scatter systems as pointed out by Lohrmann et al. (1994) and SonTek (1997). The identification of the Doppler noise is the flattening of the spectrum referred to as a noise floor because the Doppler noise is Gaussian white noise (Lohrmann et al. 1994; Nikora and Goring 1998). Fig. 3.15(a) shows the power spectrum of velocity in the region without air bubbles using raw data of MicroADV. It can be seen that the horizontal velocity components are biased due to the Doppler noise from about 15 Hz and the Doppler noise has no influence on the vertical velocity below the Nyquist frequency. Lohrmann et al. (1994) concluded that the noise floor in the case of measurements of an ADV may take place in the high frequency region, 4–10 Hz, for horizontal velocity components, while for the vertical velocity the noise floor rarely plays any role below the Nyquist frequency. Thus a MicroADV has a better resolution of turbulence frequency for the horizontal velocity components than ADV. The reason for a better resolution of MicroADV is that MicroADV has a smaller sampling volume (0.089 cm^3) and higher sampling frequency (50 Hz) than ADV (sampling volume of 0.254 cm^3 and sampling frequency of 25 Hz).

However, when the MicroADV was used in the flow with air bubbles, the air bubbles increased the noise floor level. The noise starts to influence the spectrum with elevated energy from 4–5 Hz for the horizontal velocity component and 10–12 Hz for the vertical velocity as shown in Fig. 3.15(b) using raw data of MicoADV. This observation is consistent with the finding of Nikora and Goring (1998). They found that air bubbles brought the noise energy up to 4–5 times from that caused by

SonTek seeding materials. Elevated energy at higher frequency was also found by Anderson and Lohrmann (1995) when the ADV was placed in bubble clouds. After using PSTM of Goring and Nikora (2002) to process the MicroADV data, it was found in Fig. 3.15(c) that the elevated energy disappeared and the noise floor started from about 10 Hz for all the three velocity components. But the noise floor tilted up somewhat while approaching the Nyquist frequency. The reason for this is not clear.

The inertial subrange was clearly marked by the existence of a $-5/3$ slope in the power spectra shown in Fig. 3.15. However, the turbulence is non-isotropic because the turbulence intensities of the three velocity components are not equal to each other. For a turbulent flow of a sufficiently large Reynolds number, the local isotropic state will be established in the small scale region of spectrum (Monin and Yaglom 1971). The relation $G_{uv}(f) = 0$ is a consequence of local isotropy where G_{uv} is the co-spectrum of the turbulence velocity components u' and v' (Corrsin 1949). Therefore, the correlation-coefficient spectrum

$$R_{uv}(f) = \frac{|G_{uv}(f)|}{[G_u(f)G_v(f)]^{0.5}} \quad (3.3)$$

is plotted with the frequency f in Fig. 3.16. The data show that R_{uv} falls rapidly with increasing frequency to a value of 0.14 at 15 Hz and then levels off. This level off is probably due to the influence of Doppler noise. Because of the influence of the Doppler noise, the MicroADV could only provide useful information for the frequency up to about 15 Hz. Therefore, the motion is not locally isotropic within the inertial subrange based on the frequency resolution of our measurements. But it is clear that if we extend the mean curve to $R_{uv} = 0$ in Fig. 3.16, then the motion is

locally isotropic approximately for $f > 21$ Hz. Hence, it is reasonable to use the Kolmogorov theory of local isotropic turbulence (Hinze 1975) to estimate the dissipation rate as a first approximation. According to this theory, the one dimensional spectrum, $G_u(k)$, of the longitudinal velocity in the inertial subrange is described as

$$G_u(k) = A\varepsilon^{2/3}k^{-5/3} \quad (3.4)$$

where k is the wavenumber, ε is the dissipation rate and A is a constant with a value of 0.56 for local isotropic turbulence. In order to convert a time series to a space series, Taylor's frozen turbulence hypothesis (Hinze 1975) was used,

$$\frac{\partial}{\partial t} = -u \frac{\partial}{\partial x} \quad (3.5)$$

which is valid when the velocity fluctuations are much smaller than the streamwise mean velocity (Hinze 1975). In this study, the ratio of the turbulence intensity to local streamwise mean velocity is from 5 to 50% within the jump. Therefore, the use of Taylor's hypothesis is an approximation. Then, the spectrum can be transferred from the frequency domain to the wave number domain by

$$k = 2\pi f / u \quad (3.6)$$

$$G_u(k) = \frac{u}{2\pi} G_u(f) \quad (3.7)$$

Substituting Eqs. (3.6) and (3.7) into Eq. (3.4), we could show that

$$G_u(f) = A(2\pi)^{-2/3} u^{2/3} \varepsilon^{2/3} f^{-5/3} \quad (3.8)$$

Then the energy dissipation rate could be estimated using Eq. (3.8). The distribution of energy dissipation rate is presented in Fig. 3.17. The values of energy dissipation

rate estimated for the different regions of the flow are given in Table 3.2. Fig. 3.18 shows the normalized energy dissipation rate in the form of $\varepsilon b/u_m^3 = f(y/b)$. It was found that for $y/b < 0.4$ the dissipation rates are very small, and then quickly increase with y/b within the jump.

The average energy dissipation rate per unit mass $\bar{\varepsilon}$ in the jump is defined as

$$\bar{\varepsilon} = \frac{\rho g Q \Delta h}{\rho L_j W 0.5(y_1 + y_2)} \quad (3.9)$$

where ρ is the density of water, L_j is the length of the jump, W is the width of the flume, and Δh is the energy loss in the jump expressed as a head. Then the average energy dissipation rates for the three experiments are 0.24, 0.49, and 0.86 m^2/s^3 for $F_1 = 2.0, 2.5,$ and 3.32 , respectively. This indicates that the dissipation rate increases with Froude number.

The Kolmogorov's length scale η , which corresponds to dissipative eddies, can be calculated from the relation

$$\eta = (v^3 / \varepsilon)^{1/4} \quad (3.10)$$

It is clear to see that $\eta \propto \varepsilon^{-1/4}$, which means the accuracy of estimated ε will have less effect on the accuracy of η . For example, 50% error in ε will cause only 10% difference in η . This also gives confidence on the estimation of η based on the first approximation of ε from the Kolmogorov theory of locally isotropic turbulence. The distributions of η for the three experiments are given in Fig. 3.19. The dissipative eddy size varies from 0.04 mm within the jump to 0.15 mm at the end of the transition region. These values are reasonable compared to the results of other

researchers for similar flows. Gibson (1963) found that the dissipative eddy size for a round turbulent jet with Reynolds number of 1.2×10^5 varies from 0.0126 mm off jet axis to 0.014 mm at jet axis in the plane fifty orifice diameters from the nozzle. Nikora and Smart (1997) found for a gravel bed river flow with Reynolds number of 2×10^6 that the dissipative eddy size varies from 0.05 mm near the bottom to 0.1 mm near the surface.

The mean velocity u for the three experiments measured is in the range from 50 to 180 cm/s, then the wavenumber k corresponding to the Nyquist frequency 25 Hz could be obtained using Eq. (3.6) as $k_n = 0.87\text{--}3.14 \text{ cm}^{-1}$. The wavenumber k_d corresponding to the Kolmogorov's length scale is described approximately as (Monin and Yaglom 1971)

$$k_d = 1/\eta \quad (3.11)$$

Hence $k_d = 250\text{--}67 \text{ cm}^{-1}$ for the three experiments within the measurement region. Since $k_n \ll k_d$, we can reasonably extend the inertial subrange $-5/3$ slope in the velocity spectrum down to the wavenumber k_n . Then the area under the modified velocity spectrum curve is the turbulence intensity corrected for Doppler noise. The difference between the corrected and measured turbulence intensity is up to 15%. Here “measured” means calculated from the MicroADV data after processing using PSTM. The turbulence intensities mentioned before are the corrected values. However, this correction method can not be used for Reynolds stress. Fortunately, “the contribution of the Doppler noise is zero as long as the Doppler noise is the same in all beams. Because the Doppler noise is a function of the signal strength, this

means that the signal strength should be the same in all three beams” (Lohrmann et al. 1994). In this study the signal strength is roughly equal in all three beams. Nikora and Goring (1998) found that for their ADV the ratio between the corrected and measured Reynolds stress was 0.96 to 1.13. Therefore, we would assume the effect of Doppler noise on the Reynolds stress in this study is negligible.

The power spectra of horizontal and vertical velocities are shown in Fig. 3.20. The dominant frequency was found to be in the range from 0 to 4 Hz within the jump for both velocity components. Downstream of the jump the dominant frequency ranges from 0 to 1 Hz for horizontal velocity and 0 to 2 Hz for vertical velocity. The results are similar to those of Mossa (1999) who studied the oscillating characteristics of hydraulic jumps. He found that the dominant peaks were in the 0-1 Hz frequency range for horizontal velocity components and 1–3 Hz for vertical velocity components. Similar results were also reported by Gardiner and Hay (1982) in their investigation on the dynamic forces in a stilling basin. They found that the predominant spectrum of the dynamic forces acting on the side wall of the stilling basin was concentrated in a frequency band below 2 Hz, and a peak frequency of 0.8 Hz was found.

3.4 Conclusions

This paper presents the results of a laboratory study on the turbulence structure of hydraulic jumps with low Froude numbers of 2.0, 2.5, and 3.32. A MicroADV probe was used to obtain the instantaneous velocity field. It was found that the maximum turbulence intensities and Reynolds stress decrease rapidly with

increasing longitudinal distance within the jump and gradually level off in the transition region from the jump to open channel flow. The maximum turbulence kinetic energy at any section decreases linearly with the longitudinal distance within the jump and gradually levels off in the transition region, reaching a constant value of about 0.3% of the kinetic energy of the uniform supercritical stream in front of the jump. The Reynolds stress and turbulence intensities within the jump show some degree of similarity.

The power spectrum of velocity shows the inertial subrange with $-5/3$ slope. However, the flow is not locally isotropic within the inertial subrange with the limited frequency resolution of the MicroADV. By using Kolmogorov theory of local isotropic turbulence as a first approximation, it was found that the dissipative eddy size varies from 0.04 mm within the jump to 0.15 mm at the end of the transition region. The power spectra of horizontal and vertical velocities show that the dominant frequency is in the range from 0 to 4 Hz within the jump for both velocity components. Downstream of the jump the dominant frequency ranges from 0 to 1 Hz for the horizontal velocity and 0 to 2 Hz for the vertical velocity.

3.5 Appendix: Correction to MicroADV's Mean Velocity Measurement

It was found that the MicroADV underestimates the mean velocity in bubbly two-phase flows (Robinson et al. 2000; Liu et al. 2002). Liu et al. (2002) found that the boundary effect on the measurements of MicroADV starts when the distance from the measurement point to the boundary is within about 3 cm. Two equations

were obtained for evaluating the relative errors of MicroADV measurements related to air concentration and boundary effect, respectively, as follows:

$$(u_{\text{prandtl}} - u_{\text{pstm}}) / u_{\text{prandtl}} = 0.145C + 0.036 \quad (r^2 = 0.65) \quad (\text{A1})$$

$$(u_{\text{prandtl}} - u_{\text{pstm}}) / u_{\text{prandtl}} = 0.0784y^{-0.83} \quad (r^2 = 0.74) \quad (\text{A2})$$

where u_{prandtl} is the mean velocity obtained by a Prandtl tube, u_{pstm} is the mean velocity processed from MicroADV data using PSTM, y is the vertical distance from the bed, and C is the air concentration.

Then, the longitudinal mean velocity, u , is corrected for errors caused by air and boundary as

$$u = u_{\text{pstm}} + \Delta_1 u + \Delta_2 u \quad (\text{A3})$$

where $\Delta_1 u$ and $\Delta_2 u$ are the corrections corresponding to air concentration and boundary effect, respectively. From Eqs. (A1) and (A2), $\Delta_1 u$ and $\Delta_2 u$ would be written as

$$\Delta_1 u = (0.145C + 0.036) \times u_{\text{prandtl}} \quad (\text{A4})$$

$$\Delta_2 u = 0.0784y^{-0.83} \times u_{\text{prandtl}} \quad (\text{A5})$$

The values of air concentration and mean velocity obtained from Prandtl tube were from a previous study (Liu et al. 2002).

3.5 References

Anderson, S. and Lohrmann, A. (1995). "Open water test of the SonTek acoustic Doppler velocimeter." *Proc. IEEE Fifth Working Conf. on Current*

- Measurements*, St. Petersburg, FL, IEEE Oceanic Engineering Society, 188–192.
- Gardiner, S.R.M., and Hay, D. (1982). “Dynamic force measurement on stilling basin floor and sidewalls.” *International Conference on the Hydraulic Modelling of Civil Engineering Structures*, BHRA Fluid Engineering, 123–130.
- Gibson, M. M. (1963). “Spectra of turbulence in a round jet.” *J. Fluid Mech.*, 15, 161–173.
- Corrsin, S. (1949). “An experimental verification of local isotropy.” *J. Aeronaut. Sci.*, 16, No. 12, 757–758.
- Goring, D. G., and Nikora, V. I. (2002). “Despiking acoustic Doppler velocimeter data.” *J. Hydraul. Eng.*, 128(1), 117–126.
- Hager, W. H. (1992). *Energy dissipators and hydraulic jump*, Kluwer Academic, Dordrecht.
- Hinze, J. O., (1975). *Turbulence*, McGraw-Hill, New York.
- Kraus, N. C., Lohrmann, R. A., and Cabrera, R. (1994). “New acoustic meter for measuring 3D laboratory flows.” *J. Hydraul. Eng.*, 120(3), 406–412.
- Liu, M., Zhu, D. Z., and Rajaratnam, N. (2002). “Evaluation of ADV measurements in bubbly two-phase flows.” *Proceedings of the Conference of Hydraulic Measurements & Experimental Methods 2002*, Estes Park, Colorado, USA. (CD Rom)
- Liu, Q., and Drewes, U. (1994). “Turbulence characteristics in free and forced

- hydraulic jumps.” *J. Hydraul. Res.*, 32(6), 877–898.
- Lohrmann, R. A., Cabrera, R., and Kraus, N. C. (1994). “Acoustic-Doppler velocimeter (ADV) for laboratory use.” *Proc., Symp. on Fundamentals and Advancements in Hydraul. Measurements and Experimentation*, C. A. Pugh, ed., ASCE, 351–365.
- McCorquodale, J. A. (1986). “Hydraulic jumps and internal flows,” *Encyclopedia of fluid mechanics*, N. P. Cheremisinoff, ed., Gulf Publishing, Houston, Vol. 2, Chap. 6, 120–173.
- Mossa, M. (1999). “On the oscillating characteristics of hydraulic jumps.” *J. Hydraul. Res.*, 37(4), 541–558.
- Monin, A. S., and Yaglom, A. M. (1971). *Statistical fluid mechanics: mechanics of turbulence*. Vol. 2, MIT Press, Cambridge, Mass.
- Nikora, V. I., and Smart, G. M. (1997). “Turbulence characteristics of New Zealand gravel-bed rivers.” *J. Hydraul. Eng.*, 123(9), 764–773.
- Nikora, V. I. and Goring, D. G. (1998). “ADV measurements of turbulence: Can we improve their interpretation?” *J. Hydraul. Eng.*, 124(6), 630–634.
- Ohtsu, I., Yasuda, Y., and Awazu, S. (1990). “Free and submerged hydraulic jumps in rectangular channels.” Report of the Research Institute of Science and Technology, Nihon University, No. 35, 50p.
- Peterka, A. J. (1958). “Hydraulic design of stilling basins and energy dissipators.” *Engineering Monograph No. 25*, U.S. Bureau of Reclamation, Denver, USA.
- Peterka, A. J., and Bradley, J. N. (1959). Discussion of “Turbulence characteristics

- of the hydraulic jump.” *Transactions*, ASCE, 124, 952–954.
- Rajaratnam, N. (1962). “An experimental study of the air entrainment characteristics of hydraulic jump.” *J. of Institution of Engineers, India*, 42, 247–273.
- Rajaratnam, N. (1965). “The hydraulic jump as a wall jet.” *J. Hydraul. Division*, ASCE, 91(HY5), 107–132.
- Rajaratnam, N. (1967). “Hydraulic jumps.” *Adv. Hydrosci.*, 4, 197-280, V. T. Chow, Academic Press, N.Y.
- Resch, F. J., and Leutheusser, H. J. (1972a). “Reynolds stress measurements in hydraulic jumps.” *J. Hydr. Res.*, 10(4), 409–429.
- Resch, F. J., and Leutheusser, H. J. (1972b). “Le ressaut hydraulique: mesures de turbulence dans la région diphasique.” *La Houille Blanche*, 4, 279–293.
- Robinson, K. M., Cook, K. R., and Hanson, G. J. (2000). “Velocity field measurements at an overfall.” *Transactions of ASAE*, 43(3), 665–670.
- Rouse, H., Siao, T. T., and Nagaratnam, S. (1959). “Turbulence characteristics of the hydraulic jump.” *Transactions*, ASCE, 124, 926–950.
- Schröder, R. (1963). “Die turbulente Strömung im freien Wechselsprung.” Habilitationsschrift, Mitteilung 59, Institut für Wasserbau und Wasserwirtschaft, TU Berlin, Berlin.
- SonTek. (1997). “Acoustic Doppler Velocimeter Technical Documentation.” Version 4.0, San Diego, Calif.
- Wu, S., and Rajaratnam, N. (1995). “Free jumps, submerged jumps and wall jets.” *J. Hydr. Res.*, 33(2), 197–211.

Wu, S., and Rajaratnam, N. (1996). "Transition from hydraulic jump to open channel flow." *J. Hydraul. Eng.*, 122(9), 526–528.

Table 3.1 Details of Experiments

Expt.	y_1 (mm)	U_1 (m/s)	F_1	y_2 (mm)	Q (L/s)	R_1
1	71	1.67	2.0	172	54.9	118,570
2	71	2.08	2.5	216	68.6	147,680
3	41	2.10	3.32	165	40.0	86,100

Table 3.2 Order of Energy Dissipation Rate (m^2/s^3) in Different Regions of the Flow

F_1	Surface roller ^a	Main flow under the surface roller	Transition from jump to open channel flow
2.0	1.0	0.01–0.5	0.001–0.01
2.5	1.0	0.01–0.5	0.003–0.01
3.32	1.0	0.2–0.5	0.001–0.05

^awithin the measurement area of MicroADV

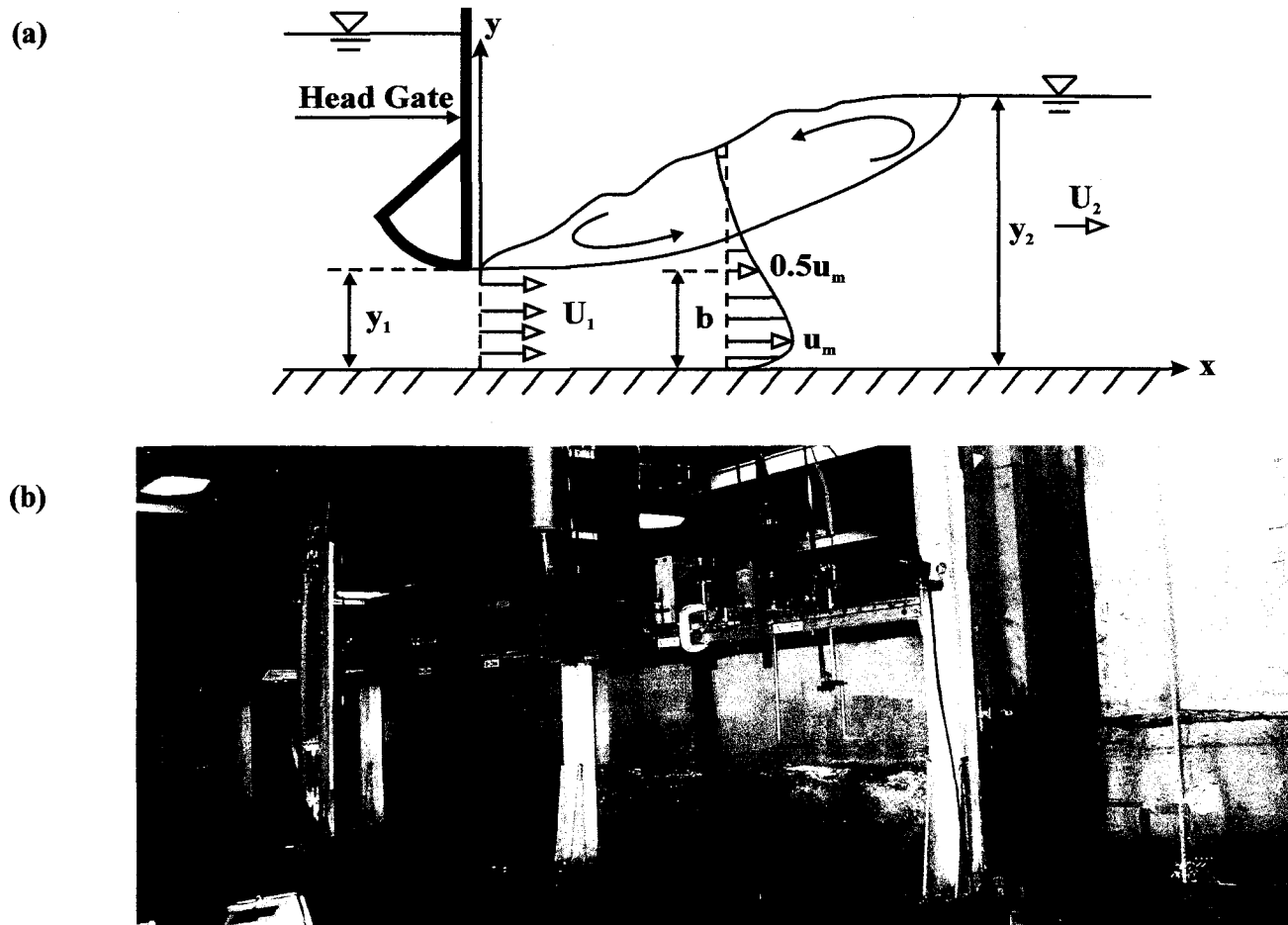


Fig. 3.1 (a) Definition sketch of free hydraulic jump; (b) experimental set-up in T. Blench Hydraulics Laboratory at the University of Alberta



Fig. 3.2(a) Experiment 1 for $F_1 = 2.0$

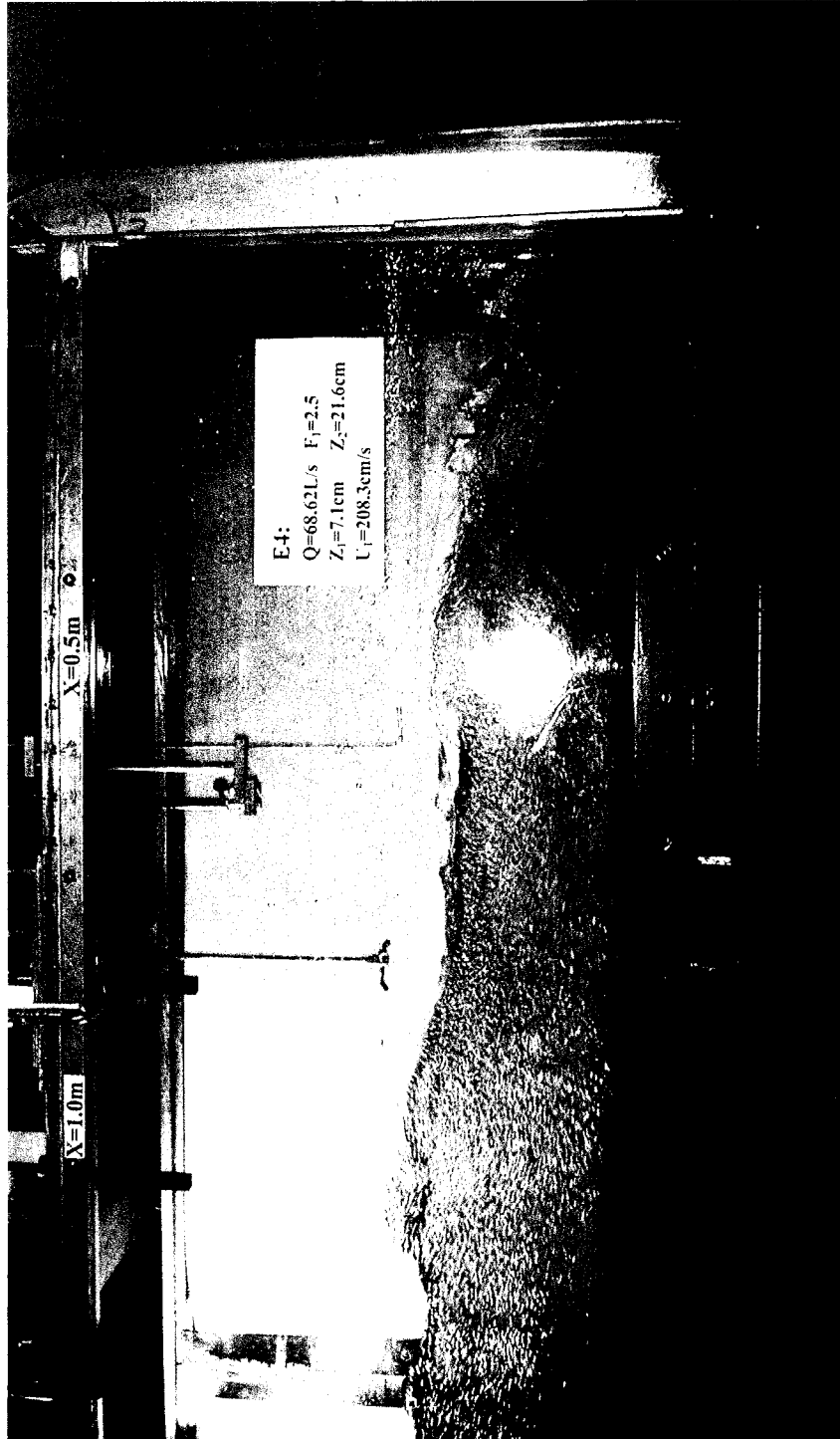


Fig. 3.2(b) Experiment 2 for $F_1 = 2.5$

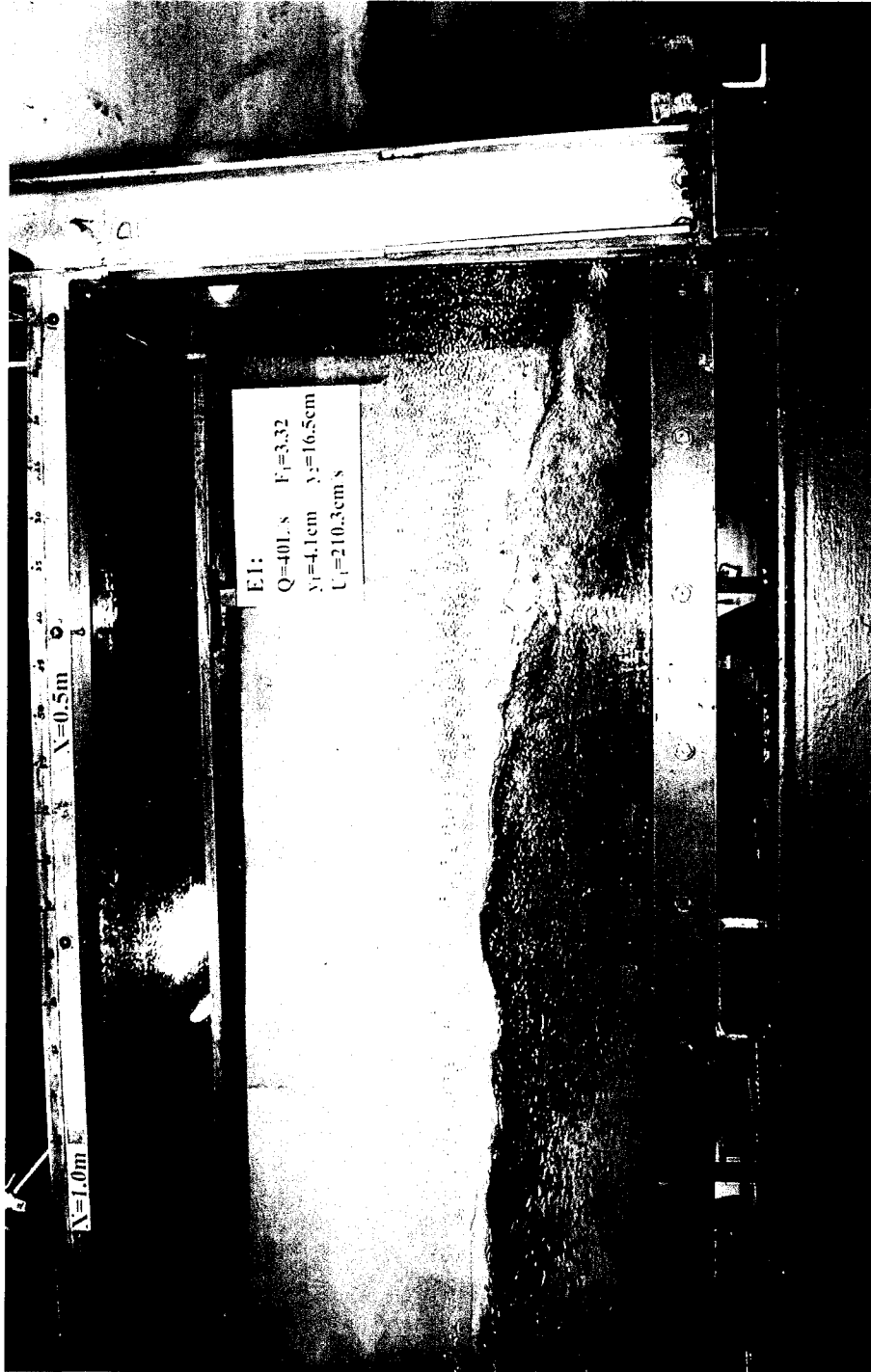


Fig. 3.2(c) Experiment 3 for $F_1 = 3.32$

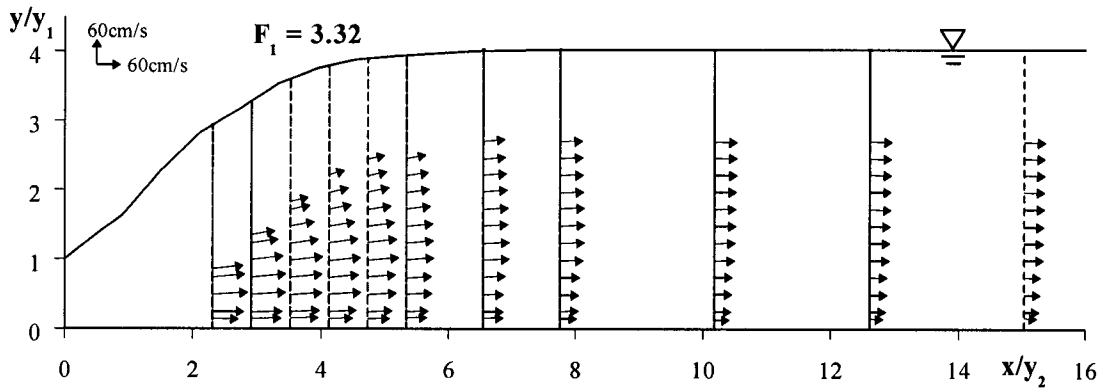
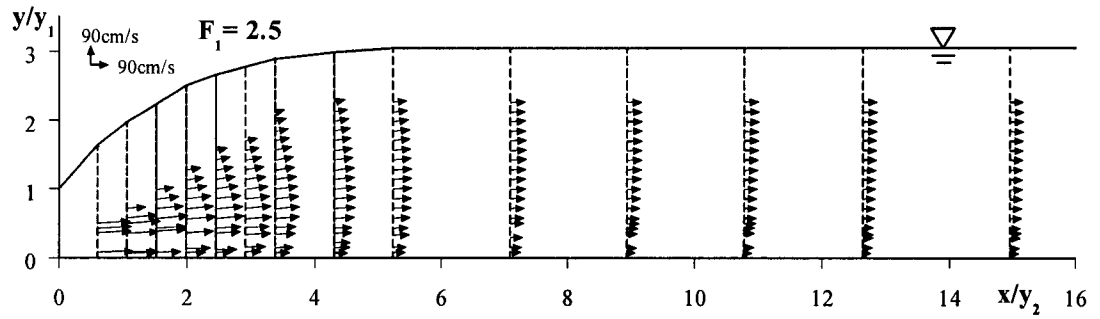
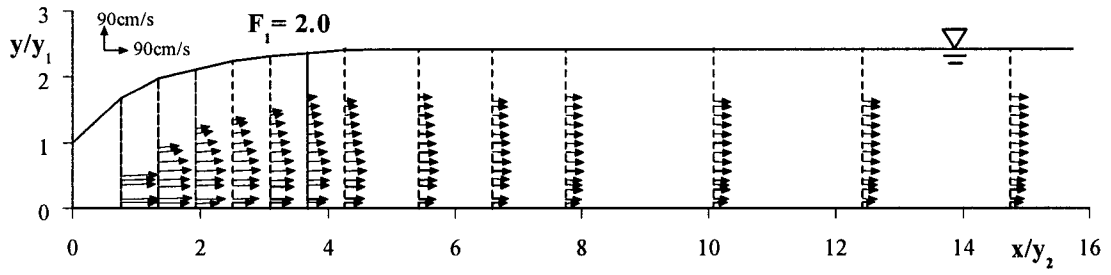


Fig. 3.3 Velocity distribution in central vertical plane

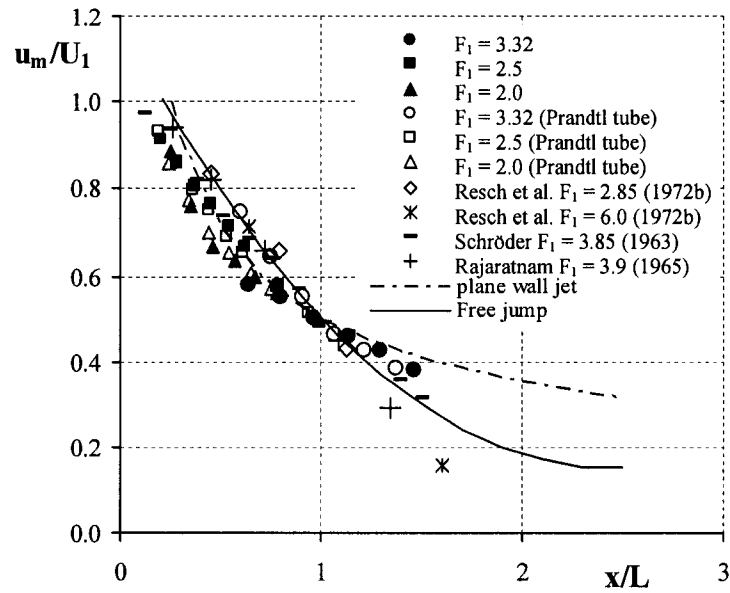


Fig. 3.4 Variation of normalized maximum velocity u_m/U_1 with x/L

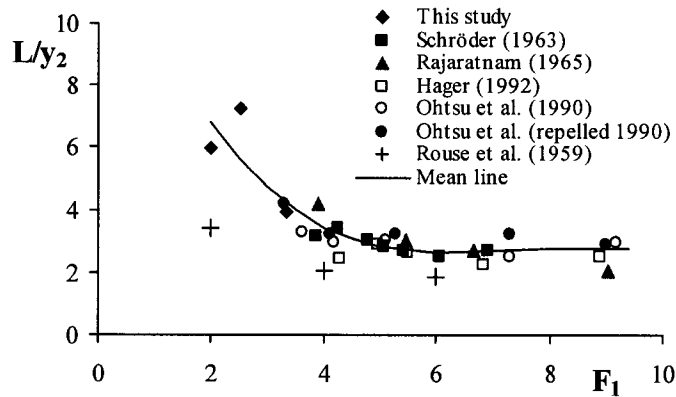


Fig. 3.5 Variation of normalized length scale L/y_2 with F_1

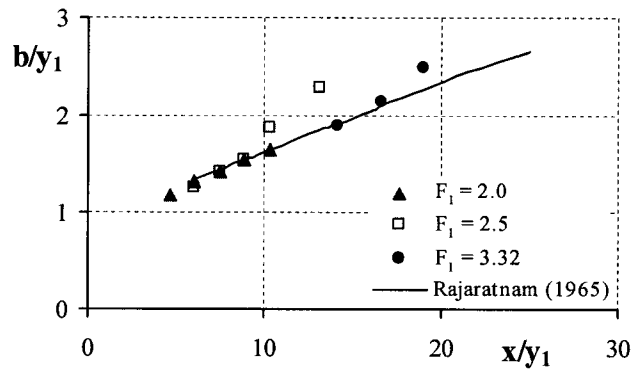


Fig. 3.6 Variation of normalized length scale b/y_1 with x/y_1

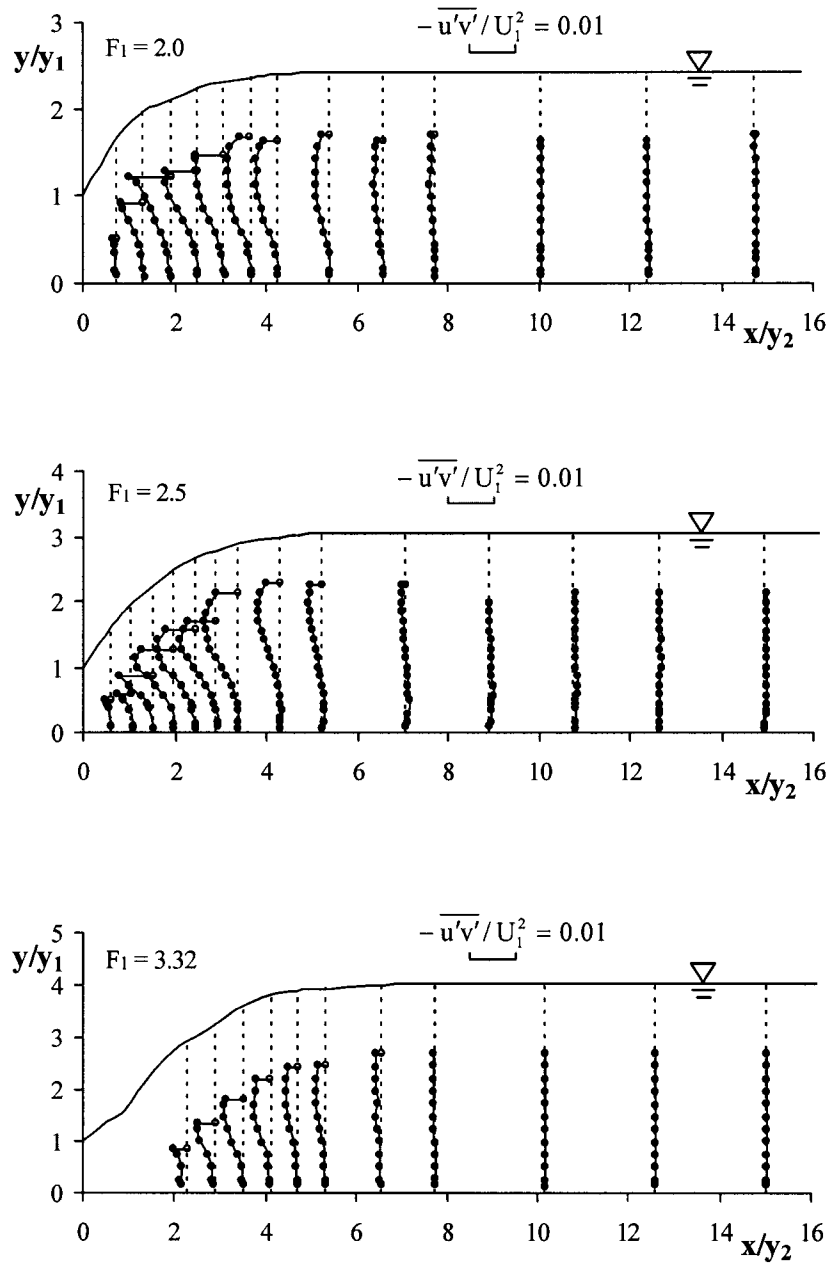


Fig. 3.7 Distribution of Reynolds shear stress in central vertical plane

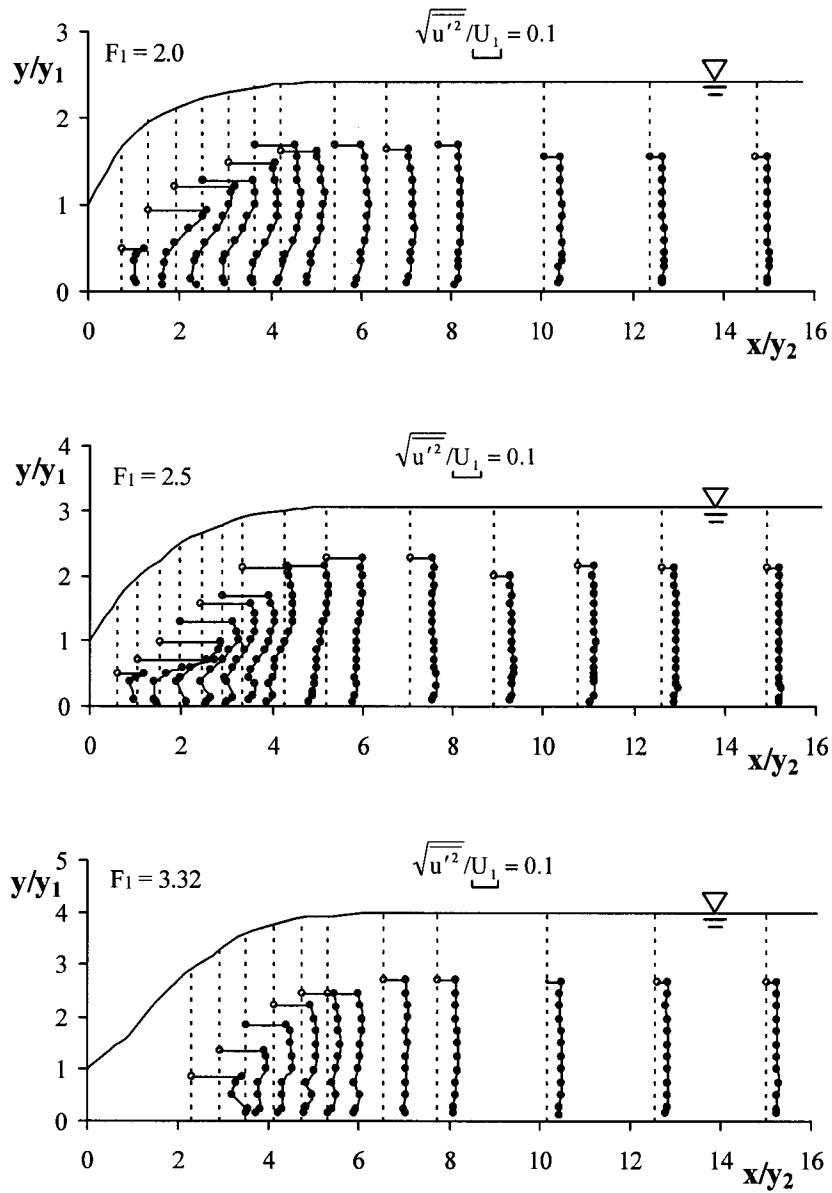


Fig. 3.8(a) Distribution of longitudinal turbulence intensity in central vertical plane

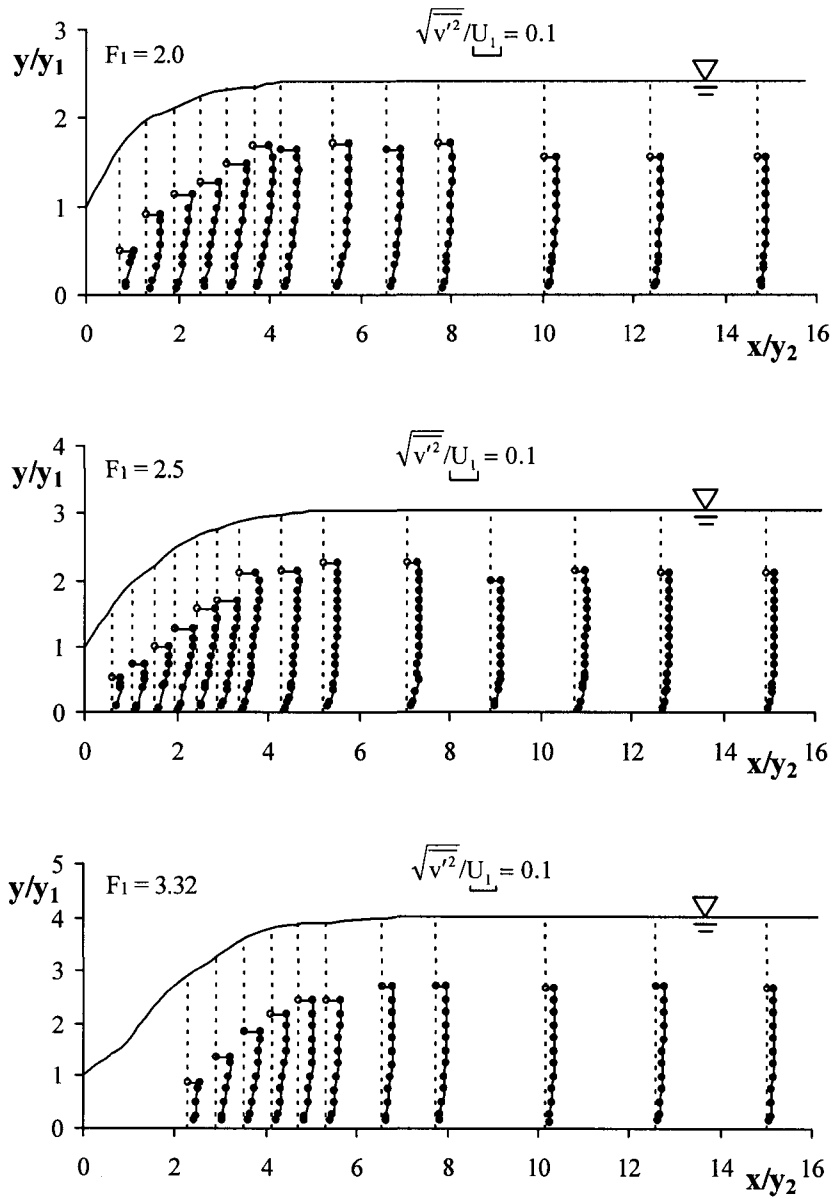


Fig. 3.8(b) Distribution of vertical turbulence intensity in central vertical plane

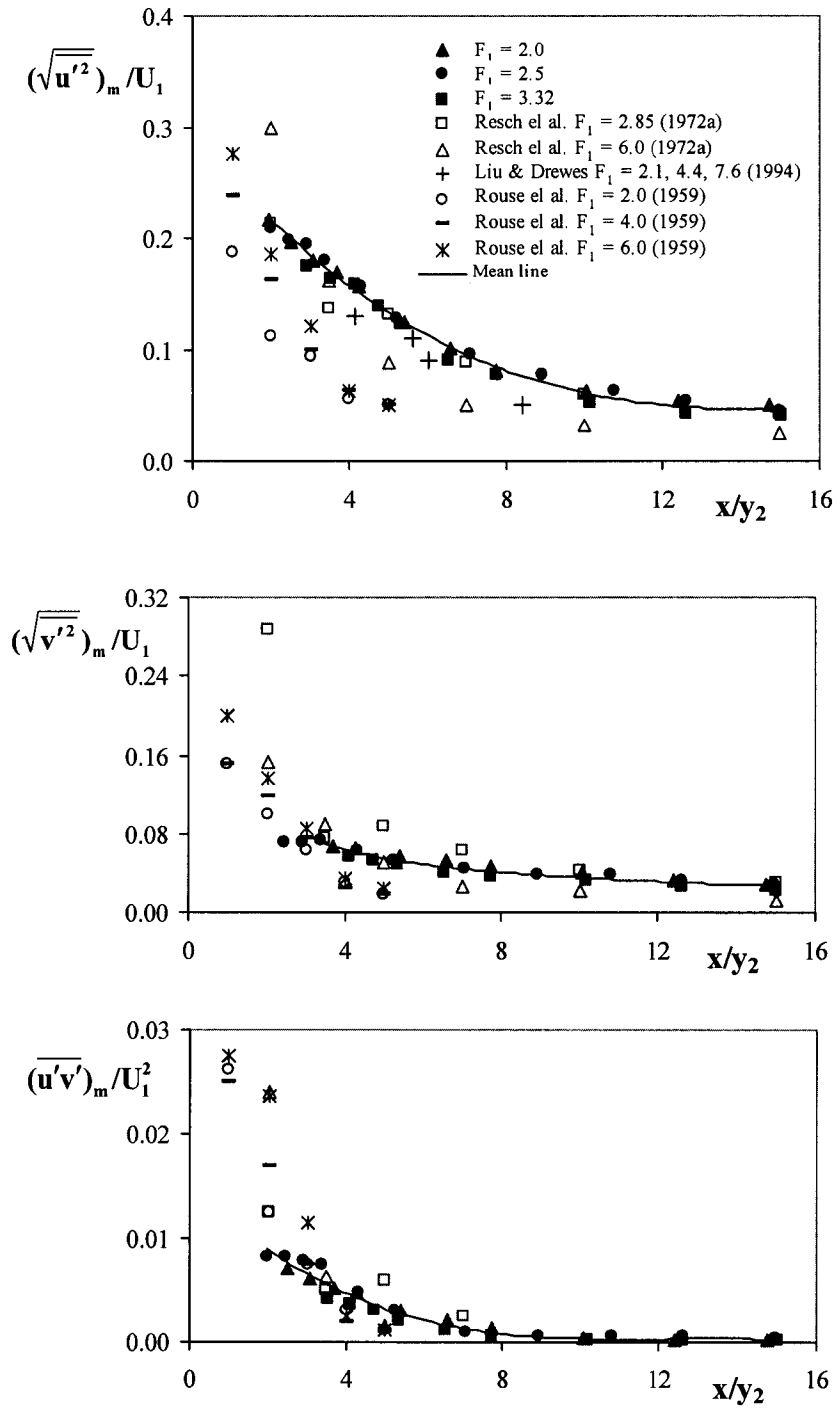


Fig. 3.9 Variation of normalized maximum turbulence intensities and Reynolds stress in central vertical plane with x/y_2

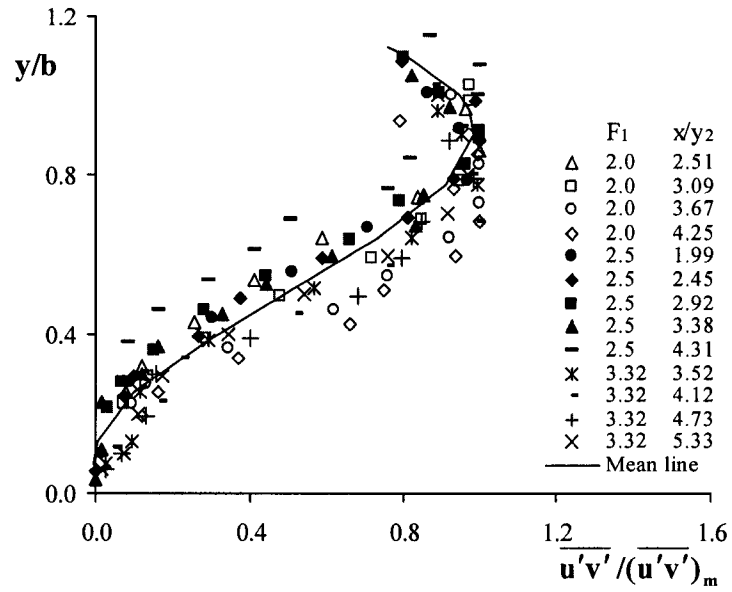


Fig. 3.10 Similarity profile of Reynolds stress

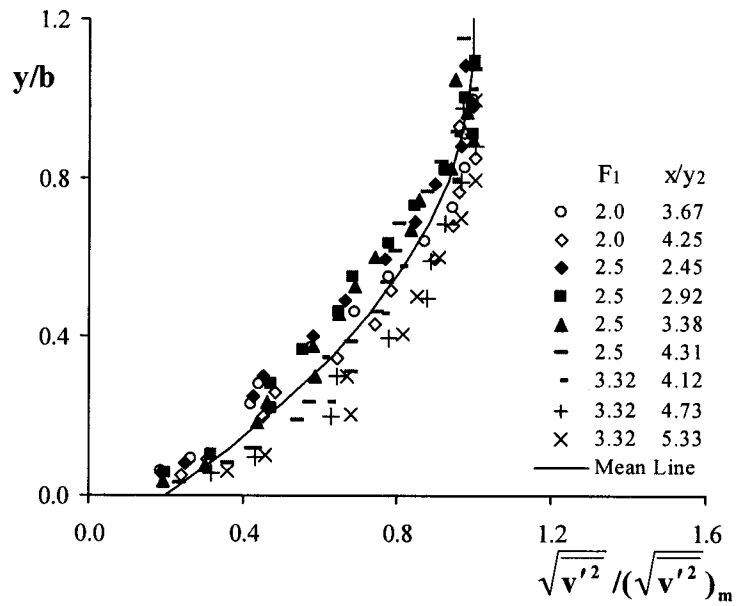


Fig. 3.11 Similarity profile of vertical turbulence intensity

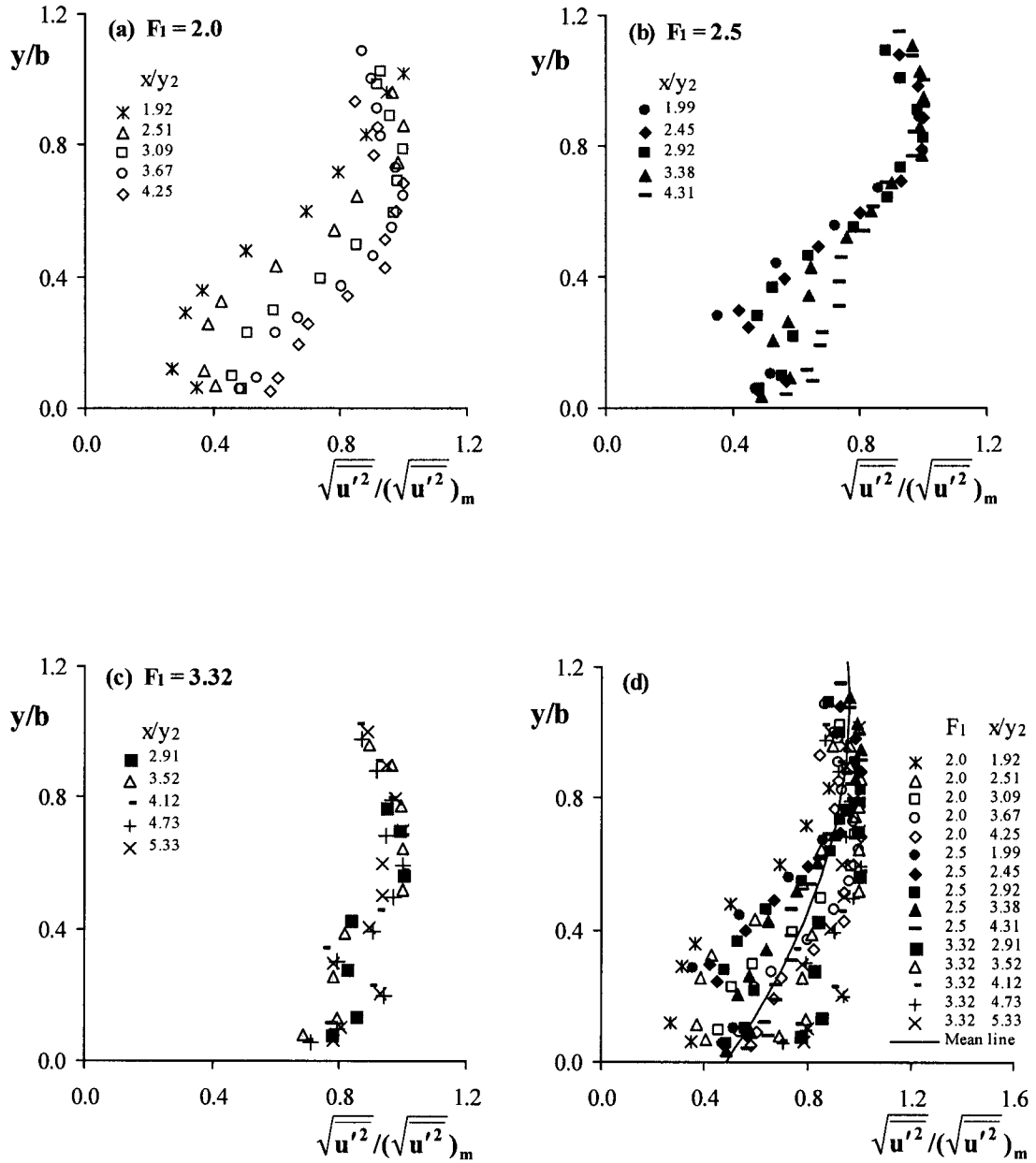


Fig. 3.12 Similarity profile of longitudinal turbulence intensity

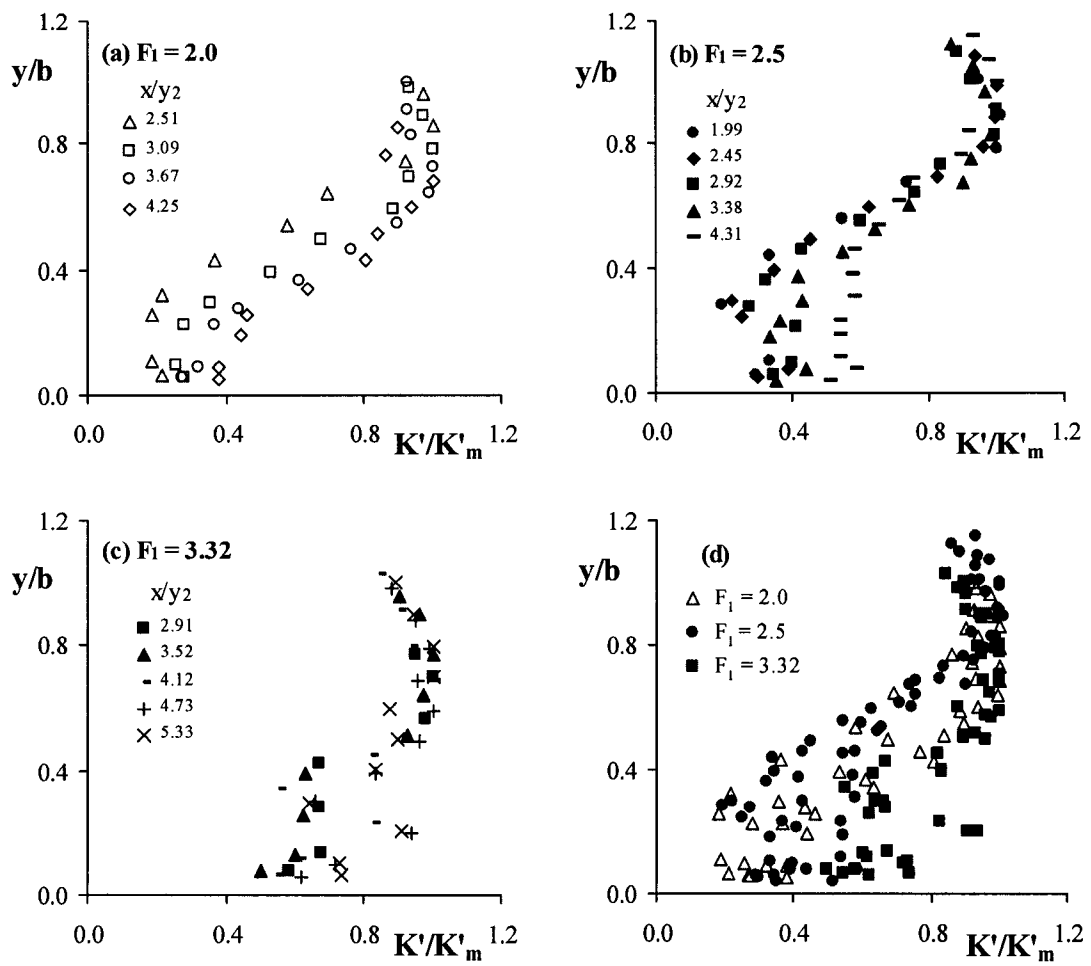


Fig. 3.13 Similarity profile of turbulence kinetic energy

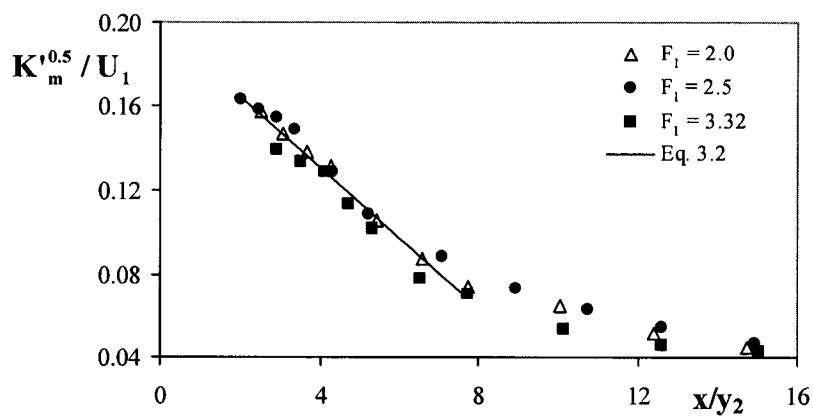


Fig. 3.14 Variation of maximum turbulence kinetic energy in central vertical plane with x/y_2

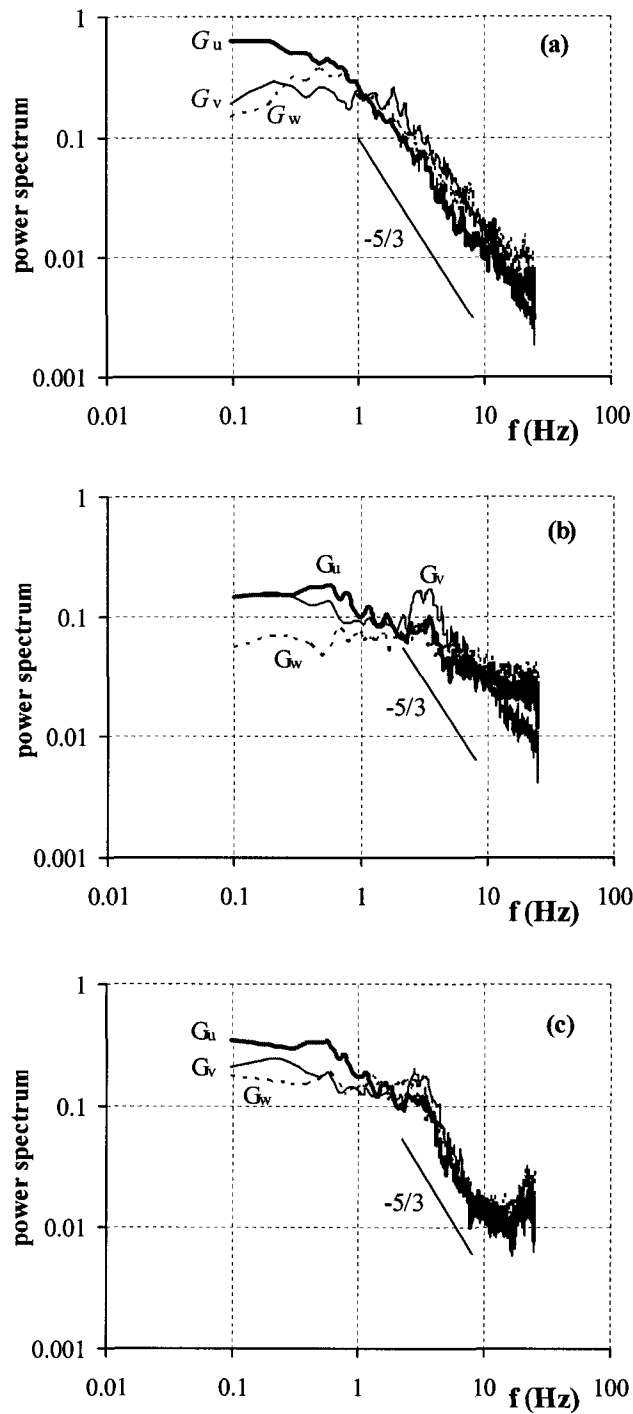


Fig. 3.15 Power spectrum of velocity: —, $G_u(f)/\overline{u'^2}$; —, $G_v(f)/\overline{v'^2}$; - - - - - , $G_w(f)/\overline{w'^2}$; (a) without air bubbles and using raw data; (b) within air bubble region and using raw data; (c) within air bubble region and data processed using PSTM

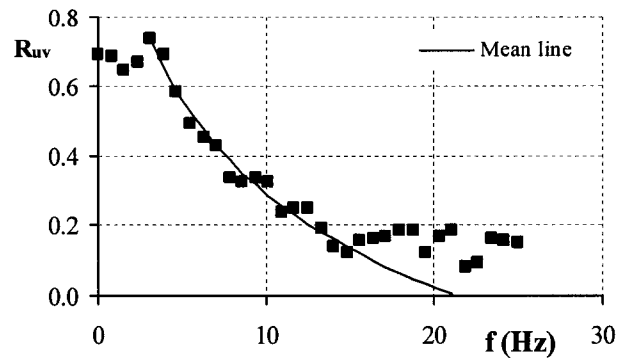


Fig. 3.16 Correlation-coefficient spectrum R_{uv} as a function of frequency f

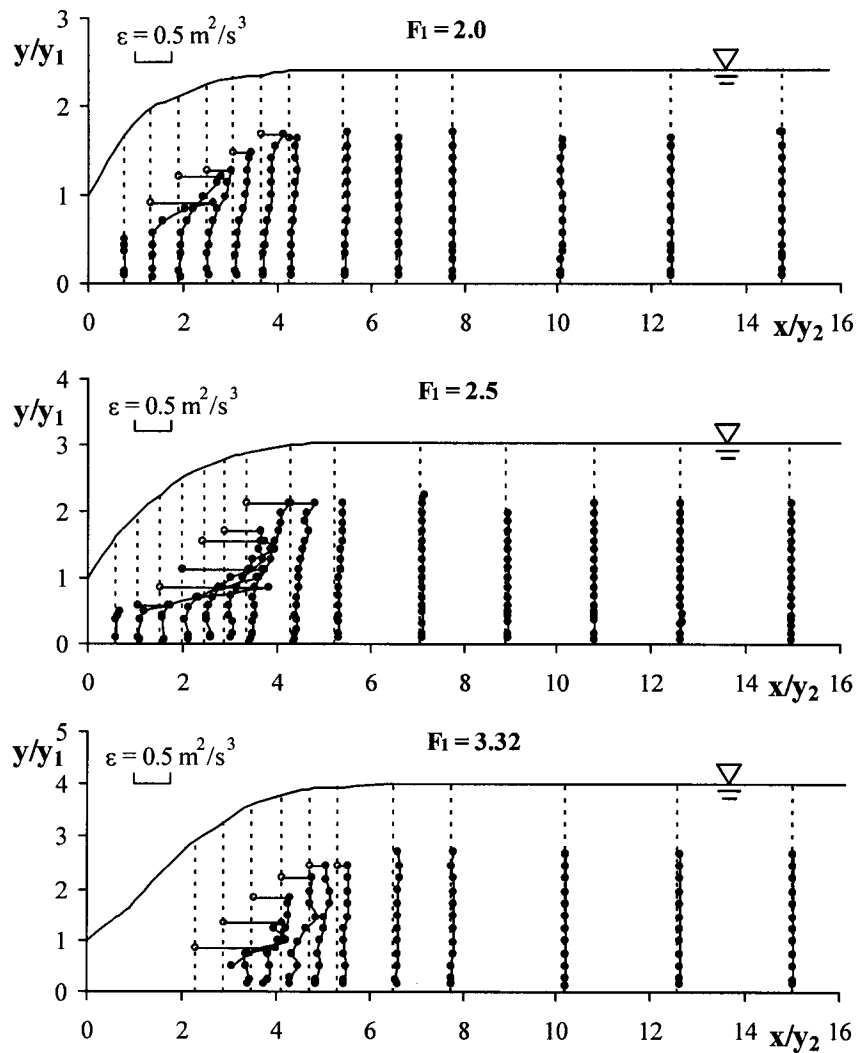


Fig. 3.17 Distribution of energy dissipation rate

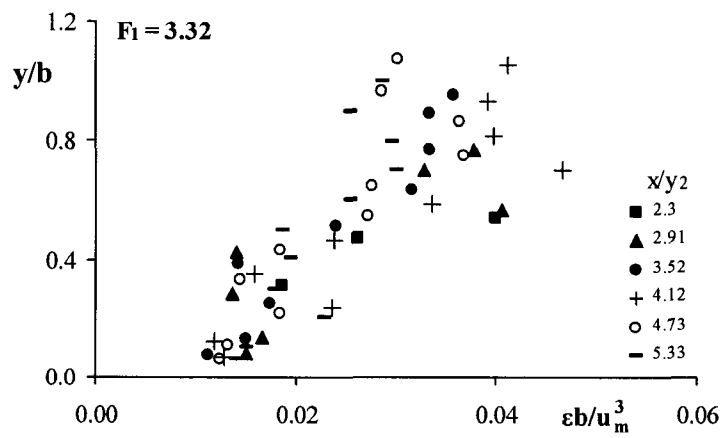
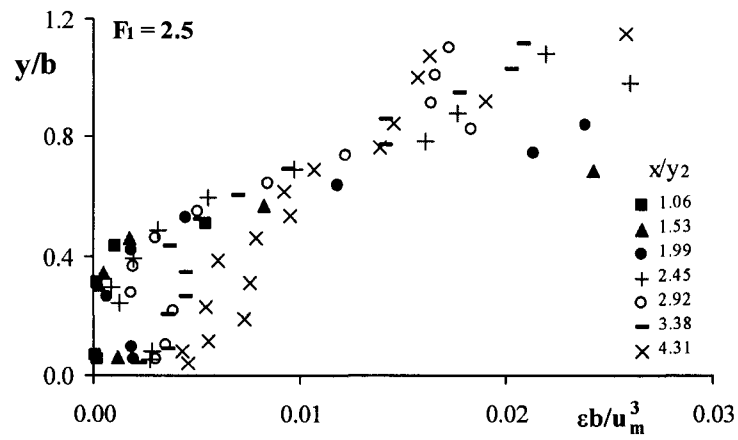
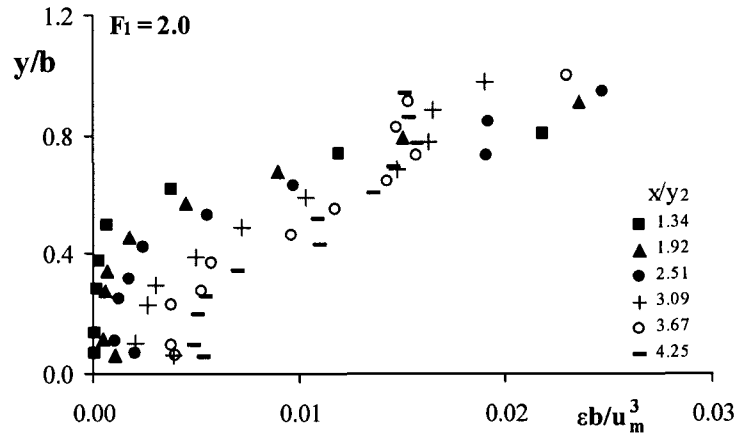


Fig. 3.18 Distribution of normalized energy dissipation rate in hydraulic jump

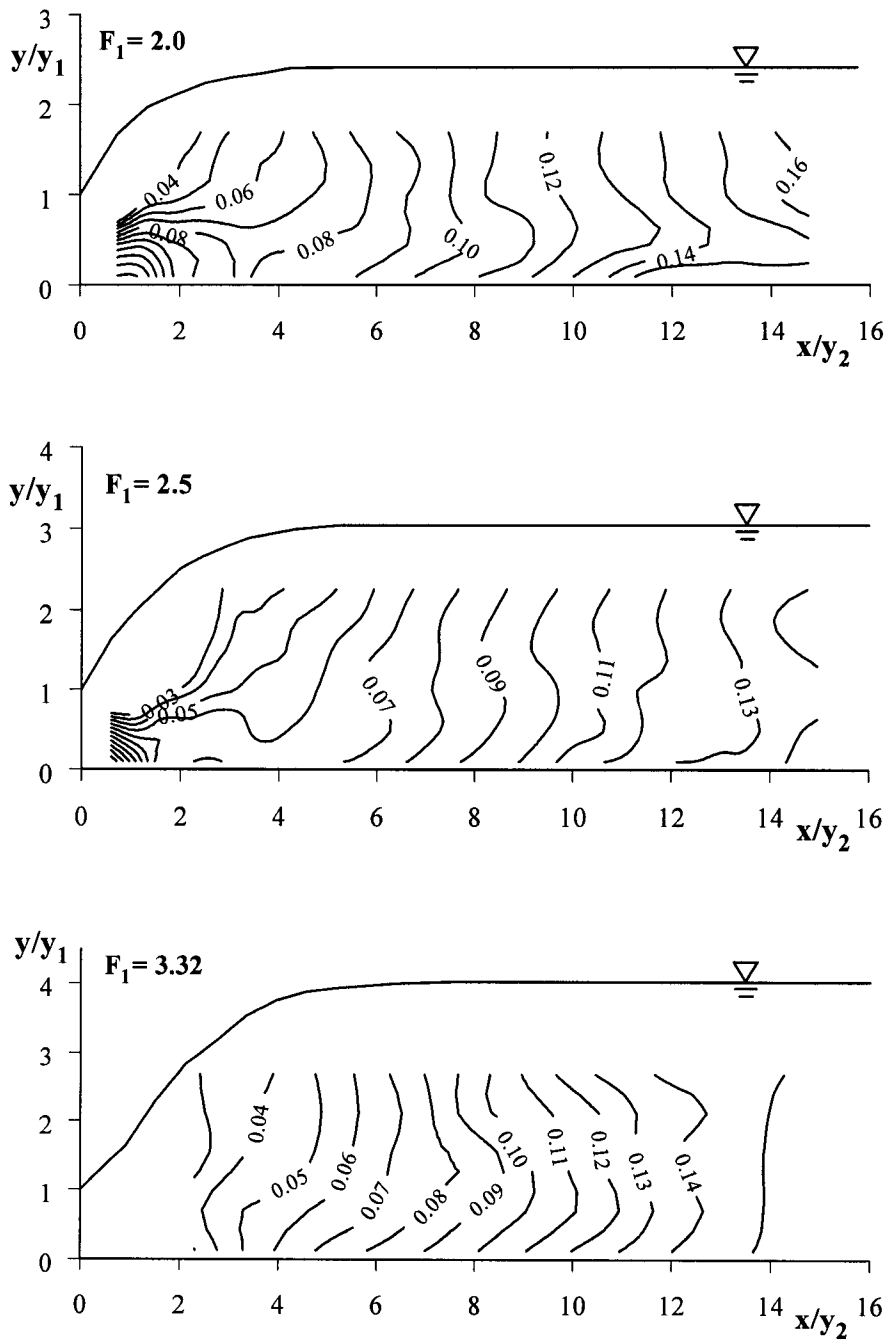


Fig. 3.19 Distribution of Kolmogorov's length scale (in mm)

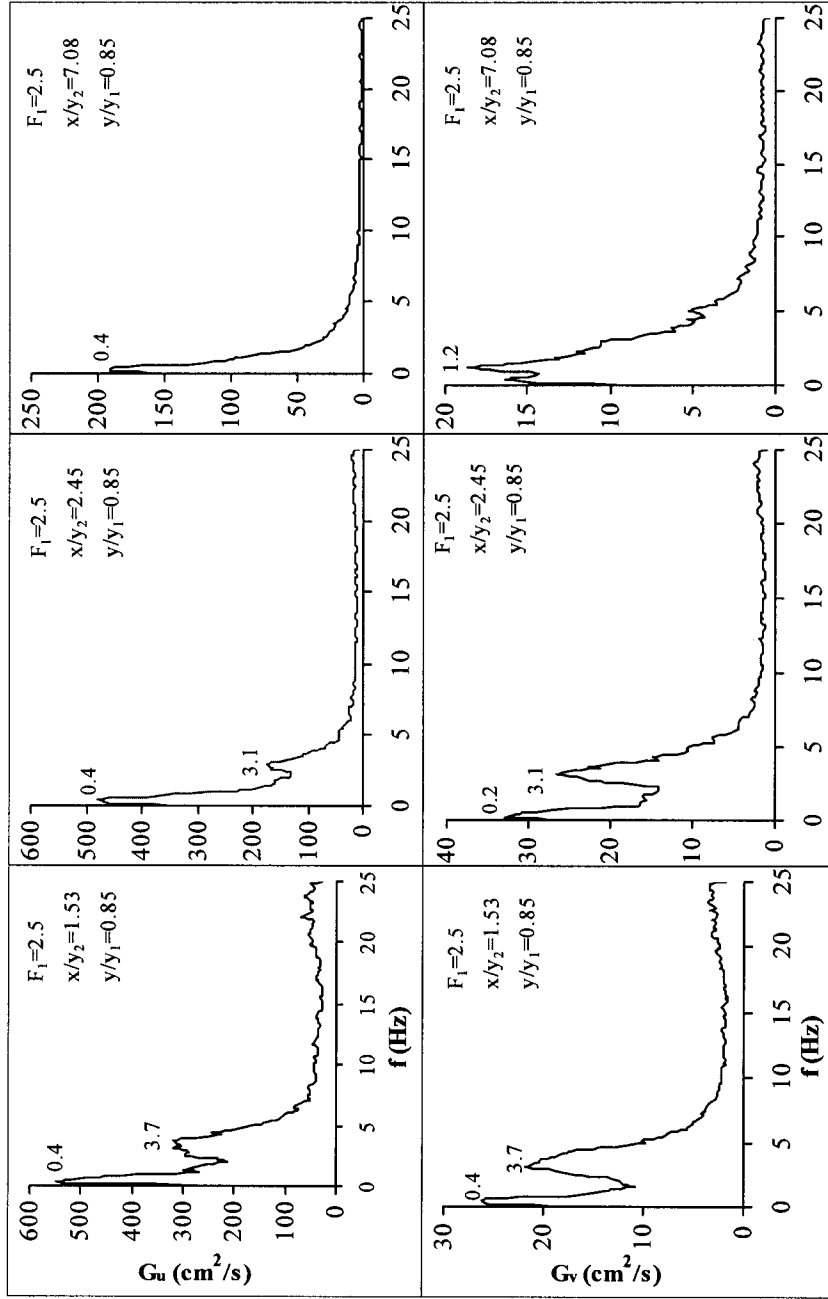


Fig. 3.20 Power spectrum: G_u for horizontal velocity and G_v for vertical velocity

Chapter 4

Turbulence Structure of Flow in Vertical Slot Fishways*

4.1 Introduction

Fishways are hydraulic structures that enable fish to overcome obstructions to reach their spawning grounds and other upstream migrations and are built when they are required for ecological, economical or legal considerations. They are so designed as to attract fish readily and allow them to enter, pass through and exit safely with no undue stress, injury and especially without any undue delay for adult spawners. Fishways are generally divided into four groups: pool and weir, Denil, vertical slot and culvert fishways (Bell 1973; Clay 1961; Katopodis 1990). Vertical slot fishways are the commonly used fish ladders in North America. The earliest vertical slot fishway was developed in about 1943 for use at Hell's Gate on the Fraser River in British Columbia, Canada (Clay 1961). A vertical slot fishway is constructed by installing baffles at certain spacing along a sloping rectangular channel to create a series of pools. The baffles are so-shaped that part of the flow is turned back upstream to create recirculation regions in the pools where the fish would rest before ascending the fishway using their burst speed. Water runs downstream through a series of vertical slots from one pool to the next. The water flow forms a jet

*Part of the content of this chapter has been published as a paper in the Proceedings of the Sixteenth Hydrotechnical Conference, Hydrotechnical Engineering, CSCE, Burlington, Ontario, Canada, 2003. (CD Rom). A paper based on the content of this chapter has been submitted for review to the Journal of Hydraulic Engineering, ASCE.

at the slot and the flow energy is dissipated by jet mixing in the pools. If Δh is the difference in water levels between two adjacent pools, the fishway is designed with a certain value of Δh depending on the burst speed of the fish that would use this fishway (Rajaratnam et al. 1986). The width of the slot b_0 of a prototype fishway is 0.305 m in most cases.

The first systematic study of vertical slot fishways was performed by Rajaratnam et al. (1986). They studied the mean flow structure in the pools of seven different designs of vertical slot fishways in models of four different scales (1:1, 1:5.33, 1:8 and 1:16). For these seven designs, the length L and width W of the pools were equal to $10b_0$ and $8b_0$, respectively. A linear relation was developed between the dimensionless discharge Q_* and the relative flow depth y_0/b_0 based on the conceptual uniform flow assumption and experimental observations, which has the following form

$$Q_* = A(y_0 / b_0) + B \quad (4.1)$$

In Eq. (4.1), y_0 is the average depth of flow approximately occurring at the center of the pools, Q_* is equal to $Q/\sqrt{gSb_0^5}$ where Q is the discharge, g is the gravitational acceleration and S is the fishway slope, and A and B are constants that depend on the geometry of the fishway. To discover the mean flow structure, some velocity profiles were obtained with a Prandtl tube, a five-hole probe and a mini-current meter. A tuft probe as well as color injection was used to observe circulation patterns in some pools. It was found that a jet that was formed at the slot traveled through the pool, losing its energy and creating recirculation patterns in the pool. The maximum

velocity at the slot V_{sm} was approximately equal to $\sqrt{2g\Delta h}$. This study also included the observations on non-uniform flow and submergence effects in the vertical slot fishways.

In a later work, Rajaratnam et al. (1992) examined 18 designs of vertical slot fishways in order to develop more effective but simple designs. They tested the sensitivity of the performance of vertical slot fishways to the length and width of pools. It was found that a length of $10b_0$ and a width of $8b_0$ could be considered as the proper length and width of pools. It should be pointed out that these dimensions are also generally used in the United States (Bell 1973). The authors also recommended Designs 6, 16 and 18 for practical use, based on overall performance and simplicity in design and construction.

Wu et al. (1999) studied the structure of the mean flow in a vertical slot fishway of Design 18 with the model scale of 1:2.67. Three slopes of 5, 10 and 20% with several discharges were studied. The flow patterns at the slots and pools were observed using dye injection. The velocities were measured by a four-tube probe and a three-tube yaw probe. Two typical flow patterns existed in the pools, referred to as patterns 1 and 2 as shown in Fig. 4.1. Pattern 1 occurs for the 5% slope in which the main flow travels from one slot to the next through the center of the pool as a 2D curved jet with two recirculation regions located on either side of the jet. In pattern 2, which occurs for the slopes of 10 and 20%, the main flow is 3D and travels towards the sidewall in between the long baffles with a recirculation region between the short baffles as well as a horizontal eddy near the long baffle on the downstream

end of the pool. It was found that the jet which is formed at the slot has no potential core and its longitudinal velocity decays much faster than that of the plane turbulent jet. The flow at the slot is not a uniform rectangular jet issuing perpendicular to the slot. The relative volume of the recirculation region between the short baffles is approximately 28% of the volume of the pool for all three slopes and all discharges whereas the corresponding volume of the recirculation region between the long baffles for the 5% slope is approximately 45%. For flow pattern 2, the horizontal eddy behind the long baffle has a relative volume of approximately 10%. They also found that the volume averaged kinetic energy heard in the pool is about 12% of Δh .

Puertas et al. (2004) conducted another research investigation on the mean flow structure of vertical slot fishways of Design 6 and 16 for two different slopes of 5.7 and 10%. A micro acoustic Doppler velocimeter (MicroADV) was used to measure the 3D velocity fields at a sampling frequency of 15 Hz and sampling time of 10 or 15 seconds. Two different flow regions were also found in their study: direct flow region and recirculation region. They also developed a linear relation between the dimensionless discharge and the relative flow depth for each design. It was found that the flow in the pools is approximately 2D flow with the vertical component of the velocity close to zero. For a given slope, the velocity at any point of the pool was found independent of the discharge and constant with the water depth. As for turbulence, only the turbulence kinetic energy information was provided.

Although the hydraulics of vertical slot fishways has been studied by several investigators, the understanding of turbulence characteristics of flow appears to be

very incomplete and such knowledge is important for the passage of migratory fish through the fishways. One of the main reasons for this incompleteness is that the flows in vertical slot fishways are bubbly two-phase flows which are difficult to measure. This study used a micro acoustic Doppler velocimeter (MicroADV) to experimentally study the turbulence characteristics of flow in a vertical slot fishway of Design 18. The results are believed to provide useful insight on the turbulence characteristics of flow in vertical slot fishways and can be used for guidance in the design of fishways in the future.

4.2 Experimental Arrangement and Experiments

Fig. 4.2 shows the experimental arrangement along with the right coordinate system (x, y, z) used. Seven pools of Design 18 (Rajaratnam et al. 1992) were built in a rectangular flume with an aluminium bed and Plexiglas sidewalls, 0.912 m wide and 0.6 m high with a length of 9.75 m. The slot width b_0 was 0.114 m, and the scale of the model was 1:2.67 assuming the standard slot width is 0.305 m. The length and width of the pools were $10b_0$ and $8b_0$ respectively. The separation baffles were made of plywood sheets and the quarter cylinders were made from polyvinyl chloride pipes. The baffles and the quarter cylinders separating the pools were made vertical for a 10% flume bed slope. The flume can be set at different slopes. The flume was connected to a head tank of the same width and partly curved bottom and equipped with stilling arrangements to provide smooth flow entrance. Two pumps were used to supply the head-tank from the laboratory sump and the discharges were monitored

by means of magnetic flowmeters located in the supply lines. Fig. 4.3 shows the experiment for $S = 10.52\%$ and $Q = 31.2$ L/s in the T. Blench Hydraulics Laboratory at the University of Alberta.

The flume was tested for two slopes of 5.06 and 10.52% and for each slope, two discharges of 31.2 and 52 L/s were run. Table 4.1 provides the details of the measurement conditions. Because the flow pattern and the head drop per pool were found to be essentially the same in almost all the pools (Wu et al. 1999), measurements were only made in the fifth pool. Detailed measurements of mean velocities, turbulence intensities and Reynolds shear stresses were performed in the planes parallel to the flume bed. The number of planes measured varied depending on the slope and discharge. In each plane, data points were distributed forming a 100 mm (in the longitudinal direction) \times 50 mm (in the transverse direction) grid.

A down-looking MicroADV was used to measure instantaneous velocity fields at a sampling frequency of 50 Hz. An investigation was carried out in order to define the sampling time of the instantaneous velocity time series to be used for the determination of the mean velocity, turbulence intensity and Reynolds shear stress. For this, the velocity time series of 20 minutes were obtained at points in the jet flow formed at the slot and the recirculating flow for all the runs. Figs. 4.4(a–c) show some typical distributions of the moving average mean velocity u , v and w , and turbulence intensities $\sqrt{u'^2}$, $\sqrt{v'^2}$ and $\sqrt{w'^2}$ in the x , y and z directions, respectively. It can be noticed that it is the mean velocity that controls the sampling time. For $S = 10.52\%$ and $Q = 31.2$ L/s, it was found that after about up to 300 seconds the mean

velocity becomes almost constant (see Fig. 4.4(a)) whereas for $S = 5.06\%$ and $Q = 31.2$ and 52 L/s, the corresponding time was about 600 seconds (see Figs. 4.4(b, c)). Therefore, the sampling time was chosen to be 300 seconds for $S = 10.52\%$ and $Q = 31.2$ L/s and 600 seconds for $S = 5.06\%$ and $Q = 31.2$ and 52 L/s. It was observed that for $S = 10.52\%$ and $Q = 52$ L/s, the flow in the pools changed from flow pattern 1 to pattern 2 and vice versa in an irregular manner. For this unstable flow, the sampling time was chosen to be 600 seconds subjectively.

It only makes sense to study the jet flow with measurements along the jet trajectory. The center-line of the jet formed at the slot is assumed to be the maximum mean plane velocity locus which can be obtained from the experiments listed in Table 4.1. Then, a new right coordinate system (x_j, y_j, z) is established where x_j is measured along the curved center-line of the jet, y_j is orthogonal to x_j in the transverse direction and z is perpendicular to the bottom of the flume, as shown in Fig. 4.2. The origin of the x_j -axis is at the point where the maximum plane velocity locus intersects with the slot line which may be defined as the line joining the tips of the long and short baffles. The measurements taken in the coordinate (x, y, z) could be transferred to the corresponding values in (x_j, y_j, z) . However, it was found that only few grid points in (x, y, z) at which measurements were taken were on the same cross section of the jet. Therefore, the second set of experiments has been performed in the coordinate system (x_j, y_j, z) to study the jet formed at the slot. The experiments conducted in the coordinate system (x, y, z) in the T. Blench Hydraulics Laboratory is referred to as the first set. Due to the construction interference, the experimental

arrangement was moved to a new Laboratory where the second set of experiments was carried out. Table 4.2 shows the primary details of the experiments. Detailed velocity measurements were made for $S = 5.06$ and 10.52% and $Q = 31.2$ L/s. The measurement points in each plane were distributed as a 100 mm (in the x_j direction) \times 50 mm (in the y_j direction) grid. In the y_j direction, the measurements were stopped when the velocity in the x_j direction changed its sign. The sampling time of MicroADV was 600 seconds for this set of experiments. In the new Laboratory, the size of the sump was reduced significantly enough not to provide stable flow pattern for the case of $S = 5.06\%$ and $Q = 31.2$ L/s. It was found that the flow in the pools switched between flow patterns 1 and 2 as shown in Fig. 4.5 instead of staying at its stable status of pattern 1 as observed in the first set of experiments. Therefore, selective sampling was decided, guided by visual observations.

Regarding the air concentration in the pools, it was observed that the jet area for $S = 10.52\%$ and $Q = 31.2$ L/s had the maximum air concentration for this study. Hence a fiber optical probe was used to obtain some air concentration measurements in the jet area at the plane of $z = 70$ mm for $S = 10.52\%$ and $Q = 31.2$ L/s, shown in Fig. 4.6. The probe was lined opposite to the velocity vector at each point. Because the fiber optical probe is generally used in one dimensional flow, the values of air concentration measured here could only be considered approximate. It can be seen that the values of air concentration at most of the points are smaller than 0.8% . The air was entrained by the jet at the slot. It can be concluded that the effect of air concentration on the measurements of MicroADV in this study could be neglected

based on the discussion in Chapter 2.

4.3 Processing Technique

The detailed descriptions and discussions about MicroADV and fiber optic probe can be found in Chapter 2. In Chapter 2 and 3, the phase-space thresholding method (PSTM) suggested by Goring and Nikora (2002) was used to process the measured MicroADV data to get rid of the spikes. The PSTM uses the mean and standard deviation as estimators for location and scale respectively to exclude spikes. Rousseeuw (1990) demonstrates that both the mean and standard deviation are very sensitive to spikes and have a breakdown point of $1/n$, where n is the number of observations, because it is sufficient to replace a single observation by a large value to change the values of mean and standard deviation. The breakdown point of an estimator is defined as “the smallest fraction of the observations that have to be replaced to carry the estimator over all bounds” (Rousseeuw 1990).

Rousseeuw (1990) shows that the sample median and the median of all absolute derivations (MAD) are the robust estimators of location and scale, respectively. MAD is expressed as

$$MAD = 1.483 \left| \text{median}_{j=1,\dots,n} x_j - \text{median}_{i=1,\dots,n} x_i \right| \quad (4.2)$$

for a sample $\{x_1, x_2, \dots, x_n\}$ where 1.483 is a factor that makes the value of MAD consistent with the standard deviation. Both of them have the best breakdown point of 50% which means that at least half of the observations have to be replaced in order to change the median.

In this Chapter, the PSTM was modified by using the sample median and MAD instead of the mean and standard deviation as estimators to locate the spikes, which were also suggested by Wahl (2003).

4.4 Experimental Results and Discussions

4.4.1 Overall structure of flow in pools

For the 5.06% slope, extensive velocity measurements were obtained at three planes parallel to the bottom of the flume for two discharges of 31.2 and 52 L/s, respectively. Figs. 4.7(a–f) show the velocity distribution in the XY-plane for each run. The velocity contour lines of V/V_{sm} are also drawn in these figures where V is the plane velocity vector at any point and V_{sm} is the maximum velocity at the slot. It can be seen that the jet flow travels through the middle of the pool from one slot to the next with high velocity, leaving one large recirculation region of low velocity on each side of the jet. The recirculation regions with low velocity will provide resting zones for fish as physiological requirements. The flow is pattern 1 as observed by Wu et al. (1999). The results of Wu et al. (1999) using a four-tube probe are compared with those of this study in Figs. 4.7(d) and 4.7(f) for $Q = 52$ L/s at $z = 10$ and 300 mm, respectively. The directions of the plane velocity vectors are almost the same for both studies and the difference between the magnitudes of the velocity is less than 10%.

Figs. 4.8(a–b) show the velocity distribution in the XY-planes which are, respectively, 10 mm and 70 mm above the bed of the flume for $S = 10.52\%$ and $Q =$

31.2 L/s. It was observed that the flow is pattern 2 and two different flow regions are formed as observed by Wu et al. (1999). One is the jet region where the flow from the slot travels towards the sidewall at high speed and a part of this jet goes to the next slot while the rest of it impinges on the sidewall. The other is a large recirculation region, which is formed on the side of the short baffles and is characterized by smaller velocities. An elliptical horizontal eddy was also observed close to the exit of the pool. It is clear to see that the jet grows much wider at $z = 10$ mm than at $z = 70$ mm. The results are compared with those of Wu et al. (1999) in Fig. 4.8(a). The directions of the plane velocity vectors are almost the same for both studies, but the magnitude of the velocity of Wu et al. (1999) is larger. This is probably due to the effect of the boundary and air bubbles on the measurements of MicroADV (Liu et al. 2002). Further experiments are needed to clearly understand this difference.

The flow in the pools for $S = 10.52\%$ and $Q = 52$ L/s was not stable and the flow pattern changed between patterns 1 and 2 irregularly, which is not consistent with the observation of Wu et al. (1999). They found that the flow belongs to pattern 2 for $S = 10.52\%$. The reason for this difference is not clear. It was observed that the fluctuation of the water level in the recirculation regions is responsible for this shift of flow patterns. When the flow shifted from pattern 1 to 2, the water level in the recirculation region between the short baffles decreased while the water level close to the long baffle at the downstream end of the pool gradually increased. The difference between the two water levels would exert a force on the jet. As the

difference increased to a certain value, the jet would be pushed towards the side of the lower water level and the stored volume of water close to the long baffle would fall into the jet. Hence the flow would switch from pattern 2 to 1. At the same time the water level would rise in the recirculation region on the left side of the jet when looking downstream and the water level in the recirculation region on the right side of the jet would drop. After enough volume of water accumulated on the left side of the jet, it would force the flow changing to pattern 2. The mean velocity field in the XY-plane is shown in Fig. 4.8(c) in which the averaging time of velocity is 600 seconds. The flow follows pattern 1 from which it is can be concluded that flow pattern 1 dominates at the conditions of $S = 10.52\%$ and $Q = 52$ L/s.

The corresponding vertical velocity contours and 3D plots for $S = 5.06\%$ are shown in Figs. 4.9(a–f) and for $S = 10.52\%$ in Figs. 4.10(a–c), which clearly demonstrate that the flow is three dimensional. It was found that the vertical velocity has a similar structure for flow pattern 1. For the planes close to the bed, the jet with downward negative vertical velocity travels through the center of the pools. The negative vertical velocity gradually reduces to zero at about the half length of the pool, then the jet is lifted with a hump on each side of the jet at the end of the pool when approaching to the next slot (see Figs. 4.9(a, d)). For the planes between the bed and half water depth, the jet is lifted at beginning for a short distance with negative vertical velocity on both sides. Then it impinges downwards to the middle of the pool and is lifted again with a hump close to the long baffle (see Figs. 4.9(b, e) and 4.10(c)). For the planes above the half water depth as shown in Figs. 4.9(c, f),

the jet travels with positive vertical velocity from one slot to the next with negative vertical velocity on both sides of the jet before reaching the middle of the pool. A big hump is created close to the long baffle.

The structure of the vertical velocity for flow pattern 2 is different from that for flow pattern 1, as shown in Figs. 4.10(a, b). The jet flow with downward negative vertical velocity travels towards the sidewall in between the long baffles. Part of this flow lifts up when approaching the sidewall, then impinges on it and reappears near the water surface and finally travels to the next slot. The vertical velocity remains at a small value in most areas of the pool for all the cases studied which would allow fish to choose any preferred swimming depth.

The mean flow kinetic energy per unit mass is defined as

$$K = \frac{1}{2}(u^2 + v^2 + w^2) \quad (4.3)$$

where u , v and w are, respectively, the mean velocity of flow in the longitudinal, transverse and vertical directions in the (x, y, z) coordinate system. The contours of K in the XY -plane are plotted in a non-dimensional form for each run in Figs. 4.11(a–f) and 4.12(a–c). It is seen from the figures that the mean flow kinetic energy decays rapidly in a small area within the jet region whereas it has a small value of less than 9% of V_{sm}^2 in the rest of the pool. The rapid decay of K is due to the entrainment of the recirculating water with negative momentum by the expanding jet (i.e. opposite to that carried by the expanding jet). The existence of reasonably small area of high K values in the pool is desirable for fish passage.

Figs. 4.13(a–f) and 4.14(a–c) show the distribution of the Reynolds shear stress $-\overline{u'v'}$ for $S = 5.06$ and 10.52% respectively. It may be noted that the results are non-dimensionalized using the velocity scale V_{sm} . It was observed that the Reynolds shear stress has a peak value for almost every section on each side of the maximum plane velocity filament for flow pattern 1 as given in Figs. 4.13(a–f). The value of the shear stress is positive on the right side of the maximum velocity filament and negative on the other side. The absolute value is larger on the right side than on the left side. The structure of the Reynolds shear stress for flow pattern 2 is different from that for flow pattern 1 as shown in Figs. 4.14(a–b). Generally speaking, there is only one peak value for almost each section which can be on either side of the maximum plane velocity filament. The Reynolds shear stress decreases as the main flow travels downstream while it remains at very small values in the recirculation region. The irregularity of the Reynolds shear stress distribution for $S = 10.52\%$ and $Q = 52$ L/s in Fig. 4.14(c) is due to the unstable flow pattern.

The distributions of the longitudinal, transverse and vertical turbulence intensities $\sqrt{\overline{u'^2}}$, $\sqrt{\overline{v'^2}}$ and $\sqrt{\overline{w'^2}}$ are shown in Figs. 4.15(a–f), 4.17(a–f) and 4.19(a–f), respectively for $S = 5.06\%$. For $S = 10.52\%$, they are given, respectively, in Figs. 4.16(a–c), 4.18(a–c) and 4.20(a–c). The turbulence intensities were corrected for the Doppler noise using the method of Liu et al. (2003) by extending the inertial subrange $-5/3$ slope in the velocity spectrum (see Fig. 4.23) down to the Nyquist frequency. Then the area under the modified velocity spectrum curve is the turbulence intensity corrected for the Doppler noise. It can be seen that in the jet

region, the longitudinal and transverse turbulence intensities decrease as the jet travels downstream while they remain at almost constant values in the recirculation regions except for the case of $S = 10.52\%$ and $Q = 52$ L/s. The distribution of the vertical turbulence intensity is close to being uniform in the planes parallel to the bottom of the flume.

The turbulence kinetic energy per unit mass K' can be calculated using Eq. (4.4)

$$K' = \frac{1}{2}(\overline{u'^2} + \overline{v'^2} + \overline{w'^2}) \quad (4.4)$$

where u' , v' , w' are the longitudinal, transverse and vertical fluctuating velocities, respectively. Figs. 4.21(a–f) and 4.22(a–c) show the contours of normalized K' by V_{sm} for $S = 5.06$ and 10.52% , respectively. The maximum turbulence kinetic energy in the pools for all the runs is less than 8% of V_{sm}^2 . Such a low value of K' would indicate relatively large energy dissipation and would enable fish to ascend without undue stress.

Fig. 4.23 shows typical power spectra $G_u(f)$, $G_v(f)$, and $G_w(f)$ for the corresponding velocity components u' , v' , and w' , where f is the frequency and the spectral density is divided by the corresponding turbulence intensity. The inertial subrange was clearly marked by the existence of a $-5/3$ slope in the power spectra. Similar to the discussion in Chapter 3 on free hydraulic jumps, it was found that the correlation-coefficient spectrum falls rapidly to zero at high wave numbers. Therefore, the Kolmogorov $-5/3$ law of local isotropic turbulence (Hinze 1975) was reasonably used to estimate the dissipation rate as a first approximation given as

$$G_u(k) = A\varepsilon^{2/3} k^{-5/3} \quad (4.5)$$

where $G_u(k)$ is the one dimensional spectrum of the longitudinal velocity in the inertial subrange, k is the wave number, ε is the dissipation rate and A is a constant with a value of 0.56 for local isotropic turbulence. The spectrum in Eq. (4.5) could be expressed in terms of frequency using Taylor's frozen turbulence hypothesis (Taylor 1938) as

$$G_u(f) = A(2\pi)^{-2/3} u^{2/3} \varepsilon^{2/3} f^{-5/3} \quad (4.6)$$

However, the turbulence intensities are of the same order of the local mean velocity and the u velocity component is not the streamwise mean velocity especially for $S = 10.52\%$, which do not satisfy the requirements for the validity of Taylor's hypothesis stated by Hinze (1975). Therefore, Taylor's hypothesis was only used as an approximation. The energy dissipation rate can be computed using Eq. (4.6) by fitting the Kolmogorov -5/3 law in the inertial subrange.

The energy dissipation rates calculated from $G_u(f)$ in the x direction are compared reasonably well in Figs. 4.24(a–d) with those obtained from $G_{u_j}(f)$ in the x_j direction in the jet region for $S = 10.52\%$ and $Q = 31.2$ L/s. In the jet region, the vertical velocity is much smaller than the horizontal velocity. The mean velocity component u_j in the x_j direction could be referred to as the streamwise velocity. Thus, it could be concluded that the effect of u being or not being the streamwise component on the use of Taylor's hypothesis is not significant.

Figs. 4.25(a–f) and 4.26(a–c) show the distribution of the energy dissipation rate, respectively, for $S = 5.06$ and 10.52% . It can be seen that the higher dissipation

rate occurs in the recirculation regions for flow pattern 1 and on the way of jet flow for flow pattern 2. Most of the areas in the pool have a lower dissipation rate which is less than $0.2 \text{ m}^2/\text{s}^3$ or $200 \text{ W}/\text{m}^3$.

The average energy dissipation rate per unit mass $\bar{\varepsilon}$ in the pool is defined as

$$\bar{\varepsilon} = \frac{\rho g Q \Delta h}{\rho L W y_0} = \frac{g Q S}{W y_0} \quad (4.7)$$

in which ρ is the density of water and y_0 is the average water depth in the pool. Wu et al. (1999) found that the relationship between the dimensionless discharge Q_* and the normalized average depth in the pool y_0/b_0 can be described for Design 18 as:

$$Q_* = 3.75 \left(\frac{y_0}{b_0} \right) \quad (4.8)$$

Combining Eqs. (4.7) and (4.8), $\bar{\varepsilon}$ reduces to the form

$$\bar{\varepsilon} = 3.75 (gS)^{1.5} \frac{b_0}{W} \sqrt{b_0} \quad (4.9)$$

which is only a function of the slope for a given flume width and slot width. Then the average energy dissipation rates per unit mass are 0.055 and $0.166 \text{ m}^2/\text{s}^3$, respectively, for $S = 5.06$ and 10.52% .

Taylor (1935) defined the microscale λ_g as

$$\lambda_g^2 = 2 \overline{u'^2} / \left(\overline{\left(\frac{\partial u'}{\partial y} \right)^2} \right) \quad (4.10)$$

For isotropic turbulence, Taylor (1935) showed that the energy dissipation reduces to

$$\varepsilon = 7.5 \nu \overline{\left(\frac{\partial u'}{\partial y} \right)^2} \quad (4.11)$$

where ν is the kinematic viscosity of the fluid. Using Eq. (4.10), one can write the isotropic dissipation as follows:

$$\varepsilon = 15\nu \frac{\overline{u'^2}}{\lambda_g^2} \quad (4.12)$$

To extend the dissipation estimate to non-isotropic turbulence, the total velocity variance $\overline{q^2}$ is used, where $\overline{q^2} = \overline{u'^2} + \overline{v'^2} + \overline{w'^2}$. In isotropic turbulence, $\overline{u'^2} = \overline{q^2} / 3$.

So that Eq. (4.12) becomes

$$\varepsilon = 5\nu \frac{\overline{q^2}}{\lambda_g^2} \quad (4.13)$$

Then the Taylor microscale λ_g is defined from Eq. (4.13) as

$$\lambda_g = \sqrt{5\nu \frac{\overline{q^2}}{\varepsilon}} \quad (4.14)$$

Figs. 4.27(a–f) and 4.28(a–c) show the contours of the microscale λ_g in the XY-plane for $S = 5.06$ and 10.52%, respectively. The value of λ_g was evaluated from the dissipation ε and Eq. (4.14). It is seen that the value of λ_g has a range from 1 to 6 mm in the pool and from 2 to 5 mm in the jet region. Gutmark and Wygnanski (1976) found that for a plane turbulent jet, λ_g has a value from 4 to 5 mm along the jet center-line and from 2 mm to 5 mm across the jet.

The Kolmogorov length scale $\eta (= (\nu^3 / \varepsilon)^{1/4})$ is shown in Figs. 4.29(a–f) and 4.30(a–c) for all the runs. The value of η varies from 0.024 to 0.152 mm in the pool and from 0.05 to 0.08 mm along the maximum plane velocity filament. The corresponding value of η for a plane turbulent jet varies from 0.073 to 0.118 mm

along the jet center-line (Gutmark and Wygnanski 1976).

4.4.2 Structure of jet flow formed at the slot

To understand the nature of the jet flow formed at the slot, extensive velocity measurements were made in the jet flow region. The transverse distributions of the mean velocity u_j in the x_j -direction are shown in Figs. 4.31(a–e) at different sections for $S = 5.06$ and 10.52% and $Q = 31.2$ L/s. The flow appeared to have a similar form to a plane turbulent jet. However, it is clear to see that the flow is not symmetric to the x_j -axis due to the existence of recirculation regions on the side of the jet. The distributions at different sections for all the runs are plotted in a dimensionless form as shown in Fig. 4.32. The velocity u_j is dimensionless by dividing it by u_{jm} which is the maximum value of u_j at that section. b_- and b_+ are, respectively, the values of y_j where u_j is equal to one-half the maximum velocity and the velocity gradient is negative on the right and left halves of the jet when looking downstream. It was found that the velocity profiles at different sections for $S = 5.06\%$ are described very well by the corresponding profile of the plane turbulent jet (Rajaratnam 1976) for $-1.5b_- < y_j < 1.5b_+$. For $S = 10.52\%$, they are described very well for $-2b_- < y_j < b_+$. The scatter at both ends for $S = 5.06\%$ and at the positive end for $S = 10.52\%$ is attributed to the effect of the recirculating flow. The expression of the curve for the plane turbulent jet is described as (Rajaratnam 1976)

$$\frac{u_j}{u_{jm}} = \exp\left(-0.693\left(\frac{y_j}{b}\right)^2\right) \quad (4.15)$$

The variation of u_{jm}/V_{sm} with $x_j/0.5b_0$ is shown in Fig. 4.33, in which the corresponding curve for the plane turbulent jet (Rajaratnam 1976) is given. The measurements of this study start from $x_j/0.5b_0$ equal to 1.75. From that point, the maximum velocity continuously decays at a faster rate than that in a plane turbulent jet which indicates that there is no potential core for the jet formed at the slot in the vertical slot fishway. The main reason for the non-existence of the potential core is probably that the jet is formed at the slot by fully developed turbulent flow traveling from upstream to downstream. At a distance of $6b_0$ which is the length of the potential core of plane turbulent jet, the value of u_{jm}/V_{sm} is only about 0.6 for the jet traveling in the pool. The mean curve describing the decay of u_{jm} can be expressed as

$$\frac{u_{jm}}{V_{sm}} = 1 - 0.035 \frac{x_j}{0.5b_0} \quad (r^2 = 0.77) \quad (4.16)$$

where r^2 is the squared correlation coefficient. This linear relation is different from that in a plane turbulent jet in fully developed flow which is described as (Rajaratnam 1976)

$$\frac{u_{jm}}{V_{sm}} = \frac{3.5}{\sqrt{x_j/0.5b_0}} \quad (4.17)$$

The rapid decay for the jet in the vertical slot fishway is attributed to the existence of the recirculating flow on the side of the jet. The negative momentum of the recirculating flow was brought into the jet through the entrainment by the expanding jet.

In Figs. 4.34(a–e), the growth of the jet half width b_+ and b_- in the pool are

plotted in a nondimensional form. It is seen that both b_+ and b_- increase linearly with the longitudinal distance till x_j equal to approximately $5b_0$. The growth rate reduces when the jet approaches the sidewall between the long baffles for flow pattern 2 with $S = 10.52\%$ and $Q = 31.2$ L/s or the jet turns to travel to the next slot for flow pattern 1 with $S = 5.06\%$ and $Q = 31.2$ L/s. The same relationship between b_- and b_+ in Figs. 4.34(a, b) for $S = 5.06\%$ at $z = 10$ and 100 mm respectively means that the jet flow is symmetric. Fig. 4.34(c) shows that the jet is approximately symmetric at $z = 150$ mm for $S = 5.06\%$. Hence, it could be concluded that the jet flow is about symmetric for $S = 5.06\%$ and $Q = 31.2$ L/s. For flow pattern 2, there is no recirculation region on the right side of the jet and the long baffle and sidewall between the long baffles confine the development of the jet on its right side. Therefore, the behavior of the right half of this jet should be different from that of the left half with a recirculation region on its side. Fig. 4.34(f) shows the variation of $b_-/0.5b_0$ with $x_j/0.5b_0$ for flow pattern 2, which can be described by

$$b_- / 0.5b_0 = 0.268(x_j / 0.5b_0) + 0.80 \quad (r^2 = 0.80) \quad (4.18)$$

It is clear to see from Figs 4.34(a–e) that the jet grows wider at the planes close to the bed which can also be detected in Figs. 4.7 and 4.8. The results of b_{\pm} for the case having a recirculation region on the side at the planes close to the bed are shown in Fig. 4.34(g). The relation between $b_{\pm} / 0.5b_0$ and $x_j/0.5b_0$ is well described by the equation

$$b_{\pm} / 0.5b_0 = 0.271(x_j / 0.5b_0) + 0.32 \quad (r^2 = 0.90) \quad (4.19)$$

whereas at the planes far from the bed, shown in Fig. 4.34(h), the results are different

and can be described by

$$b_{\pm} / 0.5b_0 = 0.188(x_j / 0.5b_0) + 0.32 \quad (r^2 = 0.90) \quad (4.20)$$

It has to be noted that the Eqs. (4.18) to (4.20) are valid for $x_j < 5b_0$. As known, the corresponding length scale for the plane turbulent jet is given as

$$b / 0.5b_0 = 0.1(x_j / 0.5b_0) \quad (4.21)$$

The growth rate of the jet in the pool is about 1.9 to 2.7 times that of the plane turbulent jet.

Figures 4.35 to 4.38 show the distributions of Reynolds stress $(-\overline{u'_j v'_j})$, and longitudinal, transverse and vertical turbulence intensities $\sqrt{\overline{u'^2_j}}$, $\sqrt{\overline{v'^2_j}}$ and $\sqrt{\overline{w'^2_j}}$, respectively for $S = 5.06$ and 10.52% and $Q = 31.2$ L/s. The turbulence intensities were corrected for the Doppler noise for $S = 10.52\%$ as discussed before. The difference between the uncorrected and corrected values is less than 10%. As for $S = 5.06\%$, the spectrum analysis is inappropriate because the selective sampling method may change the structure of the signal, therefore, no correction was made for the Doppler noise. The variations of $(-\overline{u'_j v'_j})_m / V_{sm}^2$, $(\sqrt{\overline{u'^2_j}})_m / V_{sm}$, $(\sqrt{\overline{v'^2_j}})_m / V_{sm}$ and $(\sqrt{\overline{w'^2_j}})_m / V_{sm}$ along the jet are plotted in Figs. 4.39 to 4.32, respectively, where the subscript m refers to the maximum value in a transverse profile. Because of the effect of the recirculating flow on the side of the jet, the jet in the pool is not exactly symmetric. Therefore, the maximum values of the turbulence intensities and Reynolds stress are slightly different between the right and left halves of the jet. In

Fig. 4.39, the maximum Reynolds stress reduces gradually along the jet with a linear trend on average and it is not symmetric to the jet center line. The value of $(-\overline{u'_j v'_j})_m / V_{sm}^2$ is larger for $S = 5.06\%$ than for $S = 10.52\%$. Fig. 4.40 shows that $(\sqrt{\overline{u_j'^2}})_m / V_{sm}$ reduces gradually along the jet from an average value of 0.28 to 0.21 for $S = 5.06\%$, and from 0.21 to 0.18 for $S = 10.52\%$ except for the right half of the jet at $z = 70$ mm. It might be pointed out that some points at the first section of $x_j/0.5b_0 = 1.75$ have lower value than the average trend in both Figs. 4.39 and 4.40. It is probably due to measurement errors. It was found that the normalized maximum transverse turbulence intensity is almost constant along the jet with an average value of 0.2 for $S = 5.06\%$, shown in Fig. 4.41(a). However, for $S = 10.52\%$, $(\sqrt{\overline{v_j'^2}})_m / V_{sm}$ reduces from an average value of 0.17 to 0.13 at $x_j/0.5b_0 = 8.7$ and then levels off (see Fig. 4.41(b)). The effect of the boundary on the vertical turbulence intensity is clearly demonstrated in Fig. 4.42. $(\sqrt{\overline{w_j'^2}})_m / V_{sm}$ has smaller values at the plane close to the bed than those far from the bed. At $z = 10$ mm, $(\sqrt{\overline{w_j'^2}})_m / V_{sm}$ reduces gradually along the jet for both 5.06 and 10.52% slopes. However, it stays almost constant with a value of 0.1 at $z = 70$ mm for $S = 10.52\%$. For $S = 5.06\%$ at $z = 100$ and 150 mm, $(\sqrt{\overline{w_j'^2}})_m / V_{sm}$ has a constant value of 0.15 till $x_j/0.5b_0$ reaches 8.7 and then gradually increases which is probably due to the effect of the turning of the jet. Now it can be concluded from the above discussions that the turbulence characteristics of the jet for $S = 5.06\%$ (flow pattern 1) are different from those for S

= 10.52% (flow pattern 2), which will be further corroborated by the following discussions.

The variation of the longitudinal turbulence intensity along the jet center-line is presented in Fig. 4.43 along with the results of Heskestad (1965) for the plane turbulent jet. Similar to the plane turbulent jet, $\sqrt{u_j'^2} / u_{jm}$ increase sharply at beginning and then gradually increases along the jet. The $\sqrt{u_j'^2} / u_{jm}$ profile for the jet in the pool is significantly higher than that for the plane turbulent jet.

The normalized Reynolds shear stress profile is presented in Fig. 4.44, while the normalized turbulence intensity profiles of the three components of the velocity fluctuations are shown in Figs. 4.45–4.47. Figs. 4.44–4.47 do not include the sections where the value of b_{\pm} deviates from the straight line in Fig. 4.34 and the points outside of the jet flow. The Reynolds stress and turbulence intensity profiles measured by Heskestad (1965), Bradbury (1965), Gutmark and Wygnanski (1976), and Ramaprian and Chandrasekhara (1985) for the plane turbulent jet are also plotted in Figs. 4.44–4.47 for comparison. These figures again show that the turbulent structure of the jet in the pool for flow pattern 1 is different compared to that for flow pattern 2. In Fig. 4.44, for flow pattern 2 with $S = 10.56\%$, the $\overline{-u_j'v_j'} / u_{jm}^2$ mean profile agrees well with the profile of the plane turbulent jet but with a shift of the zero point to the right side of the jet center-line. However, for flow pattern 1 with $S = 5.06\%$, the $\overline{-u_j'v_j'} / u_{jm}^2$ profile is close to symmetric but significantly higher than the profile of the plane turbulent jet. Figs. 4.45–4.46 show that for $S = 10.56\%$, the

profiles of both $\sqrt{u_j'^2} / u_{jm}$ and $\sqrt{v_j'^2} / u_{jm}$ in the left half of the jet have a good similarity and are similar to the plane turbulent jet whereas on the right half of the jet, they have different structures due to the effect of the sidewall and long baffle on the jet. Both the profiles of $\sqrt{u_j'^2} / u_{jm}$ and $\sqrt{v_j'^2} / u_{jm}$ for $S = 5.06\%$ have a higher value compared to the plane turbulent jet and are not symmetric to the jet center-line but show some similarity on either side. One may attribute this non-symmetry to the effect of the recirculating flow on both sides which may have different areas and velocities. As for $\sqrt{w_j'^2} / u_{jm}$, the boundary effect is clearly indicated in Fig. 4.47. The value of $\sqrt{w_j'^2} / u_{jm}$ at the plane near to the bed is much lower than that at the planes far from the bed. The $\sqrt{w_j'^2} / u_{jm}$ profile at $z = 100$ and 150 mm for $S = 5.06\%$ is similar to the plane turbulent jet, but for $S = 10.52\%$, it shows a linear relationship which is different from the plane turbulent jet.

The similarity of the turbulence intensities is also checked from the other perspective by normalizing them by their corresponding maximum values, shown in Figs. 4.48–50. The profiles of the longitudinal turbulence intensity are approximately similar at all the planes for $S = 5.06$ and 10.52% (see Fig. 4.48). However, the profiles of the transverse and vertical turbulence intensities are different between $S = 5.06$ and 10.52% . The $\sqrt{v_j'^2} / (\sqrt{v_j'^2})_m$ profiles show the similarity individually for each slope. For $\sqrt{w_j'^2} / (\sqrt{w_j'^2})_m$, the profiles for $S = 10.52\%$ present the similarity but

for $S = 5.06\%$, the profiles at $z = 10$ mm show a different trend from those at $z = 100$ and 150 mm. One may observe that the jet is not symmetric from Figs. 4.48–50.

4.5 Conclusions

This chapter presents the results of a laboratory study on the turbulence structure of flow in the vertical slot fishways with the slopes of 5.06 and 10.52% . A MicroADV was used to obtain the instantaneous velocity fields. There are two distinct flow patterns referred to as patterns 1 and 2. Pattern 1 occurs for $S = 5.06\%$ and pattern 2 for $S = 10.52\%$ and $Q = 31.2$ L/s. The flow for $S = 10.52\%$ and $Q = 52$ L/s was not stable and the flow pattern changed between patterns 1 and 2 irregularly. The average flow over 600 seconds shows pattern 1.

The mean velocity distributions clearly show that the flow is three dimensional and there are two different flow regions in the pools: jet flow and recirculating flow. The vertical velocity remains at a small value in most areas of the pools for all the cases studied which would allow fish to choose any preferred swimming depth. It was found that the mean flow kinetic energy decays rapidly in a small area within the jet flow region whereas it has a small value of less than 9% of V_{sm}^2 in the rest of the pool. The existence of reasonably small areas of high values of the mean flow kinetic energy in the pools is desirable for fish passage.

In the jet flow region, the Reynolds stress, longitudinal and transverse turbulence intensities decrease as the jet travels downstream while in the recirculation region they remain at very small values which can be interpreted as that

the flow structures are different between the two flow regions. The distribution of the vertical turbulence intensity is close to being uniform with small values in the planes parallel to the bottom of the flume. The maximum turbulence kinetic energy in the pool for all the runs is less than 8% of V_{sm}^2 which indicates relatively large energy dissipation and would enable fish to ascend without undue stress.

It was found that most of the areas in the pool have a lower dissipation rate which is less than $0.2 \text{ m}^2/\text{s}^3$. The average energy dissipation rates per unit mass are 0.055 and $0.166 \text{ m}^2/\text{s}^3$, respectively, for $S = 5.06$ and 10.52% . The Taylor microscale has a range from 1 to 6 mm in the pool and from 2 to 5 mm in the jet region. The Kolmogorov length scale varies from 0.024 to 0.152 mm in the pool and from 0.05 to 0.08 mm along the maximum plane velocity locus.

For the jet flow in the pool, the dimensionless mean velocity distribution can be well described by the expression for the plane turbulent jet in the center part of the jet. The scatter at the ends is attributed to the effect of the recirculating flow. The maximum velocity decays at a faster rate than that in a plane turbulent jet which indicates that there is no potential core for the jet formed at the slot in the vertical slot fishway. The jet, which is not symmetric, grows wider at the planes close to the bed. The jet half widths b_+ and b_- increase linearly with the longitudinal distance till x_j equal to about $5b_0$ and then the growth rate reduces when the jet approaches the sidewall in between the long baffles for flow pattern 2 or the jet turns to travel to the next slot for flow pattern 1. The growth rate of the jet in the pool is about 1.9 to 2.7 times that of a plane turbulent jet.

The turbulence structure of the jet flow is different between flow patterns 1 and 2. For each pattern, the following effects make the turbulence appear different between the left and right halves of the jet: the recirculating flow on both sides of the jet for flow pattern 1 and on the left side of the jet for flow pattern 2, the effect of the sidewall and long baffle on the right half of the jet for flow pattern 2, and the effect of the bed. For flow pattern 2, the $-\overline{u_j'v_j'} / u_{jm}^2$ mean profile agrees well with that of the plane turbulent jet but with a shift of the zero point to the right side of the jet center-line. However, for flow pattern 1, the shear stress profile is close to symmetric but significantly higher than that of the plane turbulent jet. For flow pattern 2, the profiles of both $\sqrt{\overline{u_j'^2}} / u_{jm}$ and $\sqrt{\overline{v_j'^2}} / u_{jm}$ in the left half of the jet have a good similarity and are similar to the plane turbulent jet whereas on the right half of the jet, they have different structures due to the effect of the sidewall and long baffle on the jet. Both the profiles of $\sqrt{\overline{u_j'^2}} / u_{jm}$ and $\sqrt{\overline{v_j'^2}} / u_{jm}$ for flow pattern 1 have a higher value than the plane turbulent jet and are not symmetric to the jet center-line but show some similarity on either side. As for $\sqrt{\overline{w_j'^2}} / u_{jm}$, the value of $\sqrt{\overline{w_j'^2}} / u_{jm}$ at the plane near to the bed is much lower than that at the planes far from the bed. The $\sqrt{\overline{w_j'^2}} / u_{jm}$ profile at $z = 100$ and 150 mm for $S = 5.06\%$ is similar to that of the plane turbulent jet, but for $S = 10.52\%$, it shows a linear relationship which is different from the plane jet.

4.6 References

- Anderson, S., and Lohrmann, A. (1995). "Open water test of the SonTek acoustic Doppler velocimeter." *Proceedings of IEEE 5th Working Conference on Current Measurements*, 188–192.
- Bell, M. C. (1973). *Fisheries handbook of engineering requirements and biological criteria*, U.S. Army Corps of Engineers, North Pacific Division, Portland, Oreg.
- Bradbury, L. J. S. (1965). "The structure of a self-preserving turbulent plane jet." *J. Fluid Mech.* 23(1), 31–64.
- Clay, C. H. (1961). *Design of fishways and other fish facilities*, Dept. of Fisheries of Canada, Ottawa.
- Goring, D. G., and Nikora, V. I. (2002.) "Despiking acoustic Doppler velocimeter data." *J. Hydraul. Eng.*, 128(1), 117–126.
- Gutmark, E., and Wygnanski, I. (1976). "The planar turbulent jet." *J. Fluid Mech.*, 73(3), 465–495.
- Heskestad, G. (1965). "Hot-wire measurements in a plane turbulent jet." *Transactions of the ASME, J. of Applied Mechanics*, December, 721–734.
- Hinze, J. Q. (1975). *Turbulence*, McGraw-Hill, New York.
- Katopodis, C. (1990). "Introduction to fishway design." *Report*, Freshwater Institute, Central and Arctic Region, Department of Fisheries and Oceans, Canada.
- Kraus, N. C., Lohrmann, R. A., and Cabrera, R. (1994). "New acoustic meter for measuring 3D laboratory flows." *J. Hydraul. Eng.*, 120(3), 406–412.

- Liu, M., Zhu, D. Z., and Rajaratnam, N. (2002). "Evaluation of ADV measurements in bubbly two-phase flows." *Proceedings of the conference of Hydraulic Measurements & Experimental Methods 2002*, Estes Park, Colorado, USA. (CD Rom)
- Liu, M., Rajaratnam, N., and Zhu, D. Z. (2003). "Turbulence structure of hydraulic jumps of low Froude numbers." *J. Hydraul. Eng.*, ASCE, will appear in June, 2004.
- Lohrmann, R. A., Cabrera, R., and Kraus, N. C. (1994). "Acoustic-Doppler velocimeter (ADV) for laboratory use." *Proc., Symp. on Fundamentals and Advancements in Hydraul. Measurements and Experimentation*, C. A. Pugh, ed., ASCE, 351–365.
- Nikora, V. I., and Goring, D. G. (1998). "ADV measurements of turbulence: Can we improve their interpretation?" *J. Hydraul. Eng.*, 124(6), 630–634.
- Puertas, J., Pena, L., and Teijeiro, T. (2004). "Experimental approach to the hydraulics of vertical slot fishways." *J. Hydraul. Eng.*, 130(1), 10–23.
- Rajaratnam, N. (1976). *Turbulent jets*, Elsevier Scientific Publishing Company, Amsterdam, Oxford, New York.
- Rajaratnam, N., Van der Vinne, G., and Katopodis, C. (1986). "Hydraulics of vertical slot fishways." *J. Hydraul. Eng.*, 112(10), 909–927.
- Rajaratnam, N., Katopodis, C., and Solanki, S. (1992). "New designs for vertical slot fishways." *Can. J. Civ. Engrg.*, 19 (3), 402–414.
- Ramaprian, B.R., and Chandrasekhara, M.S. (1985). "LDA measurements in plane

- turbulent jets.” *Transactions of the ASME, J. of Fluids Engineering*, 107, June, 264–271.
- Rousseeuw, P. J. (1990). “Robust estimation and identifying outliers.” Handbook of statistical methods for engineers and scientists, H. M. Wadsworth Jr., ed., McGraw-Hill, Inc., 16.1–16.24.
- SonTek. (1997). *Acoustic Doppler Velocimeter Technical Documentation*, Version 4.0, San Diego, Calif.
- Taylor, G. I. (1935). “Statistical theory of turbulence.” *Proc. Roy. Soc.* A151(873), 421–478.
- Taylor, G. I. (1938). “The spectrum of turbulence.” *Proc. Roy. Soc.* A164(919), 476–490.
- Wahl, Tony L. (2003). “Discussion of ‘Despiking acoustic Doppler velocimeter data’ by Derek G. Goring and Vladimir I. Nikora.” *J. Hydraul. Eng.*, 129(6), 484–487.
- Wu, S., Rajaratnam, N., and Katopodis, C. (1999). “Structure of flow in vertical slot fishway.” *J. Hydraul. Eng.*, 125(4), 351–360.

Table 4.1 Primary Details of the Experiments Undertaken in the Coordinate System (x, y, z)

Exp.	S (%)	Q (L/s)	Velocity measured at plane with z (mm)	MicroADV Sampling time (sec)
1	5.06	31.2	10, 100, 150	600
2	5.06	52.0	10, 150, 300	600
3	10.52	31.2	10, 70	300
4	10.52	52.0	100	600

Table 4.2 Primary Details of the Experiments Undertaken in the Coordinate System (x_j, y_j, z)

Exp.	S (%)	Q (L/s)	Velocity measured at plane with z (mm)	MicroADV Sampling time (sec)
5	5.06	31.2	10, 100, 150	600
6	10.52	31.2	10, 70	600

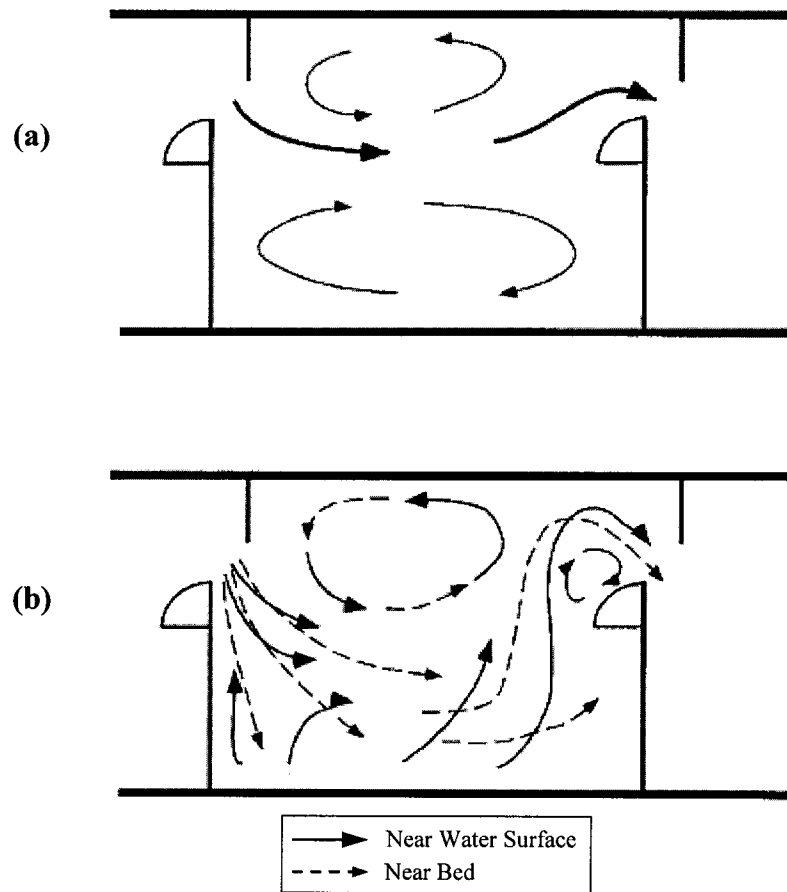


Fig. 4.1 Flow patterns in pools: (a) pattern 1 and (b) pattern 2 (Wu et al. 1999)

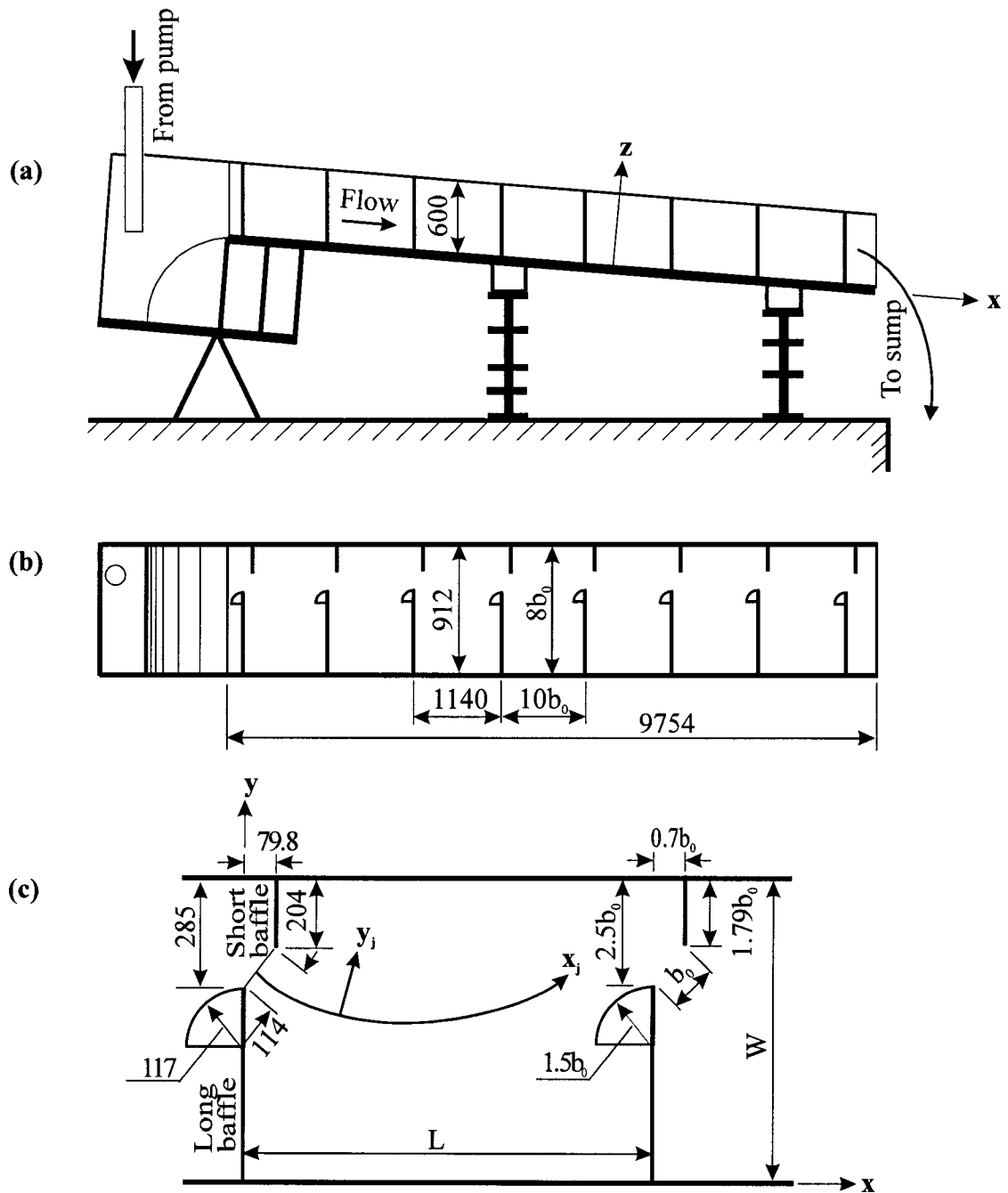


Fig. 4.2 Experimental set-up of vertical slot fishway: (a) side view; (b) plan view; (c) details of slot and pool (dimensions shown are in mm)



Fig. 4.3 Experiment for $S = 10.52\%$ and $Q = 31.2$ L/s in T. Blench Hydraulics Laboratory at the University of Alberta

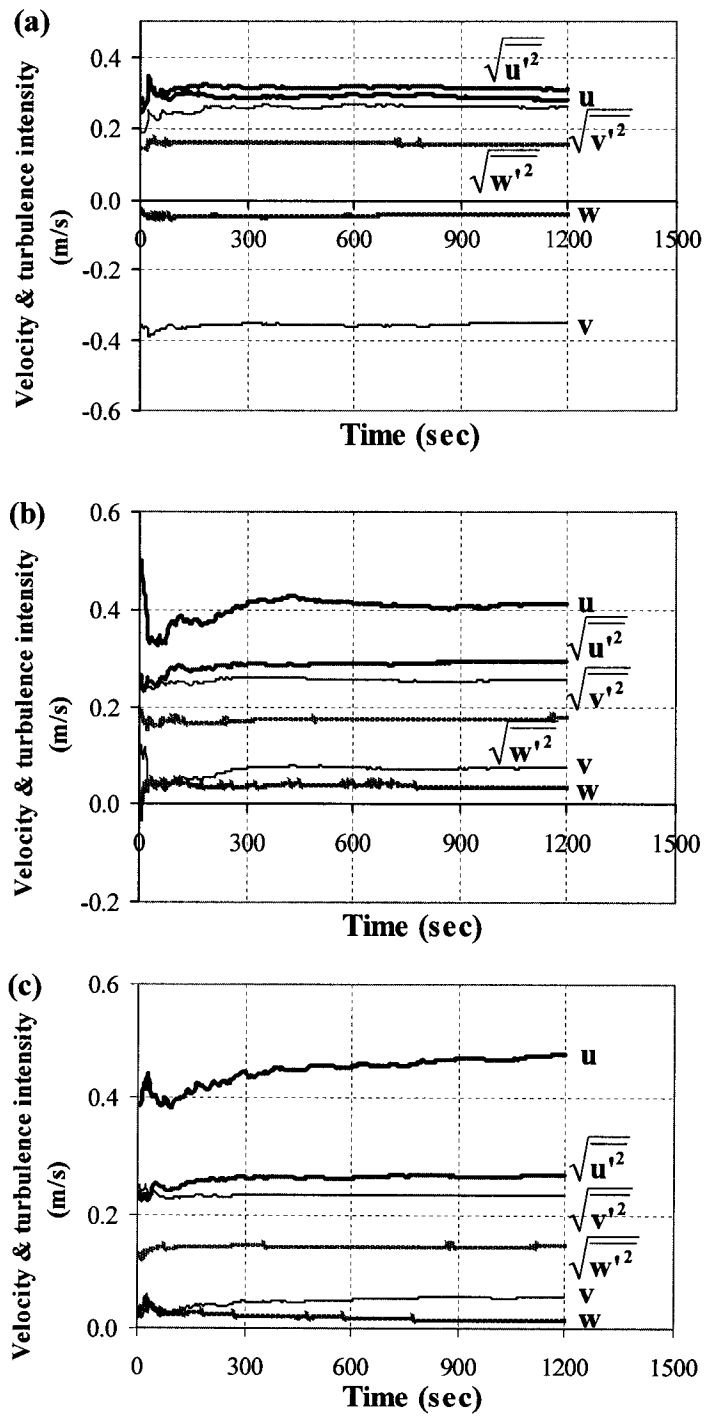


Fig. 4.4 Change of mean velocity and turbulence intensity with time:
 (a) $S = 10.52\%$, $Q = 31.2$ L/s, $x = 300$ mm, $y = 500$ mm, $z = 70$ mm;
 (b) $S = 5.06\%$, $Q = 52$ L/s, $x = 600$ mm, $y = 600$ mm, $z = 150$ mm;
 (c) $S = 5.06\%$, $Q = 31.2$ L/s, $x = 600$ mm, $y = 600$ mm, $z = 100$ mm

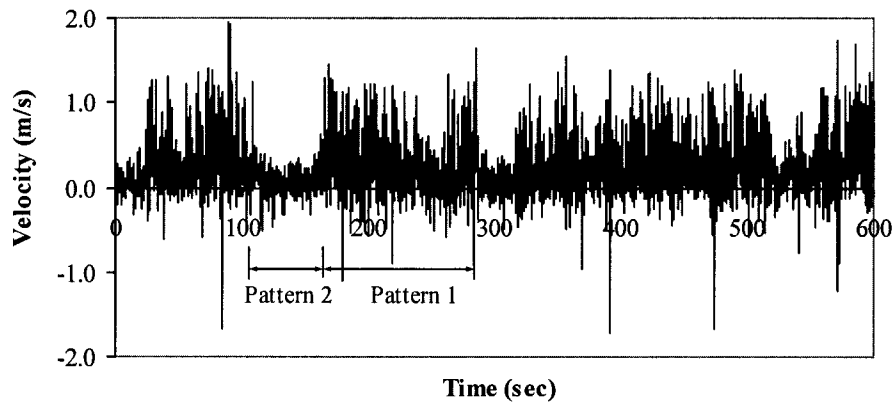


Fig. 4.5 Sample of velocity time series for $S = 5.06\%$ and $Q = 31.2$ L/s at coordinate system (x_j, y_j, z)

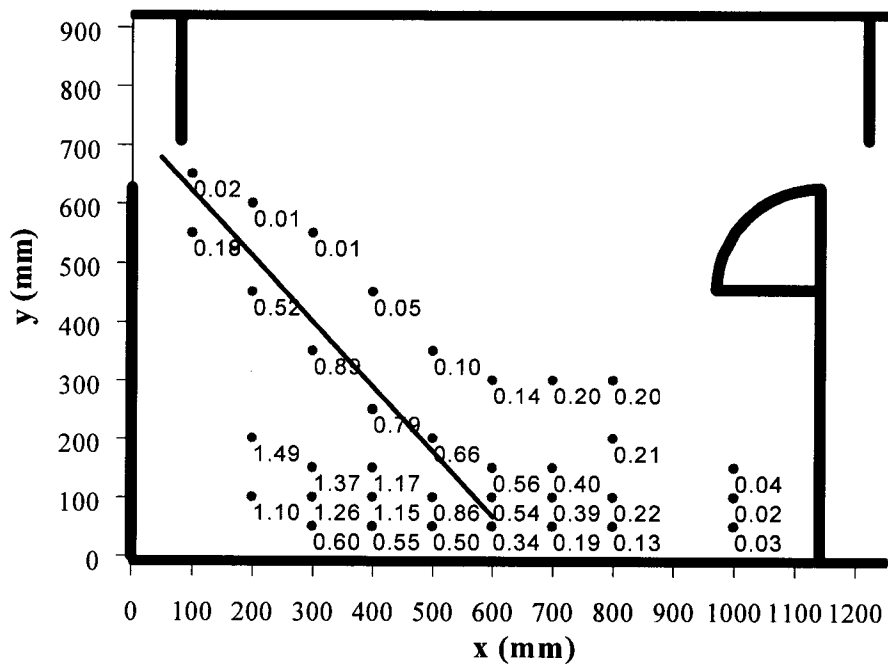


Fig. 4.6 Air concentration (%) for $S = 10.52\%$, $Q = 31.2$ L/s, $z = 70$ mm, ———, maximum plane velocity filament

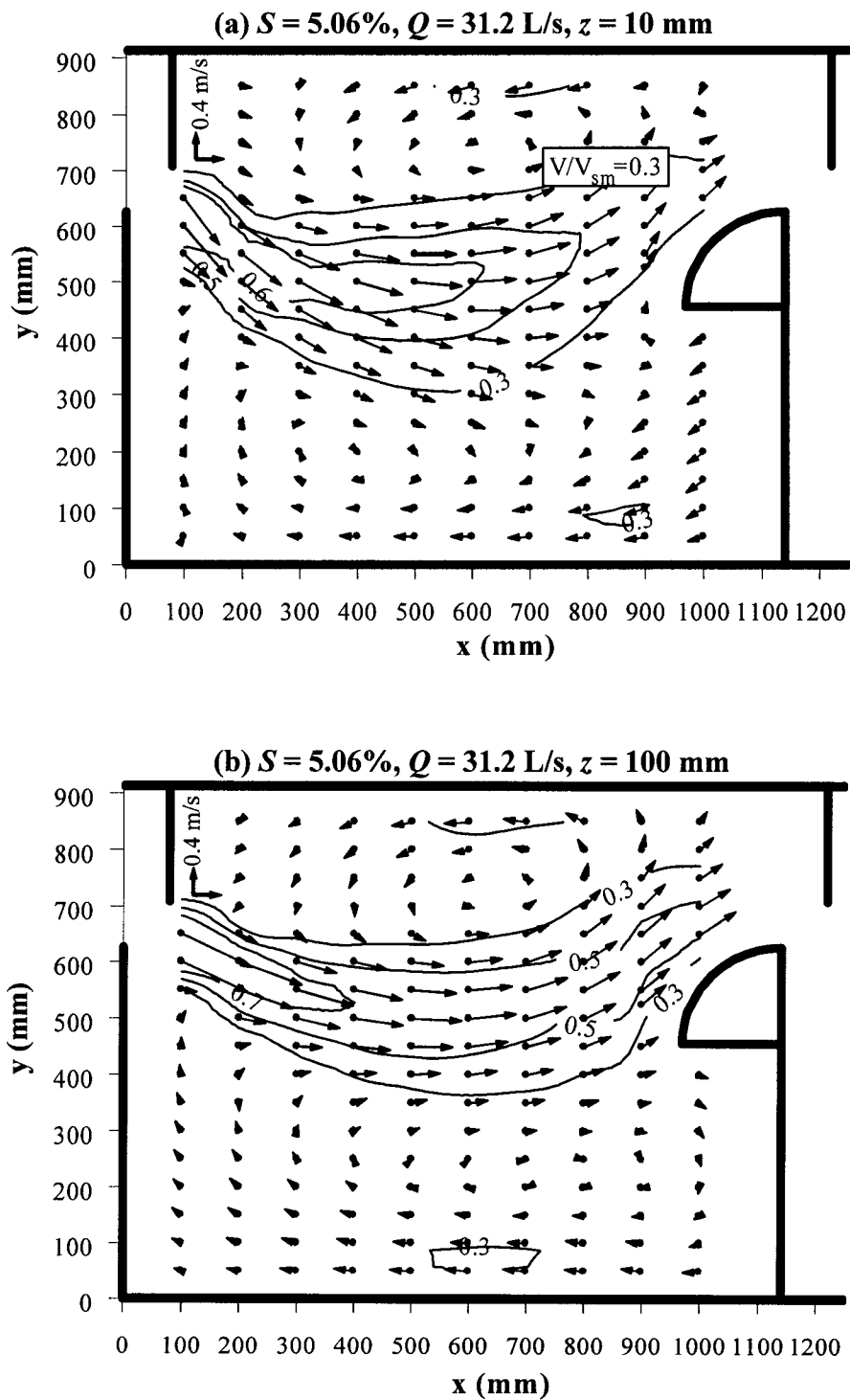


Fig. 4.7(a-f) Plane velocity field in the pool for $S = 5.06\%$: \longrightarrow , this study; \dashrightarrow , Wu et al. (1999); --- , V/V_{sm} contour: (a) $Q = 31.2$ L/s, $z = 10$ mm; (b) $Q = 31.2$ L/s, $z = 100$ mm

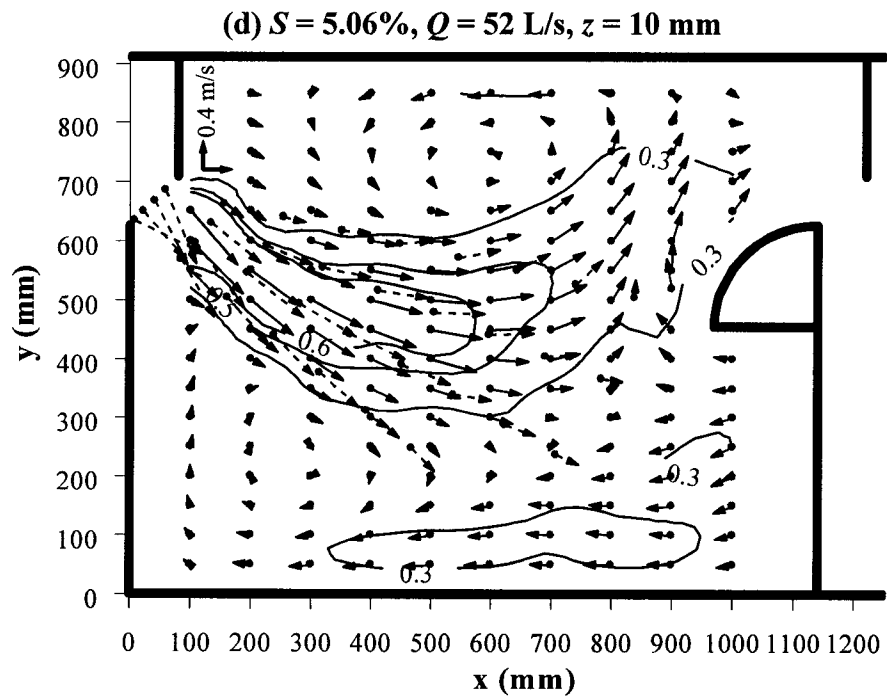
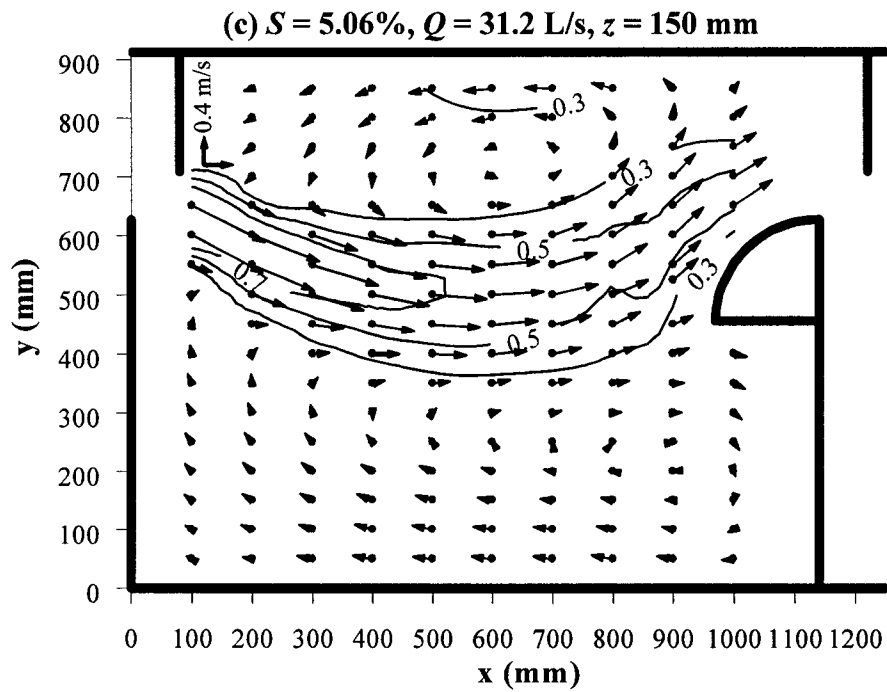


Fig. 4.7(a-f) Plane velocity field in the pool for $S = 5.06\%$: \longrightarrow , this study; \dashrightarrow , Wu et al. (1999); --- , V/V_{sm} contour: (c) $Q = 31.2$ L/s, $z = 150$ mm; (d) $Q = 52$ L/s, $z = 10$ mm

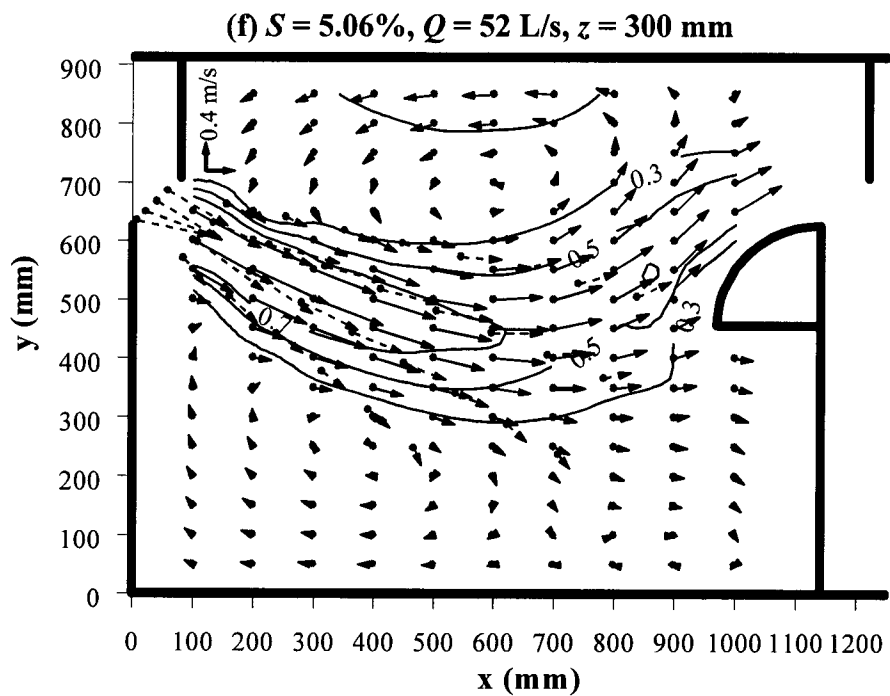
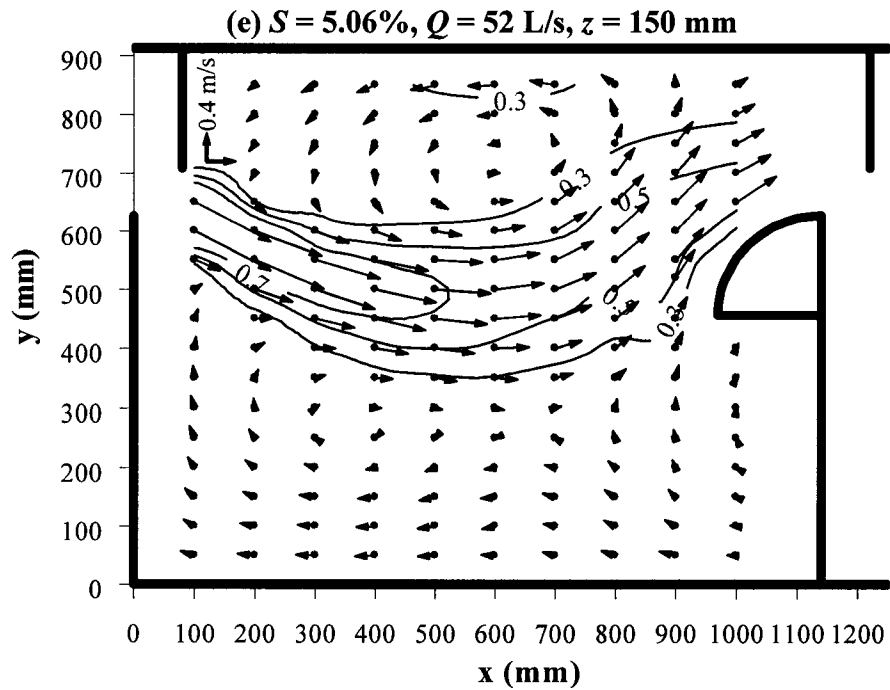


Fig. 4.7(a-f) Plane velocity field in the pool for $S = 5.06\%$: \longrightarrow , this study; \dashrightarrow , Wu et al. (1999); --- , V/V_{sm} contour: (e) $Q = 52$ L/s, $z = 150$ mm; (f) $Q = 52$ L/s, $z = 300$ mm

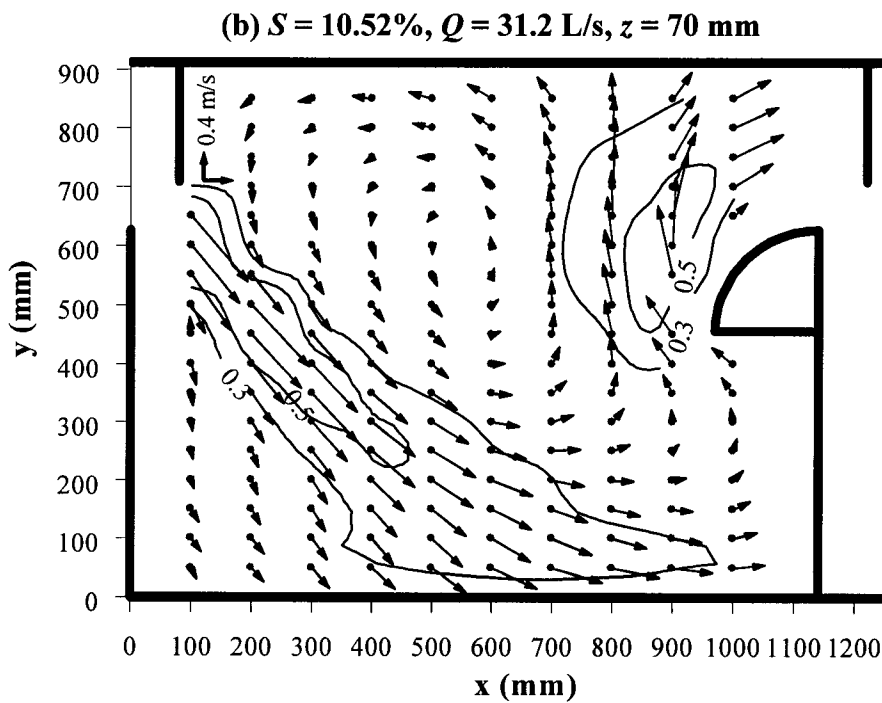
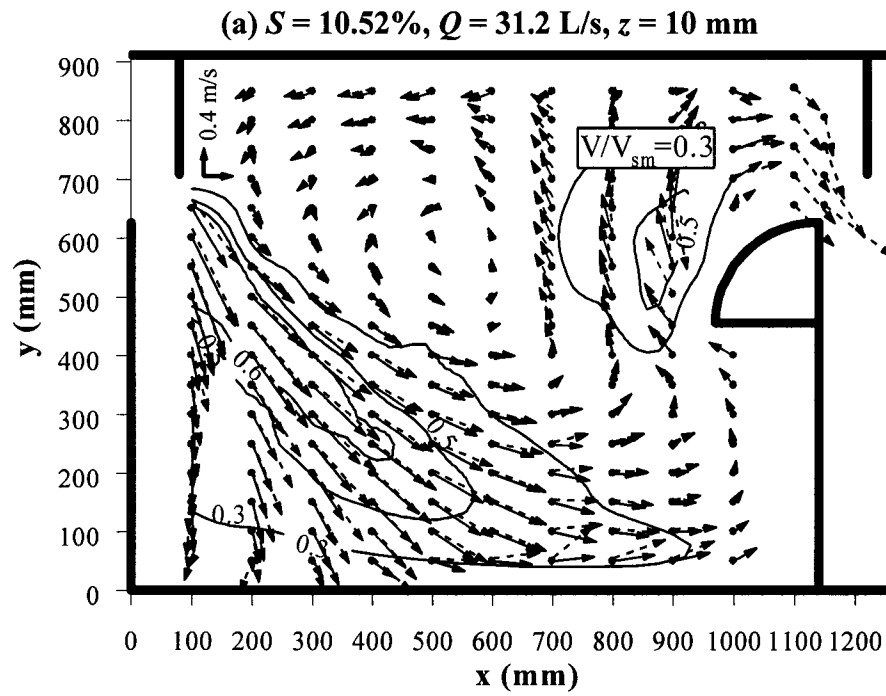


Fig. 4.8(a-c) Plane velocity field in the pool for $S = 10.52\%$: \longrightarrow , this study; \dashrightarrow , Wu et al. (1999); --- , V/V_{sm} contour: (a) $Q = 31.2$ L/s, $z = 10$ mm; (b) $Q = 31.2$ L/s, $z = 70$ mm

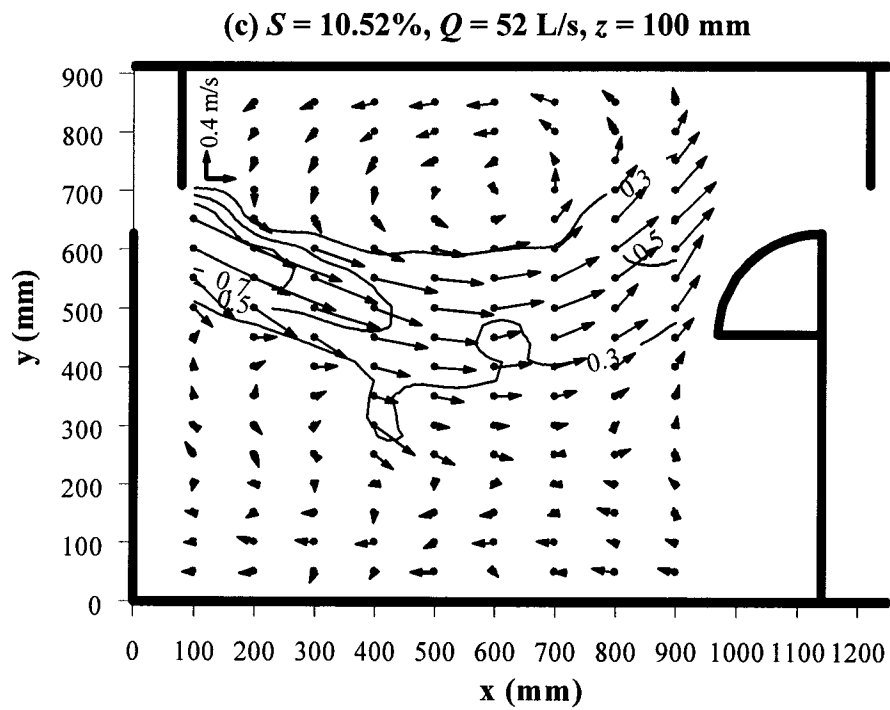
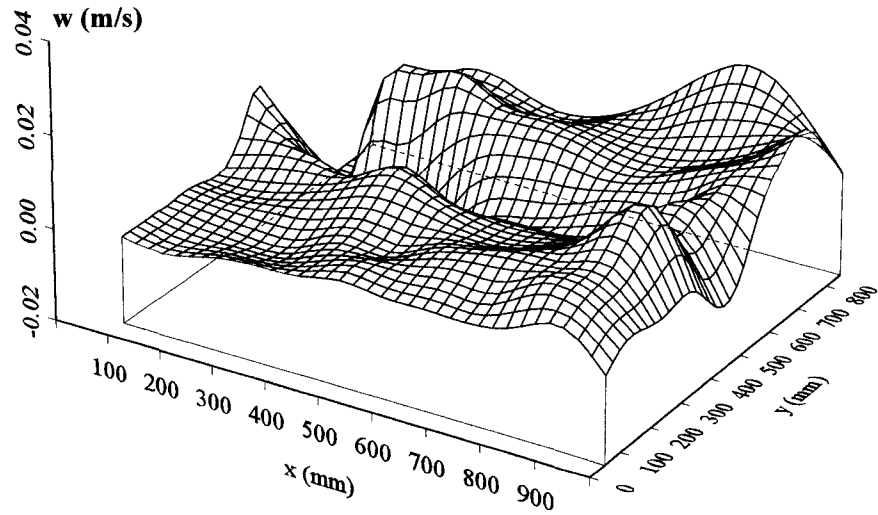
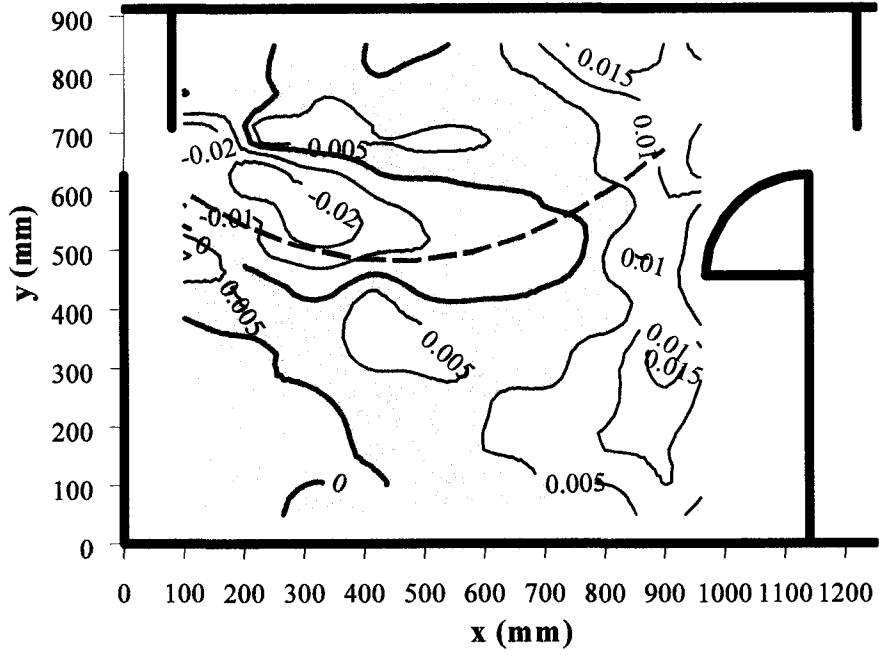


Fig. 4.8(a-c) Plane velocity field in the pool for $S = 10.52\%$: \longrightarrow , this study; \dashrightarrow , Wu et al. (1999); --- , V/V_{sm} contour: (c) $Q = 52 \text{ L/s}$, $z = 100 \text{ mm}$

(a) $S = 5.06\%$, $Q = 31.2 \text{ L/s}$, $z = 10 \text{ mm}$



**Fig. 4.9(a-f) Vertical velocity distribution in the pool for $S = 5.06\%$,
— — —, maximum plane velocity filament: (a) $Q = 31.2 \text{ L/s}$, $z = 10 \text{ mm}$**

(b) $S = 5.06\%$, $Q = 31.2 \text{ L/s}$, $z = 100 \text{ mm}$

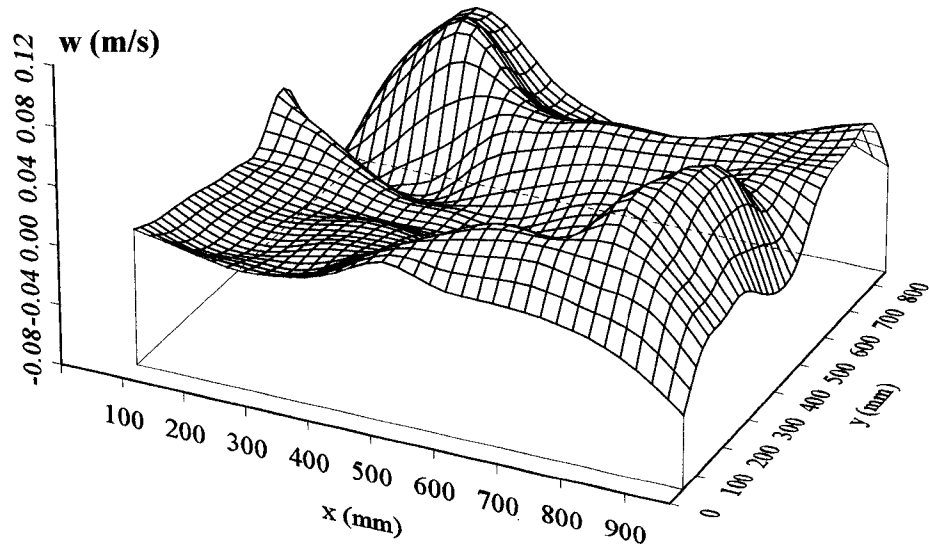
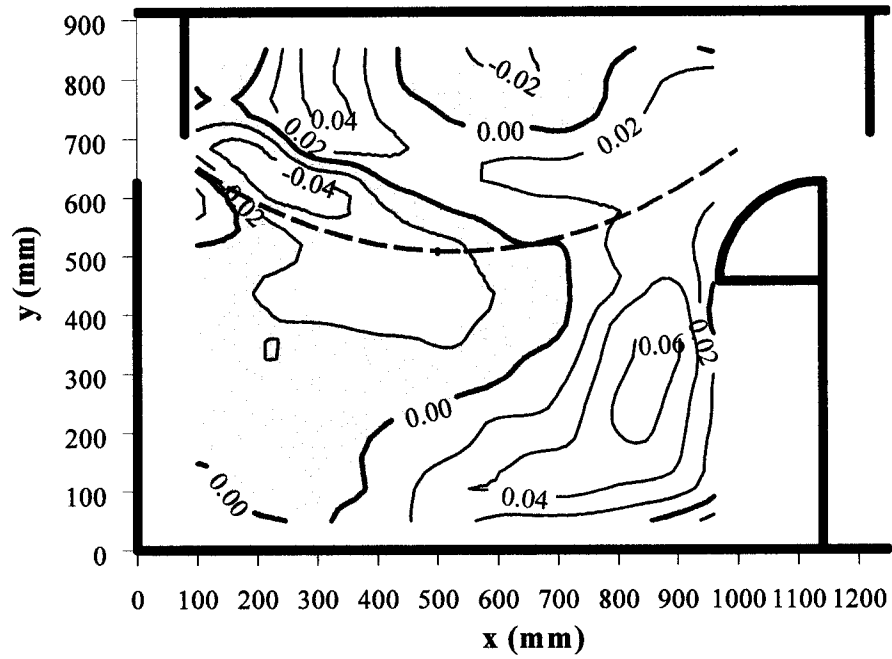


**Fig. 4.9(a-f) Vertical velocity distribution in the pool for $S = 5.06\%$,
 — — —, maximum plane velocity filament: (b) $Q = 31.2 \text{ L/s}$, $z = 100 \text{ mm}$**

(c) $S = 5.06\%$, $Q = 31.2$ L/s, $z = 150$ mm

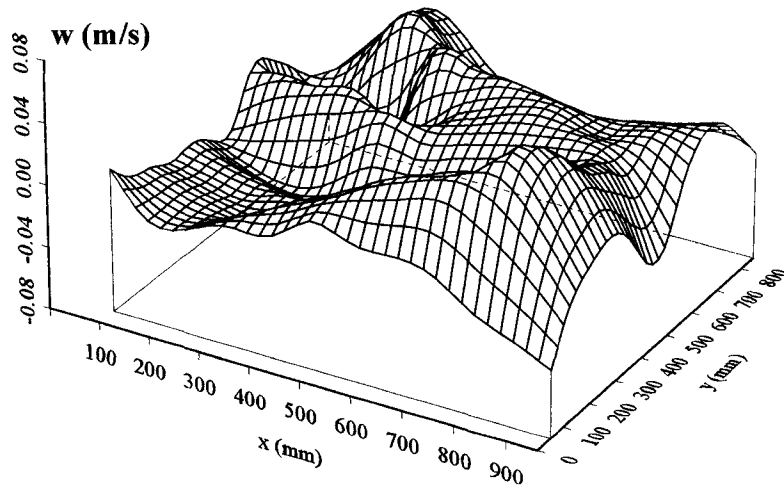
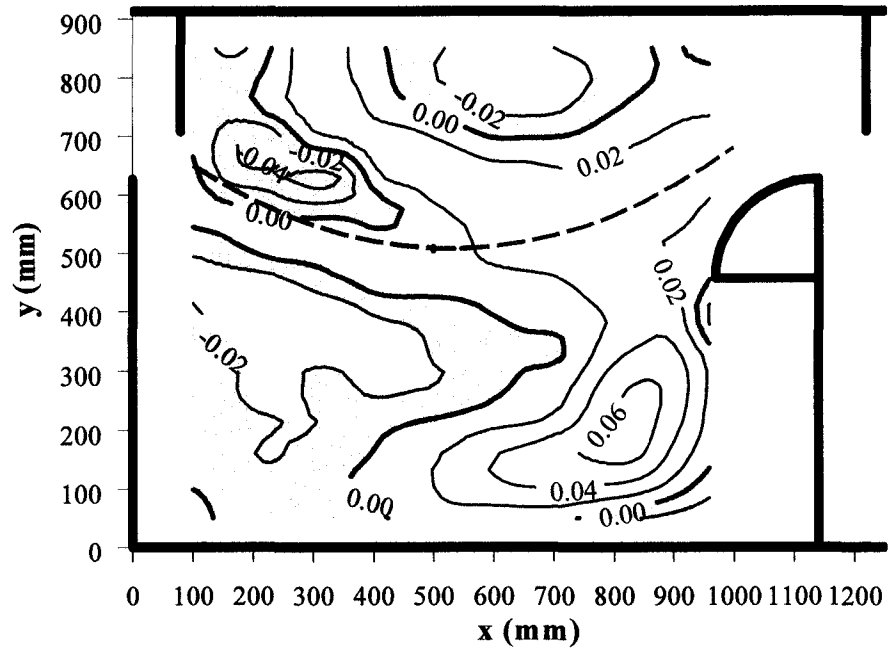


**Fig. 4.9(a-f) Vertical velocity distribution in the pool for $S = 5.06\%$,
---, maximum plane velocity filament: (c) $Q = 31.2$ L/s, $z = 150$ mm**

(d) $S = 5.06\%$, $Q = 52 \text{ L/s}$, $z = 10 \text{ mm}$

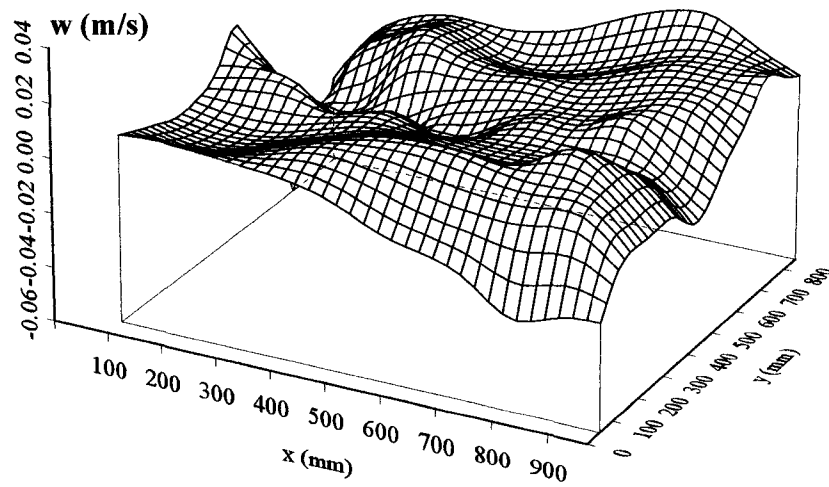
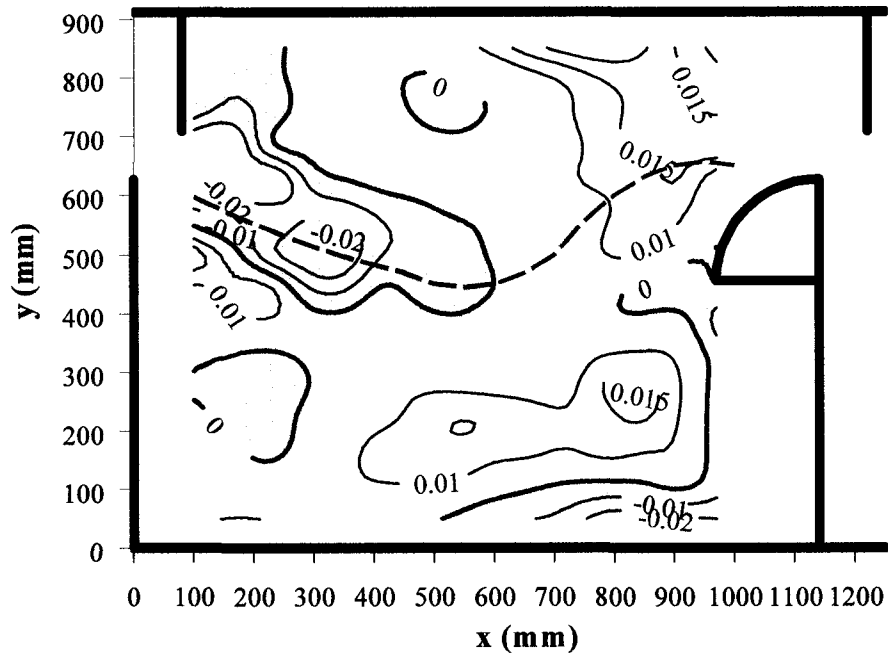


**Fig. 4.9(a-f) Vertical velocity distribution in the pool for $S = 5.06\%$,
— — —, maximum plane velocity filament: (d) $Q = 52 \text{ L/s}$, $z = 10 \text{ mm}$**

(e) $S = 5.06\%$, $Q = 52 \text{ L/s}$, $z = 150 \text{ mm}$

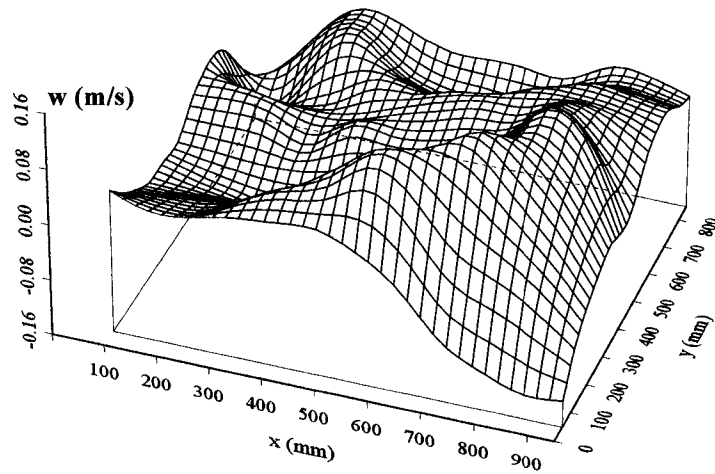
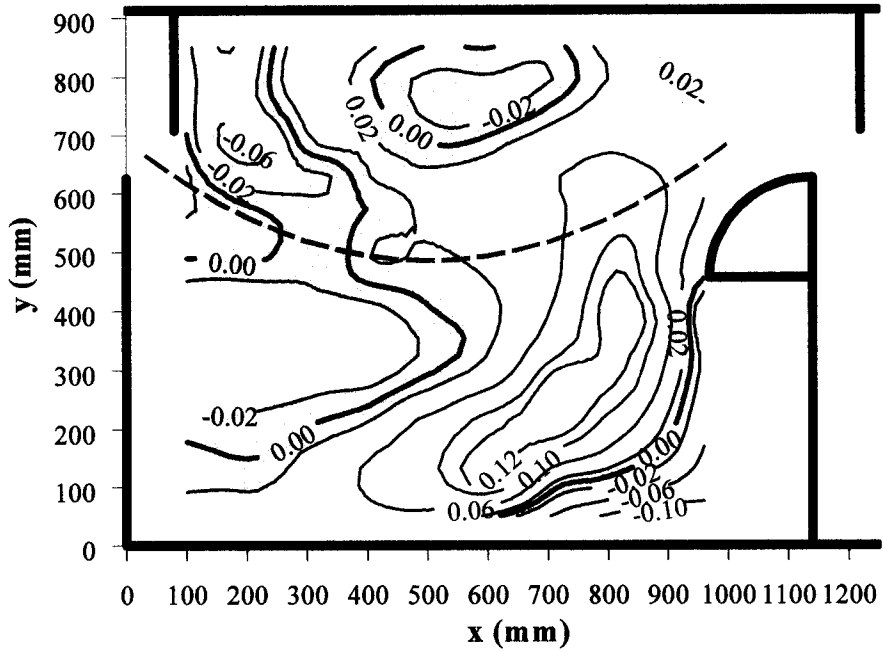


**Fig. 4.9(a-f) Vertical velocity distribution in the pool for $S = 5.06\%$,
— — —, maximum plane velocity filament: (e) $Q = 52 \text{ L/s}$, $z = 150 \text{ mm}$**

(f) $S = 5.06\%$, $Q = 52 \text{ L/s}$, $z = 300 \text{ mm}$

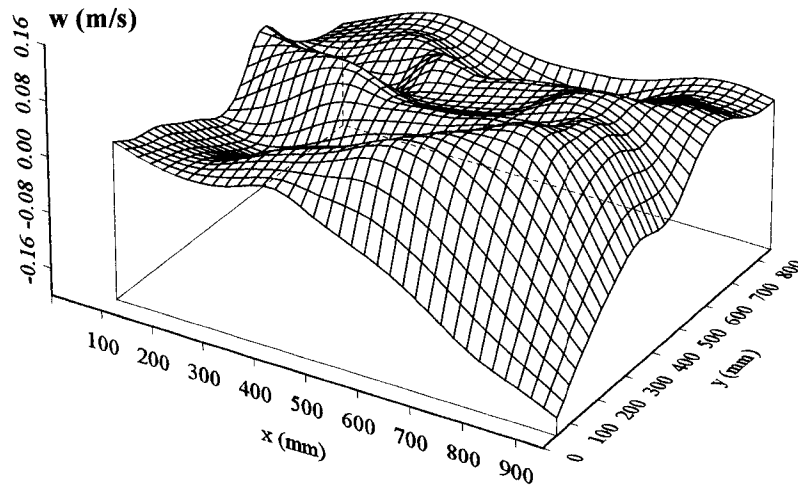
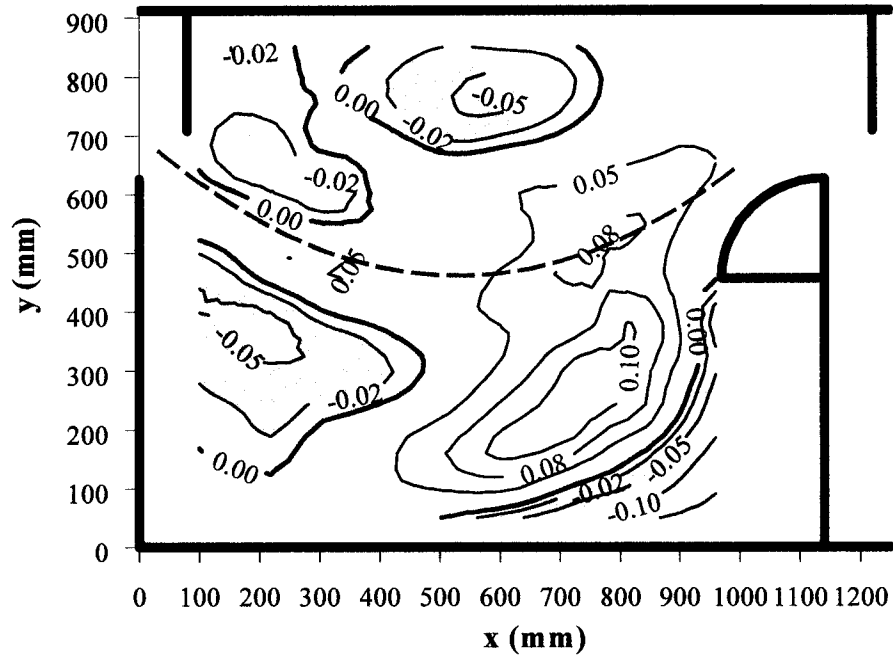


**Fig. 4.9(a-f) Vertical velocity distribution in the pool for $S = 5.06\%$,
— — —, maximum plane velocity filament: (f) $Q = 52 \text{ L/s}$, $z = 300 \text{ mm}$**

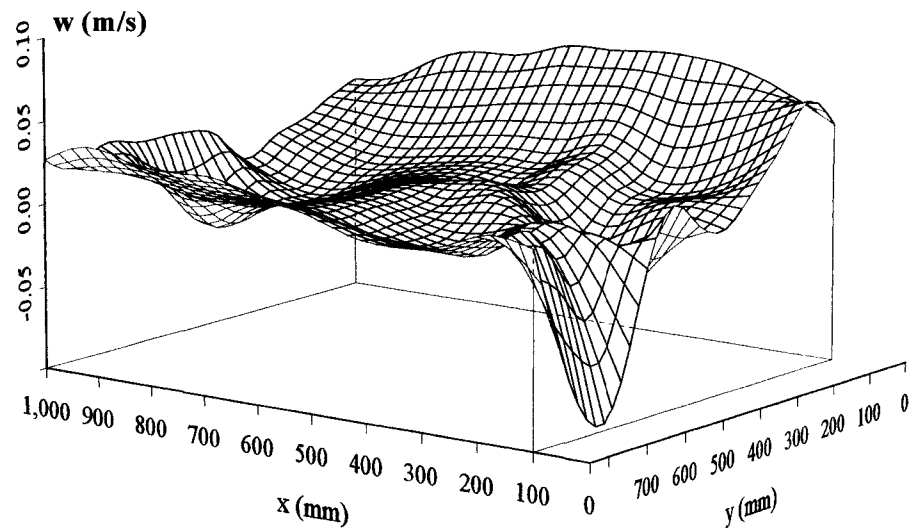
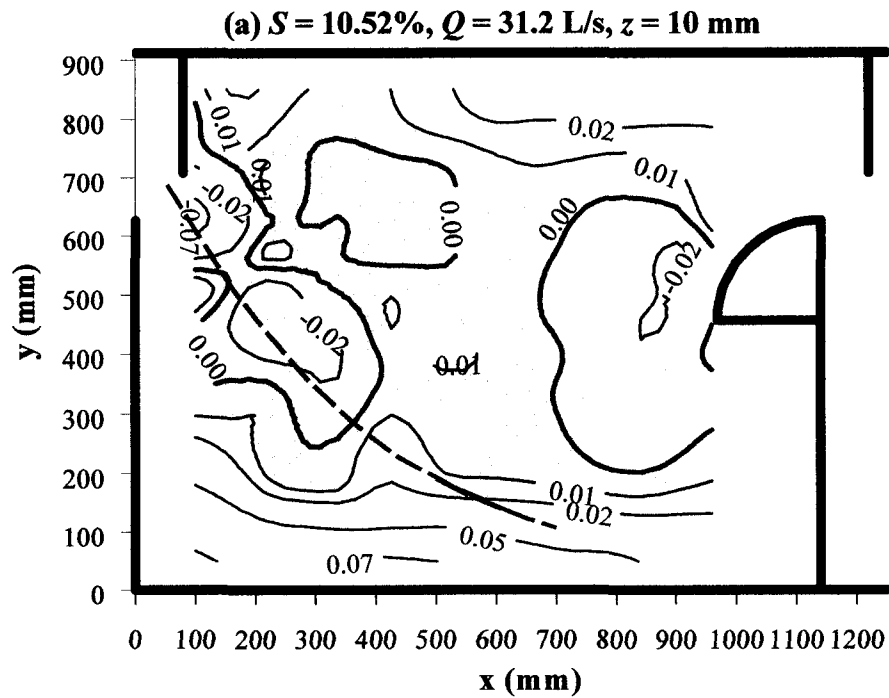


**Fig. 4.10(a-c) Vertical velocity distribution in the pool for $S = 10.52\%$,
 — — —, maximum plane velocity filament: (a) $Q = 31.2$ L/s, $z = 10$ mm**

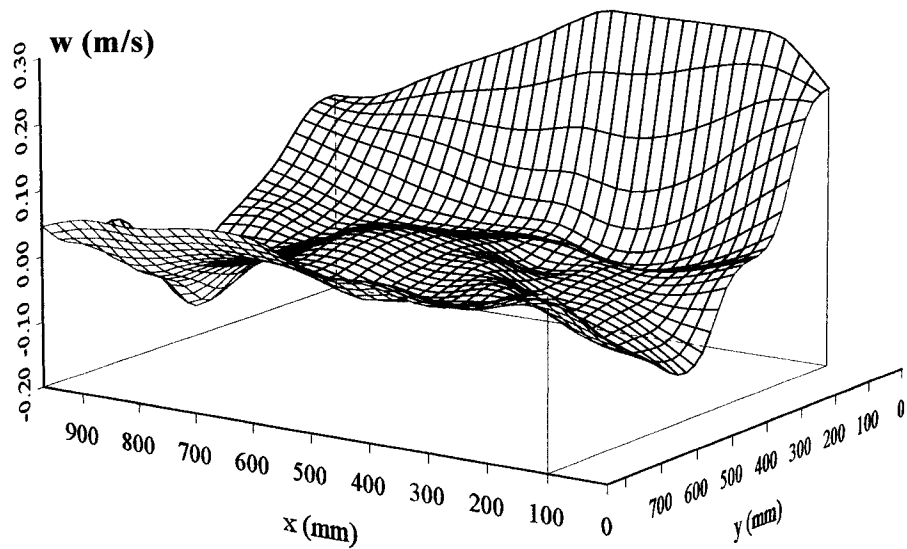
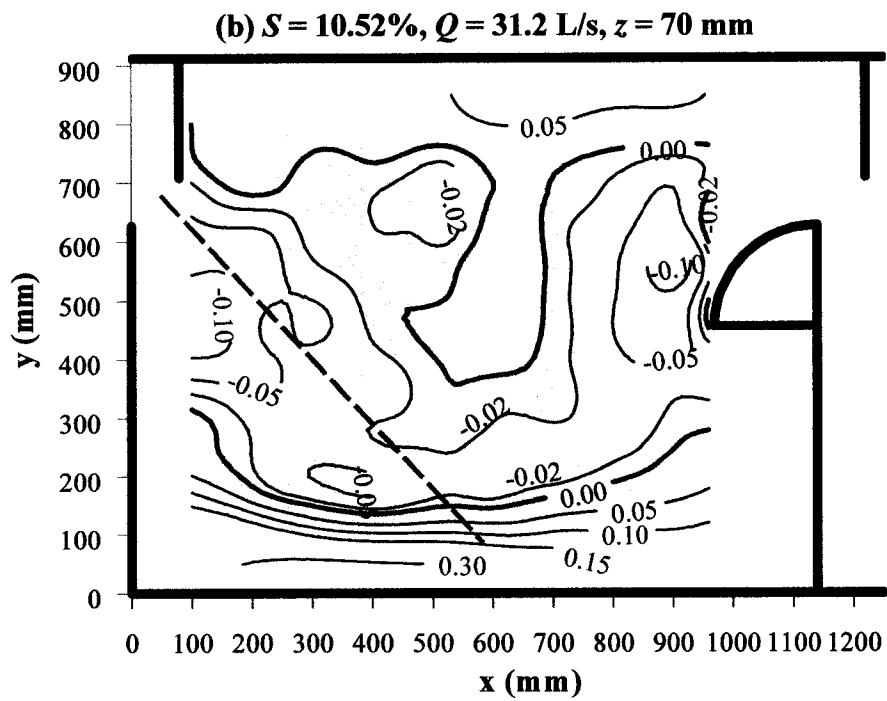


**Fig. 4.10(a-c) Vertical velocity distribution in the pool for $S = 10.52\%$:
 ---, maximum plane velocity filament: (b) $Q = 31.2$ L/s, $z = 70$ mm**

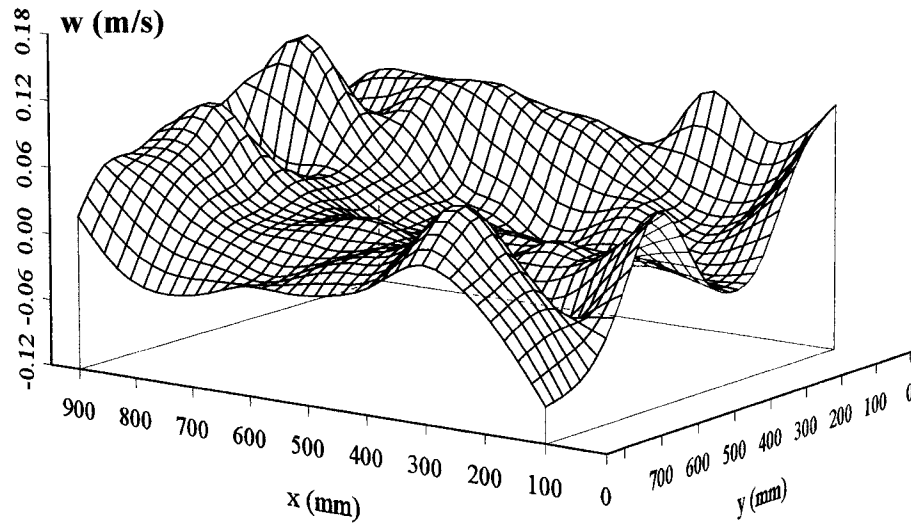
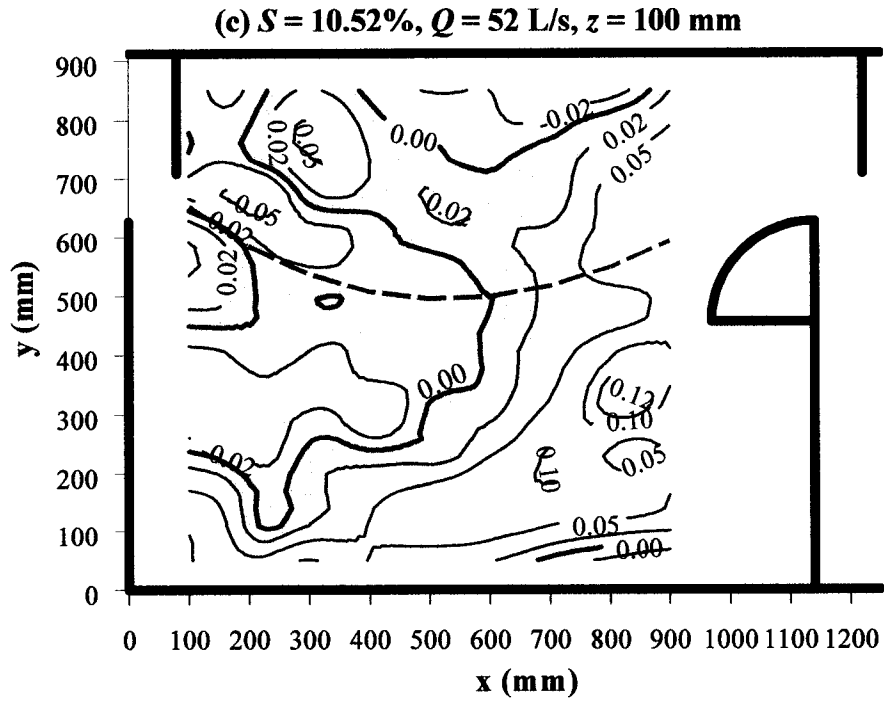


**Fig. 4.10(a-c) Vertical velocity distribution in the pool for $S = 10.52\%$:
 — — —, maximum plane velocity filament: (c) $Q = 52$ L/s, $z = 100$ mm**

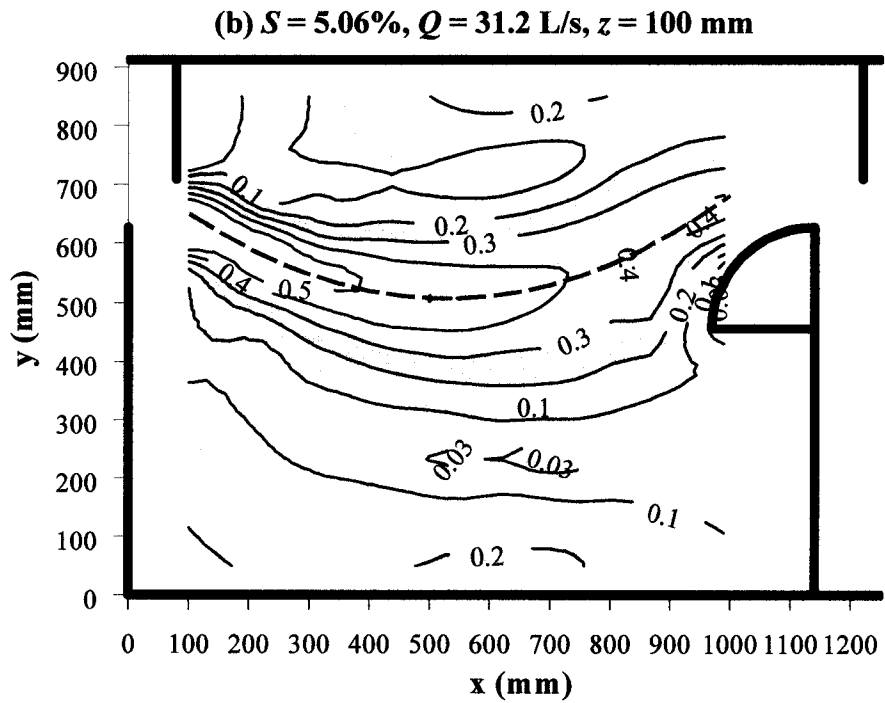
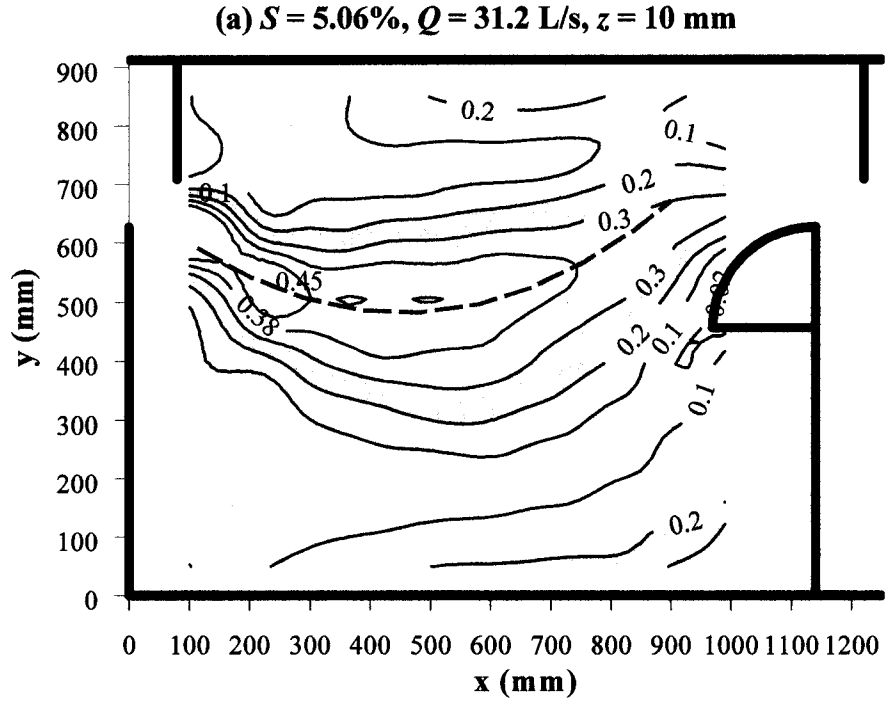


Fig. 4.11(a-f) Contours of normalized mean flow kinetic energy $K^{0.5}/V_{sm}$ for $S = 5.06\%$, — — —, maximum plane velocity filament: (a) $Q = 31.2$ L/s, $z = 10$ mm; (b) $Q = 31.2$ L/s, $z = 100$ mm

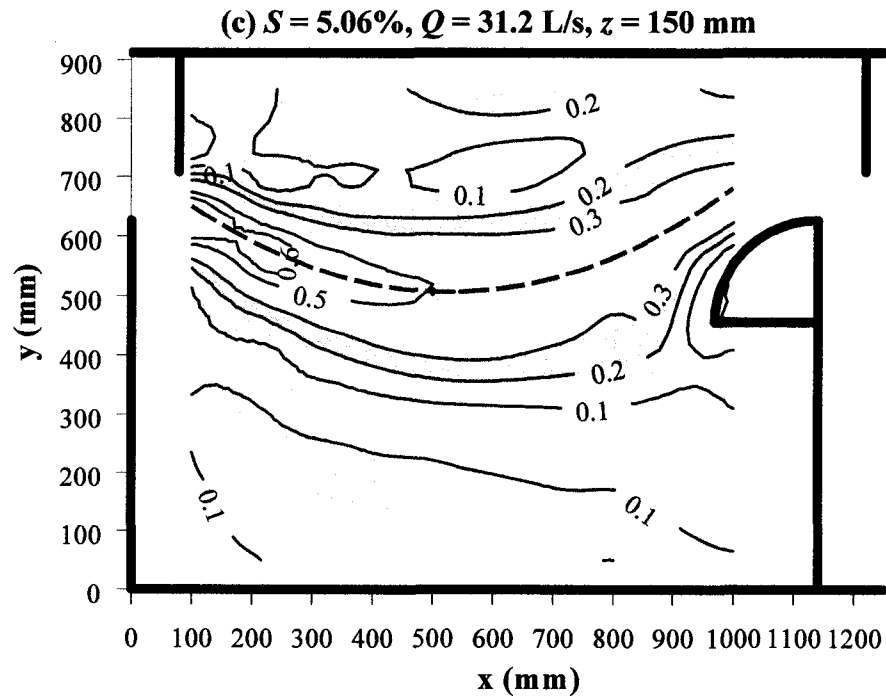


Fig. 4.11(a-f) Contours of normalized mean flow kinetic energy $K^{0.5}/V_{sm}$ for $S = 5.06\%$, — — —, maximum plane velocity filament: (c) $Q = 31.2$ L/s, $z = 150$ mm; (d) $Q = 52$ L/s, $z = 10$ mm

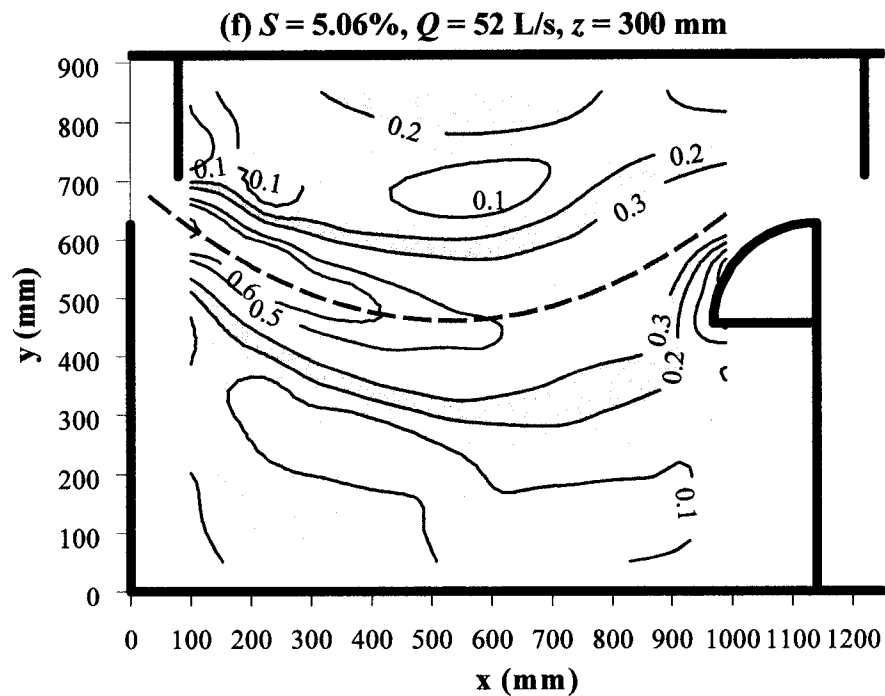
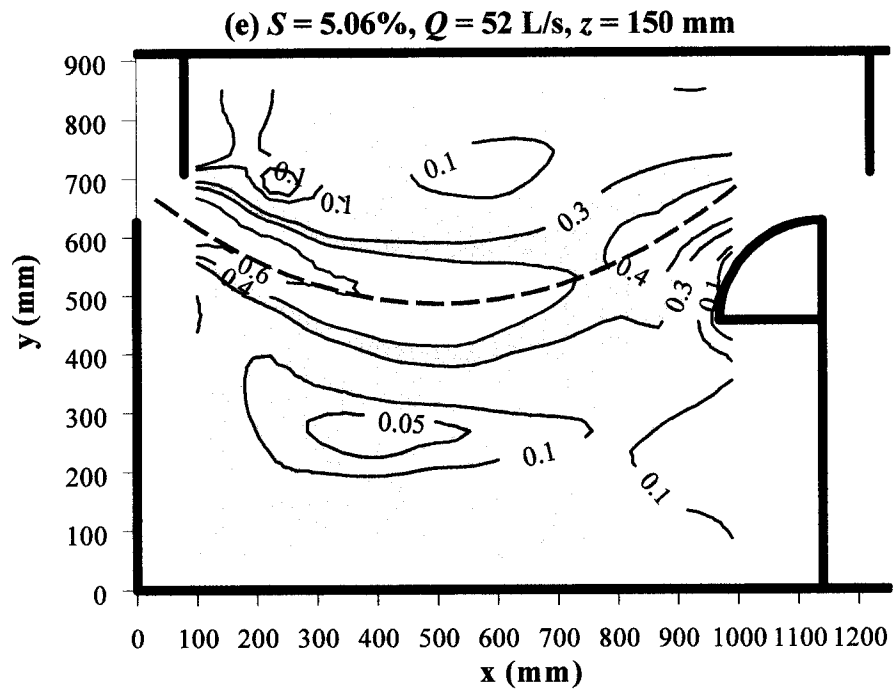


Fig. 4.11(a-f) Contours of normalized mean flow kinetic energy $K^{0.5}/V_{sm}$ for $S = 5.06\%$, — — —, maximum plane velocity filament: (e) $Q = 52 \text{ L/s}$, $z = 150 \text{ mm}$; (f) $Q = 52 \text{ L/s}$, $z = 300 \text{ mm}$

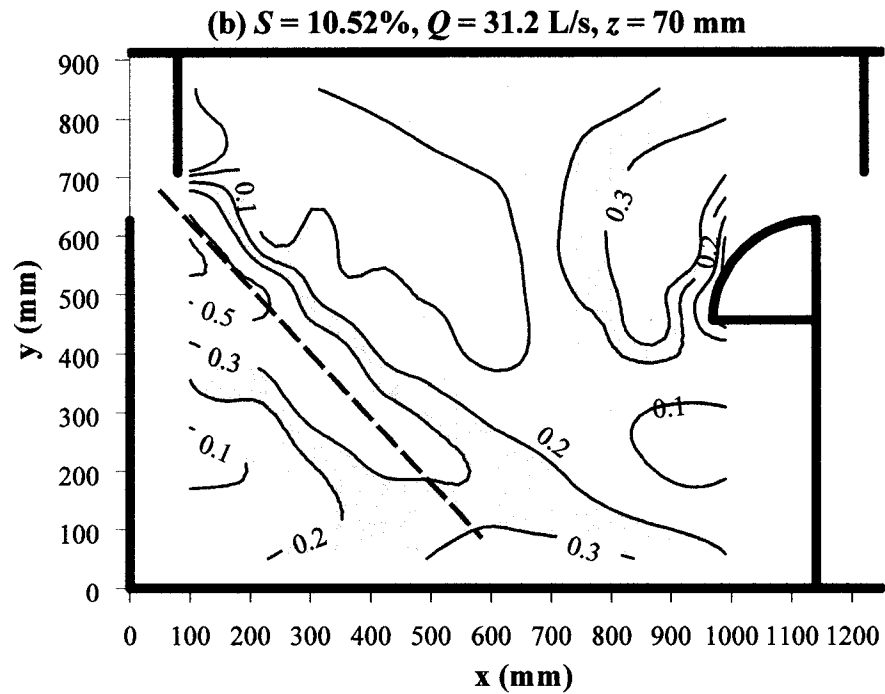
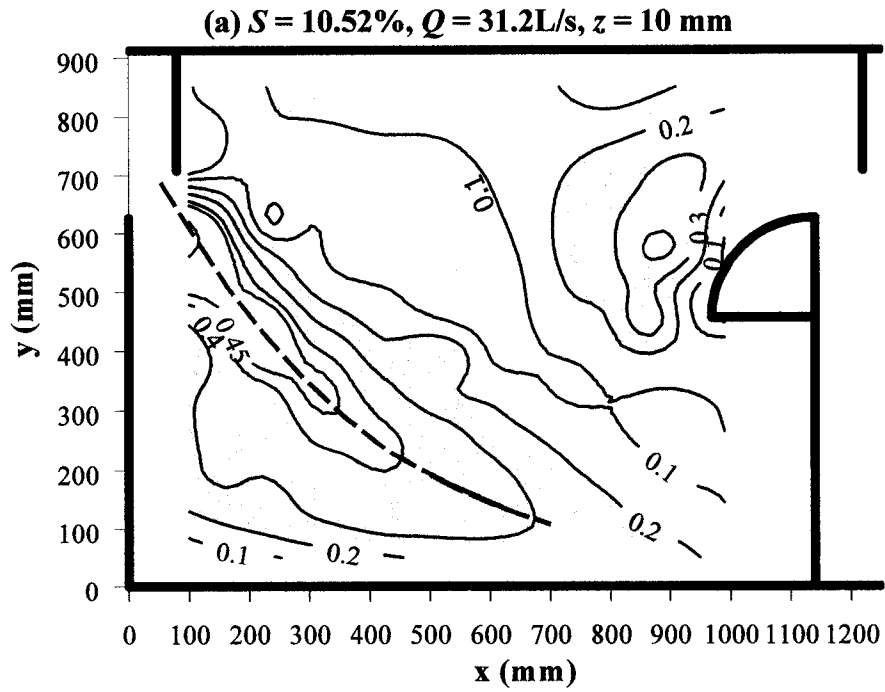


Fig. 4.12(a-c) Contours of normalized mean flow kinetic energy $K^{0.5}/V_{sm}$ for $S = 10.52\%$, — — —, maximum plane velocity filament: (a) $Q = 31.2 \text{ L/s}$, $z = 10 \text{ mm}$; (b) $Q = 31.2 \text{ L/s}$, $z = 70 \text{ mm}$

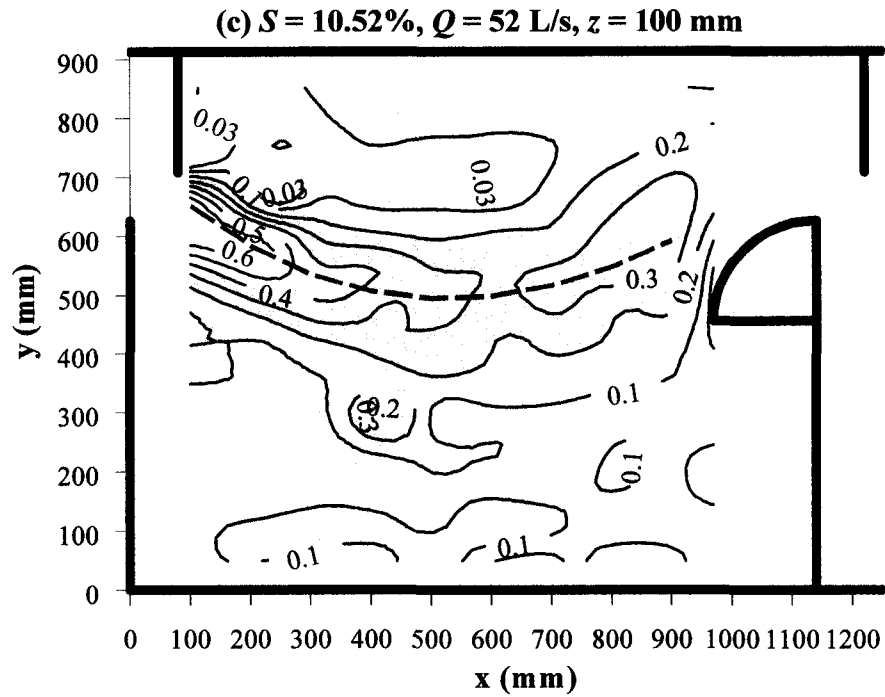


Fig. 4.12(a-c) Contours of normalized mean flow kinetic energy $K^{0.5}/V_{sm}$ for $S = 10.52\%$, — — —, maximum plane velocity filament: (c) $Q = 52$ L/s, $z = 100$ mm

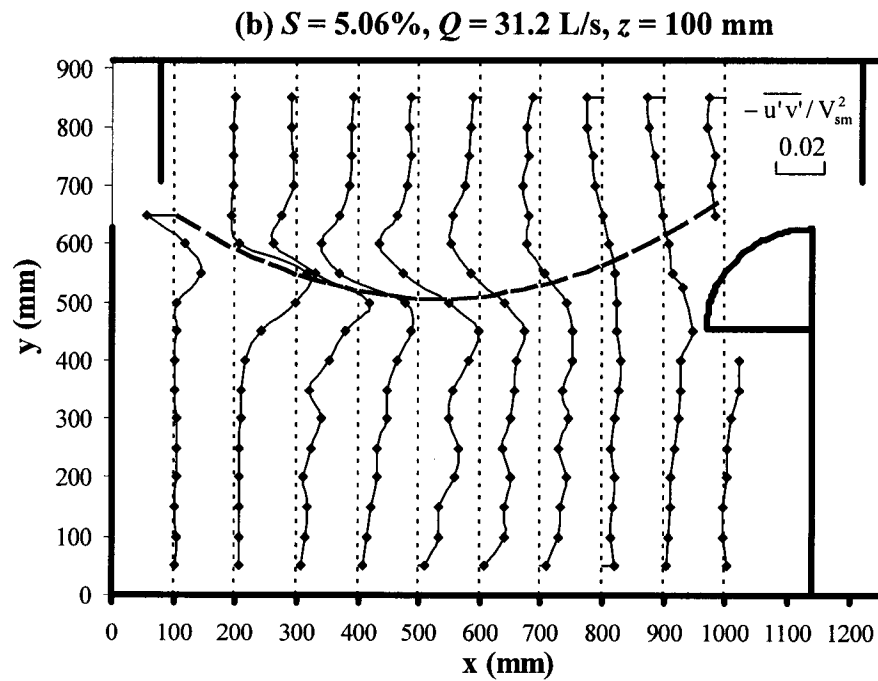
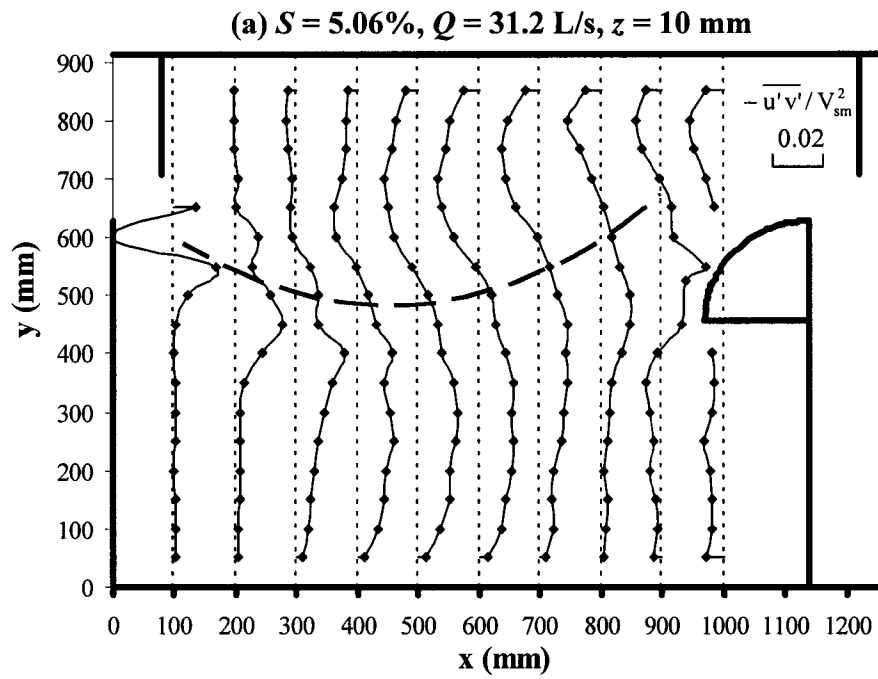


Fig. 4.13(a-f) Distribution of normalized Reynolds shear stress for $S = 5.06\%$, — — —, maximum plane velocity filament: (a) $Q = 31.2$ L/s, $z = 10$ mm; (b) $Q = 31.2$ L/s, $z = 100$ mm

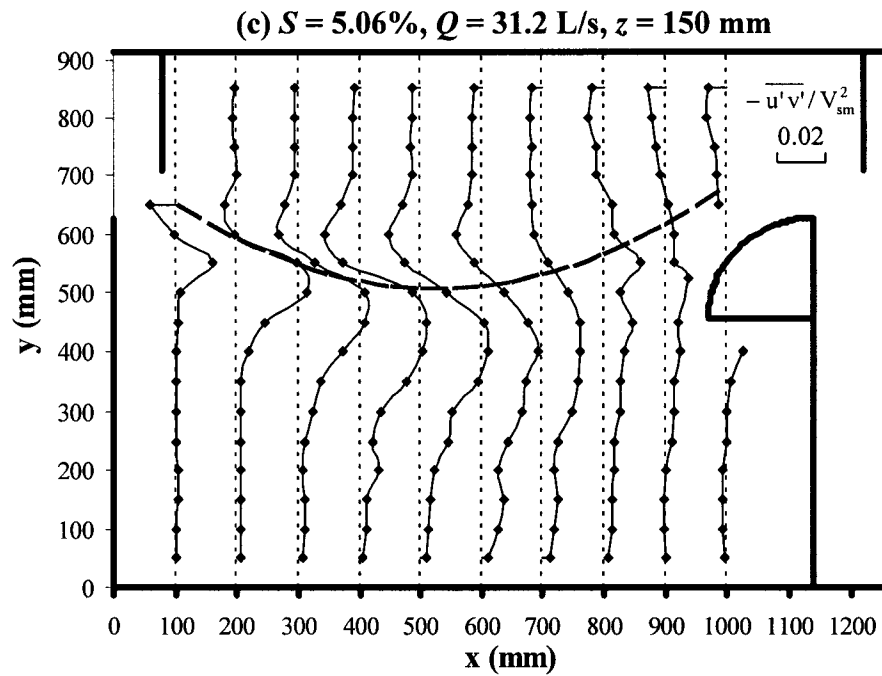


Fig. 4.13(a-f) Distribution of normalized Reynolds shear stress for $S = 5.06\%$, — — —, maximum plane velocity filament: (c) $Q = 31.2$ L/s, $z = 150$ mm; (d) $Q = 52$ L/s, $z = 10$ mm

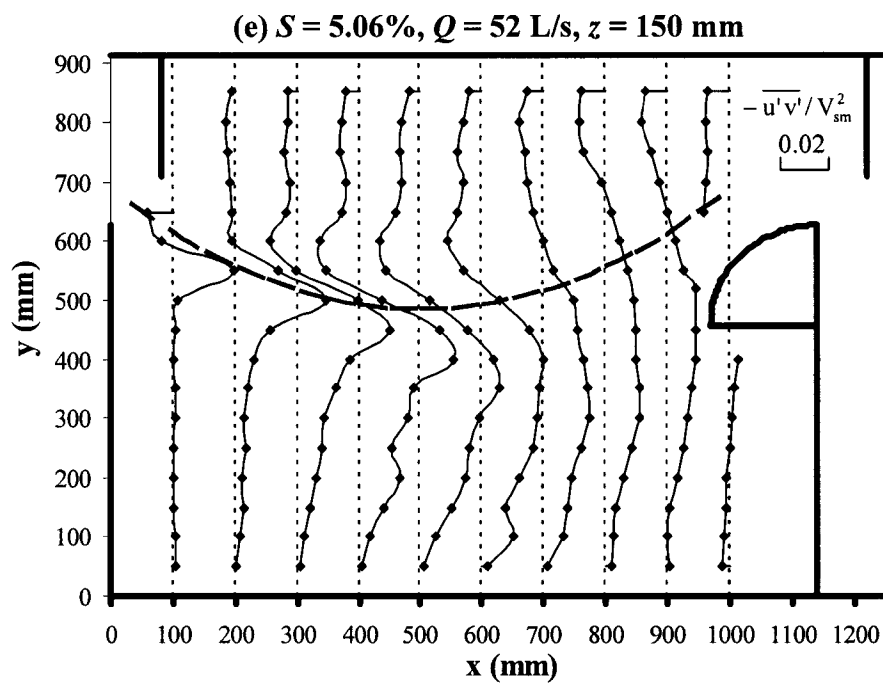


Fig. 4.13(a-f) Distribution of normalized Reynolds shear stress for $S = 5.06\%$, — — —, maximum plane velocity filament: (e) $Q = 52$ L/s, $z = 150$ mm; (f) $Q = 52$ L/s, $z = 300$ mm

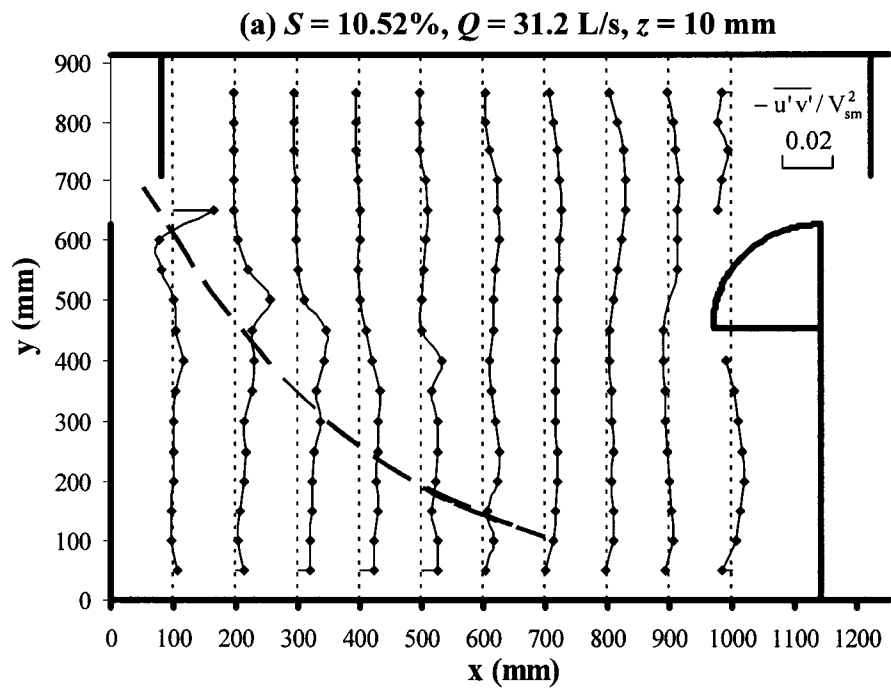


Fig. 4.14(a-c) Distribution of normalized Reynolds shear stress for $S = 10.52\%$, — — —, maximum plane velocity filament: (a) $Q = 31.2$ L/s, $z = 10$ mm; (b) $Q = 31.2$ L/s, $z = 70$ mm

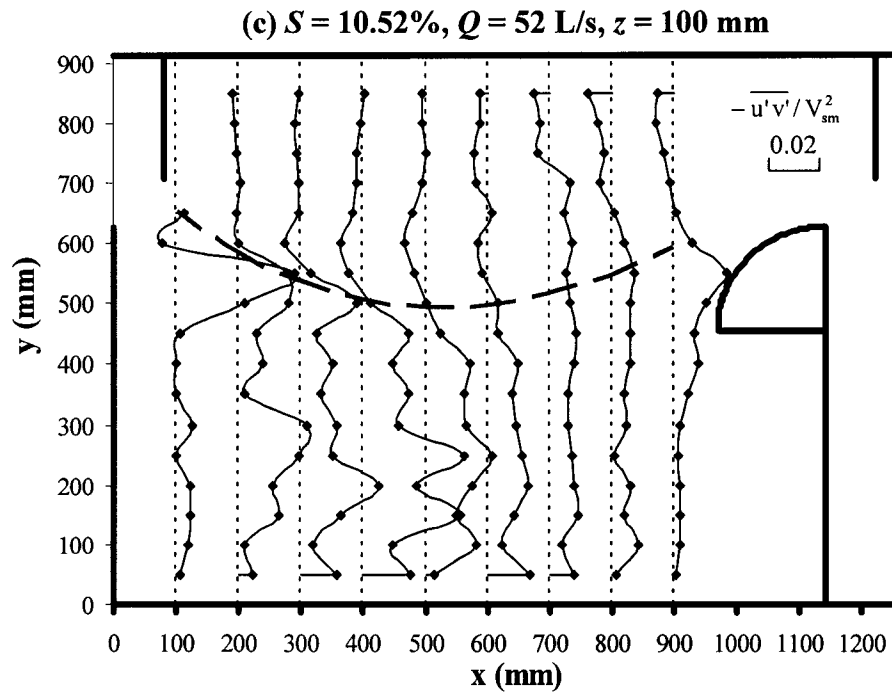


Fig. 4.14(a-c) Distribution of normalized Reynolds shear stress for $S = 10.52\%$, — — —, maximum plane velocity filament: (c) $Q = 52$ L/s, $z = 100$ mm

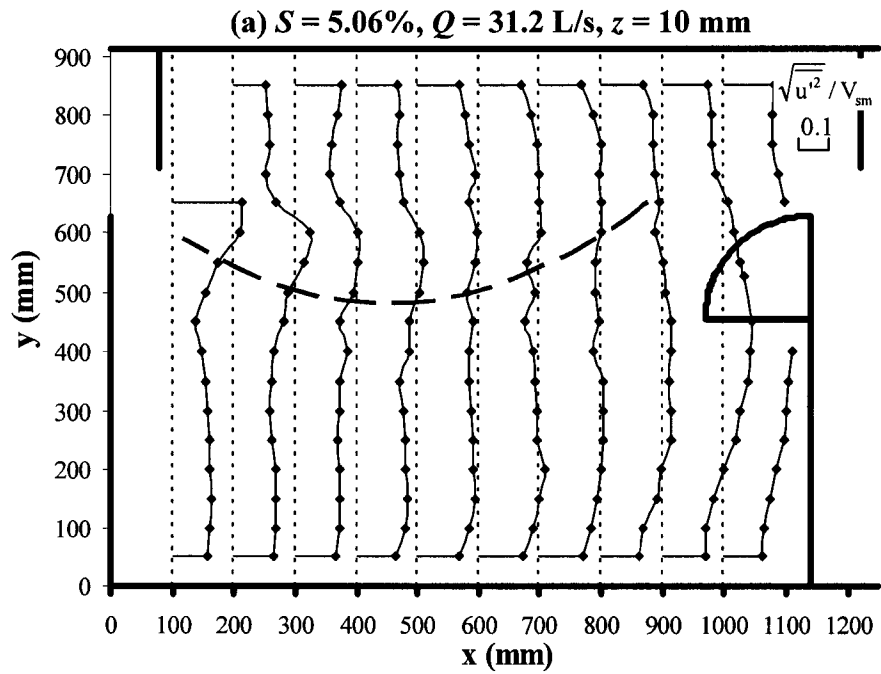


Fig. 4.15(a-f) Distribution of normalized longitudinal turbulence intensity for $S = 5.06\%$, — — —, maximum plane velocity filament: (a) $Q = 31.2$ L/s, $z = 10$ mm; (b) $Q = 31.2$ L/s, $z = 100$ mm

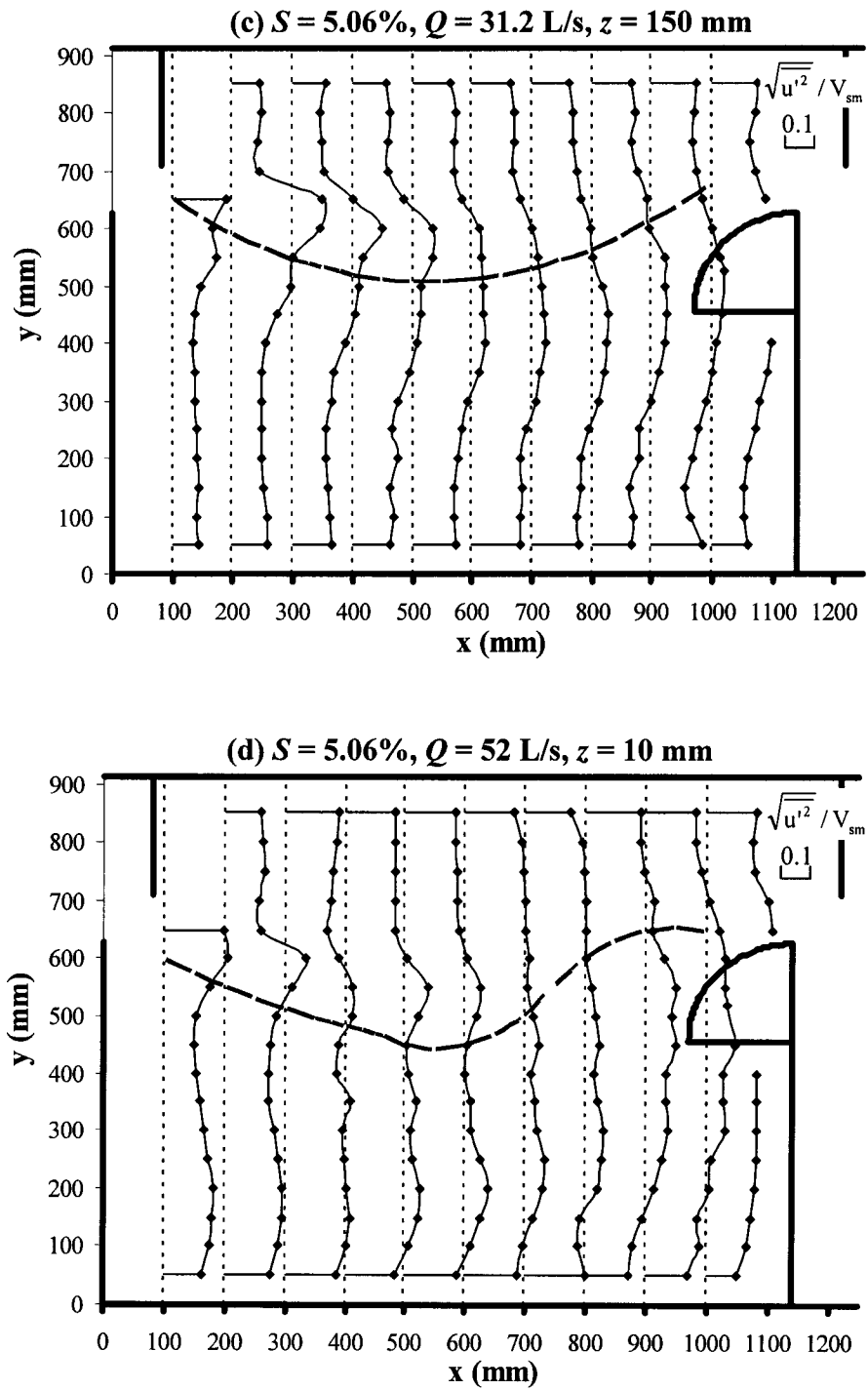


Fig. 4.15(a-f) Distribution of normalized longitudinal turbulence intensity for $S = 5.06\%$, — — —, maximum plane velocity filament: (c) $Q = 31.2$ L/s, $z = 150$ mm; (d) $Q = 52$ L/s, $z = 10$ mm

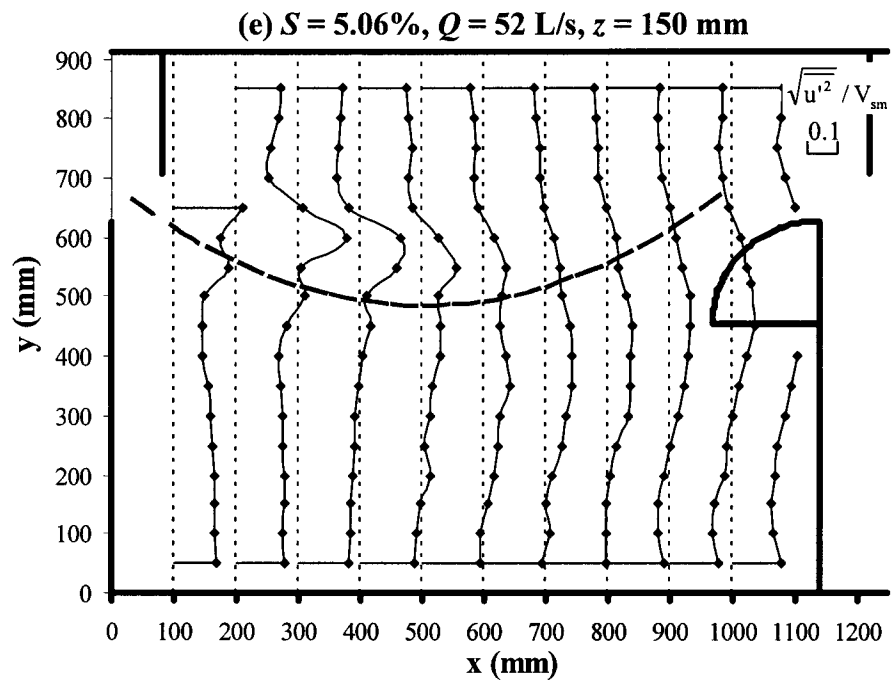


Fig. 4.15(a-f) Distribution of normalized longitudinal turbulence intensity for $S = 5.06\%$, — — —, maximum plane velocity filament: (e) $Q = 52$ L/s, $z = 150$ mm; (f) $Q = 52$ L/s, $z = 300$ mm

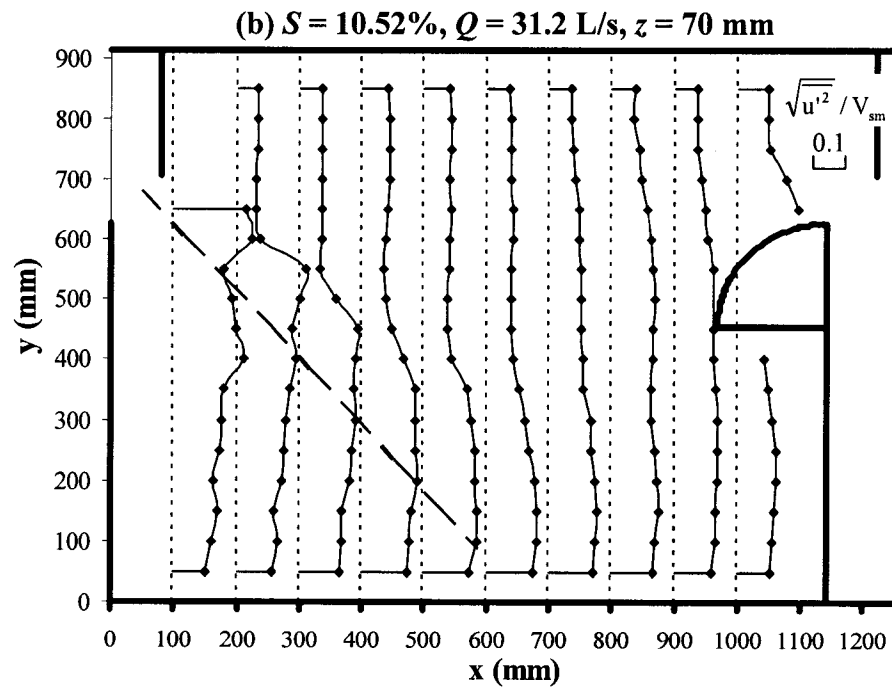
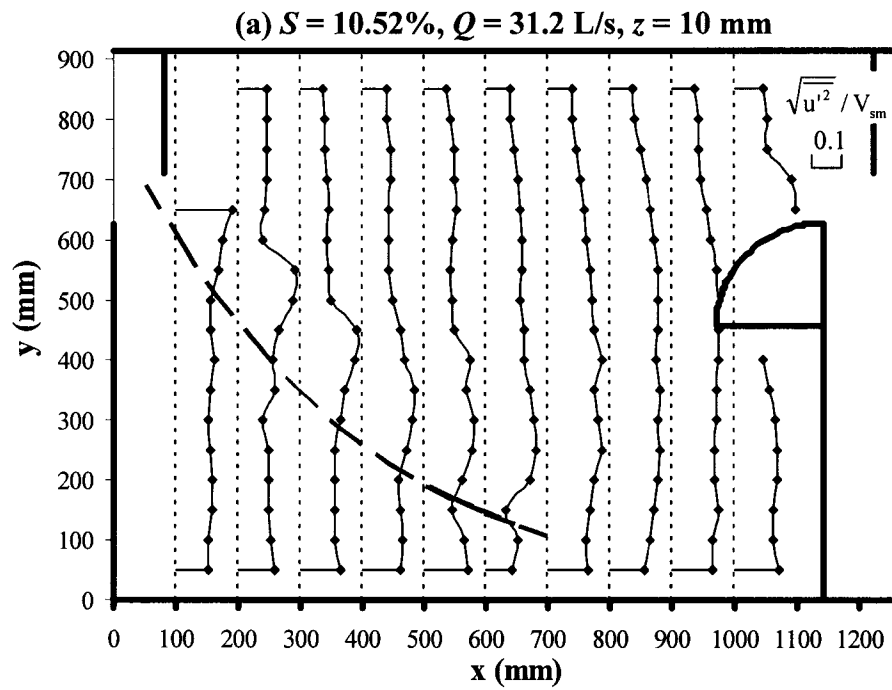


Fig. 4.16(a-c) Distribution of normalized longitudinal turbulence intensity for $S = 10.52\%$, — — —, maximum plane velocity filament: (a) $Q = 31.2$ L/s, $z = 10$ mm; (b) $Q = 31.2$ L/s, $z = 70$ mm

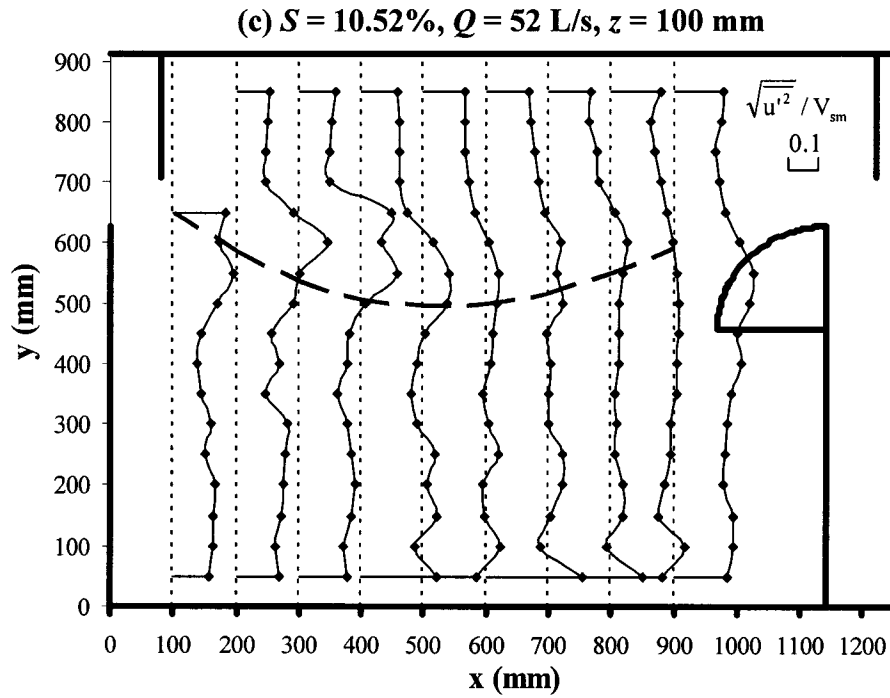


Fig. 4.16(a-c) Distribution of normalized longitudinal turbulence intensity for $S = 10.52\%$, — — —, maximum plane velocity filament: (c) $Q = 52$ L/s, $z = 100$ mm

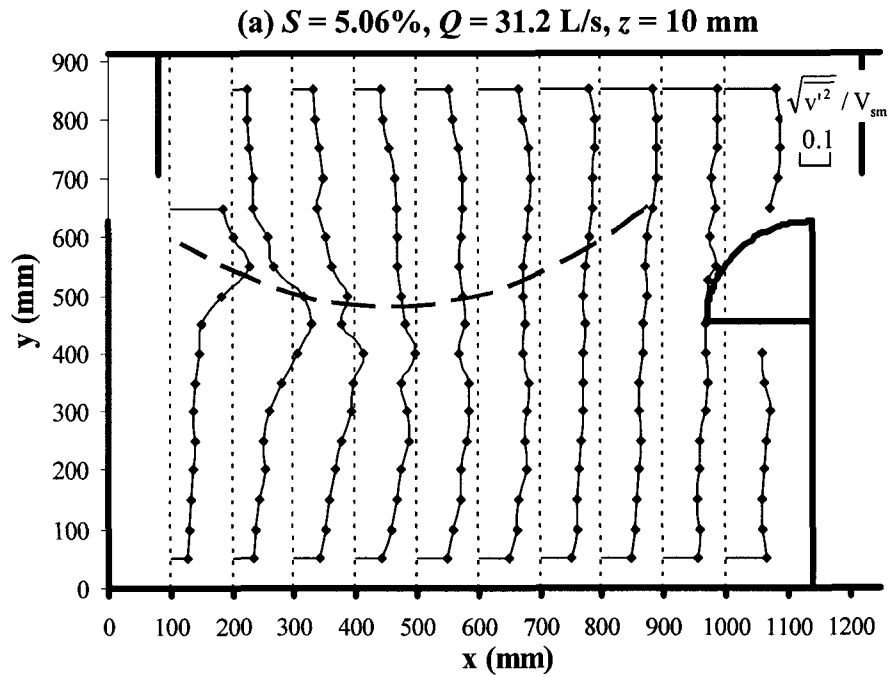


Fig. 4.17(a-f) Distribution of normalized transverse turbulence intensity for $S = 5.06\%$, — — —, maximum plane velocity filament: (a) $Q = 31.2$ L/s, $z = 10$ mm; (b) $Q = 31.2$ L/s, $z = 100$ mm

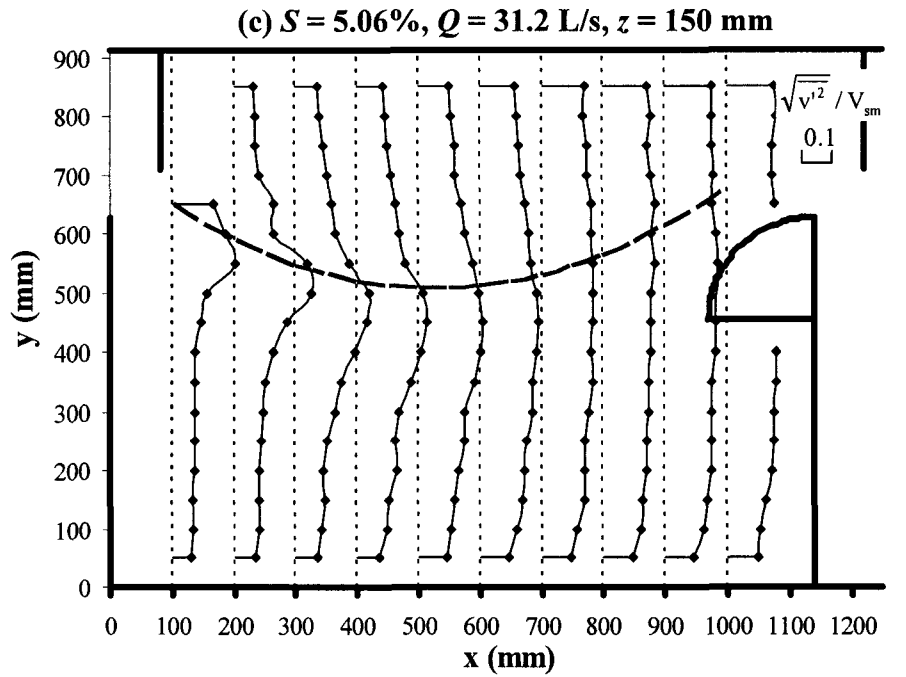


Fig. 4.17(a-f) Distribution of normalized transverse turbulence intensity for $S = 5.06\%$, — — —, maximum plane velocity filament: (c) $Q = 31.2$ L/s, $z = 150$ mm; (d) $Q = 52$ L/s, $z = 10$ mm

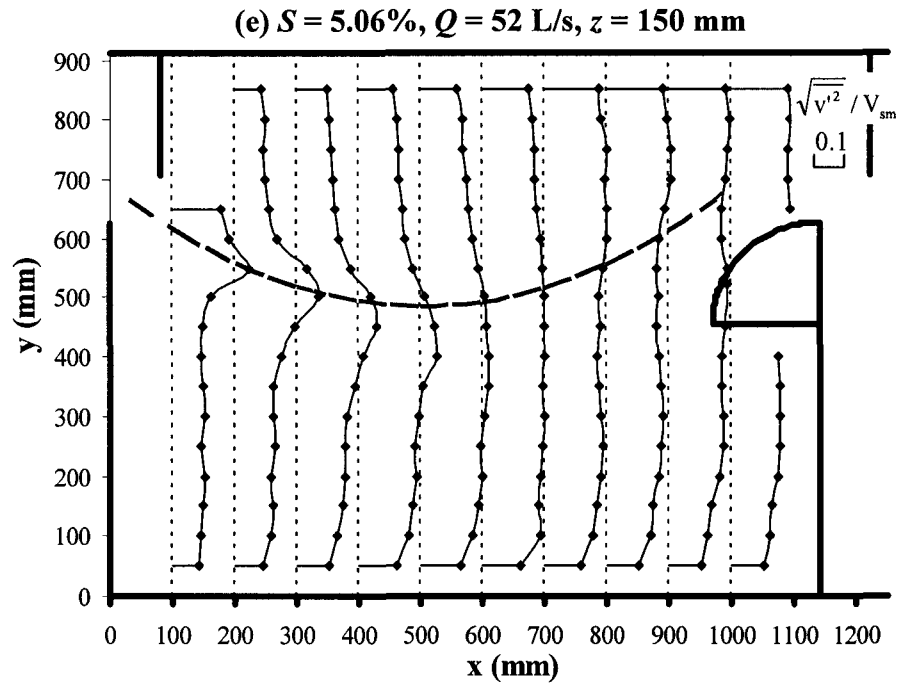


Fig. 4.17(a-f) Distribution of normalized transverse turbulence intensity for $S = 5.06\%$, — — —, maximum plane velocity filament: (e) $Q = 52$ L/s, $z = 150$ mm; (f) $Q = 52$ L/s, $z = 300$ mm

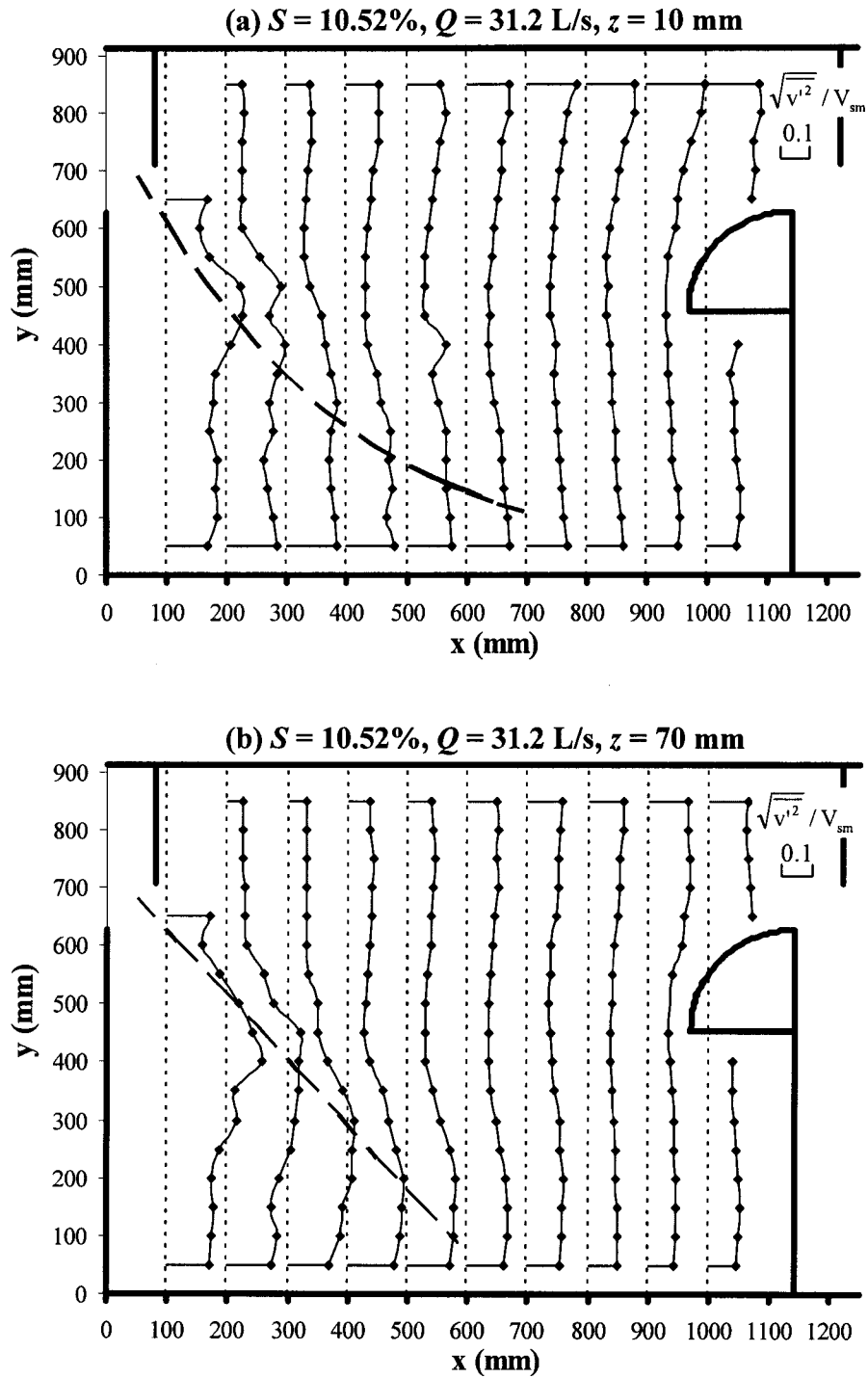


Fig. 4.18(a-c) Distribution of normalized transverse turbulence intensity for $S = 10.52\%$, — — —, maximum plane velocity filament: (a) $Q = 31.2$ L/s, $z = 10$ mm; (b) $Q = 31.2$ L/s, $z = 70$ mm

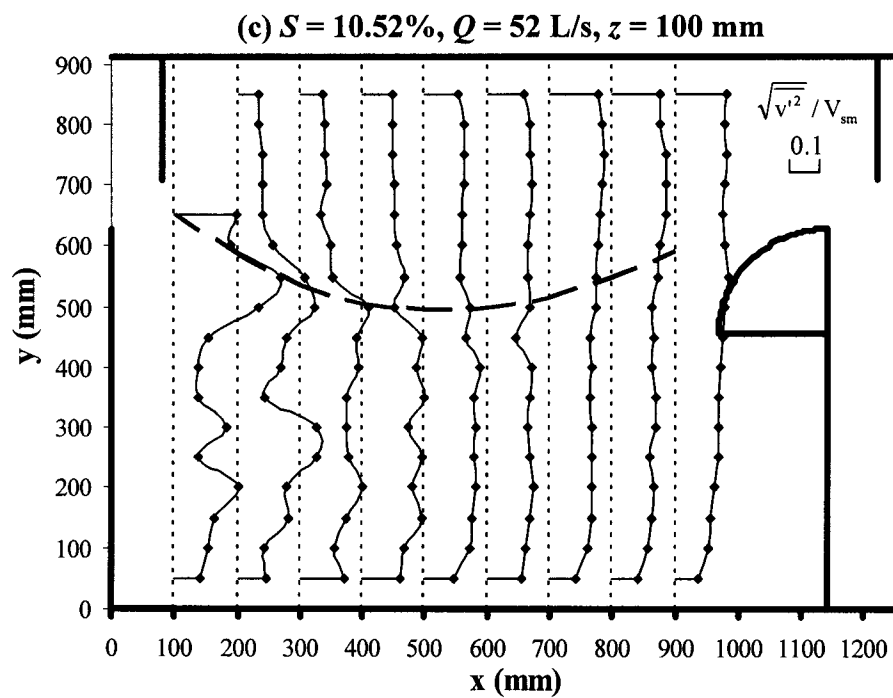


Fig. 4.18(a-c) Distribution of normalized transverse turbulence intensity for $S = 10.52\%$: — — —, maximum plane velocity filament: (c) $Q = 52$ L/s, $z = 100$ mm

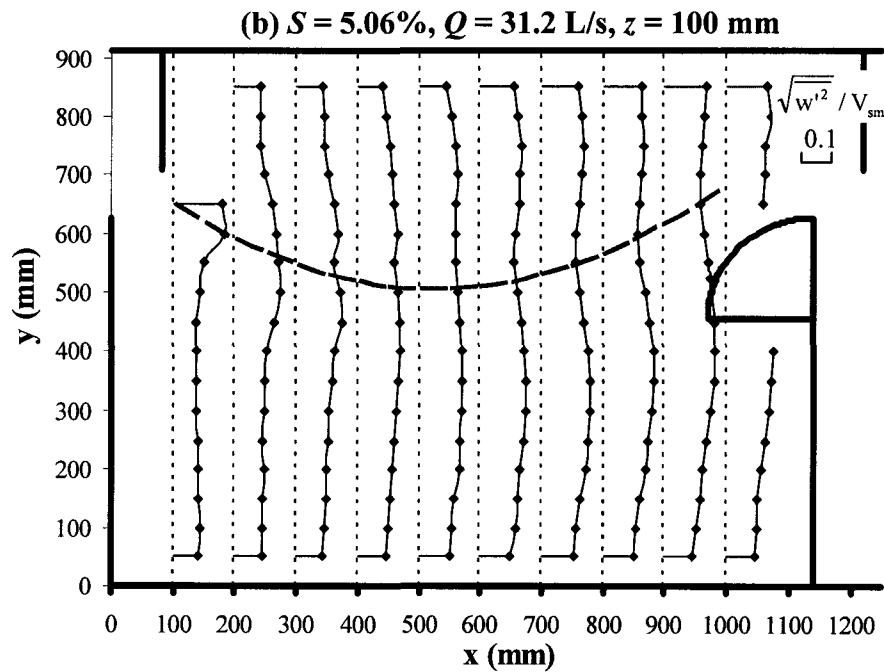
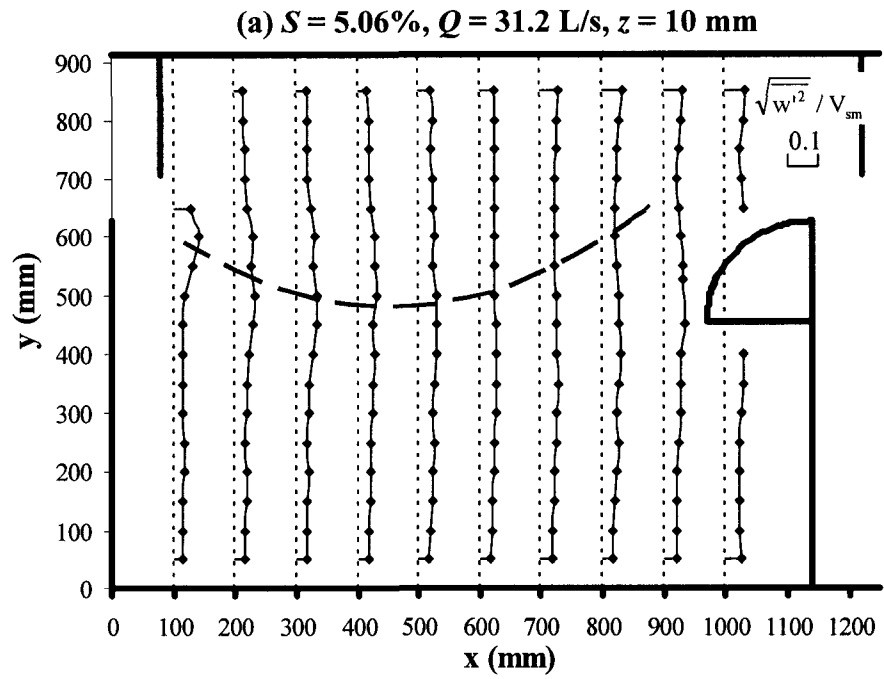


Fig. 4.19(a-f) Distribution of normalized vertical turbulence intensity for $S = 5.06\%$, — — —, maximum plane velocity filament: (a) $Q = 31.2$ L/s, $z = 10$ mm; (b) $Q = 31.2$ L/s, $z = 100$ mm

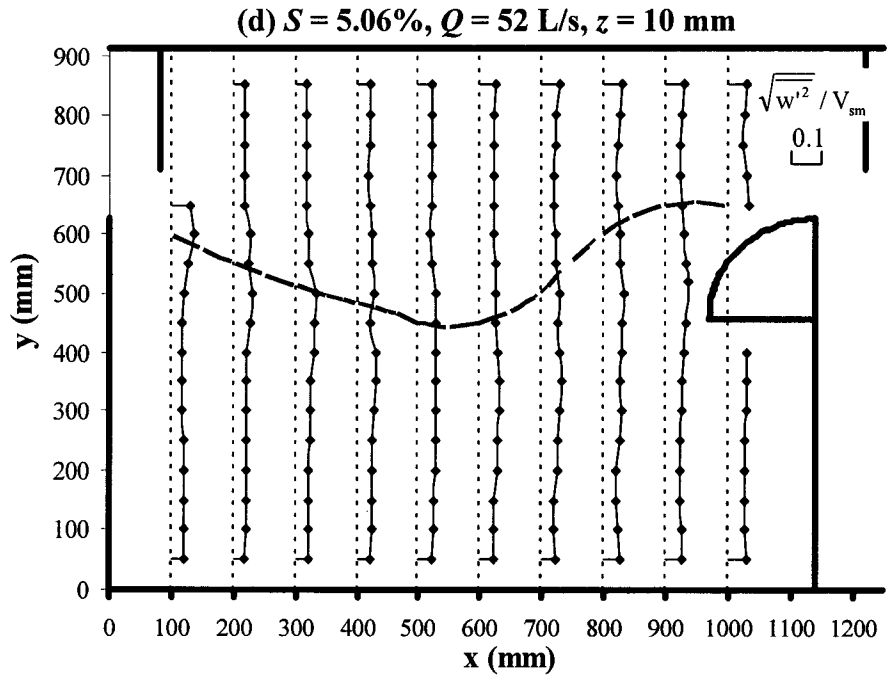
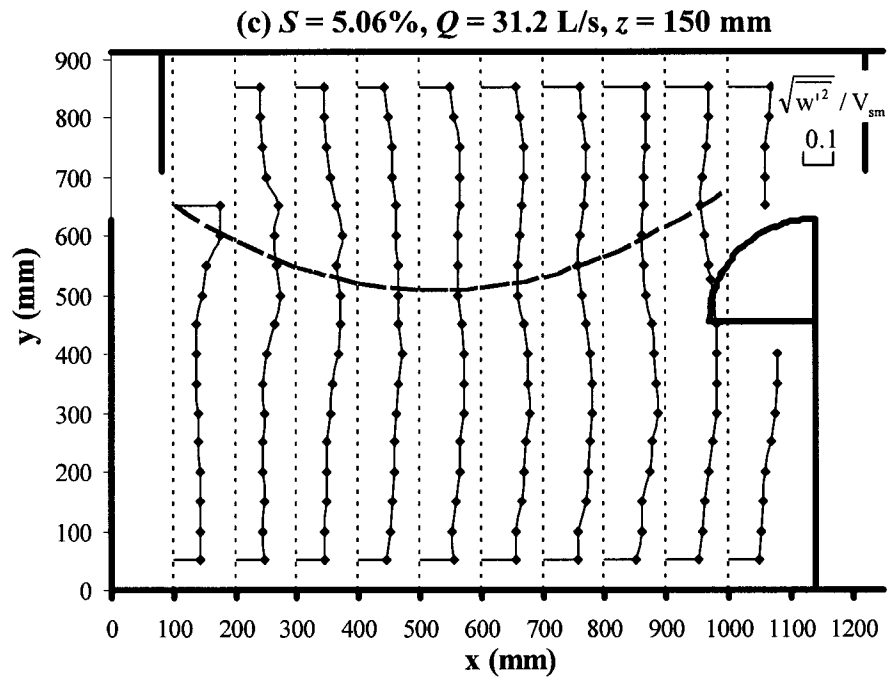


Fig. 4.19(a-f) Distribution of normalized vertical turbulence intensity for $S = 5.06\%$, — — —, maximum plane velocity filament: (c) $Q = 31.2$ L/s, $z = 150$ mm; (d) $Q = 52$ L/s, $z = 10$ mm

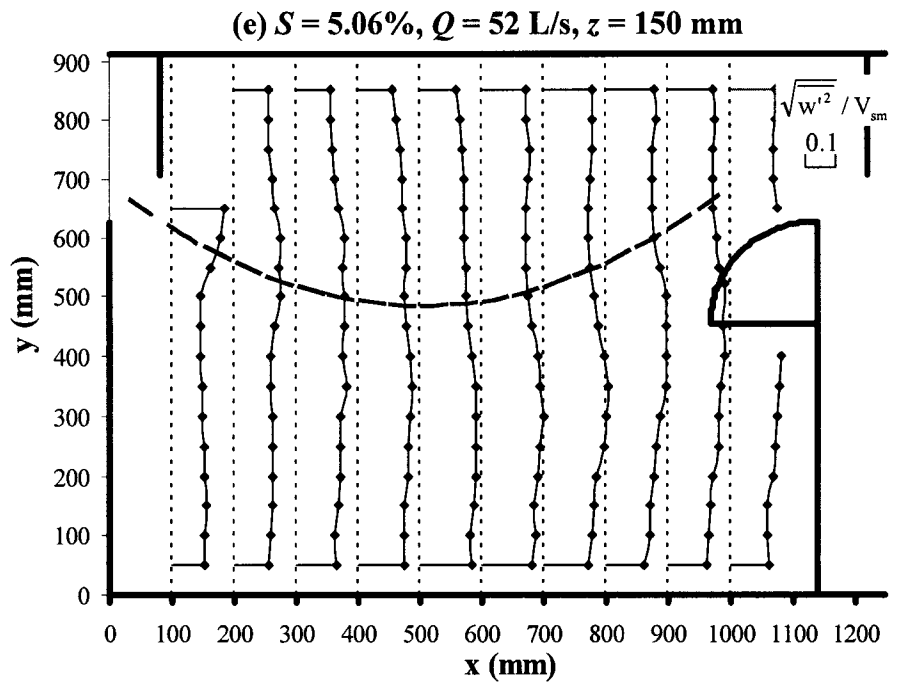


Fig. 4.19(a-f) Distribution of normalized vertical turbulence intensity for $S = 5.06\%$, — — —, maximum plane velocity filament: (e) $Q = 52$ L/s, $z = 150$ mm; (f) $Q = 52$ L/s, $z = 300$ mm

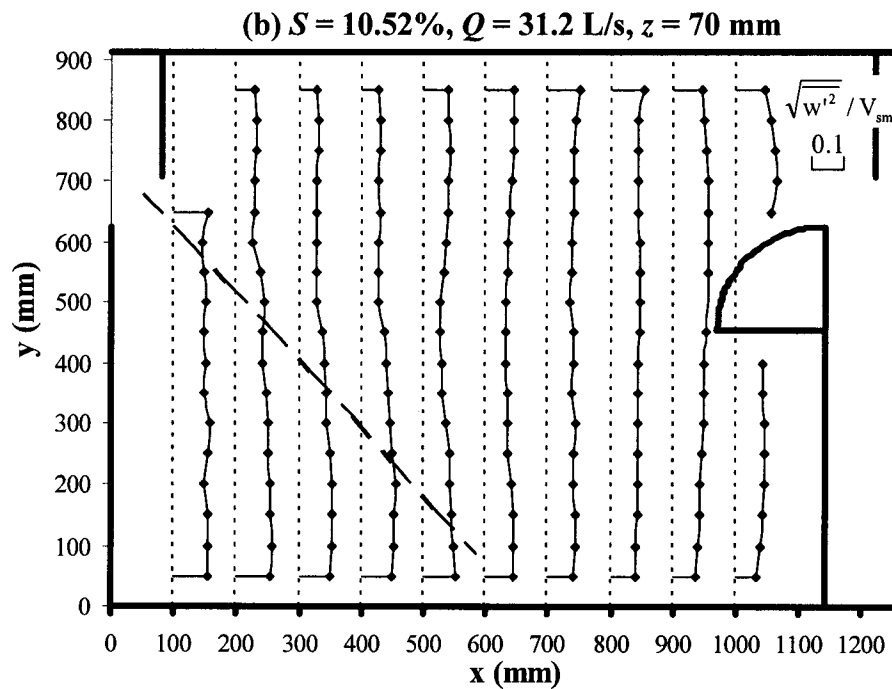
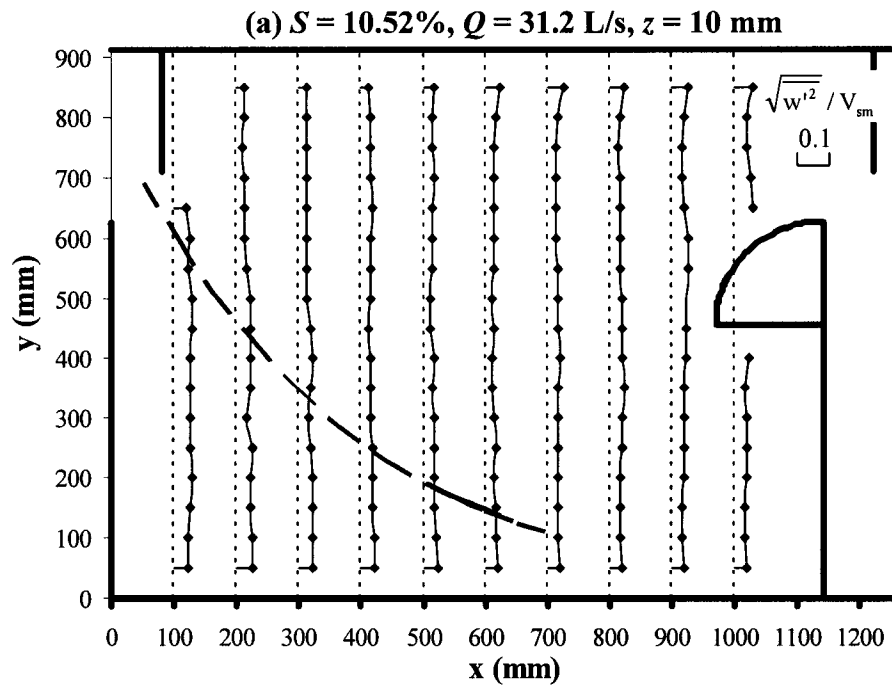


Fig. 4.20(a-c) Distribution of normalized vertical turbulence intensity for $S = 10.52\%$, — — —, maximum plane velocity filament: (a) $Q = 31.2$ L/s, $z = 10$ mm; (b) $Q = 31.2$ L/s, $z = 70$ mm

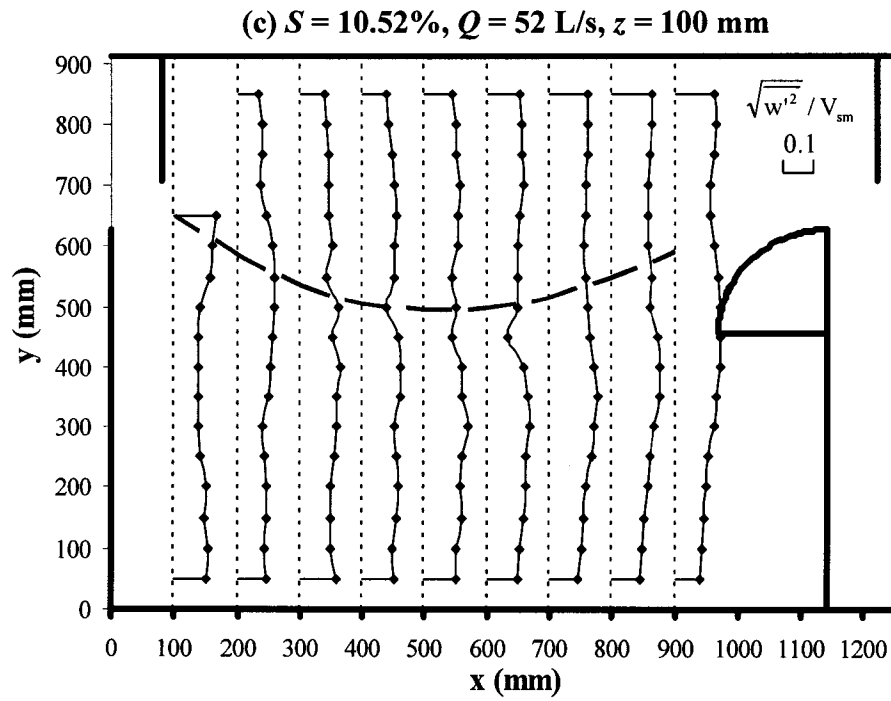


Fig. 4.20(a-c) Distribution of normalized vertical turbulence intensity for $S = 10.52\%$: — — —, maximum plane velocity filament: (c) $Q = 52$ L/s, $z = 100$ mm

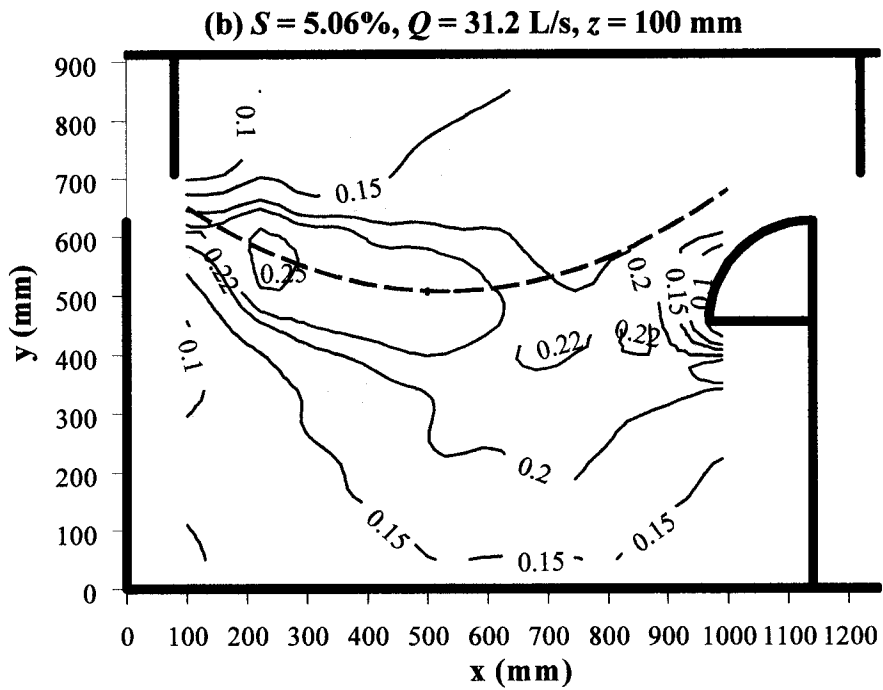
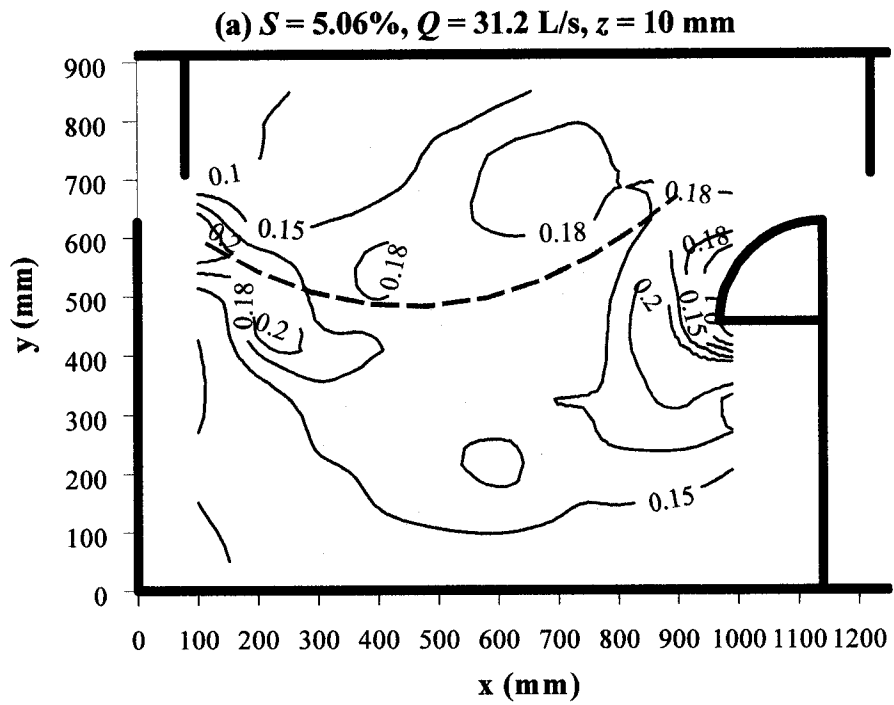


Fig. 4.21(a-f) Contours of normalized turbulence kinetic energy $K^{r0.5} / V_{sm}$ for $S = 5.06\%$, — — —, maximum plane velocity filament: (a) $Q = 31.2$ L/s, $z = 10$ mm; (b) $Q = 31.2$ L/s, $z = 100$ mm

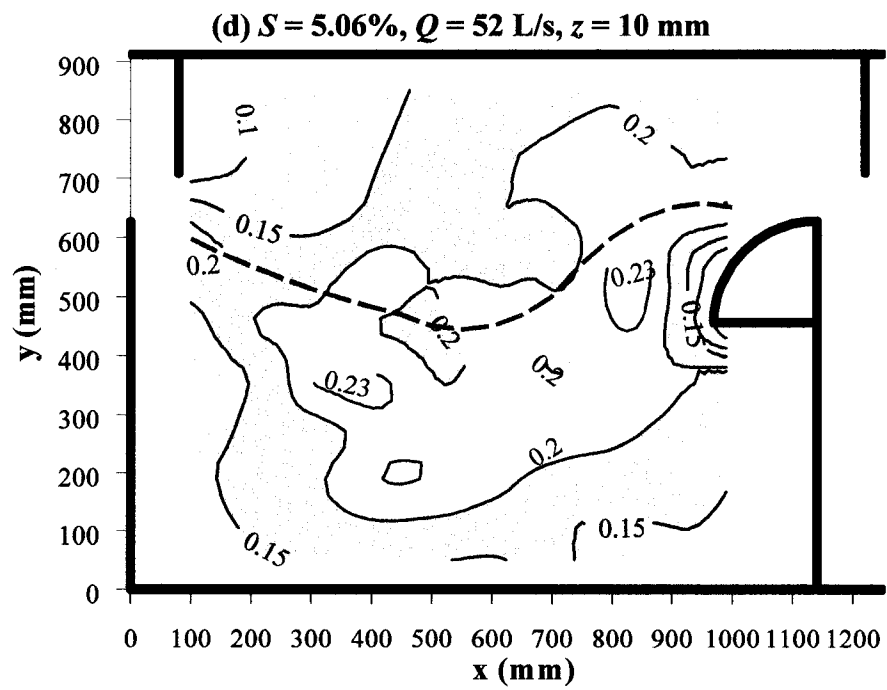
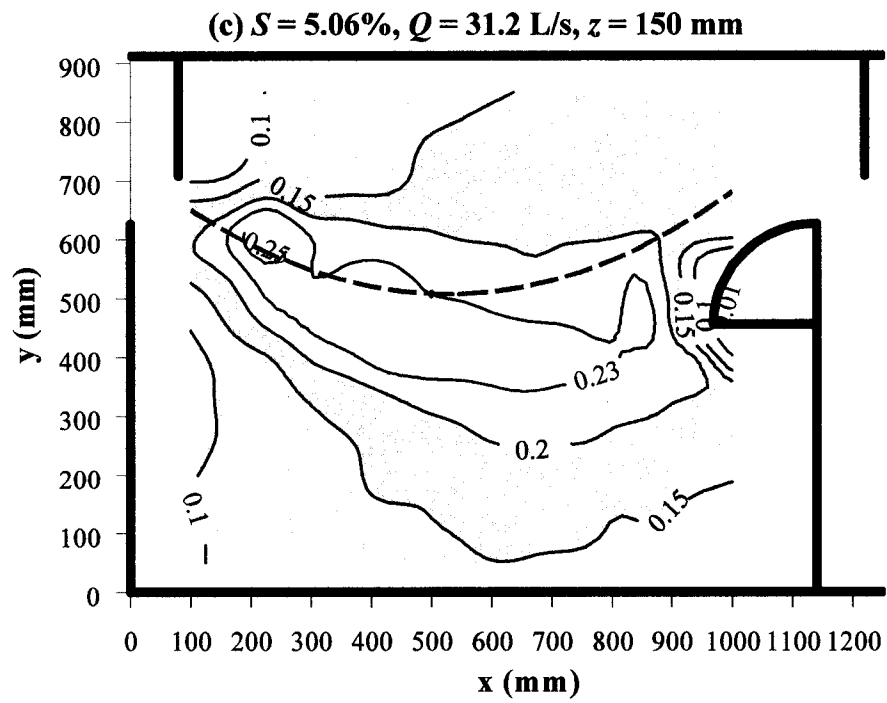


Fig. 4.21(a-f) Contours of normalized turbulence kinetic energy $K^{r0.5} / V_{sm}$ for $S = 5.06\%$, — — —, maximum plane velocity filament: (c) $Q = 31.2$ L/s, $z = 150$ mm; (d) $Q = 52$ L/s, $z = 10$ mm

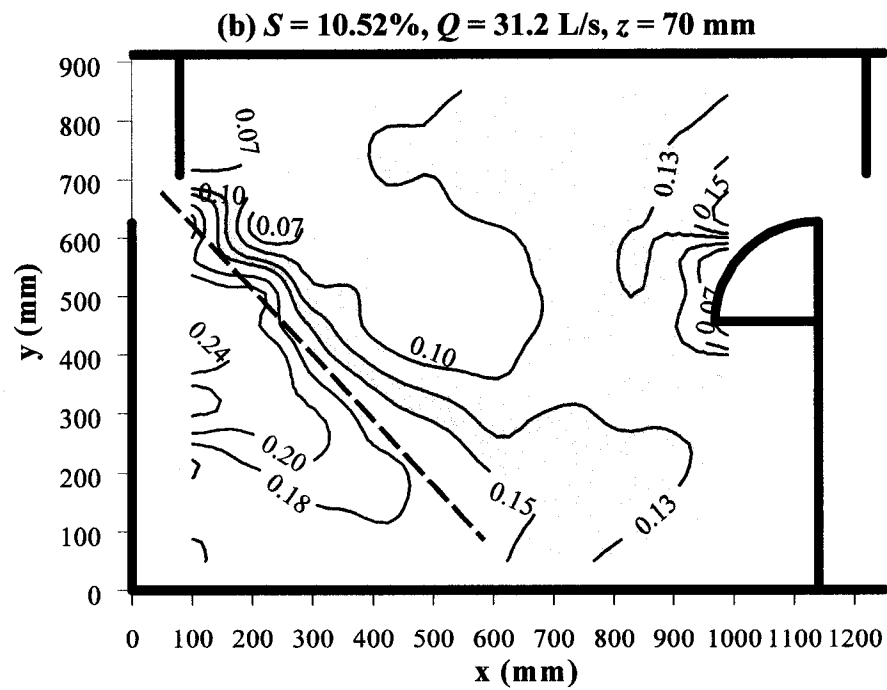
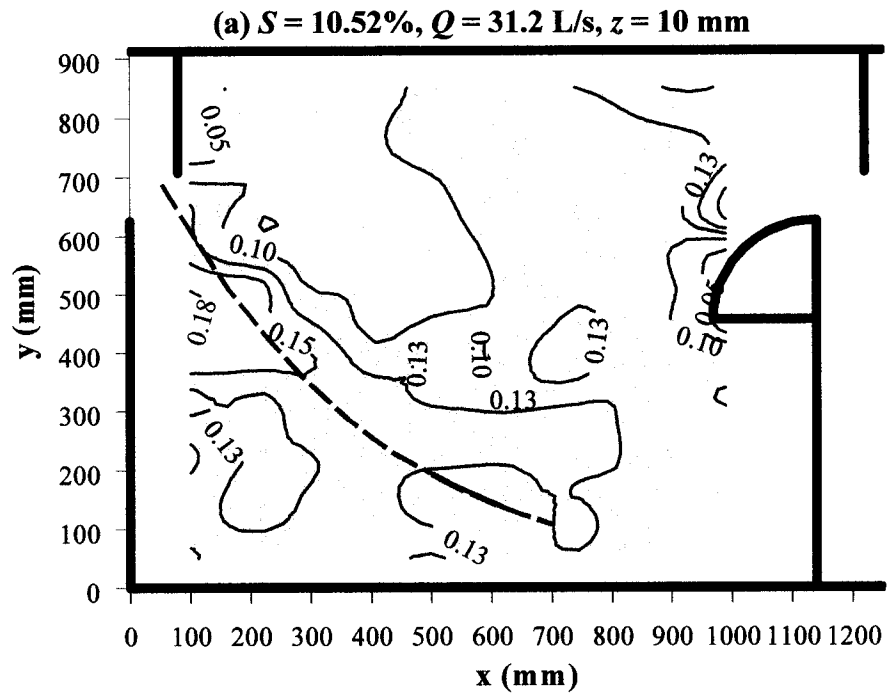


Fig. 4.22(a-c) Contours of normalized turbulence kinetic energy $K^{r0.5} / V_{sm}$ for $S = 10.52\%$, — — —, maximum plane velocity filament: (a) $Q = 31.2$ L/s, $z = 10$ mm; (b) $Q = 31.2$ L/s, $z = 70$ mm

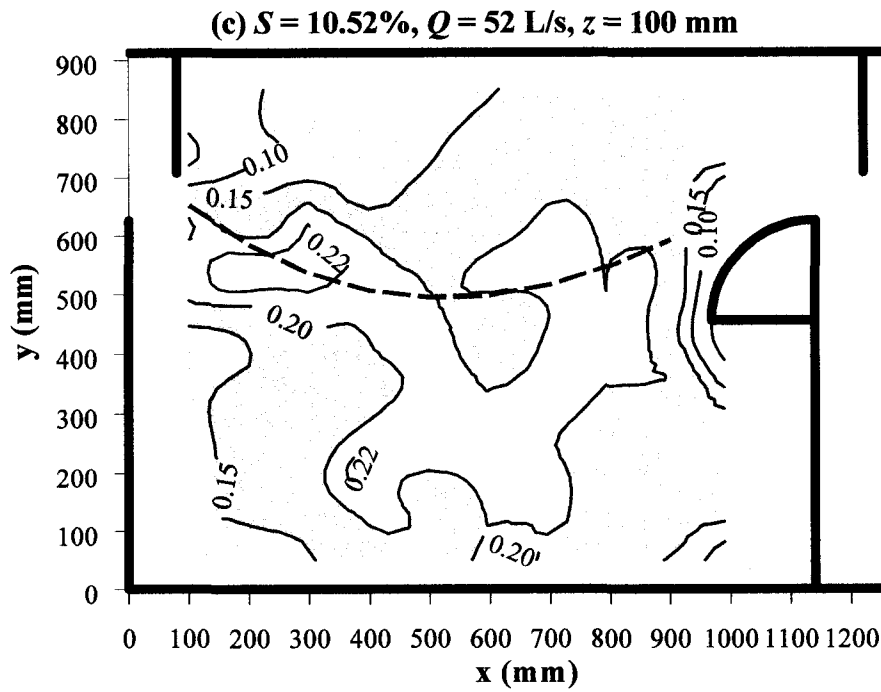


Fig. 4.22(a-c) Contours of normalized turbulence kinetic energy $K^{r0.5} / V_{sm}$ for $S = 10.52\%$, — — —, maximum plane velocity filament: (c) $Q = 52$ L/s, $z = 100$ mm

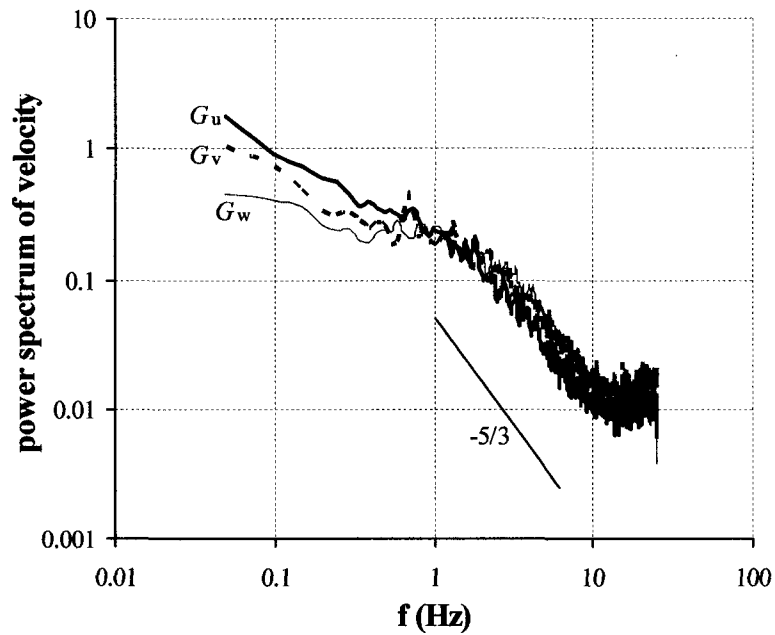
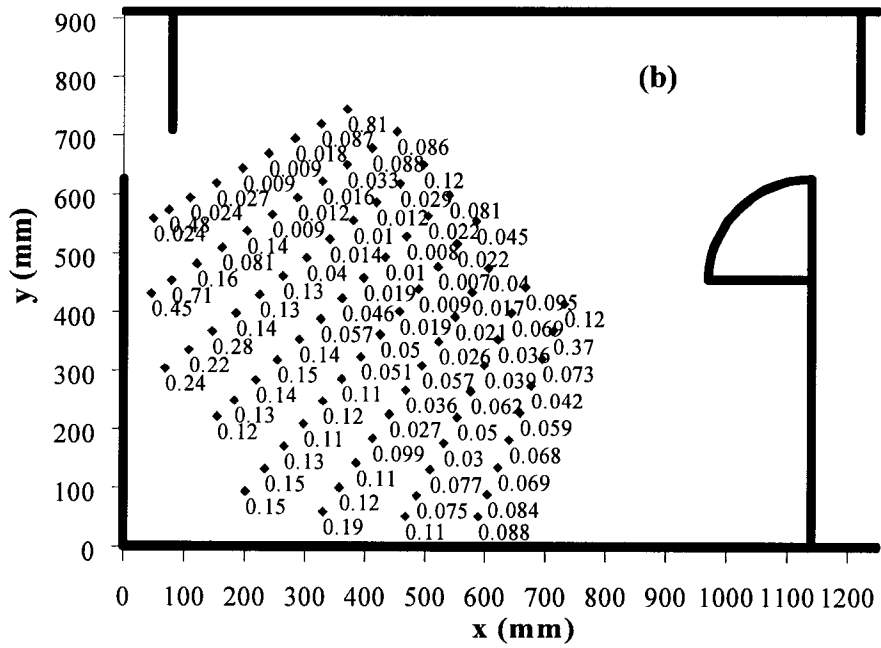
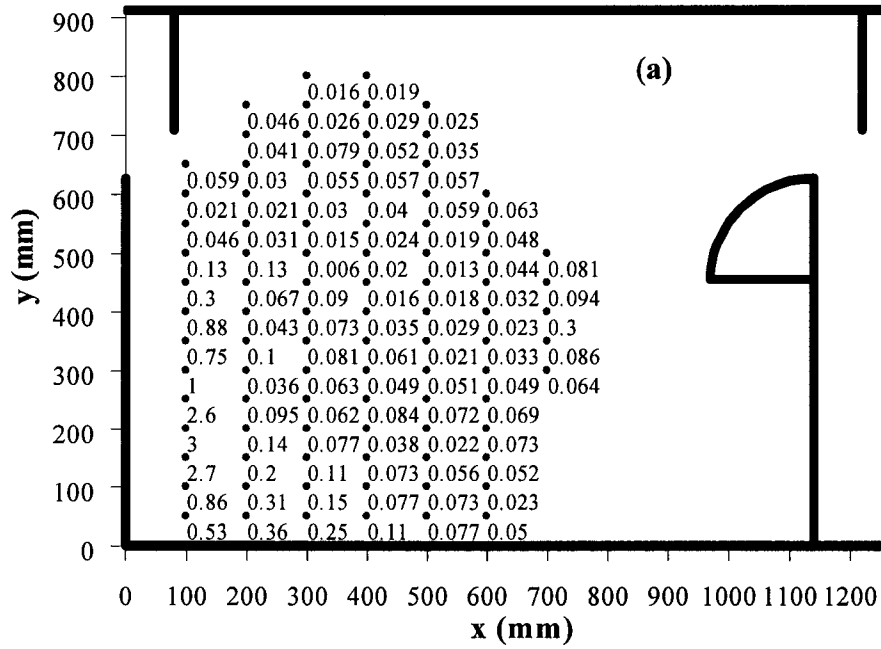
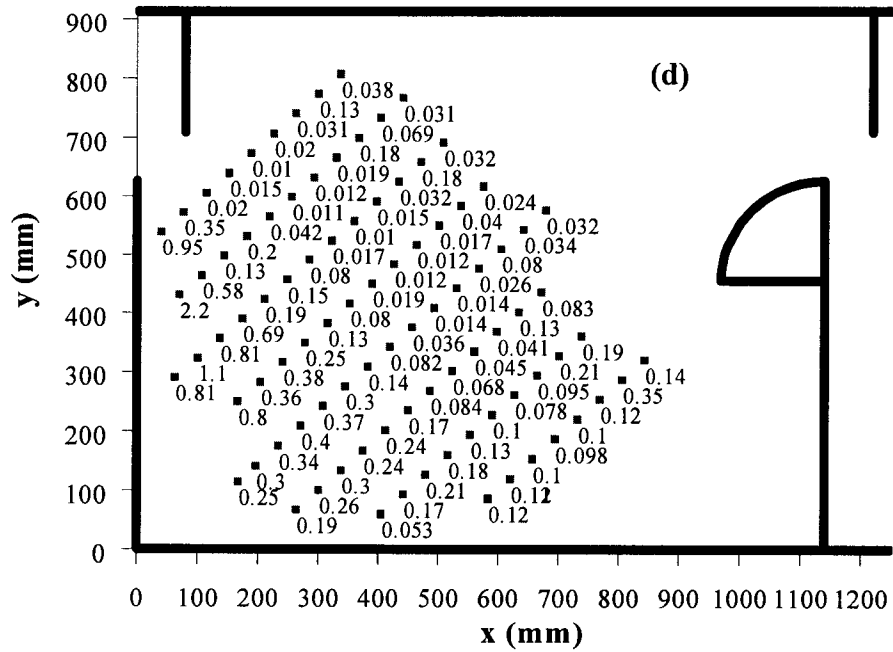
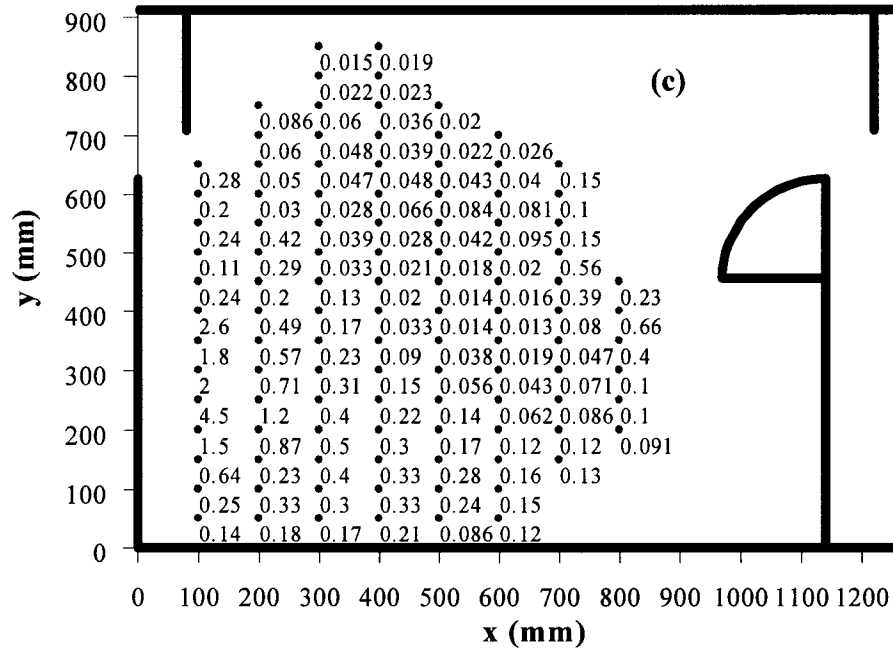


Fig. 4.23 Power spectrum of velocity: ———, $G_u(f) / \overline{u'^2}$; - - - -, $G_v(f) / \overline{v'^2}$; ·····, $G_w(f) / \overline{w'^2}$



**Fig. 4.24(a-b) Energy dissipation rate ε (m^2/s^3) for $S = 10.52\%$, $z = 10$ mm:
 (a) measured along x ; (b) measured along y**



**Fig. 4.24(c-d) Energy dissipation rate ε (m^2/s^3) for $S = 10.52\%$, $z = 70$ mm:
 (c) measured along x ; (d) measured along x_j**

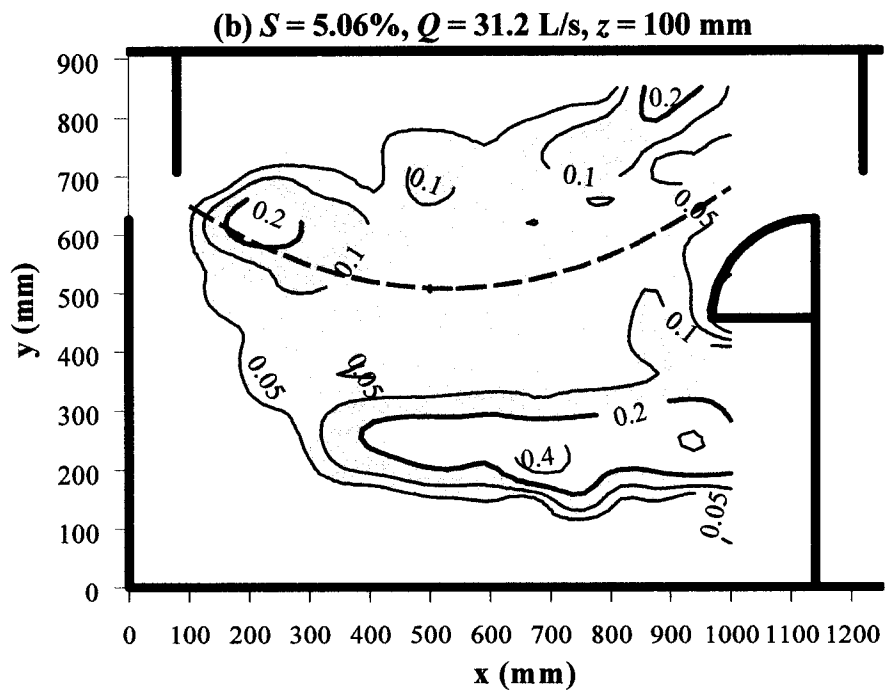
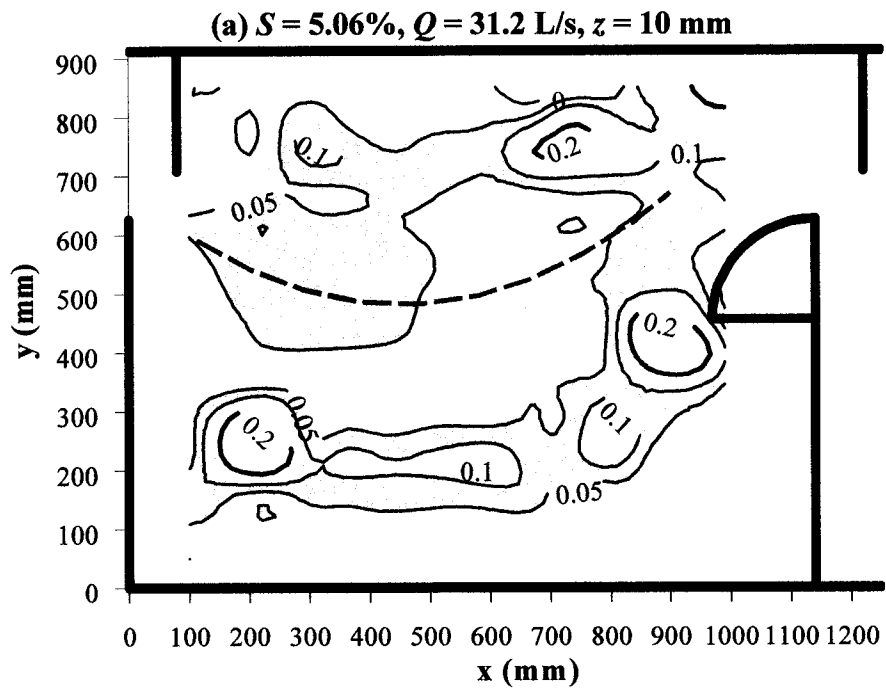


Fig. 4.25(a-f) Contours of turbulence energy dissipation rate ϵ (m^2/s^3) for $S = 5.06\%$, — — —, maximum plane velocity filament: (a) $Q = 31.2$ L/s, $z = 10$ mm; (b) $Q = 31.2$ L/s, $z = 100$ mm

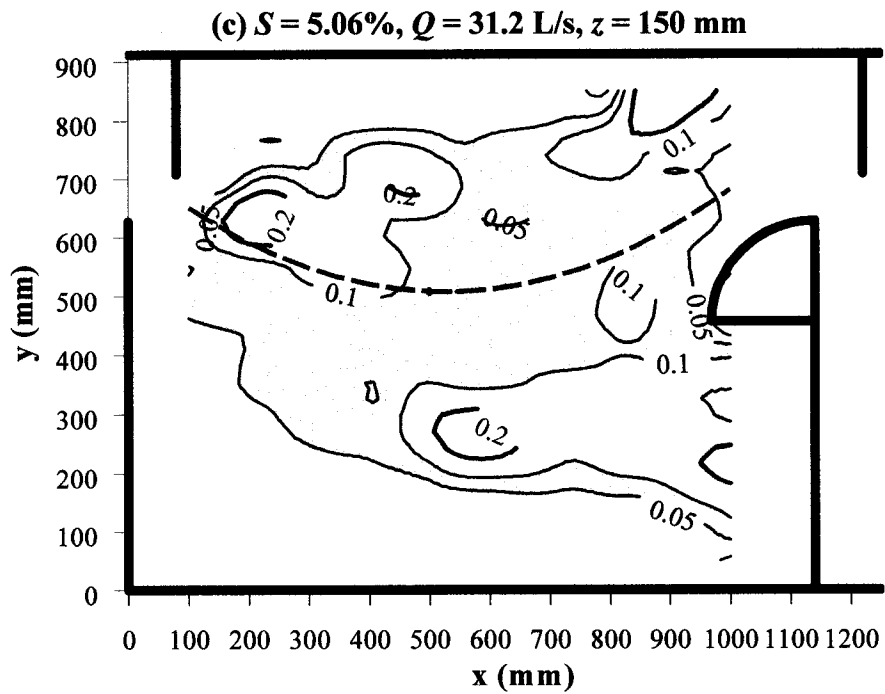


Fig. 4.25(a-f) Contours of turbulence energy dissipation rate ϵ (m^2/s^3) for $S = 5.06\%$, — — —, maximum plane velocity filament: (c) $Q = 31.2$ L/s, $z = 150$ mm; (d) $Q = 52$ L/s, $z = 10$ mm

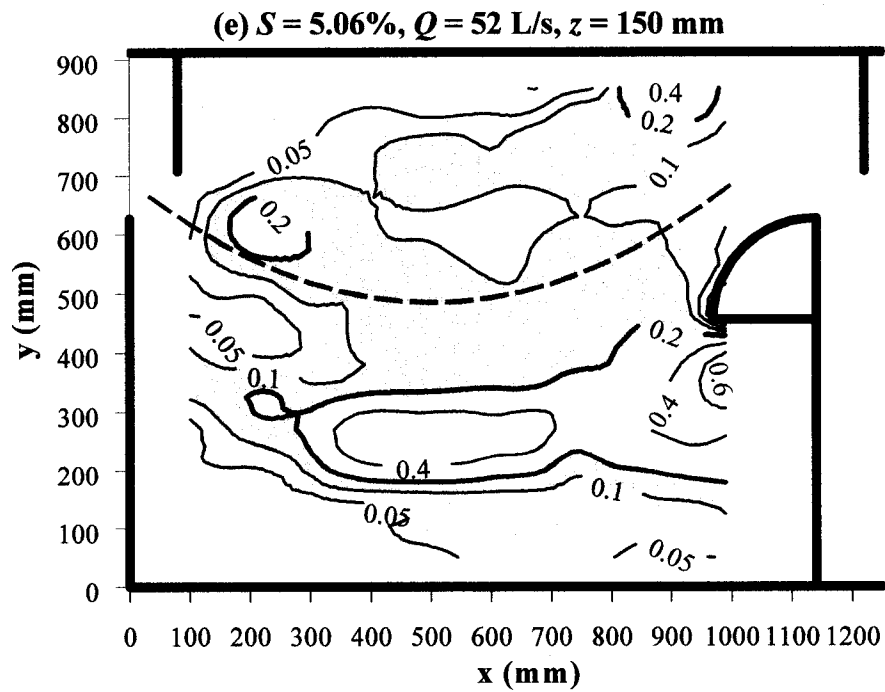


Fig. 4.25(a-f) Contours of turbulence energy dissipation rate ε (m^2/s^3) for $S = 5.06\%$, — — —, maximum plane velocity filament: (e) $Q = 52$ L/s, $z = 150$ mm; (f) $Q = 52$ L/s, $z = 300$ mm

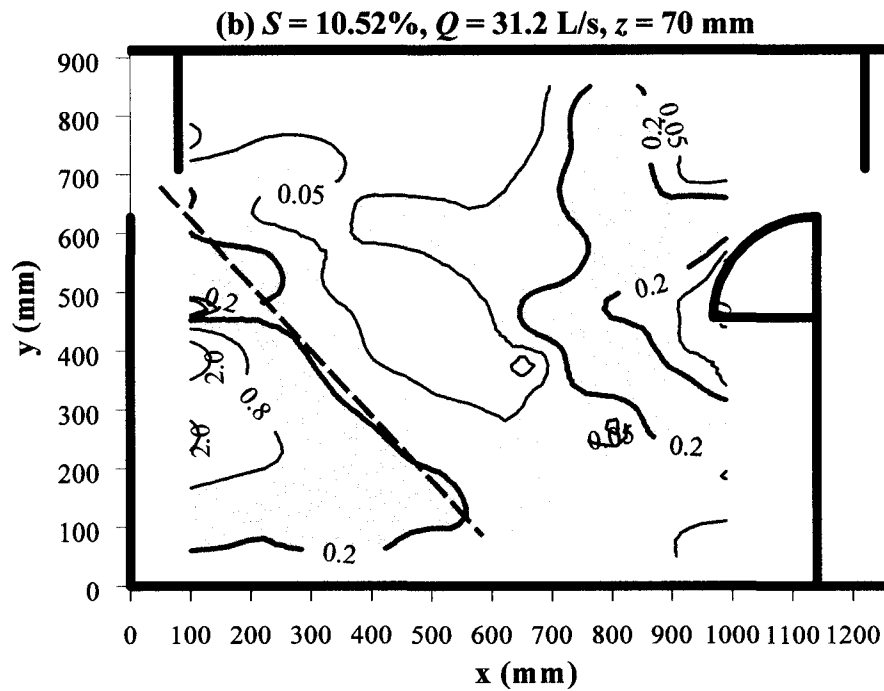
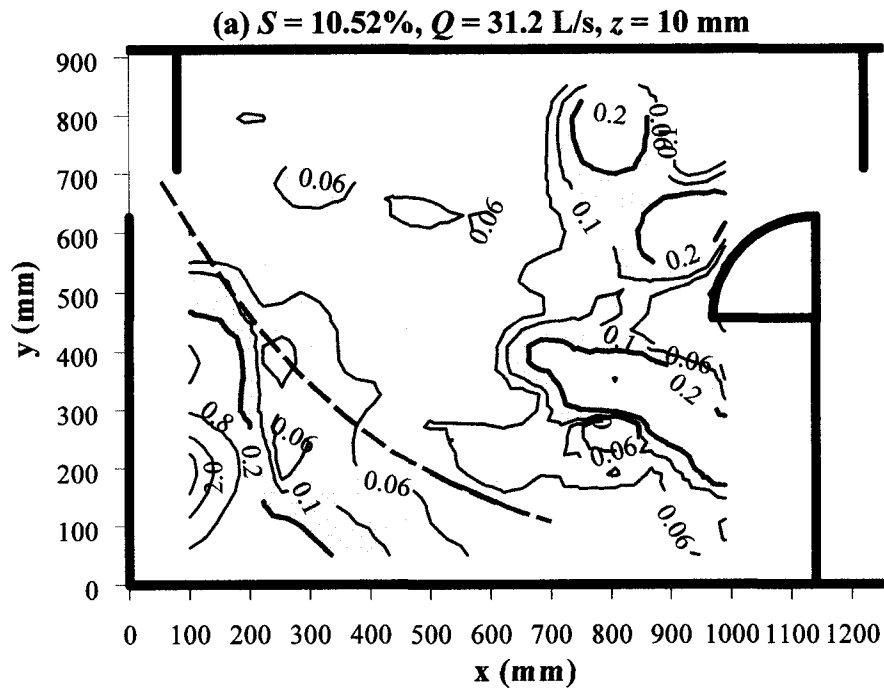


Fig. 4.26(a-c) Contours of turbulence energy dissipation rate ϵ (m^2/s^3) for $S = 10.52\%$, — — —, maximum plane velocity filament: (a) $Q = 31.2$ L/s, $z = 10$ mm; (b) $Q = 31.2$ L/s, $z = 70$ mm

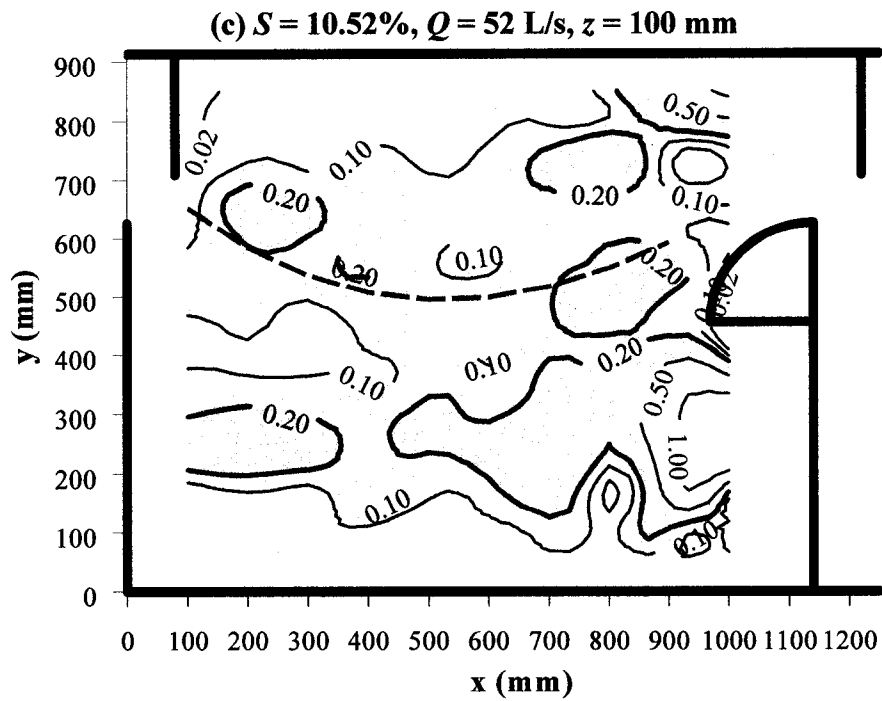
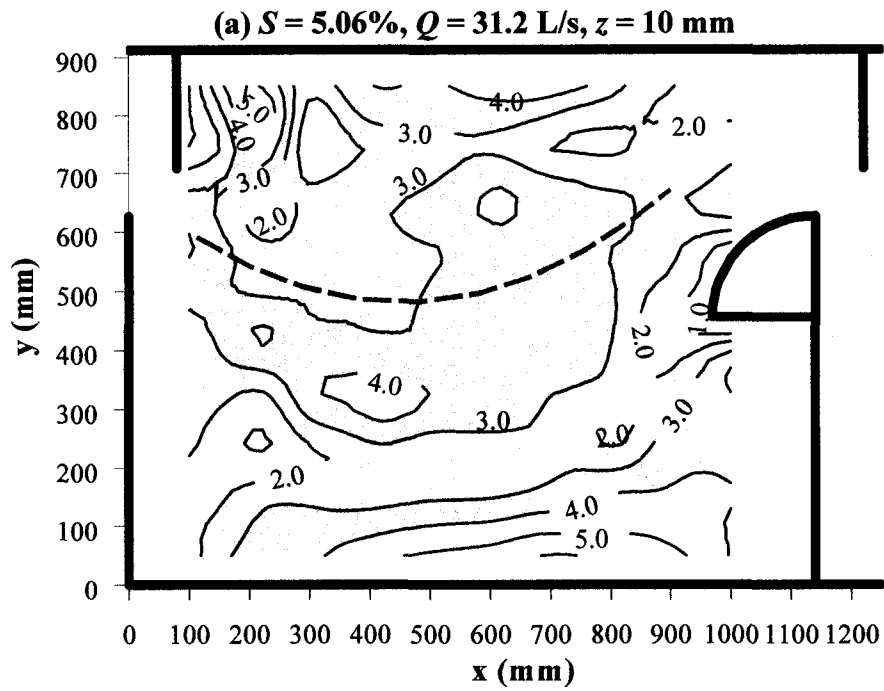
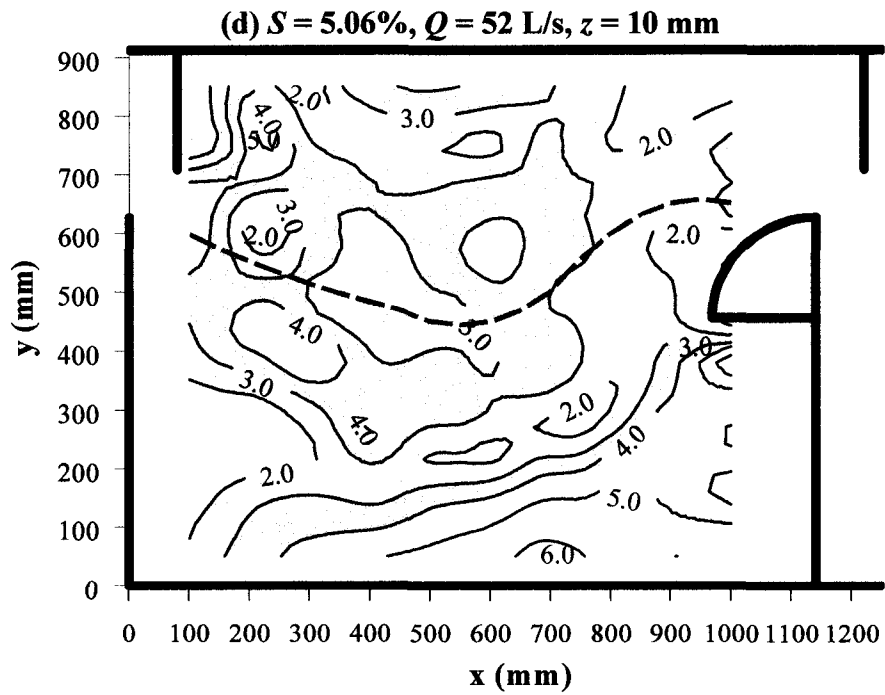
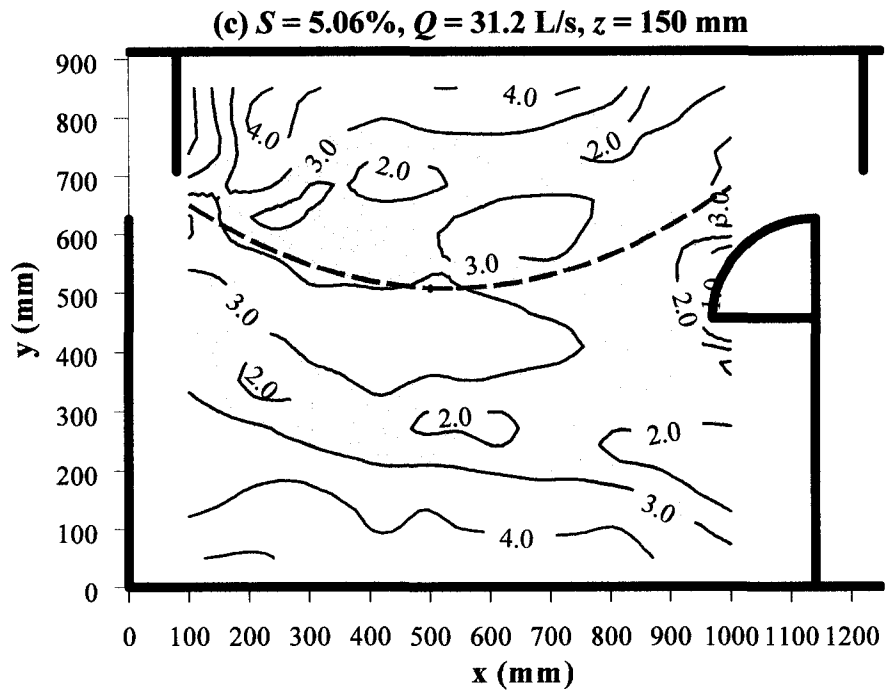


Fig. 4.26(a-c) Contours of turbulence energy dissipation rate ϵ (m^2/s^3) for $S = 10.52\%$, — — —, maximum plane velocity filament: (c) $Q = 52$ L/s, $z = 100$ mm



**Fig. 4.27(a-f) Contours of microscale λ_g (mm) for $S = 5.06\%$,
 — — —, maximum plane velocity filament: (a) $Q = 31.2$ L/s,
 $z = 10$ mm; (b) $Q = 31.2$ L/s, $z = 100$ mm**



**Fig. 4.27(a-f) Contours of microscale λ_g (mm) for $S = 5.06\%$,
 — — —, maximum plane velocity filament: (c) $Q = 31.2$ L/s,
 $z = 150$ mm; (d) $Q = 52$ L/s, $z = 10$ mm**

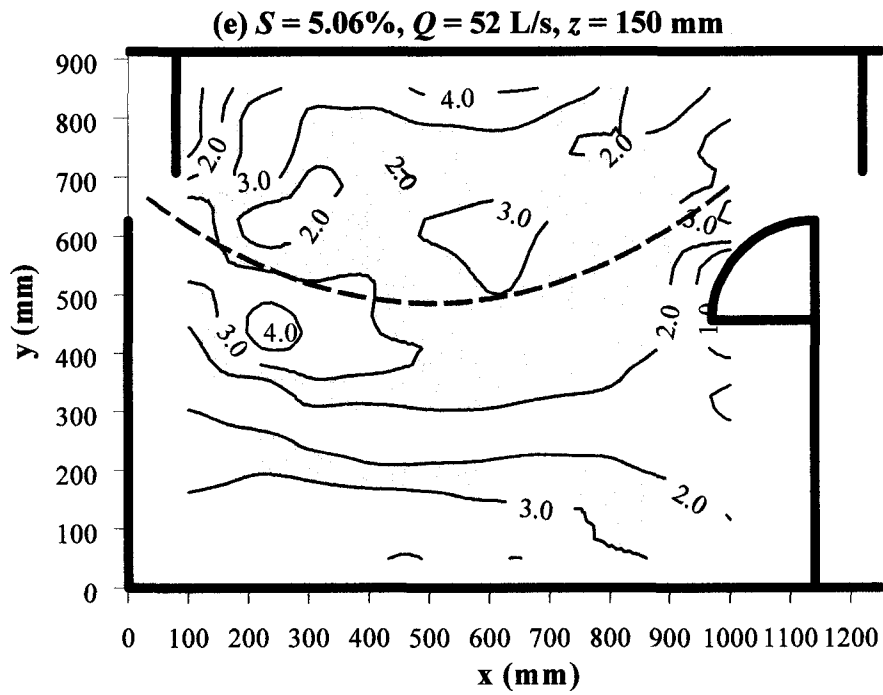


**Fig. 4.27(a-f) Contours of microscale λ_g (mm) for $S = 5.06\%$,
 — — —, maximum plane velocity filament: (e) $Q = 52$ L/s,
 $z = 150$ mm; (f) $Q = 52$ L/s, $z = 300$ mm**

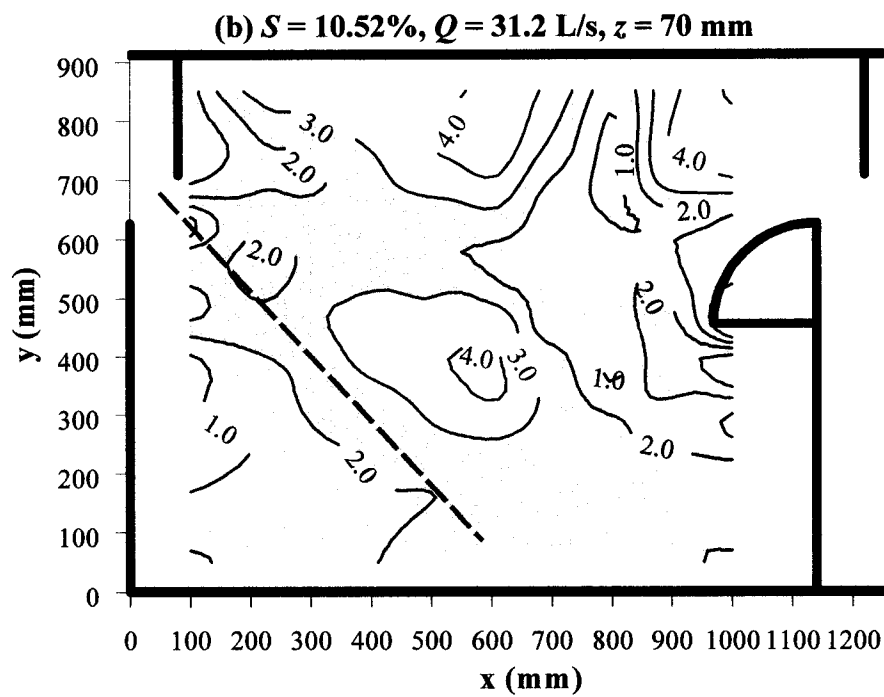
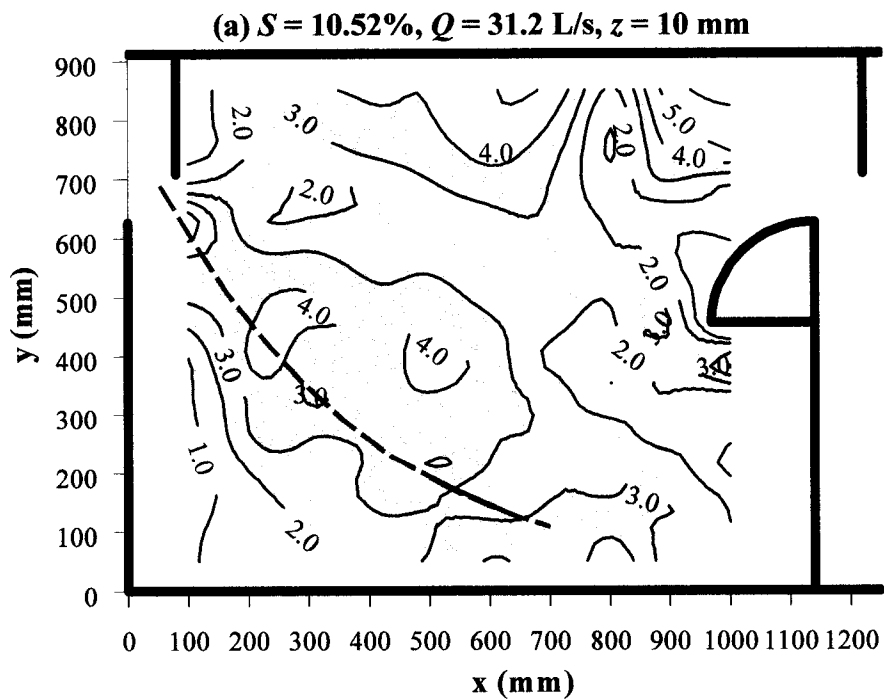
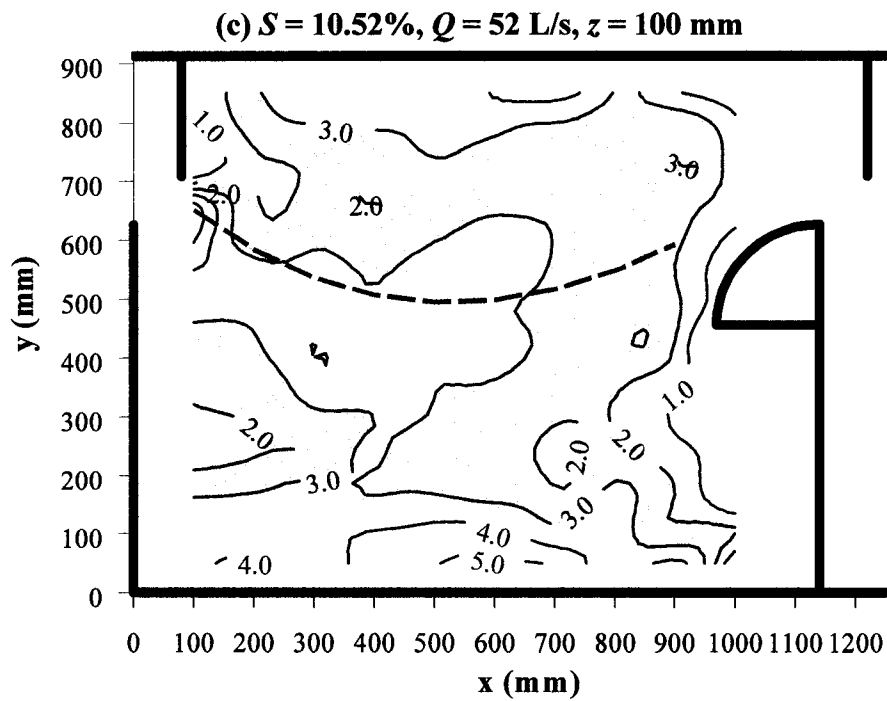


Fig. 4.28(a-c) Contours of microscale λ_g (mm) for $S = 10.52\%$,
 — — —, maximum plane velocity filament: (a) $Q = 31.2$ L/s,
 $z = 10$ mm; (b) $Q = 31.2$ L/s, $z = 70$ mm



**Fig. 4.28(a-c) Contours of microscale λ_g (mm) for $S = 10.52\%$,
 — — —, maximum plane velocity filament: (c) $Q = 52$ L/s,
 $z = 100$ mm**

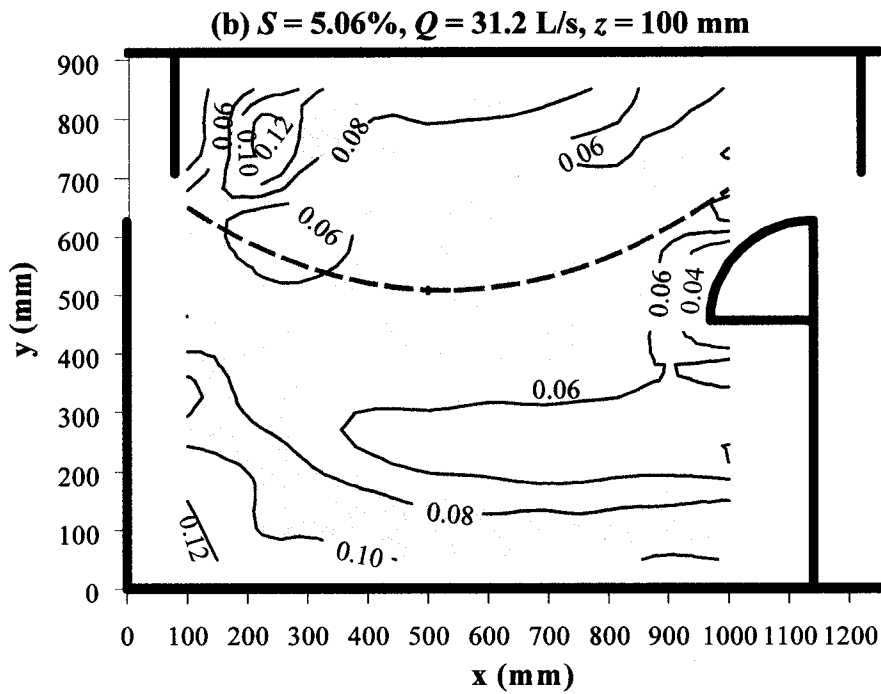
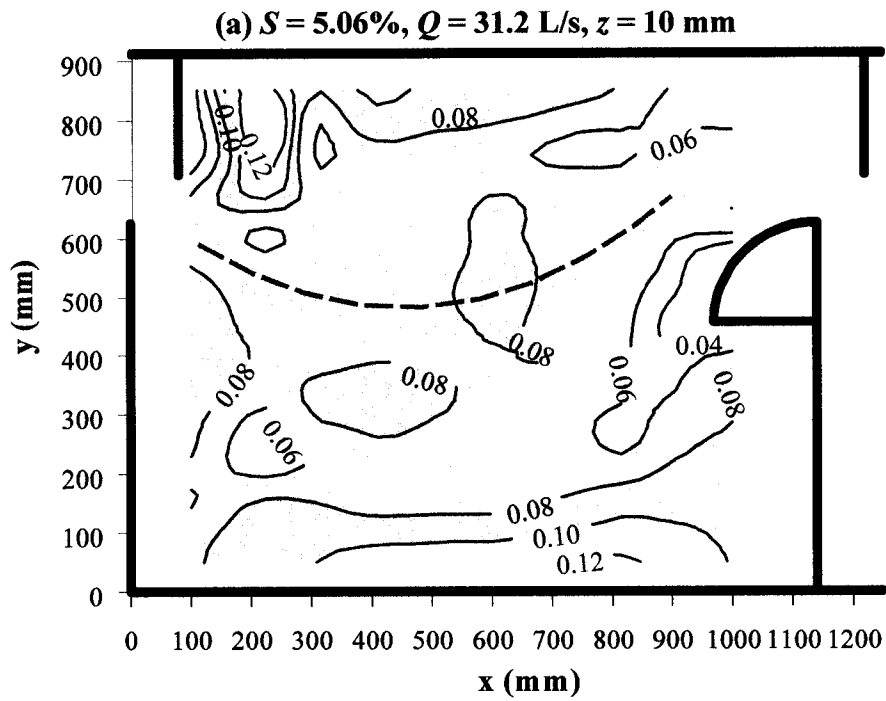


Fig. 4.29(a-f) Contours of Kolmogorov length scale η (mm) for $S = 5.06\%$, — — —, maximum plane velocity filament: (a) $Q = 31.2$ L/s, $z = 10$ mm; (b) $Q = 31.2$ L/s, $z = 100$ mm

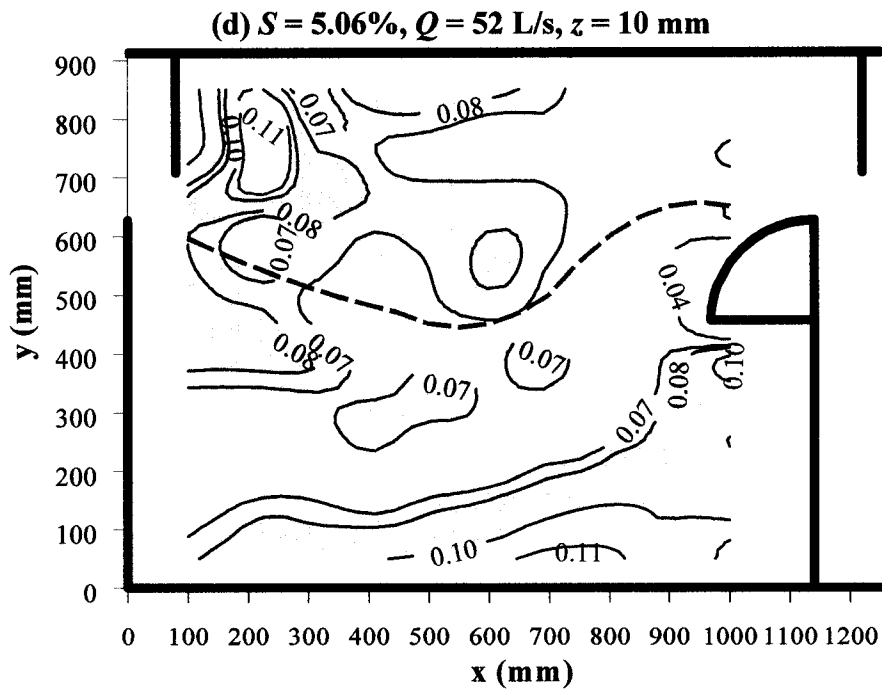
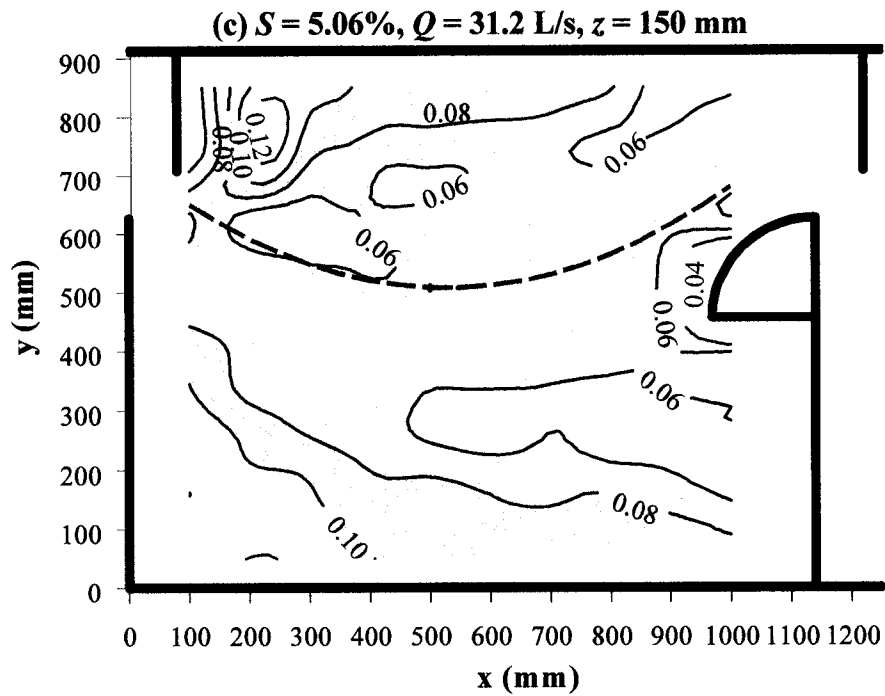
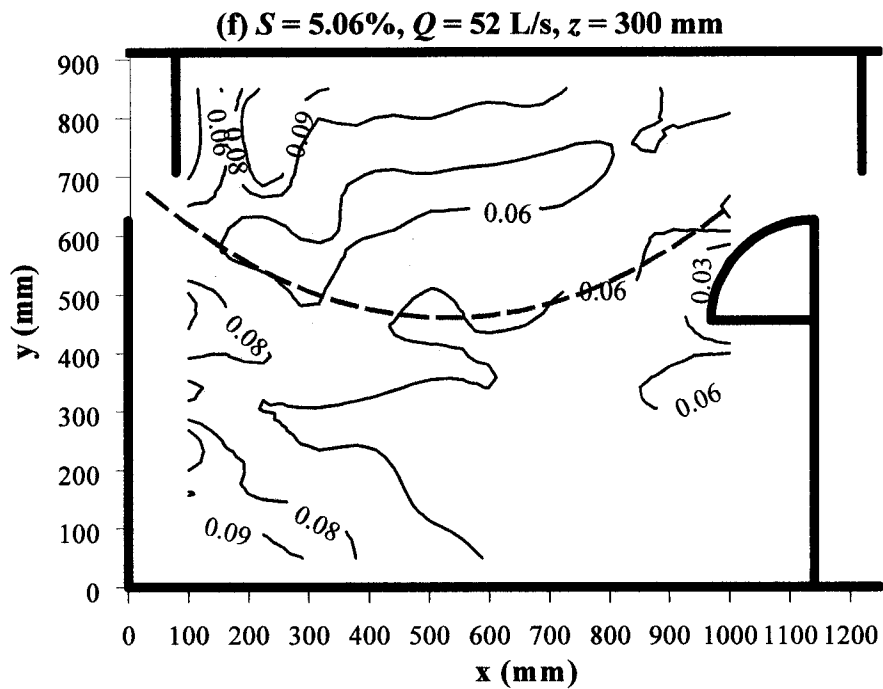
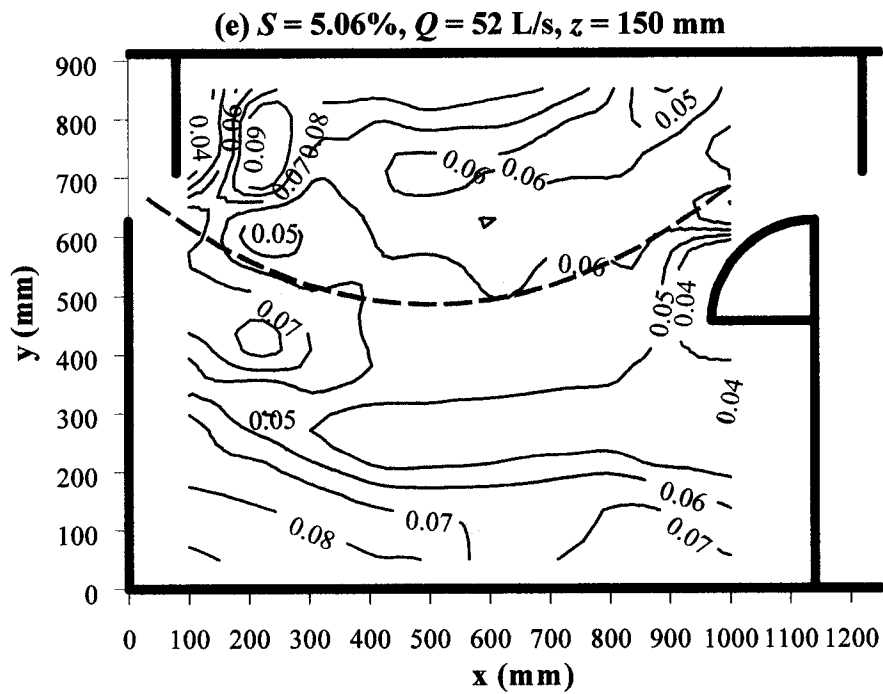


Fig. 4.29(a-f) Contours of Kolmogorov length scale η (mm) for $S = 5.06\%$,
 ---, maximum plane velocity filament: (c) $Q = 31.2$ L/s, $z = 150$ mm;
 (d) $Q = 52$ L/s, $z = 10$ mm



**Fig. 4.29(a-f) Contours of Kolmogorov length scale η (mm) for $S = 5.06\%$,
 — — —, maximum plane velocity filament: (e) $Q = 52$ L/s, $z = 150$ mm;
 (f) $Q = 52$ L/s, $z = 300$ mm**

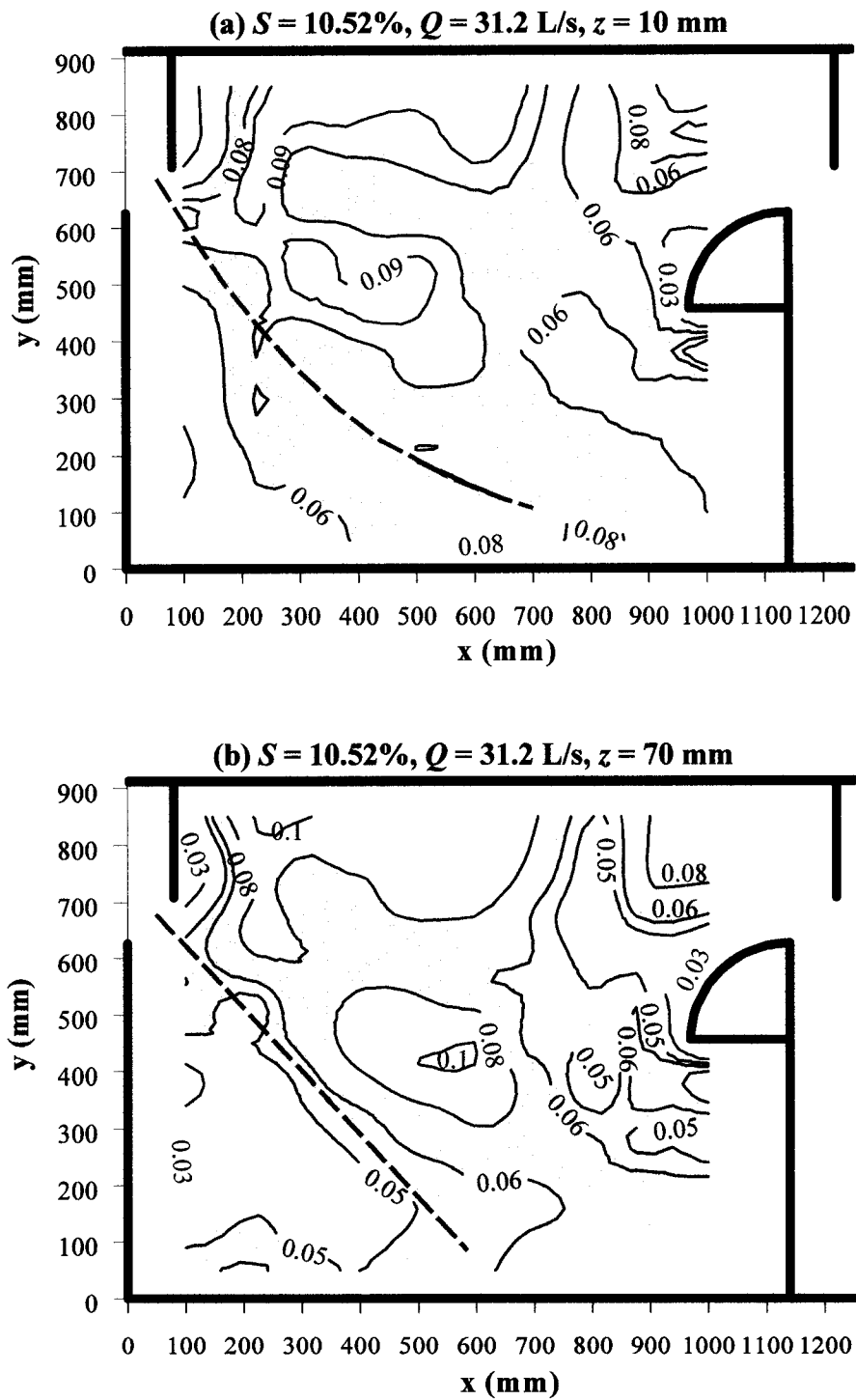
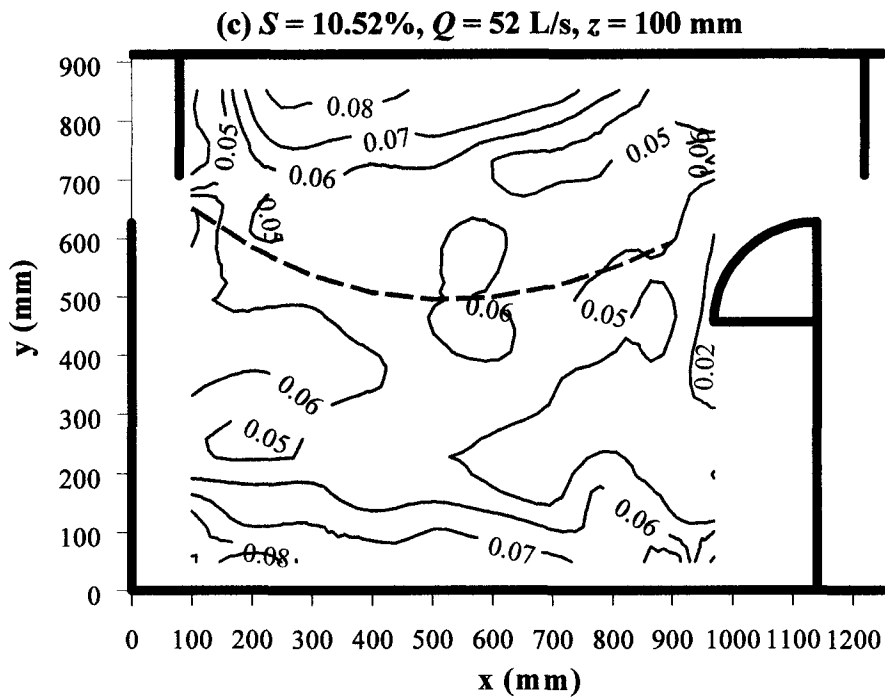


Fig. 4.30(a-c) Contours of Kolmogorov length scale η (mm) for $S = 10.52\%$, — — —, maximum plane velocity filament: (a) $Q = 31.2$ L/s, $z = 10$ mm; (b) $Q = 31.2$ L/s, $z = 70$ mm



**Fig. 4.30(a-c) Contours of Kolmogorov length scale η (mm) for $S = 10.52\%$,
 — — —, maximum plane velocity filament: (c) $Q = 52$ L/s, $z = 100$ mm**

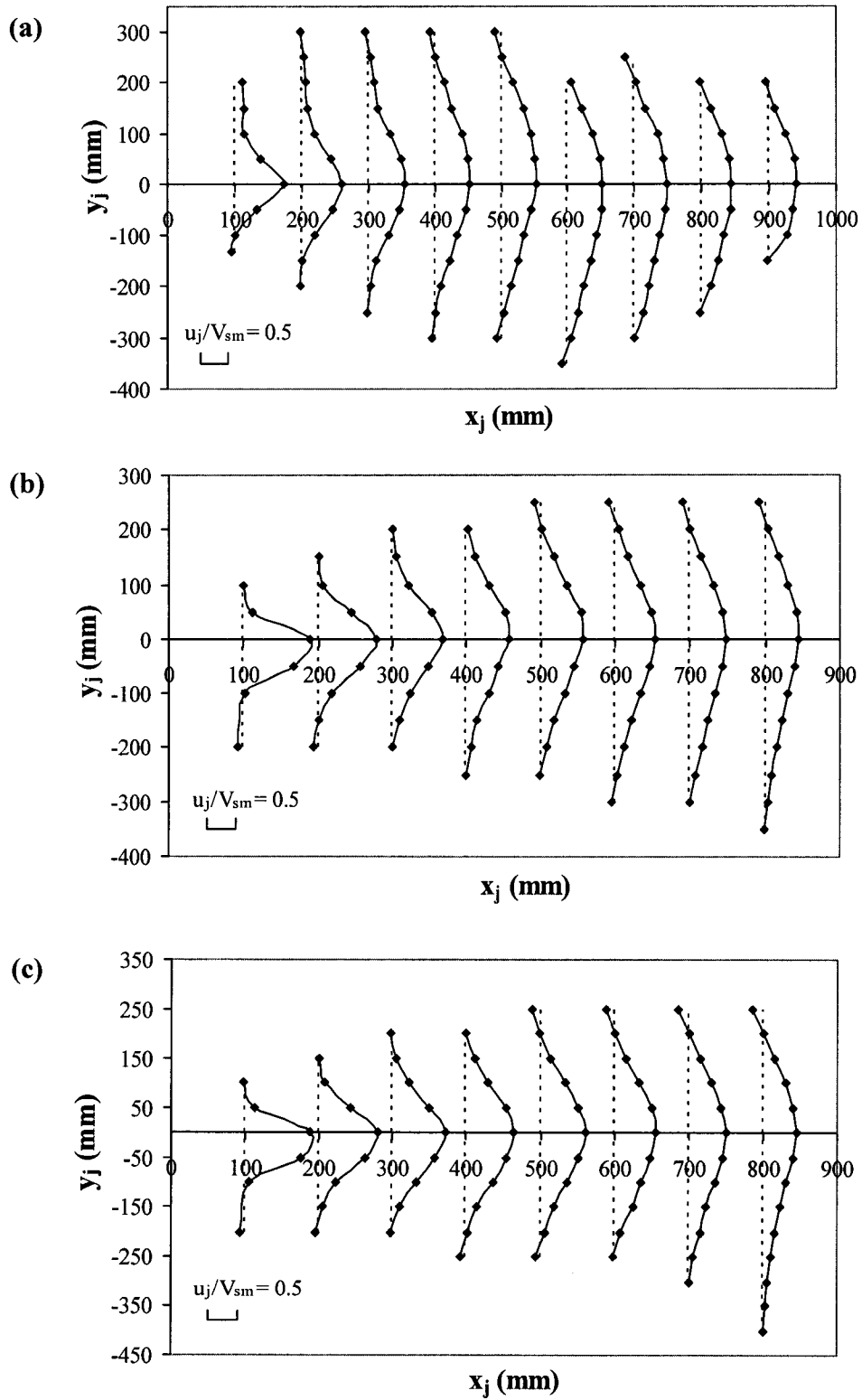


Fig. 4.31(a-c) Distribution of longitudinal mean velocity in jet for $S = 5.06\%$ and $Q = 31.2$ L/s: (a) $z = 10$ mm; (b) $z = 100$ mm; (c) $z = 150$ mm

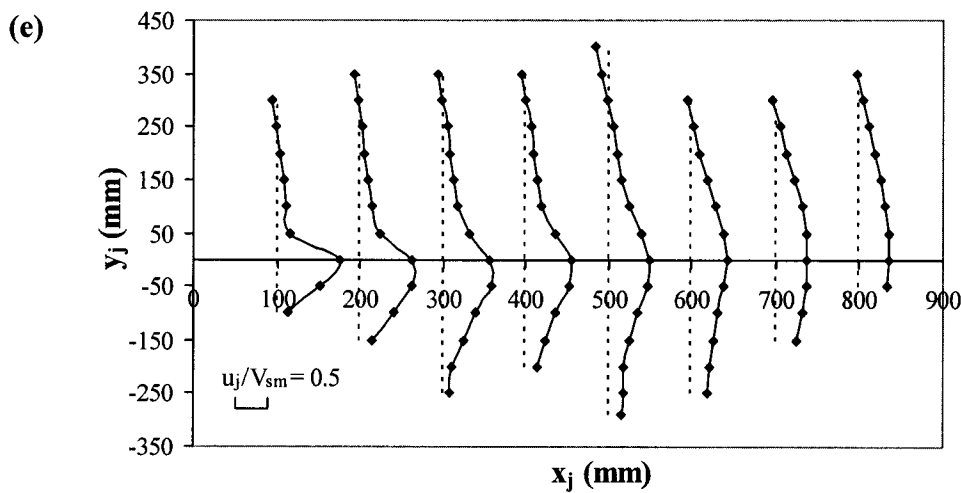
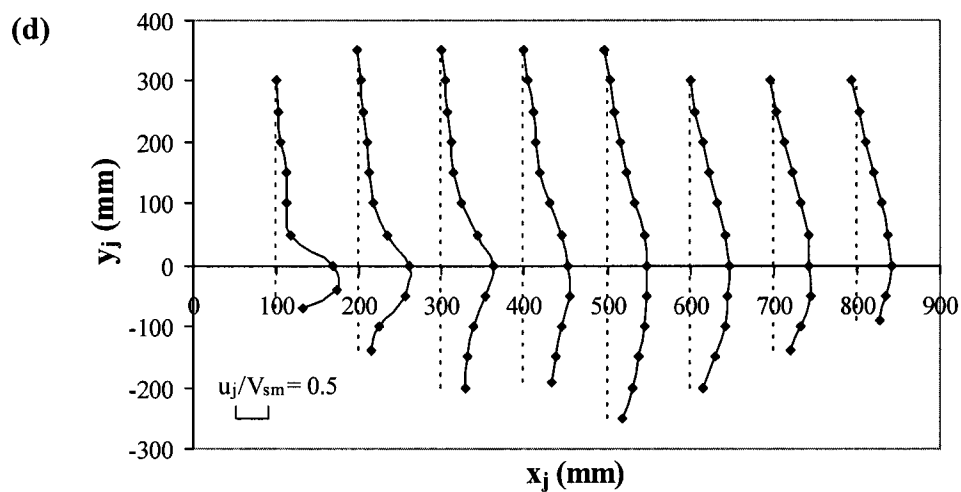


Fig. 4.31(d-e) Distribution of longitudinal mean velocity in jet for $S = 10.52\%$ and $Q = 31.2$ L/s: (d) $z = 10$ mm; (e) $z = 70$ mm

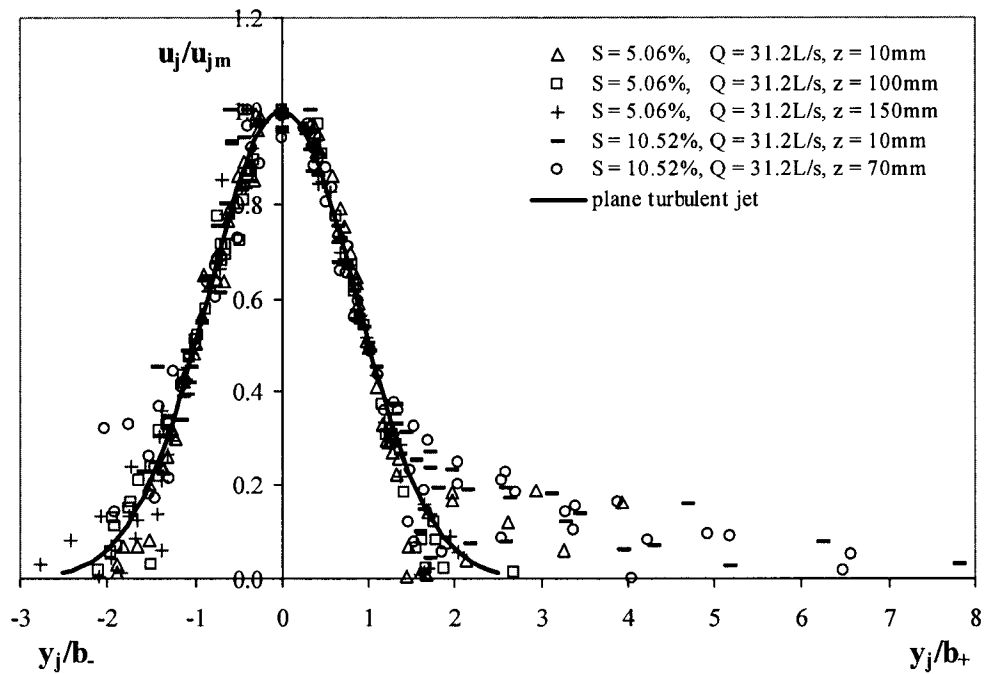


Fig. 4.32 Non-dimensional velocity profile

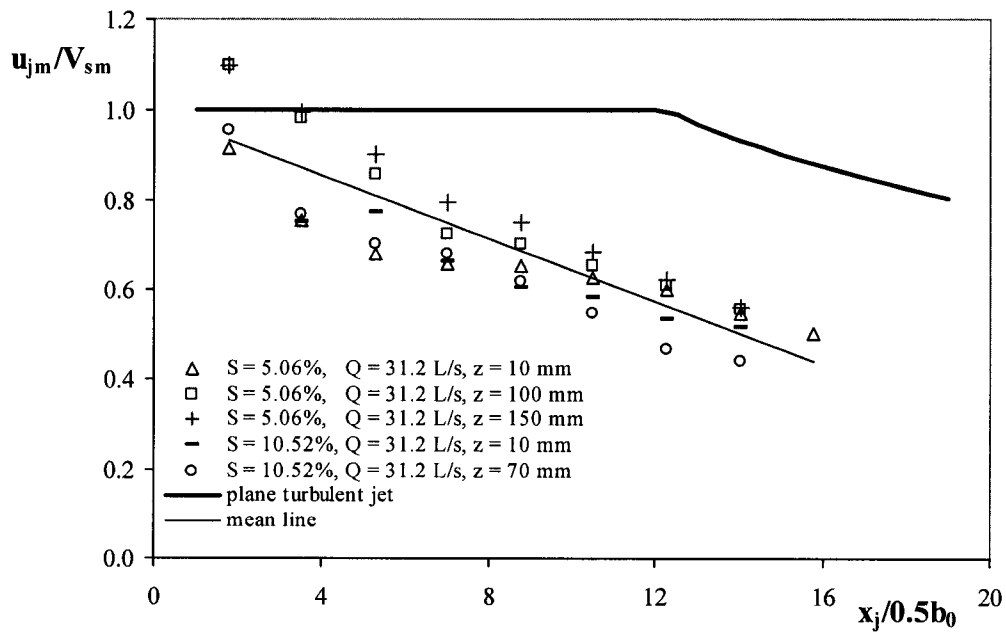


Fig. 4.33 Variation of normalized maximum velocity u_{jm}/V_{sm} with $x_j/0.5b_0$

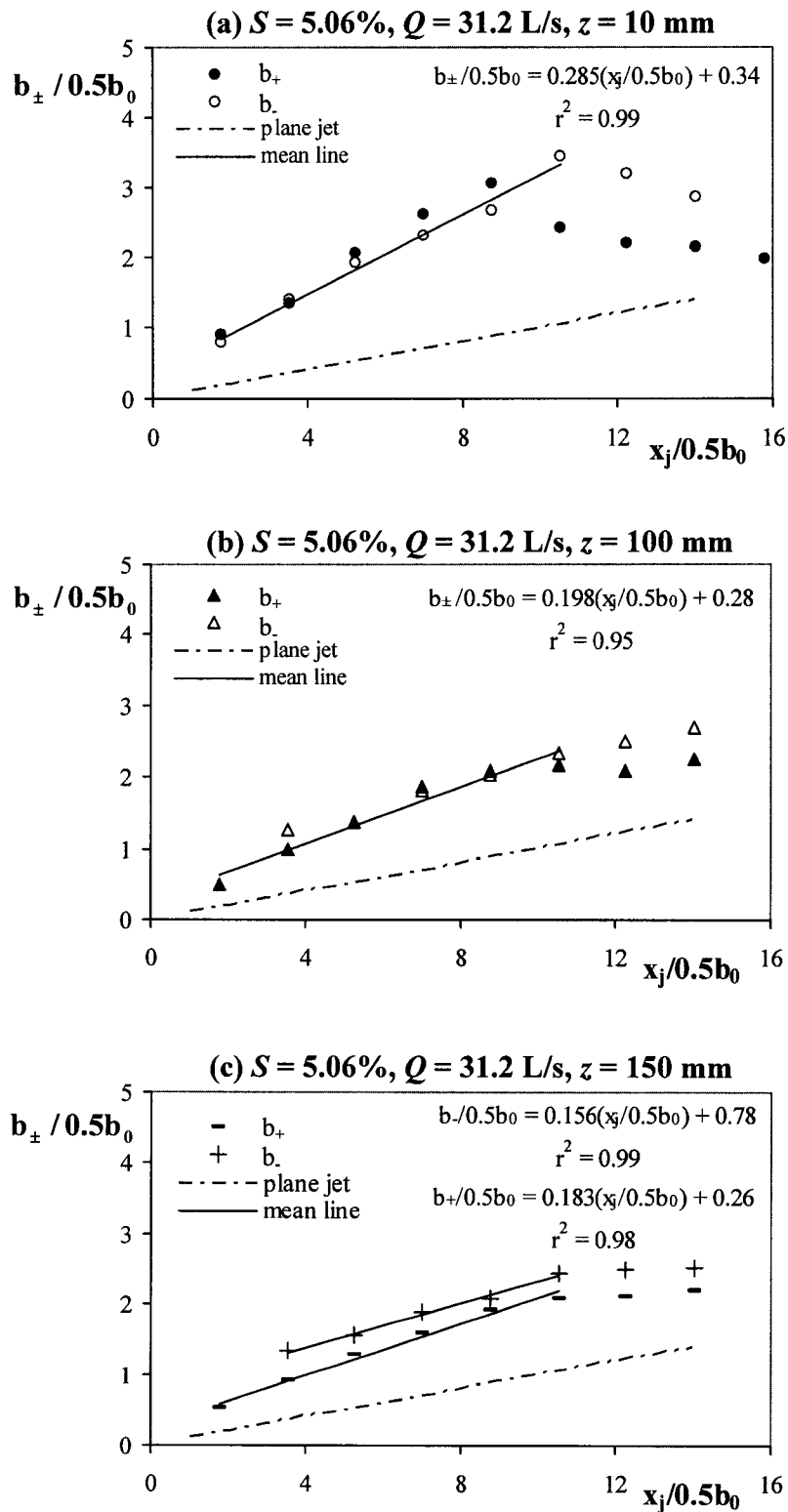


Fig. 4.34(a-c) Growth of jet half width in pool for $S = 5.06\%$ and $Q = 31.2$ L/s

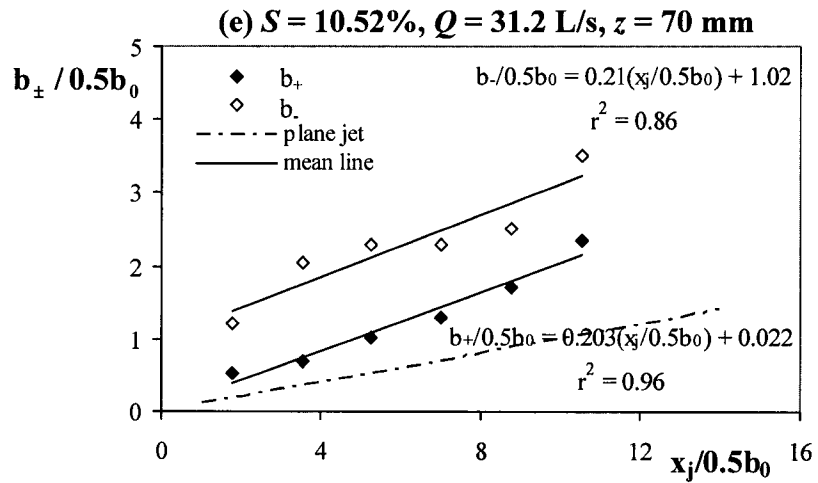
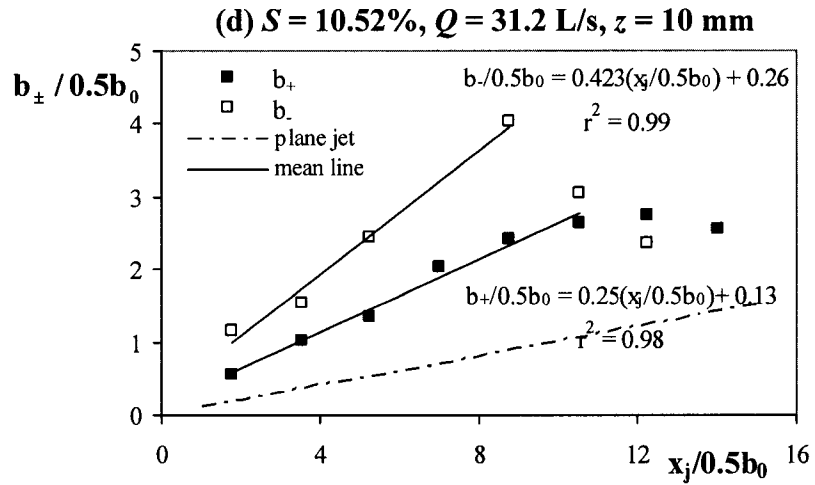


Fig. 4.34(d-e) Growth of jet half width in pool for $S = 10.52\%$ and $Q = 31.2$ L/s

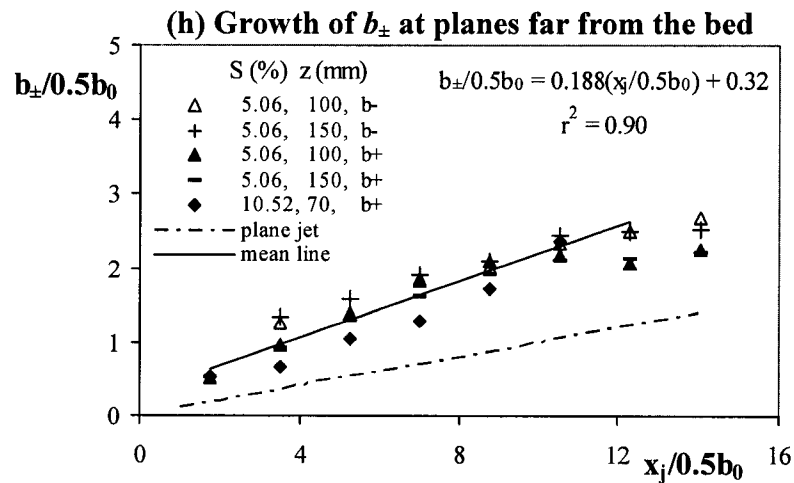
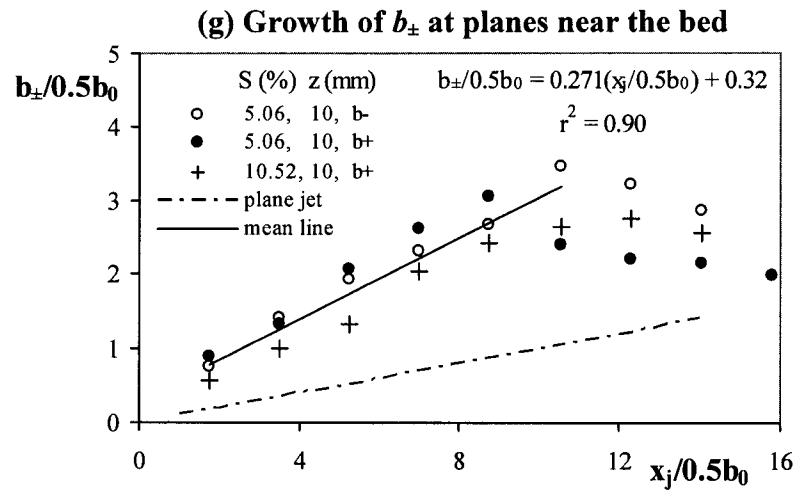
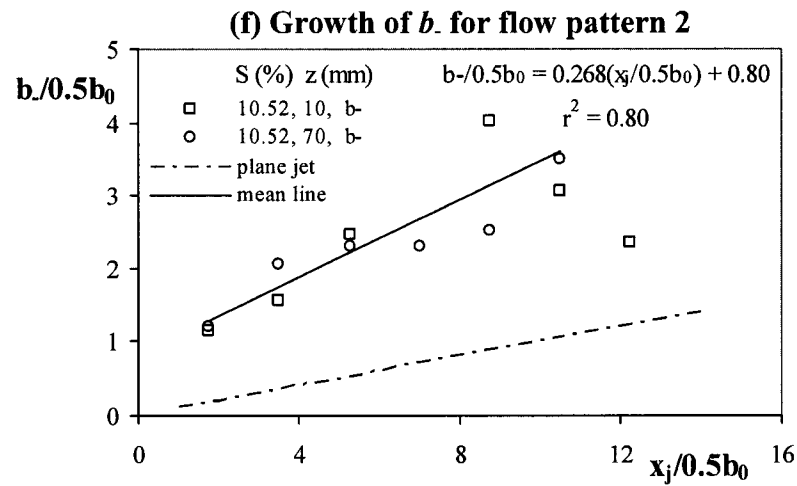


Fig. 4.34(f-h) Growth of jet half width in pool for $S = 5.06, 10.52\%$ and $Q = 31.2$ L/s

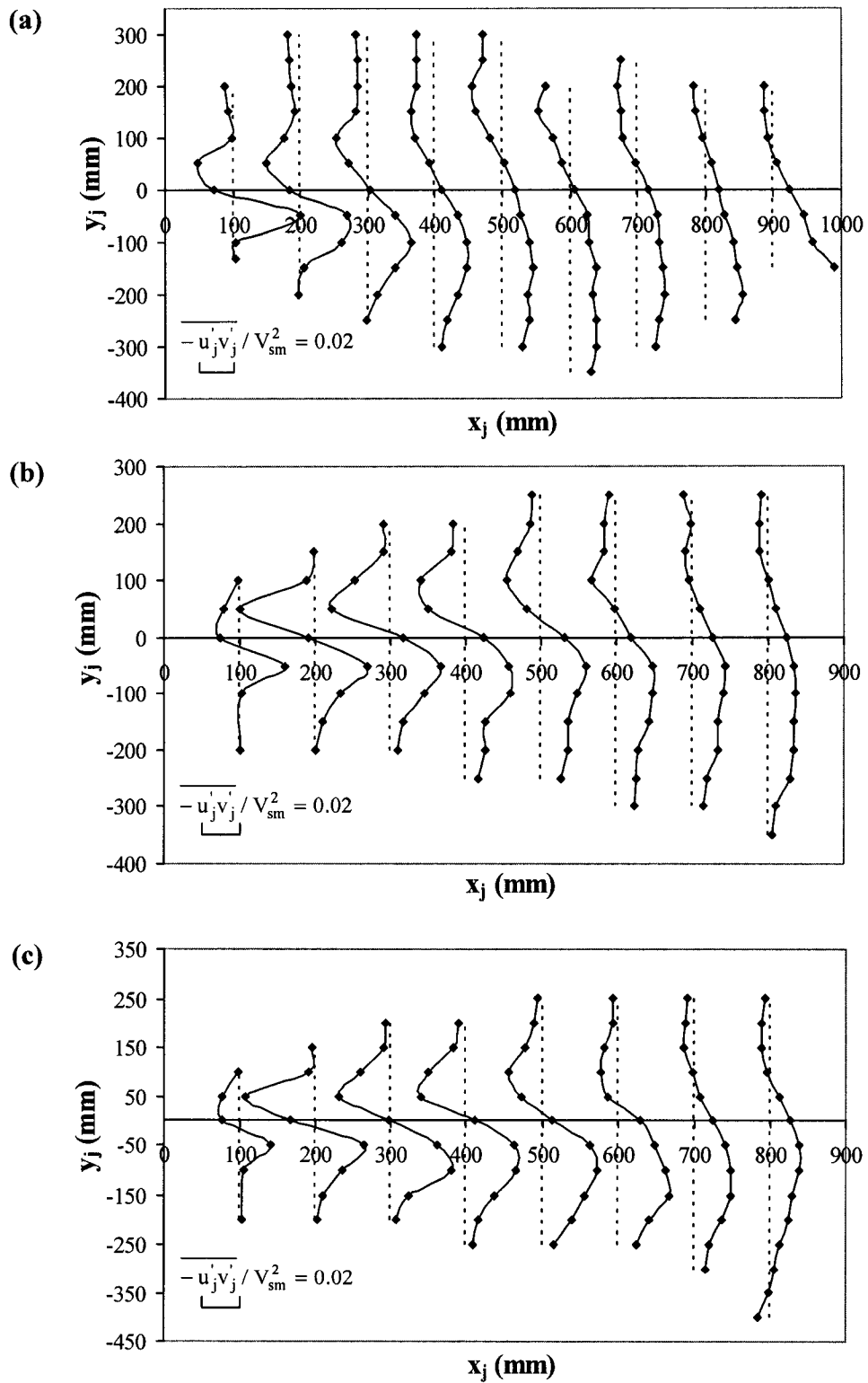


Fig. 4.35(a-c) Distribution of Reynolds shear stress in jet for $S = 5.06\%$ and $Q = 31.2 \text{ L/s}$: (a) $z = 10 \text{ mm}$; (b) $z = 100 \text{ mm}$; (c) $z = 150 \text{ mm}$

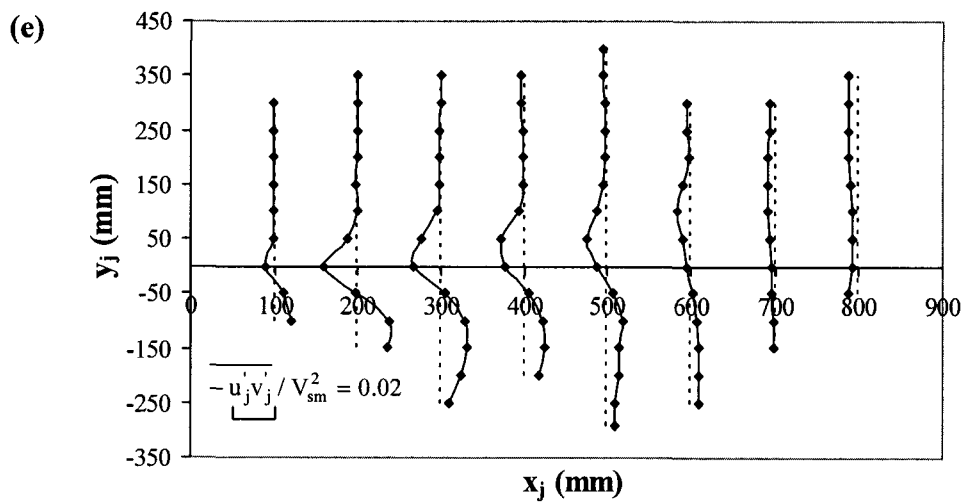
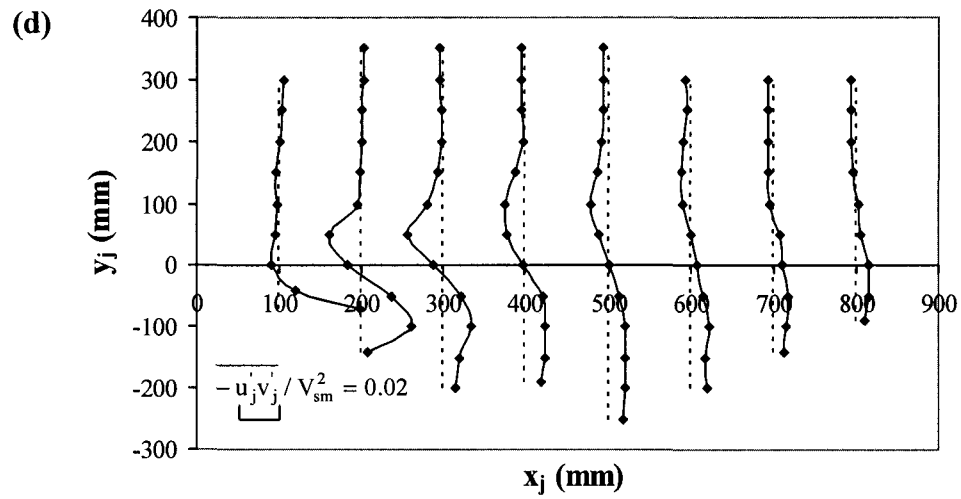


Fig. 4.35(d-e) Distribution of Reynolds shear stress in jet for $S = 10.52\%$ and $Q = 31.2$ L/s: (d) $z = 10$ mm; (e) $z = 70$ mm

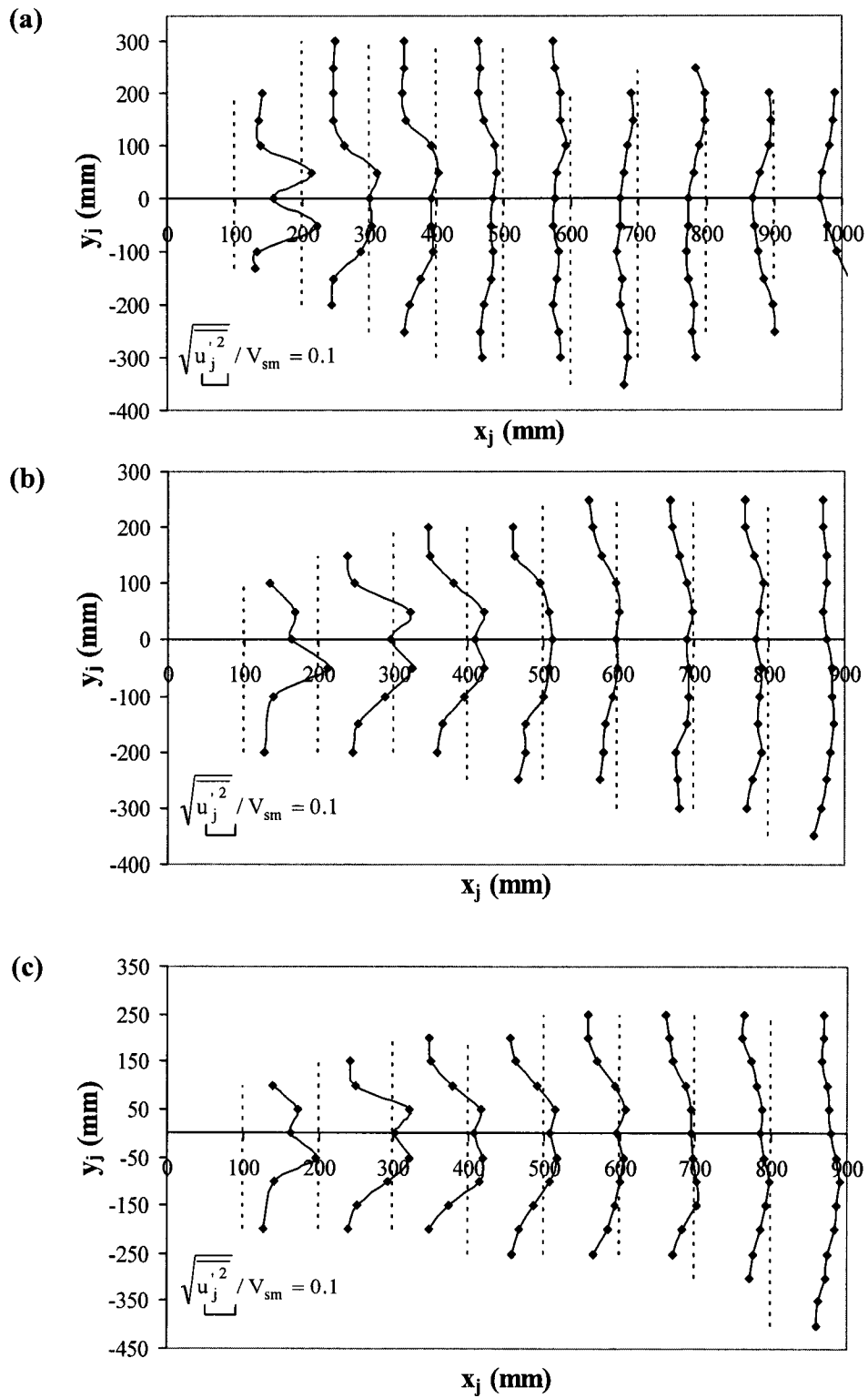


Fig. 4.36(a-c) Distribution of longitudinal turbulence intensity in jet for $S = 5.06\%$ and $Q = 31.2$ L/s: (a) $z = 10$ mm; (b) $z = 100$ mm; (c) $z = 150$ mm

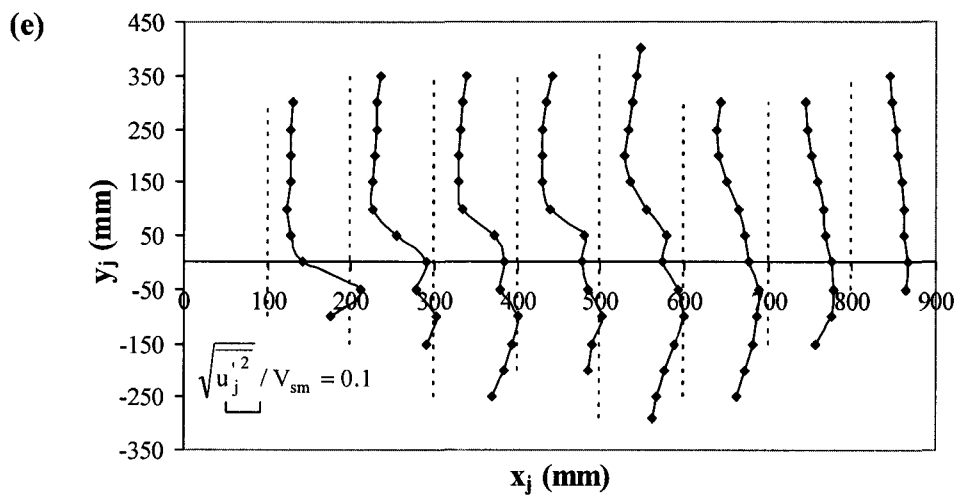
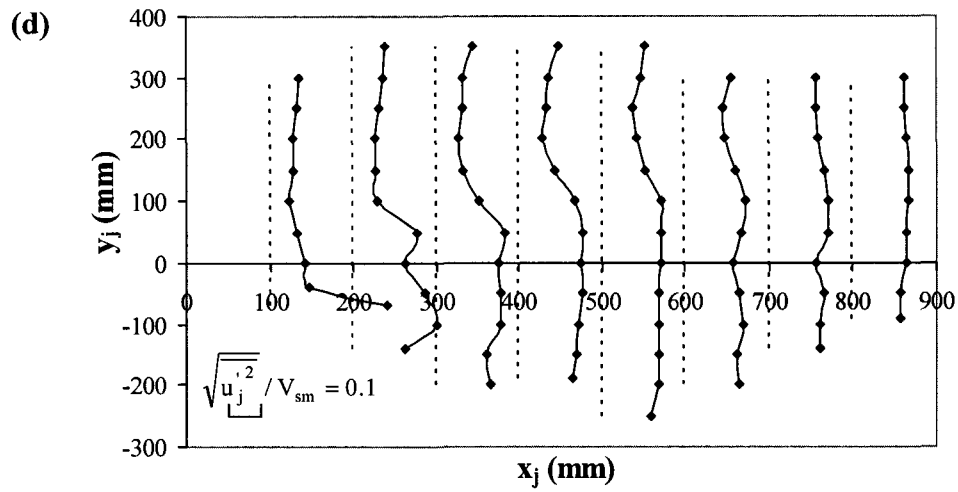


Fig. 4.36(d-e) Distribution of longitudinal turbulence intensity in jet for $S = 10.52\%$ and $Q = 31.2$ L/s: (d) $z = 10$ mm; (e) $z = 70$ mm

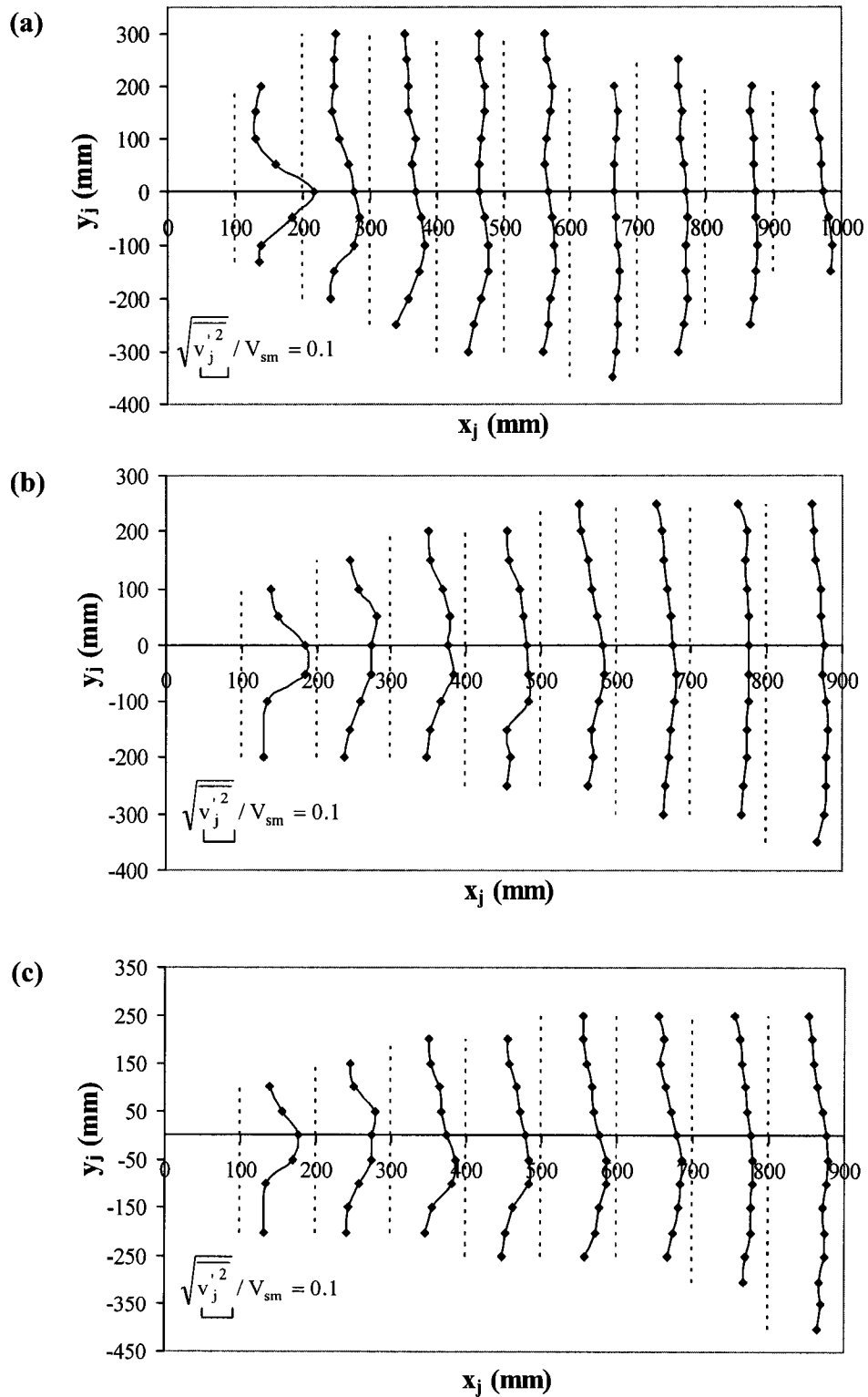


Fig. 4.37(a-c) Distribution of transverse turbulence intensity in jet for $S = 5.06\%$ and $Q = 31.2$ L/s: (a) $z = 10$ mm; (b) $z = 100$ mm; (c) $z = 150$ mm

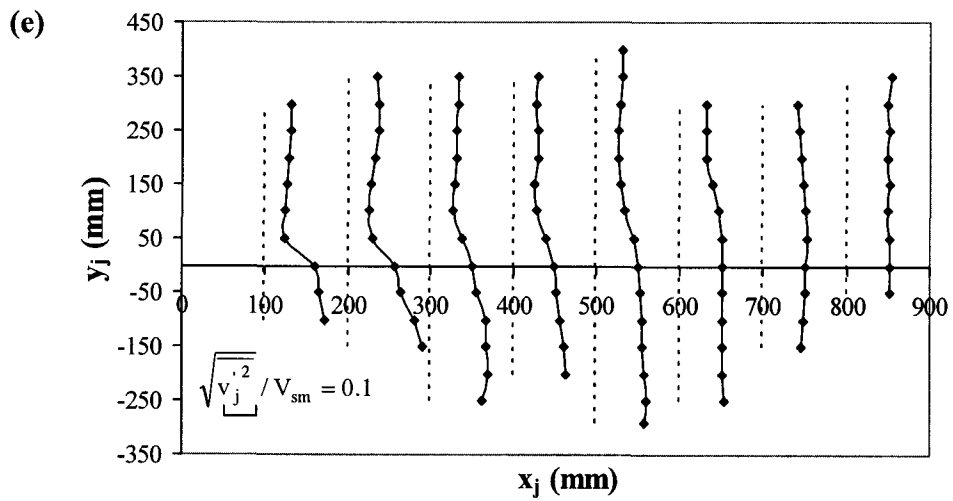
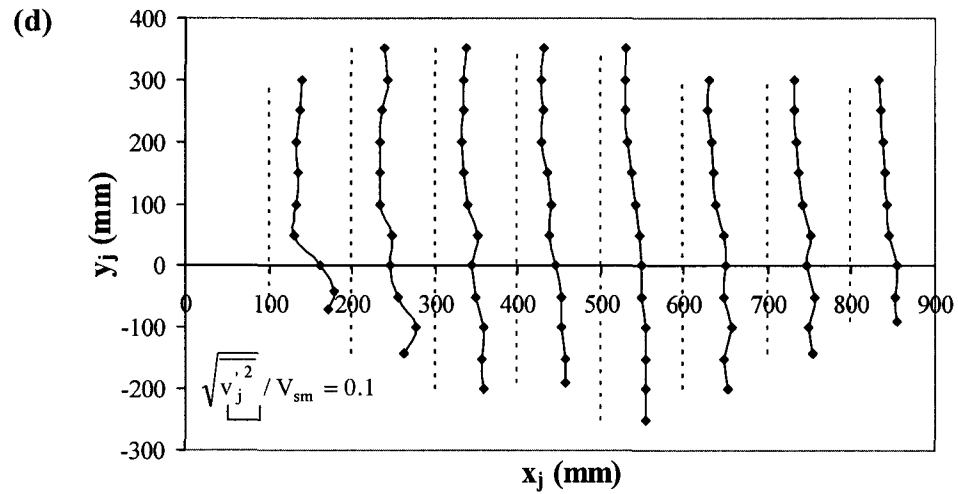


Fig. 4.37(d-e) Distribution of transverse turbulence intensity in jet for $S = 10.52\%$ and $Q = 31.2$ L/s: (d) $z = 10$ mm; (e) $z = 70$ mm

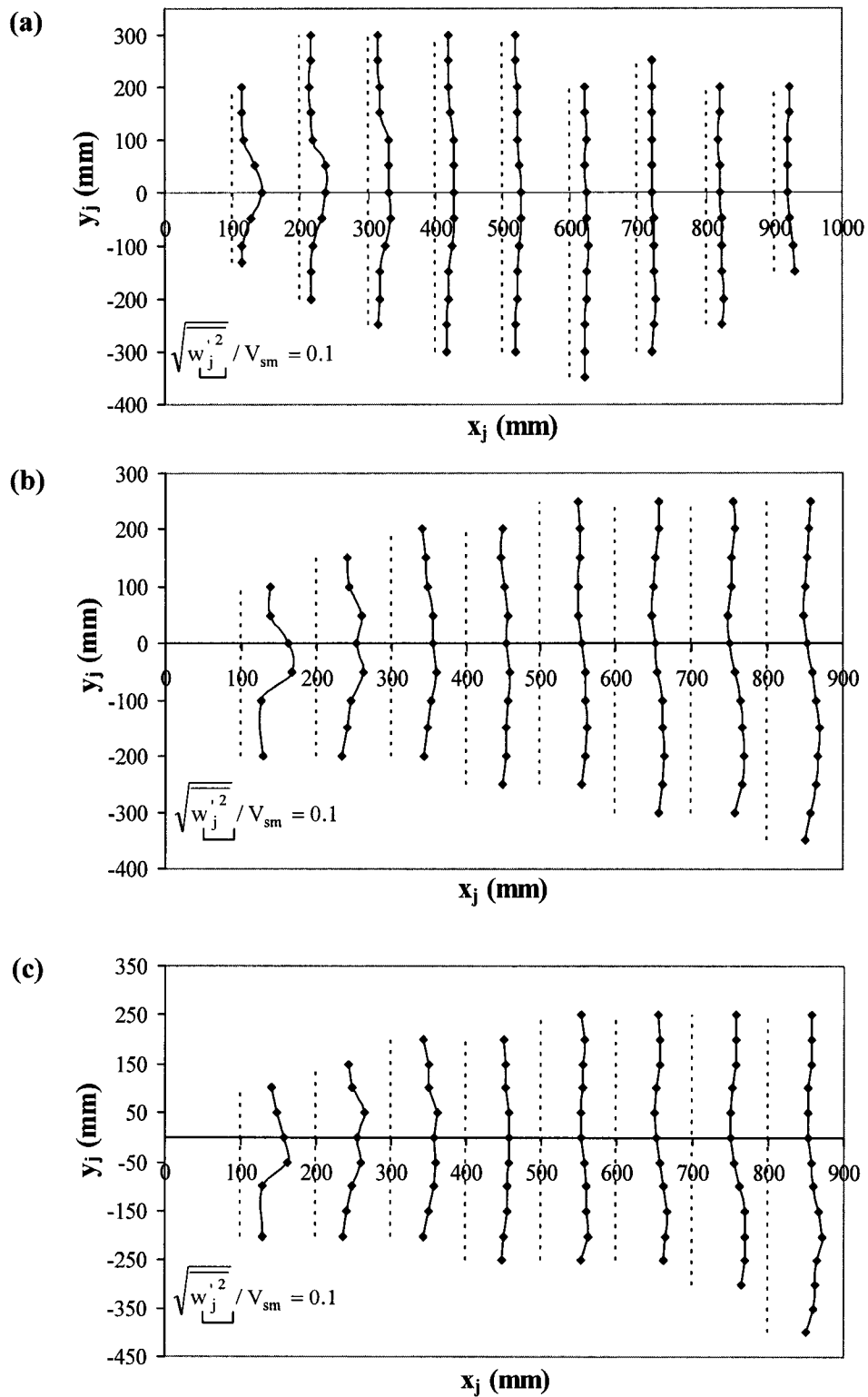


Fig. 4.38(a-c) Distribution of vertical turbulence intensity in jet for $S = 5.06\%$ and $Q = 31.2$ L/s: (a) $z = 10$ mm; (b) $z = 100$ mm; (c) $z = 150$ mm

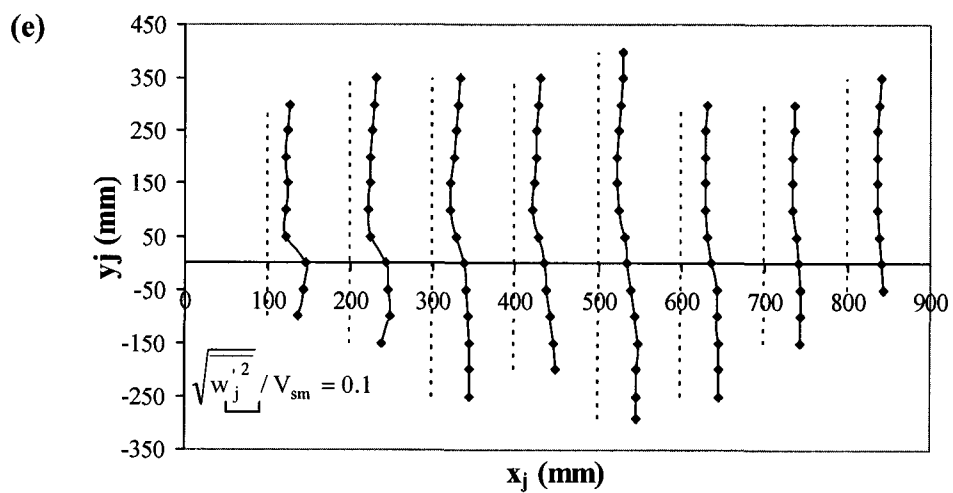
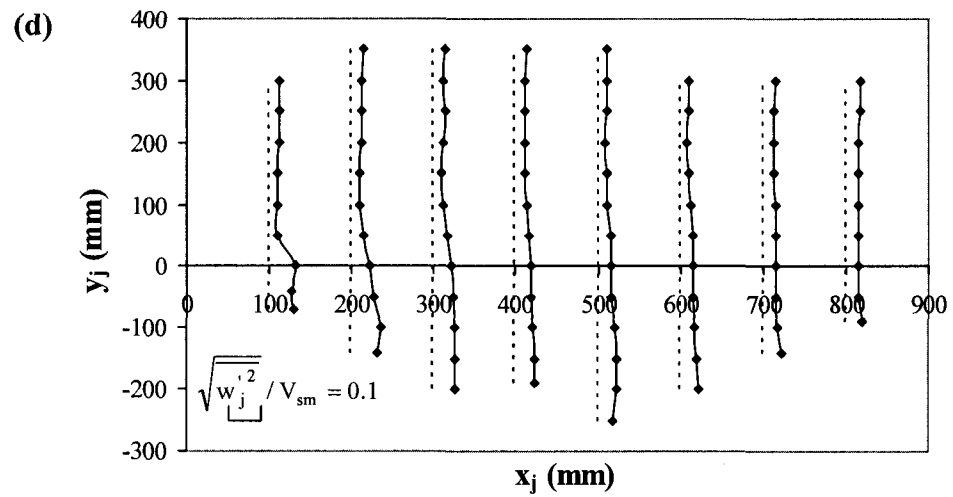


Fig. 4.38(d-e) Distribution of vertical turbulence intensity in jet for $S = 10.52\%$ and $Q = 31.2$ L/s: (d) $z = 10$ mm; (e) $z = 70$ mm

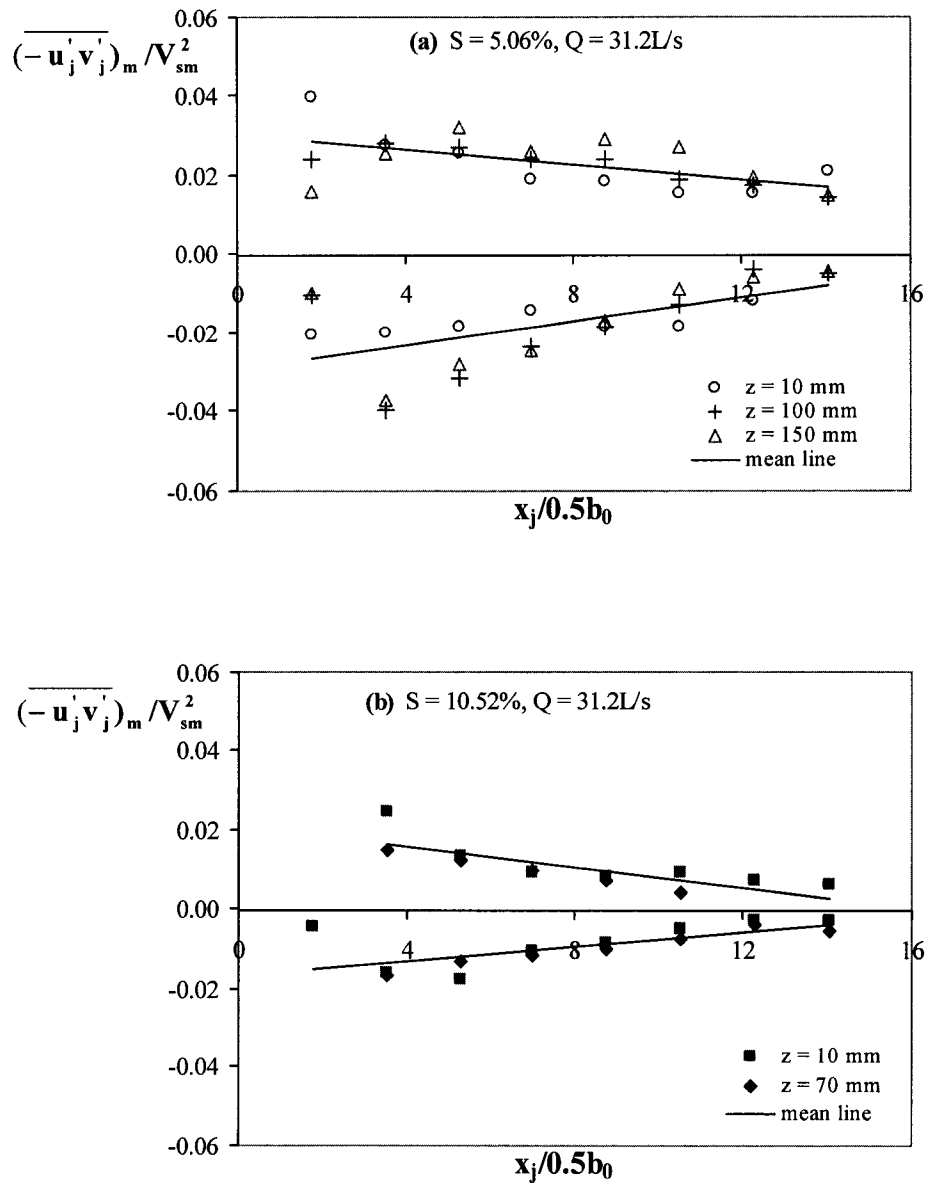


Fig. 4.39 Variation of normalized maximum Reynolds stress in jet flow with $x_j/0.5b_0$: (a) $S = 5.06\%$, $Q = 31.2 \text{ L/s}$; (b) $S = 10.52\%$, $Q = 31.2 \text{ L/s}$

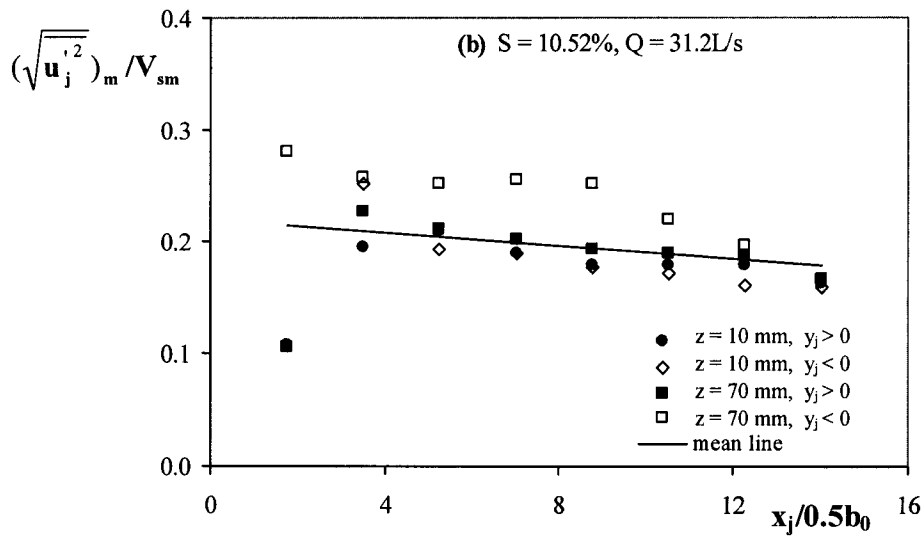
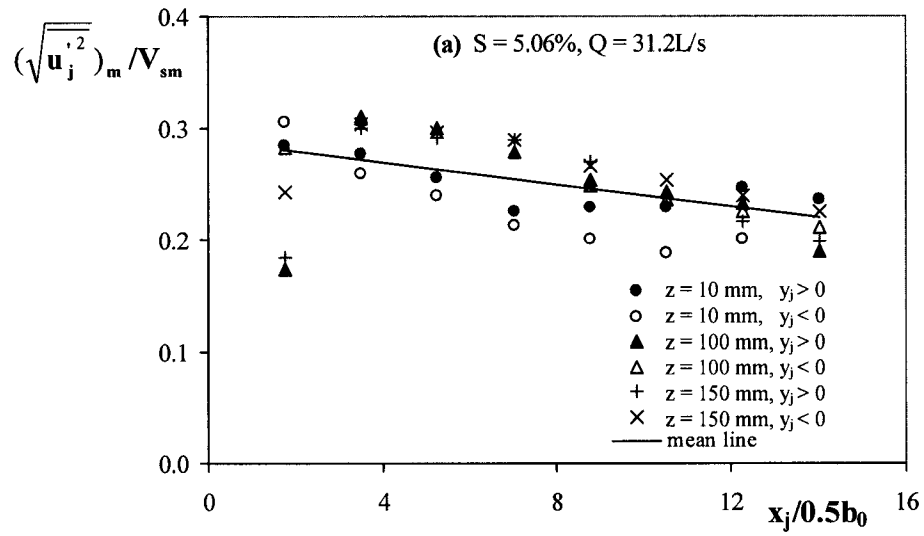


Fig. 4.40 Variation of normalized maximum longitudinal turbulence intensity in jet flow with $x_j/0.5b_0$: (a) $S = 5.06\%$, $Q = 31.2\text{ L/s}$; (b) $S = 10.52\%$, $Q = 31.2\text{ L/s}$

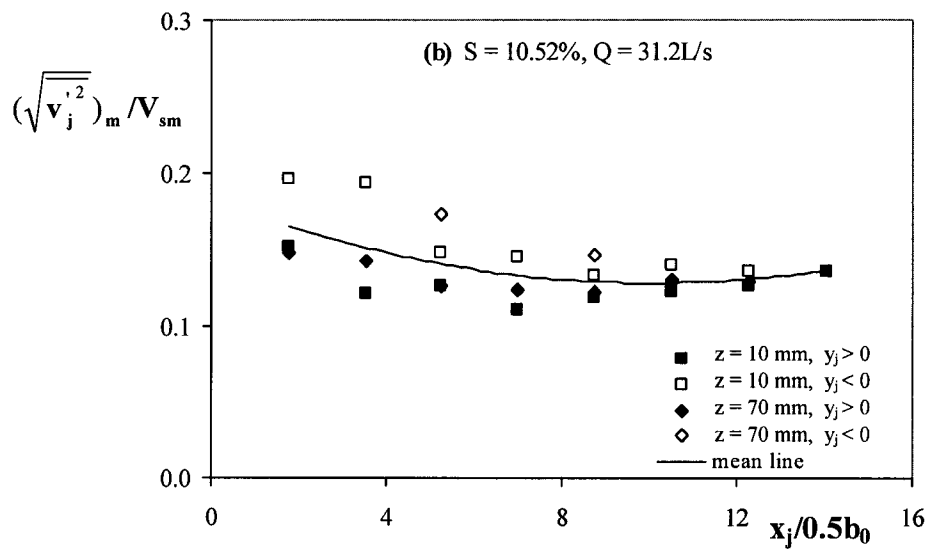
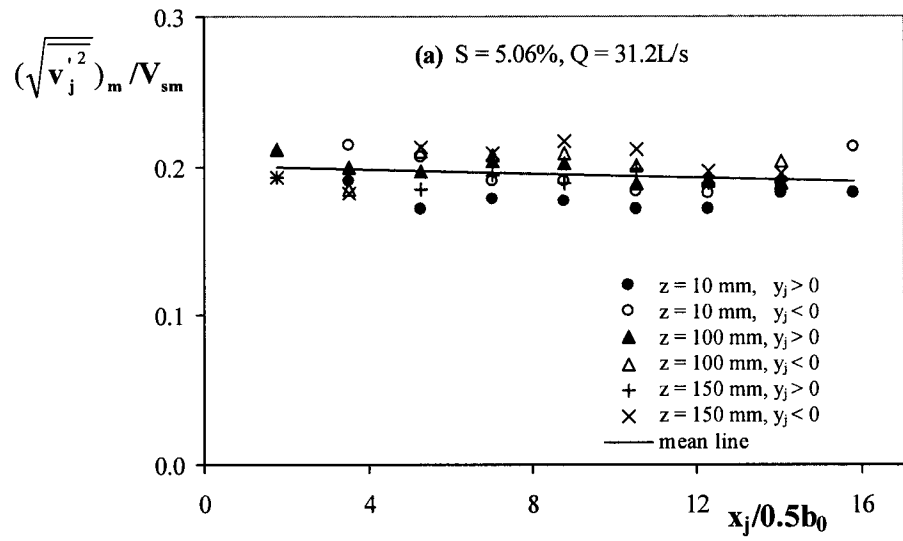


Fig. 4.41 Variation of normalized maximum transverse turbulence intensity in jet flow with $x_j/0.5b_0$: (a) $S = 5.06\%$, $Q = 31.2\text{ L/s}$; (b) $S = 10.52\%$, $Q = 31.2\text{ L/s}$

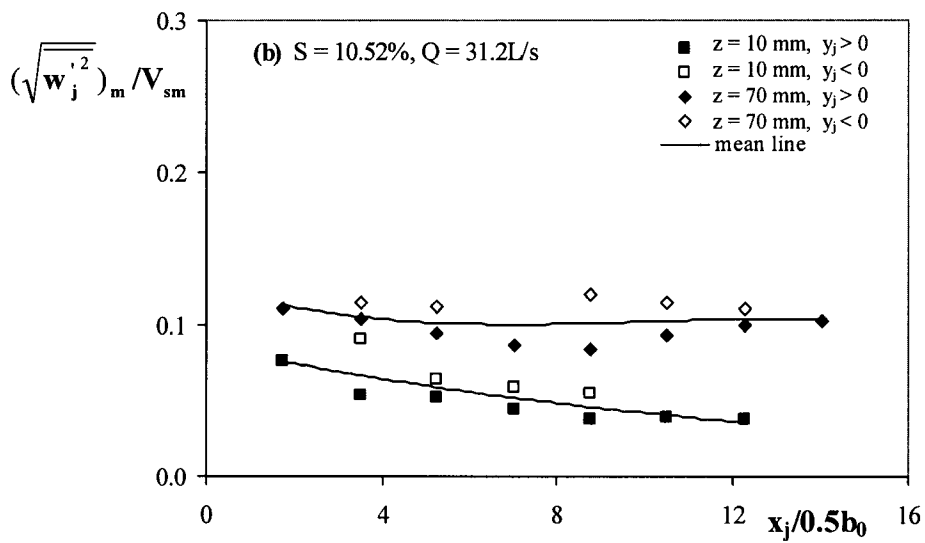
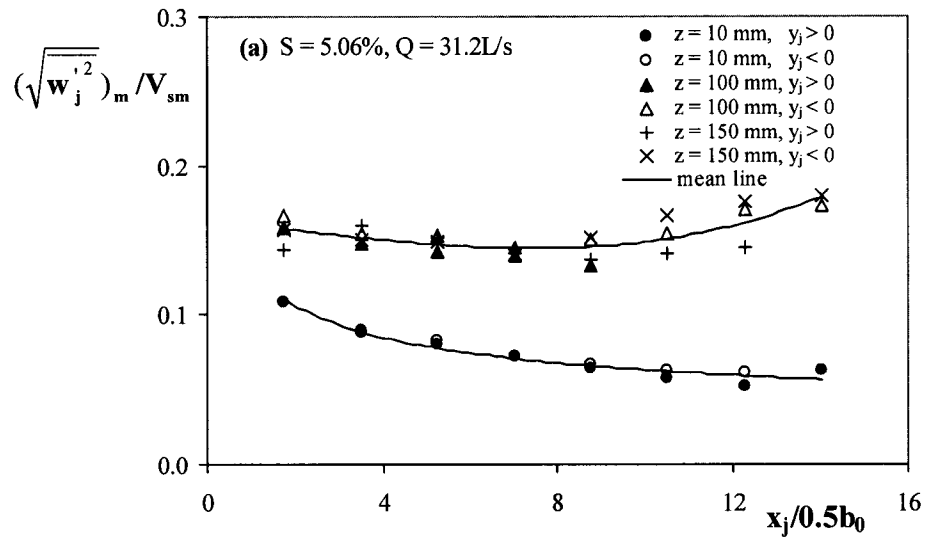


Fig. 4.42 Variation of normalized maximum vertical turbulence intensity in jet flow with $x_j/0.5b_0$: (a) $S = 5.06\%$, $Q = 31.2 \text{ L/s}$; (b) $S = 10.52\%$, $Q = 31.2 \text{ L/s}$

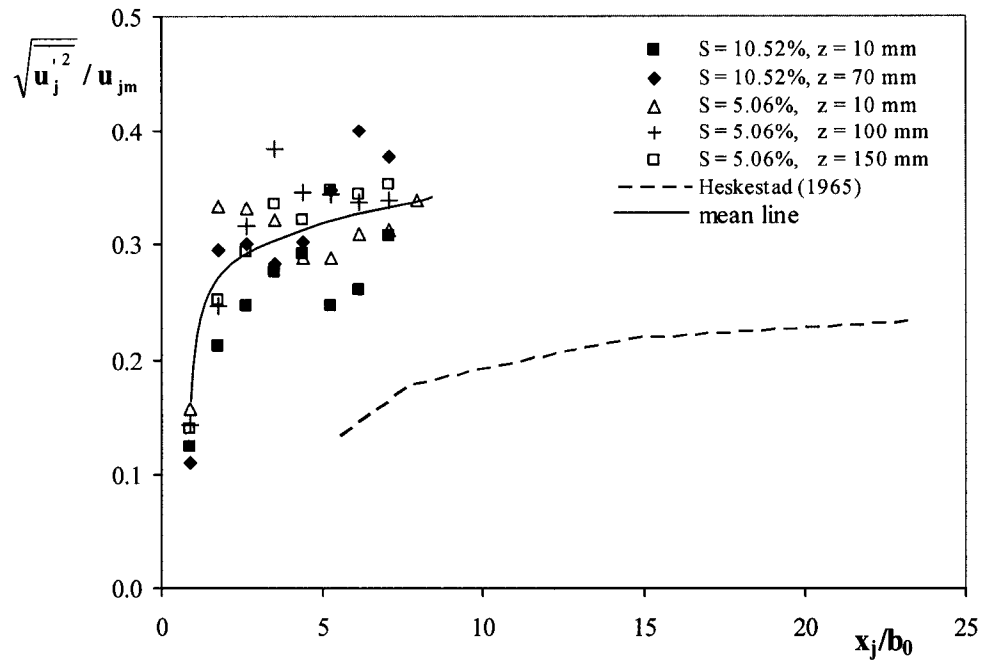


Fig. 4.43 Variation of longitudinal turbulence intensity along the jet center-line for $S = 5.06, 10.52\%$ and $Q = 31.2$ L/s

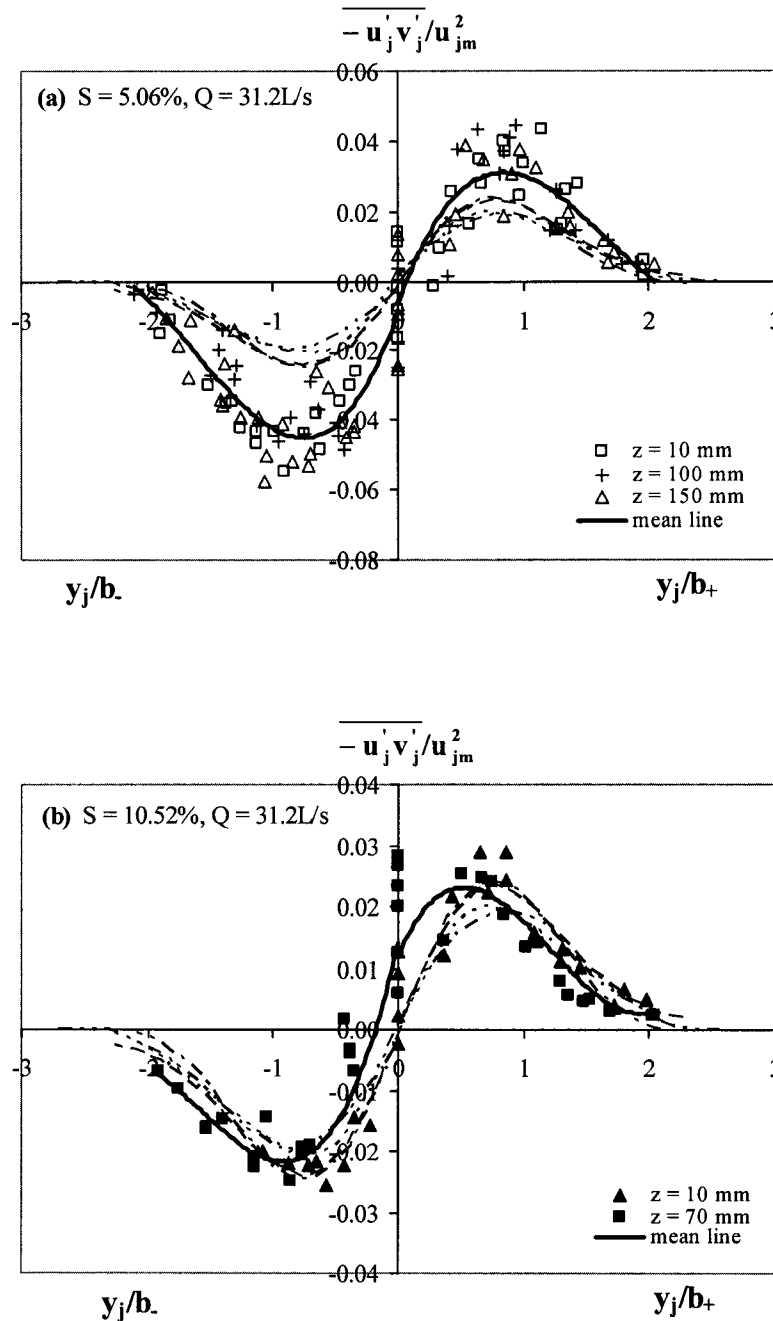


Fig. 4.44 Distribution of normalized Reynolds shear stress in jet flow:
 (a) $S = 5.06\%$, $Q = 31.2 \text{ L/s}$; (b) $S = 10.52\%$, $Q = 31.2 \text{ L/s}$; ---, Gutmark & Wygnanski (1976); - - - - -, Heskestad (1965); - · - · - ·, Bradbury (1965); - · - · - ·, Ramaprian & Chandrasekhara (1985)

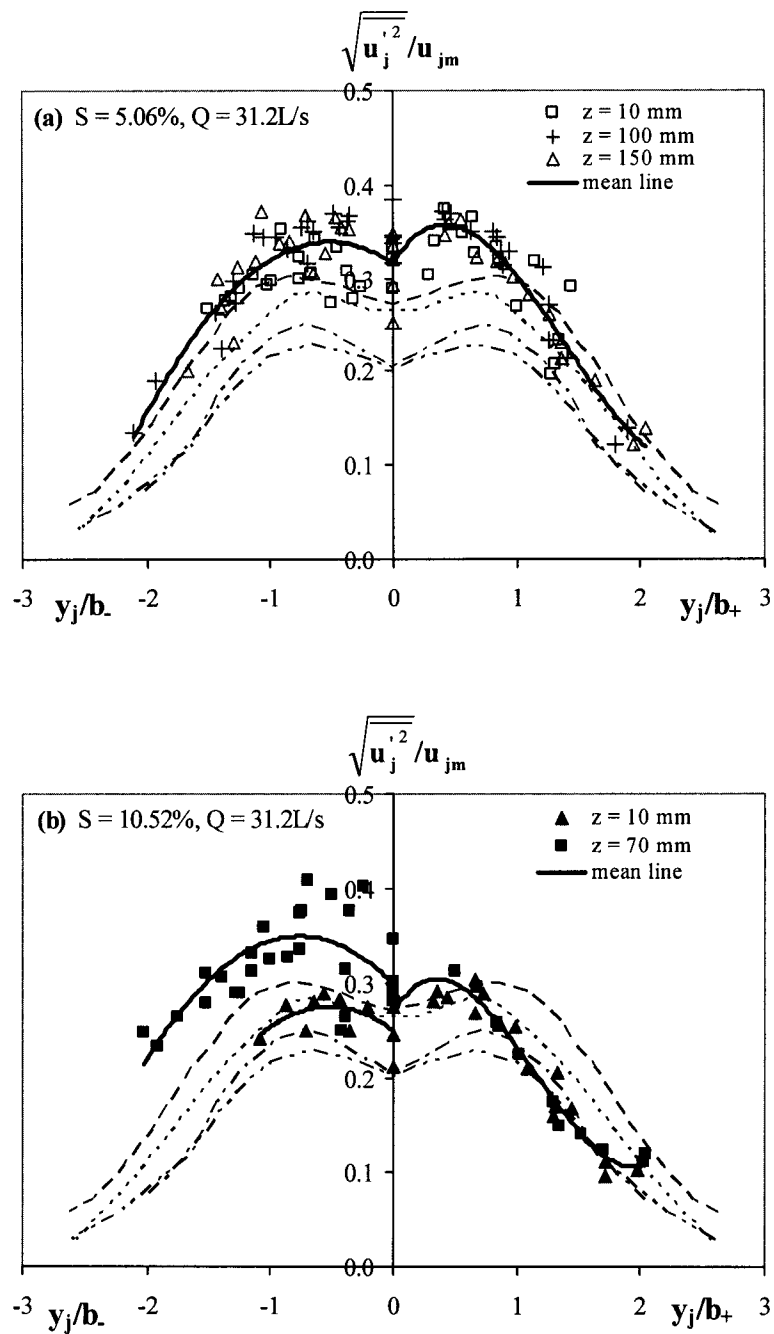


Fig. 4.45 Distribution of normalized longitudinal turbulence intensity in jet flow: (a) $S = 5.06\%$, $Q = 31.2 \text{ L/s}$; (b) $S = 10.52\%$, $Q = 31.2 \text{ L/s}$; ---, Gutmark & Wygnanski (1976); - - - - -, Heskestad (1965); - · - · - ·, Bradbury (1965); - · - · - ·, Ramaprian & Chandrasekhara (1985)

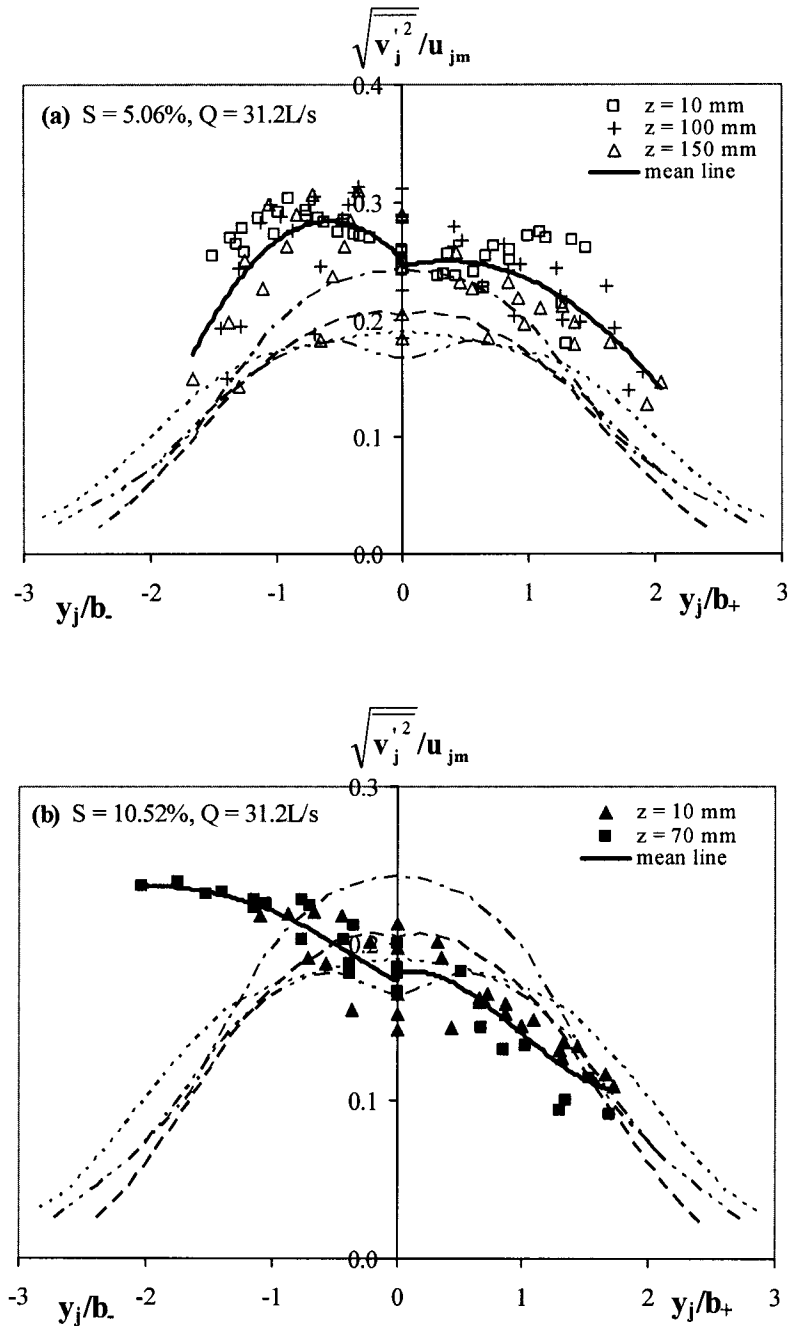


Fig. 4.46 Distribution of normalized transverse turbulence intensity in jet flow: (a) $S = 5.06\%$, $Q = 31.2 \text{ L/s}$; (b) $S = 10.52\%$, $Q = 31.2 \text{ L/s}$; ---, Gutmark & Wygnanski (1976); ----, Heskstad (1965); -·-·-, Bradbury (1965); -·-·-, Ramaprian & Chandrasekhara (1985)

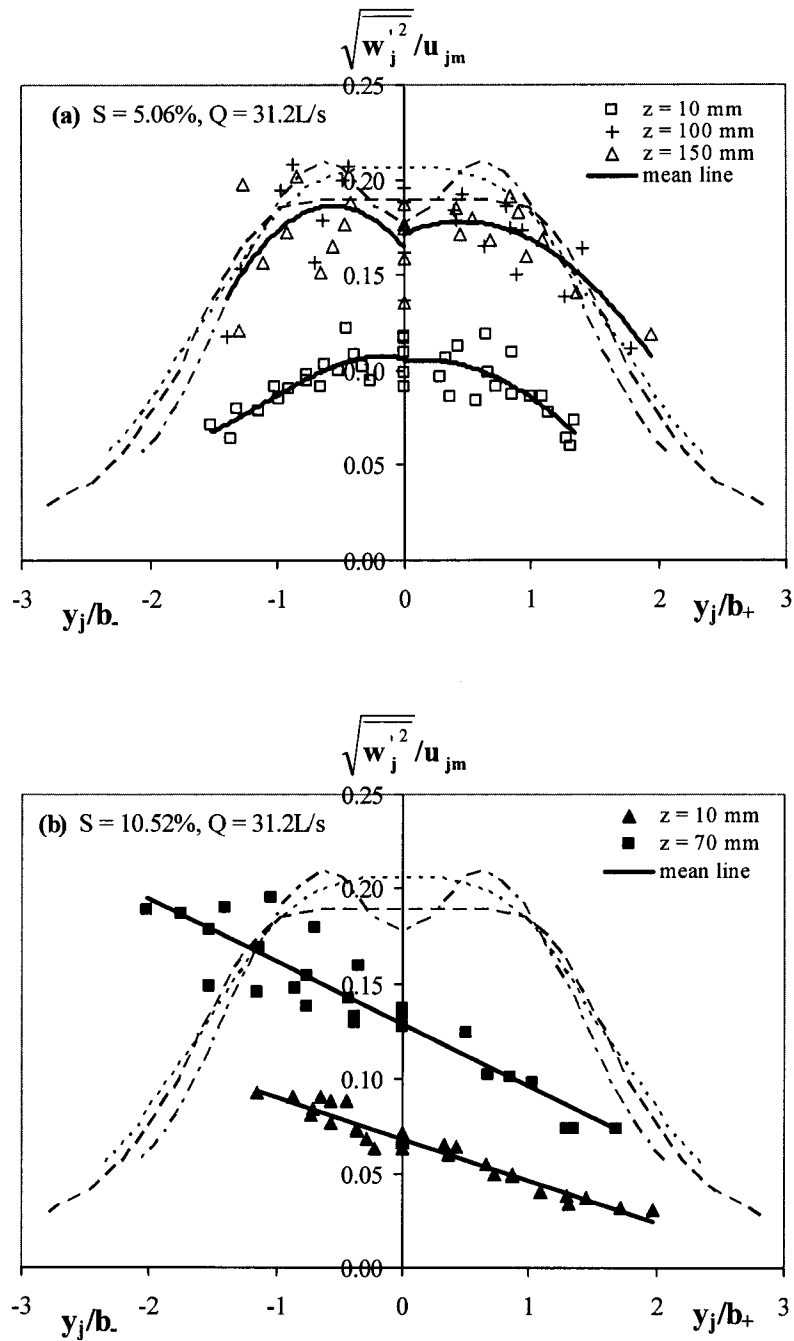


Fig. 4.47 Distribution of normalized vertical turbulence intensity in jet flow: (a) $S = 5.06\%$, $Q = 31.2 \text{ L/s}$; (b) $S = 10.52\%$, $Q = 31.2 \text{ L/s}$; ---, Gutmark & Wygnanski (1976); - - - - -, Heskestad (1965); - · - · - ·, Bradbury (1965); - · - · - ·, Ramaprian & Chandrasekhara (1985)

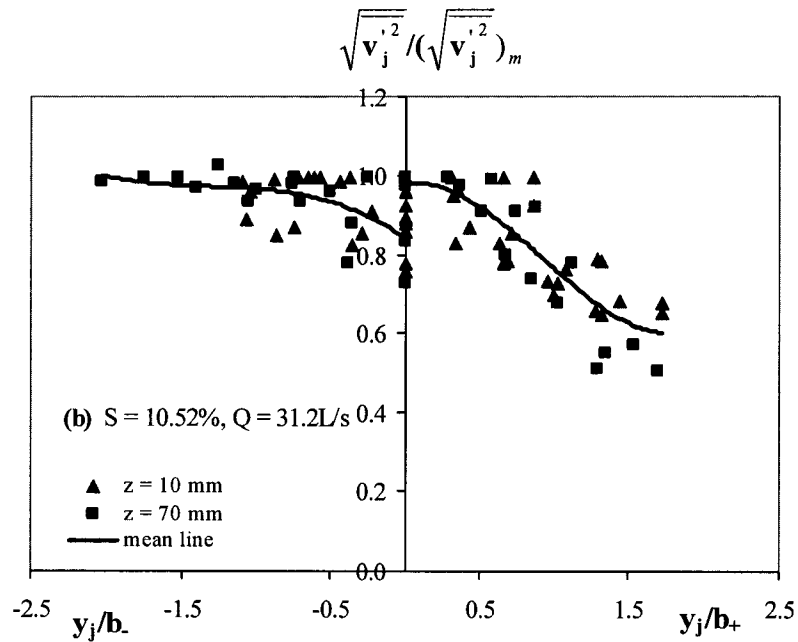
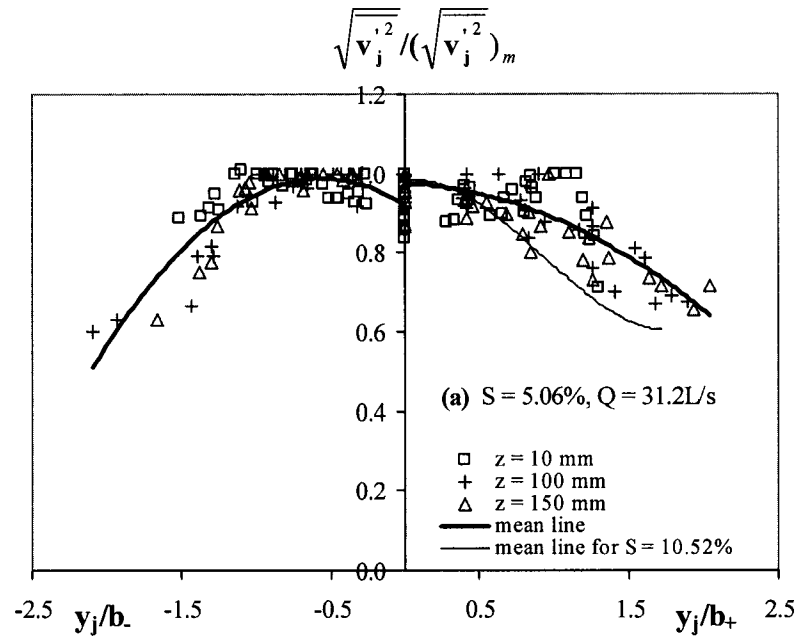


Fig. 4.49 Distribution of normalized transverse turbulence intensity in jet flow: (a) $S = 5.06\%$, $Q = 31.2\text{ L/s}$; (b) $S = 10.52\%$, $Q = 31.2\text{ L/s}$

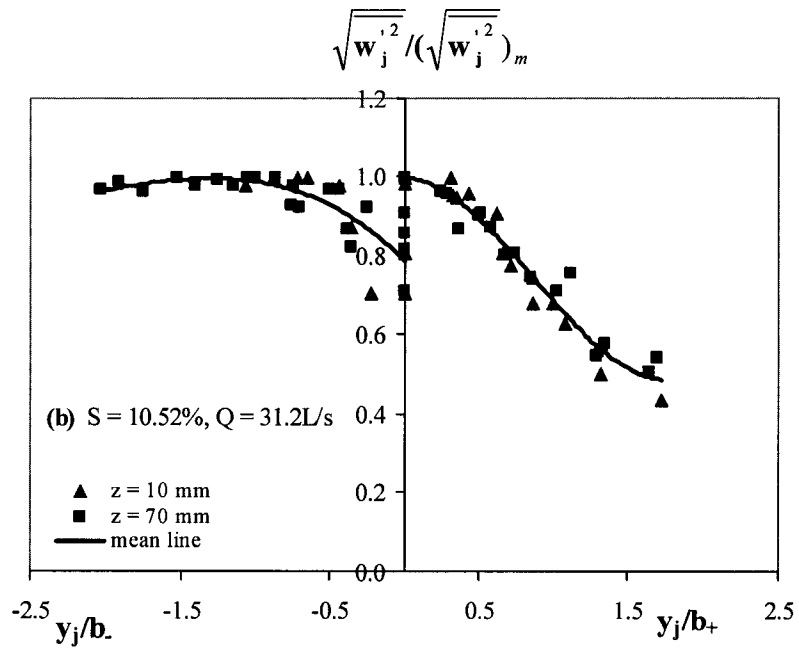
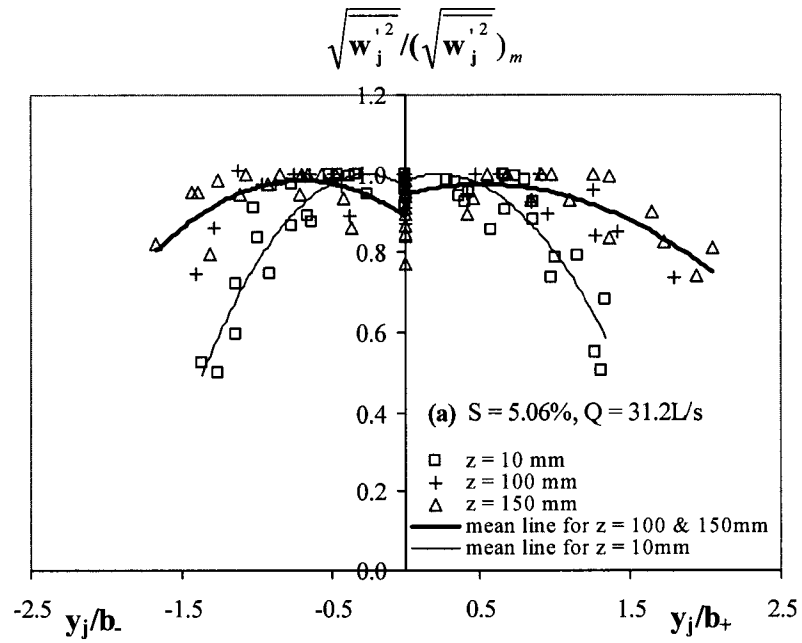


Fig. 4.50 Distribution of normalized vertical turbulence intensity in jet flow: (a) $S = 5.06\%$, $Q = 31.2 \text{ L/s}$; (b) $S = 10.52\%$, $Q = 31.2 \text{ L/s}$

Chapter 5

Conclusions and Recommendation for Further Research

In the preceding three chapters, we have presented the results of investigations of MicroADV and turbulence measurements and structure in hydraulic jumps and vertical slot fishways. A hydraulic jump may be treated as the case of a plane turbulent wall jet under adverse pressure gradient and with a finite depth of flow (Rajaratnam 1965). The jet flow in the pools of a vertical slot fishway is presented as the case of a plane turbulent free jet with recirculating flow on the sides in chapter 3 and by Wu et al. (1999). Therefore, the two problems studied here can be broadly categorized as studies on turbulent jets. This chapter summarizes the contributions made to these flows and suggests further research work.

Chapter 2 presented the finding of the air concentration and boundary effects on the measurements of MicroADV. A 16 MHz down-looking MicroADV by SonTek was tested in free hydraulic jumps. The mean velocity measured by MicroADV was compared to that obtained by Prandtl tube. For the air concentration $< 2.2\%$ in the area of sampling volume of MicroADV, the relative error of MicroADV measurements is a linear function of the air concentration with a relative error of about 15% for an air concentration of 1%. This result is different from that obtained by Matos et al. (2002). They found that ADV can provide reasonably accurate velocity measurements for the air concentration up to 8%. It is probably because that in their experiments, the air flow was produced from the bottom of the

flume whereas in hydraulic jumps the situation is different. In hydraulic jumps, the ADV probe was in a dense air bubble cloud which had a much higher value of air concentration than that at the measurement point. Special experiments may have to be carried out to understand the effect of this dense air bubble on the measurements of ADV.

The boundary shows no effect on the measurements of MicroADV if the distance from the measurement point to the boundary is larger than 3 cm. In this case, the relative error is less than 6% which is reasonable considering the measurement error of Prandtl tube in turbulent flows. However, the relative error of MicroADV measurements is about 3 ~ 15% for a distance ranging from 1 to 3 cm, and 11 ~ 23% for a distance of 0.5 cm. It is noticed that the range of the relative error is significantly large for the distance from the measurement point to the boundary equal to or less than 3 cm. It is probably because that the experiments were carried out under different flume bottom conditions. Some were on the aluminum bed and others on the bed which was carefully painted. Further experiments are needed to test the effects of bed smoothness and material on the MicroADV measurements.

Chapter 3 presented the results of an experimental study on the turbulence structure of free hydraulic jumps with Froude numbers of 2.0, 2.5 and 3.32. The instantaneous velocity field was obtained by the MicroADV studied in chapter 2. The longitudinal mean velocity was corrected for errors due to air bubbles and boundary using the results of Chapter 2 or Liu et al. (2002). The corrected values agreed very well with those obtained by Prandtl tube for $F_1 = 2.0$ and 2.5, but not for

$F_1 = 3.32$. The turbulence measurements in this study agree well with the limited observations of Resch and Leutheusser (1972a, 1972b). The study showed the existence of some degree of similarity in the Reynolds stress and turbulence intensities within the jump. The maximum turbulence intensities, turbulence kinetic energy and Reynolds stress decrease rapidly with the increasing longitudinal distance within the jump and gradually level off in the transition region from the jump to open channel flow. The maximum turbulence kinetic energy can be predicted using a linear relationship with the longitudinal distance within the jump. The Kolmogorov - 5/3 law was used to estimate the energy dissipation rate. It was observed that for $y/b < 0.4$ the dissipation rates are very small, and then quickly increase with y/b within the jump. The Kolmogorov length scale varies from 0.04 mm within the jump to 0.15 mm at the end of the transition region. The dominant frequency is in the range from 0 to 4 Hz for both horizontal and vertical velocity components. These results would also be important for testing of CFD results or any turbulence model.

Because the sampling volume of MicroADV is about 5 cm below the probe tip and the water surface fluctuates, no results were obtained in the surface roller region. The range of Froude numbers studied in this thesis is very limited due to the limitation of MicroADV used in bubbly flows. Most stilling basins are designed for Froude numbers greater than this range. Therefore, the accomplishment of the study on the turbulence structure of hydraulic jumps needs further extension to the surface roller region and higher Froude numbers.

In chapter 4, the turbulence structure of flow in the vertical slot fishways was

studied for the slopes of 5.06 and 10.52% and discharges of 31.2 and 52 L/s. A MicroADV was used to obtain the instantaneous velocity field. This contribution is related to the overall structure of flow in the pools and the structure of jet flow. It was found that two flow patterns, patterns 1 and 2 (see Fig. 4.1), existed. Pattern 1 occurs for $S = 5.06\%$ with the two discharges. For $S = 10.52\%$, pattern 2 occurs for $Q = 31.2$ L/s whereas the flow was not stable for $Q = 52$ L/s but showed pattern 1 over 600 seconds average. Two flow regions were formed in the pools: jet flow and recirculating flow. The flow is three dimensional but the vertical velocity remains at a small value in most areas of the pool which would allow fish to choose any preferred swimming depth. The experimental results showed that the mean flow kinetic energy decays rapidly in a small area in the jet flow region whereas it has a small value in the recirculation region, which is desirable for fish passage. The Reynolds stress, and longitudinal and transverse turbulence intensities decrease along the jet flow while they remain at very small values in the recirculation region. The vertical turbulence intensity is close to being uniform with small values in the planes parallel to the bottom of the flume. The maximum turbulence kinetic energy in the pools is less than 8% of V_{sm}^2 which would enable fish to ascend without undue stress. It was found that most of the areas in the pool have a lower dissipation rate which is less than $0.2 \text{ m}^2/\text{s}^3$.

As for the structure of the jet flow in the pools, it appears that the non-dimensional mean velocity profile agrees very well with that of the plane turbulent jet in the center part with some scatter at the ends, which is believed to be due to the

recirculating flow. There is no potential core for the jet formed at the slot in the vertical slot fishway. The decay rate of the maximum velocity is larger than that in a plane turbulent jet. The jet grows linearly with the longitudinal distance to approximate $5b_0$, and then the growth rate reduces when the jet approaches the sidewall between the long baffles for flow pattern 2 or the jet turns to the next slot for flow pattern 1. The growth rate of the jet in the pool is about 1.9 to 2.7 times that of the plane turbulent jet and the jet grows wider at the planes close to the bottom. The jet presents different turbulence structure for the two flow patterns and for each flow pattern the turbulence characteristics appear different between the left and right halves of the jet. These differences are due to the effect of the recirculating flow on both sides of the jet for flow pattern 1 and on the left side of the jet for flow pattern 2, the effect of the sidewall and long baffle on the right half of the jet for flow pattern 2, and the effect of the bed. For flow pattern 2, the similarity profile of the Reynolds stress agrees well with that of the plane turbulent jet but with a shift of the zero point to the right side of the jet center-line. The profiles of both longitudinal and transverse turbulence intensities on the left half of the jet show a good similarity and are similar to the plane turbulent jet whereas on the right half of the jet, they present different structures due to the effect of the sidewall and long baffle on the jet. For flow pattern 1, the profiles of Reynolds stress and longitudinal and transverse turbulence intensities have a higher value than the plane turbulent jet and are not symmetric to the jet center-line but show some similarity on either side. The vertical turbulence intensity for both flow patterns is smaller at the plane near to the bed compared to

the planes far from the bed. For the planes far from the bed, the profile is similar to that of the plane turbulent jet for $S = 5.06\%$, but it shows a linear relationship for $S = 10.52\%$ which is different from the plane jet.

There are still many aspects left to be studied such as steeper slopes, more discharges and more detailed turbulence velocity measurements. The overall flow structure indicates that the flow characteristics in the recirculation region are different from those in the jet flow. It would be useful to further study the recirculating flow which will help understand the difference between the jet produced at the slot and the plane turbulent jet.

References:

- Liu, M., Zhu, D. Z., and Rajaratnam, N. (2002). "Evaluation of ADV measurements in bubbly two-phase flows." *Proceedings of the Conference of Hydraulic Measurements & Experimental Methods 2002*, Estes Park, Colorado, USA. (CD Rom)
- Matos, Jorge, Frizell, Kathleen. H., André, Stéphanie., and Frizell, K. Warren. (2002). "On the performance of velocity measurement techniques in air-water flows." *Proceedings of the Conference of Hydraulic Measurements & Experimental Methods 2002*, Estes Park, Colorado, USA. (CD Rom)
- Rajaratnam, N. (1965). "The hydraulic jump as a wall jet." *J. Hydraul. Division*, ASCE, 91(HY5), 107–132.
- Resch, F. J., and Leutheusser, H. J. (1972a). "Reynolds stress measurements in

hydraulic jumps.” *J. Hydraul. Res.*, 10(4), 409–429.

Resch, F. J., and Leutheusser, H. J. (1972b). “Le ressaut hydraulique: mesures de turbulence dans la région diphasique.” *La Houille Blanche*, 4, 279–293.

Wu, S., Rajaratnam, N. and Katopodis, C. (1999). “Structure of flow in vertical slot fishway.” *J. Hydraul. Eng.*, 125(4), 351–360.

Appendix

A1. Experimental Study on Turbulence Structure in Hydraulic Jumps

A1.1 Water surface profile for $F_1 = 2.0, 2.5, 3.32$

$F_1 = 2.0, Q = 54.9 \text{ L/s}$

$x \text{ (cm)}$	$y \text{ (cm)}$
0	7.1
13	11.9
23	14.0
33	15.0
43	15.9
53	16.4
63	16.7
73	17.1
93	17.16
113	17.16
133	17.16
253	17.16
270	17.16

$F_1 = 2.5, Q = 68.6 \text{ L/s}$

$x \text{ (cm)}$	$y \text{ (cm)}$
0	7.1
13	11.6
23	14.0
33	15.9
43	17.8
53	18.9
63	19.7
73	20.5
93	21.2
113	21.6
153	21.6
193	21.6
233	21.6
350	21.6

$F_1 = 3.32, Q = 40 \text{ L/s}$

$x \text{ (cm)}$	$y \text{ (cm)}$
0	4.1
8.5	5.6
15	6.7
25	9.4
35	11.6
45	13.0
55	14.5
65	15.4
75	15.9
85	16.1
105	16.4
125	16.5
165	16.5
270	16.5

A1.2 Mean velocity for $F_1 = 2.0$, $Q = 54.9$ L/s, $y_1 = 7.1$ cm

x (cm)	Processed MicroADV data				Prandtl tube measurements	
	y (cm)	u (cm/s)	v (cm/s)	w (cm/s)	y (cm)	u (cm/s)
13	0.61	139.73	1.60	-5.62	0.52	157.1
13	1.02	146.99	1.31	-2.47	1.02	157.8
13	2.51	135.32	2.67	1.24	2.51	157.8
13	3.03	133.93	3.65	4.13	3.04	157.8
13	3.50	143.54	5.29	4.39	3.99	157.1
23	0.56	121.43	0.72	-3.30	0.56	137.2
23	1.08	131.91	1.75	-1.15	1.03	142.8
23	2.31	124.02	1.95	0.65	2.31	142.8
23	3.06	122.36	3.25	2.80	3.03	142.8
23	4.01	128.96	5.04	4.48	4.01	140.0
23	5.00	115.23	7.34	6.27	5.00	133.6
23	6.00	94.65	8.89	5.40	6.00	126.8
23	6.52	80.96	10.17	5.21	7.01	110.2
33	0.53	91.31	0.68	-5.37	0.51	118.8
33	1.02	116.81	0.64	-2.11	1.02	127.5
33	2.44	110.45	1.26	0.60	2.44	128.3
33	3.02	109.04	2.02	1.40	3.02	129.1
33	4.00	116.06	3.93	2.91	4.00	123.6
33	5.03	106.40	5.61	4.22	5.03	116.3
33	6.00	96.77	7.38	4.33	6.00	111.1
33	6.99	83.05	9.03	4.41	6.99	101.9
33	8.06	67.52	9.76	3.83	8.06	86.3
33	8.57	55.07	9.26	3.40	9.02	71.4
43	0.63	81.72	-0.03	-5.79	0.56	107.5
43	1.05	101.76	0.26	-0.22	1.05	114.6
43	2.40	101.45	1.02	0.61	2.40	117.1
43	3.03	100.65	1.89	1.79	3.03	115.4
43	4.04	107.30	3.32	1.68	4.04	113.7
43	5.06	98.45	4.64	3.05	5.06	104.8
43	6.05	90.84	5.97	3.68	6.05	99.0
43	7.00	77.67	6.54	3.56	7.00	90.7
43	8.08	67.35	7.36	3.51	8.08	77.9
43	9.05	58.55	8.19	3.77	9.05	70.0
43	9.52	49.09	7.24	2.91	10.08	59.4
53	0.60	80.94	-0.18	-2.00	0.53	89.6
53	1.01	92.09	-0.13	0.74	1.01	101.0
53	2.31	92.70	0.38	1.41	2.31	106.6
53	3.00	91.60	1.34	1.79	3.00	109.3
53	4.01	96.84	2.43	2.50	4.01	102.9
53	5.05	91.09	3.62	2.99	5.05	99.0

A1.2 Mean velocity for $F_1 = 2.0$, $Q = 54.9$ L/s, $y_1 = 7.1$ cm (continued)

x (cm)	Processed MicroADV data				Prandtl tube measurements	
	y (cm)	u (cm/s)	v (cm/s)	w (cm/s)	y (cm)	u (cm/s)
53	6.02	80.35	4.20	2.97	6.02	87.4
53	7.04	75.50	4.69	3.84	7.04	84.0
53	8.01	65.38	5.24	3.54	8.01	76.7
53	9.07	57.57	5.26	3.18	9.07	71.4
53	10.03	51.58	5.71	2.97	10.03	57.7
53	10.43	44.80	5.07	2.34	10.88	52.4
63	0.64	69.92	-0.25	-1.48	0.64	87.4
63	1.01	80.40	-0.25	-1.05	1.01	95.0
63	2.48	85.64	0.36	1.16	2.48	103.8
63	3.03	84.97	0.86	1.14	3.03	101.0
63	4.04	92.32	1.85	1.16	4.04	100.0
63	5.07	87.98	2.42	1.92	5.07	92.9
63	6.02	77.35	2.71	2.10	6.02	86.3
63	7.05	69.21	2.60	2.12	7.05	81.6
63	8.00	62.26	2.76	2.15	8.00	76.7
63	9.08	60.27	3.78	2.85	9.08	67.1
63	10.04	52.98	3.48	2.45	10.04	62.6
63	10.98	46.67	3.70	2.08	11.00	59.4
63	11.95	37.00	4.69	2.33	11.95	50.5
73	0.59	69.94	-0.29	-1.33	0.55	80.4
73	1.07	78.75	0.10	0.28	1.07	87.4
73	2.30	79.99	0.19	1.09	2.30	92.9
73	3.01	80.07	0.86	1.33	3.01	95.0
73	4.02	86.58	1.56	1.60	4.02	92.9
73	5.04	80.82	1.93	2.23	5.04	85.2
73	6.04	75.41	2.13	2.31	6.04	81.6
73	7.05	68.88	1.90	2.11	7.05	79.2
73	8.04	65.54	2.40	2.23	8.04	74.1
73	9.03	59.56	2.24	2.30	9.03	70.0
73	10.04	56.23	2.54	2.43	10.04	62.6
73	11.01	49.52	1.95	2.77	11.01	59.4
73	11.55	46.49	2.15	2.84	12.03	54.2
93	0.57	60.00	0.24	-1.13	0.57	74.1
93	1.00	68.82	0.00	0.21	1.00	77.9
93	2.41	71.16	-0.03	0.37	2.41	85.2
93	3.05	71.93	-0.07	0.70	3.05	86.3
93	4.05	77.49	0.32	1.53	4.05	80.4
93	5.04	76.01	0.33	1.89	5.04	79.2
93	6.02	73.10	0.28	1.49	6.02	77.9
93	7.02	69.37	0.13	2.29	7.02	74.1
93	8.04	63.54	-0.49	2.53	8.04	71.4

A1.2 Mean velocity for $F_1 = 2.0$, $Q = 54.9$ L/s, $y_1 = 7.1$ cm (continued)

x (cm)	Processed MicroADV data				Prandtl tube measurements	
	y (cm)	u (cm/s)	v (cm/s)	w (cm/s)	y (cm)	u (cm/s)
93	9.02	63.67	0.15	2.56	9.02	70.0
93	10.00	58.91	-0.09	2.71	10.00	67.1
93	11.04	56.62	0.11	3.21	11.04	62.6
93	12.04	53.21	-0.15	3.22	12.04	64.2
113	0.58	59.50	-0.07	-0.41	0.53	70.0
113	1.07	65.22	-0.06	-0.33	1.07	74.1
113	2.45	66.06	-0.73	0.27	2.45	77.9
113	3.17	68.01	-0.50	0.96	3.04	77.9
113	4.00	74.65	-0.18	1.01	4.00	77.9
113	5.04	73.21	-0.17	1.47	5.04	76.7
113	6.07	70.07	-0.86	1.39	6.07	75.4
113	7.09	70.05	-0.58	2.31	7.09	74.1
113	8.00	66.19	-1.46	1.98	8.00	71.4
113	9.04	64.66	-1.23	2.44	9.04	68.6
113	10.03	62.70	-1.55	2.74	10.03	68.6
113	11.02	61.13	-1.22	3.14	11.02	67.1
113	11.58	59.56	-1.69	3.71	12.01	64.2
133	0.53	53.89	0.22	-2.12	0.53	62.6
133	0.98	62.36	0.10	0.38	0.98	67.1
133	2.01	66.35	-0.56	0.36	2.01	70.0
133	2.53	63.88	-0.60	0.34	2.53	72.7
133	3.04	64.11	-0.55	1.23	3.04	75.4
133	4.00	72.29	-0.26	1.42	4.00	74.1
133	5.03	71.69	-0.46	1.82	5.03	71.4
133	6.05	70.84	-0.85	1.86	6.05	71.4
133	7.05	69.41	-0.91	2.30	7.05	71.4
133	8.03	68.12	-1.08	2.34	8.03	68.6
133	9.06	67.67	-1.20	3.04	9.06	67.1
133	10.06	65.56	-1.45	3.18	10.06	67.1
133	11.04	64.84	-1.83	4.00	11.04	67.1
133	12.03	63.26	-1.62	4.12	12.03	65.7
173	0.61	54.08	0.08	-0.11	0.57	62.6
173	1.04	58.71	0.01	0.75	1.04	64.2
173	2.01	63.41	-0.03	1.12	2.01	65.7
173	2.53	60.48	-0.62	1.19	2.53	68.6
173	3.00	62.57	-0.56	1.57	3.00	70.0
173	4.01	69.83	-0.39	1.65	4.01	70.0
173	5.04	69.83	-0.66	2.09	5.04	70.0
173	6.02	69.45	-0.92	2.79	6.02	70.0
173	7.07	69.50	-1.00	2.78	7.07	70.0
173	8.05	69.15	-1.30	3.33	8.05	70.0

A1.2 Mean velocity for $F_1 = 2.0$, $Q = 54.9$ L/s, $y_1 = 7.1$ cm (continued)

x (cm)	Processed MicroADV data				Prandtl tube measurements	
	y (cm)	u (cm/s)	v (cm/s)	w (cm/s)	y (cm)	u (cm/s)
173	9.06	68.80	-1.68	3.66	9.06	71.4
173	10.03	68.19	-1.65	3.95	10.03	71.4
173	11.04	68.26	-1.57	4.43	11.04	71.4
213	0.66	50.26	-0.43	-0.96	0.52	59.4
213	1.04	57.69	-0.57	0.70	1.04	62.6
213	2.01	60.85	-0.45	0.94	2.01	65.7
213	2.53	59.40	-0.91	1.44	2.53	67.1
213	3.06	60.46	-1.25	1.50	3.06	67.1
213	4.03	68.86	-0.97	1.71	4.03	68.6
213	5.06	68.90	-1.03	2.12	5.06	68.6
213	6.07	69.75	-1.37	2.49	6.07	68.6
213	7.02	69.91	-1.34	2.83	7.02	70.0
213	8.06	70.01	-1.65	3.02	8.06	70.0
213	9.01	70.44	-1.92	3.58	9.01	70.0
213	10.01	69.26	-1.85	3.77	10.01	71.4
213	11.04	70.04	-1.90	4.23	11.04	71.4
253	0.63	49.68	-0.22	-1.70	0.55	56.0
253	1.05	55.85	-0.29	0.76	1.05	59.4
253	2.02	60.81	-0.22	1.35	2.02	62.6
253	2.47	59.20	-0.75	1.17	2.47	64.2
253	3.08	60.03	-0.92	1.46	3.08	65.7
253	4.01	68.42	-0.49	1.55	4.01	67.1
253	5.01	69.12	-0.72	2.11	5.01	67.1
253	6.02	69.64	-0.86	2.53	6.02	68.6
253	7.05	69.99	-1.00	2.83	7.05	68.6
253	8.06	70.39	-1.40	3.21	8.06	70.0
253	9.02	71.12	-1.53	3.52	9.02	70.0
253	10.06	70.93	-1.46	3.85	10.06	70.0
253	11.01	70.47	-1.61	4.12	11.01	70.0

A1.3 Mean velocity for $F_1 = 2.5$, $Q = 68.6$ L/s, $y_1 = 7.1$ cm

x (cm)	Processed MicroADV data				Prandtl tube measurements	
	y (cm)	u (cm/s)	v (cm/s)	w (cm/s)	y (cm)	u (cm/s)
13	0.57	187.50	3.82	3.14	0.71	205.8
13	2.55	174.00	9.14	2.19	2.79	207.2
13	2.99	175.68	9.81	5.56	3.78	209.5
13	3.54	169.90	9.75	5.50		
23	0.43	148.63	4.32	6.35	0.58	183.1
23	0.56	164.60	3.65	3.27	1.06	192.0
23	2.50	164.20	8.90	4.22	2.70	194.0
23	3.52	173.58	12.19	5.09	3.52	194.0
23	4.10	157.45	12.55	5.02	4.10	191.4
23	5.05	96.40	7.96	3.53	5.05	188.9
33	0.52	124.97	4.69	-3.32	0.43	159.0
33	2.69	151.72	9.45	4.84	2.69	178.2
33	3.01	150.62	10.03	2.83	3.01	179.3
33	4.04	161.30	13.24	5.01	4.04	176.5
33	5.03	140.45	13.96	4.62	5.03	170.3
33	6.01	113.91	13.09	3.96	6.01	156.5
33	7.00	88.12	11.41	2.71	7.00	141.4
43	0.52	100.67	2.77	-4.05	0.43	141.4
43	0.92	125.83	3.46	-0.26	2.74	165.7
43	2.54	140.29	7.11	3.11	3.97	164.5
43	3.97	151.32	11.94	4.37	5.01	151.4
43	5.01	142.07	13.93	3.72	6.03	145.5
43	6.03	126.70	15.06	4.07	7.05	132.8
43	7.05	106.70	14.23	4.52	7.99	120.4
43	7.99	90.15	13.96	3.28	9.03	96.0
43	9.03	74.21	12.04	2.50		
53	0.54	83.24	1.98	-5.84	0.47	115.4
53	0.82	109.02	1.81	-1.09	1.00	130.6
53	2.51	127.66	5.74	2.50	2.45	149.5
53	3.01	129.37	7.23	3.17	3.01	154.6
53	4.04	143.99	11.39	3.19	4.04	156.5
53	5.01	139.74	12.98	3.42	5.01	150.1
53	6.06	129.39	14.75	3.41	6.06	144.8
53	7.07	115.55	15.40	3.56	7.07	137.2
53	8.04	99.27	14.78	3.33	8.04	122.8
53	9.01	88.49	14.97	2.60	9.01	114.6
53	10.04	73.80	14.47	2.39	10.04	98.0
53	11.04	59.29	12.98	1.94	11.04	86.3

A1.3 Mean velocity for $F_1 = 2.5$, $Q = 68.6$ L/s, $y_1 = 7.1$ cm (continued)

x (cm)	Processed MicroADV data				Prandtl tube measurements	
	y (cm)	u (cm/s)	v (cm/s)	w (cm/s)	y (cm)	u (cm/s)
63	0.61	81.22	0.86	-2.38	0.45	104.8
63	1.10	104.61	1.64	-0.64	1.00	118.8
63	2.36	130.25	5.33	0.62	2.00	131.3
63	3.07	121.07	6.39	1.87	2.56	137.9
63	4.00	135.24	9.30	2.03	3.06	141.4
63	5.07	133.71	11.76	3.29	4.00	143.5
63	6.03	125.11	13.26	3.30	5.07	142.8
63	7.01	116.87	14.43	3.87	6.03	135.7
63	8.04	104.99	14.60	3.53	7.01	129.8
63	9.05	94.65	15.20	4.18	8.04	126.0
63	10.02	82.41	14.40	3.04	9.05	111.1
63	11.04	70.62	13.68	2.64	10.02	99.0
63	12.03	60.88	12.93	2.31	11.04	92.9
63					12.03	79.2
73	0.49	75.28	1.44	-5.26	0.40	99.0
73	1.04	93.11	1.91	0.00	1.00	105.7
73	2.40	106.28	4.36	0.24	2.00	122.8
73	3.09	109.35	6.14	1.54	2.40	126.8
73	4.02	125.48	8.63	1.55	3.04	129.8
73	5.01	127.44	10.72	1.76	4.02	135.7
73	6.05	122.43	12.76	3.96	5.01	133.6
73	7.04	117.02	14.27	3.91	6.05	130.6
73	8.04	112.56	15.33	3.75	7.04	125.2
73	9.01	101.22	15.25	4.47	8.04	123.6
73	10.02	93.96	15.69	3.99	9.01	112.0
73	11.07	85.58	15.87	4.10	10.02	108.4
73	12.01	74.30	14.94	3.27	11.07	98.0
73	12.99	67.92	14.53	2.91	12.02	89.6
73	14.07	57.27	13.84	2.84	13.00	76.7
73	15.01	47.97	13.13	2.31	13.99	71.4
73					15.01	62.6
93	0.49	70.00	0.49	-1.81	0.40	84.0
93	1.05	80.16	1.33	-1.27	1.03	91.8
93	1.53	83.82	1.97	-0.63	2.38	103.8
93	2.48	90.38	2.85	1.00	3.05	106.6
93	3.03	91.70	3.75	2.10	4.04	112.9
93	4.04	105.82	5.69	0.31	5.02	116.3
93	5.02	110.07	7.33	0.87	6.03	119.6
93	6.03	111.42	8.78	1.70	7.03	117.1
93	7.03	110.10	10.14	2.50	8.05	113.7
93	8.05	106.89	11.08	3.32	9.01	112.0

A1.3 Mean velocity for $F_1 = 2.5$, $Q = 68.6$ L/s, $y_1 = 7.1$ cm (continued)

x (cm)	Processed MicroADV data				Prandtl tube measurements	
	y (cm)	u (cm/s)	v (cm/s)	w (cm/s)	y (cm)	u (cm/s)
93	9.01	104.66	12.31	3.68	10.03	108.4
93	10.03	98.54	12.15	3.90	11.02	104.8
93	11.02	94.29	13.08	3.95	12.05	97.0
93	12.05	87.87	12.69	3.88	13.09	90.7
93	13.09	81.67	12.64	4.65	14.07	85.2
93	14.07	75.70	12.36	3.71	15.08	77.9
93	15.08	68.12	11.28	4.02	16.08	72.7
93	16.08	56.78	10.80	4.01		
113	0.54	64.01	0.71	-1.20	0.45	71.4
113	1.08	70.94	1.20	0.25	1.01	80.4
113	2.31	84.94	2.60	0.88	2.30	85.2
113	3.02	80.33	2.69	2.10	3.09	93.9
113	4.05	89.06	3.69	1.42	4.05	97.0
113	5.07	93.69	4.52	2.09	5.07	101.0
113	6.03	95.61	5.53	2.94	6.03	101.9
113	7.04	97.36	6.68	3.05	7.04	103.8
113	8.06	98.04	7.50	3.18	8.06	106.6
113	9.02	96.98	7.94	3.47	9.02	104.8
113	10.04	94.49	8.24	4.08	10.04	103.8
113	11.04	92.07	9.11	3.98	11.04	97.0
113	12.06	90.13	9.09	4.45	12.06	93.9
113	13.01	87.96	9.36	5.18	13.01	92.9
113	14.02	80.97	8.76	5.11	14.02	90.7
113	15.04	77.11	8.32	4.98	15.04	82.8
113	16.03	72.61	8.52	5.27	16.03	81.6
153	0.56	57.75	1.12	-0.10	0.56	62.6
153	1.06	62.27	0.98	0.15	1.06	65.7
153	2.07	67.20	1.36	1.35	2.00	68.6
153	3.52	71.56	1.58	1.85	3.06	76.7
153	4.05	73.80	1.77	3.06	4.05	76.7
153	5.05	76.94	2.33	3.10	5.05	79.2
153	6.06	80.28	2.47	3.40	6.06	80.4
153	7.02	82.13	2.41	3.60	7.02	82.8
153	8.04	83.33	3.11	3.67	8.04	86.3
153	9.05	85.21	3.18	4.23	9.05	89.6
153	10.05	86.64	3.36	4.60	10.05	88.5
153	11.02	85.96	3.46	4.66	11.02	87.4
153	12.04	85.76	3.62	5.10	12.04	89.6
153	13.02	83.38	3.43	4.91	13.02	86.3
153	14.04	83.13	3.62	4.46	14.04	85.2
153	15.03	81.21	3.52	5.15	15.03	85.2
153	15.99	79.18	4.14	4.15	15.99	82.8

A1.3 Mean velocity for $F_1 = 2.5$, $Q = 68.6$ L/s, $y_1 = 7.1$ cm (continued)

x (cm)	Processed MicroADV data				Prandtl tube measurements	
	y (cm)	u (cm/s)	v (cm/s)	w (cm/s)	y (cm)	u (cm/s)
193	0.55	44.25	0.01	-1.18	0.52	54.2
193	1.02	50.60	0.11	0.70	1.03	57.7
193	2.45	54.94	0.14	1.33	2.40	64.2
193	3.02	57.73	0.06	2.10	3.03	67.1
193	3.50	63.97	0.64	1.89	4.02	68.6
193	4.02	65.42	0.95	2.30	5.05	71.4
193	5.05	67.89	0.93	3.00	6.07	72.7
193	6.07	71.37	1.05	3.56	7.01	75.4
193	7.01	72.05	1.06	3.86	8.09	76.7
193	8.09	74.30	1.12	4.19	9.06	75.4
193	9.06	75.78	1.01	4.58	10.02	77.9
193	10.02	77.76	1.04	4.81	11.01	77.9
193	11.01	78.36	0.95	5.14	12.01	80.4
193	12.01	79.46	1.02	5.33	13.07	81.6
193	13.07	79.10	1.08	5.12	14.02	82.8
193	14.02	79.07	0.45	5.71	15.04	84.0
193	15.04	78.65	0.70	5.40	16.00	84.0
193	16.00	76.35	1.96	4.36		
233	0.50	39.24	-0.66	-0.21	0.48	50.5
233	1.08	50.76	-0.03	0.51	1.08	56.0
233	2.53	54.03	-0.28	1.23	2.44	61.0
233	3.09	54.69	0.12	1.62	3.09	62.6
233	3.53	61.38	0.26	1.61	4.06	65.7
233	4.06	63.13	0.49	2.11	5.06	67.1
233	5.06	65.39	0.62	2.95	6.08	67.1
233	6.08	66.61	0.25	3.15	7.03	71.4
233	7.03	68.04	0.15	3.57	8.03	72.7
233	8.03	69.86	0.35	4.19	9.01	74.1
233	9.01	71.41	0.25	4.41	10.03	74.1
233	10.03	73.03	0.49	4.47	11.05	75.4
233	11.05	73.69	0.11	4.47	12.06	75.4
233	12.06	75.53	-0.07	4.63	13.01	75.4
233	13.01	76.40	-0.07	4.83	14.02	76.7
233	14.02	77.03	-0.34	4.52	15.08	80.4
233	15.08	77.11	-0.14	5.10	16.05	80.4
273	0.48	42.43	0.16	0.35	0.45	52.4
273	1.04	50.51	0.37	0.78	1.04	56.0
273	2.05	53.82	0.55	0.99	2.40	59.4
273	2.40	53.33	0.00	1.29	3.12	61.0
273	3.12	55.17	0.16	1.61	4.05	62.6
273	4.05	62.99	0.72	2.27	5.02	64.2

A1.3 Mean velocity for $F_1 = 2.5$, $Q = 68.6$ L/s, $y_1 = 7.1$ cm (continued)

x (cm)	Processed MicroADV data				Prandtl tube measurements	
	y (cm)	u (cm/s)	v (cm/s)	w (cm/s)	y (cm)	u (cm/s)
273	5.02	64.46	0.76	2.66	6.04	65.7
273	6.04	65.39	0.88	3.05	7.05	67.1
273	7.05	67.01	0.66	3.63	8.02	68.6
273	8.02	68.13	0.47	3.89	9.02	71.4
273	9.02	69.71	0.38	4.03	10.04	74.1
273	10.04	70.84	0.27	4.42	11.04	74.1
273	11.04	71.78	-0.04	4.82	12.07	74.1
273	12.07	73.34	-0.09	5.07	13.04	74.1
273	13.04	74.19	-0.38	5.21	14.01	76.7
273	14.01	74.55	-0.42	5.39	15.02	77.9
273	15.02	75.02	-0.73	5.37	16.05	76.7
323	0.45	46.86	0.05	1.22	0.45	52.4
323	0.97	51.89	-0.17	1.08	0.96	54.2
323	2.03	55.31	0.22	0.69	2.03	57.7
323	2.49	61.70	0.57	1.41	2.44	59.4
323	3.02	55.22	0.20	1.90	3.02	62.6
323	4.03	63.39	0.64	2.09	4.03	62.6
323	5.03	64.89	0.39	2.31	5.03	64.2
323	6.03	65.79	0.49	2.91	6.03	65.7
323	7.00	67.60	0.16	3.43	7.00	67.1
323	8.01	67.57	0.35	3.47	8.01	68.6
323	9.04	68.51	0.28	3.98	9.04	70.0
323	10.04	69.72	0.15	4.05	10.04	70.0
323	11.02	71.35	-0.22	4.46	11.02	71.4
323	12.03	71.77	-0.58	4.52	12.03	71.4
323	13.02	72.75	-0.69	4.98	13.02	72.7
323	14.01	73.39	-0.83	4.65	14.01	72.7
323	15.02	73.93	-0.89	5.06	15.02	72.7

A1.4 Mean velocity for $F_1 = 3.32$, $Q = 40$ L/s, $y_1 = 4.1$ cm

x (cm)	Processed MicroADV data				Prandtl tube measurements	
	y (cm)	u (cm/s)	v (cm/s)	w (cm/s)	y (cm)	u (cm/s)
38	0.56	67.91	-0.56	-2.63	0.54	148.8
38	1.00	82.38	-0.34	-1.22	1.00	157.1
38	2.01	92.33	5.55	-0.51	2.03	156.5
38	3.04	84.76	7.05	1.64	3.04	139.3
38	3.50	79.98	7.88	2.14	3.50	134.3
48	0.57	76.89	0.96	-3.57	0.55	125.2
48	0.98	79.42	0.98	-2.43	1.02	131.3
48	2.01	88.49	5.43	-0.68	2.01	135.7
48	3.04	89.32	7.30	1.48	3.04	126.0
48	4.05	82.33	9.20	0.98	4.05	112.0
48	5.03	69.13	10.06	1.11	5.03	99.0
48	5.51	60.65	9.39	1.62	5.51	89.6
58	0.60	72.27	1.66	-2.85	0.52	103.8
58	1.01	75.83	2.19	-3.33	1.00	112.9
58	1.99	81.18	5.15	-1.72	2.02	116.3
58	3.03	81.97	7.02	1.01	3.03	111.1
58	4.02	83.78	9.12	1.11	4.02	100.0
58	5.01	72.10	9.90	1.06	5.01	91.8
58	6.03	61.95	10.20	0.94	6.03	84.0
58	7.00	49.95	10.25	0.64	7.00	72.7
58	7.48	45.97	10.28	0.38	7.48	64.2
68	0.57	61.67	1.56	-3.41	0.53	84.0
68	1.02	71.40	2.50	-3.29	1.04	90.7
68	2.02	82.82	5.17	-3.01	2.02	97.0
68	3.02	77.72	6.35	0.64	3.02	97.0
68	3.98	82.17	8.54	0.73	3.98	92.9
68	5.04	76.15	9.86	1.31	5.04	89.6
68	6.02	67.66	10.77	1.03	6.02	81.6
68	7.01	57.36	10.66	1.32	7.01	76.7
68	8.00	49.90	11.17	0.94	8.00	67.1
68	9.04	40.20	11.13	0.78	9.04	56.0
78	0.56	56.60	1.09	-2.74	0.59	76.7
78	1.00	63.51	1.86	-2.71	1.01	81.6
78	2.01	74.47	3.82	-2.56	2.04	87.4
78	3.05	71.88	5.04	0.22	3.05	89.6
78	4.02	79.86	6.88	0.79	4.02	87.4
78	5.06	74.65	8.41	1.17	5.06	81.6
78	6.02	69.42	9.16	1.00	6.02	79.2
78	6.99	60.33	9.30	1.09	6.99	72.7

A1.4 Mean velocity for $F_1 = 3.32$, $Q = 40$ L/s, $y_1 = 4.1$ cm (continued)

x (cm)	Processed MicroADV data				Prandtl tube measurements	
	y (cm)	u (cm/s)	v (cm/s)	w (cm/s)	y (cm)	u (cm/s)
78	8.05	55.25	9.44	1.88	8.05	61.0
78	8.99	49.60	9.75	1.07	8.99	56.0
78	9.99	42.76	9.51	2.08	9.99	52.4
88	0.62	54.34	0.50	-2.05	0.55	64.2
88	1.01	57.81	1.12	-1.94	1.02	74.1
88	2.03	67.68	2.47	-1.56	2.03	76.7
88	2.99	66.46	3.18	1.11	2.99	76.7
88	4.04	72.97	4.96	1.35	4.04	80.4
88	5.03	71.50	5.89	1.50	5.03	76.7
88	6.01	69.97	6.45	2.20	6.01	76.7
88	7.03	63.51	7.21	2.24	7.03	71.4
88	8.01	60.33	7.67	2.33	8.01	68.6
88	9.00	57.45	7.97	2.61	9.00	64.2
88	10.03	51.22	8.09	2.31	10.03	61.0
108	0.61	52.15	0.60	-0.88	0.51	57.7
108	0.99	52.11	0.44	0.26	0.99	62.6
108	2.00	52.37	0.99	0.03	2.05	65.7
108	3.05	56.84	1.52	2.47	3.05	68.6
108	4.04	67.11	2.55	2.09	4.04	67.1
108	5.00	66.86	2.92	2.66	5.00	71.4
108	6.06	64.16	3.21	2.50	6.06	68.6
108	7.02	64.62	3.75	2.91	7.02	67.1
108	8.06	62.10	3.96	3.21	8.06	67.1
108	9.03	59.39	4.00	3.17	9.03	67.1
108	9.99	56.93	4.41	3.53	9.99	64.2
108	11.05	55.28	4.55	3.41		
128	0.58	43.05	-0.12	-0.48	0.57	46.4
128	1.04	47.95	0.38	0.97	1.04	48.5
128	1.98	48.15	0.42	0.47	2.05	54.2
128	3.01	51.04	0.13	1.64	3.01	57.7
128	3.99	60.07	1.24	1.57	3.99	59.4
128	5.03	62.95	1.59	2.35	5.03	61.0
128	6.04	63.95	2.43	2.42	6.04	57.7
128	7.06	63.64	2.15	3.41	7.06	59.4
128	8.01	60.86	1.07	2.95	8.01	61.0
128	9.03	59.86	1.29	3.25	9.03	61.0
128	10.05	59.21	1.42	3.54	10.05	61.0
128	11.04	57.27	1.25	3.62	11.04	61.0

A1.4 Mean velocity for $F_1 = 3.32$, $Q = 40$ L/s, $y_1 = 4.1$ cm (continued)

x (cm)	Processed MicroADV data				Prandtl tube measurements	
	y (cm)	u (cm/s)	v (cm/s)	w (cm/s)	y (cm)	u (cm/s)
168	0.51	38.63	0.04	0.37	0.51	46.4
168	1.02	42.93	0.03	0.80	1.02	48.5
168	2.04	45.80	0.31	1.32	2.04	50.5
168	3.04	46.77	-0.24	2.12	3.04	54.2
168	4.00	52.62	0.24	2.25	4.00	54.2
168	5.03	54.56	0.49	2.79	5.03	56.0
168	6.04	56.02	0.26	3.20	6.04	57.7
168	7.04	56.54	0.43	3.27	7.04	59.4
168	8.04	57.04	0.15	3.53	8.04	61.0
168	9.04	59.03	0.04	3.97	9.04	59.4
168	10.06	58.88	-0.31	4.36	10.06	59.4
168	11.00	58.57	-0.23	4.26		
208	0.58	34.31	-0.35	-0.96	0.51	42.0
208	1.02	41.06	-0.23	0.10	1.02	46.4
208	2.01	44.07	0.13	0.86	2.01	48.5
208	3.04	44.02	-0.51	1.76	3.04	50.5
208	4.02	50.43	-0.22	1.80	4.02	52.4
208	5.03	52.15	-0.02	2.26	5.03	54.2
208	6.02	52.84	-0.18	2.57	6.02	56.0
208	7.01	54.79	-0.46	3.02	7.01	56.0
208	8.05	55.11	-0.54	2.98	8.05	56.0
208	9.05	55.95	-0.69	3.27	9.05	57.7
208	10.04	56.35	-0.77	3.24	10.04	57.7
208	11.03	57.50	-0.81	3.74	11.03	59.4
248	0.62	33.42	-0.61	-1.41	0.58	42.0
248	0.99	40.31	-0.18	0.39	0.99	46.4
248	2.01	42.30	-0.06	1.09	2.01	47.5
248	3.03	43.43	-0.62	1.57	3.03	48.5
248	4.03	50.38	-0.26	2.19	4.03	50.5
248	5.01	51.38	-0.07	2.69	5.01	52.4
248	5.99	52.56	-0.19	3.08	5.99	53.3
248	7.04	53.93	-0.59	3.24	7.04	53.3
248	8.04	54.03	-0.60	3.30	8.04	54.2
248	9.04	54.85	-0.71	3.64	9.04	55.1
248	10.04	55.42	-0.85	3.77	10.04	56.0
248	10.99	56.18	-0.74	4.21	10.99	57.7

A1.5 Processed turbulence data for $F_1 = 2.0$, $Q = 54.9$ L/s, $y_1 = 7.1$ cm

x (cm)	y (cm)	$\sqrt{u'^2}$ (cm/s)	$\sqrt{v'^2}$ (cm/s)	$\sqrt{w'^2}$ (cm/s)	$-\overline{u'v'}$ (cm ² /s ²)	$-\overline{u'w'}$ (cm ² /s ²)	$-\overline{v'w'}$ (cm ² /s ²)	ε (m ² /s ³)	η (mm)
13	0.61	8.76	2.85	12.40	-4.59	-6.73	-0.11	0.004	0.139
13	1.02	7.68	3.53	12.38	-9.96	-4.10	-1.04	0.002	0.158
13	2.51	7.22	6.24	9.99	-15.12	3.45	7.91	0.003	0.150
13	3.03	8.83	6.74	9.31	-21.09	7.40	6.00	0.005	0.130
13	3.50	13.96	7.84	11.21	-28.89	13.83	6.86	0.021	0.091
23	0.56	8.13	2.11	11.86	4.43	-2.43	0.52	0.005	0.132
23	1.08	8.51	3.57	10.66	-9.55	1.03	-1.12	0.005	0.131
23	2.31	9.38	5.74	10.31	-17.23	4.37	5.07	0.008	0.117
23	3.06	10.43	6.35	9.26	-25.05	9.42	5.97	0.010	0.111
23	4.01	15.77	7.88	9.50	-53.71	15.11	9.95	0.028	0.085
23	5.00	24.74	8.24	10.40	-89.30	6.57	4.99	0.152	0.056
23	6.00	32.23	7.84	12.92	-122.95	-22.57	-0.72	0.473	0.042
23	6.52	34.84	8.20	14.83	-144.38	-6.81	-4.31	0.865	0.036
33	0.53	12.71	2.06	10.56	0.49	4.71	-1.22	0.026	0.086
33	1.02	9.75	2.93	10.79	-6.84	-0.76	-0.35	0.010	0.109
33	2.44	11.35	4.94	9.85	-20.06	13.37	3.65	0.013	0.103
33	3.02	13.19	5.68	9.16	-30.43	7.98	3.58	0.015	0.099
33	4.00	18.20	7.02	9.61	-56.11	6.48	3.56	0.041	0.077
33	5.03	25.12	7.90	9.72	-96.49	6.14	2.93	0.104	0.061
33	6.00	28.73	8.35	10.71	-123.59	-3.99	-1.42	0.207	0.051
33	6.99	31.95	9.27	12.42	-158.01	-21.47	-4.34	0.351	0.045
33	8.06	34.34	11.07	14.14	-207.03	-23.38	-7.69	0.551	0.040
33	8.57	36.21	12.63	15.35	-253.45	-29.10	-8.58	0.607	0.039
43	0.63	13.33	2.17	10.55	1.22	11.64	-2.94	0.030	0.083
43	1.05	12.18	2.77	9.92	-2.93	4.67	0.07	0.015	0.099
43	2.40	12.59	4.28	8.76	-16.06	8.37	1.51	0.018	0.095
43	3.03	13.97	4.87	8.85	-23.61	5.62	1.80	0.025	0.088
43	4.04	19.44	6.48	9.11	-50.75	-2.08	0.35	0.035	0.080
43	5.06	25.49	7.18	9.92	-82.27	2.86	1.91	0.080	0.065
43	6.05	27.77	8.37	10.71	-116.88	4.22	1.07	0.140	0.057
43	7.00	32.04	9.81	11.98	-166.82	-27.99	-8.09	0.276	0.048
43	8.08	32.70	11.31	13.50	-199.07	-9.79	-2.93	0.278	0.048
43	9.05	31.43	11.44	14.94	-191.53	-36.56	-14.33	0.358	0.045
43	9.52	32.66	12.67	15.79	-224.13	-10.25	-3.37	0.428	0.043
53	0.60	14.68	2.43	10.48	3.16	1.94	-1.29	0.045	0.075
53	1.01	13.88	3.11	10.17	1.08	3.36	0.00	0.024	0.088
53	2.31	15.21	4.38	9.16	-12.59	6.72	0.33	0.030	0.083
53	3.00	17.76	4.83	9.31	-23.51	8.31	0.50	0.034	0.081
53	4.01	22.23	6.51	9.99	-50.04	9.79	-0.57	0.057	0.071

A1.5 Processed turbulence data for $F_1 = 2.0$, $Q = 54.9$ L/s, $y_1 = 7.1$ cm (cont'd)

x (cm)	y (cm)	$\sqrt{u'^2}$ (cm/s)	$\sqrt{v'^2}$ (cm/s)	$\sqrt{w'^2}$ (cm/s)	$-\overline{u'v'}$ (cm ² /s ²)	$-\overline{u'w'}$ (cm ² /s ²)	$-\overline{v'w'}$ (cm ² /s ²)	ε (m ² /s ³)	η (mm)
53	5.05	25.55	7.45	9.98	-83.31	1.77	-1.09	0.083	0.065
53	6.02	29.16	8.85	11.43	-125.39	-2.75	-4.03	0.118	0.059
53	7.04	29.48	9.76	12.24	-148.06	-3.58	-2.52	0.170	0.054
53	8.01	30.06	10.50	13.50	-165.39	-11.28	-4.92	0.188	0.053
53	9.07	28.71	11.41	14.44	-174.01	-17.82	-10.06	0.190	0.052
53	10.03	27.49	11.87	14.76	-169.75	-6.91	-7.06	0.220	0.051
53	10.43	27.85	12.31	16.21	-169.21	-11.35	-6.03	0.233	0.050
63	0.64	13.73	2.13	9.81	2.17	-0.15	-0.80	0.036	0.080
63	1.01	15.22	3.00	10.16	2.25	-1.73	-0.19	0.034	0.080
63	2.48	16.87	4.73	9.18	-13.29	8.96	-1.25	0.034	0.081
63	3.03	18.84	5.00	9.16	-18.60	5.73	-0.33	0.047	0.075
63	4.04	22.72	6.54	9.64	-49.96	14.82	-0.16	0.052	0.073
63	5.07	25.56	7.80	10.07	-89.90	9.16	-0.66	0.086	0.064
63	6.02	27.25	8.82	11.59	-110.82	-10.85	-2.74	0.105	0.061
63	7.05	28.31	9.86	12.67	-133.81	5.90	-0.64	0.128	0.058
63	8.00	27.60	10.70	13.81	-145.27	-0.08	-2.36	0.141	0.057
63	9.08	26.33	11.00	13.63	-145.26	-9.67	-2.86	0.132	0.057
63	10.04	25.91	11.02	13.98	-138.16	-3.50	-6.21	0.138	0.057
63	10.98	25.46	11.29	14.55	-134.62	-0.57	-2.12	0.207	0.051
63	11.95	24.52	9.26	14.62	-71.91	-6.27	-6.13	0.308	0.047
73	0.59	15.20	2.60	11.21	2.17	9.63	-1.12	0.038	0.079
73	1.07	15.78	3.36	10.25	1.37	4.35	0.78	0.034	0.081
73	2.30	17.55	4.95	9.56	-15.58	8.79	0.37	0.035	0.080
73	3.01	18.29	5.30	8.90	-21.36	12.32	0.34	0.038	0.078
73	4.02	21.60	7.02	9.61	-48.36	13.81	-0.49	0.049	0.074
73	5.04	24.62	8.14	10.11	-86.77	13.05	-0.69	0.077	0.066
73	6.04	24.68	8.59	11.13	-98.32	10.41	-2.15	0.077	0.066
73	7.05	25.59	9.81	12.17	-123.10	1.20	0.79	0.095	0.062
73	8.04	26.27	10.33	12.78	-131.45	-4.78	-2.56	0.103	0.061
73	9.03	23.68	10.51	12.56	-122.54	-5.75	-3.24	0.110	0.060
73	10.04	24.01	10.92	12.96	-130.83	-0.08	0.54	0.108	0.060
73	11.01	22.21	10.48	13.09	-103.83	-12.14	-3.38	0.106	0.061
73	11.55	21.26	10.10	13.97	-80.04	-6.69	-3.14	0.123	0.058
93	0.57	12.71	2.12	9.95	0.45	5.50	-0.77	0.027	0.086
93	1.00	14.42	3.31	10.59	0.71	-1.36	-0.02	0.024	0.088
93	2.41	15.85	5.05	9.30	-5.94	4.72	-0.83	0.034	0.081
93	3.05	16.41	5.51	8.91	-17.93	3.93	-0.52	0.031	0.082
93	4.05	19.18	7.64	9.45	-42.29	3.55	-2.68	0.041	0.077
93	5.04	20.28	7.98	9.46	-55.63	2.99	-0.64	0.043	0.076
93	6.02	20.46	8.79	9.96	-77.14	-3.11	-0.84	0.052	0.073

A1.5 Processed turbulence data for $F_1 = 2.0$, $Q = 54.9$ L/s, $y_1 = 7.1$ cm (cont'd)

x (cm)	y (cm)	$\sqrt{u'^2}$ (cm/s)	$\sqrt{v'^2}$ (cm/s)	$\sqrt{w'^2}$ (cm/s)	$-\overline{u'v'}$ (cm ² /s ²)	$-\overline{u'w'}$ (cm ² /s ²)	$-\overline{v'w'}$ (cm ² /s ²)	ε (m ² /s ³)	η (mm)
93	7.02	20.76	9.15	10.14	-87.65	4.50	1.25	0.044	0.076
93	8.04	20.25	9.55	10.44	-87.34	7.66	0.83	0.045	0.075
93	9.02	20.20	9.35	10.87	-87.92	-4.03	2.85	0.053	0.072
93	10.00	19.10	9.48	11.44	-83.73	2.36	2.75	0.045	0.075
93	11.04	18.68	9.48	11.18	-74.91	-4.93	-0.92	0.049	0.074
93	12.04	16.76	8.86	11.71	-47.77	-10.58	0.61	0.053	0.072
113	0.58	12.47	2.25	10.11	0.43	4.10	-0.09	0.016	0.097
113	1.07	13.23	3.39	9.85	0.41	-3.34	0.94	0.019	0.094
113	2.45	14.47	4.86	8.72	-8.23	1.87	1.15	0.029	0.084
113	3.17	14.93	5.77	8.82	-16.56	3.00	0.24	0.024	0.088
113	4.00	16.28	6.64	9.09	-21.98	0.67	-0.38	0.025	0.087
113	5.04	16.94	7.41	9.06	-39.98	4.35	-1.14	0.026	0.087
113	6.07	16.53	8.05	8.93	-47.27	-0.78	-0.42	0.023	0.089
113	7.09	16.30	8.25	9.27	-51.30	0.32	-0.20	0.031	0.083
113	8.00	16.22	8.66	9.34	-58.11	-1.42	1.44	0.029	0.084
113	9.04	15.51	8.59	9.56	-49.92	-7.83	0.05	0.029	0.084
113	10.03	14.59	8.67	9.60	-48.14	-1.13	2.12	0.025	0.088
113	11.02	13.99	8.28	9.99	-41.01	-1.38	1.00	0.024	0.088
113	11.58	13.89	8.32	9.82	-35.13	-3.40	1.44	0.023	0.089
133	0.53	9.79	1.78	8.29	0.96	-0.33	-0.51	0.011	0.107
133	0.98	11.36	2.85	9.09	1.65	-3.02	0.13	0.012	0.105
133	2.01	12.42	4.25	8.44	-4.06	-4.22	-0.20	0.013	0.102
133	2.53	12.26	4.59	8.24	-4.11	-6.03	0.77	0.015	0.100
133	3.04	12.25	4.95	8.11	-7.61	-1.84	0.16	0.021	0.091
133	4.00	13.40	6.15	7.83	-13.78	0.93	-1.14	0.014	0.101
133	5.03	13.66	6.50	7.89	-20.13	-1.44	0.46	0.015	0.099
133	6.05	13.58	7.28	7.93	-31.69	-1.55	-0.78	0.013	0.103
133	7.05	13.39	7.49	7.97	-32.38	-2.15	-0.16	0.016	0.097
133	8.03	13.54	7.50	8.04	-35.11	-4.42	1.70	0.014	0.101
133	9.06	13.00	7.68	8.07	-32.45	-2.79	2.45	0.014	0.101
133	10.06	12.34	7.69	8.20	-31.93	-1.72	1.13	0.012	0.104
133	11.04	12.12	7.72	8.24	-28.97	-0.64	3.75	0.015	0.099
133	12.03	11.96	7.34	8.44	-23.45	-5.75	0.74	0.014	0.101
173	0.61	8.95	2.60	8.32	1.68	-1.33	-0.30	0.005	0.131
173	1.04	9.21	3.31	8.65	0.96	-4.00	-0.28	0.005	0.132
173	2.01	9.02	3.25	7.04	-1.35	-6.67	-0.07	0.004	0.136
173	2.53	10.58	4.75	9.78	0.15	-2.51	0.38	0.009	0.112
173	3.00	10.44	4.96	9.43	-0.39	-2.95	0.36	0.007	0.121
173	4.01	10.62	5.92	8.52	-2.19	-7.01	-0.26	0.007	0.119
173	5.04	10.26	6.20	8.64	-3.29	-6.80	-0.08	0.006	0.124

A1.5 Processed turbulence data for $F_1 = 2.0$, $Q = 54.9$ L/s, $y_1 = 7.1$ cm (cont'd)

x (cm)	y (cm)	$\sqrt{u'^2}$ (cm/s)	$\sqrt{v'^2}$ (cm/s)	$\sqrt{w'^2}$ (cm/s)	$-\overline{u'v'}$ (cm ² /s ²)	$-\overline{u'w'}$ (cm ² /s ²)	$-\overline{v'w'}$ (cm ² /s ²)	ε (m ² /s ³)	η (mm)
173	6.02	10.45	6.49	8.50	-5.98	-4.93	0.95	0.006	0.123
173	7.07	10.34	6.45	8.57	-7.72	-6.79	0.24	0.008	0.116
173	8.05	9.89	6.68	8.39	-10.15	-3.29	1.04	0.006	0.125
173	9.06	9.92	6.81	8.46	-9.86	-2.09	0.74	0.006	0.125
173	10.03	9.74	6.87	8.70	-7.89	-1.56	1.78	0.006	0.125
173	11.04	9.83	6.84	8.77	-8.35	-1.67	1.46	0.007	0.120
213	0.66	7.04	2.11	6.78	1.58	-0.31	-0.41	0.002	0.161
213	1.04	7.72	2.76	7.07	2.90	-4.04	0.14	0.003	0.149
213	2.01	9.01	3.62	7.03	1.51	-3.98	0.20	0.003	0.155
213	2.53	8.91	3.83	8.64	2.69	-3.29	-0.16	0.005	0.128
213	3.06	8.82	3.95	8.20	2.08	-2.96	-0.47	0.005	0.129
213	4.03	8.28	4.72	7.43	2.05	-4.74	0.65	0.003	0.144
213	5.06	8.28	4.92	7.25	1.29	-5.62	0.59	0.003	0.150
213	6.07	8.16	5.23	7.16	-0.22	-2.88	0.60	0.003	0.143
213	7.02	8.05	5.26	7.11	0.14	-3.21	0.43	0.003	0.145
213	8.06	7.73	5.34	7.09	-0.68	-2.57	0.26	0.003	0.146
213	9.01	7.74	5.56	7.24	-0.72	-1.51	0.98	0.003	0.144
213	10.01	7.55	5.36	7.24	-1.55	-3.07	1.06	0.003	0.149
213	11.04	7.71	5.42	7.26	-0.59	-2.22	1.12	0.003	0.146
253	0.63	6.74	1.88	6.04	1.85	-2.22	-0.34	0.003	0.155
253	1.05	6.75	2.32	6.50	2.63	-1.33	-0.04	0.002	0.162
253	2.02	7.36	3.04	6.04	2.76	-4.06	0.59	0.002	0.164
253	2.47	8.49	3.36	8.17	2.94	-1.30	-0.24	0.004	0.138
253	3.08	8.04	3.45	7.54	2.25	-2.25	-0.15	0.004	0.139
253	4.01	7.20	3.87	6.55	2.75	-4.92	0.78	0.002	0.160
253	5.01	6.95	4.12	6.37	3.19	-3.17	0.00	0.002	0.167
253	6.02	6.87	4.34	6.43	3.11	-3.06	-0.19	0.002	0.166
253	7.05	6.82	4.42	6.32	3.02	-1.66	0.51	0.002	0.166
253	8.06	6.54	4.53	6.27	2.40	-2.17	0.55	0.002	0.171
253	9.02	6.49	4.59	6.22	1.73	-2.27	1.04	0.002	0.163
253	10.06	6.60	4.54	6.39	1.98	-1.27	0.62	0.002	0.170
253	11.01	6.29	4.59	6.31	0.90	-2.18	0.77	0.002	0.167

A1.6 Processed turbulence data for $F_1 = 2.5$, $Q = 68.6$ L/s, $y_1 = 7.1$ cm

x (cm)	y (cm)	$\sqrt{u'^2}$ (cm/s)	$\sqrt{v'^2}$ (cm/s)	$\sqrt{w'^2}$ (cm/s)	$-\overline{u'v'}$ (cm ² /s ²)	$-\overline{u'w'}$ (cm ² /s ²)	$-\overline{v'w'}$ (cm ² /s ²)	ε (m ² /s ³)	η (mm)
13	0.57	13.35	3.85	17.77	12.42	-13.90	0.76	0.003	0.143
13	2.55	10.46	6.81	12.60	-22.07	-16.10	-0.23	0.007	0.120
13	2.99	13.81	7.31	9.88	-41.18	-13.01	-1.36	0.017	0.096
13	3.54	20.24	7.27	10.24	-56.89	-14.23	-1.87	0.042	0.076
23	0.43	13.59	2.50	14.86	9.84	-24.75	4.15	0.017	0.096
23	0.56	12.29	3.13	16.75	14.23	-22.52	3.04	0.012	0.106
23	2.50	12.24	6.61	12.59	-27.22	-12.46	-3.89	0.016	0.097
23	3.52	20.93	8.85	12.02	-75.60	-12.76	-5.28	0.092	0.063
23	4.10	34.29	9.07	12.24	-145.37	-19.09	-3.26	0.454	0.042
23	5.05	58.77	9.36	16.90	-304.39	-31.83	-2.31		
33	0.52	20.46	3.06	17.29	1.33	-17.65	5.31	0.072	0.067
33	2.69	13.12	6.86	12.43	-32.01	-3.12	-0.99	0.020	0.092
33	3.01	15.30	7.26	11.40	-53.43	-10.54	-3.67	0.032	0.082
33	4.04	23.53	9.31	11.73	-106.93	-13.34	-3.80	0.109	0.060
33	5.03	36.19	10.76	12.14	-226.09	-13.54	-2.87	0.527	0.041
33	6.01	45.90	11.19	14.36	-312.71	-19.95	-5.24	1.551	0.031
33	7.00	46.35	11.38	17.86	-295.95	-7.46	-3.11		
43	0.52	20.61	2.65	15.58	1.53	-10.34	0.51	0.098	0.062
43	0.92	22.67	3.78	15.41	-6.44	-11.11	1.96	0.092	0.063
43	2.54	15.44	6.23	12.82	-31.66	-5.27	-2.31	0.033	0.081
43	3.97	23.54	9.14	11.56	-109.72	-0.11	-2.01	0.093	0.063
43	5.01	31.63	10.33	11.85	-184.11	-25.93	-8.88	0.223	0.050
43	6.03	37.46	11.29	12.36	-257.62	-15.00	-5.78	0.589	0.040
43	7.05	43.70	12.89	14.59	-351.32	-23.57	-9.66	1.059	0.034
43	7.99	43.14	13.60	16.42	-362.31	-19.38	-3.95	1.187	0.033
43	9.03	40.35	13.92	18.49	-313.80	-0.61	1.55		
53	0.54	19.75	2.75	15.88	-0.87	6.79	-4.04	0.107	0.061
53	0.82	23.37	3.74	16.79	2.87	0.29	0.69	0.113	0.060
53	2.51	18.41	6.36	13.00	-26.29	-0.24	-0.20	0.049	0.074
53	3.01	17.28	6.74	11.91	-35.20	-2.74	-2.24	0.033	0.081
53	4.04	23.19	8.68	11.75	-94.89	-5.41	-4.64	0.076	0.066
53	5.01	27.42	9.89	11.26	-135.34	-10.92	-4.48	0.123	0.059
53	6.06	32.79	11.47	11.87	-212.33	-10.67	-3.97	0.217	0.051
53	7.07	38.09	12.63	13.11	-292.86	-13.16	-4.36	0.383	0.044
53	8.04	40.81	13.37	14.95	-335.52	-5.28	-7.76	0.633	0.039
53	9.01	41.14	14.42	15.85	-360.00	-5.02	0.99	0.696	0.038
53	10.04	40.30	14.88	17.73	-357.31	-4.24	-7.42	1.024	0.034
53	11.04	37.89	14.52	19.46	-286.80	-5.18	-0.88	0.863	0.036

A1.6 Processed turbulence data for $F_1 = 2.5$, $Q = 68.6$ L/s, $y_1 = 7.1$ cm (cont'd)

x (cm)	y (cm)	$\sqrt{u'^2}$ (cm/s)	$\sqrt{v'^2}$ (cm/s)	$\sqrt{w'^2}$ (cm/s)	$-\overline{u'v'}$ (cm ² /s ²)	$-\overline{u'w'}$ (cm ² /s ²)	$-\overline{v'w'}$ (cm ² /s ²)	ε (m ² /s ³)	η (mm)
63	0.61	19.60	2.85	18.08	3.73	-24.97	-0.26	0.088	0.064
63	1.10	22.55	4.65	17.35	5.04	-35.28	-1.99	0.103	0.061
63	2.36	24.00	6.93	15.20	-10.03	0.08	0.14	0.114	0.060
63	3.07	19.32	6.89	12.43	-22.27	-8.96	-4.24	0.056	0.071
63	4.00	21.35	8.12	11.99	-50.73	-2.25	-2.51	0.057	0.071
63	5.07	25.90	9.53	11.18	-96.76	-6.46	-3.35	0.088	0.064
63	6.03	31.54	10.03	11.97	-150.24	-7.20	-4.35	0.148	0.056
63	7.01	35.86	11.42	12.29	-225.91	-5.76	-2.07	0.251	0.049
63	8.04	37.51	12.41	13.05	-270.15	-28.17	-6.40	0.361	0.045
63	9.05	40.46	13.54	15.31	-328.12	-11.26	-3.62	0.544	0.040
63	10.02	39.82	14.60	16.55	-341.02	-19.68	-4.51	0.486	0.042
63	11.04	37.48	14.30	17.36	-305.67	-18.20	-6.00	0.492	0.041
63	12.03	35.57	14.65	18.64	-273.93	-15.00	-6.06	0.512	0.041
73	0.49	18.41	2.97	18.20	0.55	-0.87	-10.23	0.052	0.073
73	1.04	21.92	4.67	18.53	4.67	-22.13	-0.74	0.082	0.065
73	2.40	19.88	6.75	14.36	9.60	-11.85	-2.44	0.083	0.065
73	3.09	21.54	7.18	13.82	-4.39	-16.19	-1.17	0.101	0.061
73	4.02	24.12	9.04	12.70	-40.09	-14.77	-3.60	0.103	0.061
73	5.01	24.27	9.02	11.34	-53.72	-3.97	-3.80	0.084	0.064
73	6.05	28.62	10.08	11.20	-107.80	-10.76	-1.43	0.117	0.059
73	7.04	31.46	10.72	11.39	-145.81	-12.28	-5.41	0.160	0.055
73	8.04	33.87	11.45	12.14	-201.36	-21.39	-6.14	0.214	0.051
73	9.01	37.40	12.92	12.96	-272.63	-16.77	-3.92	0.322	0.046
73	10.02	37.13	13.27	14.83	-279.71	-15.28	-4.45	0.322	0.046
73	11.07	37.69	14.54	15.87	-312.42	-11.01	0.12	0.406	0.043
73	12.01	37.14	15.46	17.44	-327.33	-6.92	1.09	0.462	0.042
73	12.99	36.26	15.21	17.44	-301.43	-22.40	-12.16	0.476	0.042
73	14.07	34.55	14.70	19.46	-269.79	3.37	4.57	0.491	0.041
73	15.01	34.04	12.69	18.44	-200.48	4.45	-0.41	0.599	0.039
93	0.49	18.48	3.15	19.61	3.91	-60.81	-1.83	0.061	0.070
93	1.05	21.08	4.74	19.29	8.77	-62.89	-6.28	0.058	0.071
93	1.53	20.58	5.77	17.81	7.02	-38.96	-4.47	0.074	0.066
93	2.48	22.00	7.19	15.62	14.18	-34.04	-3.78	0.097	0.062
93	3.03	22.06	7.62	15.14	8.06	-39.09	-5.75	0.073	0.067
93	4.04	23.78	9.09	13.57	3.37	-34.59	-4.09	0.102	0.061
93	5.02	23.84	9.05	13.10	-17.60	-25.89	-2.23	0.081	0.065
93	6.03	23.97	9.95	12.68	-33.90	-28.93	-0.86	0.105	0.061
93	7.03	26.37	10.27	11.74	-61.50	-18.02	2.65	0.127	0.058
93	8.05	27.36	10.61	12.46	-86.53	-15.95	5.94	0.123	0.059
93	9.01	28.55	10.74	12.14	-106.28	-11.51	3.12	0.143	0.056
93	10.03	31.36	11.67	12.72	-159.90	-24.74	1.36	0.185	0.053

A1.6 Processed turbulence data for $F_1 = 2.5$, $Q = 68.6$ L/s, $y_1 = 7.1$ cm (cont'd)

x (cm)	y (cm)	$\sqrt{u'^2}$ (cm/s)	$\sqrt{v'^2}$ (cm/s)	$\sqrt{w'^2}$ (cm/s)	$-\overline{u'v'}$ (cm ² /s ²)	$-\overline{u'w'}$ (cm ² /s ²)	$-\overline{v'w'}$ (cm ² /s ²)	ε (m ² /s ³)	η (mm)
93	11.02	31.53	12.18	13.21	-172.55	-15.03	-0.77	0.195	0.052
93	12.05	32.52	12.73	14.25	-201.11	-25.74	2.94	0.254	0.049
93	13.09	32.45	13.02	14.51	-210.07	-31.92	-0.77	0.210	0.051
93	14.07	31.24	13.31	15.58	-210.56	-21.73	-3.98	0.219	0.051
93	15.08	30.07	12.90	16.19	-183.08	-7.19	2.35	0.346	0.045
93	16.08	32.32	10.82	16.48	-141.43	-21.90	1.03		
113	0.54	19.18	3.19	19.14	4.24	-57.26	-5.33	0.055	0.072
113	1.08	21.03	5.10	18.37	9.74	-77.37	-6.22	0.058	0.071
113	2.31	22.59	7.73	18.20	21.50	-66.60	-8.75	0.067	0.068
113	3.02	20.62	7.58	15.08	14.66	-34.62	-2.29	0.070	0.067
113	4.05	22.91	8.96	15.63	11.12	-64.86	-6.85	0.077	0.066
113	5.07	22.19	9.35	14.58	6.23	-62.19	-2.82	0.073	0.067
113	6.03	22.89	9.29	13.42	-12.83	-48.58	-3.26	0.070	0.067
113	7.04	22.87	9.39	12.30	-28.98	-43.51	1.32	0.077	0.066
113	8.06	22.40	10.11	12.91	-41.14	-41.13	1.51	0.109	0.060
113	9.02	23.57	10.10	12.68	-59.83	-22.91	4.35	0.095	0.062
113	10.04	25.61	10.20	12.79	-80.62	-30.91	2.04	0.085	0.064
113	11.04	26.23	10.64	13.00	-103.72	-30.22	1.81	0.114	0.060
113	12.06	26.44	11.20	12.67	-119.21	-29.69	3.65	0.128	0.058
113	13.01	26.13	10.92	12.82	-114.58	-25.34	2.70	0.122	0.059
113	14.02	26.75	11.00	13.49	-131.97	-15.36	2.37	0.119	0.059
113	15.04	26.04	10.94	14.40	-120.74	-22.92	1.54	0.136	0.057
113	16.03	26.33	9.99	14.40	-107.09	-22.19	-0.84		
153	0.56	16.30	2.98	16.36	3.52	-53.68	-3.63	0.026	0.087
153	1.06	17.96	4.54	16.35	10.91	-52.82	-5.72	0.030	0.083
153	2.07	19.11	6.56	15.77	19.17	-59.30	-6.23	0.029	0.084
153	3.52	19.92	8.40	14.58	31.83	-52.77	-7.98	0.040	0.077
153	4.05	18.71	8.25	14.19	23.87	-44.01	-4.91	0.031	0.082
153	5.05	18.64	8.42	13.57	19.22	-47.50	-2.80	0.033	0.082
153	6.06	18.87	8.80	13.03	14.23	-37.00	-2.93	0.036	0.080
153	7.02	18.23	8.88	12.68	9.79	-40.35	-3.86	0.033	0.081
153	8.04	17.85	8.93	12.15	-5.83	-29.50	-2.33	0.036	0.079
153	9.05	17.74	8.91	12.06	-10.92	-27.43	2.27	0.032	0.082
153	10.05	17.39	9.09	12.11	-14.86	-25.20	2.12	0.036	0.080
153	11.02	17.37	9.30	11.69	-25.70	-17.76	-0.49	0.033	0.081
153	12.04	17.16	8.86	11.38	-23.72	-15.78	-0.61	0.038	0.079
153	13.02	18.01	8.90	11.30	-34.49	-23.08	2.11	0.036	0.079
153	14.04	17.87	8.70	11.66	-39.18	-17.02	-1.33	0.030	0.083
153	15.03	18.73	8.55	11.58	-44.61	-22.75	-1.95	0.037	0.079
153	15.99	18.15	8.28	12.48	-40.16	-18.92	-0.30	0.045	0.075

A1.6 Processed turbulence data for $F_1 = 2.5$, $Q = 68.6$ L/s, $y_1 = 7.1$ cm (cont'd)

x (cm)	y (cm)	$\sqrt{u'^2}$ (cm/s)	$\sqrt{v'^2}$ (cm/s)	$\sqrt{w'^2}$ (cm/s)	$-\overline{u'v'}$ (cm ² /s ²)	$-\overline{u'w'}$ (cm ² /s ²)	$-\overline{v'w'}$ (cm ² /s ²)	ε (m ² /s ³)	η (mm)
193	0.55	12.57	2.22	11.48	3.15	-31.54	-2.48	0.013	0.102
193	1.02	13.54	3.32	12.14	6.12	-34.10	-1.30	0.014	0.102
193	2.45	15.08	5.31	12.66	12.80	-39.38	-1.98	0.018	0.095
193	3.02	14.99	5.84	12.27	13.13	-31.51	-4.26	0.020	0.092
193	3.50	16.06	6.68	12.57	20.58	-44.16	-2.13	0.019	0.094
193	4.02	15.58	7.26	12.53	25.17	-40.42	-5.45	0.016	0.098
193	5.05	15.07	7.24	11.61	23.46	-35.17	-2.19	0.013	0.103
193	6.07	14.46	7.50	10.76	19.69	-27.28	-1.18	0.017	0.096
193	7.01	14.48	7.46	10.83	19.97	-29.13	0.30	0.018	0.094
193	8.09	14.50	7.83	10.78	19.52	-22.00	-1.47	0.014	0.100
193	9.06	14.49	7.94	10.32	16.78	-25.81	-0.09	0.016	0.097
193	10.02	13.54	7.94	10.01	8.59	-20.35	-1.68	0.015	0.099
193	11.01	13.09	8.06	10.03	2.54	-20.35	0.15	0.017	0.095
193	12.01	13.17	7.71	9.63	0.37	-22.48	1.44	0.017	0.095
193	13.07	13.07	7.84	9.55	-0.58	-14.09	-0.15	0.015	0.099
193	14.02	13.07	7.38	9.38	-6.99	-15.45	-1.15	0.012	0.104
193	15.04	12.84	7.66	9.87	-11.57	-13.88	2.77	0.013	0.104
193	16.00	14.04	7.10	10.91	-11.81	-20.16	4.63		
233	0.50	9.80	2.39	8.95	2.12	-12.26	-0.69	0.006	0.123
233	1.08	11.95	3.89	11.00	5.42	-20.88	-0.25	0.006	0.122
233	2.53	12.09	5.53	11.83	10.97	-25.10	-0.74	0.009	0.112
233	3.09	12.37	5.84	11.13	14.09	-24.83	0.12	0.011	0.108
233	3.53	12.66	6.72	11.68	18.15	-26.89	-0.44	0.008	0.116
233	4.06	12.92	6.71	11.28	21.33	-28.19	-1.08	0.011	0.108
233	5.06	12.50	7.03	11.11	21.60	-19.91	-2.48	0.008	0.114
233	6.08	12.89	7.36	11.04	20.94	-21.45	0.56	0.009	0.113
233	7.03	13.04	7.57	10.88	20.38	-24.88	-1.53	0.008	0.118
233	8.03	12.38	7.66	10.48	18.66	-18.38	0.55	0.010	0.110
233	9.01	12.35	7.86	10.19	20.44	-18.57	0.48	0.009	0.113
233	10.03	12.10	7.95	10.35	17.61	-11.45	0.59	0.009	0.114
233	11.05	12.09	7.93	10.27	16.51	-15.01	0.94	0.009	0.111
233	12.06	11.64	7.80	10.18	13.36	-10.39	0.94	0.009	0.111
233	13.01	11.50	7.80	10.00	9.51	-9.71	1.05	0.008	0.115
233	14.02	11.24	7.66	9.92	8.12	-9.86	0.20	0.008	0.117
233	15.08	11.96	7.58	11.19	6.93	-8.95	-0.36	0.007	0.119
273	0.48	8.76	2.18	8.86	2.07	-8.14	-0.28	0.006	0.127
273	1.04	9.92	3.25	9.42	4.69	-18.44	0.41	0.003	0.143
273	2.05	12.19	4.38	9.72	6.24	-18.53	-0.19	0.004	0.138
273	2.40	10.71	4.56	10.62	8.09	-8.81	0.11	0.009	0.112
273	3.12	10.56	5.02	10.21	9.95	-11.05	0.69	0.010	0.111
273	4.05	11.01	5.98	9.91	16.62	-19.56	-0.47	0.005	0.131

A1.6 Processed turbulence data for $F_1 = 2.5$, $Q = 68.6$ L/s, $y_1 = 7.1$ cm (cont'd)

x (cm)	y (cm)	$\sqrt{u'^2}$ (cm/s)	$\sqrt{v'^2}$ (cm/s)	$\sqrt{w'^2}$ (cm/s)	$-\overline{u'v'}$ (cm ² /s ²)	$-\overline{u'w'}$ (cm ² /s ²)	$-\overline{v'w'}$ (cm ² /s ²)	ε (m ² /s ³)	η (mm)
273	5.02	10.83	6.15	9.90	18.22	-14.79	-0.95	0.005	0.130
273	6.04	10.76	6.38	9.40	18.17	-16.35	-0.54	0.005	0.133
273	7.05	11.08	6.60	9.38	21.42	-13.17	-0.73	0.005	0.127
273	8.02	10.83	6.69	9.27	18.50	-15.45	0.27	0.006	0.127
273	9.02	10.31	6.67	9.11	17.01	-13.76	0.88	0.005	0.134
273	10.04	10.56	6.88	9.12	19.30	-9.22	-0.87	0.006	0.126
273	11.04	10.15	6.83	8.91	14.66	-8.35	-0.59	0.006	0.127
273	12.07	10.06	6.98	9.11	16.28	-8.05	0.14	0.004	0.135
273	13.04	9.87	6.80	8.93	12.99	-6.19	-0.60	0.005	0.129
273	14.01	9.83	6.83	8.90	10.08	-8.47	-0.73	0.005	0.133
273	15.02	9.70	6.66	8.91	7.45	-6.96	-1.75	0.005	0.130
323	0.45	8.33	1.93	7.82	2.40	-8.62	0.19	0.003	0.150
323	0.97	8.27	2.89	8.39	4.47	-7.88	0.68	0.003	0.144
323	2.03	9.80	3.88	8.66	6.24	-13.75	0.84	0.003	0.152
323	2.49	8.79	4.22	8.97	8.47	-10.46	0.56	0.003	0.151
323	3.02	9.31	4.35	9.22	9.07	-8.18	-0.47	0.005	0.128
323	4.03	9.04	5.05	8.52	12.34	-12.91	0.89	0.003	0.146
323	5.03	9.42	5.40	8.56	15.40	-10.60	0.04	0.003	0.151
323	6.03	9.42	5.57	8.29	15.77	-10.82	0.26	0.003	0.144
323	7.00	9.36	5.81	8.45	16.53	-12.99	0.84	0.004	0.139
323	8.01	9.28	5.98	8.32	15.52	-9.72	-0.48	0.003	0.148
323	9.04	9.21	5.93	8.21	16.78	-10.68	0.71	0.003	0.149
323	10.04	9.31	6.09	7.92	17.57	-8.31	0.79	0.003	0.144
323	11.02	8.90	6.09	7.93	15.16	-4.46	-0.66	0.003	0.149
323	12.03	9.13	6.14	7.94	15.52	-6.39	-0.80	0.003	0.149
323	13.02	8.71	6.04	7.66	13.05	-5.82	-0.67	0.003	0.150
323	14.01	8.76	5.99	7.80	11.72	-6.01	-0.10	0.003	0.147
323	15.02	8.75	5.78	8.31	9.14	-5.74	-0.30	0.003	0.145

A1.7 Processed turbulence data for $F_1 = 3.32$, $Q = 40$ L/s, $y_1 = 4.1$ cm

x (cm)	y (cm)	$\sqrt{u'^2}$ (cm/s)	$\sqrt{v'^2}$ (cm/s)	$\sqrt{w'^2}$ (cm/s)	$-\overline{u'v'}$ (cm ² /s ²)	$-\overline{u'w'}$ (cm ² /s ²)	$-\overline{v'w'}$ (cm ² /s ²)	ε (m ² /s ³)	η (mm)
38	0.56	42.48	4.21	12.49	-61.39	28.27	0.73		
38	1.00	43.31	5.12	12.11	-84.92	24.08	-0.38	0.525	0.041
38	2.01	31.90	6.41	15.45	-71.41	3.98	0.44	0.741	0.037
38	3.04	33.74	6.76	14.40	-108.80	-13.59	-2.86	1.130	0.034
38	3.50	38.22	8.39	18.32	-134.15	-9.91	-6.97		
48	0.57	28.38	4.01	13.37	-21.23	25.62	-1.30	0.325	0.046
48	0.98	31.29	5.14	12.39	-35.73	14.23	-0.24	0.361	0.045
48	2.01	30.10	6.38	14.36	-41.87	5.08	0.49	0.296	0.047
48	3.04	30.63	7.28	12.72	-87.08	3.11	-2.36	0.307	0.047
48	4.05	36.75	9.40	15.71	-156.68	-7.93	-0.22	0.887	0.036
48	5.03	36.30	10.22	17.30	-173.03	16.66	1.55	0.715	0.038
48	5.51	34.86	10.60	17.48	-173.84	-12.05	-7.22	0.824	0.036
58	0.60	23.74	3.69	14.28	-4.49	5.52	-1.29	0.167	0.054
58	1.01	27.29	4.91	13.17	-18.30	-5.41	0.43	0.225	0.050
58	1.99	26.83	6.73	14.44	-21.85	7.41	0.30	0.259	0.049
58	3.03	28.11	7.40	11.88	-55.48	-6.54	-0.67	0.213	0.051
58	4.02	34.48	8.97	13.52	-108.24	3.88	-2.19	0.358	0.045
58	5.01	34.51	10.43	14.83	-156.92	-6.63	-3.49	0.471	0.042
58	6.03	34.34	11.44	15.95	-189.27	-17.07	-2.57	0.498	0.041
58	7.00	33.19	11.98	16.08	-181.30	-4.46	2.59	0.499	0.041
58	7.48	30.84	12.27	17.67	-169.58	-7.84	0.81	0.535	0.041
68	0.57	23.24	3.49	15.63	-3.62	8.79	-2.71	0.134	0.057
68	1.02	25.33	4.80	15.16	-7.63	1.77	-2.83	0.123	0.059
68	2.02	29.94	7.38	16.01	-27.17	15.23	-0.65	0.248	0.049
68	3.02	25.03	7.17	11.30	-36.96	-6.15	-0.36	0.166	0.054
68	3.98	30.73	9.00	13.16	-85.11	-10.98	-0.58	0.251	0.049
68	5.04	33.38	9.59	13.99	-124.34	7.88	0.25	0.352	0.045
68	6.02	33.35	11.09	15.04	-163.27	0.75	2.50	0.489	0.041
68	7.01	31.89	11.13	15.05	-160.27	-19.57	-1.68	0.417	0.043
68	8.00	30.62	11.22	16.04	-152.88	-22.09	-0.89	0.410	0.043
68	9.04	28.64	11.70	16.60	-144.04	17.75	2.70	0.432	0.043
78	0.56	20.77	3.51	16.05	-3.51	-6.56	-1.78	0.097	0.062
78	1.00	23.18	4.80	15.91	-9.30	-15.79	-2.34	0.103	0.061
78	2.01	27.51	6.97	15.92	-17.42	-23.68	-1.85	0.144	0.056
78	3.05	23.30	7.16	12.28	-20.62	-18.75	-0.84	0.113	0.060
78	4.02	26.46	8.65	12.83	-53.04	-10.04	1.35	0.144	0.056
78	5.06	28.50	9.77	13.28	-90.38	-4.47	1.23	0.213	0.051
78	6.02	29.34	9.84	13.15	-105.87	-6.51	0.19	0.216	0.051
78	6.99	27.80	10.24	14.13	-112.60	3.57	1.33	0.287	0.047

A1.7 Processed turbulence data for $F_1 = 3.32$, $Q = 40$ L/s, $y_1 = 4.1$ cm (cont'd)

x (cm)	y (cm)	$\sqrt{u'^2}$ (cm/s)	$\sqrt{v'^2}$ (cm/s)	$\sqrt{w'^2}$ (cm/s)	$-\overline{u'v'}$ (cm ² /s ²)	$-\overline{u'w'}$ (cm ² /s ²)	$-\overline{v'w'}$ (cm ² /s ²)	ε (m ² /s ³)	η (mm)
78	8.05	28.19	10.75	14.45	-130.71	-3.15	0.09	0.284	0.047
78	8.99	26.97	11.10	14.95	-122.68	-3.38	1.87	0.223	0.050
78	9.99	25.44	10.80	15.25	-106.02	-2.75	-2.37	0.235	0.050
88	0.62	20.27	3.63	15.95	-1.43	-22.27	-0.53	0.072	0.067
88	1.01	20.83	4.60	14.80	-7.33	-19.18	0.01	0.077	0.066
88	2.03	24.06	6.86	14.53	-10.65	-16.03	-0.06	0.116	0.059
88	2.99	20.22	6.80	11.58	-16.57	-18.72	-2.72	0.091	0.063
88	4.04	23.09	8.25	12.86	-33.63	-19.17	-0.36	0.099	0.062
88	5.03	24.27	8.63	12.76	-52.66	-9.48	-2.46	0.095	0.062
88	6.01	24.21	9.18	11.77	-73.89	-14.63	-0.09	0.130	0.058
88	7.03	25.92	9.74	12.50	-89.46	-16.96	-0.51	0.153	0.055
88	8.01	25.26	10.11	13.52	-94.47	-10.42	-0.63	0.151	0.056
88	9.00	24.52	10.05	12.93	-96.39	-11.81	-1.21	0.130	0.058
88	10.03	22.95	10.12	14.01	-86.80	-1.43	-1.66	0.147	0.056
108	0.61	17.89	3.14	15.39	0.71	-24.84	-1.53	0.036	0.079
108	0.99	15.83	3.95	13.10	-0.91	-27.13	-2.94	0.025	0.087
108	2.00	17.41	5.97	12.52	-8.15	-31.51	-2.82	0.045	0.075
108	3.05	17.00	6.16	11.32	-9.57	-15.80	-2.17	0.045	0.075
108	4.04	17.69	7.48	11.73	-8.28	-19.74	-2.64	0.040	0.078
108	5.00	18.13	7.91	11.84	-22.71	-19.99	-0.72	0.042	0.077
108	6.06	18.95	8.25	11.44	-40.35	-25.52	0.02	0.054	0.072
108	7.02	18.14	8.21	11.37	-38.92	-16.69	-1.74	0.052	0.072
108	8.06	18.37	8.44	11.17	-46.20	-11.25	0.04	0.056	0.071
108	9.03	18.59	8.34	10.97	-45.42	-17.24	-0.96	0.066	0.068
108	9.99	18.13	8.55	11.34	-51.77	-8.40	0.54	0.063	0.069
108	11.05	17.59	8.51	11.13	-45.69	-7.21	-0.49	0.048	0.074
128	0.58	12.50	2.64	11.80	1.75	-18.25	-1.40	0.017	0.097
128	1.04	13.09	3.43	11.38	0.33	-25.07	-1.01	0.017	0.096
128	1.98	13.92	4.84	11.01	0.68	-23.60	-4.04	0.019	0.094
128	3.01	13.67	5.64	10.12	-0.45	-15.59	-1.73	0.026	0.086
128	3.99	15.15	6.84	10.96	-5.23	-27.34	-2.10	0.023	0.089
128	5.03	15.62	7.29	10.74	-13.18	-25.10	-2.23	0.022	0.090
128	6.04	16.04	7.73	11.09	-17.05	-23.39	-3.09	0.037	0.079
128	7.06	16.13	7.71	10.45	-26.48	-14.64	-1.90	0.029	0.084
128	8.01	14.30	7.55	10.38	-18.70	-17.16	0.32	0.021	0.091
128	9.03	14.06	7.60	9.33	-25.85	-10.98	-1.38	0.023	0.089
128	10.05	14.06	7.45	9.92	-21.77	-15.66	0.17	0.019	0.094
128	11.04	13.43	7.41	9.56	-23.65	-12.50	2.78	0.021	0.091

A1.7 Processed turbulence data for $F_1 = 3.32$, $Q = 40$ L/s, $y_1 = 4.1$ cm (cont'd)

x (cm)	y (cm)	$\sqrt{u'^2}$ (cm/s)	$\sqrt{v'^2}$ (cm/s)	$\sqrt{w'^2}$ (cm/s)	$-\overline{u'v'}$ (cm ² /s ²)	$-\overline{u'w'}$ (cm ² /s ²)	$-\overline{v'w'}$ (cm ² /s ²)	ε (m ² /s ³)	η (mm)
168	0.51	9.22	2.70	9.09	2.01	-10.92	-0.34	0.006	0.122
168	1.02	9.73	3.71	9.71	3.40	-16.38	-0.17	0.005	0.129
168	2.04	10.63	4.85	9.49	4.85	-18.65	-2.10	0.007	0.122
168	3.04	10.99	5.31	10.13	4.75	-13.46	-1.27	0.010	0.111
168	4.00	10.78	6.23	9.77	6.99	-15.45	-1.77	0.007	0.119
168	5.03	10.71	6.39	9.20	5.66	-13.12	-1.38	0.008	0.114
168	6.04	10.84	6.78	9.61	6.00	-18.04	-0.49	0.008	0.114
168	7.04	10.91	6.77	9.07	4.14	-14.21	0.30	0.007	0.118
168	8.04	10.34	6.87	9.17	0.38	-12.02	0.99	0.008	0.115
168	9.04	10.36	6.90	9.15	-0.33	-13.64	0.36	0.007	0.118
168	10.06	10.47	6.91	9.16	-1.83	-10.58	0.68	0.008	0.117
168	11.00	10.56	6.91	9.06	-2.55	-12.40	0.12	0.007	0.121
208	0.58	7.17	2.15	7.51	1.81	-7.24	-0.62	0.003	0.152
208	1.02	7.93	2.86	8.01	3.21	-11.74	-0.02	0.003	0.147
208	2.01	8.34	3.82	8.10	4.43	-11.86	-1.44	0.003	0.150
208	3.04	9.25	4.32	9.07	5.40	-7.78	-0.14	0.007	0.120
208	4.02	8.95	4.96	8.35	7.84	-14.49	-1.51	0.004	0.142
208	5.03	8.75	5.40	8.22	9.19	-10.40	-0.39	0.004	0.141
208	6.02	8.31	5.40	7.95	8.17	-7.73	-1.35	0.003	0.144
208	7.01	8.62	5.64	8.06	8.60	-11.43	-0.99	0.004	0.138
208	8.05	8.47	5.59	7.90	7.28	-7.13	-0.64	0.004	0.141
208	9.05	7.80	5.70	7.81	4.70	-7.40	-1.86	0.004	0.136
208	10.04	8.07	5.66	7.86	4.14	-8.17	-0.56	0.004	0.138
208	11.03	8.41	5.58	7.75	4.28	-7.51	-0.17	0.003	0.144
248	0.62	6.83	1.91	6.82	1.83	-4.48	-0.61	0.003	0.152
248	0.99	6.88	2.50	7.47	2.64	-8.11	-0.48	0.002	0.163
248	2.01	7.40	3.27	7.61	3.52	-8.70	-0.40	0.002	0.169
248	3.03	8.73	3.75	8.61	5.62	-5.03	-1.04	0.006	0.124
248	4.03	7.75	4.24	7.82	5.46	-9.58	-0.99	0.003	0.154
248	5.01	7.85	4.45	7.60	7.89	-8.86	-0.77	0.002	0.155
248	5.99	7.50	4.76	7.44	8.14	-6.69	-1.50	0.002	0.157
248	7.04	7.85	4.87	7.58	7.74	-9.44	-1.33	0.002	0.161
248	8.04	7.76	5.01	7.58	8.79	-7.65	-0.90	0.003	0.153
248	9.04	7.46	4.87	7.37	6.52	-5.27	-0.66	0.002	0.163
248	10.04	7.37	4.79	7.35	5.51	-5.55	-1.05	0.002	0.158
248	10.99	7.90	4.87	7.20	5.00	-5.19	-0.15	0.003	0.153

A1.8 Air concentration for $F_1 = 2.0$, $Q = 54.9$ L/s, $y_1 = 7.1$ cm

x (cm)	y (cm)	C (%)	C_e (%)	No. of Bubbles	V_{mean} (cm/s)	D_{mean} (cm)
13	1	0.00	0.606	0	0.00	0.00
13	2	0.00	0.755	0	0.00	0.00
13	3	0.01	0.667	6	101.32	3.50
13	4	0.04	0.972	10	114.35	2.98
13	5	0.17	1.176	68	90.33	2.70
13	6	0.88	1.123	260	85.71	3.05
13	7	2.56	2.93	648	82.79	3.12
13	8	5.79	5.411	865	71.72	3.31
13	9	8.93	7.751	617	59.31	3.81
23	1	0.00	0.919	0	0.00	0.00
23	2	0.02	0.95	7	99.34	2.95
23	3	0.12	0.965	37	83.88	2.85
23	4	0.13	1.013	49	86.08	2.94
23	5	0.25	1.273	96	86.23	2.81
23	6	0.61	1.253	176	80.24	2.93
23	7	1.23	1.508	349	79.26	3.05
23	8	1.85	1.857	396	73.40	3.15
23	9	2.69	2.406	392	68.66	3.30
23	10	3.08	2.654	337	64.54	3.38
23	11	3.34	3.129	202	57.39	3.58
23	11.5	4.46	4.71	144	52.57	3.82
33	1	0.01	0.8	2	72.18	3.00
33	2	0.04	0.969	12	89.26	2.66
33	3	0.12	0.908	51	77.21	2.52
33	4	0.15	0.902	55	71.83	2.47
33	5	0.39	1.228	113	80.84	3.12
33	6	0.54	1.024	132	75.97	2.94
33	7	0.69	1.057	163	76.95	3.01
33	8	0.88	1.134	186	70.89	3.01
33	9	1.16	0.98	186	63.44	3.00
33	10	1.28	1.079	183	64.58	3.48
33	11	1.43	1.296	135	54.92	3.40
33	12	1.53	1.856	114	53.14	3.48
33	13	2.75	3.237	89	52.23	3.70
43	1	0.02	0.764	6	89.14	3.50
43	2	0.05	0.582	20	90.07	2.73
43	3	0.10	0.694	27	68.50	2.48
43	4	0.17	0.857	39	81.65	3.29
43	5	0.25	0.842	51	73.56	3.16

Note: C – air concentration by fiber optic probe;
 C_e – air concentration by electrical probe;
 V_{mean} – average bubble velocity;
 D_{mean} – average bubble diameter.

A1.8 Air concentration for $F_1 = 2.0$, $Q = 54.9$ L/s, $y_1 = 7.1$ cm (cont'd)

x (cm)	y (cm)	C (%)	C_e (%)	No. of Bubbles	V_{mean} (cm/s)	D_{mean} (cm)
43	6	0.37	0.872	68	70.08	2.97
43	7	0.57	0.637	108	69.00	3.58
43	8	0.59	0.638	119	65.16	3.19
43	9	0.77	0.655	102	67.43	3.52
43	10	0.75	0.656	102	64.40	3.37
43	11	0.89	0.883	107	59.43	3.48
43	12	0.91	0.834	77	59.09	3.29
43	13	0.92	0.953	50	51.77	3.29
43	13.5	1.18		58	52.99	3.98
53	1	0.01	0.51	2	98.33	3.89
53	2	0.04	0.464	13	69.70	2.69
53	3	0.08	0.652	23	66.72	2.54
53	4	0.14	0.799	32	76.10	3.41
53	5	0.19	0.736	46	71.91	2.93
53	6	0.28	0.757	52	69.68	3.28
53	7	0.34	0.812	71	67.12	3.25
53	8	0.38	0.89	70	64.87	3.01
53	9	0.39	0.822	39	56.64	2.86
53	10	0.56	0.55	82	58.00	3.35
53	11	0.53	0.437	57	55.45	3.43
53	12	0.54	0.501	43	53.45	2.99
53	13	0.60	0.594	36	54.31	3.42
53	14	0.70	0.997	44	51.10	3.52
53	14.5	1.06		53	48.26	3.62
63	1	0.02	0.483	6	51.29	2.28
63	2	0.01	0.473	3	59.27	3.30
63	3	0.05	0.428	8	77.88	3.67
63	4	0.08	0.574	16	73.00	3.72
63	5	0.13	0.446	30	68.00	3.05
63	6	0.23	0.567	40	64.46	3.11
63	7	0.25	0.554	41	57.78	3.11
63	8	0.21	0.608	38	67.30	3.64
63	9	0.31	0.661	33	70.71	3.60
63	10	0.34	0.64	30	51.05	3.38
63	11	0.38	0.661	37	56.11	3.35
63	12	0.44	0.65	39	49.73	3.39
63	13	0.48	0.656	41	48.32	3.83
63	14	0.60	0.782	54	53.09	3.75
63	15	0.72	1.846	42	54.29	3.49
73	1	0.01	0.46	2	79.96	4.50
73	2	0.02	0.386	4	70.30	3.74
73	3	0.04	0.56	10	68.21	2.91
73	4	0.09	0.754	15	64.34	3.35

A1.8 Air concentration for $F_1 = 2.0$, $Q = 54.9$ L/s, $y_1 = 7.1$ cm (cont'd)

x (cm)	y (cm)	C (%)	C_e (%)	No. of Bubbles	V_{mean} (cm/s)	D_{mean} (cm)
73	5	0.08	0.516	12	66.56	3.58
73	6	0.12	0.467	19	72.97	3.52
73	7	0.17	0.46	23	63.63	3.37
73	8	0.21	0.784	34	57.12	3.10
73	9	0.16	0.699	14	53.85	3.37
73	10	0.28	0.793	28	54.69	3.03
73	11	0.29	0.869	32	51.28	3.26
73	12	0.32	0.856	34	49.61	3.38
73	13	0.32	0.827	26	53.18	3.37
73	14	0.38	0.635	29	52.76	3.80
73	15	0.40	0.785	34	49.64	3.33
73	15.5	0.81		38	54.66	3.66
93	1	0.00	0.361	0	0.00	0.00
93	2	0.01	0.425	0	0.00	0.00
93	3	0.01	0.594	2	96.01	4.31
93	4	0.03	0.535	4	66.27	4.51
93	5	0.03	0.555	7	59.13	3.39
93	6	0.05	0.539	4	68.62	3.06
93	7	0.04	0.516	10	59.75	2.95
93	8	0.07	0.499	9	51.11	3.34
93	9	0.07	0.497	9	60.14	4.33
93	10	0.09	0.441	16	65.38	3.52
93	11	0.11	0.523	10	52.51	2.93
93	12	0.10	0.5	13	59.20	3.70
93	13	0.20	0.491	27	49.68	3.64
93	14	0.25	0.501	33	56.78	3.53
93	15	0.20	0.699	18	48.93	3.27
93	16	0.53		32	59.03	4.02
113	1	0.00	0.35	0	0.00	0.00
113	2	0.00	0.316	0	0.00	0.00
113	3	0.00	0.278	0	0.00	0.00
113	4	0.01	0.282	1	29.86	4.30
113	5	0.00	0.276	0	0.00	0.00
113	6	0.02	0.338	3	61.28	3.94
113	7	0.02	0.335	1	96.01	4.00
113	8	0.01	0.314	3	60.51	3.34
113	9	0.03	0.351	2	46.39	4.52
113	10	0.03	0.345	5	53.80	2.89
113	11	0.06	0.36	10	52.85	3.07
113	12	0.06	0.419	8	54.08	3.10
113	13	0.11	0.436	18	48.89	3.10
113	14	0.10	0.431	14	49.95	2.72
113	15	0.09	0.567	11	59.33	3.81
113	16	0.15	0.891	6	58.98	4.58

A1.9 Air concentration for $F_1 = 2.5$, $Q = 68.6$ L/s, $y_1 = 7.1$ cm

x (cm)	y (cm)	C (%)	No. of Bubbles	V_{mean} (cm/s)	D_{mean} (cm)
13	1	0.002	0	0.00	0.00
13	2	0.000	0	0.00	0.00
13	3	0.001	0	0.00	0.00
13	4	0.016	13	138.07	2.14
13	5	0.208	110	125.41	2.37
13	6	1.48	395	120.62	3.26
13	7	5.061	1655	106.67	2.88
13	8	13.334	2600	91.22	3.21
23	1	0.00051	0	0.00	0.00
23	2	0.00445	2	128.41	2.02
23	3	0.05055	26	124.79	2.35
23	4	0.11823	77	110.69	2.19
23	5	0.41040	206	111.37	2.35
23	6	1.47747	623	110.57	2.57
23	7	3.25447	1162	103.35	2.78
23	8	5.14539	1474	96.42	2.95
23	9	8.04593	1725	89.10	3.16
23	10	9.58917	1157	76.22	3.35
33	1	0.00	1	68.23	1.24
33	2	0.03	16	127.78	2.69
33	3	0.10	68	107.68	2.10
33	4	0.27	148	114.10	2.40
33	5	0.47	241	110.49	2.42
33	6	1.15	493	106.12	2.60
33	7	1.78	700	99.71	2.66
33	8	2.80	998	96.15	2.82
33	9	3.49	1094	92.31	2.76
33	10	4.67	1058	83.02	3.02
33	11	5.59	965	78.67	3.14
33	12	5.60	669	71.33	3.17
33	13	5.72	494	64.26	3.21
43	1	0.01	7	125.52	1.87
43	2	0.03	25	110.66	2.02
43	3	0.14	74	105.43	2.44
43	4	0.32	166	104.12	2.40
43	5	0.62	297	103.61	2.49
43	6	0.95	377	98.00	2.75
43	7	1.34	526	97.29	2.70
43	8	1.73	634	93.60	2.74
43	9	2.14	674	87.65	2.82
43	10	2.77	769	86.16	3.03
43	11	2.74	654	78.82	3.04
43	12	2.90	532	76.06	3.01

A1.9 Air concentration for $F_1 = 2.5$, $Q = 68.6$ L/s, $y_1 = 7.1$ cm (cont'd)

x (cm)	y (cm)	C (%)	No. of Bubbles	V_{mean} (cm/s)	D_{mean} (cm)
43	13	3.16	449	69.53	3.07
43	14	3.25	413	67.22	3.17
53	1	0.00	3	104.12	1.66
53	2	0.08	37	105.66	2.64
53	3	0.15	67	102.77	2.46
53	4	0.25	101	103.54	2.65
53	5	0.45	168	96.75	2.87
53	6	0.64	231	98.45	2.84
53	7	0.99	322	94.30	3.02
53	8	1.25	401	92.40	3.02
53	9	1.33	398	88.04	2.82
53	10	1.65	460	87.50	3.04
53	11	2.15	441	77.90	3.28
53	12	1.89	380	78.24	3.20
53	13	2.21	379	72.29	3.13
53	14	2.49	409	74.02	3.40
53	15	2.66	283	70.16	3.40
53	16	3.06	225	62.83	3.32
63	1	0.01	6.00	108.60	2.44
63	2	0.05	17.00	99.90	2.46
63	3	0.14	51.00	88.29	2.50
63	4	0.20	85.00	97.12	2.81
63	5	0.30	121.00	96.05	2.71
63	6	0.45	165.00	94.17	2.94
63	7	0.59	212.00	91.84	2.88
63	8	0.76	263.00	89.11	2.80
63	9	1.00	329.00	84.55	2.99
63	10	1.04	298.00	86.97	2.97
63	11	1.33	356.00	78.66	3.00
63	12	1.45	333.00	77.44	3.18
63	13	1.61	348.00	75.58	3.13
63	14	1.42	282.00	74.22	3.02
63	15	1.87	323.00	68.60	3.14
63	16	1.82	235.00	65.32	3.40
63	17	2.24	209.00	62.79	3.27
73	1	0.01	2	62.47	1.94
73	2	0.05	18	93.97	2.86
73	3	0.08	36	87.68	2.86
73	5	0.18	76	97.64	2.59
73	6	0.28	105	96.93	3.03
73	7	0.46	160	87.77	3.05
73	8	0.58	175	90.71	3.08
73	9	0.73	215	83.77	3.14

A1.9 Air concentration for $F_1 = 2.5$, $Q = 68.6$ L/s, $y_1 = 7.1$ cm (cont'd)

x (cm)	y (cm)	C (%)	No. of Bubbles	V_{mean} (cm/s)	D_{mean} (cm)
73	10	0.93	265	80.51	3.05
73	11	0.87	233	80.77	3.05
73	12	0.88	224	78.89	2.91
73	13	1.14	254	75.53	3.04
73	14	1.23	249	76.36	3.25
73	15	1.24	240	68.72	3.13
73	16	1.36	229	66.75	3.38
73	17	1.26	185	65.12	3.09
73	18	2.47	239	63.43	3.28
93	1	0.00	2	88.30	2.04
93	2	0.04	11	85.95	3.10
93	3	0.05	18	76.05	2.58
93	4	0.09	28	81.72	2.51
93	5	0.12	44	83.33	3.04
93	6	0.16	58	85.45	2.98
93	7	0.20	67	80.83	2.82
93	8	0.23	78	87.78	3.02
93	9	0.34	101	80.15	3.26
93	10	0.38	113	79.53	2.93
93	11	0.40	124	83.02	3.13
93	12	0.50	138	79.51	3.05
93	13	0.55	137	76.84	3.08
93	14	0.61	140	72.40	2.93
93	15	0.79	190	72.61	3.18
93	16	0.87	186	69.78	3.32
93	17	0.79	168	72.50	3.37
93	18	0.81	138	67.68	3.50
93	19	1.00	130	64.48	3.23
113	1	0.00	0	0.00	0.00
113	2	0.01	0	0.00	0.00
113	3	0.02	8	80.72	2.97
113	4	0.05	16	82.06	3.24
113	5	0.04	11	88.53	4.18
113	6	0.08	25	79.95	3.08
113	7	0.11	33	79.51	3.10
113	8	0.12	31	79.65	3.12
113	9	0.16	52	83.30	3.15
113	10	0.20	54	87.89	3.49
113	11	0.23	69	80.45	3.21
113	12	0.25	72	75.13	2.93
113	13	0.26	77	80.86	2.97
113	14	0.36	91	76.84	3.35
113	15	0.41	96	75.82	3.27
113	16	0.38	77	77.93	3.62

A1.9 Air concentration for $F_1 = 2.5$, $Q = 68.6$ L/s, $y_1 = 7.1$ cm (cont'd)

x (cm)	y (cm)	C (%)	No. of Bubbles	V_{mean} (cm/s)	D_{mean} (cm)
113	17	0.43	93	70.26	3.45
113	18	0.55	105	67.38	3.47
113	19	0.53	97	68.02	3.48
153	1	0.00	0	0.00	0.00
153	2	0.00	0	0.00	0.00
153	3	0.00	0	0.00	0.00
153	4	0.00	1	61.10	2.93
153	5	0.01	0	0.00	0.00
153	6	0.01	2	60.06	3.21
153	7	0.02	4	68.95	3.76
153	8	0.03	11	93.16	2.98
153	9	0.04	11	82.94	3.07
153	10	0.04	11	85.78	3.89
153	11	0.06	14	64.16	2.92
153	12	0.07	19	90.66	3.74
153	13	0.07	17	77.11	2.99
153	14	0.07	21	76.00	3.24
153	15	0.08	21	82.47	3.01
153	16	0.11	27	76.44	3.55
153	17	0.10	21	72.72	3.72
153	18	0.17	39	63.18	3.10
153	19	0.16	40	66.02	3.04
153	20	0.15	31	66.69	3.47
193	1	0.01	0	0.00	0.00
193	2	0.00	0	0.00	0.00
193	3	0.00	0	0.00	0.00
193	4	0.01	0	0.00	0.00
193	5	0.02	0	0.00	0.00
193	6	0.00	0	0.00	0.00
193	7	0.00	0	0.00	0.00
193	8	0.00	0	0.00	0.00
193	9	0.01	1	33.09	2.37
193	10	0.01	0	0.00	0.00
193	11	0.00	1	73.98	3.52
193	12	0.01	3	67.42	3.56
193	13	0.01	4	54.25	2.69
193	14	0.01	4	83.83	3.76
193	15	0.01	3	68.78	3.00
193	16	0.02	7	65.66	2.87
193	17	0.03	5	85.49	4.32
193	18	0.05	12	81.18	3.51
193	19	0.02	2	70.82	3.74
193	20	0.03	8	72.31	3.38

A1.10 Air concentration for $F_1 = 3.32$, $Q = 40$ L/s, $y_1 = 4.1$ cm

x (cm)	y (cm)	C (%)	No. of Bubbles	V_{mean} (cm/s)	D_{mean} (cm)
28	1	0.15	91	116.11	2.48
28	2	0.77	355	109.92	2.71
28	3	2.00	749	102.62	2.83
28	4	3.62	1177	95.40	2.92
28	5	5.56	1346	86.61	3.10
28	6	7.41	1237	77.48	3.23
28	7	7.14	834	69.76	3.33
28	7.5	7.13	607	64.72	3.49
28	8	7.60	479	62.28	3.39
28	8.5	9.02	364	58.77	3.51
28	9	9.83	268	52.42	3.70
38	1	0.26	110	102.45	2.48
38	2	0.75	288	97.70	2.65
38	3	1.50	548	90.92	2.71
38	4	2.07	673	89.53	2.89
38	5	3.02	786	82.50	3.08
38	6	3.61	744	76.23	3.02
38	7	3.59	620	73.08	3.20
38	8	3.63	422	67.28	3.27
38	9	3.31	306	58.97	3.19
38	9.5	3.67	222	56.46	3.37
38	10	4.11	203	56.62	3.32
38	10.5	5.69	166	52.16	3.38
48	1	0.22	87	85.11	2.65
48	2	0.54	168	88.39	2.86
48	3	1.03	337	83.03	2.74
48	4	1.45	404	81.75	2.88
48	5	1.78	451	80.94	3.11
48	6	2.14	483	78.03	3.13
48	7	2.26	411	73.14	3.23
48	8	2.36	357	67.78	3.17
48	9	2.38	275	62.88	3.28
48	10	2.39	215	57.40	3.09
48	10.5	2.17	175	55.22	3.46
48	11	2.07	156	55.56	2.99
48	11.5	2.73	143	55.36	3.17
58	1	0.14	44	73.16	2.68
58	2	0.43	126	82.44	2.94
58	3	0.68	173	76.95	2.94
58	4	0.86	240	79.18	3.04
58	5	1.17	260	75.50	2.95

A1.10 Air concentration for $F_1 = 3.32$, $Q = 40$ L/s, $y_1 = 4.1$ cm (cont'd)

x (cm)	y (cm)	C (%)	No. of Bubbles	V_{mean} (cm/s)	D_{mean} (cm)
58	6	1.33	289	76.61	3.09
58	7	1.31	230	71.88	3.15
58	8	1.59	243	67.67	3.14
58	9	1.76	222	66.94	3.27
58	10	1.69	204	61.85	3.34
58	11	1.57	133	55.79	3.23
58	12	1.89	122	51.26	3.06
58	12.5	2.12	125	55.54	3.35
68	1	0.08	15	71.69	2.68
68	2	0.24	65	69.81	2.84
68	3	0.35	80	74.44	2.90
68	4	0.44	115	71.90	2.66
68	5	0.71	157	72.57	2.96
68	6	0.75	166	74.39	3.15
68	7	0.92	178	65.31	3.04
68	8	1.06	165	65.00	3.07
68	9	1.24	183	64.56	3.34
68	10	1.29	163	58.79	3.15
68	11	1.22	128	60.17	3.22
68	12	1.29	114	55.76	3.07
68	13	1.29	115	51.19	3.24
78	1	0.04	12	64.69	2.60
78	2	0.13	28	56.12	2.75
78	3	0.21	45	67.82	3.02
78	4	0.27	63	72.64	2.90
78	5	0.42	90	68.16	3.18
78	6	0.46	90	63.97	3.10
78	7	0.70	121	66.66	3.26
78	8	0.76	126	63.74	3.12
78	9	0.94	151	64.77	3.14
78	10	0.98	152	62.16	3.39
78	11	0.86	100	58.45	3.08
78	12	1.00	125	57.58	3.19
78	13	1.06	119	56.71	3.49
78	13.5	1.15	111	51.76	3.36
88	1	0.02	2	35.77	3.17
88	2	0.06	14	59.61	3.44
88	3	0.12	32	65.74	2.72
88	4	0.19	32	64.78	3.22
88	5	0.22	53	66.97	3.32

A1.10 Air concentration for $F_1 = 3.32$, $Q = 40$ L/s, $y_1 = 4.1$ cm (cont'd)

x (cm)	y (cm)	C (%)	No. of Bubbles	V_{mean} (cm/s)	D_{mean} (cm)
88	6	0.29	63	67.12	3.02
88	7	0.35	64	60.15	3.01
88	8	0.42	76	65.18	3.35
88	9	0.53	101	63.97	3.19
88	10	0.56	75	62.45	3.29
88	11	0.70	81	61.95	3.73
88	12	0.90	116	57.59	3.47
88	13	0.74	85	59.90	3.57
88	14	0.93	98	54.50	3.29
108	1	0.00	0	0.00	0.00
108	2	0.01	2	56.15	4.81
108	3	0.01	3	61.85	2.44
108	4	0.03	6	73.92	2.75
108	5	0.05	9	57.11	3.95
108	6	0.06	9	71.50	3.52
108	7	0.10	18	68.44	3.64
108	8	0.19	31	54.58	3.24
108	9	0.18	32	55.67	3.15
108	10	0.21	37	58.48	3.19
108	11	0.27	31	52.42	3.31
108	12	0.34	41	52.98	3.03
108	13	0.26	41	58.95	3.28
108	14	0.32	47	54.87	3.26
108	14.5	0.37	50	60.07	3.36
128	1	0.00	0	0.00	0.00
128	2	0.00	1	39.80	2.94
128	3	0.00	0	0.00	0.00
128	4	0.01	0	0.00	0.00
128	5	0.01	3	55.80	1.86
128	6	0.01	0	0.00	0.00
128	7	0.03	5	48.44	3.37
128	8	0.03	4	55.16	3.49
128	9	0.02	3	57.68	3.01
128	10	0.06	11	56.36	2.67
128	11	0.10	15	53.31	3.58
128	12	0.09	14	55.02	3.74
128	13	0.07	13	54.88	3.27
128	14	0.13	22	50.00	3.37
128	14.5	0.12	15	56.89	3.12

A2. Experimental Study on Turbulence Structure in Vertical Slot Fishways

A2.1 Overall structure of flow in the pool with coordinates (x, y, z)

A2.1.1 Mean velocity for $S = 5.06\%$, $Q = 31.2$ L/s, $z = 10$ mm

x (mm)	y (mm)	u (m/s)	v (m/s)	w (m/s)	x (mm)	y (mm)	u (m/s)	v (m/s)	w (m/s)
100	50	0.0109	0.0246	-0.0007	300	500	0.6098	-0.3308	-0.0180
100	100	-0.0283	0.0548	-0.0006	300	550	0.5648	-0.2288	-0.0282
100	150	-0.0130	0.0769	-0.0010	300	600	0.3900	-0.0950	-0.0299
100	200	0.0208	0.1002	-0.0013	300	650	0.1852	-0.0366	-0.0020
100	250	0.0259	0.1101	0.0001	300	700	0.0659	-0.0584	0.0085
100	300	0.0436	0.1084	-0.0028	300	750	0.0091	-0.1009	0.0038
100	350	0.0522	0.1169	-0.0019	300	800	-0.0197	-0.0880	0.0039
100	400	0.0569	0.1089	0.0012	300	850	-0.0268	-0.0493	0.0036
100	450	0.0793	0.0623	0.0052					
100	500	0.1517	-0.0649	0.0109	400	50	-0.2559	0.0131	0.0013
100	550	0.3566	-0.3537	-0.0099	400	100	-0.1552	0.0027	-0.0006
100	600	0.6082	-0.7460	0.0100	400	150	-0.0751	-0.0040	0.0012
100	650	0.5047	-0.6894	-0.0489	400	200	0.0268	-0.0267	0.0009
					400	250	0.1250	-0.0451	0.0027
200	50	-0.1211	0.0381	-0.0021	400	300	0.2218	-0.0890	0.0042
200	100	-0.0756	0.0630	-0.0024	400	350	0.3268	-0.1319	0.0070
200	150	-0.0552	0.0850	-0.0044	400	400	0.4953	-0.2175	0.0062
200	200	-0.0258	0.0846	-0.0020	400	450	0.5793	-0.2316	0.0016
200	250	0.0032	0.0839	-0.0022	400	500	0.6528	-0.1849	-0.0141
200	300	0.0484	0.0587	-0.0001	400	550	0.6052	-0.0918	-0.0185
200	350	0.0839	-0.0053	-0.0014	400	600	0.4466	-0.0197	-0.0090
200	400	0.1820	-0.0937	0.0044	400	650	0.2204	-0.0232	0.0014
200	450	0.3427	-0.2975	0.0037	400	700	0.0591	-0.0876	0.0069
200	500	0.5097	-0.4310	-0.0052	400	750	-0.0510	-0.1054	0.0026
200	550	0.5577	-0.4631	-0.0057	400	800	-0.1441	-0.1197	0.0003
200	600	0.4678	-0.2986	-0.0372	400	850	-0.1924	-0.0837	0.0003
200	650	0.1469	-0.0993	-0.0082					
200	700	0.1349	-0.0902	0.0000	500	50	-0.3006	0.0027	0.0030
200	750	0.1225	-0.0772	-0.0017	500	100	-0.2020	-0.0029	0.0034
200	800	0.1333	-0.0493	-0.0036	500	150	-0.0733	-0.0499	0.0041
200	850	0.1314	-0.0245	-0.0063	500	200	0.0402	-0.0516	0.0010
					500	250	0.1485	-0.0539	0.0023
300	50	-0.1831	0.0218	0.0014	500	300	0.2869	-0.0950	0.0055
300	100	-0.1218	0.0377	-0.0002	500	350	0.4168	-0.1320	0.0059
300	150	-0.0762	0.0440	-0.0027	500	400	0.5348	-0.1380	0.0033
300	200	-0.0170	0.0343	-0.0032	500	450	0.6092	-0.1257	-0.0036
300	250	0.0559	0.0103	-0.0009	500	500	0.6801	-0.0650	-0.0101
300	300	0.1446	-0.0421	0.0008	500	550	0.6014	0.0027	-0.0089
300	350	0.2276	-0.1134	0.0017	500	600	0.4770	0.0304	-0.0044
300	400	0.3675	-0.2152	0.0017	500	650	0.2823	0.0023	0.0046
300	450	0.4991	-0.2965	-0.0050	500	700	0.0741	-0.0616	0.0065

A2.1.1 Mean velocity for $S = 5.06\%$, $Q = 31.2$ L/s, $z = 10$ mm (cont'd)

x (mm)	y (mm)	u (m/s)	v (m/s)	w (m/s)	x (mm)	y (mm)	u (m/s)	v (m/s)	w (m/s)
500	750	-0.0779	-0.0905	0.0009	800	300	0.0891	-0.0380	0.0084
500	800	-0.1773	-0.0968	0.0008	800	350	0.1876	-0.0021	0.0073
500	850	-0.2889	-0.0894	-0.0009	800	400	0.2837	0.0591	0.0024
600	50	-0.3092	0.0004	0.0018	800	450	0.3389	0.1254	0.0044
600	100	-0.2133	-0.0286	0.0034	800	500	0.4280	0.1980	0.0044
600	150	-0.1043	-0.0469	0.0053	800	550	0.4460	0.2568	0.0011
600	200	0.0430	-0.0609	0.0048	800	600	0.4516	0.2836	0.0041
600	250	0.1826	-0.0683	0.0036	800	650	0.3493	0.2941	0.0072
600	300	0.2879	-0.0618	0.0051	800	700	0.2171	0.2350	0.0049
600	350	0.4018	-0.0718	0.0032	800	750	0.0413	0.1745	0.0074
600	400	0.5300	-0.0505	0.0017	800	800	-0.1330	0.0978	0.0145
600	450	0.5838	-0.0075	-0.0039	800	850	-0.2837	-0.0494	0.0201
600	500	0.6392	0.0427	-0.0055					
600	550	0.6205	0.0824	-0.0061	900	50	-0.2970	-0.0487	0.0067
600	600	0.5114	0.1033	-0.0001	900	100	-0.3021	-0.0918	0.0102
600	650	0.3104	0.0603	0.0049	900	150	-0.2388	-0.1163	0.0099
600	700	0.1630	0.0146	0.0055	900	200	-0.1976	-0.1122	0.0113
600	750	-0.0912	-0.0372	0.0040	900	250	-0.1744	-0.1165	0.0150
600	800	-0.2096	-0.0618	0.0040	900	300	-0.1019	-0.0786	0.0156
600	850	-0.3439	-0.0873	0.0026	900	350	-0.0776	-0.0475	0.0169
					900	400	-0.0284	0.0227	0.0096
700	50	-0.3153	-0.0192	0.0017	900	450	0.0180	0.1203	0.0073
700	100	-0.2434	-0.0355	0.0049	900	525	0.1442	0.2720	0.0100
700	150	-0.1465	-0.0556	0.0049	900	550	0.1958	0.3360	0.0086
700	200	-0.0021	-0.0534	0.0078	900	600	0.2877	0.3458	0.0098
700	250	0.1158	-0.0424	0.0052	900	650	0.2810	0.3587	0.0106
700	300	0.2114	-0.0264	0.0040	900	700	0.2480	0.3051	0.0101
700	350	0.3290	-0.0157	0.0035	900	750	0.1231	0.2141	0.0110
700	400	0.4093	0.0350	0.0021	900	800	-0.0422	0.1146	0.0138
700	450	0.4827	0.0882	-0.0013	900	850	-0.1638	-0.0269	0.0148
700	500	0.5559	0.1290	-0.0056					
700	550	0.5739	0.1685	-0.0013	1000	50	-0.2303	-0.0686	-0.0009
700	600	0.4774	0.1941	0.0004	1000	100	-0.2442	-0.1457	0.0035
700	650	0.3421	0.1521	0.0024	1000	150	-0.2458	-0.1817	0.0032
700	700	0.1931	0.1058	0.0033	1000	200	-0.2325	-0.1691	0.0019
700	750	-0.0291	0.0607	0.0040	1000	250	-0.2174	-0.1521	0.0029
700	800	-0.2107	0.0173	0.0061	1000	300	-0.2310	-0.1379	0.0003
700	850	-0.3484	-0.0776	0.0107	1000	350	-0.1914	-0.1265	0.0020
					1000	400	-0.1951	-0.1056	-0.0039
800	50	-0.3103	-0.0279	0.0024	1000	650	0.3145	0.3203	0.0165
800	100	-0.2666	-0.0516	0.0054	1000	700	0.2887	0.2177	0.0190
800	150	-0.2035	-0.0762	0.0099	1000	750	0.1817	0.1034	0.0134
800	200	-0.1129	-0.0794	0.0088	1000	800	0.0218	-0.0181	0.0101
800	250	-0.0296	-0.0684	0.0100	1000	850	-0.0635	-0.1170	0.0024

A2.1.2 Mean velocity for $S = 5.06\%$, $Q = 31.2$ L/s, $z = 100$ mm

x (mm)	y (mm)	u (m/s)	v (m/s)	w (m/s)	x (mm)	y (mm)	u (m/s)	v (m/s)	w (m/s)
100	50	-0.0922	0.0337	0.0114	300	650	0.1351	-0.1197	-0.0142
100	100	-0.1272	0.0621	0.0097	300	700	-0.0387	-0.1175	0.0376
100	150	-0.1283	0.0993	-0.0033	300	750	-0.0822	-0.1230	0.0469
100	200	-0.1089	0.1118	0.0006	300	800	-0.1064	-0.1028	0.0443
100	250	-0.1032	0.1283	-0.0009	300	850	-0.1250	-0.0691	0.0473
100	300	-0.0822	0.1373	-0.0045					
100	350	-0.0586	0.1419	-0.0068	400	50	-0.2799	0.0400	0.0081
100	400	-0.0243	0.1403	-0.0090	400	100	-0.2401	0.0629	0.0028
100	450	-0.0008	0.1333	-0.0074	400	150	-0.1937	0.0656	0.0052
100	500	0.0621	0.1012	-0.0063	400	200	-0.1139	0.0845	-0.0019
100	550	0.2173	-0.0256	0.0137	400	250	-0.0206	0.0649	-0.0030
100	600	0.9534	-0.4501	0.0510	400	300	0.0871	0.0617	-0.0148
100	650	1.0108	-0.4980	-0.0366	400	350	0.1808	0.0625	-0.0146
					400	400	0.3223	0.0320	-0.0249
					400	450	0.5220	-0.0479	-0.0238
200	50	-0.1645	0.0369	0.0030	400	500	0.7069	-0.1042	-0.0247
200	100	-0.1751	0.0735	-0.0089	400	550	0.6955	-0.1401	-0.0295
200	150	-0.1549	0.1023	-0.0112	400	600	0.4807	-0.1128	-0.0241
200	200	-0.1286	0.1244	-0.0169	400	650	0.1588	-0.1234	0.0162
200	250	-0.0951	0.1310	-0.0171	400	700	0.0012	-0.1471	0.0283
200	300	-0.0439	0.1371	-0.0128	400	750	-0.0836	-0.1452	0.0165
200	350	-0.0070	0.1179	-0.0196	400	800	-0.1556	-0.1210	0.0107
200	400	0.0700	0.0861	-0.0166	400	850	-0.2163	-0.1043	0.0111
200	450	0.1628	0.0432	-0.0205					
200	500	0.3830	-0.0700	-0.0076	500	50	-0.3044	0.0249	0.0258
200	550	0.7719	-0.2730	-0.0096	500	100	-0.2573	0.0280	0.0321
200	600	0.9057	-0.3361	-0.0284	500	150	-0.1857	0.0380	0.0175
200	650	0.2563	-0.1431	-0.0708	500	200	-0.0638	0.0025	0.0103
200	700	-0.0899	-0.0833	-0.0157	500	250	0.0243	0.0280	-0.0017
200	750	-0.0839	-0.0714	0.0072	500	300	0.1211	0.0497	-0.0098
200	800	-0.0639	-0.0544	0.0051	500	350	0.2257	0.0506	-0.0214
200	850	-0.0366	-0.0404	-0.0081	500	400	0.4104	0.0270	-0.0243
					500	450	0.5928	-0.0037	-0.0248
300	50	-0.2294	0.0399	-0.0012	500	500	0.7218	-0.0316	-0.0278
300	100	-0.2089	0.0689	-0.0038	500	550	0.6481	-0.0440	-0.0138
300	150	-0.1664	0.0874	-0.0106	500	600	0.4596	-0.0500	0.0043
300	200	-0.1266	0.1077	-0.0079	500	650	0.1970	-0.0984	0.0188
300	250	-0.0547	0.0993	-0.0130	500	700	0.0307	-0.1218	0.0088
300	300	0.0203	0.0881	-0.0093	500	750	-0.1099	-0.1230	-0.0013
300	350	0.0810	0.1024	-0.0139	500	800	-0.2183	-0.1012	-0.0116
300	400	0.2013	0.0501	-0.0218	500	850	-0.2929	-0.0620	-0.0135
300	450	0.3609	-0.0134	-0.0300					
300	500	0.6189	-0.1410	-0.0228					
300	550	0.8191	-0.2292	-0.0331					
300	600	0.5702	-0.1674	-0.0614					

A2.1.2 Mean velocity for $S = 5.06\%$, $Q = 31.2$ L/s, $z = 100$ mm (cont'd)

x (mm)	y (mm)	u (m/s)	v (m/s)	w (m/s)	x (mm)	y (mm)	u (m/s)	v (m/s)	w (m/s)
600	50	-0.3448	0.0324	0.0151	800	450	0.3794	0.1574	0.0163
600	100	-0.2553	0.0175	0.0406	800	500	0.4462	0.2220	0.0257
600	150	-0.1943	0.0311	0.0322	800	550	0.5029	0.2747	0.0189
600	200	-0.0661	0.0119	0.0329	800	600	0.4589	0.3145	0.0224
600	250	0.0260	0.0264	0.0040	800	650	0.3862	0.2974	0.0327
600	300	0.1521	0.0238	-0.0022	800	700	0.2200	0.2482	0.0245
600	350	0.2754	0.0429	-0.0109	800	750	0.0456	0.2161	0.0060
600	400	0.4017	0.0625	-0.0184	800	800	-0.0999	0.1555	0.0036
600	450	0.5594	0.0778	-0.0193	800	850	-0.2711	0.1233	-0.0028
600	500	0.6793	0.0721	-0.0087					
600	550	0.6216	0.0610	0.0014	900	50	-0.2891	0.0446	-0.0091
600	600	0.4783	0.0503	0.0152	900	100	-0.2169	0.0398	0.0267
600	650	0.2806	0.0080	0.0247	900	150	-0.1319	-0.0099	0.0408
600	700	0.0705	-0.0190	0.0113	900	200	-0.0426	-0.0120	0.0413
600	750	-0.0997	-0.0474	-0.0140	900	250	0.0141	-0.0270	0.0571
600	800	-0.2465	-0.0424	-0.0200	900	300	0.0752	-0.0074	0.0526
600	850	-0.3657	-0.0234	-0.0228	900	350	0.1276	0.0247	0.0642
					900	400	0.1981	0.0696	0.0568
700	50	-0.3318	0.0314	0.0142	900	450	0.2278	0.1503	0.0399
700	100	-0.2614	0.0183	0.0461	900	525	0.3398	0.2958	0.0304
700	150	-0.1835	0.0016	0.0432	900	550	0.3877	0.3251	0.0331
700	200	-0.0173	-0.0096	0.0329	900	600	0.4143	0.3678	0.0313
700	250	0.0293	0.0054	0.0239	900	650	0.4172	0.3739	0.0278
700	300	0.1488	0.0208	0.0145	900	700	0.3281	0.3341	0.0282
700	350	0.2628	0.0561	0.0047	900	750	0.1839	0.2661	0.0292
700	400	0.3806	0.0866	-0.0043	900	800	0.0371	0.2259	0.0240
700	450	0.4865	0.1352	-0.0033	900	850	-0.0882	0.1775	0.0040
700	500	0.5726	0.1743	-0.0019					
700	550	0.5834	0.1900	0.0057	1000	50	-0.2379	-0.0120	-0.0418
700	600	0.4952	0.1750	0.0214	1000	100	-0.1391	-0.0389	-0.0099
700	650	0.3155	0.1520	0.0264	1000	150	-0.0743	-0.0479	-0.0132
700	700	0.1301	0.0924	0.0078	1000	200	-0.0190	-0.0787	-0.0125
700	750	-0.0626	0.0613	-0.0172	1000	250	0.0163	-0.0871	-0.0125
700	800	-0.2125	0.0436	-0.0178	1000	300	0.0571	-0.0784	-0.0225
700	850	-0.3371	0.0411	-0.0147	1000	350	0.0865	-0.0628	-0.0387
					1000	400	0.1114	-0.0364	-0.0470
800	50	-0.2758	0.0298	0.0075	1000	650	0.5087	0.3439	0.0317
800	100	-0.2566	0.0402	0.0371	1000	700	0.4261	0.2587	0.0368
800	150	-0.1602	0.0043	0.0507	1000	750	0.3151	0.2160	0.0397
800	200	-0.0504	-0.0220	0.0643	1000	800	0.1812	0.1882	0.0378
800	250	0.0256	-0.0070	0.0633	1000	850	0.0906	0.1482	-0.0104
800	300	0.1083	0.0043	0.0578					
800	350	0.2069	0.0470	0.0500					
800	400	0.2888	0.0935	0.0421					

A2.1.3 Mean velocity for $S = 5.06\%$, $Q = 31.2$ L/s, $z = 150$ mm

x (mm)	y (mm)	u (m/s)	v (m/s)	w (m/s)	x (mm)	y (mm)	u (m/s)	v (m/s)	w (m/s)
100	50	-0.0732	0.0372	0.0122	300	650	0.1662	-0.1380	-0.0316
100	100	-0.0896	0.0555	-0.0005	300	700	-0.0560	-0.1229	0.0205
100	150	-0.1001	0.0815	-0.0049	300	750	-0.1129	-0.1352	0.0317
100	200	-0.0941	0.1036	-0.0075	300	800	-0.1440	-0.1179	0.0265
100	250	-0.0932	0.1269	-0.0144	300	850	-0.1747	-0.0840	0.0301
100	300	-0.0737	0.1323	-0.0113					
100	350	-0.0577	0.1357	-0.0113	400	50	-0.2758	0.0485	-0.0039
100	400	-0.0271	0.1271	-0.0176	400	100	-0.2517	0.0794	0.0086
100	450	0.0177	0.1025	-0.0235	400	150	-0.2186	0.0924	0.0022
100	500	0.0897	0.0667	-0.0192	400	200	-0.1642	0.0966	-0.0059
100	550	0.2745	-0.0893	0.0072	400	250	-0.0866	0.1080	-0.0123
100	600	0.9772	-0.5201	0.0120	400	300	-0.0004	0.0999	-0.0352
100	650	0.9986	-0.5134	-0.0005	400	350	0.1684	0.0425	-0.0292
					400	400	0.3689	0.0019	-0.0187
200	50	-0.1346	0.0274	-0.0188	400	450	0.5749	-0.0909	0.0086
200	100	-0.1606	0.0658	-0.0138	400	500	0.7806	-0.1493	0.0164
200	150	-0.1374	0.0937	-0.0204	400	550	0.7413	-0.1765	-0.0078
200	200	-0.1287	0.1196	-0.0174	400	600	0.4646	-0.1346	-0.0083
200	250	-0.1082	0.1331	-0.0177	400	650	0.1581	-0.1374	0.0295
200	300	-0.0631	0.1399	-0.0287	400	700	-0.0131	-0.1565	0.0281
200	350	-0.0221	0.1283	-0.0212	400	750	-0.0960	-0.1511	0.0150
200	400	0.0621	0.0858	-0.0339	400	800	-0.1939	-0.1275	0.0087
200	450	0.2143	0.0062	-0.0311	400	850	-0.2365	-0.0992	0.0062
200	500	0.4568	-0.1504	0.0032					
200	550	0.8514	-0.3493	0.0114	500	50	-0.2768	0.0351	0.0152
200	600	0.9169	-0.3651	-0.0031	500	100	-0.2839	0.0617	0.0197
200	650	0.3174	-0.1538	-0.0742	500	150	-0.2362	0.0710	0.0204
200	700	-0.1044	-0.0981	-0.0218	500	200	-0.1846	0.0821	0.0047
200	750	-0.1309	-0.0855	-0.0063	500	250	-0.0512	0.0679	-0.0080
200	800	-0.1206	-0.0664	-0.0020	500	300	0.0528	0.0650	-0.0266
200	850	-0.1177	-0.0338	-0.0163	500	350	0.2457	0.0269	-0.0151
					500	400	0.4666	-0.0131	-0.0122
300	50	-0.2165	0.0444	-0.0042	500	450	0.6546	-0.0324	0.0111
300	100	-0.1924	0.0721	-0.0047	500	500	0.7495	-0.0586	0.0133
300	150	-0.1779	0.0975	-0.0150	500	550	0.7141	-0.0650	0.0103
300	200	-0.1524	0.1184	-0.0226	500	600	0.4449	-0.0748	0.0291
300	250	-0.1083	0.1274	-0.0166	500	650	0.1887	-0.0984	0.0320
300	300	-0.0330	0.1108	-0.0202	500	700	0.0161	-0.1127	0.0198
300	350	0.0713	0.0913	-0.0268	500	750	-0.1338	-0.1307	-0.0037
300	400	0.2286	0.0218	-0.0366	500	800	-0.2398	-0.0964	-0.0199
300	450	0.4218	-0.0521	-0.0133	500	850	-0.3273	-0.0609	-0.0172
300	500	0.7115	-0.2174	0.0101					
300	550	0.9057	-0.2783	0.0130					
300	600	0.6191	-0.2042	-0.0566					

A2.1.3 Mean velocity for $S = 5.06\%$, $Q = 31.2$ L/s, $z = 150$ mm (cont'd)

x (mm)	y (mm)	u (m/s)	v (m/s)	w (m/s)	x (mm)	y (mm)	u (m/s)	v (m/s)	w (m/s)
600	50	-0.2912	0.0396	0.0057	800	450	0.3679	0.1788	0.0308
600	100	-0.2667	0.0465	0.0365	800	500	0.4822	0.2127	0.0325
600	150	-0.2096	0.0409	0.0400	800	550	0.4624	0.2981	0.0256
600	200	-0.1573	0.0550	0.0199	800	600	0.4545	0.3109	0.0243
600	250	-0.0309	0.0497	-0.0016	800	650	0.3275	0.2947	0.0240
600	300	0.1089	0.0420	-0.0089	800	700	0.2120	0.2534	0.0126
600	350	0.2481	0.0529	-0.0058	800	750	0.0380	0.2068	-0.0016
600	400	0.4669	0.0408	0.0006	800	800	-0.1359	0.1410	-0.0137
600	450	0.6206	0.0569	0.0128	800	850	-0.3004	0.0862	-0.0104
600	500	0.7036	0.0427	0.0236					
600	550	0.6402	0.0538	0.0281	900	50	-0.2201	0.0378	-0.0275
600	600	0.4595	0.0293	0.0328	900	100	-0.1525	0.0433	0.0113
600	650	0.2368	0.0110	0.0267	900	150	-0.1111	0.0101	0.0311
600	700	0.0614	-0.0238	-0.0026	900	200	-0.0354	-0.0064	0.0459
600	750	-0.1152	-0.0364	-0.0238	900	250	0.0456	0.0069	0.0525
600	800	-0.2816	-0.0431	-0.0288	900	300	0.1132	0.0053	0.0533
600	850	-0.4031	-0.0325	-0.0275	900	350	0.1521	0.0078	0.0398
					900	400	0.2118	0.0846	0.0280
700	50	-0.2708	0.0394	0.0059	900	450	0.2659	0.1198	0.0226
700	100	-0.2668	0.0426	0.0400	900	525	0.3325	0.2951	0.0153
700	150	-0.1724	0.0267	0.0576	900	550	0.3658	0.3352	0.0291
700	200	-0.1213	0.0308	0.0271	900	600	0.4057	0.3885	0.0306
700	250	-0.0056	0.0366	0.0198	900	650	0.4001	0.3696	0.0304
700	300	0.1195	0.0318	0.0048	900	700	0.2957	0.3287	0.0232
700	350	0.2516	0.0530	-0.0040	900	750	0.1660	0.2644	0.0155
700	400	0.3935	0.0892	0.0098	900	800	0.0163	0.2008	0.0041
700	450	0.5235	0.1266	0.0182	900	850	-0.1325	0.1369	0.0016
700	500	0.6208	0.1562	0.0301					
700	550	0.6031	0.1686	0.0328	1000	50	-0.1675	-0.0141	-0.0455
700	600	0.4557	0.1678	0.0276	1000	100	-0.0844	-0.0379	-0.0290
700	650	0.2828	0.1389	0.0233	1000	150	-0.0216	-0.0581	-0.0161
700	700	0.1086	0.0891	-0.0015	1000	200	0.0193	-0.0747	-0.0203
700	750	-0.0746	0.0660	-0.0232	1000	250	0.0716	-0.1053	-0.0182
700	800	-0.2506	0.0411	-0.0312	1000	300	0.1033	-0.0881	-0.0246
700	850	-0.3895	0.0130	-0.0204	1000	350	0.1514	-0.0788	-0.0320
					1000	400	0.1719	-0.0397	-0.0579
800	50	-0.2978	0.0517	-0.0132	1000	650	0.5115	0.3593	0.0277
800	100	-0.2276	0.0526	0.0353	1000	700	0.4320	0.2679	0.0336
800	150	-0.1717	0.0344	0.0669	1000	750	0.2965	0.2031	0.0161
800	200	-0.0587	0.0076	0.0662	1000	800	0.1673	0.1631	0.0061
800	250	0.0034	0.0068	0.0582	1000	850	0.0635	0.1003	-0.0198
800	300	0.1108	0.0105	0.0479					
800	350	0.2177	0.0378	0.0283					
800	400	0.3180	0.0978	0.0222					

A2.1.4 Mean velocity for $S = 5.06\%$, $Q = 52$ L/s, $z = 10$ mm

x (mm)	y (mm)	u (m/s)	v (m/s)	w (m/s)	x (mm)	y (mm)	u (m/s)	v (m/s)	w (m/s)
100	50	-0.0808	0.0609	0.0087	300	650	0.2078	-0.0705	0.0039
100	100	-0.0730	0.0913	0.0064	300	700	0.1313	-0.1020	0.0061
100	150	-0.0355	0.1301	0.0049	300	750	0.0963	-0.1130	0.0061
100	200	-0.0012	0.1559	0.0024	300	800	0.0309	-0.1088	0.0029
100	250	0.0298	0.1596	-0.0001	300	850	-0.0264	-0.0643	0.0044
100	300	0.0217	0.1654	0.0004					
100	350	0.0516	0.1644	0.0023	400	50	-0.3804	-0.0303	0.0056
100	400	0.0677	0.1394	0.0058	400	100	-0.2748	-0.0665	0.0090
100	450	0.0965	0.0683	0.0099	400	150	-0.1319	-0.0903	0.0117
100	500	0.1780	-0.0967	0.0181	400	200	-0.0327	-0.1049	0.0085
100	550	0.3774	-0.3851	-0.0071	400	250	0.1189	-0.1328	0.0062
100	600	0.7210	-0.7400	0.0053	400	300	0.2425	-0.1421	0.0065
100	650	0.6435	-0.7555	-0.0487	400	350	0.3728	-0.1937	0.0060
					400	400	0.5340	-0.2401	0.0053
					400	450	0.6195	-0.2357	-0.0017
200	50	-0.2381	0.0226	0.0098	400	500	0.7013	-0.1759	-0.0126
200	100	-0.1827	0.0346	0.0049	400	550	0.5761	-0.1027	-0.0119
200	150	-0.1108	0.0502	-0.0004	400	600	0.3618	-0.0559	-0.0006
200	200	-0.0318	0.0556	-0.0018	400	650	0.1521	-0.0747	0.0046
200	250	0.0189	0.0549	-0.0027	400	700	0.0981	-0.1120	0.0063
200	300	0.0357	0.0545	-0.0030	400	750	0.0064	-0.1355	0.0035
200	350	0.0910	0.0382	0.0005	400	800	-0.1089	-0.1334	0.0021
200	400	0.1903	-0.1041	0.0105	400	850	-0.1859	-0.0899	0.0033
200	450	0.3719	-0.3140	0.0106					
200	500	0.5784	-0.4883	-0.0090	500	50	-0.3834	-0.0259	0.0007
200	550	0.6769	-0.4973	-0.0083	500	100	-0.3073	-0.0421	0.0093
200	600	0.5135	-0.3211	-0.0349	500	150	-0.2003	-0.0760	0.0134
200	650	0.1954	-0.1261	-0.0128	500	200	-0.0517	-0.1264	0.0139
200	700	0.1896	-0.0995	-0.0108	500	250	0.1163	-0.1325	0.0115
200	750	0.1674	-0.0906	-0.0094	500	300	0.2437	-0.1139	0.0072
200	800	0.1500	-0.0631	-0.0057	500	350	0.4011	-0.1329	0.0046
200	850	0.1219	-0.0258	-0.0062	500	400	0.6293	-0.1768	0.0013
					500	450	0.7033	-0.1190	-0.0067
300	50	-0.2963	-0.0279	0.0078	500	500	0.6814	-0.0493	-0.0091
300	100	-0.2045	-0.0314	0.0078	500	550	0.5228	-0.0124	-0.0032
300	150	-0.1439	-0.0328	0.0042	500	600	0.3288	-0.0078	0.0023
300	200	-0.0459	-0.0320	0.0034	500	650	0.2225	-0.0359	0.0042
300	250	0.0272	-0.0368	0.0011	500	700	0.0665	-0.0939	0.0018
300	300	0.1582	-0.0814	-0.0003	500	750	-0.0404	-0.0919	-0.0026
300	350	0.2776	-0.1801	0.0025	500	800	-0.1505	-0.0844	-0.0008
300	400	0.4433	-0.2994	0.0025	500	850	-0.2831	-0.0917	0.0046
300	450	0.5901	-0.3721	-0.0138					
300	500	0.7063	-0.3750	-0.0309					
300	550	0.5874	-0.2298	-0.0206					
300	600	0.3589	-0.1035	-0.0165					

A2.1.4 Mean velocity for $S = 5.06\%$, $Q = 52$ L/s, $z = 10$ mm (cont'd)

x (mm)	y (mm)	u (m/s)	v (m/s)	w (m/s)	x (mm)	y (mm)	u (m/s)	v (m/s)	w (m/s)
600	50	-0.3693	-0.0088	-0.0077	800	450	0.1484	0.2481	0.0042
600	100	-0.3121	-0.0198	0.0043	800	500	0.1852	0.3305	0.0110
600	150	-0.2615	-0.0371	0.0100	800	550	0.2650	0.3838	0.0099
600	200	-0.0577	-0.0773	0.0156	800	600	0.3020	0.4138	0.0108
600	250	0.0627	-0.0702	0.0096	800	650	0.2942	0.3956	0.0130
600	300	0.2968	-0.0877	0.0061	800	700	0.2273	0.3910	0.0150
600	350	0.4188	-0.0758	0.0043	800	750	0.0749	0.3084	0.0148
600	400	0.5197	-0.0260	0.0026	800	800	-0.0699	0.2101	0.0158
600	450	0.6094	0.0264	0.0000	800	850	-0.1825	0.0440	0.0236
600	500	0.5772	0.0802	0.0021					
600	550	0.5423	0.1087	0.0021	900	50	-0.3370	0.0109	-0.0218
600	600	0.3948	0.0933	0.0022	900	100	-0.2948	0.0207	0.0013
600	650	0.2583	0.0767	0.0069	900	150	-0.3439	-0.0316	0.0073
600	700	0.1006	0.0124	0.0029	900	200	-0.2977	-0.0627	0.0099
600	750	-0.0281	0.0108	0.0010	900	250	-0.3096	-0.0833	0.0104
600	800	-0.1539	-0.0103	0.0039	900	300	-0.2253	-0.0375	0.0113
600	850	-0.3256	-0.0503	0.0116	900	350	-0.2083	0.0706	0.0072
					900	400	-0.1657	0.1675	0.0005
700	50	-0.2922	0.0102	-0.0122	900	450	-0.2082	0.2392	-0.0063
700	100	-0.3365	0.0284	-0.0006	900	520	-0.0737	0.4232	0.0067
700	150	-0.3068	0.0269	0.0082	900	550	0.0054	0.4097	0.0104
700	200	-0.1963	-0.0265	0.0126	900	600	0.1292	0.4059	0.0137
700	250	-0.0353	-0.0423	0.0084	900	650	0.2093	0.4205	0.0154
700	300	0.0915	-0.0086	0.0070	900	700	0.2146	0.3662	0.0158
700	350	0.3004	0.0201	0.0042	900	750	0.1319	0.2701	0.0161
700	400	0.3981	0.0891	0.0020	900	800	0.0436	0.1700	0.0164
700	450	0.4499	0.1717	0.0048	900	850	-0.0316	0.0277	0.0153
700	500	0.4816	0.2264	0.0051					
700	550	0.4606	0.2585	0.0044	1000	50	-0.2155	-0.0327	-0.0217
700	600	0.4245	0.2746	0.0079	1000	100	-0.2407	-0.0570	-0.0101
700	650	0.2947	0.2317	0.0064	1000	150	-0.2657	-0.0950	-0.0107
700	700	0.1733	0.1948	0.0088	1000	200	-0.2915	-0.1317	-0.0107
700	750	-0.0042	0.1397	0.0085	1000	250	-0.2923	-0.1364	-0.0098
700	800	-0.1518	0.0837	0.0095	1000	300	-0.3010	-0.0787	-0.0133
700	850	-0.3192	-0.0130	0.0206	1000	350	-0.2683	-0.0166	-0.0113
					1000	400	-0.2539	0.0407	-0.0168
800	50	-0.3759	0.0081	-0.0260	1000	650	0.2160	0.3140	0.0062
800	100	-0.3426	0.0434	-0.0038	1000	700	0.2277	0.1911	0.0189
800	150	-0.3039	0.0165	0.0100	1000	750	0.2195	0.1025	0.0136
800	200	-0.2617	-0.0320	0.0122	1000	800	0.1256	-0.0009	0.0090
800	250	-0.1953	-0.0479	0.0172	1000	850	0.0665	-0.0540	0.0056
800	300	-0.0468	-0.0209	0.0157					
800	350	0.0855	0.0613	0.0084					
800	400	0.1504	0.1906	0.0009					

A2.1.5 Mean velocity for $S = 5.06\%$, $Q = 52$ L/s, $z = 150$ mm

x (mm)	y (mm)	u (m/s)	v (m/s)	w (m/s)	x (mm)	y (mm)	u (m/s)	v (m/s)	w (m/s)
100	50	-0.1857	0.0592	0.0454	300	650	0.0638	-0.1343	-0.0114
100	100	-0.1505	0.0994	0.0144	300	700	-0.0367	-0.1455	0.0232
100	150	-0.1309	0.1178	0.0108	300	750	-0.0855	-0.1481	0.0341
100	200	-0.0899	0.1475	-0.0120	300	800	-0.1317	-0.1329	0.0429
100	250	-0.0706	0.1676	-0.0240	300	850	-0.1912	-0.0994	0.0399
100	300	-0.0543	0.1632	-0.0282					
100	350	-0.0229	0.1691	-0.0251	400	50	-0.2839	-0.0098	0.0477
100	400	0.0187	0.1574	-0.0292	400	100	-0.2625	-0.0154	0.0652
100	450	0.0465	0.1359	-0.0219	400	150	-0.2364	-0.0182	0.0585
100	500	0.1021	0.0795	0.0066	400	200	-0.1311	-0.0267	0.0314
100	550	0.3508	-0.1473	0.0156	400	250	-0.0201	-0.0187	-0.0089
100	600	1.0476	-0.5663	0.0314	400	300	0.0819	0.0026	-0.0322
100	650	1.0437	-0.5703	0.0158	400	350	0.2438	-0.0112	-0.0442
					400	400	0.4566	-0.0751	-0.0307
					400	450	0.6982	-0.1627	0.0023
200	50	-0.2354	0.0262	0.0251	400	500	0.8437	-0.1815	0.0181
200	100	-0.2010	0.0429	0.0182	400	550	0.7306	-0.1489	-0.0012
200	150	-0.1632	0.0717	-0.0010	400	600	0.3554	-0.1355	0.0113
200	200	-0.1326	0.1053	-0.0101	400	650	0.0998	-0.1527	0.0229
200	250	-0.0828	0.1201	-0.0270	400	700	-0.0056	-0.1671	0.0211
200	300	-0.0192	0.1246	-0.0384	400	750	-0.0795	-0.1557	0.0110
200	350	0.0417	0.1157	-0.0465	400	800	-0.1618	-0.1350	0.0033
200	400	0.1294	0.0780	-0.0372	400	850	-0.2602	-0.1037	0.0244
200	450	0.2390	0.0034	-0.0220					
200	500	0.5162	-0.1735	0.0095	500	50	-0.2431	-0.0114	0.0505
200	550	0.9469	-0.4071	0.0105	500	100	-0.2470	-0.0332	0.0881
200	600	0.9201	-0.3530	-0.0023	500	150	-0.2236	-0.0458	0.0876
200	650	0.1460	-0.1452	-0.0836	500	200	-0.1368	-0.0512	0.0862
200	700	-0.0692	-0.1054	-0.0640	500	250	-0.0286	-0.0327	0.0285
200	750	-0.0855	-0.1034	-0.0430	500	300	0.0997	-0.0208	-0.0026
200	800	-0.1128	-0.0995	-0.0329	500	350	0.2996	-0.0439	-0.0187
200	850	-0.0966	-0.0725	-0.0469	500	400	0.5477	-0.0703	-0.0044
					500	450	0.7206	-0.0778	0.0103
300	50	-0.2646	0.0075	0.0397	500	500	0.7667	-0.0581	0.0178
300	100	-0.2457	0.0215	0.0333	500	550	0.6519	-0.0309	0.0241
300	150	-0.2155	0.0328	0.0265	500	600	0.3636	-0.0576	0.0286
300	200	-0.1515	0.0473	0.0031	500	650	0.1795	-0.0963	0.0182
300	250	-0.0354	0.0311	-0.0249	500	700	0.0264	-0.1249	-0.0064
300	300	0.0549	0.0484	-0.0346	500	750	-0.0976	-0.1218	-0.0296
300	350	0.1416	0.0412	-0.0615	500	800	-0.2178	-0.0995	-0.0251
300	400	0.2784	0.0013	-0.0417	500	850	-0.3382	-0.0681	-0.0005
300	450	0.5394	-0.1260	-0.0183					
300	500	0.8296	-0.2777	-0.0187					
300	550	0.8997	-0.2622	-0.0052					
300	600	0.4677	-0.1732	-0.0362					

A2.1.5 Mean velocity for $S = 5.06\%$, $Q = 52$ L/s, $z = 150$ mm (cont'd)

x (mm)	y (mm)	u (m/s)	v (m/s)	w (m/s)	x (mm)	y (mm)	u (m/s)	v (m/s)	w (m/s)
600	50	-0.1892	0.0103	0.0149	800	450	0.3118	0.2492	0.1218
600	100	-0.1804	-0.0392	0.1265	800	500	0.3971	0.3335	0.1043
600	150	-0.2002	-0.0126	0.1245	800	550	0.4550	0.3938	0.0883
600	200	-0.1512	-0.0226	0.1249	800	600	0.4420	0.4195	0.0738
600	250	-0.0353	-0.0116	0.0781	800	650	0.3787	0.3966	0.0587
600	300	0.1280	-0.0261	0.0290	800	700	0.2556	0.3581	0.0594
600	350	0.3109	-0.0209	0.0126	800	750	0.0795	0.2758	0.0349
600	400	0.4679	0.0209	0.0124	800	800	-0.0777	0.2126	0.0169
600	450	0.6337	0.0534	0.0188	800	850	-0.1933	0.1391	0.0253
600	500	0.6709	0.0899	0.0298					
600	550	0.6126	0.1006	0.0465	900	50	-0.2242	0.0573	-0.1287
600	600	0.4096	0.0697	0.0354	900	100	-0.1446	0.0904	-0.0594
600	650	0.2356	0.0256	0.0378	900	150	-0.1003	0.1019	-0.0162
600	700	0.0630	0.0050	-0.0035	900	200	-0.0451	0.1120	0.0078
600	750	-0.0979	-0.0099	-0.0329	900	250	-0.0299	0.1158	0.0311
600	800	-0.2479	-0.0193	-0.0240	900	300	0.0028	0.1466	0.0509
600	850	-0.3759	-0.0132	0.0011	900	350	0.0479	0.1808	0.0645
					900	400	0.0974	0.2372	0.0718
700	50	-0.1719	0.0503	-0.0577	900	450	0.1562	0.3119	0.0413
700	100	-0.1602	0.0389	0.0204	900	520	0.2572	0.3987	0.0461
700	150	-0.1702	0.0514	0.0860	900	550	0.3784	0.4517	0.0559
700	200	-0.1432	0.0353	0.1367	900	600	0.4157	0.4576	0.0612
700	250	-0.0493	0.0317	0.1355	900	650	0.4213	0.4430	0.0508
700	300	0.0872	0.0270	0.1186	900	700	0.3243	0.3830	0.0459
700	350	0.2421	0.0634	0.0723	900	750	0.2285	0.3096	0.0344
700	400	0.3646	0.1111	0.0601	900	800	0.0805	0.2298	0.0186
700	450	0.4960	0.1919	0.0506	900	850	-0.0204	0.1448	0.0184
700	500	0.5624	0.2387	0.0515					
700	550	0.5246	0.2731	0.0541	1000	50	-0.1303	0.0038	-0.1165
700	600	0.4203	0.2668	0.0562	1000	100	-0.0842	0.0145	-0.1035
700	650	0.3072	0.2262	0.0579	1000	150	-0.0629	0.0230	-0.1016
700	700	0.1329	0.1845	0.0266	1000	200	-0.0338	0.0175	-0.0970
700	750	-0.0585	0.1396	0.0010	1000	250	-0.0147	0.0358	-0.0905
700	800	-0.2114	0.0980	-0.0235	1000	300	0.0055	0.0478	-0.1018
700	850	-0.3478	0.0564	-0.0082	1000	350	0.0225	0.0504	-0.1178
					1000	400	0.0282	0.0735	-0.1153
800	50	-0.1931	0.0672	-0.1051	1000	650	0.5445	0.3693	0.0181
800	100	-0.1602	0.0827	-0.0236	1000	700	0.4643	0.2607	0.0408
800	150	-0.1498	0.0939	0.0417	1000	750	0.3684	0.2074	0.0177
800	200	-0.1020	0.0928	0.0815	1000	800	0.2476	0.1456	-0.0047
800	250	-0.0379	0.1030	0.1139	1000	850	0.1453	0.0975	-0.0112
800	300	0.0168	0.1204	0.1319					
800	350	0.1422	0.1305	0.1243					
800	400	0.2105	0.1816	0.1323					

A2.1.6 Mean velocity for $S = 5.06\%$, $Q = 52$ L/s, $z = 300$ mm

x (mm)	y (mm)	u (m/s)	v (m/s)	w (m/s)	x (mm)	y (mm)	u (m/s)	v (m/s)	w (m/s)
100	50	-0.1086	0.0527	0.0265	300	650	0.0915	-0.1591	-0.0015
100	100	-0.1040	0.0857	0.0147	300	700	-0.0604	-0.1614	0.0109
100	150	-0.0860	0.1125	0.0007	300	750	-0.1403	-0.1673	0.0028
100	200	-0.0824	0.1247	0.0019	300	800	-0.2000	-0.1425	0.0018
100	250	-0.0592	0.1537	-0.0096	300	850	-0.2654	-0.1063	0.0078
100	300	-0.0517	0.1625	-0.0281					
100	350	-0.0159	0.1570	-0.0338	400	50	-0.2135	0.0022	0.0283
100	400	0.0253	0.1390	-0.0496	400	100	-0.1803	0.0062	0.0404
100	450	0.1075	0.0611	-0.0483	400	150	-0.1773	0.0041	0.0395
100	500	0.2283	-0.0527	-0.0176	400	200	-0.1101	0.0122	0.0348
100	550	0.5394	-0.3212	0.0314	400	250	0.0186	-0.0112	-0.0069
100	600	1.0892	-0.6108	0.0192	400	300	0.1698	-0.0393	-0.0296
100	650	0.9204	-0.5218	-0.0102	400	350	0.4033	-0.1129	-0.0134
					400	400	0.6348	-0.1870	0.0166
200	50	-0.1659	0.0308	0.0073	400	450	0.8274	-0.2563	0.0489
200	100	-0.1597	0.0636	0.0057	400	500	0.8521	-0.2718	0.0235
200	150	-0.1462	0.0965	-0.0084	400	550	0.6186	-0.2165	0.0070
200	200	-0.1091	0.1047	-0.0184	400	600	0.3049	-0.1582	0.0108
200	250	-0.0808	0.1303	-0.0360	400	650	0.0900	-0.1543	0.0371
200	300	-0.0185	0.1108	-0.0378	400	700	-0.0515	-0.1525	0.0058
200	350	0.0797	0.0637	-0.0564	400	750	-0.1632	-0.1434	-0.0126
200	400	0.2439	-0.0400	-0.0544	400	800	-0.2557	-0.1247	-0.0181
200	450	0.4366	-0.1463	-0.0044	400	850	-0.3522	-0.0916	-0.0041
200	500	0.7288	-0.3488	0.0387					
200	550	1.0298	-0.4831	0.0237	500	50	-0.1582	-0.0087	0.0014
200	600	0.8000	-0.3525	-0.0115	500	100	-0.1259	-0.0397	0.0540
200	650	0.1477	-0.1573	-0.0551	500	150	-0.1056	-0.0657	0.0784
200	700	-0.0683	-0.1375	-0.0229	500	200	-0.0468	-0.0617	0.0590
200	750	-0.1211	-0.1447	-0.0166	500	250	0.0961	-0.0727	0.0338
200	800	-0.1683	-0.1253	-0.0167	500	300	0.2868	-0.0952	0.0095
200	850	-0.1943	-0.1067	-0.0177	500	350	0.5261	-0.1359	0.0123
					500	400	0.6960	-0.1554	0.0381
300	50	-0.2056	0.0271	0.0072	500	450	0.7954	-0.1591	0.0324
300	100	-0.1633	0.0346	0.0195	500	500	0.7230	-0.1254	0.0196
300	150	-0.1670	0.0674	0.0169	500	550	0.5361	-0.0954	0.0218
300	200	-0.1283	0.0780	0.0057	500	600	0.2777	-0.0842	0.0378
300	250	-0.0399	0.0753	-0.0244	500	650	0.0893	-0.0899	0.0150
300	300	0.0811	0.0203	-0.0425	500	700	-0.0626	-0.0857	-0.0226
300	350	0.2512	-0.0340	-0.0435	500	750	-0.1982	-0.0941	-0.0464
300	400	0.4664	-0.1272	-0.0083	500	800	-0.3308	-0.0870	-0.0393
300	450	0.7316	-0.2784	0.0418	500	850	-0.4245	-0.0568	-0.0195
300	500	0.9522	-0.3662	0.0473					
300	550	0.8369	-0.3270	-0.0036					
300	600	0.4499	-0.2150	-0.0554					

A2.1.6 Mean velocity for $S = 5.06\%$, $Q = 52$ L/s, $z = 300$ mm (cont'd)

x (mm)	y (mm)	u (m/s)	v (m/s)	w (m/s)	x (mm)	y (mm)	u (m/s)	v (m/s)	w (m/s)
600	50	-0.0778	-0.0167	-0.0344	800	450	0.4659	0.2159	0.0772
600	100	-0.0763	-0.0426	0.0643	800	500	0.5182	0.2997	0.0823
600	150	-0.0322	-0.0900	0.1023	800	550	0.5205	0.3459	0.0843
600	200	0.0438	-0.1174	0.0976	800	600	0.4273	0.3655	0.0683
600	250	0.1577	-0.1086	0.0813	800	650	0.2819	0.3359	0.0428
600	300	0.3293	-0.0983	0.0564	800	700	0.1572	0.2906	0.0356
600	350	0.5079	-0.0796	0.0435	800	750	-0.0028	0.2316	0.0199
600	400	0.7022	-0.0566	0.0542	800	800	-0.1589	0.1618	0.0102
600	450	0.7624	-0.0102	0.0578	800	850	-0.2620	0.0822	0.0182
600	500	0.6683	0.0404	0.0343					
600	550	0.5049	0.0461	0.0401	900	50	-0.0724	0.0136	-0.1588
600	600	0.3273	0.0480	0.0496	900	100	0.0430	0.0014	-0.1083
600	650	0.1234	0.0352	0.0264	900	150	0.1069	-0.0168	-0.0788
600	700	-0.0346	0.0058	-0.0195	900	200	0.1320	-0.0144	-0.0212
600	750	-0.1938	-0.0119	-0.0572	900	250	0.1789	-0.0127	0.0154
600	800	-0.3512	-0.0213	-0.0579	900	300	0.2009	0.0240	0.0331
600	850	-0.4441	-0.0179	-0.0170	900	350	0.2966	0.0408	0.0551
					900	400	0.3179	0.1142	0.0463
700	50	-0.0564	-0.0087	-0.0770	900	450	0.3421	0.1771	0.0346
700	100	0.0251	-0.0346	0.0070	900	520	0.3475	0.3371	0.0381
700	150	0.0578	-0.0684	0.0826	900	550	0.4257	0.4345	0.0513
700	200	0.0842	-0.0766	0.1007	900	600	0.4575	0.4533	0.0621
700	250	0.2152	-0.0980	0.1091	900	650	0.4071	0.4157	0.0619
700	300	0.3131	-0.0573	0.0954	900	700	0.2991	0.3434	0.0434
700	350	0.4337	-0.0016	0.0827	900	750	0.1543	0.2581	0.0226
700	400	0.5507	0.0763	0.0557	900	800	-0.0007	0.1857	0.0211
700	450	0.6492	0.1349	0.0809	900	850	-0.1005	0.0993	0.0250
700	500	0.6531	0.1972	0.0705					
700	550	0.5240	0.2221	0.0688	1000	50	-0.0565	-0.0496	-0.1915
700	600	0.3567	0.2260	0.0503	1000	100	0.0427	-0.0718	-0.1631
700	650	0.1951	0.1875	0.0416	1000	150	0.0800	-0.0760	-0.1523
700	700	0.0341	0.1552	-0.0024	1000	200	0.1221	-0.0976	-0.1426
700	750	-0.1346	0.1171	-0.0216	1000	250	0.1247	-0.0858	-0.1313
700	800	-0.3012	0.0684	-0.0315	1000	300	0.1766	-0.0557	-0.1266
700	850	-0.4099	0.0237	-0.0072	1000	350	0.2202	-0.0554	-0.1303
					1000	400	0.2421	-0.0268	-0.1251
800	50	-0.0534	0.0085	-0.1274	1000	650	0.6166	0.3828	0.0323
800	100	0.0115	0.0063	-0.0450	1000	700	0.4743	0.2417	0.0282
800	150	0.0936	-0.0274	0.0149	1000	750	0.3154	0.1740	0.0198
800	200	0.1351	-0.0451	0.0687	1000	800	0.1496	0.1001	0.0070
800	250	0.2068	-0.0403	0.1149	1000	850	0.0423	0.0557	0.0056
800	300	0.2502	-0.0011	0.1010					
800	350	0.3599	0.0377	0.1015					
800	400	0.4401	0.1169	0.0957					

A2.1.7 Mean velocity for $S = 10.52\%$, $Q = 31.2$ L/s, $z = 10$ mm

x (mm)	y (mm)	u (m/s)	v (m/s)	w (m/s)	x (mm)	y (mm)	u (m/s)	v (m/s)	w (m/s)
100	50	-0.0328	-0.0598	0.0426	300	650	0.0509	-0.1527	-0.0033
100	100	0.0271	-0.2844	0.0597	300	700	-0.0346	-0.1322	-0.0032
100	150	0.0169	-0.5399	0.0607	300	750	-0.1085	-0.1071	-0.0014
100	200	0.0193	-0.6211	0.0378	300	800	-0.1952	-0.1028	0.0037
100	250	0.0193	-0.6058	0.0222	300	850	-0.2838	-0.1008	0.0090
100	300	0.0485	-0.6282	0.0120					
100	350	0.0702	-0.5861	-0.0015	400	50	0.3012	-0.2275	0.0731
100	400	0.0941	-0.4721	0.0038	400	100	0.4561	-0.5027	0.0515
100	450	0.1844	-0.6602	0.0034	400	150	0.5330	-0.5540	0.0270
100	500	0.2823	-0.9640	0.0212	400	200	0.6355	-0.5688	0.0175
100	550	0.4518	-1.2162	-0.0102	400	250	0.7293	-0.5716	0.0147
100	600	0.5922	-1.2332	-0.0692	400	300	0.7043	-0.5043	0.0084
100	650	0.4792	-0.8271	-0.0860	400	350	0.6040	-0.4075	0.0000
					400	400	0.4874	-0.3107	-0.0012
200	50	0.0046	-0.1400	0.0594	400	450	0.3235	-0.2266	0.0058
200	100	0.1011	-0.4350	0.0594	400	500	0.1975	-0.1659	0.0076
200	150	0.1420	-0.5716	0.0321	400	550	0.1272	-0.1466	-0.0008
200	200	0.1875	-0.6041	0.0127	400	600	0.0580	-0.1290	-0.0060
200	250	0.2632	-0.6685	0.0079	400	650	-0.0098	-0.1066	-0.0085
200	300	0.3361	-0.6414	0.0076	400	700	-0.0779	-0.0757	-0.0052
200	350	0.4359	-0.6763	0.0028	400	750	-0.1704	-0.0686	-0.0003
200	400	0.5888	-0.8307	-0.0199	400	800	-0.2464	-0.0576	0.0058
200	450	0.6958	-0.8898	-0.0458	400	850	-0.2983	-0.0850	0.0084
200	500	0.6418	-0.6597	-0.0313					
200	550	0.5720	-0.4926	0.0080	500	50	0.4477	-0.1376	0.0705
200	600	0.2158	-0.2381	-0.0181	500	100	0.5867	-0.4047	0.0531
200	650	0.1398	-0.2026	0.0037	500	150	0.6621	-0.4536	0.0234
200	700	0.1092	-0.1966	0.0077	500	200	0.6990	-0.4182	0.0121
200	750	0.0256	-0.1877	0.0134	500	250	0.6905	-0.3666	0.0084
200	800	-0.0652	-0.1818	0.0154	500	300	0.6148	-0.2923	0.0043
200	850	-0.1270	-0.1396	0.0210	500	350	0.4436	-0.1959	0.0011
					500	400	0.6219	-0.1180	0.0121
300	50	0.1421	-0.2309	0.0715	500	450	0.2248	-0.1127	0.0038
300	100	0.2521	-0.5250	0.0531	500	500	0.1605	-0.1093	0.0042
300	150	0.3125	-0.5901	0.0173	500	550	0.1130	-0.0960	-0.0010
300	200	0.4228	-0.6528	0.0025	500	600	0.0296	-0.0621	-0.0028
300	250	0.5361	-0.6708	0.0007	500	650	-0.0468	-0.0203	-0.0022
300	300	0.6508	-0.6885	-0.0078	500	700	-0.1255	0.0014	-0.0032
300	350	0.7324	-0.7100	-0.0189	500	750	-0.1876	0.0346	0.0038
300	400	0.7125	-0.6223	-0.0273	500	800	-0.2685	-0.0007	0.0149
300	450	0.5561	-0.4604	-0.0295	500	850	-0.3532	-0.1117	0.0178
300	500	0.3310	-0.2800	-0.0091					
300	550	0.2025	-0.2118	0.0028					
300	600	0.1139	-0.1714	0.0018					

A2.1.7 Mean velocity for $S = 10.52\%$, $Q = 31.2$ L/s, $z = 10$ mm (cont'd)

x (mm)	y (mm)	u (m/s)	v (m/s)	w (m/s)	x (mm)	y (mm)	u (m/s)	v (m/s)	w (m/s)
600	50	0.5466	-0.0466	0.0680	800	450	-0.1547	0.4152	-0.0131
600	100	0.6296	-0.2695	0.0453	800	500	-0.1801	0.5083	-0.0131
600	150	0.6770	-0.3097	0.0207	800	550	-0.1768	0.5699	-0.0101
600	200	0.6456	-0.2554	0.0100	800	600	-0.1490	0.6150	-0.0071
600	250	0.5631	-0.1791	0.0050	800	650	-0.0758	0.5809	-0.0011
600	300	0.4404	-0.1093	0.0058	800	700	-0.0473	0.5472	0.0026
600	350	0.3273	-0.0410	0.0031	800	750	-0.0210	0.4415	0.0108
600	400	0.1925	0.0024	0.0065	800	800	-0.0174	0.2698	0.0225
600	450	0.1049	0.0364	0.0064	800	850	-0.0472	0.0126	0.0295
600	500	0.0580	0.0667	0.0081					
600	550	-0.0183	0.1119	0.0070	900	50	0.5018	0.1205	0.0360
600	600	-0.0622	0.1358	0.0074	900	100	0.3895	0.0162	0.0257
600	650	-0.1184	0.1544	0.0067	900	150	0.3077	0.0013	0.0145
600	700	-0.1721	0.1574	0.0069	900	200	0.2065	0.0274	0.0033
600	750	-0.2275	0.1499	0.0110	900	250	0.0976	0.0748	-0.0016
600	800	-0.2799	0.0520	0.0210	900	300	-0.0107	0.1406	-0.0089
600	850	-0.3319	-0.1345	0.0238	900	350	-0.1163	0.2190	-0.0157
					900	400	-0.2246	0.3239	-0.0107
700	50	0.5734	0.0661	0.0574	900	450	-0.3504	0.4755	-0.0176
700	100	0.5995	-0.1419	0.0380	900	550	-0.2178	0.8113	-0.0262
700	150	0.5684	-0.1447	0.0179	900	600	-0.0418	0.8487	-0.0113
700	200	0.5048	-0.0988	0.0060	900	650	0.1109	0.7955	-0.0037
700	250	0.4072	-0.0193	0.0020	900	700	0.2390	0.6729	0.0114
700	300	0.2813	0.0694	0.0001	900	750	0.2783	0.5132	0.0140
700	350	0.1392	0.1356	-0.0007	900	800	0.2482	0.3054	0.0225
700	400	0.0012	0.2123	0.0009	900	850	0.1947	0.0325	0.0394
700	450	-0.0970	0.2759	-0.0016					
700	500	-0.1262	0.3274	-0.0046	1000	50	0.3029	0.1840	0.0290
700	550	-0.1612	0.3598	-0.0021	1000	100	0.1897	0.1551	0.0238
700	600	-0.1679	0.3937	0.0008	1000	150	0.1146	0.1650	0.0180
700	650	-0.1566	0.3835	0.0019	1000	200	0.0301	0.1827	0.0109
700	700	-0.1626	0.3643	0.0070	1000	250	-0.0493	0.2175	0.0086
700	750	-0.1835	0.2988	0.0125	1000	300	-0.1111	0.2287	-0.0005
700	800	-0.2031	0.2104	0.0205	1000	350	-0.1956	0.2369	-0.0038
700	850	-0.2289	-0.0869	0.0331	1000	400	-0.3367	0.1847	0.0125
					1000	450	0.0405	0.1966	0.0245
800	50	0.5757	0.0891	0.0563	1000	500	0.3700	0.2434	0.0280
800	100	0.4952	-0.0566	0.0312	1000	550	0.5596	0.1973	0.0163
800	150	0.4377	-0.0722	0.0144	1000	600	0.4753	0.0562	0.0187
800	200	0.3337	-0.0114	0.0005	1000	650	0.3593	-0.1054	0.0269
800	250	0.2633	0.0672	-0.0057					
800	300	0.1469	0.1501	-0.0102					
800	350	0.0234	0.2403	-0.0146					
800	400	-0.0763	0.3288	-0.0162					

A2.1.8 Mean velocity for $S = 10.52\%$, $Q = 31.2$ L/s, $z = 70$ mm

x (mm)	y (mm)	u (m/s)	v (m/s)	w (m/s)	x (mm)	y (mm)	u (m/s)	v (m/s)	w (m/s)
100	50	0.0811	-0.1558	0.2256	300	650	0.0566	-0.1863	-0.0054
100	100	0.1384	-0.1882	0.2237	300	700	0.0092	-0.1555	-0.0135
100	150	0.1116	-0.1885	0.1413	300	750	-0.0520	-0.1103	-0.0020
100	200	0.0430	-0.1210	0.0443	300	800	-0.1219	-0.0645	0.0125
100	250	0.0250	-0.1268	0.0143	300	850	-0.2023	-0.0366	0.0179
100	300	0.0640	-0.2932	-0.0636					
100	350	0.1126	-0.4167	-0.1442	400	50	0.3277	-0.2947	0.3156
100	400	0.1453	-0.4805	-0.1727	400	100	0.2995	-0.3627	0.0966
100	450	0.4496	-0.7286	-0.1258	400	150	0.3451	-0.3890	-0.0333
100	500	0.7438	-0.8836	-0.0939	400	200	0.4519	-0.4421	-0.0489
100	550	0.9792	-1.0371	-0.0873	400	250	0.5948	-0.5145	-0.0187
100	600	0.6611	-0.8076	-0.0657	400	300	0.5992	-0.4956	-0.0186
100	650	0.7715	-0.9279	-0.0536	400	350	0.4915	-0.4366	-0.0365
					400	400	0.3386	-0.3394	-0.0284
					400	450	0.2012	-0.2520	-0.0164
200	50	0.1743	-0.1923	0.3059	400	500	0.1562	-0.2253	-0.0088
200	100	0.1767	-0.2193	0.1968	400	550	0.1071	-0.1993	-0.0088
200	150	0.1240	-0.2211	0.0531	400	600	0.0450	-0.1706	-0.0176
200	200	0.0851	-0.2107	-0.0147	400	650	-0.0243	-0.1287	-0.0205
200	250	0.0958	-0.2341	-0.0182	400	700	-0.0766	-0.0794	-0.0165
200	300	0.1665	-0.2967	-0.0270	400	750	-0.1145	-0.0818	0.0075
200	350	0.2926	-0.4533	-0.0500	400	800	-0.1976	0.0006	0.0303
200	400	0.4472	-0.5671	-0.0661	400	850	-0.2805	0.0388	0.0361
200	450	0.6802	-0.7564	-0.0604					
200	500	0.7891	-0.8686	-0.0704	500	50	0.4770	-0.3447	0.2949
200	550	0.4306	-0.5393	-0.0781	500	100	0.4294	-0.3930	0.0988
200	600	0.1465	-0.3041	-0.0676	500	150	0.4766	-0.3809	-0.0100
200	650	0.0552	-0.2364	-0.0181	500	200	0.5729	-0.3871	-0.0277
200	700	0.0019	-0.2316	0.0099	500	250	0.6046	-0.3730	-0.0158
200	750	-0.0274	-0.2110	0.0234	500	300	0.5076	-0.3112	-0.0123
200	800	-0.0971	-0.1792	0.0363	500	350	0.3439	-0.2356	-0.0068
200	850	-0.1660	-0.1275	0.0411	500	400	0.2182	-0.1879	-0.0025
					500	450	0.1749	-0.1602	0.0069
300	50	0.2499	-0.2831	0.3350	500	500	0.1292	-0.1510	-0.0024
300	100	0.2132	-0.2988	0.1295	500	550	0.0638	-0.1422	-0.0069
300	150	0.1905	-0.3137	-0.0085	500	600	-0.0298	-0.0583	-0.0102
300	200	0.2158	-0.3372	-0.0487	500	650	-0.0726	-0.0701	-0.0164
300	250	0.3158	-0.4197	-0.0383	500	700	-0.1407	-0.0375	-0.0291
300	300	0.4844	-0.5668	-0.0315	500	750	-0.2130	0.0117	-0.0128
300	350	0.6311	-0.7051	-0.0340	500	800	-0.2735	0.0684	0.0305
300	400	0.6253	-0.6887	-0.0384	500	850	-0.3317	0.0963	0.0402
300	450	0.4460	-0.5254	-0.0554					
300	500	0.2599	-0.3662	-0.0495					
300	550	0.1575	-0.2587	-0.0262					
300	600	0.1067	-0.2232	-0.0138					

A2.1.8 Mean velocity for $S = 10.52\%$, $Q = 31.2$ L/s, $z = 70$ mm (cont'd)

x (mm)	y (mm)	u (m/s)	v (m/s)	w (m/s)	x (mm)	y (mm)	u (m/s)	v (m/s)	w (m/s)
600	50	0.6322	-0.2882	0.2458	800	450	-0.1086	0.4800	-0.0438
600	100	0.5401	-0.3223	0.0859	800	500	-0.1356	0.5827	-0.0461
600	150	0.5548	-0.2817	-0.0100	800	550	-0.1155	0.6476	-0.0477
600	200	0.5701	-0.2232	-0.0290	800	600	-0.0819	0.6868	-0.0443
600	250	0.4733	-0.1114	-0.0261	800	650	-0.0207	0.6480	-0.0323
600	300	0.3798	-0.0613	-0.0168	800	700	0.0244	0.5957	-0.0200
600	350	0.2692	-0.0220	-0.0088	800	750	0.0295	0.5521	-0.0061
600	400	0.1772	0.0189	0.0110	800	800	0.0134	0.4334	0.0327
600	450	0.1155	0.0462	0.0229	800	850	-0.0248	0.3598	0.0652
600	500	0.0843	0.0792	0.0243					
600	550	0.0223	0.1037	0.0234	900	50	0.5571	-0.0666	0.1122
600	600	-0.0300	0.1253	0.0137	900	100	0.4045	-0.0500	0.1027
600	650	-0.0901	0.1340	0.0040	900	150	0.2846	-0.0247	0.0512
600	700	-0.1578	0.1540	0.0019	900	200	0.1879	0.0326	0.0209
600	750	-0.2336	0.1766	0.0133	900	250	0.0868	0.0997	-0.0071
600	800	-0.2756	0.2028	0.0501	900	300	-0.0182	0.1850	-0.0104
600	850	-0.3477	0.2045	0.0768	900	350	-0.1333	0.2682	-0.0279
					900	400	-0.2744	0.3701	-0.0519
700	50	0.6961	-0.2054	0.1967	900	450	-0.3682	0.5492	-0.0780
700	100	0.5543	-0.2285	0.1023	900	550	-0.2048	0.9780	-0.1303
700	150	0.4933	-0.1759	0.0150	900	600	0.0377	0.9684	-0.0882
700	200	0.4447	-0.0814	-0.0268	900	650	0.1916	0.8894	-0.0651
700	250	0.3900	0.0208	-0.0314	900	700	0.3027	0.7655	-0.0460
700	300	0.2926	0.1045	-0.0178	900	750	0.3424	0.6206	-0.0179
700	350	0.1924	0.1857	-0.0113	900	800	0.2988	0.4522	0.0295
700	400	0.1005	0.2487	-0.0121	900	850	0.2480	0.3735	0.0646
700	450	0.0224	0.3013	-0.0094					
700	500	-0.0152	0.3370	-0.0085	1000	50	0.4373	0.0497	0.1070
700	550	-0.0526	0.3788	-0.0073	1000	100	0.3313	0.0875	0.1160
700	600	-0.0666	0.3847	-0.0137	1000	150	0.2325	0.1189	0.0842
700	650	-0.0530	0.3925	-0.0052	1000	200	0.1299	0.1454	0.0474
700	700	-0.0666	0.3710	0.0008	1000	250	0.0407	0.1830	0.0138
700	750	-0.1190	0.3576	0.0090	1000	300	-0.0403	0.2089	-0.0090
700	800	-0.1690	0.3378	0.0492	1000	350	-0.1644	0.2315	-0.0355
700	850	-0.2154	0.3047	0.0772	1000	400	-0.2965	0.2414	-0.0566
					1000	650	0.1828	0.1882	0.0608
800	50	0.6577	-0.1358	0.1544	1000	700	0.5269	0.3302	0.0405
800	100	0.4788	-0.1367	0.1027	1000	750	0.6724	0.3267	-0.0034
800	150	0.3871	-0.0895	0.0379	1000	800	0.6057	0.2929	0.0238
800	200	0.2973	-0.0164	-0.0091	1000	850	0.4912	0.2706	0.0389
800	250	0.2425	0.0947	-0.0284					
800	300	0.1509	0.1999	-0.0349					
800	350	0.0532	0.2947	-0.0433					
800	400	-0.0314	0.3864	-0.0399					

A2.1.9 Mean velocity for $S = 10.52\%$, $Q = 52$ L/s, $z = 100$ mm

x (mm)	y (mm)	u (m/s)	v (m/s)	w (m/s)	x (mm)	y (mm)	u (m/s)	v (m/s)	w (m/s)
100	50	-0.1557	0.0079	0.1005	300	650	0.0844	-0.1876	-0.0080
100	100	-0.1263	0.0151	0.0968	300	700	-0.0545	-0.1742	0.0449
100	150	-0.1074	0.0401	0.0597	300	750	-0.0909	-0.1579	0.0500
100	200	-0.0284	-0.0970	0.0317	300	800	-0.1301	-0.1379	0.0553
100	250	-0.1326	0.1945	-0.0055	300	850	-0.2076	-0.0810	0.0234
100	300	-0.0498	0.0665	-0.0425					
100	350	-0.0699	0.2317	-0.0119	400	50	-0.0752	-0.0854	0.0464
100	400	-0.0358	0.2194	-0.0143	400	100	-0.2709	-0.0171	0.0500
100	450	0.0483	0.1786	-0.0043	400	150	-0.0281	-0.1264	0.0482
100	500	0.2437	-0.2117	0.0372	400	200	-0.0906	-0.0080	0.0215
100	550	0.5483	-0.5549	0.0520	400	250	0.2412	-0.1875	-0.0019
100	600	1.3216	-0.6473	0.0481	400	300	0.5459	-0.4174	-0.0438
100	650	1.4120	-0.6108	-0.0184	400	350	0.3074	-0.0823	-0.0203
					400	400	0.4669	-0.1143	-0.0075
200	50	-0.2125	-0.0072	0.0559	400	450	0.7193	-0.1314	-0.0013
200	100	-0.2350	0.0808	0.0095	400	500	0.6441	-0.2328	-0.0231
200	150	-0.1007	-0.0344	0.0167	400	550	0.8489	-0.1919	-0.0038
200	200	-0.0848	0.0423	-0.0119	400	600	0.4547	-0.1701	-0.0069
200	250	0.0602	-0.1771	-0.0292	400	650	0.1237	-0.1572	0.0070
200	300	0.1084	-0.1174	-0.0366	400	700	-0.0422	-0.1847	0.0225
200	350	0.0174	0.1827	-0.0261	400	750	-0.1221	-0.1781	0.0151
200	400	0.1489	0.1058	-0.0135	400	800	-0.2084	-0.1319	0.0092
200	450	0.2740	0.0559	0.0019	400	850	-0.3215	-0.0556	-0.0057
200	500	0.5619	-0.3980	0.0032					
200	550	1.1182	-0.4535	0.0009	500	50	-0.3431	0.0000	0.0273
200	600	1.2176	-0.4533	-0.0135	500	100	-0.1539	-0.0703	0.0728
200	650	0.1978	-0.1898	-0.0667	500	150	-0.2172	-0.0352	0.0661
200	700	-0.0070	-0.2228	-0.0053	500	200	-0.0298	-0.0748	0.0518
200	750	-0.0715	-0.1393	-0.0077	500	250	0.2731	-0.1318	-0.0083
200	800	-0.0904	-0.1114	0.0003	500	300	0.1962	-0.0106	0.0051
200	850	-0.1609	-0.1147	-0.0157	500	350	0.3914	-0.0715	-0.0136
					500	400	0.5608	-0.0301	-0.0071
300	50	-0.0741	-0.1364	0.0993	500	450	0.5731	-0.0669	-0.0154
300	100	-0.2645	0.0367	0.0163	500	500	0.7964	-0.0869	-0.0113
300	150	-0.1773	0.0136	0.0201	500	550	0.6428	-0.0666	-0.0061
300	200	-0.0078	-0.0908	0.0061	500	600	0.3946	-0.0922	0.0105
300	250	-0.0499	0.0640	0.0018	500	650	0.1660	-0.1080	0.0243
300	300	0.0887	0.0780	-0.0159	500	700	-0.0449	-0.1183	0.0073
300	350	0.1515	0.0880	-0.0311	500	750	-0.1912	-0.0581	0.0098
300	400	0.3047	0.0314	-0.0109	500	800	-0.2604	-0.0667	-0.0041
300	450	0.4274	-0.2913	-0.0281	500	850	-0.3564	-0.0544	-0.0203
300	500	0.8906	-0.2809	0.0065					
300	550	0.8643	-0.3355	-0.0201					
300	600	0.6316	-0.2370	-0.0308					

A2.1.9 Mean velocity for $S = 10.52\%$, $Q = 52$ L/s, $z = 100$ mm (cont'd)

x (mm)	y (mm)	u (m/s)	v (m/s)	w (m/s)	x (mm)	y (mm)	u (m/s)	v (m/s)	w (m/s)
600	50	0.0543	-0.0529	0.0211	800	400	0.2568	0.2098	0.0804
600	100	-0.3065	-0.0060	0.0652	800	450	0.4212	0.2619	0.0757
600	150	-0.2049	-0.0285	0.0826	800	500	0.2988	0.3513	-0.0185
600	200	-0.0618	-0.0492	0.0899	800	550	0.5805	0.4569	0.0772
600	250	0.2480	-0.0510	0.0294	800	600	0.5820	0.4601	0.0615
600	300	0.1871	0.0094	0.0146	800	650	0.4138	0.4619	0.0693
600	350	0.3584	0.0272	0.0043	800	700	0.2837	0.3560	0.0529
600	400	0.4975	0.0590	0.0046	800	750	0.0727	0.3522	0.0269
600	450	0.3305	0.0909	0.0091	800	800	-0.1236	0.2035	0.0119
600	500	0.6643	0.1029	-0.0042	800	850	-0.1863	0.1761	-0.0337
600	550	0.6130	0.0980	0.0096					
600	600	0.4628	0.0960	0.0183	900	50	-0.2431	0.0609	-0.0474
600	650	0.1328	0.0619	0.0151	900	100	-0.1370	0.0599	0.0261
600	700	0.0245	-0.0453	0.0100	900	150	-0.0309	0.0890	0.0459
600	750	-0.1419	-0.0748	-0.0196	900	200	-0.0902	0.0942	0.0545
600	800	-0.2911	-0.0247	-0.0147	900	250	-0.0222	0.0979	0.0639
600	850	-0.3938	-0.0367	-0.0203	900	300	0.0154	0.1483	0.0737
					900	350	0.0429	0.1727	0.1030
700	50	-0.0091	0.0019	-0.0065	900	400	0.1137	0.2323	0.1021
700	100	-0.2566	0.0243	0.0432	900	450	0.2338	0.2893	0.0927
700	150	-0.1025	-0.0163	0.0831	900	500	0.3184	0.4656	0.0812
700	200	-0.0668	-0.0087	0.1008	900	550	0.3623	0.6139	0.0814
700	250	-0.0241	0.0023	0.1008	900	600	0.5128	0.5802	0.0815
700	300	0.1708	0.0389	0.0651	900	650	0.5427	0.5348	0.0767
700	350	0.2906	0.0794	0.0465	900	700	0.4134	0.4863	0.0637
700	400	0.4262	0.1365	0.0347	900	750	0.3096	0.4192	0.0788
700	450	0.5335	0.2257	0.0260	900	800	0.1411	0.3087	0.0432
700	500	0.6674	0.2636	0.0274	900	850	-0.0490	0.2131	0.0192
700	550	0.5898	0.3097	0.0279					
700	600	0.3601	0.3244	0.0270					
700	650	0.2223	0.2819	0.0116					
700	700	-0.0071	0.3133	0.0110					
700	750	-0.0667	0.1196	0.0101					
700	800	-0.2228	0.1756	-0.0140					
700	850	-0.3384	0.1228	-0.0353					
800	50	-0.3255	0.0527	-0.0249					
800	100	-0.1109	0.0443	0.0312					
800	150	-0.2529	0.0788	0.0687					
800	200	-0.1571	0.0553	0.0999					
800	250	0.2082	0.0960	0.0308					
800	300	0.0377	0.0673	0.1274					
800	350	0.1753	0.1285	0.1271					

A2.1.10 Processed turbulence data for $S = 5.06\%$, $Q = 31.2$ L/s, $z = 10$ mm

x (mm)	y (mm)	$\sqrt{u'^2}$ (m/s)	$\sqrt{v'^2}$ (m/s)	$\sqrt{w'^2}$ (m/s)	$-\overline{u'v'}$ (m ² /s ²)	$-\overline{u'w'}$ (m ² /s ²)	$-\overline{v'w'}$ (m ² /s ²)	ε (m ² /s ³)	λ_g (mm)	η (mm)
100	50	0.119	0.053	0.030	0.000138	0.000130	0.000073	0.0500	1.55	0.073
100	100	0.126	0.063	0.033	0.000807	0.000308	0.000046	0.0383	1.92	0.078
100	150	0.131	0.070	0.033	0.000775	0.000043	0.000027	0.1047	1.22	0.061
100	200	0.128	0.079	0.034	-0.000213	0.000136	0.000062	0.0503	1.79	0.073
100	250	0.127	0.081	0.034	0.000566	0.000115	-0.000049	0.0480	1.82	0.074
100	300	0.122	0.078	0.032	0.000293	0.000315	0.000032	0.0262	2.36	0.086
100	350	0.110	0.085	0.032	0.000302	0.000150	-0.000047	0.0239	2.39	0.088
100	400	0.101	0.097	0.031	-0.000338	0.000197	-0.000008	0.0276	2.23	0.085
100	450	0.076	0.108	0.031	0.000035	-0.000067	0.000081	0.0098	3.54	0.110
100	500	0.115	0.172	0.039	0.005717	-0.000055	-0.000360	0.0401	2.72	0.077
100	550	0.155	0.269	0.062	0.019132	-0.001268	0.004870	0.0393	4.12	0.078
100	600	0.229	0.218	0.089	-0.029665	0.002048	-0.002250	0.0490	3.84	0.074
100	650	0.240	0.181	0.057	0.009589	0.000849	-0.002589	0.0395	3.98	0.078
200	50	0.136	0.074	0.033	0.001234	0.000019	0.000248	0.0132	3.57	0.102
200	100	0.144	0.082	0.036	0.001278	-0.000239	0.000061	0.0236	2.85	0.088
200	150	0.143	0.089	0.037	0.001804	-0.000052	0.000123	0.0315	2.52	0.082
200	200	0.142	0.112	0.038	0.002293	-0.000346	0.000222	0.0629	1.91	0.069
200	250	0.129	0.106	0.035	0.001785	-0.000319	0.000149	0.4468	0.66	0.042
200	300	0.126	0.128	0.039	0.001576	-0.000413	0.000397	0.0496	2.14	0.073
200	350	0.129	0.166	0.040	0.003871	-0.000579	0.000193	0.0576	2.31	0.071
200	400	0.140	0.223	0.044	0.012295	-0.000241	0.000424	0.0294	4.03	0.084
200	450	0.174	0.274	0.060	0.021050	-0.000632	0.001375	0.0714	3.20	0.067
200	500	0.183	0.243	0.067	0.015712	-0.000444	0.001611	0.0706	3.03	0.067
200	550	0.241	0.143	0.057	0.007087	0.000006	-0.001654	0.0661	2.88	0.068
200	600	0.265	0.120	0.063	0.010125	0.002610	-0.002007	0.0948	2.50	0.062
200	650	0.141	0.071	0.041	-0.000300	0.000363	0.000040	0.0803	1.49	0.065
200	700	0.111	0.069	0.033	0.000634	0.000281	0.000030	0.0155	2.81	0.098
200	750	0.123	0.059	0.030	-0.000893	0.000203	-0.000037	0.0082	3.99	0.115
200	800	0.114	0.049	0.028	-0.001012	0.000190	-0.000030	0.0053	4.53	0.129
200	850	0.109	0.049	0.029	-0.000576	0.000260	-0.000154	0.0027	6.16	0.152
300	50	0.142	0.089	0.033	0.002449	-0.000334	0.000460	0.0133	3.82	0.102
300	100	0.154	0.105	0.037	0.005431	-0.000400	0.000233	0.0244	3.14	0.088
300	150	0.150	0.118	0.036	0.005697	-0.000061	0.000205	0.0269	3.07	0.086
300	200	0.154	0.141	0.042	0.007606	-0.000143	0.000354	0.1760	1.31	0.054
300	250	0.150	0.166	0.039	0.009564	-0.000336	0.000420	0.0750	2.14	0.066
300	300	0.150	0.194	0.043	0.012865	-0.000557	0.000537	0.0371	3.35	0.079
300	350	0.155	0.204	0.044	0.016285	-0.000583	0.000235	0.0273	4.08	0.085
300	400	0.181	0.237	0.056	0.021557	-0.001186	0.001096	0.0533	3.41	0.072
300	450	0.152	0.166	0.071	0.009514	-0.000858	0.000717	0.0317	3.43	0.082
300	500	0.203	0.187	0.069	0.009546	0.000161	-0.001116	0.0875	2.49	0.064
300	550	0.219	0.127	0.055	0.005975	0.001306	-0.001290	0.0679	2.58	0.068

A2.1.10 Processed turbulence data for $S = 5.06\%$, $Q = 31.2\text{L/s}$, $z = 10\text{mm}$ (cont'd)

x (mm)	y (mm)	$\sqrt{u'^2}$ (m/s)	$\sqrt{v'^2}$ (m/s)	$\sqrt{w'^2}$ (m/s)	$-\overline{u'v'}$ (m ² /s ²)	$-\overline{u'w'}$ (m ² /s ²)	$-\overline{v'w'}$ (m ² /s ²)	ε (m ² /s ³)	λ_g (mm)	η (mm)
300	600	0.213	0.108	0.063	-0.002283	0.001914	-0.000367	0.0742	2.35	0.066
300	650	0.157	0.079	0.048	-0.003635	-0.000160	0.000087	0.0517	2.07	0.073
300	700	0.117	0.099	0.033	-0.002124	-0.000764	-0.000497	0.0423	1.98	0.076
300	750	0.126	0.090	0.032	-0.003866	-0.000582	-0.000304	0.1604	1.02	0.055
300	800	0.145	0.074	0.034	-0.005127	-0.000626	-0.000221	0.0565	1.81	0.071
300	850	0.157	0.063	0.033	-0.004141	-0.000677	-0.000231	0.0497	2.01	0.073
400	50	0.134	0.090	0.035	0.002972	-0.000698	0.000680	0.0092	4.44	0.112
400	100	0.168	0.120	0.037	0.009138	-0.000901	0.000747	0.0175	4.12	0.095
400	150	0.178	0.144	0.043	0.012412	-0.000923	0.000942	0.0486	2.73	0.074
400	200	0.170	0.157	0.045	0.013237	-0.000934	0.000881	0.1611	1.52	0.055
400	250	0.169	0.184	0.047	0.016508	-0.001161	0.001269	0.0399	3.29	0.078
400	300	0.160	0.177	0.049	0.014924	-0.000748	0.001206	0.0229	4.16	0.089
400	350	0.149	0.161	0.051	0.012344	-0.000612	0.000982	0.0184	4.30	0.094
400	400	0.181	0.203	0.060	0.015719	-0.000398	0.001663	0.0476	3.30	0.074
400	450	0.180	0.171	0.055	0.008834	0.000432	0.001170	0.0557	2.79	0.071
400	500	0.215	0.157	0.064	0.004691	0.001464	0.000412	0.0852	2.43	0.064
400	550	0.229	0.143	0.060	-0.001135	0.001836	-0.000079	0.0773	2.57	0.066
400	600	0.219	0.144	0.056	-0.010261	0.001147	0.000376	0.0726	2.58	0.067
400	650	0.165	0.146	0.046	-0.010609	-0.000130	0.000470	0.0394	2.94	0.078
400	700	0.148	0.134	0.040	-0.007516	0.000139	0.000012	0.0738	1.94	0.067
400	750	0.139	0.116	0.035	-0.005164	0.000128	0.000190	0.0447	2.26	0.075
400	800	0.148	0.098	0.037	-0.005652	0.000266	0.000272	0.0200	3.32	0.092
400	850	0.140	0.088	0.033	-0.004411	0.000080	0.000002	0.0127	3.88	0.103
500	50	0.147	0.102	0.036	0.002904	-0.000425	0.000883	0.0110	4.51	0.107
500	100	0.179	0.127	0.040	0.009917	-0.000975	0.000615	0.0155	4.65	0.098
500	150	0.201	0.155	0.050	0.014075	-0.001059	0.001085	0.0531	2.90	0.072
500	200	0.195	0.153	0.049	0.014615	-0.001208	0.001013	0.1402	1.75	0.057
500	250	0.192	0.174	0.051	0.017157	-0.001340	0.001365	0.0508	3.03	0.073
500	300	0.189	0.181	0.051	0.017844	-0.000877	0.001226	0.0328	3.81	0.081
500	350	0.178	0.178	0.056	0.016295	-0.000747	0.001610	0.0255	4.19	0.087
500	400	0.182	0.147	0.058	0.010652	-0.000444	0.001127	0.0424	3.03	0.076
500	450	0.192	0.166	0.058	0.009364	0.000753	0.000951	0.0499	3.02	0.073
500	500	0.169	0.160	0.060	0.003852	0.000915	0.000684	0.0329	3.43	0.081
500	550	0.198	0.143	0.049	-0.003193	0.000778	-0.000126	0.0530	2.80	0.072
500	600	0.210	0.152	0.051	-0.011847	0.000759	0.000222	0.0523	2.99	0.072
500	650	0.182	0.162	0.050	-0.014726	0.000019	0.000426	0.0259	4.00	0.086
500	700	0.198	0.157	0.045	-0.015950	0.000112	0.000225	0.0949	2.16	0.062
500	750	0.179	0.142	0.042	-0.012377	0.000284	0.000437	0.0484	2.74	0.074
500	800	0.166	0.127	0.046	-0.010277	0.000459	0.000434	0.0196	3.96	0.093
500	850	0.145	0.113	0.043	-0.006233	0.000117	-0.000005	0.0226	3.26	0.089

A2.1.10 Processed turbulence data for $S = 5.06\%$, $Q = 31.2\text{L/s}$, $z = 10\text{mm}$ (cont'd)

x (mm)	y (mm)	$\sqrt{u'^2}$ (m/s)	$\sqrt{v'^2}$ (m/s)	$\sqrt{w'^2}$ (m/s)	$-\overline{u'v'}$ (m ² /s ²)	$-\overline{u'w'}$ (m ² /s ²)	$-\overline{v'w'}$ (m ² /s ²)	ε (m ² /s ³)	λ_g (mm)	η (mm)
600	50	0.155	0.106	0.039	0.003697	-0.000641	0.000865	0.0094	5.11	0.111
600	100	0.186	0.131	0.043	0.009910	-0.000837	0.000700	0.0174	4.55	0.095
600	150	0.208	0.140	0.045	0.011804	-0.000705	0.000384	0.0468	3.05	0.075
600	200	0.231	0.164	0.053	0.014900	-0.001079	0.000932	0.1942	1.69	0.052
600	250	0.205	0.159	0.047	0.016096	-0.000964	0.001119	0.0452	3.21	0.075
600	300	0.199	0.167	0.054	0.015429	-0.000858	0.001034	0.0402	3.42	0.077
600	350	0.194	0.172	0.059	0.015509	-0.000263	0.000940	0.0452	3.24	0.075
600	400	0.190	0.154	0.056	0.011788	0.000024	0.000899	0.0391	3.29	0.078
600	450	0.161	0.157	0.054	0.007505	0.000585	0.000402	0.0202	4.22	0.092
600	500	0.198	0.156	0.053	0.005433	0.000879	0.000222	0.0447	3.15	0.075
600	550	0.169	0.156	0.052	-0.001415	0.000558	-0.000090	0.0255	3.82	0.087
600	600	0.220	0.169	0.051	-0.011728	0.000816	-0.000019	0.0468	3.37	0.075
600	650	0.210	0.176	0.047	-0.017860	0.000179	0.000160	0.0225	4.79	0.089
600	700	0.209	0.181	0.048	-0.019279	-0.000381	-0.000193	0.0507	3.23	0.073
600	750	0.206	0.174	0.049	-0.015959	0.000041	0.000157	0.0838	2.45	0.064
600	800	0.180	0.155	0.049	-0.014099	0.000576	0.000641	0.0185	4.62	0.094
600	850	0.146	0.141	0.053	-0.007311	0.000272	-0.000165	0.0261	3.36	0.086
700	50	0.147	0.104	0.039	0.002602	-0.000304	0.000915	0.0056	6.37	0.127
700	100	0.178	0.127	0.041	0.006297	-0.000198	0.000706	0.0165	4.48	0.097
700	150	0.195	0.129	0.046	0.005686	-0.000268	0.000507	0.0331	3.38	0.081
700	200	0.213	0.136	0.049	0.006609	-0.000395	0.000570	0.0830	2.31	0.065
700	250	0.217	0.140	0.052	0.009609	-0.001012	0.000872	0.0610	2.76	0.070
700	300	0.219	0.147	0.055	0.011034	-0.000967	0.001128	0.0546	2.99	0.072
700	350	0.218	0.147	0.056	0.012561	-0.000408	0.000982	0.0493	3.13	0.074
700	400	0.186	0.148	0.054	0.011493	-0.000233	0.000558	0.0286	3.74	0.084
700	450	0.205	0.154	0.051	0.012524	0.000176	0.000285	0.0386	3.45	0.078
700	500	0.189	0.149	0.049	0.007853	0.000567	0.000157	0.0469	2.94	0.074
700	550	0.188	0.153	0.043	0.004032	0.000672	-0.000308	0.0383	3.26	0.078
700	600	0.209	0.171	0.045	-0.001227	0.000606	-0.000497	0.0425	3.44	0.076
700	650	0.210	0.180	0.044	-0.011911	-0.000177	-0.000490	0.0461	3.37	0.075
700	700	0.204	0.185	0.045	-0.016191	-0.000555	-0.000485	0.0543	3.10	0.072
700	750	0.211	0.191	0.049	-0.018251	0.000168	-0.000488	0.2587	1.47	0.049
700	800	0.184	0.190	0.053	-0.014762	0.000644	0.000112	0.0347	3.75	0.080
700	850	0.145	0.168	0.061	-0.006750	0.000573	0.000163	0.0231	3.92	0.089
800	50	0.128	0.103	0.037	0.001136	0.000161	0.000796	0.0052	6.07	0.129
800	100	0.148	0.116	0.037	0.001807	0.000542	0.000588	0.0131	4.32	0.102
800	150	0.192	0.123	0.042	0.002699	0.000422	0.000610	0.0212	4.12	0.091
800	200	0.208	0.126	0.044	0.001059	0.000698	0.000957	0.0496	2.87	0.073
800	250	0.240	0.136	0.053	0.002879	0.000632	0.001106	0.2531	1.45	0.049
800	300	0.241	0.130	0.050	0.003935	0.000584	0.000854	0.1236	2.05	0.058
800	350	0.238	0.130	0.056	0.004802	0.000163	0.000960	0.0621	2.87	0.069

A2.1.10 Processed turbulence data for $S = 5.06\%$, $Q = 31.2\text{L/s}$, $z = 10\text{mm}$ (cont'd)

x (mm)	y (mm)	$\sqrt{u'^2}$ (m/s)	$\sqrt{v'^2}$ (m/s)	$\sqrt{w'^2}$ (m/s)	$-\overline{u'v'}$ (m ² /s ²)	$-\overline{u'w'}$ (m ² /s ²)	$-\overline{v'w'}$ (m ² /s ²)	ε (m ² /s ³)	λ_g (mm)	η (mm)
800	400	0.239	0.144	0.060	0.009543	-0.000072	0.000979	0.0639	2.93	0.069
800	450	0.243	0.144	0.057	0.012705	0.000684	0.000594	0.0566	3.14	0.071
800	500	0.224	0.156	0.053	0.012751	0.000533	0.000077	0.0571	3.01	0.071
800	550	0.214	0.150	0.050	0.008525	0.000346	-0.000090	0.0560	2.91	0.071
800	600	0.186	0.159	0.042	0.004754	0.000303	-0.000376	0.0405	3.19	0.077
800	650	0.198	0.177	0.043	0.001134	0.000168	-0.001103	0.0493	3.13	0.074
800	700	0.190	0.187	0.045	-0.004692	0.000025	-0.001332	0.0605	2.85	0.070
800	750	0.182	0.188	0.048	-0.010314	0.000080	-0.001254	0.2138	1.49	0.051
800	800	0.182	0.192	0.055	-0.015529	0.000929	-0.000026	0.0822	2.44	0.065
800	850	0.147	0.176	0.066	-0.007300	0.000748	0.000784	0.0341	3.34	0.081
900	50	0.148	0.114	0.042	-0.004259	0.000581	0.001256	0.0093	5.13	0.112
900	100	0.148	0.120	0.042	-0.002526	0.000886	0.001024	0.0103	4.98	0.109
900	150	0.173	0.119	0.043	-0.003347	0.001137	0.000956	0.0164	4.35	0.097
900	200	0.207	0.125	0.045	-0.005817	0.000912	0.000995	0.0247	4.05	0.087
900	250	0.249	0.126	0.050	-0.004239	0.001544	0.000951	0.0424	3.57	0.076
900	300	0.268	0.141	0.055	-0.006122	0.002060	0.001326	0.0734	2.93	0.067
900	350	0.292	0.148	0.059	-0.008088	0.002214	0.001566	0.1505	2.22	0.056
900	400	0.299	0.140	0.059	-0.002442	0.001550	0.001419	0.4556	1.29	0.042
900	450	0.306	0.144	0.068	0.008651	0.000551	0.001487	0.9150	0.93	0.035
900	525	0.280	0.153	0.065	0.010910	0.001200	0.001119	0.1571	2.13	0.055
900	550	0.266	0.178	0.063	0.019830	-0.000126	0.001845	0.0983	2.69	0.062
900	600	0.246	0.158	0.054	0.004882	0.001660	0.000347	0.0810	2.70	0.065
900	650	0.222	0.177	0.047	0.004011	0.000677	-0.000155	0.0724	2.76	0.067
900	700	0.182	0.167	0.046	-0.001384	0.000648	-0.000720	0.0527	2.83	0.072
900	750	0.168	0.188	0.048	-0.009188	0.000148	-0.001103	0.0849	2.28	0.064
900	800	0.172	0.187	0.055	-0.012661	0.000831	-0.000006	0.2288	1.41	0.050
900	850	0.153	0.183	0.065	-0.007938	0.000746	0.000795	0.0526	2.79	0.072
1000	50	0.129	0.137	0.054	-0.007912	0.000468	0.001007	0.0140	4.30	0.101
1000	100	0.136	0.126	0.043	-0.004976	0.000205	0.000690	0.0184	3.63	0.094
1000	150	0.155	0.126	0.044	-0.004991	0.000139	0.000700	0.0172	4.04	0.096
1000	200	0.175	0.131	0.046	-0.006019	-0.000056	0.000718	0.0232	3.80	0.089
1000	250	0.208	0.137	0.048	-0.008737	-0.000219	0.000601	0.0257	4.11	0.087
1000	300	0.214	0.149	0.054	-0.005358	-0.000540	0.000669	0.0337	3.75	0.081
1000	350	0.220	0.129	0.056	-0.004500	-0.000381	0.000887	0.0308	3.85	0.083
1000	400	0.236	0.126	0.059	-0.005147	-0.001190	-0.000023	0.0503	3.16	0.073
1000	650	0.206	0.153	0.062	-0.004678	0.000688	0.000208	0.0495	3.07	0.073
1000	700	0.184	0.178	0.053	-0.008043	0.001624	-0.000248	0.0469	3.13	0.074
1000	750	0.161	0.189	0.049	-0.013399	0.000706	-0.000153	0.0544	2.80	0.072
1000	800	0.161	0.188	0.057	-0.015768	0.001233	0.001145	0.3405	1.13	0.045
1000	850	0.170	0.175	0.067	-0.008622	0.000060	-0.000477	0.1264	1.84	0.058

A2.1.11 Processed turbulence data for $S = 5.06\%$, $Q = 31.2$ L/s, $z = 100$ mm

x (mm)	y (mm)	$\sqrt{u'^2}$ (m/s)	$\sqrt{v'^2}$ (m/s)	$\sqrt{w'^2}$ (m/s)	$-\overline{u'v'}$ (m ² /s ²)	$-\overline{u'w'}$ (m ² /s ²)	$-\overline{v'w'}$ (m ² /s ²)	ε (m ² /s ³)	λ_g (mm)	η (mm)
100	50	0.0838	0.0632	0.0859	0.000577	0.000942	-0.000296	0.0047	0.132	5.115
100	100	0.1066	0.0764	0.0895	0.001200	0.001849	0.000133	0.0060	0.124	5.304
100	150	0.1019	0.0749	0.0885	0.000788	0.001899	-0.000023	0.0069	0.120	4.811
100	200	0.0995	0.0771	0.0869	0.001043	0.001532	-0.000382	0.0096	0.111	4.036
100	250	0.0968	0.0827	0.0829	0.001196	0.000906	0.000393	0.0126	0.103	3.498
100	300	0.0937	0.0851	0.0814	0.000901	0.000864	0.000405	0.0155	0.098	3.130
100	350	0.0771	0.0784	0.0789	0.000518	0.000623	0.000044	0.0125	0.104	3.127
100	400	0.0779	0.0816	0.0811	0.000562	0.000387	0.000092	0.0315	0.082	2.027
100	450	0.0729	0.0854	0.0762	0.000913	-0.000032	0.000272	0.0350	0.080	1.878
100	500	0.0904	0.1043	0.0899	0.001234	0.000068	0.000320	0.0413	0.077	2.098
100	550	0.1369	0.1957	0.1064	0.012662	-0.001496	0.001815	0.0391	0.078	3.422
100	600	0.1587	0.2070	0.1727	0.004944	-0.002788	-0.004589	0.0400	0.078	4.051
100	650	0.1764	0.1636	0.1702	-0.012213	-0.005561	-0.004935	0.0325	0.082	4.232
200	50	0.1222	0.0784	0.0947	0.001382	0.000353	0.000339	0.0108	0.108	4.321
200	100	0.1193	0.0834	0.0966	0.001131	0.000040	-0.000120	0.0118	0.105	4.167
200	150	0.1184	0.0878	0.0953	0.001365	0.000167	0.000330	0.0149	0.099	3.729
200	200	0.1149	0.0923	0.0975	0.001417	0.000009	0.000648	0.0130	0.103	4.017
200	250	0.1089	0.0931	0.0957	0.001610	-0.000107	0.000088	0.0216	0.090	3.032
200	300	0.1139	0.1101	0.1008	0.002735	-0.000434	0.000503	0.0467	0.075	2.250
200	350	0.1117	0.1139	0.1013	0.002461	-0.000750	0.000644	0.0500	0.073	2.188
200	400	0.1144	0.1320	0.1055	0.004723	-0.001302	0.000698	0.0513	0.073	2.333
200	450	0.1514	0.1779	0.1375	0.011982	-0.000365	0.000575	0.0500	0.073	3.137
200	500	0.1978	0.2554	0.1565	0.027484	-0.002368	0.002459	0.0653	0.069	3.637
200	550	0.2333	0.2608	0.1488	0.032923	-0.001819	-0.000920	0.0954	0.062	3.186
200	600	0.3000	0.1539	0.1393	0.001605	-0.004951	-0.001801	0.1480	0.056	2.454
200	650	0.3004	0.1138	0.1275	-0.002113	0.005956	0.000473	0.3819	0.044	1.448
200	700	0.0907	0.0911	0.1027	-0.000793	0.001114	0.001097	0.0274	0.085	2.575
200	750	0.0848	0.0727	0.0874	-0.001597	0.001379	0.000860	0.0081	0.116	4.086
200	800	0.0933	0.0681	0.0868	-0.001135	0.001132	0.000521	0.0131	0.102	3.270
200	850	0.1020	0.0641	0.0845	-0.000700	0.001089	-0.000211	0.0285	0.084	2.256
300	50	0.1402	0.0800	0.0919	0.002216	0.001300	0.000616	0.0119	0.105	4.408
300	100	0.1363	0.1015	0.0935	0.003571	-0.000513	0.001288	0.0151	0.099	4.079
300	150	0.1448	0.1075	0.1035	0.004841	-0.000489	0.001274	0.0209	0.091	3.720
300	200	0.1283	0.1071	0.1057	0.003126	-0.000341	0.000972	0.0235	0.088	3.337
300	250	0.1373	0.1255	0.1072	0.006487	-0.001150	0.000880	0.0713	0.067	2.082
300	300	0.1543	0.1482	0.1131	0.010998	-0.001440	-0.000041	0.0600	0.070	2.557
300	350	0.1353	0.1346	0.1203	0.005812	-0.002012	0.000373	0.0525	0.072	2.548
300	400	0.1709	0.1841	0.1322	0.014955	-0.000873	0.000223	0.0589	0.070	3.029
300	450	0.1944	0.2184	0.1549	0.022107	-0.000388	-0.000322	0.0670	0.068	3.308
300	500	0.2438	0.2476	0.1514	0.033384	-0.001151	0.000244	0.0865	0.064	3.336
300	550	0.2811	0.1959	0.1308	0.008461	-0.000589	-0.002267	0.1484	0.056	2.464

A2.1.11 Processed turbulence data for $S = 5.06\%$, $Q = 31.2\text{L/s}$, $z = 100\text{mm}$ (cont'd)

x (mm)	y (mm)	$\sqrt{u'^2}$ (m/s)	$\sqrt{v'^2}$ (m/s)	$\sqrt{w'^2}$ (m/s)	$-\overline{u'v'}$ (m ² /s ²)	$-\overline{u'w'}$ (m ² /s ²)	$-\overline{v'w'}$ (m ² /s ²)	ε (m ² /s ³)	λ_g (mm)	η (mm)
300	600	0.3328	0.1371	0.1421	-0.011059	0.002978	-0.000701	0.2120	0.051	2.175
300	650	0.1887	0.1294	0.1306	-0.007355	0.005428	0.002971	0.1546	0.055	1.735
300	700	0.1052	0.1080	0.1094	-0.001844	0.000273	0.001627	0.0720	0.067	1.797
300	750	0.0929	0.0913	0.0993	-0.001987	-0.000459	0.000188	0.0175	0.095	3.204
300	800	0.1004	0.0829	0.0939	-0.002727	-0.001170	-0.000376	0.0142	0.100	3.491
300	850	0.1186	0.0786	0.0922	-0.002956	-0.002245	-0.001254	0.0153	0.099	3.546
400	50	0.1403	0.0834	0.1010	0.001826	0.000119	0.002102	0.0125	0.104	4.439
400	100	0.1452	0.1036	0.1046	0.004306	-0.001367	0.002127	0.0191	0.093	3.874
400	150	0.1554	0.1191	0.1136	0.006170	-0.000742	0.001609	0.0277	0.085	3.520
400	200	0.1650	0.1289	0.1180	0.008399	-0.001932	0.000982	0.0428	0.076	3.008
400	250	0.1621	0.1509	0.1281	0.008950	-0.002612	0.001169	0.2764	0.048	1.260
400	300	0.1728	0.1662	0.1327	0.013113	-0.003588	0.000648	0.0872	0.064	2.402
400	350	0.1742	0.1717	0.1398	0.012948	-0.001844	-0.000385	0.0548	0.072	3.116
400	400	0.1950	0.1905	0.1448	0.017583	-0.000728	0.000217	0.0555	0.071	3.391
400	450	0.2286	0.2225	0.1483	0.024314	0.000556	0.002041	0.0834	0.064	3.153
400	500	0.2413	0.2228	0.1398	0.021501	0.002073	0.000488	0.0935	0.063	3.021
400	550	0.2731	0.1793	0.1284	-0.008385	0.003451	0.000233	0.0936	0.063	2.970
400	600	0.2652	0.1570	0.1393	-0.017581	0.007099	0.001733	0.1067	0.061	2.680
400	650	0.1813	0.1374	0.1239	-0.008444	0.003165	0.002370	0.0753	0.066	2.444
400	700	0.1364	0.1236	0.1171	-0.004043	0.000154	0.001390	0.0600	0.070	2.305
400	750	0.1296	0.1076	0.1102	-0.003638	-0.000703	0.000813	0.0480	0.074	2.378
400	800	0.1348	0.0995	0.0986	-0.003576	-0.002006	0.001250	0.0310	0.083	2.857
400	850	0.1273	0.0852	0.0873	-0.002696	-0.001972	0.000301	0.0202	0.092	3.214
500	50	0.1597	0.0992	0.1069	0.003039	-0.002900	0.003341	0.0148	0.099	4.602
500	100	0.1796	0.1312	0.1155	0.008950	-0.002834	0.004008	0.0268	0.086	3.965
500	150	0.1788	0.1400	0.1196	0.009310	-0.001365	0.001981	0.0355	0.080	3.525
500	200	0.2080	0.1643	0.1393	0.016531	-0.004051	0.000935	0.1432	0.056	2.048
500	250	0.2008	0.1763	0.1401	0.018306	-0.002621	0.000585	0.4081	0.043	1.222
500	300	0.1941	0.1678	0.1461	0.013669	-0.003923	-0.000033	0.0992	0.062	2.427
500	350	0.1996	0.1774	0.1492	0.015491	-0.002322	0.000264	0.0644	0.069	3.121
500	400	0.2262	0.1981	0.1511	0.022523	0.000171	-0.000131	0.0668	0.068	3.370
500	450	0.2417	0.2160	0.1419	0.027756	0.000418	0.000938	0.0883	0.064	3.081
500	500	0.2387	0.2058	0.1334	0.013445	0.003289	0.000373	0.0892	0.063	2.967
500	550	0.2556	0.1819	0.1255	-0.007781	0.003963	0.000969	0.0981	0.062	2.792
500	600	0.2538	0.1699	0.1291	-0.018232	0.004204	0.001996	0.0736	0.067	3.163
500	650	0.1831	0.1462	0.1287	-0.010724	0.001378	0.001544	0.0561	0.071	2.922
500	700	0.1576	0.1361	0.1319	-0.005737	0.000190	0.000760	0.2160	0.051	1.373
500	750	0.1510	0.1200	0.1274	-0.004150	-0.000926	0.000035	0.0532	0.072	2.595
500	800	0.1547	0.1114	0.1141	-0.004934	-0.001518	0.000014	0.0335	0.081	3.140
500	850	0.1448	0.0984	0.0958	-0.003857	-0.002342	-0.000072	0.0216	0.090	3.513

A2.1.11 Processed turbulence data for $S = 5.06\%$, $Q = 31.2\text{L/s}$, $z = 100\text{mm}$ (cont'd)

x (mm)	y (mm)	$\sqrt{u'^2}$ (m/s)	$\sqrt{v'^2}$ (m/s)	$\sqrt{w'^2}$ (m/s)	$-\overline{u'v'}$ (m ² /s ²)	$-\overline{u'w'}$ (m ² /s ²)	$-\overline{v'w'}$ (m ² /s ²)	ε (m ² /s ³)	λ_g (mm)	η (mm)
600	50	0.1489	0.0922	0.1019	0.001566	-0.000595	0.002870	0.0137	0.101	4.480
600	100	0.1956	0.1373	0.1216	0.010972	-0.003851	0.004143	0.0321	0.082	3.877
600	150	0.1896	0.1488	0.1328	0.011325	-0.003255	0.002312	0.0423	0.076	3.464
600	200	0.2123	0.1555	0.1361	0.013600	-0.002692	0.000845	0.1630	0.055	1.899
600	250	0.1954	0.1607	0.1504	0.010548	-0.003184	0.000409	0.3942	0.044	1.213
600	300	0.2203	0.1702	0.1603	0.014206	-0.003623	-0.000509	0.1148	0.060	2.454
600	350	0.2271	0.1741	0.1556	0.016178	0.000307	-0.000566	0.0873	0.064	2.853
600	400	0.2306	0.1751	0.1469	0.016389	-0.000530	0.000987	0.0700	0.067	3.177
600	450	0.2493	0.1929	0.1399	0.020296	0.001460	0.001298	0.0790	0.065	3.176
600	500	0.2322	0.1947	0.1312	0.011220	0.001942	0.000752	0.0848	0.064	2.935
600	550	0.2441	0.1803	0.1189	-0.004211	0.002318	0.000527	0.0768	0.066	3.044
600	600	0.2210	0.1815	0.1251	-0.013403	0.002230	0.001042	0.0626	0.069	3.230
600	650	0.1893	0.1684	0.1341	-0.012683	0.001234	0.001148	0.0451	0.075	3.492
600	700	0.1722	0.1533	0.1359	-0.006949	-0.000654	0.000637	0.1051	0.061	2.137
600	750	0.1564	0.1384	0.1410	-0.005555	-0.001826	-0.000130	0.0596	0.070	2.671
600	800	0.1523	0.1240	0.1301	-0.004476	-0.002320	-0.000146	0.0343	0.081	3.292
600	850	0.1460	0.1131	0.1145	-0.003825	-0.003738	-0.001266	0.0238	0.088	3.642
700	50	0.1577	0.1011	0.1077	0.001999	-0.001458	0.003030	0.0131	0.102	4.885
700	100	0.1872	0.1304	0.1168	0.007574	-0.002531	0.004316	0.0275	0.085	3.999
700	150	0.1909	0.1438	0.1309	0.008855	-0.002206	0.002341	0.0418	0.077	3.452
700	200	0.2379	0.1512	0.1493	0.011639	-0.000623	0.000929	0.7067	0.038	0.982
700	250	0.2005	0.1487	0.1560	0.007890	-0.000978	0.001189	0.3658	0.045	1.260
700	300	0.2292	0.1627	0.1657	0.012400	-0.001144	-0.000273	0.1260	0.058	2.379
700	350	0.2214	0.1565	0.1659	0.009913	-0.000841	-0.000315	0.0746	0.066	3.013
700	400	0.2438	0.1650	0.1616	0.014479	0.000511	0.000395	0.0891	0.063	2.912
700	450	0.2475	0.1686	0.1444	0.013964	0.000811	0.000765	0.0801	0.065	3.040
700	500	0.2403	0.1690	0.1308	0.011555	0.000826	0.000697	0.0781	0.066	2.978
700	550	0.2088	0.1708	0.1174	0.001801	0.001115	0.000385	0.0667	0.068	2.950
700	600	0.1946	0.1795	0.1189	-0.006481	0.000485	-0.000008	0.0502	0.073	3.352
700	650	0.1984	0.1802	0.1290	-0.005941	-0.001255	-0.000294	0.0535	0.072	3.328
700	700	0.1688	0.1670	0.1397	-0.008806	-0.002402	-0.000690	0.0855	0.064	2.439
700	750	0.1573	0.1549	0.1449	-0.006130	-0.000608	-0.000031	0.1148	0.060	2.018
700	800	0.1545	0.1482	0.1384	-0.007173	-0.003506	-0.001249	0.0416	0.077	3.234
700	850	0.1487	0.1341	0.1268	-0.004415	-0.003851	-0.002108	0.0293	0.084	3.581
800	50	0.1942	0.1044	0.1037	0.005718	-0.002228	0.002965	0.0183	0.094	4.664
800	100	0.1481	0.1254	0.1118	0.003246	0.000027	0.003104	0.0204	0.092	4.055
800	150	0.1610	0.1398	0.1247	0.004696	-0.000794	0.002219	0.0372	0.079	3.315
800	200	0.2045	0.1474	0.1470	0.005654	-0.000890	0.002490	0.2183	0.051	1.617
800	250	0.2023	0.1490	0.1560	0.003181	-0.000546	0.002425	0.4087	0.043	1.197
800	300	0.2146	0.1518	0.1666	0.005406	0.000470	0.002092	0.1228	0.059	2.298
800	350	0.2240	0.1541	0.1716	0.006836	0.001174	0.000879	0.0931	0.063	2.727

A2.1.11 Processed turbulence data for $S = 5.06\%$, $Q = 31.2\text{L/s}$, $z = 100\text{mm}$ (cont'd)

x (mm)	y (mm)	$\sqrt{u'^2}$ (m/s)	$\sqrt{v'^2}$ (m/s)	$\sqrt{w'^2}$ (m/s)	$-\overline{u'v'}$ (m ² /s ²)	$-\overline{u'w'}$ (m ² /s ²)	$-\overline{v'w'}$ (m ² /s ²)	ε (m ² /s ³)	λ_g (mm)	η (mm)
800	400	0.2305	0.1586	0.1750	0.007817	0.001247	-0.000030	0.0876	0.064	2.886
800	450	0.2329	0.1489	0.1617	0.006159	0.001757	-0.000053	0.0869	0.064	2.812
800	500	0.2335	0.1593	0.1490	0.006523	0.001449	-0.000798	0.0839	0.064	2.855
800	550	0.2241	0.1578	0.1293	0.005855	0.000351	0.000020	0.0737	0.067	2.889
800	600	0.1966	0.1607	0.1223	0.003037	-0.000846	-0.001043	0.0660	0.068	2.840
800	650	0.1762	0.1707	0.1242	0.000143	-0.001950	-0.000763	0.0587	0.070	2.937
800	700	0.1646	0.1791	0.1362	-0.004189	-0.002013	-0.001247	0.0673	0.068	2.782
800	750	0.1535	0.1628	0.1397	-0.004743	-0.001632	-0.001569	0.2084	0.051	1.495
800	800	0.1611	0.1558	0.1351	-0.007310	-0.002585	-0.003035	0.1081	0.060	2.060
800	850	0.1515	0.1500	0.1346	-0.007714	-0.003376	-0.003746	0.0354	0.080	3.471
900	50	0.1367	0.1025	0.0958	0.001062	-0.000213	0.001895	0.0133	0.102	4.389
900	100	0.1336	0.1258	0.1067	0.001862	0.000560	0.001295	0.0207	0.091	3.817
900	150	0.1368	0.1422	0.1212	0.002638	-0.000874	0.001832	0.0346	0.080	3.222
900	200	0.1612	0.1515	0.1294	0.002868	-0.001104	0.003162	0.1406	0.057	1.769
900	250	0.1705	0.1545	0.1449	0.004581	-0.001070	0.003375	0.6119	0.039	0.900
900	300	0.1978	0.1638	0.1588	0.006353	-0.001291	0.003425	0.1692	0.054	1.900
900	350	0.2147	0.1632	0.1700	0.007414	-0.002220	0.001795	0.1205	0.059	2.378
900	400	0.2406	0.1552	0.1730	0.007441	-0.001838	-0.000169	0.1181	0.059	2.520
900	450	0.2490	0.1867	0.1676	0.012710	-0.004996	-0.000726	0.1224	0.059	2.616
900	525	0.2486	0.1836	0.1537	0.008133	-0.003767	-0.000975	0.1045	0.061	2.763
900	550	0.2178	0.1673	0.1489	0.003641	-0.003854	-0.000865	0.0900	0.063	2.696
900	600	0.2047	0.1695	0.1334	0.001916	-0.001626	-0.000129	0.0725	0.067	2.857
900	650	0.1742	0.1483	0.1193	-0.000665	-0.001988	-0.000675	0.0600	0.070	2.725
900	700	0.1524	0.1526	0.1209	-0.002188	-0.001762	-0.001220	0.0546	0.072	2.739
900	750	0.1457	0.1612	0.1265	-0.004776	-0.001629	-0.001808	0.0626	0.069	2.602
900	800	0.1526	0.1568	0.1380	-0.007288	-0.001876	-0.002717	0.3360	0.046	1.155
900	850	0.1597	0.1703	0.1402	-0.008006	-0.002563	-0.005226	0.1180	0.059	2.052
1000	50	0.1053	0.1031	0.0988	0.000311	-0.001627	0.001062	0.0121	0.105	4.177
1000	100	0.1167	0.1219	0.1024	-0.001324	-0.001742	0.000747	0.0272	0.085	3.101
1000	150	0.1076	0.1325	0.1035	-0.001118	-0.001613	0.001448	0.0318	0.082	2.897
1000	200	0.1234	0.1299	0.1157	0.000264	-0.002821	0.001536	0.2187	0.051	1.180
1000	250	0.1473	0.1399	0.1300	0.000832	-0.002371	0.001534	0.4315	0.043	0.950
1000	300	0.1721	0.1561	0.1466	0.002849	-0.004889	0.001719	0.1885	0.053	1.638
1000	350	0.1871	0.1560	0.1525	0.005831	-0.006082	0.002287	0.1471	0.056	1.939
1000	400	0.2018	0.1561	0.1562	0.006095	-0.005916	0.001674	0.1358	0.057	2.101
1000	650	0.1740	0.1474	0.1230	-0.004616	-0.000948	-0.000119	0.0400	0.078	3.354
1000	700	0.1548	0.1563	0.1281	-0.006505	0.000095	0.000076	0.0412	0.077	3.245
1000	750	0.1329	0.1523	0.1317	-0.005327	-0.000199	-0.000817	0.0313	0.082	3.531
1000	800	0.1474	0.1656	0.1498	-0.008273	-0.001825	-0.004119	0.0574	0.071	2.890
1000	850	0.1548	0.1664	0.1393	-0.007621	-0.000782	-0.003080	0.0967	0.062	2.219

A2.1.12 Processed turbulence data for $S = 5.06\%$, $Q = 31.2$ L/s, $z = 150$ mm

x (mm)	y (mm)	$\sqrt{u'^2}$ (m/s)	$\sqrt{v'^2}$ (m/s)	$\sqrt{w'^2}$ (m/s)	$-\overline{u'v'}$ (m ² /s ²)	$-\overline{u'w'}$ (m ² /s ²)	$-\overline{v'w'}$ (m ² /s ²)	ε (m ² /s ³)	λ_g (mm)	η (mm)
100	50	0.09	0.06	0.09	0.000011	0.000558	-0.000558	0.008	4.030	0.115
100	100	0.08	0.07	0.09	0.000784	0.000618	-0.000119	0.006	4.720	0.124
100	150	0.09	0.07	0.09	0.001053	0.000399	0.000368	0.013	3.430	0.103
100	200	0.09	0.08	0.09	0.001123	0.000293	0.000569	0.010	3.748	0.109
100	250	0.09	0.08	0.09	0.000478	0.000520	0.000733	0.010	3.642	0.109
100	300	0.08	0.08	0.08	0.000571	0.000097	0.000513	0.011	3.359	0.107
100	350	0.07	0.08	0.08	0.000532	0.000300	0.000295	0.015	2.823	0.099
100	400	0.07	0.08	0.08	0.000487	0.000025	0.000276	0.020	2.330	0.092
100	450	0.08	0.10	0.08	0.001699	0.000082	0.000247	0.079	1.370	0.065
100	500	0.10	0.12	0.10	0.002253	0.000976	-0.000486	0.036	2.467	0.079
100	550	0.15	0.22	0.11	0.016820	0.001378	-0.001892	0.047	3.467	0.075
100	600	0.14	0.18	0.16	-0.000399	-0.001396	-0.005261	0.034	3.984	0.081
100	650	0.19	0.14	0.16	-0.011558	-0.003484	-0.003348	0.040	3.613	0.077
200	50	0.12	0.07	0.10	0.001465	0.002117	-0.000352	0.012	4.102	0.104
200	100	0.12	0.08	0.09	0.001818	0.001637	-0.000148	0.014	3.810	0.101
200	150	0.11	0.09	0.10	0.001903	0.000332	0.000277	0.010	4.473	0.111
200	200	0.10	0.09	0.09	0.001547	-0.000017	0.000298	0.014	3.591	0.101
200	250	0.10	0.09	0.09	0.001237	0.000291	0.000155	0.015	3.493	0.099
200	300	0.10	0.10	0.10	0.001419	0.000141	0.000330	0.029	2.590	0.084
200	350	0.10	0.10	0.10	0.002021	-0.000056	-0.000094	0.072	1.675	0.067
200	400	0.12	0.13	0.10	0.005611	0.000941	-0.000478	0.043	2.568	0.076
200	450	0.16	0.18	0.13	0.012544	0.003155	-0.001520	0.042	3.424	0.076
200	500	0.21	0.27	0.15	0.031643	0.002152	-0.001869	0.069	3.658	0.068
200	550	0.21	0.25	0.14	0.027031	0.000928	-0.004555	0.070	3.471	0.067
200	600	0.31	0.14	0.13	-0.001378	-0.006920	-0.002844	0.094	3.082	0.063
200	650	0.32	0.14	0.15	-0.005732	0.001876	-0.000363	0.455	1.436	0.042
200	700	0.09	0.08	0.11	-0.000221	-0.000771	0.000703	0.022	2.883	0.090
200	750	0.09	0.07	0.09	-0.001009	-0.000447	-0.000065	0.010	3.777	0.110
200	800	0.10	0.07	0.09	-0.001704	-0.000135	-0.000041	0.010	3.822	0.108
200	850	0.10	0.07	0.09	-0.000862	-0.000335	-0.000509	0.009	3.928	0.112
300	50	0.14	0.07	0.10	0.001881	0.001974	0.000252	0.011	4.445	0.106
300	100	0.13	0.09	0.09	0.003045	0.000737	0.000628	0.012	4.384	0.105
300	150	0.12	0.10	0.10	0.002891	0.001144	0.000377	0.013	4.265	0.103
300	200	0.12	0.10	0.10	0.002021	0.000677	0.000138	0.017	3.654	0.096
300	250	0.12	0.11	0.10	0.002666	-0.000512	0.000225	0.022	3.258	0.090
300	300	0.14	0.13	0.11	0.006511	-0.000417	-0.000242	0.134	1.578	0.057
300	350	0.14	0.16	0.12	0.010045	-0.000673	-0.000332	0.066	2.457	0.068
300	400	0.19	0.20	0.14	0.019953	0.002004	-0.001009	0.062	3.242	0.069
300	450	0.22	0.24	0.15	0.030491	0.003793	-0.001020	0.069	3.585	0.068
300	500	0.24	0.25	0.15	0.030834	0.001049	-0.002468	0.083	3.398	0.065
300	550	0.25	0.18	0.14	0.007294	-0.002566	-0.003407	0.113	2.584	0.060

A2.1.12 Processed turbulence data for $S = 5.06\%$, $Q = 31.2\text{L/s}$, $z = 150\text{mm}$ (cont'd)

x (mm)	y (mm)	$\sqrt{u'^2}$ (m/s)	$\sqrt{v'^2}$ (m/s)	$\sqrt{w'^2}$ (m/s)	$-\overline{u'v'}$ (m ² /s ²)	$-\overline{u'w'}$ (m ² /s ²)	$-\overline{v'w'}$ (m ² /s ²)	ε (m ² /s ³)	λ_g (mm)	η (mm)
300	600	0.32	0.14	0.16	-0.009532	-0.001225	-0.001913	0.194	2.229	0.052
300	650	0.21	0.12	0.14	-0.006100	0.005812	0.000935	0.183	1.700	0.053
300	700	0.11	0.11	0.11	-0.001490	-0.000702	0.001531	0.054	2.125	0.072
300	750	0.10	0.09	0.10	-0.001637	-0.000526	0.000194	0.020	3.109	0.092
300	800	0.10	0.08	0.09	-0.001975	-0.000301	0.000085	0.010	4.023	0.109
300	850	0.11	0.08	0.09	-0.001701	-0.000979	-0.000613	0.013	3.728	0.103
400	50	0.14	0.08	0.10	0.001156	0.001866	0.000584	0.012	4.393	0.105
400	100	0.15	0.10	0.11	0.003334	0.001089	0.001628	0.020	3.837	0.092
400	150	0.13	0.11	0.11	0.002812	-0.000476	0.000959	0.019	3.891	0.093
400	200	0.16	0.14	0.12	0.008685	-0.000450	0.000835	0.035	3.351	0.080
400	250	0.14	0.13	0.12	0.006319	-0.001342	0.000832	0.060	2.431	0.070
400	300	0.16	0.14	0.13	0.009620	-0.000973	-0.000134	0.060	2.643	0.070
400	350	0.20	0.19	0.14	0.021699	-0.000268	-0.000538	0.069	3.017	0.068
400	400	0.23	0.22	0.15	0.029055	0.002431	-0.000023	0.068	3.520	0.068
400	450	0.24	0.24	0.14	0.031109	0.001713	0.001047	0.075	3.482	0.066
400	500	0.24	0.23	0.14	0.024613	0.002761	-0.000419	0.089	3.136	0.063
400	550	0.28	0.17	0.14	-0.008317	0.001336	-0.001599	0.128	2.575	0.058
400	600	0.28	0.14	0.13	-0.015972	0.002143	0.000148	0.141	2.360	0.057
400	650	0.18	0.13	0.13	-0.008435	0.000537	0.000715	0.087	2.266	0.064
400	700	0.13	0.12	0.12	-0.002933	-0.002594	0.000297	0.279	1.011	0.048
400	750	0.13	0.10	0.11	-0.003239	-0.001994	0.000576	0.037	2.685	0.079
400	800	0.14	0.09	0.10	-0.003424	-0.001775	0.000266	0.028	2.978	0.085
400	850	0.12	0.09	0.09	-0.002553	-0.001028	0.000794	0.016	3.582	0.098
500	50	0.16	0.10	0.12	0.002596	-0.000580	0.001603	0.016	4.406	0.097
500	100	0.15	0.11	0.11	0.003775	0.000277	0.001331	0.020	4.009	0.093
500	150	0.15	0.13	0.12	0.004038	0.000881	0.001048	0.023	3.920	0.089
500	200	0.16	0.13	0.14	0.006514	0.000199	0.000373	0.035	3.465	0.080
500	250	0.18	0.16	0.14	0.012328	-0.001004	-0.000270	0.156	1.799	0.055
500	300	0.20	0.16	0.15	0.014621	-0.002014	-0.000449	0.206	1.690	0.051
500	350	0.24	0.19	0.15	0.026602	0.000983	0.000235	0.083	3.064	0.065
500	400	0.26	0.21	0.15	0.030938	0.002266	0.001440	0.082	3.332	0.065
500	450	0.25	0.22	0.14	0.029306	0.002676	0.001092	0.077	3.420	0.066
500	500	0.26	0.21	0.13	0.012128	0.001478	-0.000557	0.102	2.850	0.061
500	550	0.24	0.18	0.13	-0.007689	0.000301	-0.001802	0.088	2.906	0.064
500	600	0.24	0.16	0.13	-0.014916	0.000685	0.000056	0.077	2.939	0.066
500	650	0.18	0.14	0.14	-0.008654	-0.003401	0.000179	0.064	2.718	0.069
500	700	0.15	0.13	0.14	-0.003533	-0.003049	-0.000628	0.359	1.036	0.045
500	750	0.15	0.12	0.14	-0.004984	-0.003607	0.000132	0.050	2.733	0.073
500	800	0.15	0.11	0.12	-0.004210	-0.003141	0.000379	0.025	3.642	0.087
500	850	0.14	0.11	0.10	-0.003424	-0.002177	0.000172	0.020	3.710	0.092

A2.1.12 Processed turbulence data for $S = 5.06\%$, $Q = 31.2\text{L/s}$, $z = 150\text{mm}$ (cont'd)

x (mm)	y (mm)	$\sqrt{u'^2}$ (m/s)	$\sqrt{v'^2}$ (m/s)	$\sqrt{w'^2}$ (m/s)	$-\overline{u'v'}$ (m ² /s ²)	$-\overline{u'w'}$ (m ² /s ²)	$-\overline{v'w'}$ (m ² /s ²)	ε (m ² /s ³)	λ_g (mm)	η (mm)
600	50	0.17	0.10	0.12	0.002944	0.000167	0.001533	0.017	4.499	0.096
600	100	0.17	0.13	0.12	0.007661	-0.000331	0.002502	0.027	3.820	0.085
600	150	0.18	0.15	0.14	0.010042	0.000420	0.002602	0.036	3.666	0.080
600	200	0.17	0.15	0.15	0.007920	0.001519	0.000198	0.046	3.277	0.075
600	250	0.19	0.16	0.15	0.012458	0.001396	-0.000920	0.360	1.267	0.045
600	300	0.23	0.18	0.17	0.018177	0.002071	0.000190	0.166	2.112	0.054
600	350	0.24	0.18	0.16	0.020467	0.002745	0.000136	0.091	2.952	0.063
600	400	0.26	0.20	0.16	0.026262	0.001572	0.001689	0.085	3.237	0.064
600	450	0.26	0.20	0.14	0.021031	0.001338	0.001120	0.084	3.187	0.064
600	500	0.25	0.19	0.13	0.009923	0.001842	-0.000930	0.092	2.893	0.063
600	550	0.23	0.18	0.12	-0.003885	0.000251	-0.001304	0.082	2.866	0.065
600	600	0.21	0.17	0.13	-0.012111	-0.000886	0.000026	0.058	3.232	0.071
600	650	0.17	0.16	0.14	-0.006656	-0.002315	-0.000269	0.043	3.387	0.076
600	700	0.15	0.14	0.15	-0.004603	-0.002350	-0.000617	0.110	1.951	0.060
600	750	0.15	0.13	0.14	-0.004268	-0.002282	-0.000521	0.056	2.724	0.071
600	800	0.15	0.13	0.13	-0.004129	-0.002033	0.000445	0.032	3.445	0.082
600	850	0.14	0.12	0.12	-0.003723	-0.001292	0.000476	0.020	3.928	0.092
700	50	0.16	0.10	0.12	0.003429	0.000046	0.001640	0.019	4.290	0.094
700	100	0.16	0.12	0.12	0.005508	-0.000666	0.002980	0.022	4.138	0.090
700	150	0.17	0.15	0.15	0.007088	0.002366	0.002586	0.045	3.334	0.075
700	200	0.18	0.14	0.15	0.005502	0.002465	0.000791	0.061	2.865	0.070
700	250	0.20	0.15	0.16	0.007297	0.003654	-0.000653	0.090	2.567	0.063
700	300	0.23	0.16	0.17	0.013467	0.001543	-0.000338	0.154	2.177	0.055
700	350	0.25	0.17	0.17	0.016501	0.003171	0.000057	0.105	2.811	0.061
700	400	0.26	0.17	0.16	0.016745	0.002631	0.000777	0.083	3.166	0.065
700	450	0.27	0.17	0.14	0.016803	0.002080	0.000500	0.096	2.937	0.062
700	500	0.25	0.17	0.13	0.011302	0.001693	-0.000145	0.087	2.921	0.064
700	550	0.22	0.18	0.12	0.002264	-0.000380	-0.001422	0.073	2.917	0.067
700	600	0.21	0.17	0.13	-0.004162	-0.002577	-0.001177	0.056	3.279	0.071
700	650	0.17	0.17	0.14	-0.004902	-0.002813	-0.001252	0.048	3.281	0.074
700	700	0.16	0.16	0.15	-0.005712	-0.002824	-0.001090	0.075	2.520	0.066
700	750	0.15	0.15	0.15	-0.004891	-0.001032	-0.000523	0.090	2.233	0.063
700	800	0.14	0.14	0.14	-0.005725	-0.002798	-0.000690	0.031	3.600	0.083
700	850	0.13	0.15	0.13	-0.004797	-0.002513	-0.000466	0.022	4.075	0.090
800	50	0.14	0.10	0.11	0.001607	0.001301	0.001038	0.013	4.565	0.102
800	100	0.15	0.13	0.13	0.003669	0.000368	0.001918	0.024	3.821	0.088
800	150	0.13	0.13	0.13	0.003194	-0.000028	0.001471	0.026	3.675	0.086
800	200	0.17	0.15	0.16	0.004448	0.001028	0.001954	0.127	2.026	0.058
800	250	0.17	0.15	0.16	0.004505	0.001664	0.001255	0.130	1.982	0.058
800	300	0.21	0.16	0.18	0.007125	0.004488	0.000227	0.146	2.165	0.056
800	350	0.24	0.16	0.18	0.007633	0.004107	-0.000540	0.111	2.601	0.060

A2.1.12 Processed turbulence data for $S = 5.06\%$, $Q = 31.2\text{L/s}$, $z = 150\text{mm}$ (cont'd)

x (mm)	y (mm)	$\sqrt{u'^2}$ (m/s)	$\sqrt{v'^2}$ (m/s)	$\sqrt{w'^2}$ (m/s)	$-\overline{u'v'}$ (m ² /s ²)	$-\overline{u'w'}$ (m ² /s ²)	$-\overline{v'w'}$ (m ² /s ²)	ε (m ² /s ³)	λ_g (mm)	η (mm)
800	400	0.26	0.16	0.17	0.009182	0.004438	0.000153	0.096	2.922	0.062
800	450	0.26	0.16	0.16	0.012398	0.001532	-0.000753	0.111	2.709	0.060
800	500	0.26	0.16	0.14	0.007168	0.002085	-0.000174	0.099	2.753	0.062
800	550	0.26	0.18	0.13	0.016724	-0.004581	0.002699	0.103	2.731	0.061
800	600	0.20	0.16	0.13	0.004069	-0.001914	-0.000991	0.072	2.787	0.067
800	650	0.19	0.18	0.13	0.003816	-0.003449	0.000106	0.068	2.923	0.068
800	700	0.16	0.16	0.14	-0.003354	-0.002445	-0.001505	0.061	2.783	0.070
800	750	0.14	0.15	0.14	-0.003713	-0.001388	-0.001010	0.216	1.393	0.051
800	800	0.15	0.16	0.14	-0.007343	-0.002795	-0.001055	0.076	2.457	0.066
800	850	0.14	0.15	0.14	-0.005929	-0.001877	-0.000289	0.032	3.591	0.082
900	50	0.18	0.10	0.11	0.000541	0.002687	0.001047	0.020	4.181	0.092
900	100	0.14	0.13	0.12	-0.000753	0.001867	0.002225	0.034	3.114	0.080
900	150	0.12	0.14	0.13	-0.000545	0.000278	0.001208	0.036	3.066	0.080
900	200	0.14	0.15	0.14	0.000665	-0.000485	-0.000485	0.151	1.685	0.056
900	250	0.17	0.16	0.16	0.002847	-0.000147	-0.000935	0.174	1.723	0.054
900	300	0.19	0.16	0.17	0.003697	-0.000547	0.000152	0.111	2.333	0.060
900	350	0.21	0.16	0.17	0.003751	0.001152	-0.000334	0.108	2.476	0.060
900	400	0.23	0.17	0.17	0.006234	0.000369	-0.000299	0.095	2.799	0.062
900	450	0.24	0.17	0.17	0.006060	0.001403	-0.000360	0.099	2.841	0.062
900	525	0.25	0.18	0.15	0.010232	-0.001521	0.000669	0.105	2.756	0.061
900	550	0.24	0.18	0.15	0.003656	0.000331	-0.001778	0.106	2.624	0.061
900	600	0.21	0.17	0.13	0.004225	-0.000257	0.000369	0.084	2.710	0.064
900	650	0.18	0.16	0.12	0.000880	-0.000516	-0.000329	0.072	2.563	0.067
900	700	0.16	0.16	0.12	-0.002236	-0.001465	-0.001286	0.060	2.723	0.070
900	750	0.14	0.16	0.14	-0.004817	-0.002086	-0.001549	0.071	2.440	0.067
900	800	0.15	0.16	0.14	-0.006527	-0.001750	-0.002023	0.605	0.859	0.039
900	850	0.15	0.16	0.14	-0.008066	-0.002577	-0.001519	0.067	2.594	0.068
1000	50	0.12	0.10	0.10	-0.001140	0.000684	0.000623	0.023	3.248	0.089
1000	100	0.11	0.11	0.11	-0.002463	-0.000359	0.000340	0.041	2.440	0.077
1000	150	0.11	0.13	0.12	-0.002048	-0.000369	0.001459	0.166	1.314	0.054
1000	200	0.13	0.15	0.13	-0.002305	-0.000594	0.001025	0.227	1.269	0.050
1000	250	0.15	0.16	0.14	-0.000070	-0.000388	0.001002	0.121	1.924	0.059
1000	300	0.17	0.16	0.16	-0.000175	-0.001260	0.000095	0.105	2.213	0.061
1000	350	0.19	0.17	0.17	0.001642	-0.000054	0.001514	0.094	2.549	0.063
1000	400	0.21	0.16	0.17	0.006559	-0.001154	0.001174	0.104	2.525	0.061
1000	650	0.18	0.16	0.13	-0.004035	-0.000199	-0.000144	0.041	3.502	0.077
1000	700	0.15	0.16	0.12	-0.005262	-0.000426	-0.000892	0.039	3.255	0.078
1000	750	0.13	0.15	0.12	-0.006151	-0.001388	-0.001426	0.037	3.172	0.079
1000	800	0.15	0.17	0.14	-0.009684	-0.002657	-0.001920	0.062	2.724	0.069
1000	850	0.16	0.16	0.14	-0.008372	-0.000518	-0.001186	0.127	1.946	0.058

A2.1.13 Processed turbulence data for $S = 5.06\%$, $Q = 52 \text{ L/s}$, $z = 10 \text{ mm}$

x (mm)	y (mm)	$\sqrt{u'^2}$ (m/s)	$\sqrt{v'^2}$ (m/s)	$\sqrt{w'^2}$ (m/s)	$-\overline{u'v'}$ (m ² /s ²)	$-\overline{u'w'}$ (m ² /s ²)	$-\overline{v'w'}$ (m ² /s ²)	ε (m ² /s ³)	λ_g (mm)	η (mm)
100	50	0.134	0.085	0.040	-0.000336	-0.000126	0.000084	0.041	2.087	0.077
100	100	0.160	0.100	0.041	0.001342	0.000245	-0.000182	0.070	1.888	0.067
100	150	0.169	0.102	0.042	0.001332	0.000400	-0.000148	0.113	1.551	0.060
100	200	0.176	0.102	0.041	0.001108	0.000791	-0.000125	0.120	1.550	0.059
100	250	0.150	0.101	0.040	-0.000186	0.000517	-0.000203	0.098	1.530	0.062
100	300	0.142	0.105	0.038	0.000291	0.000414	-0.000108	0.148	1.213	0.056
100	350	0.128	0.109	0.038	0.000627	-0.000032	-0.000299	0.055	1.895	0.071
100	400	0.108	0.128	0.035	0.000693	-0.000041	0.000070	0.028	2.660	0.085
100	450	0.104	0.142	0.034	0.001376	-0.000068	0.000079	0.034	2.517	0.090
100	500	0.110	0.226	0.042	0.008456	-0.000068	-0.000602	0.029	3.867	0.084
100	550	0.162	0.298	0.059	0.025270	-0.001769	0.005526	0.042	4.358	0.077
100	600	0.225	0.215	0.074	-0.030239	0.001454	-0.001751	0.031	4.737	0.080
100	650	0.205	0.150	0.063	0.004797	-0.000048	-0.002736	0.013	6.023	0.103
200	50	0.160	0.113	0.038	0.003116	-0.000271	0.000339	0.030	2.970	0.083
200	100	0.190	0.134	0.041	0.006053	0.000058	0.000399	0.026	3.779	0.086
200	150	0.200	0.145	0.044	0.008566	0.000298	0.000091	0.054	2.799	0.072
200	200	0.200	0.147	0.043	0.006198	0.000224	0.000229	0.134	1.781	0.057
200	250	0.185	0.151	0.045	0.004968	0.000201	0.000277	0.253	1.250	0.049
200	300	0.173	0.156	0.045	0.005310	-0.000248	0.000276	0.134	1.676	0.057
200	350	0.153	0.172	0.044	0.007800	-0.000401	0.000287	0.056	2.561	0.071
200	400	0.153	0.191	0.040	0.012584	-0.000112	0.000113	0.024	4.184	0.088
200	450	0.162	0.270	0.054	0.021743	-0.000722	0.000620	0.025	5.279	0.088
200	500	0.184	0.254	0.062	0.018682	-0.000729	0.000726	0.053	3.597	0.072
200	550	0.234	0.148	0.052	0.006195	0.000139	-0.001548	0.062	2.913	0.069
200	600	0.282	0.115	0.054	0.010393	0.002110	-0.001235	0.126	2.256	0.058
200	650	0.125	0.056	0.033	0.000191	0.000569	-0.000020	0.039	1.862	0.078
200	700	0.122	0.076	0.038	0.000286	0.000674	0.000003	0.014	3.257	0.101
200	750	0.137	0.076	0.036	-0.002145	0.000771	0.000110	0.009	4.461	0.114
200	800	0.131	0.070	0.035	-0.002003	0.000297	-0.000049	0.007	4.780	0.121
200	850	0.128	0.072	0.037	-0.002676	0.000265	-0.000140	0.010	3.831	0.108
300	50	0.180	0.118	0.042	0.005060	-0.000781	0.000784	0.02	4.035	0.092
300	100	0.216	0.152	0.045	0.014292	-0.000124	0.000666	0.03	4.156	0.085
300	150	0.230	0.173	0.043	0.015822	0.000009	0.000557	0.05	3.234	0.072
300	200	0.218	0.174	0.047	0.013740	-0.000255	0.000680	0.15	1.870	0.055
300	250	0.211	0.190	0.049	0.016469	-0.000209	0.000177	0.23	1.543	0.050
300	300	0.204	0.178	0.048	0.016246	-0.000694	0.000516	0.06	2.856	0.069
300	350	0.230	0.281	0.054	0.036062	-0.001060	0.001351	0.06	3.876	0.070
300	400	0.178	0.281	0.066	0.028041	-0.000557	0.000647	0.026	5.425	0.086
300	450	0.188	0.222	0.062	0.016518	-0.000282	-0.000274	0.07	3.018	0.069
300	500	0.239	0.183	0.068	0.009574	0.001013	-0.001904	0.13	2.179	0.057
300	550	0.237	0.117	0.047	0.004224	0.001137	-0.000928	0.05	3.223	0.075

A2.1.13 Processed turbulence data for $S = 5.06\%$, $Q = 52\text{L/s}$, $z = 10\text{mm}$ (cont'd)

x (mm)	y (mm)	$\sqrt{u'^2}$ (m/s)	$\sqrt{v'^2}$ (m/s)	$\sqrt{w'^2}$ (m/s)	$-\overline{u'v'}$ (m ² /s ²)	$-\overline{u'w'}$ (m ² /s ²)	$-\overline{v'w'}$ (m ² /s ²)	ε (m ² /s ³)	λ_g (mm)	η (mm)
300	600	0.189	0.105	0.046	-0.002197	0.000628	-0.000134	0.04	2.913	0.078
300	650	0.149	0.082	0.038	-0.003260	-0.000349	-0.000104	0.03	2.565	0.083
300	700	0.160	0.102	0.035	-0.004542	-0.000529	-0.000327	0.02	3.771	0.095
300	750	0.165	0.095	0.034	-0.004524	-0.000723	-0.000233	0.02	3.260	0.088
300	800	0.179	0.094	0.037	-0.005409	-0.000359	-0.000142	0.08	1.878	0.065
300	850	0.191	0.086	0.038	-0.006120	-0.000553	-0.000170	0.12	1.612	0.059
400	50	0.178	0.123	0.045	0.003847	-0.000639	0.001349	0.016	4.580	0.098
400	100	0.227	0.170	0.048	0.016144	-0.001394	0.001714	0.031	4.257	0.083
400	150	0.257	0.193	0.051	0.027488	-0.000844	0.001762	0.075	3.067	0.066
400	200	0.267	0.204	0.054	0.027882	-0.001444	0.001253	0.297	1.615	0.047
400	250	0.235	0.222	0.052	0.027933	-0.000786	0.001219	0.044	4.030	0.076
400	300	0.230	0.213	0.058	0.028310	-0.001270	0.001776	0.061	3.354	0.070
400	350	0.253	0.249	0.068	0.035999	-0.001454	0.002395	0.075	3.420	0.066
400	400	0.221	0.226	0.063	0.024688	0.000049	0.001850	0.084	2.890	0.064
400	450	0.215	0.163	0.046	0.011680	0.000823	0.000845	0.064	2.806	0.069
400	500	0.261	0.160	0.060	0.004038	0.001881	0.000311	0.113	2.407	0.060
400	550	0.295	0.143	0.053	-0.007091	0.002279	0.000055	0.110	2.591	0.060
400	600	0.219	0.140	0.050	-0.010180	0.000331	0.000361	0.056	2.905	0.071
400	650	0.172	0.138	0.042	-0.008842	-0.000045	0.000174	0.039	2.940	0.078
400	700	0.172	0.134	0.041	-0.007946	-0.000577	-0.000009	0.040	2.887	0.078
400	750	0.175	0.128	0.041	-0.006326	-0.000439	0.000034	0.060	2.329	0.070
400	800	0.174	0.123	0.042	-0.005984	-0.000016	0.000159	0.034	3.046	0.081
400	850	0.178	0.115	0.042	-0.006533	0.000290	0.000000	0.021	3.830	0.091
500	50	0.180	0.118	0.048	0.003176	-0.000749	0.001404	0.013	5.028	0.103
500	100	0.229	0.174	0.049	0.015377	-0.001161	0.001720	0.025	4.774	0.087
500	150	0.263	0.192	0.055	0.025950	-0.000948	0.001233	0.052	3.747	0.073
500	200	0.293	0.188	0.056	0.030215	-0.001303	0.001321	0.246	1.840	0.049
500	250	0.268	0.201	0.057	0.030669	-0.001961	0.001877	0.142	2.335	0.056
500	300	0.231	0.161	0.062	0.021090	-0.001640	0.001228	0.032	4.173	0.082
500	350	0.228	0.200	0.062	0.025179	-0.000927	0.001477	0.050	3.565	0.073
500	400	0.213	0.194	0.058	0.016565	0.000371	0.001198	0.068	2.927	0.068
500	450	0.215	0.176	0.057	0.008408	0.000955	0.000518	0.073	2.717	0.067
500	500	0.249	0.170	0.058	0.000474	0.001249	-0.000003	0.096	2.566	0.062
500	550	0.263	0.154	0.044	-0.010496	0.001141	0.000027	0.059	3.282	0.070
500	600	0.215	0.159	0.040	-0.012915	0.000135	0.000410	0.045	3.300	0.075
500	650	0.188	0.168	0.044	-0.015161	-0.000273	0.000151	0.036	3.479	0.079
500	700	0.186	0.164	0.046	-0.012384	0.000130	-0.000050	0.074	2.398	0.066
500	750	0.182	0.149	0.044	-0.010474	0.000268	0.000270	0.107	1.895	0.061
500	800	0.179	0.152	0.045	-0.010668	0.000354	0.000294	0.030	3.556	0.083
500	850	0.176	0.138	0.046	-0.009310	0.000700	-0.000138	0.025	3.713	0.087

A2.1.13 Processed turbulence data for $S = 5.06\%$, $Q = 52\text{L/s}$, $z = 10\text{mm}$ (cont'd)

x (mm)	y (mm)	$\sqrt{u'^2}$ (m/s)	$\sqrt{v'^2}$ (m/s)	$\sqrt{w'^2}$ (m/s)	$-\overline{u'v'}$ (m ² /s ²)	$-\overline{u'w'}$ (m ² /s ²)	$-\overline{v'w'}$ (m ² /s ²)	ε (m ² /s ³)	λ_g (mm)	η (mm)
600	50	0.184	0.109	0.050	0.002945	-0.001160	0.001489	0.011	5.430	0.107
600	100	0.207	0.153	0.047	0.013037	-0.000814	0.001395	0.018	5.097	0.095
600	150	0.238	0.172	0.048	0.019919	-0.000512	0.001005	0.030	4.472	0.084
600	200	0.277	0.181	0.058	0.024463	-0.001174	0.001033	0.216	1.870	0.051
600	250	0.278	0.177	0.063	0.023096	-0.001460	0.001187	0.214	1.877	0.051
600	300	0.251	0.185	0.067	0.023863	-0.001346	0.001315	0.071	3.093	0.067
600	350	0.245	0.183	0.066	0.022701	-0.000634	0.001159	0.067	3.135	0.068
600	400	0.235	0.181	0.058	0.019065	0.000162	0.000656	0.070	2.946	0.067
600	450	0.261	0.182	0.055	0.012667	0.000130	0.000121	0.068	3.218	0.068
600	500	0.242	0.168	0.050	0.004000	0.000704	-0.000427	0.058	3.219	0.071
600	550	0.221	0.181	0.053	-0.005598	0.000793	-0.000052	0.025	4.725	0.087
600	600	0.225	0.190	0.045	-0.014846	0.000251	-0.000104	0.040	3.873	0.078
600	650	0.212	0.199	0.045	-0.014136	-0.000033	-0.000257	0.036	4.007	0.079
600	700	0.212	0.196	0.046	-0.015943	-0.000444	-0.000426	0.061	3.067	0.070
600	750	0.208	0.189	0.046	-0.014068	-0.000047	-0.000665	0.214	1.595	0.051
600	800	0.195	0.178	0.048	-0.013651	0.000375	-0.000315	0.059	2.865	0.070
600	850	0.171	0.162	0.056	-0.009004	0.001232	-0.000282	0.030	3.628	0.083
700	50	0.216	0.113	0.048	-0.004701	-0.001708	0.001179	0.010	6.448	0.110
700	100	0.186	0.140	0.043	0.010317	-0.000391	0.001349	0.010	6.026	0.109
700	150	0.195	0.148	0.041	0.011085	0.000058	0.000710	0.016	5.073	0.097
700	200	0.254	0.151	0.051	0.014850	0.000406	0.000490	0.041	3.814	0.077
700	250	0.269	0.158	0.055	0.012452	0.000078	0.000440	0.327	1.433	0.046
700	300	0.273	0.157	0.060	0.011815	0.000033	0.000993	0.176	1.980	0.054
700	350	0.254	0.160	0.066	0.016684	-0.000113	0.001012	0.054	3.421	0.072
700	400	0.240	0.170	0.062	0.016132	-0.000453	0.000766	0.039	3.946	0.078
700	450	0.263	0.167	0.057	0.019022	-0.000304	0.000278	0.076	2.975	0.066
700	500	0.248	0.177	0.058	0.014523	0.000666	-0.000301	0.066	3.118	0.068
700	550	0.232	0.177	0.049	0.009833	0.000629	-0.000601	0.052	3.353	0.072
700	600	0.213	0.197	0.046	0.004596	0.000732	-0.000969	0.043	3.659	0.076
700	650	0.215	0.209	0.041	-0.001787	0.000179	-0.000868	0.053	3.406	0.072
700	700	0.209	0.220	0.042	-0.006039	0.000253	-0.001007	0.064	3.127	0.069
700	750	0.209	0.231	0.049	-0.011345	0.000374	-0.001865	0.060	3.329	0.070
700	800	0.199	0.214	0.050	-0.015442	0.000454	-0.001379	0.069	2.922	0.068
700	850	0.159	0.191	0.062	-0.009910	0.001137	-0.000700	0.035	3.574	0.080
800	50	0.149	0.108	0.052	-0.001122	-0.000815	0.001335	0.008	5.402	0.114
800	100	0.164	0.134	0.045	0.004631	-0.000201	0.001357	0.012	5.084	0.104
800	150	0.198	0.142	0.044	0.006695	0.000234	0.001052	0.015	5.282	0.100
800	200	0.238	0.132	0.044	0.003874	0.001304	0.000798	0.025	4.498	0.087
800	250	0.272	0.134	0.052	0.002582	0.001228	0.000887	0.043	3.826	0.076
800	300	0.290	0.143	0.060	0.001045	0.002149	0.001300	0.270	1.639	0.048
800	350	0.283	0.149	0.058	0.008147	0.000906	0.001274	0.145	2.206	0.056

A2.1.13 Processed turbulence data for $S = 5.06\%$, $Q = 52\text{L/s}$, $z = 10\text{mm}$ (cont'd)

x (mm)	y (mm)	$\sqrt{u'^2}$ (m/s)	$\sqrt{v'^2}$ (m/s)	$\sqrt{w'^2}$ (m/s)	$-\overline{u'v'}$ (m ² /s ²)	$-\overline{u'w'}$ (m ² /s ²)	$-\overline{v'w'}$ (m ² /s ²)	ε (m ² /s ³)	λ_g (mm)	η (mm)
800	400	0.285	0.151	0.061	0.016091	0.000351	0.000476	0.127	2.379	0.058
800	450	0.316	0.148	0.064	0.012363	0.000822	0.000938	0.182	2.150	0.053
800	500	0.305	0.151	0.067	0.015477	0.002674	0.000288	0.213	1.949	0.051
800	550	0.313	0.163	0.057	0.019039	0.000810	-0.000076	0.116	2.724	0.059
800	600	0.273	0.169	0.054	0.018076	0.001215	-0.000551	0.106	2.582	0.061
800	650	0.231	0.190	0.045	0.011379	0.000643	-0.000700	0.075	2.852	0.066
800	700	0.243	0.210	0.044	0.008989	0.001073	-0.001379	0.084	2.896	0.064
800	750	0.209	0.238	0.050	-0.004270	0.000446	-0.002506	0.204	1.838	0.052
800	800	0.195	0.232	0.053	-0.013988	0.000430	-0.002238	0.198	1.791	0.052
800	850	0.190	0.215	0.063	-0.013334	0.000388	-0.000413	0.085	2.612	0.064
900	50	0.148	0.133	0.057	-0.001819	-0.000260	0.001745	0.012	4.834	0.104
900	100	0.190	0.151	0.052	-0.003039	0.000340	0.000737	0.015	5.200	0.099
900	150	0.182	0.141	0.051	-0.002830	0.000823	0.000814	0.014	5.116	0.100
900	200	0.224	0.142	0.050	-0.002157	0.000726	0.000815	0.024	4.542	0.088
900	250	0.225	0.135	0.051	-0.005983	0.000996	0.001412	0.023	4.535	0.089
900	300	0.273	0.150	0.057	-0.007444	0.000890	0.001734	0.037	4.234	0.079
900	350	0.266	0.152	0.057	-0.002820	0.000447	0.001868	0.043	3.876	0.076
900	400	0.270	0.142	0.059	0.001837	0.000304	0.001191	0.060	3.283	0.070
900	450	0.309	0.146	0.072	0.004375	-0.002496	0.001094	0.078	3.239	0.066
900	520	0.281	0.149	0.075	0.007897	-0.001473	0.001462	0.267	1.640	0.048
900	550	0.273	0.194	0.072	0.007901	-0.000286	0.002294	0.300	1.618	0.047
900	600	0.275	0.194	0.066	-0.004202	0.001110	0.000729	0.250	1.775	0.049
900	650	0.254	0.179	0.056	-0.003790	0.001296	-0.000310	0.114	2.421	0.060
900	700	0.222	0.201	0.052	-0.004577	0.000940	-0.000708	0.089	2.630	0.063
900	750	0.195	0.230	0.049	-0.008778	0.000371	-0.001242	0.128	2.209	0.058
900	800	0.172	0.217	0.056	-0.011696	0.000016	-0.001343	0.280	1.381	0.048
900	850	0.176	0.193	0.062	-0.007495	0.000311	-0.000788	0.348	1.178	0.045
1000	50	0.107	0.152	0.067	-0.002949	-0.000078	0.000963	0.014	4.306	0.101
1000	100	0.137	0.161	0.059	-0.008006	-0.000754	0.000452	0.009	6.048	0.113
1000	150	0.151	0.150	0.058	-0.006149	-0.000772	0.000552	0.030	3.322	0.084
1000	200	0.168	0.147	0.057	-0.007352	-0.000721	0.000613	0.019	4.301	0.093
1000	250	0.172	0.143	0.055	-0.007048	-0.001025	0.000730	0.017	4.536	0.095
1000	300	0.176	0.163	0.062	-0.008329	-0.000948	0.000788	0.017	4.979	0.097
1000	350	0.173	0.168	0.061	-0.007260	-0.000293	0.001110	0.016	5.033	0.097
1000	400	0.172	0.160	0.061	-0.001362	-0.000744	0.000417	0.011	6.070	0.108
1000	650	0.229	0.197	0.071	-0.011456	-0.000079	0.000629	0.074	2.957	0.067
1000	700	0.216	0.228	0.061	-0.014210	0.002018	-0.000401	0.071	3.119	0.067
1000	750	0.167	0.230	0.051	-0.013938	0.000498	-0.000461	0.047	3.438	0.074
1000	800	0.161	0.218	0.058	-0.012827	0.000254	-0.000519	0.079	2.549	0.065
1000	850	0.171	0.199	0.065	-0.010020	0.000276	-0.000778	0.148	1.821	0.056

A2.1.14 Processed turbulence data for $S = 5.06\%$, $Q = 52 \text{ L/s}$, $z = 150 \text{ mm}$

x (mm)	y (mm)	$\sqrt{u'^2}$ (m/s)	$\sqrt{v'^2}$ (m/s)	$\sqrt{w'^2}$ (m/s)	$-\overline{u'v'}$ (m ² /s ²)	$-\overline{u'w'}$ (m ² /s ²)	$-\overline{v'w'}$ (m ² /s ²)	ε (m ² /s ³)	λ_g (mm)	η (mm)
100	50	0.15	0.09	0.11	0.001300	0.002584	-0.000274	0.020	3.698	0.092
100	100	0.14	0.10	0.11	0.001160	0.001649	0.000886	0.024	3.377	0.088
100	150	0.14	0.10	0.12	0.000041	0.002672	0.001171	0.030	3.121	0.083
100	200	0.14	0.11	0.11	-0.000219	0.001720	0.001077	0.041	2.646	0.077
100	250	0.13	0.10	0.11	-0.000220	0.002884	0.000539	0.054	2.185	0.072
100	300	0.13	0.11	0.10	0.000648	0.001905	0.000452	0.060	2.067	0.070
100	350	0.12	0.10	0.10	0.000574	0.001932	-0.000514	0.117	1.413	0.059
100	400	0.10	0.09	0.10	0.000186	0.000846	0.000101	0.107	1.329	0.061
100	450	0.10	0.11	0.09	0.001053	0.000658	-0.000143	0.042	2.171	0.077
100	500	0.10	0.13	0.10	0.002306	0.000274	0.000250	0.033	2.762	0.081
100	550	0.19	0.26	0.13	0.027970	0.001359	-0.002152	0.066	3.495	0.068
100	600	0.16	0.19	0.16	-0.005661	-0.002535	-0.004576	0.041	3.837	0.077
100	650	0.23	0.16	0.18	-0.011937	-0.004477	-0.003462	0.059	3.578	0.070
200	50	0.17	0.10	0.12	0.000523	0.004258	0.001014	0.024	3.826	0.088
200	100	0.16	0.12	0.12	0.002142	0.001745	0.001967	0.029	3.618	0.084
200	150	0.16	0.13	0.13	0.003466	0.002516	0.001576	0.035	3.378	0.080
200	200	0.16	0.12	0.13	0.002793	0.003569	0.001100	0.049	2.828	0.074
200	250	0.16	0.14	0.13	0.004730	0.002007	0.000110	0.074	2.374	0.066
200	300	0.16	0.13	0.13	0.003522	0.001052	-0.000221	0.255	1.249	0.049
200	350	0.15	0.13	0.13	0.005450	0.001333	-0.000619	0.118	1.787	0.059
200	400	0.15	0.16	0.13	0.008794	0.000454	0.000259	0.030	3.733	0.083
200	450	0.17	0.20	0.14	0.016258	0.000008	-0.000017	0.044	3.677	0.075
200	500	0.23	0.29	0.16	0.041260	0.000203	0.000029	0.069	3.948	0.068
200	550	0.22	0.25	0.15	0.019616	-0.002802	-0.002473	0.075	3.439	0.066
200	600	0.38	0.14	0.16	-0.001269	-0.012119	-0.002206	0.299	2.045	0.047
200	650	0.23	0.12	0.14	-0.001761	0.002506	0.001656	0.279	1.434	0.048
200	700	0.11	0.10	0.13	-0.002336	0.001493	0.002687	0.034	2.808	0.081
200	750	0.12	0.09	0.12	-0.003162	0.001587	0.001583	0.022	3.382	0.090
200	800	0.14	0.10	0.12	-0.004385	0.001503	0.000498	0.036	2.887	0.079
200	850	0.15	0.09	0.11	-0.001774	0.001570	-0.000223	0.036	2.838	0.080
300	50	0.17	0.11	0.14	0.001256	0.003103	0.003012	0.029	3.772	0.084
300	100	0.18	0.14	0.13	0.003417	0.001788	0.003085	0.033	3.749	0.082
300	150	0.18	0.16	0.15	0.005953	0.003762	0.003339	0.044	3.442	0.076
300	200	0.19	0.16	0.15	0.008346	0.001383	0.000357	0.069	2.873	0.068
300	250	0.19	0.17	0.15	0.011309	0.001617	-0.000620	0.244	1.562	0.049
300	300	0.20	0.17	0.16	0.011950	0.001129	-0.001001	0.204	1.733	0.052
300	350	0.21	0.20	0.17	0.018067	0.001013	-0.000486	0.093	2.818	0.063
300	400	0.22	0.23	0.16	0.024145	-0.000598	0.001752	0.058	3.791	0.071
300	450	0.25	0.27	0.17	0.042382	-0.000662	0.000614	0.057	4.386	0.071
300	500	0.24	0.26	0.17	0.027444	-0.001292	-0.001868	0.080	3.544	0.065
300	550	0.34	0.19	0.16	-0.000496	-0.009975	-0.002941	0.213	2.338	0.051

A2.1.14 Processed turbulence data for $S = 5.06\%$, $Q = 52\text{L/s}$, $z = 150\text{mm}$ (cont'd)

x (mm)	y (mm)	$\sqrt{u'^2}$ (m/s)	$\sqrt{v'^2}$ (m/s)	$\sqrt{w'^2}$ (m/s)	$-\overline{u'v'}$ (m ² /s ²)	$-\overline{u'w'}$ (m ² /s ²)	$-\overline{v'w'}$ (m ² /s ²)	ε (m ² /s ³)	λ_g (mm)	η (mm)
300	600	0.35	0.14	0.17	-0.012946	0.001495	0.000690	0.208	2.369	0.051
300	650	0.17	0.13	0.15	-0.005065	0.003024	0.003650	0.169	1.637	0.054
300	700	0.13	0.12	0.13	-0.003168	0.002112	0.002861	0.100	1.812	0.062
300	750	0.14	0.11	0.13	-0.005738	0.000532	0.001854	0.046	2.662	0.075
300	800	0.14	0.11	0.12	-0.004640	-0.000724	-0.000034	0.036	2.954	0.080
300	850	0.15	0.10	0.12	-0.004319	-0.001779	-0.000817	0.029	3.281	0.084
400	50	0.19	0.13	0.16	0.001192	0.005782	0.004669	0.031	4.050	0.082
400	100	0.20	0.17	0.16	0.005387	0.003202	0.006323	0.045	3.685	0.075
400	150	0.21	0.18	0.16	0.011772	0.005895	0.003173	0.056	3.505	0.071
400	200	0.24	0.20	0.17	0.018817	0.003736	0.000495	0.144	2.411	0.056
400	250	0.22	0.19	0.18	0.015385	0.004167	-0.003271	0.738	1.022	0.037
400	300	0.24	0.20	0.18	0.022085	0.005056	-0.000424	0.260	1.841	0.049
400	350	0.25	0.22	0.19	0.025638	0.002189	0.001310	0.124	2.809	0.058
400	400	0.28	0.26	0.18	0.043202	0.000163	0.003082	0.113	3.248	0.060
400	450	0.28	0.26	0.17	0.036855	0.001461	0.001334	0.137	2.907	0.057
400	500	0.27	0.23	0.16	0.010766	0.000397	-0.000842	0.120	2.874	0.059
400	550	0.33	0.19	0.17	-0.015063	-0.001159	-0.000270	0.151	2.775	0.056
400	600	0.27	0.16	0.16	-0.018129	0.005161	0.003323	0.107	2.778	0.061
400	650	0.18	0.15	0.15	-0.008058	0.002334	0.004217	0.105	2.226	0.061
400	700	0.16	0.14	0.15	-0.006402	0.001255	0.003435	0.120	1.947	0.059
400	750	0.18	0.14	0.15	-0.008978	-0.002628	0.003194	0.095	2.273	0.063
400	800	0.17	0.13	0.13	-0.008063	-0.002105	0.002342	0.048	2.936	0.074
400	850	0.16	0.12	0.12	-0.005571	-0.003019	0.000790	0.032	3.372	0.082
500	50	0.20	0.14	0.18	0.001193	0.003404	0.006290	0.040	3.892	0.078
500	100	0.20	0.18	0.17	0.006979	0.003410	0.007690	0.049	3.745	0.074
500	150	0.23	0.20	0.19	0.014365	0.007459	0.003886	0.079	3.262	0.065
500	200	0.25	0.21	0.20	0.021169	0.009929	-0.000549	0.184	2.306	0.053
500	250	0.26	0.21	0.20	0.022861	0.010099	-0.002110	0.878	1.065	0.036
500	300	0.27	0.22	0.20	0.027400	0.006080	-0.002676	0.238	2.097	0.050
500	350	0.30	0.23	0.19	0.036501	0.001788	0.000030	0.168	2.690	0.054
500	400	0.29	0.23	0.18	0.033367	0.003645	0.000631	0.128	3.009	0.058
500	450	0.27	0.23	0.17	0.021403	0.001325	0.001310	0.125	2.862	0.058
500	500	0.28	0.22	0.16	0.004201	0.001718	-0.001296	0.129	2.784	0.058
500	550	0.29	0.19	0.16	-0.015775	0.002135	-0.000309	0.143	2.623	0.056
500	600	0.25	0.18	0.15	-0.018601	0.001489	0.002560	0.077	3.185	0.066
500	650	0.20	0.16	0.15	-0.011476	0.000030	0.003707	0.067	2.972	0.068
500	700	0.18	0.15	0.15	-0.008777	-0.003458	0.002862	0.282	1.380	0.048
500	750	0.18	0.14	0.15	-0.009289	-0.002417	0.001293	0.094	2.313	0.063
500	800	0.18	0.14	0.14	-0.008647	-0.003932	-0.000265	0.038	3.520	0.078
500	850	0.17	0.12	0.13	-0.005215	-0.003439	-0.001120	0.025	4.001	0.087

A2.1.14 Processed turbulence data for $S = 5.06\%$, $Q = 52\text{L/s}$, $z = 150\text{mm}$ (cont'd)

x (mm)	y (mm)	$\sqrt{u'^2}$ (m/s)	$\sqrt{v'^2}$ (m/s)	$\sqrt{w'^2}$ (m/s)	$-\overline{u'v'}$ (m ² /s ²)	$-\overline{u'w'}$ (m ² /s ²)	$-\overline{v'w'}$ (m ² /s ²)	ε (m ² /s ³)	λ_g (mm)	η (mm)
600	50	0.20	0.13	0.17	0.002371	-0.000241	0.005607	0.051	3.352	0.073
600	100	0.23	0.20	0.19	0.014763	0.004206	0.006826	0.113	2.745	0.060
600	150	0.22	0.19	0.18	0.011048	0.005948	0.006750	0.080	3.097	0.065
600	200	0.23	0.20	0.19	0.017610	0.008383	0.002324	0.143	2.478	0.056
600	250	0.27	0.21	0.20	0.023232	0.010150	-0.000129	0.717	1.209	0.038
600	300	0.29	0.21	0.21	0.025017	0.008548	-0.001283	0.274	2.035	0.048
600	350	0.30	0.20	0.20	0.026226	0.009295	-0.001113	0.176	2.568	0.053
600	400	0.30	0.21	0.19	0.028066	0.007796	-0.000053	0.138	2.891	0.057
600	450	0.30	0.21	0.17	0.021631	0.004794	-0.000554	0.130	2.889	0.058
600	500	0.27	0.21	0.16	0.007654	0.003078	-0.001235	0.127	2.733	0.058
600	550	0.26	0.20	0.15	-0.008091	0.001154	0.000352	0.080	3.356	0.065
600	600	0.24	0.20	0.15	-0.015776	0.001120	0.001070	0.073	3.364	0.067
600	650	0.21	0.18	0.16	-0.011186	-0.002535	0.001294	0.052	3.593	0.073
600	700	0.19	0.18	0.16	-0.008664	-0.004130	0.000036	0.160	1.980	0.055
600	750	0.19	0.18	0.16	-0.011623	-0.006392	-0.003122	0.088	2.706	0.064
600	800	0.18	0.17	0.15	-0.008234	-0.004347	-0.003120	0.043	3.625	0.076
600	850	0.17	0.15	0.15	-0.005594	-0.003945	-0.003989	0.034	3.917	0.081
700	50	0.21	0.12	0.16	0.001450	0.000324	0.005223	0.053	3.222	0.072
700	100	0.21	0.16	0.17	0.008917	0.001132	0.006243	0.083	2.798	0.065
700	150	0.21	0.18	0.17	0.010843	0.002989	0.005760	0.076	3.015	0.066
700	200	0.22	0.19	0.18	0.012284	0.007772	0.003741	0.120	2.577	0.059
700	250	0.24	0.20	0.21	0.017648	0.009387	0.000101	0.448	1.455	0.042
700	300	0.28	0.19	0.22	0.020875	0.014212	-0.001777	0.409	1.633	0.043
700	350	0.29	0.18	0.22	0.019992	0.014206	-0.001651	0.185	2.463	0.053
700	400	0.29	0.18	0.21	0.018362	0.011741	-0.002731	0.126	2.915	0.058
700	450	0.30	0.19	0.19	0.015562	0.008688	-0.002206	0.140	2.753	0.057
700	500	0.28	0.18	0.17	0.013670	0.005862	-0.002919	0.125	2.732	0.058
700	550	0.25	0.19	0.16	0.004717	0.001328	-0.003031	0.120	2.647	0.059
700	600	0.24	0.21	0.16	0.000031	0.001548	-0.002932	0.104	2.856	0.061
700	650	0.21	0.21	0.15	-0.004373	-0.001044	-0.001271	0.077	3.122	0.066
700	700	0.18	0.20	0.16	-0.007267	-0.002683	-0.004122	0.119	2.354	0.059
700	750	0.18	0.21	0.17	-0.008791	-0.002991	-0.004867	0.201	1.886	0.052
700	800	0.18	0.19	0.17	-0.010789	-0.007871	-0.006595	0.061	3.241	0.070
700	850	0.16	0.18	0.16	-0.007816	-0.003343	-0.006321	0.045	3.598	0.075
800	50	0.20	0.11	0.14	0.002552	-0.002484	0.003299	0.051	3.008	0.073
800	100	0.17	0.15	0.15	0.004077	-0.000084	0.005880	0.056	2.991	0.071
800	150	0.18	0.16	0.15	0.004508	0.000993	0.005445	0.062	2.940	0.070
800	200	0.19	0.18	0.17	0.008168	0.002553	0.004180	0.110	2.433	0.060
800	250	0.22	0.18	0.18	0.012242	0.004176	0.001406	0.430	1.317	0.043
800	300	0.24	0.19	0.19	0.015977	0.004890	0.000055	0.355	1.551	0.045
800	350	0.27	0.18	0.20	0.015184	0.007532	-0.001984	0.213	2.139	0.051

A2.1.14 Processed turbulence data for $S = 5.06\%$, $Q = 52\text{L/s}$, $z = 150\text{mm}$ (cont'd)

x (mm)	y (mm)	$\sqrt{u'^2}$ (m/s)	$\sqrt{v'^2}$ (m/s)	$\sqrt{w'^2}$ (m/s)	$-\overline{u'v'}$ (m ² /s ²)	$-\overline{u'w'}$ (m ² /s ²)	$-\overline{v'w'}$ (m ² /s ²)	ε (m ² /s ³)	λ_g (mm)	η (mm)
800	400	0.27	0.17	0.21	0.014007	0.011865	-0.004124	0.198	2.258	0.052
800	450	0.29	0.17	0.21	0.013360	0.010705	-0.005252	0.142	2.707	0.056
800	500	0.28	0.18	0.21	0.013144	0.008401	-0.005166	0.136	2.768	0.057
800	550	0.26	0.17	0.19	0.009991	0.005161	-0.004885	0.110	2.821	0.060
800	600	0.24	0.18	0.17	0.006681	0.002031	-0.004506	0.105	2.738	0.061
800	650	0.21	0.20	0.16	0.003023	0.000307	-0.002576	0.093	2.800	0.063
800	700	0.19	0.21	0.16	-0.001798	-0.001224	-0.005541	0.100	2.691	0.062
800	750	0.18	0.22	0.16	-0.009966	-0.002456	-0.004766	0.208	1.848	0.051
800	800	0.18	0.21	0.18	-0.012025	-0.005867	-0.008562	0.213	1.816	0.051
800	850	0.18	0.19	0.17	-0.011152	-0.005565	-0.007726	0.070	3.004	0.067
900	50	0.17	0.11	0.14	0.001185	-0.001949	0.002546	0.043	2.996	0.076
900	100	0.15	0.13	0.14	0.000227	0.000518	0.003383	0.054	2.696	0.072
900	150	0.15	0.14	0.15	0.001004	-0.000679	0.003259	0.067	2.568	0.068
900	200	0.19	0.17	0.15	0.004998	-0.002856	0.002711	0.243	1.545	0.049
900	250	0.19	0.18	0.17	0.007590	-0.001291	0.004721	0.427	1.259	0.043
900	300	0.21	0.19	0.17	0.009679	-0.004278	0.001509	0.480	1.242	0.042
900	350	0.24	0.18	0.18	0.011194	-0.003724	0.002084	0.367	1.476	0.045
900	400	0.27	0.18	0.19	0.012791	-0.007282	-0.000743	0.277	1.833	0.048
900	450	0.29	0.19	0.19	0.013037	-0.005367	-0.001138	0.230	2.142	0.050
900	520	0.28	0.19	0.20	0.012952	-0.003933	-0.000695	0.202	2.265	0.052
900	550	0.26	0.19	0.18	0.007001	-0.002830	-0.002881	0.137	2.588	0.057
900	600	0.24	0.18	0.17	0.003373	-0.002109	-0.001695	0.102	2.771	0.061
900	650	0.20	0.18	0.16	0.000111	-0.000491	-0.003228	0.095	2.620	0.062
900	700	0.18	0.19	0.15	-0.003965	-0.001813	-0.002844	0.090	2.640	0.063
900	750	0.17	0.20	0.16	-0.007552	-0.002829	-0.004626	0.091	2.590	0.063
900	800	0.18	0.20	0.16	-0.011876	-0.004551	-0.005356	0.256	1.595	0.049
900	850	0.18	0.19	0.16	-0.009987	-0.004478	-0.004339	0.731	0.924	0.037
1000	50	0.16	0.10	0.13	-0.003304	-0.006769	-0.000395	0.056	2.580	0.071
1000	100	0.14	0.13	0.13	-0.002797	-0.003364	-0.000223	0.082	2.066	0.065
1000	150	0.13	0.14	0.13	-0.001943	-0.002506	0.000811	0.118	1.746	0.059
1000	200	0.15	0.16	0.15	-0.001980	-0.005457	0.000787	0.270	1.291	0.048
1000	250	0.16	0.16	0.15	0.000137	-0.004018	0.001547	0.647	0.878	0.039
1000	300	0.18	0.16	0.16	0.000936	-0.006376	0.000957	0.560	1.006	0.040
1000	350	0.20	0.16	0.17	0.001830	-0.007647	0.001997	0.796	0.889	0.037
1000	400	0.22	0.16	0.18	0.004074	-0.007475	-0.000502	0.694	1.008	0.038
1000	650	0.21	0.20	0.16	-0.012000	-0.001353	-0.000348	0.049	3.879	0.074
1000	700	0.18	0.19	0.15	-0.010366	-0.000257	-0.001639	0.055	3.302	0.072
1000	750	0.16	0.19	0.15	-0.009972	-0.001653	-0.003207	0.046	3.437	0.075
1000	800	0.17	0.19	0.16	-0.010694	-0.001564	-0.003215	0.059	3.233	0.070
1000	850	0.17	0.19	0.15	-0.010153	-0.001742	-0.002938	0.087	2.636	0.064

A2.1.15 Processed turbulence data for $S = 5.06\%$, $Q = 52\text{L/s}$, $z = 300\text{mm}$

x (mm)	y (mm)	$\sqrt{u'^2}$ (m/s)	$\sqrt{v'^2}$ (m/s)	$\sqrt{w'^2}$ (m/s)	$-\overline{u'v'}$ (m ² /s ²)	$-\overline{u'w'}$ (m ² /s ²)	$-\overline{v'w'}$ (m ² /s ²)	ε (m ² /s ³)	λ_g (mm)	η (mm)
100	50	0.131	0.069	0.107	0.000969	-0.000899	-0.000360	0.016	3.756	0.0977
100	100	0.130	0.087	0.105	0.001999	-0.000098	0.000111	0.020	3.470	0.0925
100	150	0.126	0.095	0.107	0.002490	-0.000625	0.000651	0.032	2.764	0.0820
100	200	0.116	0.098	0.104	0.002343	-0.000839	0.001337	0.020	3.384	0.0924
100	250	0.119	0.101	0.105	0.002451	-0.000889	0.001162	0.045	2.311	0.0754
100	300	0.108	0.101	0.101	0.001200	-0.000409	0.000529	0.039	2.340	0.0778
100	350	0.103	0.109	0.099	0.001361	-0.000976	0.000779	0.103	1.450	0.0612
100	400	0.093	0.110	0.096	0.001942	-0.000362	0.000242	0.033	2.476	0.0816
100	450	0.099	0.129	0.107	0.003046	0.000050	-0.000877	0.017	3.918	0.0966
100	500	0.127	0.188	0.126	0.009248	0.002024	-0.001890	0.020	4.786	0.0925
100	550	0.204	0.317	0.160	0.034630	0.000674	-0.002264	0.082	3.710	0.0648
100	600	0.181	0.173	0.164	-0.008850	-0.002177	-0.002501	0.050	3.449	0.0731
100	650	0.349	0.141	0.189	0.001316	-0.005669	-0.002969	0.206	2.404	0.0515
200	50	0.163	0.080	0.116	0.001501	0.004814	-0.000445	0.023	3.680	0.0889
200	100	0.154	0.101	0.114	0.002722	0.003050	-0.000081	0.022	3.752	0.0897
200	150	0.152	0.111	0.116	0.003847	0.001524	0.000105	0.030	3.301	0.0832
200	200	0.144	0.124	0.120	0.003657	0.001251	0.000035	0.038	2.979	0.0785
200	250	0.134	0.122	0.119	0.003312	0.000355	-0.000277	0.047	2.594	0.0746
200	300	0.136	0.138	0.126	0.004278	0.000292	0.000023	0.161	1.491	0.0548
200	350	0.151	0.176	0.127	0.010341	0.001475	-0.000504	0.047	3.169	0.0746
200	400	0.163	0.204	0.143	0.014553	0.001985	-0.000960	0.037	3.981	0.0788
200	450	0.183	0.238	0.163	0.019790	0.002298	-0.000811	0.051	3.914	0.0730
200	500	0.217	0.272	0.165	0.030953	0.000979	-0.002613	0.089	3.342	0.0635
200	550	0.238	0.197	0.142	0.008855	-0.002340	-0.002428	0.085	3.017	0.0642
200	600	0.369	0.143	0.171	0.002136	-0.004738	-0.001753	0.237	2.298	0.0497
200	650	0.180	0.117	0.151	-0.002711	-0.000243	-0.000176	0.129	1.892	0.0579
200	700	0.119	0.094	0.117	-0.001248	-0.003641	-0.000332	0.043	2.387	0.0760
200	750	0.115	0.090	0.107	-0.001878	-0.001644	0.000296	0.020	3.316	0.0922
200	800	0.123	0.088	0.097	-0.002335	-0.001346	0.000416	0.017	3.590	0.0964
200	850	0.144	0.082	0.095	-0.002133	-0.001158	0.000343	0.021	3.369	0.0906
300	50	0.158	0.094	0.131	0.001595	0.006448	0.000138	0.018	4.429	0.0953
300	100	0.174	0.124	0.127	0.003892	0.005365	0.000118	0.037	3.344	0.0790
300	150	0.166	0.130	0.134	0.003770	0.003795	0.000853	0.039	3.280	0.0780
300	200	0.174	0.146	0.146	0.006498	0.002829	0.000100	0.051	3.104	0.0730
300	250	0.169	0.162	0.152	0.007917	0.001347	0.001151	0.188	1.666	0.0526
300	300	0.189	0.211	0.162	0.016033	0.000747	0.002008	0.122	2.418	0.0586
300	350	0.208	0.215	0.168	0.019903	0.003148	0.000373	0.067	3.429	0.0681
300	400	0.229	0.260	0.172	0.031796	0.000801	0.002969	0.091	3.312	0.0631
300	450	0.234	0.276	0.172	0.033600	0.000420	0.000293	0.106	3.183	0.0607
300	500	0.245	0.214	0.151	0.013786	-0.000881	-0.003091	0.107	2.844	0.0606
300	550	0.337	0.157	0.170	-0.003848	-0.004012	-0.002717	0.202	2.352	0.0517

A2.1.15 Processed turbulence data for $S = 5.06\%$, $Q = 52\text{L/s}$, $z = 300\text{mm}$ (cont'd)

x (mm)	y (mm)	$\sqrt{u'^2}$ (m/s)	$\sqrt{v'^2}$ (m/s)	$\sqrt{w'^2}$ (m/s)	$-\overline{u'v'}$ (m ² /s ²)	$-\overline{u'w'}$ (m ² /s ²)	$-\overline{v'w'}$ (m ² /s ²)	ε (m ² /s ³)	λ_g (mm)	η (mm)
300	600	0.265	0.144	0.183	-0.007921	0.005595	-0.001546	0.122	2.617	0.0587
300	650	0.158	0.092	0.158	-0.003058	-0.003244	-0.000053	0.036	3.303	0.0795
300	700	0.158	0.120	0.137	-0.003224	-0.004288	-0.000142	0.085	2.143	0.0642
300	750	0.157	0.114	0.120	-0.003680	-0.002717	0.000943	0.040	2.940	0.0774
300	800	0.152	0.108	0.108	-0.003626	-0.000782	0.001547	0.028	3.310	0.0845
300	850	0.147	0.097	0.104	-0.003331	0.000353	0.000956	0.020	3.730	0.0920
400	50	0.187	0.129	0.161	0.003911	0.007415	0.000666	0.036	3.804	0.0797
400	100	0.183	0.149	0.150	0.003656	0.005560	0.000567	0.048	3.316	0.0742
400	150	0.183	0.168	0.162	0.007178	0.006157	0.000113	0.051	3.393	0.0729
400	200	0.189	0.183	0.169	0.009589	0.005456	0.001438	0.073	2.986	0.0666
400	250	0.224	0.204	0.174	0.019888	0.005072	0.001921	0.178	2.142	0.0534
400	300	0.243	0.222	0.184	0.026118	0.002214	0.002976	0.144	2.571	0.0562
400	350	0.246	0.254	0.176	0.033463	0.002531	0.003750	0.090	3.405	0.0633
400	400	0.246	0.263	0.176	0.034508	0.001445	0.004626	0.087	3.509	0.0637
400	450	0.243	0.247	0.159	0.022355	0.001754	0.000875	0.100	3.126	0.0617
400	500	0.286	0.192	0.157	-0.000603	0.000438	-0.001259	0.147	2.558	0.0560
400	550	0.288	0.150	0.167	-0.009016	0.003992	-0.001420	0.062	3.806	0.0696
400	600	0.254	0.141	0.166	-0.009837	0.000995	-0.000998	0.094	2.823	0.0626
400	650	0.195	0.141	0.164	-0.008232	-0.005016	-0.001668	0.126	2.120	0.0581
400	700	0.176	0.135	0.148	-0.006631	-0.006460	-0.001074	0.146	1.807	0.0560
400	750	0.180	0.136	0.139	-0.008405	-0.003204	-0.000861	0.050	3.058	0.0732
400	800	0.168	0.122	0.120	-0.006046	-0.001863	0.001192	0.037	3.223	0.0790
400	850	0.150	0.107	0.116	-0.004150	0.000317	0.001921	0.024	3.633	0.0880
500	50	0.185	0.135	0.166	0.002025	0.008182	0.001499	0.053	3.170	0.0721
500	100	0.193	0.175	0.178	0.004628	0.008323	0.000946	0.088	2.752	0.0636
500	150	0.216	0.200	0.192	0.012120	0.009417	0.000418	0.175	2.179	0.0536
500	200	0.229	0.205	0.191	0.017161	0.009705	-0.001284	0.431	1.428	0.0428
500	250	0.257	0.215	0.196	0.024641	0.010588	0.000277	0.269	1.935	0.0481
500	300	0.285	0.241	0.192	0.034753	0.005602	0.002168	0.150	2.809	0.0557
500	350	0.280	0.246	0.189	0.035471	-0.000349	0.004732	0.118	3.149	0.0591
500	400	0.266	0.232	0.173	0.026199	0.001828	0.001416	0.103	3.169	0.0612
500	450	0.264	0.218	0.151	0.012372	0.001089	-0.000310	0.140	2.590	0.0566
500	500	0.307	0.177	0.152	-0.004576	-0.001709	-0.001319	0.152	2.563	0.0555
500	550	0.289	0.160	0.153	-0.010531	0.000267	-0.000950	0.086	3.222	0.0641
500	600	0.227	0.155	0.160	-0.012039	-0.003908	-0.002327	0.069	3.137	0.0676
500	650	0.200	0.150	0.164	-0.009019	-0.006822	-0.002021	0.132	2.130	0.0575
500	700	0.196	0.151	0.156	-0.009671	-0.004800	-0.001288	0.158	1.906	0.0550
500	750	0.186	0.147	0.150	-0.007641	-0.001613	0.000427	0.051	3.214	0.0729
500	800	0.172	0.140	0.134	-0.006131	-0.001146	0.000948	0.034	3.662	0.0810
500	850	0.150	0.132	0.127	-0.003944	0.000224	0.002783	0.025	3.869	0.0871

A2.1.15 Processed turbulence data for $S = 5.06\%$, $Q = 52\text{L/s}$, $z = 300\text{mm}$ (cont'd)

x (mm)	y (mm)	$\sqrt{u'^2}$ (m/s)	$\sqrt{v'^2}$ (m/s)	$\sqrt{w'^2}$ (m/s)	$\overline{-u'v'}$ (m ² /s ²)	$\overline{-u'w'}$ (m ² /s ²)	$\overline{-v'w'}$ (m ² /s ²)	ε (m ² /s ³)	λ_g (mm)	η (mm)
600	50	0.196	0.152	0.167	0.004458	0.004063	0.003133	0.180	1.826	0.0532
600	100	0.197	0.187	0.189	0.008965	0.005976	0.002906	0.167	2.094	0.0542
600	150	0.216	0.200	0.190	0.014902	0.006818	0.004098	0.424	1.392	0.0430
600	200	0.255	0.218	0.208	0.024557	0.012650	0.001734	0.661	1.256	0.0384
600	250	0.288	0.217	0.206	0.030150	0.011978	-0.000347	0.228	2.250	0.0501
600	300	0.307	0.227	0.201	0.032937	0.008604	0.001906	0.159	2.806	0.0549
600	350	0.297	0.207	0.194	0.029117	0.004092	0.002509	0.103	3.318	0.0612
600	400	0.279	0.221	0.173	0.025241	0.000544	0.001483	0.114	3.037	0.0597
600	450	0.269	0.203	0.160	0.012731	0.000849	-0.000950	0.112	2.878	0.0599
600	500	0.294	0.194	0.154	0.002571	-0.004753	-0.000560	0.113	2.962	0.0598
600	550	0.267	0.171	0.152	-0.008879	-0.001463	-0.001418	0.082	3.179	0.0648
600	600	0.227	0.161	0.149	-0.008319	-0.001675	-0.001223	0.055	3.491	0.0717
600	650	0.192	0.162	0.160	-0.008791	-0.004233	-0.001306	0.083	2.678	0.0645
600	700	0.180	0.172	0.166	-0.008000	-0.001014	-0.000213	0.261	1.517	0.0485
600	750	0.184	0.161	0.158	-0.008845	-0.000820	0.000385	0.057	3.147	0.0708
600	800	0.170	0.167	0.150	-0.007675	0.001025	0.002438	0.037	3.806	0.0792
600	850	0.157	0.156	0.154	-0.004840	0.000796	0.002633	0.035	3.734	0.0802
700	50	0.214	0.155	0.166	0.007479	-0.000116	0.002487	0.251	1.612	0.0490
700	100	0.210	0.187	0.181	0.010636	0.004161	0.003996	0.581	1.136	0.0397
700	150	0.236	0.208	0.198	0.016534	0.007749	0.002807	0.328	1.681	0.0458
700	200	0.259	0.206	0.211	0.020261	0.010764	0.002713	0.288	1.891	0.0473
700	250	0.284	0.206	0.226	0.024772	0.009718	0.002459	0.172	2.605	0.0538
700	300	0.308	0.205	0.222	0.026858	0.009662	0.001431	0.158	2.816	0.0550
700	350	0.308	0.198	0.202	0.025024	0.004998	0.002402	0.123	3.083	0.0585
700	400	0.298	0.193	0.200	0.023310	-0.002361	0.003468	0.142	2.797	0.0565
700	450	0.278	0.190	0.175	0.014147	0.001621	-0.001931	0.111	2.954	0.0601
700	500	0.257	0.192	0.162	0.006766	-0.000344	-0.002939	0.107	2.841	0.0606
700	550	0.259	0.191	0.162	-0.000600	-0.000284	-0.003921	0.098	2.984	0.0620
700	600	0.242	0.195	0.160	-0.000875	-0.006253	-0.001563	0.087	3.061	0.0637
700	650	0.207	0.186	0.164	-0.006985	-0.004343	-0.002265	0.091	2.766	0.0631
700	700	0.176	0.186	0.165	-0.007504	-0.001420	-0.001582	0.314	1.408	0.0463
700	750	0.171	0.186	0.166	-0.009283	-0.001244	-0.001732	0.082	2.734	0.0648
700	800	0.165	0.190	0.167	-0.009546	-0.000743	0.000877	0.043	3.756	0.0760
700	850	0.150	0.177	0.170	-0.006050	-0.001069	0.000285	0.029	4.343	0.0837
800	50	0.202	0.145	0.156	0.004991	0.000885	0.001674	0.224	1.604	0.0504
800	100	0.198	0.167	0.169	0.007013	0.004459	0.000860	0.265	1.557	0.0483
800	150	0.219	0.188	0.179	0.010818	0.006057	0.000803	0.176	2.096	0.0535
800	200	0.234	0.184	0.200	0.014626	0.008095	-0.001236	0.119	2.696	0.0591
800	250	0.260	0.185	0.213	0.014493	0.009937	-0.000681	0.143	2.626	0.0563
800	300	0.282	0.185	0.214	0.017953	0.005510	-0.000887	0.137	2.796	0.0570
800	350	0.293	0.173	0.208	0.017548	0.007602	-0.000945	0.126	2.916	0.0582

A2.1.15 Processed turbulence data for $S = 5.06\%$, $Q = 52\text{L/s}$, $z = 300\text{mm}$ (cont'd)

x (mm)	y (mm)	$\sqrt{u'^2}$ (m/s)	$\sqrt{v'^2}$ (m/s)	$\sqrt{w'^2}$ (m/s)	$-\overline{u'v'}$ (m ² /s ²)	$-\overline{u'w'}$ (m ² /s ²)	$-\overline{v'w'}$ (m ² /s ²)	ε (m ² /s ³)	λ_g (mm)	η (mm)
800	400	0.283	0.176	0.205	0.012584	0.005255	-0.001365	0.134	2.766	0.0573
800	450	0.304	0.156	0.198	0.015690	-0.001945	0.000608	0.121	2.944	0.0588
800	500	0.293	0.179	0.186	0.015005	0.000999	-0.001877	0.153	2.581	0.0554
800	550	0.239	0.173	0.167	0.004986	0.001612	-0.002917	0.099	2.779	0.0617
800	600	0.212	0.171	0.166	0.001390	-0.001343	-0.003954	0.086	2.820	0.0641
800	650	0.192	0.188	0.162	-0.002559	-0.004255	-0.002859	0.089	2.717	0.0634
800	700	0.175	0.186	0.164	-0.006450	-0.002694	-0.003055	0.122	2.252	0.0586
800	750	0.167	0.184	0.158	-0.009083	-0.002911	-0.003613	0.102	2.384	0.0613
800	800	0.171	0.189	0.164	-0.011405	-0.002977	-0.001169	0.098	2.511	0.0620
800	850	0.181	0.191	0.168	-0.008997	-0.002024	-0.001345	0.082	2.821	0.0647
900	50	0.182	0.129	0.144	0.002553	0.002251	0.000766	0.159	1.722	0.0549
900	100	0.184	0.155	0.151	0.003067	0.003765	-0.001397	0.284	1.379	0.0475
900	150	0.194	0.168	0.168	0.004377	0.005779	-0.000015	0.116	2.331	0.0594
900	200	0.215	0.176	0.187	0.006664	0.006437	-0.002135	0.143	2.294	0.0564
900	250	0.235	0.175	0.192	0.008309	0.008666	-0.002217	0.119	2.625	0.0590
900	300	0.256	0.180	0.207	0.013211	0.005937	-0.003567	0.125	2.741	0.0582
900	350	0.259	0.163	0.205	0.009244	0.004201	-0.002889	0.091	3.168	0.0631
900	400	0.293	0.173	0.215	0.010712	0.005096	-0.003374	0.131	2.875	0.0576
900	450	0.294	0.178	0.196	0.011320	0.006054	-0.002894	0.143	2.707	0.0563
900	520	0.278	0.197	0.184	0.011850	0.002549	-0.002359	0.173	2.410	0.0538
900	550	0.239	0.187	0.175	0.003252	0.002289	-0.003822	0.127	2.543	0.0581
900	600	0.213	0.177	0.160	0.001198	0.000613	-0.002744	0.112	2.471	0.0598
900	650	0.188	0.179	0.154	-0.001350	-0.001369	-0.003076	0.082	2.725	0.0647
900	700	0.165	0.176	0.149	-0.004100	-0.002308	-0.002979	0.074	2.703	0.0665
900	750	0.151	0.183	0.153	-0.006679	-0.002906	-0.001490	0.106	2.249	0.0607
900	800	0.168	0.199	0.163	-0.011831	-0.001981	0.000298	0.110	2.397	0.0602
900	850	0.164	0.198	0.161	-0.007819	-0.001963	0.000367	0.120	2.266	0.0589
1000	50	0.156	0.129	0.135	-0.002003	0.003236	-0.002118	0.187	1.460	0.0527
1000	100	0.146	0.141	0.143	-0.000619	0.003221	-0.002236	0.181	1.508	0.0531
1000	150	0.168	0.163	0.158	0.000973	0.003117	-0.003943	0.148	1.902	0.0559
1000	200	0.180	0.166	0.173	0.002133	0.004328	-0.002294	0.126	2.186	0.0582
1000	250	0.197	0.165	0.175	0.003357	0.004275	-0.001910	0.129	2.240	0.0578
1000	300	0.221	0.171	0.193	0.003820	0.003509	-0.002156	0.132	2.421	0.0575
1000	350	0.231	0.169	0.190	0.004727	0.002998	-0.000771	0.130	2.466	0.0577
1000	400	0.231	0.155	0.205	0.004751	0.000456	-0.002098	0.087	3.021	0.0637
1000	650	0.182	0.176	0.151	-0.006403	0.000313	-0.002030	0.046	3.554	0.0749
1000	700	0.156	0.187	0.148	-0.009060	-0.001423	-0.001963	0.043	3.567	0.0762
1000	750	0.153	0.188	0.151	-0.012054	-0.002224	-0.001709	0.050	3.311	0.0733
1000	800	0.165	0.198	0.165	-0.013483	-0.001980	-0.000386	0.072	2.949	0.0669
1000	850	0.164	0.184	0.158	-0.009458	-0.000342	0.000420	0.254	1.505	0.0488

A2.1.16 Processed turbulence data for $S = 10.52\%$, $Q = 31.2$ L/s, $z = 10$ mm

x (mm)	y (mm)	$\sqrt{u'^2}$ (m/s)	$\sqrt{v'^2}$ (m/s)	$\sqrt{w'^2}$ (m/s)	$-\overline{u'v'}$ (m ² /s ²)	$-\overline{u'w'}$ (m ² /s ²)	$-\overline{v'w'}$ (m ² /s ²)	ε (m ² /s ³)	λ_g (mm)	η (mm)
100	50	0.157	0.210	0.065	0.003255	0.000639	0.002004	0.530	0.962	0.041
100	100	0.153	0.253	0.071	-0.002916	0.000892	0.005969	0.856	0.851	0.036
100	150	0.172	0.247	0.081	-0.001074	-0.000655	0.003673	2.660	0.494	0.027
100	200	0.181	0.259	0.087	0.000366	-0.000935	0.003484	3.016	0.488	0.026
100	250	0.163	0.211	0.078	0.000659	-0.000330	0.002185	2.615	0.445	0.027
100	300	0.162	0.238	0.077	0.000821	-0.000136	0.000997	0.998	0.771	0.035
100	350	0.163	0.240	0.080	0.002092	0.000274	-0.000199	0.753	0.898	0.037
100	400	0.185	0.324	0.078	0.009873	-0.000023	0.002399	0.877	1.054	0.036
100	450	0.171	0.383	0.092	0.001216	0.000667	0.002261	0.301	2.025	0.047
100	500	0.167	0.377	0.089	0.000748	0.001411	-0.001172	0.125	3.090	0.058
100	550	0.205	0.213	0.072	-0.011299	0.001646	-0.002641	0.046	3.686	0.075
100	600	0.226	0.170	0.080	-0.012970	-0.001969	-0.005071	0.021	5.206	0.091
100	650	0.279	0.207	0.059	0.037248	0.003175	-0.003864	0.059	3.749	0.070
200	50	0.179	0.252	0.077	0.007611	0.000766	0.002349	0.360	1.375	0.045
200	100	0.158	0.235	0.073	0.001851	-0.000816	0.003640	0.314	1.352	0.046
200	150	0.151	0.202	0.069	0.003612	-0.000620	0.001348	0.196	1.531	0.052
200	200	0.151	0.189	0.066	0.006486	-0.000316	0.001114	0.143	1.717	0.056
200	250	0.151	0.238	0.072	0.008997	-0.000009	0.000574	0.095	2.444	0.062
200	300	0.121	0.215	0.048	0.007912	0.000674	-0.000507	0.036	3.414	0.079
200	350	0.181	0.251	0.066	0.014528	0.001534	-0.002359	0.100	2.586	0.062
200	400	0.170	0.290	0.064	0.017799	0.002237	-0.005713	0.043	4.260	0.076
200	450	0.198	0.213	0.065	0.015930	0.002220	-0.006220	0.067	2.969	0.068
200	500	0.260	0.273	0.068	0.032016	0.002232	-0.005040	0.125	2.808	0.058
200	550	0.275	0.162	0.046	0.011286	0.001014	-0.000159	0.031	4.701	0.082
200	600	0.113	0.076	0.033	0.000899	0.000748	0.000141	0.021	2.480	0.091
200	650	0.131	0.080	0.039	-0.002021	0.000068	0.000110	0.030	2.355	0.083
200	700	0.137	0.081	0.037	-0.002337	-0.000701	0.000208	0.041	2.088	0.077
200	750	0.138	0.073	0.029	-0.001353	-0.000770	-0.000046	0.046	1.921	0.075
200	800	0.134	0.082	0.036	-0.001336	-0.000707	0.000154	0.070	1.572	0.067
200	850	0.141	0.076	0.041	-0.002248	-0.000559	0.000139	0.034	2.325	0.081
300	50	0.191	0.251	0.070	0.011503	-0.000372	0.003238	0.248	1.683	0.049
300	100	0.167	0.238	0.070	0.011579	-0.001613	0.002452	0.154	1.974	0.055
300	150	0.171	0.227	0.066	0.012517	-0.000901	0.001088	0.113	2.243	0.060
300	200	0.171	0.209	0.064	0.012929	-0.000111	0.000358	0.077	2.588	0.066
300	250	0.167	0.222	0.055	0.014044	0.000709	-0.000445	0.062	2.952	0.070
300	300	0.195	0.252	0.048	0.021305	0.001266	-0.002503	0.063	3.338	0.069
300	350	0.213	0.218	0.051	0.017297	0.001131	-0.002960	0.081	2.810	0.065
300	400	0.267	0.195	0.061	0.025033	0.000791	-0.002457	0.073	3.221	0.067
300	450	0.271	0.173	0.055	0.025833	0.000796	-0.001029	0.090	2.818	0.063
300	500	0.147	0.112	0.038	0.005712	0.000615	-0.000439	0.006	6.534	0.127
300	550	0.138	0.082	0.034	-0.000503	-0.000164	-0.000072	0.015	3.506	0.099

A2.1.16 Processed turbulence data for $S = 10.52\%$, $Q = 31.2\text{L/s}$, $z = 10\text{mm}$ (cont'd)

x (mm)	y (mm)	$\sqrt{\overline{u'^2}}$ (m/s)	$\sqrt{\overline{v'^2}}$ (m/s)	$\sqrt{\overline{w'^2}}$ (m/s)	$-\overline{u'v'}$ (m ² /s ²)	$-\overline{u'w'}$ (m ² /s ²)	$-\overline{v'w'}$ (m ² /s ²)	ε (m ² /s ³)	λ_g (mm)	η (mm)
300	600	0.132	0.088	0.036	-0.001239	-0.000539	-0.000186	0.030	2.431	0.083
300	650	0.133	0.091	0.037	-0.001695	0.000044	-0.000125	0.055	1.821	0.071
300	700	0.124	0.109	0.040	-0.002785	0.000092	0.000124	0.079	1.563	0.065
300	750	0.118	0.123	0.040	-0.003233	0.000461	0.000300	0.026	2.788	0.086
300	800	0.113	0.125	0.036	-0.004200	0.000380	0.000255	0.016	3.501	0.097
300	850	0.107	0.113	0.033	-0.003670	0.000380	-0.000097	0.014	3.517	0.101
400	50	0.188	0.238	0.066	0.012179	-0.001712	0.003123	0.113	2.391	0.060
400	100	0.193	0.198	0.063	0.012896	-0.001832	0.001987	0.077	2.655	0.066
400	150	0.181	0.227	0.058	0.016136	-0.001030	0.001332	0.073	2.832	0.067
400	200	0.173	0.207	0.053	0.014777	-0.000593	0.000518	0.038	3.666	0.079
400	250	0.214	0.222	0.050	0.017089	-0.000707	-0.000317	0.084	2.794	0.064
400	300	0.241	0.175	0.043	0.017558	-0.001288	-0.000077	0.049	3.500	0.073
400	350	0.255	0.157	0.046	0.019231	-0.000896	-0.000253	0.061	3.182	0.070
400	400	0.205	0.103	0.045	0.010414	0.000104	-0.000245	0.035	3.239	0.080
400	450	0.186	0.095	0.034	0.004608	-0.000174	-0.000050	0.016	4.331	0.097
400	500	0.144	0.091	0.042	-0.000327	-0.000536	-0.000205	0.020	3.239	0.093
400	550	0.125	0.097	0.042	-0.001299	-0.000564	-0.000233	0.024	2.750	0.088
400	600	0.124	0.101	0.042	-0.000194	-0.000266	0.000154	0.040	2.131	0.077
400	650	0.131	0.123	0.052	-0.000856	-0.000051	-0.000054	0.057	2.036	0.071
400	700	0.133	0.136	0.048	-0.002953	-0.000018	0.000711	0.052	2.228	0.073
400	750	0.133	0.159	0.044	-0.005015	0.000397	0.000651	0.029	3.209	0.084
400	800	0.119	0.167	0.041	-0.004644	0.000093	0.000338	0.019	3.896	0.093
400	850	0.113	0.161	0.039	-0.004829	0.000275	0.000023	0.017	4.030	0.096
500	50	0.219	0.231	0.069	0.014550	-0.001949	0.002377	0.077	3.041	0.066
500	100	0.198	0.224	0.062	0.014882	-0.002148	0.001891	0.073	2.923	0.067
500	150	0.138	0.203	0.055	0.009611	-0.000787	0.000940	0.056	2.756	0.071
500	200	0.184	0.205	0.053	0.013546	-0.001118	0.000425	0.022	4.908	0.090
500	250	0.236	0.204	0.051	0.014276	-0.001533	0.000286	0.072	3.049	0.067
500	300	0.245	0.161	0.050	0.015268	-0.001453	-0.000317	0.051	3.420	0.073
500	350	0.208	0.127	0.041	0.008360	-0.000492	-0.000226	0.021	4.423	0.091
500	400	0.228	0.203	0.057	0.018787	-0.000864	0.000983	0.029	4.714	0.084
500	450	0.147	0.094	0.034	0.000066	-0.000507	-0.000008	0.018	3.439	0.095
500	500	0.133	0.094	0.036	-0.000172	-0.000358	-0.000194	0.013	3.763	0.102
500	550	0.125	0.095	0.041	0.001630	-0.000246	-0.000021	0.019	3.062	0.094
500	600	0.132	0.112	0.043	0.003290	-0.000033	-0.000022	0.059	1.904	0.070
500	650	0.151	0.129	0.046	0.004839	-0.000025	0.000159	0.057	2.219	0.071
500	700	0.150	0.149	0.049	0.002588	0.000380	0.000204	0.035	3.010	0.080
500	750	0.143	0.169	0.044	-0.001537	0.000670	0.000470	0.025	3.707	0.087
500	800	0.126	0.198	0.045	-0.002909	0.000400	0.000278	0.024	4.026	0.088
500	850	0.109	0.172	0.049	-0.001529	0.000944	-0.000448	0.020	3.853	0.092

A2.1.16 Processed turbulence data for $S = 10.52\%$, $Q = 31.2\text{L/s}$, $z = 10\text{mm}$ (cont'd)

x (mm)	y (mm)	$\sqrt{u'^2}$ (m/s)	$\sqrt{v'^2}$ (m/s)	$\sqrt{w'^2}$ (m/s)	$-\overline{u'v'}$ (m ² /s ²)	$-\overline{u'w'}$ (m ² /s ²)	$-\overline{v'w'}$ (m ² /s ²)	ε (m ² /s ³)	λ_g (mm)	η (mm)
600	50	0.129	0.221	0.065	0.001422	-0.001087	0.001153	0.050	3.057	0.073
600	100	0.156	0.211	0.053	0.008754	-0.001363	0.001044	0.023	4.537	0.089
600	150	0.093	0.194	0.051	0.003514	-0.000186	0.000584	0.052	2.511	0.073
600	200	0.219	0.176	0.046	0.012044	-0.001329	0.000278	0.073	2.725	0.067
600	250	0.247	0.172	0.047	0.014436	-0.001362	0.000284	0.069	2.999	0.068
600	300	0.238	0.145	0.041	0.011778	-0.000712	-0.000061	0.049	3.286	0.074
600	350	0.210	0.125	0.037	0.007332	-0.000354	-0.000066	0.033	3.541	0.081
600	400	0.182	0.111	0.036	0.005801	-0.000040	0.000167	0.023	3.719	0.089
600	450	0.186	0.116	0.039	0.008081	0.000125	0.000191	0.032	3.242	0.082
600	500	0.165	0.115	0.036	0.008862	0.000295	0.000048	0.044	2.502	0.075
600	550	0.172	0.131	0.038	0.011241	0.000435	-0.000019	0.048	2.585	0.074
600	600	0.175	0.142	0.040	0.013811	0.000677	-0.000154	0.063	2.367	0.069
600	650	0.169	0.156	0.040	0.013363	0.000759	-0.000203	0.042	2.948	0.077
600	700	0.157	0.178	0.043	0.012057	0.000918	-0.000031	0.025	3.962	0.087
600	750	0.136	0.183	0.043	0.004764	0.000835	-0.000376	0.018	4.431	0.094
600	800	0.118	0.222	0.048	0.001364	0.000775	0.000440	0.020	4.724	0.093
600	850	0.111	0.217	0.067	0.001137	0.001155	-0.000909	0.017	5.045	0.096
700	50	0.192	0.209	0.061	-0.000474	-0.001882	0.000849	0.050	3.377	0.073
700	100	0.183	0.190	0.049	0.007934	-0.001249	0.000859	0.061	2.814	0.070
700	150	0.202	0.180	0.051	0.009481	-0.001270	0.000634	0.061	2.876	0.070
700	200	0.229	0.170	0.051	0.011566	-0.001296	0.000381	0.056	3.175	0.071
700	250	0.260	0.160	0.051	0.010466	-0.001463	0.000324	0.081	2.815	0.065
700	300	0.243	0.146	0.049	0.009052	-0.000697	0.000183	0.064	2.929	0.069
700	350	0.227	0.135	0.048	0.009423	0.000130	-0.000239	0.086	2.372	0.064
700	400	0.261	0.149	0.063	0.009185	0.000729	-0.000018	0.301	1.450	0.047
700	450	0.225	0.116	0.050	0.010381	0.001509	-0.000332	0.094	2.181	0.063
700	500	0.209	0.121	0.047	0.010501	0.000786	-0.000087	0.081	2.242	0.065
700	550	0.203	0.128	0.047	0.012175	0.001223	-0.000449	0.066	2.459	0.068
700	600	0.187	0.135	0.042	0.013246	0.001475	-0.000724	0.043	2.921	0.076
700	650	0.178	0.152	0.042	0.015188	0.000888	-0.000144	0.047	2.854	0.075
700	700	0.151	0.173	0.040	0.013089	0.001148	-0.000608	0.038	3.087	0.078
700	750	0.134	0.188	0.040	0.010616	0.001077	-0.000634	0.029	3.552	0.084
700	800	0.115	0.207	0.046	0.007098	0.001180	-0.000922	0.025	3.945	0.087
700	850	0.111	0.256	0.079	0.003663	0.001239	0.000069	0.020	5.274	0.092
800	50	0.165	0.186	0.063	-0.002729	-0.001563	0.000464	0.017	5.134	0.096
800	100	0.196	0.182	0.047	0.005743	-0.001008	-0.000019	0.051	3.117	0.073
800	150	0.215	0.155	0.050	0.005654	-0.001031	0.000112	0.055	2.980	0.072
800	200	0.238	0.144	0.049	0.003875	-0.001416	0.000289	0.064	2.883	0.069
800	250	0.247	0.147	0.061	0.004862	-0.001619	0.000560	0.076	2.759	0.066
800	300	0.236	0.133	0.064	0.002529	-0.000678	0.000458	0.124	2.047	0.058
800	350	0.241	0.125	0.065	0.002379	-0.001148	0.000345	0.723	0.849	0.038

A2.1.16 Processed turbulence data for $S = 10.52\%$, $Q = 31.2\text{L/s}$, $z = 10\text{mm}$ (cont'd)

x (mm)	y (mm)	$\sqrt{u'^2}$ (m/s)	$\sqrt{v'^2}$ (m/s)	$\sqrt{w'^2}$ (m/s)	$-\overline{u'v'}$ (m ² /s ²)	$-\overline{u'w'}$ (m ² /s ²)	$-\overline{v'w'}$ (m ² /s ²)	ε (m ² /s ³)	λ_g (mm)	η (mm)
800	400	0.227	0.115	0.062	0.001669	0.000197	0.000401	0.229	1.418	0.050
800	450	0.237	0.100	0.064	0.002064	0.000889	0.000113	0.101	2.163	0.062
800	500	0.231	0.104	0.063	0.005378	0.000978	0.000389	0.104	2.095	0.061
800	550	0.232	0.103	0.052	0.008110	0.000927	0.000152	0.090	2.242	0.063
800	600	0.216	0.119	0.052	0.012946	0.000673	0.000347	0.114	1.931	0.060
800	650	0.197	0.144	0.047	0.016159	0.001378	0.000132	0.123	1.835	0.059
800	700	0.174	0.164	0.047	0.016349	0.001124	0.000348	0.206	1.386	0.051
800	750	0.148	0.196	0.044	0.014507	0.001021	0.000327	0.383	1.041	0.044
800	800	0.120	0.251	0.054	0.009710	0.000949	-0.000474	0.464	1.076	0.042
800	850	0.108	0.250	0.072	0.002098	0.000795	-0.001009	0.150	1.886	0.056
900	50	0.195	0.157	0.059	-0.004671	-0.001666	0.001056	0.052	2.918	0.073
900	100	0.189	0.170	0.048	0.004031	-0.000869	-0.000535	0.055	2.848	0.072
900	150	0.227	0.158	0.053	0.000544	-0.000669	-0.000071	0.048	3.313	0.074
900	200	0.202	0.129	0.056	-0.001218	-0.001017	-0.000088	0.059	2.614	0.070
900	250	0.204	0.127	0.055	-0.002103	-0.000714	0.000388	0.097	2.052	0.062
900	300	0.218	0.122	0.060	-0.003789	-0.001250	-0.000244	0.947	0.683	0.035
900	350	0.215	0.112	0.063	-0.005310	0.000137	0.000350	0.107	1.975	0.061
900	400	0.226	0.106	0.066	-0.005545	-0.000883	-0.000034	0.077	2.415	0.066
900	450	0.221	0.098	0.068	-0.006565	-0.000388	-0.000164	0.030	3.723	0.083
900	550	0.214	0.103	0.078	0.007353	-0.003601	0.001034	0.077	2.324	0.066
900	600	0.186	0.143	0.073	0.007786	-0.001033	0.001770	0.577	0.838	0.040
900	650	0.160	0.161	0.058	0.006905	-0.000025	0.001457	0.143	1.602	0.056
900	700	0.139	0.184	0.052	0.009103	0.000085	0.001253	0.041	3.040	0.077
900	750	0.125	0.229	0.051	0.005381	0.000327	0.000897	0.030	3.969	0.083
900	800	0.120	0.273	0.055	0.002219	0.000569	0.000223	0.022	5.351	0.090
900	850	0.109	0.295	0.081	-0.002403	0.000799	0.000433	0.028	5.003	0.085
1000	50	0.217	0.147	0.055	-0.010108	-0.000721	-0.000368	0.069	2.629	0.068
1000	100	0.187	0.164	0.046	0.002729	0.000059	-0.001129	0.092	2.162	0.063
1000	150	0.188	0.161	0.052	0.007278	0.000787	-0.001278	0.143	1.732	0.056
1000	200	0.205	0.146	0.053	0.009697	0.001093	-0.000642	0.507	0.935	0.041
1000	250	0.208	0.139	0.055	0.008615	0.001051	-0.000806	0.309	1.195	0.047
1000	300	0.190	0.131	0.055	0.005604	0.000982	-0.001137	0.129	1.709	0.058
1000	350	0.166	0.116	0.051	0.001741	0.000303	-0.000756	0.056	2.289	0.071
1000	400	0.134	0.151	0.066	-0.006283	0.001836	0.002338	0.013	4.789	0.102
1000	650	0.291	0.221	0.091	-0.013463	0.002553	-0.002688	0.220	2.077	0.051
1000	700	0.271	0.239	0.074	-0.011033	0.001646	-0.002862	0.126	2.696	0.058
1000	750	0.150	0.232	0.059	-0.005009	-0.000235	-0.000526	0.020	5.155	0.092
1000	800	0.150	0.270	0.061	-0.013562	0.000979	0.002079	0.014	6.931	0.101
1000	850	0.139	0.262	0.085	-0.011059	0.000231	-0.000637	0.019	5.805	0.094

A2.1.17 Processed turbulence data for $S = 10.52\%$, $Q = 31.2$ L/s, $z = 70$ mm

x (mm)	y (mm)	$\sqrt{u'^2}$ (m/s)	$\sqrt{v'^2}$ (m/s)	$\sqrt{w'^2}$ (m/s)	$-\overline{u'v'}$ (m ² /s ²)	$-\overline{u'w'}$ (m ² /s ²)	$-\overline{v'w'}$ (m ² /s ²)	ε (m ² /s ³)	λ_g (mm)	η (mm)
100	50	0.16	0.21	0.17	0.005684	-0.000475	0.015912	0.135	2.197	0.057
100	100	0.18	0.23	0.16	0.004756	-0.001840	0.010945	0.248	1.730	0.049
100	150	0.21	0.24	0.17	0.001401	-0.003377	0.007658	0.640	1.161	0.039
100	200	0.19	0.22	0.15	0.000040	-0.002650	0.008136	1.497	0.696	0.031
100	250	0.23	0.27	0.17	0.001605	-0.005184	0.011619	4.514	0.473	0.024
100	300	0.23	0.35	0.17	0.008440	-0.003302	0.005511	1.967	0.830	0.029
100	350	0.24	0.34	0.15	0.016376	0.001642	-0.003298	1.780	0.857	0.030
100	400	0.34	0.48	0.15	0.083192	0.005806	-0.010927	2.576	0.981	0.027
100	450	0.30	0.43	0.15	0.074151	0.006320	-0.009775	0.241	2.891	0.049
100	500	0.28	0.36	0.15	0.055906	0.005113	-0.010969	0.108	3.790	0.060
100	550	0.24	0.27	0.15	0.010128	0.001855	-0.006297	0.240	2.043	0.050
100	600	0.38	0.50	0.10	0.045679	0.011890	-0.020739	0.203	3.719	0.052
100	650	0.35	0.21	0.16	0.040842	-0.005522	0.000790	0.276	2.163	0.048
200	50	0.17	0.22	0.16	0.001816	-0.002776	0.010976	0.177	2.002	0.053
200	100	0.20	0.25	0.17	0.000539	-0.004899	0.008193	0.331	1.616	0.046
200	150	0.18	0.23	0.16	-0.000130	-0.004607	0.005968	0.232	1.769	0.050
200	200	0.22	0.27	0.16	0.008065	-0.007638	0.010549	0.874	1.050	0.036
200	250	0.23	0.32	0.16	0.015132	-0.007031	0.012357	1.248	0.989	0.033
200	300	0.24	0.34	0.15	0.022137	-0.006172	0.010501	0.708	1.358	0.038
200	350	0.26	0.36	0.14	0.033973	-0.002045	0.005906	0.575	1.586	0.040
200	400	0.29	0.36	0.13	0.049195	-0.000747	0.001743	0.492	1.765	0.041
200	450	0.27	0.37	0.12	0.056604	-0.000044	-0.000639	0.203	2.712	0.052
200	500	0.30	0.23	0.13	0.036109	0.003022	-0.004212	0.293	1.934	0.047
200	550	0.33	0.18	0.11	0.037584	0.000688	-0.000530	0.421	1.579	0.043
200	600	0.11	0.09	0.07	0.002689	0.000863	0.000238	0.030	2.446	0.083
200	650	0.10	0.09	0.08	0.000093	0.001721	0.001345	0.050	1.755	0.073
200	700	0.10	0.08	0.08	-0.000099	0.002065	0.001267	0.060	1.603	0.070
200	750	0.10	0.08	0.09	-0.000154	0.002587	0.001252	0.086	1.364	0.064
200	800	0.10	0.08	0.09	-0.000126	0.002202	0.000625	0.024	2.619	0.088
200	850	0.10	0.08	0.08	-0.000787	0.002041	0.000094	0.016	3.083	0.098
300	50	0.19	0.21	0.15	0.003732	-0.005702	0.004732	0.167	2.035	0.054
300	100	0.21	0.26	0.16	0.009206	-0.006380	0.005949	0.304	1.757	0.047
300	150	0.21	0.28	0.16	0.012404	-0.005922	0.009984	0.404	1.577	0.043
300	200	0.25	0.32	0.16	0.024035	-0.008802	0.012817	0.500	1.602	0.041
300	250	0.26	0.33	0.15	0.036868	-0.008092	0.009052	0.399	1.817	0.044
300	300	0.27	0.34	0.13	0.037878	-0.005604	0.005724	0.308	2.113	0.047
300	350	0.26	0.28	0.13	0.026032	-0.003146	0.001816	0.226	2.198	0.050
300	400	0.28	0.20	0.12	0.025781	-0.002855	0.000498	0.169	2.272	0.054
300	450	0.28	0.15	0.11	0.023373	0.000773	-0.001193	0.134	2.382	0.057
300	500	0.18	0.15	0.08	0.013505	0.002621	-0.001420	0.033	3.563	0.082
300	550	0.10	0.10	0.08	0.001945	0.000667	-0.000039	0.039	2.134	0.078

A2.1.17 Processed turbulence data for $S = 10.52\%$, $Q = 31.2\text{L/s}$, $z = 70\text{mm}$ (cont'd)

x (mm)	y (mm)	$\sqrt{u'^2}$ (m/s)	$\sqrt{v'^2}$ (m/s)	$\sqrt{w'^2}$ (m/s)	$-\overline{u'v'}$ (m ² /s ²)	$-\overline{u'w'}$ (m ² /s ²)	$-\overline{v'w'}$ (m ² /s ²)	ε (m ² /s ³)	λ_g (mm)	η (mm)
300	600	0.11	0.09	0.08	-0.000092	0.000346	-0.000182	0.028	2.499	0.085
300	650	0.11	0.09	0.09	-0.000375	0.000028	-0.000021	0.047	1.983	0.075
300	700	0.11	0.09	0.08	-0.001464	0.000099	0.000087	0.048	1.980	0.074
300	750	0.11	0.09	0.09	-0.001234	0.001534	0.000411	0.060	1.803	0.070
300	800	0.11	0.09	0.09	-0.000981	0.001844	0.000216	0.022	2.943	0.090
300	850	0.11	0.09	0.08	-0.000835	0.001560	-0.000594	0.015	3.437	0.099
400	50	0.22	0.23	0.16	0.010565	-0.008931	0.004770	0.209	2.042	0.051
400	100	0.24	0.26	0.16	0.018553	-0.006566	0.006270	0.329	1.740	0.046
400	150	0.25	0.27	0.16	0.023683	-0.007595	0.008279	0.325	1.820	0.046
400	200	0.28	0.29	0.14	0.032855	-0.009041	0.008727	0.301	2.011	0.047
400	250	0.26	0.25	0.13	0.022552	-0.007385	0.005827	0.216	2.159	0.051
400	300	0.26	0.21	0.12	0.018288	-0.004706	0.003217	0.154	2.322	0.055
400	350	0.26	0.18	0.10	0.021022	-0.001512	0.000932	0.090	2.870	0.063
400	400	0.20	0.11	0.08	0.011967	0.000358	-0.000437	0.033	3.546	0.082
400	450	0.14	0.08	0.08	0.003919	0.000421	0.000043	0.020	3.412	0.093
400	500	0.12	0.09	0.08	0.001025	-0.000760	-0.000366	0.021	3.034	0.091
400	550	0.11	0.10	0.09	0.000592	-0.000737	-0.000889	0.028	2.676	0.085
400	600	0.12	0.11	0.09	-0.000974	-0.001355	-0.000672	0.066	1.858	0.068
400	650	0.13	0.12	0.10	-0.002852	-0.001331	-0.001556	0.048	2.388	0.074
400	700	0.13	0.12	0.11	-0.003284	-0.000211	-0.000995	0.039	2.770	0.078
400	750	0.14	0.13	0.11	-0.002525	0.000475	-0.000698	0.036	2.990	0.080
400	800	0.13	0.11	0.10	-0.001813	0.001879	-0.000598	0.023	3.447	0.089
400	850	0.13	0.11	0.10	0.000643	0.001810	-0.002096	0.019	3.642	0.093
500	50	0.23	0.22	0.15	0.013994	-0.008289	0.004853	0.086	3.098	0.064
500	100	0.26	0.24	0.15	0.022457	-0.008244	0.007530	0.243	1.987	0.049
500	150	0.26	0.24	0.14	0.020009	-0.006310	0.006400	0.276	1.867	0.048
500	200	0.25	0.24	0.13	0.015978	-0.006517	0.006567	0.175	2.272	0.054
500	250	0.25	0.22	0.13	0.015001	-0.006080	0.004821	0.139	2.455	0.057
500	300	0.23	0.17	0.11	0.012557	-0.003671	0.001498	0.056	3.374	0.071
500	350	0.21	0.13	0.09	0.010965	-0.001017	0.000883	0.038	3.455	0.079
500	400	0.13	0.09	0.08	0.003196	-0.000294	0.000321	0.014	4.003	0.102
500	450	0.11	0.09	0.08	0.001164	-0.000741	0.000083	0.014	3.509	0.101
500	500	0.11	0.09	0.08	0.000880	-0.000502	-0.000978	0.018	3.176	0.094
500	550	0.12	0.10	0.09	0.001310	-0.000045	-0.001071	0.042	2.352	0.077
500	600	0.13	0.12	0.11	0.002516	0.000610	-0.001398	0.084	1.818	0.064
500	650	0.13	0.12	0.12	0.000282	-0.000615	-0.001794	0.043	2.662	0.076
500	700	0.12	0.12	0.11	-0.000589	-0.000026	-0.001118	0.022	3.626	0.090
500	750	0.13	0.14	0.12	-0.001730	0.001241	-0.001454	0.020	4.121	0.092
500	800	0.14	0.12	0.12	-0.000659	0.001979	-0.001791	0.026	3.518	0.086
500	850	0.13	0.11	0.12	0.000552	0.001800	-0.003304	0.019	3.839	0.093

A2.1.17 Processed turbulence data for $S = 10.52\%$, $Q = 31.2\text{L/s}$, $z = 70\text{mm}$ (cont'd)

x (mm)	y (mm)	$\sqrt{u'^2}$ (m/s)	$\sqrt{v'^2}$ (m/s)	$\sqrt{w'^2}$ (m/s)	$\overline{-u'v'}$ (m ² /s ²)	$\overline{-u'w'}$ (m ² /s ²)	$\overline{-v'w'}$ (m ² /s ²)	ε (m ² /s ³)	λ_g (mm)	η (mm)
600	50	0.23	0.18	0.14	0.008389	-0.006630	0.003265	0.120	2.412	0.059
600	100	0.25	0.21	0.14	0.015148	-0.008838	0.005949	0.153	2.318	0.055
600	150	0.24	0.21	0.13	0.011999	-0.006479	0.005641	0.158	2.253	0.055
600	200	0.23	0.20	0.12	0.009857	-0.004954	0.004771	0.118	2.471	0.059
600	250	0.20	0.17	0.11	0.006912	-0.000942	0.003035	0.062	2.967	0.069
600	300	0.19	0.15	0.11	0.004773	-0.000266	0.002489	0.043	3.295	0.076
600	350	0.16	0.12	0.11	0.002718	0.001492	0.002236	0.019	4.255	0.094
600	400	0.13	0.11	0.10	0.001895	0.001634	0.001031	0.013	4.336	0.102
600	450	0.12	0.10	0.09	0.002725	0.000860	0.000974	0.016	3.770	0.098
600	500	0.12	0.11	0.10	0.002791	0.000601	0.000415	0.020	3.424	0.092
600	550	0.12	0.12	0.10	0.005177	0.000489	-0.000121	0.095	1.660	0.062
600	600	0.13	0.12	0.11	0.005257	0.001075	-0.001849	0.081	1.900	0.065
600	650	0.13	0.14	0.12	0.005368	0.000645	-0.002777	0.040	2.921	0.078
600	700	0.13	0.16	0.13	0.005943	0.001061	-0.004948	0.026	3.807	0.086
600	750	0.12	0.15	0.14	0.002101	0.002312	-0.003728	0.017	4.539	0.095
600	800	0.12	0.15	0.14	0.002175	0.002714	-0.005203	0.021	4.243	0.091
600	850	0.11	0.14	0.13	0.002043	0.002616	-0.007438	0.015	4.700	0.098
700	50	0.22	0.17	0.13	0.006983	-0.007361	0.003417	0.083	2.693	0.064
700	100	0.22	0.17	0.13	0.007755	-0.007661	0.003053	0.086	2.750	0.064
700	150	0.24	0.18	0.13	0.008725	-0.005219	0.003874	0.134	2.284	0.057
700	200	0.23	0.18	0.12	0.006662	-0.004592	0.004983	0.121	2.335	0.059
700	250	0.20	0.16	0.12	0.004134	-0.002072	0.004662	0.086	2.544	0.064
700	300	0.20	0.17	0.13	0.007875	-0.001824	0.004561	0.071	2.872	0.067
700	350	0.17	0.14	0.12	0.002824	0.001218	0.002671	0.047	2.935	0.074
700	400	0.17	0.12	0.13	0.003557	0.001754	0.002711	0.080	2.233	0.065
700	450	0.16	0.11	0.12	0.002754	0.001905	0.001887	0.392	0.942	0.044
700	500	0.16	0.10	0.11	0.004543	0.001280	0.000876	0.562	0.756	0.040
700	550	0.15	0.11	0.12	0.005497	0.000664	0.000368	0.147	1.505	0.056
700	600	0.15	0.11	0.11	0.005394	0.000961	-0.000122	0.102	1.782	0.061
700	650	0.15	0.14	0.12	0.008809	0.000789	-0.000734	0.152	1.589	0.055
700	700	0.13	0.16	0.12	0.007584	0.001872	-0.002053	0.109	1.853	0.060
700	750	0.12	0.15	0.13	0.005036	0.002893	-0.001736	0.044	2.783	0.075
700	800	0.11	0.17	0.14	0.003332	0.002421	-0.004735	0.037	3.235	0.079
700	850	0.11	0.17	0.15	0.002821	0.002946	-0.009392	0.028	3.908	0.085
800	50	0.20	0.15	0.12	0.005134	-0.008315	0.002402	0.066	2.789	0.068
800	100	0.21	0.15	0.12	0.004066	-0.007069	0.001104	0.073	2.739	0.067
800	150	0.23	0.15	0.13	0.004041	-0.007171	0.002407	0.097	2.535	0.062
800	200	0.23	0.15	0.13	0.001673	-0.005174	0.003665	0.091	2.558	0.063
800	250	0.22	0.14	0.13	0.000641	-0.004782	0.003976	0.104	2.333	0.061
800	300	0.20	0.13	0.14	-0.000269	-0.002199	0.003279	0.101	2.231	0.062
800	350	0.19	0.12	0.13	-0.000328	-0.000560	0.002358	0.397	1.098	0.044

A2.1.17 Processed turbulence data for $S = 10.52\%$, $Q = 31.2\text{L/s}$, $z = 70\text{mm}$ (cont'd)

x (mm)	y (mm)	$\sqrt{u'^2}$ (m/s)	$\sqrt{v'^2}$ (m/s)	$\sqrt{w'^2}$ (m/s)	$-\overline{u'v'}$ (m ² /s ²)	$-\overline{u'w'}$ (m ² /s ²)	$-\overline{v'w'}$ (m ² /s ²)	ε (m ² /s ³)	λ_g (mm)	η (mm)
800	400	0.20	0.11	0.14	-0.000922	0.000241	0.002102	0.660	0.856	0.038
800	450	0.20	0.11	0.14	0.000874	0.002241	0.001888	0.226	1.464	0.050
800	500	0.21	0.12	0.14	0.002703	0.001285	0.002290	0.204	1.625	0.052
800	550	0.21	0.12	0.14	0.005908	0.000767	0.001518	0.244	1.451	0.049
800	600	0.20	0.13	0.14	0.009070	-0.000360	0.003011	0.312	1.275	0.046
800	650	0.18	0.15	0.13	0.011213	0.000753	0.002193	0.950	0.707	0.035
800	700	0.14	0.16	0.13	0.009790	0.001406	0.001259	0.538	0.878	0.040
800	750	0.13	0.16	0.13	0.008293	0.002176	0.000888	0.448	0.952	0.042
800	800	0.11	0.18	0.13	0.004815	0.002350	-0.002824	0.519	0.905	0.041
800	850	0.11	0.18	0.16	0.003378	0.003928	-0.008492	0.285	1.283	0.047
900	50	0.18	0.13	0.11	0.002437	-0.005991	0.001192	0.051	2.818	0.073
900	100	0.20	0.14	0.12	0.001522	-0.007121	0.000094	0.053	3.048	0.072
900	150	0.20	0.14	0.13	0.000468	-0.006975	0.000660	0.059	2.956	0.070
900	200	0.21	0.14	0.13	-0.002283	-0.006156	0.001348	0.084	2.520	0.064
900	250	0.21	0.13	0.14	-0.000965	-0.006033	0.003134	0.160	1.856	0.055
900	300	0.21	0.13	0.15	-0.001674	-0.005377	0.002810	0.750	0.857	0.037
900	350	0.20	0.12	0.15	-0.003250	-0.003716	0.002714	0.112	2.130	0.060
900	400	0.19	0.11	0.15	-0.001942	-0.005836	0.001653	0.060	2.788	0.070
900	450	0.20	0.10	0.15	-0.002637	-0.006187	0.001152	0.054	2.995	0.072
900	550	0.19	0.12	0.17	0.006771	-0.006999	0.005773	0.140	1.936	0.057
900	600	0.16	0.17	0.17	0.004983	-0.001738	0.007407	0.611	0.953	0.039
900	650	0.15	0.18	0.17	0.004870	-0.001418	0.006488	0.112	2.239	0.060
900	700	0.13	0.21	0.17	0.006586	-0.000423	0.009948	0.050	3.480	0.073
900	750	0.11	0.21	0.16	0.002943	0.001025	0.006441	0.029	4.312	0.084
900	800	0.11	0.20	0.15	-0.000822	0.001451	0.002164	0.027	4.270	0.085
900	850	0.12	0.19	0.14	-0.002346	0.001686	-0.006735	0.034	3.711	0.081
1000	50	0.16	0.14	0.10	0.000343	-0.003765	0.001885	0.036	3.108	0.079
1000	100	0.17	0.15	0.12	0.001504	-0.005454	-0.000517	0.048	2.996	0.074
1000	150	0.18	0.15	0.13	0.002194	-0.006939	-0.000802	0.057	2.943	0.071
1000	200	0.19	0.14	0.14	0.002198	-0.007567	0.000365	0.095	2.312	0.062
1000	250	0.19	0.13	0.14	0.003992	-0.007823	0.000816	0.309	1.261	0.046
1000	300	0.17	0.13	0.14	0.003483	-0.005609	0.001532	0.264	1.287	0.048
1000	350	0.15	0.12	0.13	0.001868	-0.004105	0.001815	0.054	2.598	0.072
1000	400	0.13	0.12	0.13	-0.000171	-0.003191	0.001995	0.027	3.443	0.085
1000	650	0.29	0.21	0.17	-0.025982	-0.002357	-0.002581	0.468	1.512	0.042
1000	700	0.23	0.21	0.20	-0.015289	0.005533	-0.003956	0.067	3.680	0.068
1000	750	0.16	0.19	0.19	-0.006956	0.003257	-0.001234	0.025	5.062	0.087
1000	800	0.15	0.19	0.17	-0.009147	0.002416	-0.002528	0.022	5.124	0.090
1000	850	0.15	0.20	0.14	-0.007954	0.000991	-0.006860	0.020	5.195	0.092

A2.1.18 Processed turbulence data for $S = 10.52\%$, $Q = 52$ L/s, $z = 100$ mm

x (mm)	y (mm)	$\sqrt{u'^2}$ (m/s)	$\sqrt{v'^2}$ (m/s)	$\sqrt{w'^2}$ (m/s)	$-\overline{u'v'}$ (m ² /s ²)	$-\overline{u'w'}$ (m ² /s ²)	$-\overline{v'w'}$ (m ² /s ²)	ε (m ² /s ³)	λ_g (mm)	η (mm)
100	50	0.178	0.125	0.158	0.004348	-0.002711	0.010055	0.038	3.553	0.078
100	100	0.191	0.160	0.159	0.011942	-0.009549	0.013310	0.059	3.155	0.070
100	150	0.193	0.189	0.142	0.013215	-0.004813	0.010068	0.054	3.412	0.072
100	200	0.201	0.314	0.156	0.013757	-0.003072	0.007281	0.175	2.500	0.054
100	250	0.158	0.116	0.122	-0.000393	0.004323	0.000886	0.280	1.129	0.048
100	300	0.180	0.251	0.115	0.014700	0.005316	-0.009200	0.187	1.971	0.053
100	350	0.134	0.110	0.117	0.000155	0.002591	-0.000259	0.049	2.452	0.074
100	400	0.116	0.114	0.116	0.000614	0.001819	0.000008	0.067	2.001	0.068
100	450	0.133	0.163	0.117	0.003320	0.001878	-0.001414	0.112	1.859	0.060
100	500	0.211	0.409	0.122	0.064180	-0.000752	0.004608	0.116	3.623	0.059
100	550	0.286	0.517	0.170	0.111180	-0.004568	0.002514	0.128	4.442	0.058
100	600	0.223	0.271	0.183	-0.012849	-0.006788	-0.007871	0.047	4.748	0.075
100	650	0.255	0.300	0.201	0.007727	-0.007876	0.005639	0.035	6.147	0.080
200	50	0.212	0.140	0.146	0.011987	-0.006028	0.007449	0.046	3.516	0.075
200	100	0.187	0.131	0.129	0.005621	0.000045	0.002874	0.020	4.811	0.092
200	150	0.224	0.252	0.139	0.036536	-0.003467	0.007540	0.101	2.973	0.062
200	200	0.229	0.244	0.138	0.031524	0.001693	0.000952	0.133	2.570	0.057
200	250	0.238	0.390	0.135	0.056340	0.003866	-0.007882	0.545	1.669	0.040
200	300	0.250	0.387	0.127	0.064060	0.002762	-0.008631	0.247	2.491	0.049
200	350	0.143	0.133	0.151	0.004850	0.001166	-0.001027	0.144	1.684	0.056
200	400	0.211	0.214	0.166	0.022338	-0.001092	0.001556	0.115	2.626	0.060
200	450	0.174	0.239	0.169	0.016867	-0.001399	0.001548	0.104	2.731	0.061
200	500	0.274	0.375	0.185	0.046975	-0.000546	-0.002904	0.127	3.635	0.058
200	550	0.303	0.326	0.179	0.044017	-0.003686	-0.003357	0.159	3.113	0.055
200	600	0.447	0.172	0.170	-0.000712	-0.010581	-0.001849	0.231	2.735	0.050
200	650	0.279	0.117	0.139	-0.001740	0.002837	0.001550	0.382	1.396	0.044
200	700	0.140	0.117	0.117	0.001854	0.002564	0.001923	0.190	1.287	0.052
200	750	0.138	0.119	0.123	-0.002990	0.002845	0.002921	0.060	2.320	0.070
200	800	0.148	0.106	0.124	-0.004796	0.002462	0.001744	0.045	2.682	0.075
200	850	0.162	0.099	0.102	-0.005841	0.002826	-0.000072	0.032	3.114	0.082
300	50	0.241	0.216	0.178	0.032428	-0.013333	0.014775	0.097	3.074	0.062
300	100	0.217	0.167	0.144	0.010484	0.000577	0.004976	0.038	4.138	0.079
300	150	0.260	0.227	0.145	0.037744	-0.000639	0.005185	0.062	3.898	0.070
300	200	0.280	0.306	0.149	0.072570	0.003462	-0.000068	0.173	2.743	0.054
300	250	0.254	0.232	0.169	0.029684	0.001807	0.001875	0.260	1.947	0.049
300	300	0.240	0.222	0.174	0.033188	-0.000816	0.000824	0.180	2.258	0.053
300	350	0.189	0.222	0.181	0.018248	0.001153	0.001202	0.053	3.848	0.072
300	400	0.234	0.283	0.195	0.030015	-0.000041	0.000210	0.058	4.469	0.071
300	450	0.249	0.277	0.155	0.015384	0.000197	-0.005734	0.126	2.945	0.058
300	500	0.320	0.334	0.183	0.051370	-0.002316	-0.001470	0.104	3.990	0.061
300	550	0.478	0.163	0.128	0.009472	-0.006221	-0.000161	0.159	3.382	0.055

A2.1.18 Processed turbulence data for $S = 10.52\%$, $Q = 52\text{L/s}$, $z = 100\text{mm}$ (cont'd)

x (mm)	y (mm)	$\sqrt{u'^2}$ (m/s)	$\sqrt{v'^2}$ (m/s)	$\sqrt{w'^2}$ (m/s)	$-\overline{u'v'}$ (m ² /s ²)	$-\overline{u'w'}$ (m ² /s ²)	$-\overline{v'w'}$ (m ² /s ²)	ε (m ² /s ³)	λ_g (mm)	η (mm)
300	600	0.407	0.147	0.161	-0.015286	0.003065	0.000436	0.227	2.509	0.050
300	650	0.449	0.103	0.141	-0.001707	0.004447	0.000953	0.223	2.642	0.050
300	700	0.149	0.132	0.137	-0.002508	0.001720	0.002683	0.131	1.730	0.058
300	750	0.148	0.124	0.137	-0.005035	-0.000602	0.000768	0.061	2.477	0.070
300	800	0.162	0.115	0.129	-0.005942	-0.001327	0.000005	0.042	2.980	0.076
300	850	0.178	0.110	0.120	-0.003314	-0.004071	-0.000764	0.032	3.491	0.082
400	50	0.370	0.185	0.156	0.044022	-0.008260	0.007939	0.065	4.488	0.069
400	100	0.266	0.202	0.147	0.028099	-0.005463	0.009128	0.062	3.809	0.070
400	150	0.375	0.290	0.165	0.092395	-0.003352	0.005980	0.150	3.359	0.056
400	200	0.323	0.246	0.172	0.050263	0.002667	0.004175	0.238	2.340	0.050
400	250	0.357	0.293	0.169	0.094639	0.004803	-0.003766	0.146	3.338	0.056
400	300	0.269	0.222	0.160	0.032605	0.002845	-0.003929	0.156	2.513	0.055
400	350	0.247	0.298	0.181	0.043045	0.001556	-0.002195	0.088	3.739	0.064
400	400	0.269	0.266	0.184	0.028353	-0.001209	-0.002388	0.097	3.499	0.062
400	450	0.311	0.294	0.175	0.042114	-0.001351	-0.001135	0.118	3.476	0.059
400	500	0.423	0.155	0.114	0.007154	-0.002512	-0.000302	0.157	3.035	0.055
400	550	0.428	0.202	0.159	-0.014466	0.002465	-0.002049	0.226	2.717	0.050
400	600	0.349	0.161	0.160	-0.021730	0.004527	0.001447	0.203	2.393	0.052
400	650	0.224	0.155	0.165	-0.010131	0.005842	0.003142	0.146	2.158	0.056
400	700	0.187	0.152	0.153	-0.005728	0.000877	0.002399	0.215	1.590	0.051
400	750	0.189	0.146	0.144	-0.005778	-0.001274	0.001663	0.084	2.489	0.064
400	800	0.187	0.144	0.130	-0.003521	-0.002407	0.002161	0.045	3.287	0.075
400	850	0.176	0.142	0.120	0.000265	-0.003667	0.000312	0.031	3.786	0.083
500	50	0.257	0.143	0.154	0.007545	-0.000151	0.005935	0.037	4.448	0.079
500	100	0.373	0.218	0.152	0.048681	-0.003852	0.009085	0.060	4.843	0.070
500	150	0.298	0.226	0.178	0.029988	-0.000116	0.006817	0.090	3.565	0.063
500	200	0.291	0.248	0.173	0.043383	0.005249	0.001815	0.308	1.957	0.047
500	250	0.367	0.243	0.187	0.062599	0.008702	-0.004698	0.205	2.735	0.052
500	300	0.319	0.253	0.211	0.039486	-0.000913	0.002416	0.237	2.437	0.050
500	350	0.288	0.239	0.186	0.035946	0.002874	-0.003252	0.101	3.414	0.062
500	400	0.330	0.270	0.184	0.042007	-0.000992	-0.000252	0.144	3.165	0.056
500	450	0.336	0.205	0.135	0.013863	-0.001737	-0.000609	0.080	3.809	0.065
500	500	0.360	0.219	0.152	0.000665	0.000320	-0.000516	0.136	3.146	0.057
500	550	0.364	0.172	0.138	-0.010618	0.002679	-0.000188	0.108	3.347	0.060
500	600	0.319	0.183	0.164	-0.020927	0.005707	0.003368	0.111	3.129	0.060
500	650	0.254	0.185	0.165	-0.011753	0.004940	0.002580	0.150	2.372	0.056
500	700	0.219	0.192	0.168	-0.003324	0.001844	0.001786	0.242	1.769	0.049
500	750	0.202	0.188	0.152	0.000926	0.002496	-0.001653	0.057	3.429	0.071
500	800	0.199	0.189	0.152	-0.003415	-0.000360	-0.001970	0.050	3.621	0.073
500	850	0.200	0.158	0.134	-0.003860	-0.005359	-0.002021	0.041	3.657	0.077

A2.1.18 Processed turbulence data for $S = 10.52\%$, $Q = 52\text{L/s}$, $z = 100\text{mm}$ (cont'd)

x (mm)	y (mm)	$\sqrt{u'^2}$ (m/s)	$\sqrt{v'^2}$ (m/s)	$\sqrt{w'^2}$ (m/s)	$-\overline{u'v'}$ (m ² /s ²)	$-\overline{u'w'}$ (m ² /s ²)	$-\overline{v'w'}$ (m ² /s ²)	ε (m ² /s ³)	λ_g (mm)	η (mm)
600	50	0.471	0.167	0.154	0.039765	-0.011554	0.006649	0.060	5.530	0.070
600	100	0.270	0.191	0.158	0.014703	-0.003811	0.009053	0.054	4.068	0.072
600	150	0.320	0.213	0.183	0.024733	0.001214	0.007129	0.111	3.304	0.060
600	200	0.376	0.225	0.193	0.038605	0.009667	0.006315	0.566	1.648	0.040
600	250	0.370	0.211	0.190	0.033039	0.017543	-0.002234	0.232	2.507	0.050
600	300	0.310	0.201	0.206	0.026084	0.004757	0.000378	0.171	2.645	0.054
600	350	0.304	0.208	0.201	0.023771	-0.000066	-0.000320	0.155	2.759	0.055
600	400	0.319	0.222	0.182	0.029519	-0.001558	-0.000560	0.103	3.468	0.061
600	450	0.295	0.142	0.105	0.009461	0.001189	-0.000973	0.068	3.403	0.068
600	500	0.378	0.205	0.145	0.010171	-0.000787	0.000178	0.148	3.056	0.056
600	550	0.350	0.194	0.146	-0.004872	0.000642	0.001059	0.078	3.937	0.066
600	600	0.361	0.200	0.147	-0.008665	0.001475	0.001629	0.072	4.235	0.067
600	650	0.287	0.211	0.156	0.003888	0.002122	0.000427	0.112	3.004	0.060
600	700	0.256	0.214	0.176	-0.010144	-0.000993	0.000421	0.656	1.206	0.039
600	750	0.235	0.212	0.172	-0.013240	-0.004290	-0.002091	0.107	2.851	0.061
600	800	0.216	0.207	0.166	-0.007108	-0.004427	-0.005174	0.058	3.689	0.071
600	850	0.209	0.175	0.161	-0.007522	-0.008736	-0.004960	0.050	3.671	0.073
700	50	0.459	0.132	0.133	0.022520	-0.006649	0.004040	0.080	4.534	0.065
700	100	0.287	0.186	0.153	0.012121	-0.003104	0.008082	0.064	3.820	0.069
700	150	0.366	0.204	0.164	0.027246	0.004859	0.006049	0.251	2.325	0.049
700	200	0.360	0.202	0.180	0.023806	0.007496	0.003961	0.450	1.737	0.042
700	250	0.319	0.206	0.206	0.020708	0.006564	0.004794	0.420	1.724	0.043
700	300	0.329	0.201	0.218	0.017191	0.005664	0.002562	0.251	2.289	0.049
700	350	0.320	0.200	0.231	0.018235	0.001573	0.001651	0.180	2.697	0.053
700	400	0.341	0.209	0.216	0.022445	0.001073	-0.000506	0.217	2.526	0.051
700	450	0.342	0.197	0.195	0.024007	-0.004476	0.000547	0.162	2.833	0.055
700	500	0.344	0.228	0.183	0.019914	-0.000131	0.000502	0.210	2.552	0.051
700	550	0.361	0.229	0.172	0.014982	0.000515	-0.001182	0.184	2.778	0.053
700	600	0.379	0.235	0.165	0.020534	-0.008873	0.002789	0.178	2.912	0.053
700	650	0.319	0.248	0.173	0.014195	-0.011343	0.004798	0.168	2.771	0.054
700	700	0.245	0.253	0.172	0.019139	-0.005607	0.006256	0.250	2.028	0.049
700	750	0.239	0.264	0.187	-0.010426	-0.003311	-0.007356	0.299	1.904	0.047
700	800	0.199	0.255	0.184	-0.008907	-0.002186	-0.005941	0.074	3.545	0.066
700	850	0.203	0.237	0.185	-0.014103	-0.001655	-0.005017	0.052	4.136	0.073
800	50	0.253	0.124	0.137	0.004128	-0.001705	0.004772	0.038	4.165	0.079
800	100	0.358	0.177	0.144	0.024530	-0.005476	0.006345	0.174	2.636	0.054
800	150	0.228	0.191	0.158	0.012081	0.001772	0.005909	0.052	3.805	0.072
800	200	0.260	0.204	0.175	0.017409	0.002633	0.005084	0.125	2.742	0.058
800	250	0.291	0.181	0.179	0.001202	0.010309	0.001092	0.185	2.325	0.053
800	300	0.289	0.211	0.208	0.012533	0.007907	0.003049	0.952	1.099	0.035
800	350	0.318	0.211	0.231	0.012334	0.005289	0.003154	0.247	2.324	0.049

A2.1.18 Processed turbulence data for $S = 10.52\%$, $Q = 52\text{L/s}$, $z = 100\text{mm}$ (cont'd)

x (mm)	y (mm)	$\sqrt{u'^2}$ (m/s)	$\sqrt{v'^2}$ (m/s)	$\sqrt{w'^2}$ (m/s)	$-\overline{u'v'}$ (m ² /s ²)	$-\overline{u'w'}$ (m ² /s ²)	$-\overline{v'w'}$ (m ² /s ²)	ε (m ² /s ³)	λ_g (mm)	η (mm)
800	400	0.322	0.198	0.235	0.016304	-0.007525	0.005372	0.180	2.716	0.053
800	450	0.330	0.207	0.222	0.016427	0.000695	-0.000811	0.172	2.796	0.054
800	500	0.333	0.198	0.185	0.017062	-0.010115	0.006092	0.341	1.899	0.045
800	550	0.322	0.223	0.198	0.020286	0.001609	-0.005020	0.224	2.399	0.050
800	600	0.297	0.230	0.175	0.012357	-0.001345	-0.002805	0.173	2.578	0.054
800	650	0.273	0.258	0.177	0.002748	-0.001834	-0.004150	0.154	2.737	0.055
800	700	0.241	0.260	0.178	-0.010597	-0.004580	-0.004464	0.171	2.482	0.054
800	750	0.214	0.265	0.186	-0.007764	-0.004588	-0.002269	0.365	1.662	0.045
800	800	0.196	0.235	0.194	-0.013911	-0.006248	-0.008328	0.142	2.488	0.056
800	850	0.242	0.235	0.193	-0.023427	-0.000482	-0.005964	0.125	2.842	0.058
900	50	0.260	0.115	0.125	0.002143	-0.002891	0.003087	0.050	3.600	0.073
900	100	0.287	0.156	0.135	0.005975	-0.006077	0.004076	0.105	2.820	0.061
900	150	0.292	0.166	0.145	0.006284	-0.004939	0.002861	0.616	1.207	0.039
900	200	0.240	0.189	0.155	0.005897	-0.002613	0.003892	0.182	2.076	0.053
900	250	0.249	0.205	0.166	0.003878	0.001150	0.004000	0.937	0.970	0.035
900	300	0.256	0.213	0.186	0.005179	-0.002723	0.005580	0.870	1.059	0.036
900	350	0.276	0.213	0.200	0.012754	-0.003274	0.004964	0.732	1.214	0.037
900	400	0.331	0.223	0.217	0.021827	-0.008810	0.002769	0.434	1.785	0.043
900	450	0.306	0.226	0.225	0.018468	-0.009801	0.000131	0.092	3.765	0.063
900	500	0.366	0.237	0.223	0.030963	-0.012206	0.001820	0.266	2.455	0.048
900	550	0.387	0.255	0.211	0.048291	-0.012750	0.001004	0.332	2.287	0.046
900	600	0.313	0.236	0.190	0.017422	-0.007056	-0.000371	0.210	2.463	0.051
900	650	0.253	0.228	0.170	0.002351	-0.003316	-0.002915	0.145	2.591	0.056
900	700	0.216	0.236	0.173	-0.003776	-0.004598	-0.002461	0.109	2.848	0.060
900	750	0.197	0.248	0.190	-0.009900	-0.006485	-0.003579	0.101	2.998	0.061
900	800	0.227	0.244	0.201	-0.016789	-0.008731	-0.010860	0.255	1.997	0.049
900	850	0.238	0.249	0.191	-0.016117	-0.007205	-0.012460	0.631	1.283	0.039

A2.2 Structure of jet flow in the pool with coordinates (x_j, y_j, z)

A2.2.1 Maximum plane velocity locus

$S = 5.06\%, Q = 31.2 \text{ L/s}$								
$z = 10 \text{ mm}$			$z = 100 \text{ mm}$			$z = 150 \text{ mm}$		
$x_j \text{ (mm)}$	$x \text{ (mm)}$	$y \text{ (mm)}$	$x_j \text{ (mm)}$	$x \text{ (mm)}$	$y \text{ (mm)}$	$x_j \text{ (mm)}$	$x \text{ (mm)}$	$y \text{ (mm)}$
0	32.0	649.7	0	59.0	682.0	0	59.0	682.0
100	113.0	591.0	100	140.0	623.0	100	140.0	623.0
200	200.0	542.0	200	227.0	575.0	200	227.0	575.0
300	290.0	506.3	300	318.0	541.0	300	318.0	541.0
400	386.0	485.3	400	415.0	516.0	400	415.0	516.0
500	483.0	481.8	500	516.0	507.0	500	516.0	507.0
600	578.5	495.8	600	615.0	512.0	600	615.0	512.0
700	666.9	524.2	700	713.0	532.0	700	713.0	532.0
800	754.3	567.0	800	800.6	565.0	800	800.6	565.0
900	837.2	620.8						
$S = 5.06\%, Q = 52 \text{ L/s}$								
$z = 10 \text{ mm}$			$z = 150 \text{ mm}$			$z = 300 \text{ mm}$		
$x_j \text{ (mm)}$	$x \text{ (mm)}$	$y \text{ (mm)}$	$x_j \text{ (mm)}$	$x \text{ (mm)}$	$y \text{ (mm)}$	$x_j \text{ (mm)}$	$x \text{ (mm)}$	$y \text{ (mm)}$
	100	597.2		30.3	665.5		30.3	675.5
	200	551.5		100.0	616.1		50.0	658.9
	300	513.1		200.0	559.0		100.0	619.7
	400	481.9		300.0	518.1		200.0	554.1
	500	450.0		400.0	493.4		300.0	505.8
	550	443.8		450.0	487.1		400.0	474.6
	600	450.0		500.0	484.9		500.0	460.7
	650	468.8		550.0	486.7		550.0	460.2
	700	500.0		600.0	492.5		600.0	464.0
	750	556.3		650.0	502.5		650.0	472.0
	800	600.0		700.0	516.4		700.0	484.4
	850	631.3		800.0	556.5		800.0	522.1
	900	650.0		900.0	612.8		900.0	576.9
$S = 10.52\%, Q = 31.2 \text{ L/s}$						$S = 10.52\%, Q = 52 \text{ L/s}$		
$z = 10 \text{ mm}$			$z = 70 \text{ mm}$			$z = 100 \text{ mm}$		
$x_j \text{ (mm)}$	$x \text{ (mm)}$	$y \text{ (mm)}$	$x_j \text{ (mm)}$	$x \text{ (mm)}$	$y \text{ (mm)}$	$x_j \text{ (mm)}$	$x \text{ (mm)}$	$y \text{ (mm)}$
0	52.2	688.3	0	48.2	679.2		100	651.7
100	109.0	594.0	100	115.1	604.9		200	584.1
200	162.0	510.0	200	182.1	530.7		300	536.1
300	224.0	430.0	300	249.1	456.4		400	506.6
400	290.0	354.0	400	316.1	382.2		500	494.2
500	361.0	286.0	500	383.1	307.9		600	497.8
600	440.0	225.5	600	450.1	233.7		700	516.2
700	531.0	176.0	700	517.1	159.4		800	548.2
800	622.0	135.0	800	584.1	85.2		900	592.7

A2.2.2 Measurement points in (x_j, y_j) and its corresponding points in (x, y) for $S = 5.06\%$, $Q = 31.2$ L/s, $z = 10$ mm

x_j (mm)	y_j (mm)	x (mm)	y (mm)	x_j (mm)	y_j (mm)	x (mm)	y (mm)	x_j (mm)	y_j (mm)	x (mm)	y (mm)
100	-130	40.5	483.1	400	100	406.3	583.2	700	150	627.8	669.0
100	-100	57.2	508.0	400	150	416.5	632.2	700	200	614.8	717.3
100	-50	85.1	549.5	400	200	426.6	681.1	700	250	601.7	765.6
100	0	113.0	591.0	400	250	436.8	730.1				
100	50	140.9	632.5	400	300	447.0	779.0	800	-250	850.9	336.4
100	100	168.8	674.0					800	-200	831.6	382.5
100	150	196.6	715.5	500	-300	470.2	182.1	800	-150	812.3	428.6
100	200	224.5	757.0	500	-250	472.4	232.0	800	-100	793.0	474.7
				500	-200	474.5	282.0	800	-50	773.6	520.8
200	-200	107.2	364.8	500	-150	476.6	331.9	800	0	754.3	567.0
200	-150	130.4	409.1	500	-100	478.7	381.9	800	50	735.0	613.1
200	-100	153.6	453.4	500	-50	480.9	431.8	800	100	715.7	659.2
200	-50	176.8	497.7	500	0	483.0	481.8	800	150	696.4	705.3
200	0	200.0	542.0	500	50	485.1	531.8	800	200	673.2	760.7
200	50	223.2	586.3	500	100	487.3	581.7				
200	100	246.4	630.6	500	150	489.4	631.7	900	-150	910.4	489.9
200	150	269.6	674.9	500	200	491.5	681.6	900	-100	886.0	533.6
200	200	292.8	719.2	500	250	493.6	731.6	900	-50	861.6	577.2
200	250	316.0	763.5	500	300	495.8	781.5	900	0	837.2	620.8
200	300	339.2	807.8					900	50	812.8	664.5
				600	-350	620.1	148.3	900	100	788.3	708.1
300	-250	203.1	271.9	600	-300	614.2	197.9	900	150	763.9	751.7
300	-200	220.5	318.8	600	-250	608.2	247.6	900	200	739.5	795.4
300	-150	237.9	365.7	600	-200	602.3	297.2				
300	-100	255.2	412.5	600	-150	596.3	346.9				
300	-50	272.6	459.4	600	-100	590.4	396.5				
300	0	290.0	506.3	600	-50	584.4	446.2				
300	50	307.4	553.2	600	0	578.5	495.8				
300	100	324.8	600.1	600	50	572.6	545.4				
300	150	342.1	646.9	600	100	566.6	595.1				
300	200	359.5	693.8	600	150	560.7	644.7				
300	250	376.9	740.7	600	200	554.7	694.4				
300	300	394.3	787.6								
				700	-300	745.1	234.6				
400	-300	325.0	191.6	700	-250	732.1	282.8				
400	-250	335.2	240.5	700	-200	719.0	331.1				
400	-200	345.4	289.5	700	-150	706.0	379.4				
400	-150	355.5	338.4	700	-100	693.0	427.7				
400	-100	365.7	387.4	700	-50	679.9	475.9				
400	-50	375.8	436.3	700	0	666.9	524.2				
400	0	386.0	485.4	700	50	653.9	572.5				
400	50	396.2	534.3	700	100	640.8	620.7				

A2.2.3 Measurement points in (x_j, y_j) and its corresponding points in (x, y) for $S = 5.06\%$, $Q = 31.2$ L/s, $z = 100$ mm

x_j (mm)	y_j (mm)	x (mm)	y (mm)	x_j (mm)	y_j (mm)	x (mm)	y (mm)
100	-200	36.4	451.9	500	100	517.9	607.0
100	-100	88.2	537.5	500	150	518.8	657.0
100	-50	114.1	580.2	500	200	519.8	707.0
100	0	140.0	623.0	500	250	520.7	757.0
100	50	165.9	665.8				
100	100	191.8	708.5	600	-300	574.7	809.3
				600	-250	581.4	759.7
200	-200	142.0	394.0	600	-200	588.1	710.2
200	-150	163.2	439.2	600	-150	594.9	660.6
200	-100	184.5	484.5	600	-100	601.6	611.1
200	-50	205.7	529.7	600	-50	608.3	561.5
200	0	227.0	575.0	600	0	615.0	512.0
200	50	248.3	620.3	600	50	621.7	462.5
200	100	269.5	665.5	600	100	628.4	412.9
200	150	290.8	710.8	600	150	635.1	363.4
				600	200	641.9	313.8
				600	250	648.6	264.3
300	-200	255.7	351.0				
300	-150	271.3	398.5				
300	-100	286.8	446.0	700	-300	629.9	820.3
300	-50	302.4	493.5	700	-250	643.7	772.2
300	0	318.0	541.0	700	-200	657.6	724.2
300	50	333.6	588.5	700	-150	671.4	676.1
300	100	349.2	636.0	700	-100	685.3	628.1
300	150	364.7	683.5	700	-50	699.1	580.0
300	200	380.3	731.0	700	0	713.0	532.0
				700	50	726.9	484.0
400	-250	371.5	269.8	700	100	740.7	435.9
400	-200	380.2	319.0	700	150	754.6	387.9
400	-150	388.9	368.3	700	200	768.4	339.8
400	-100	397.6	417.5	700	250	782.3	291.8
400	-50	406.3	466.8				
400	0	415.0	516.0	800	-350	663.7	887.1
400	50	423.7	565.2	800	-300	683.2	841.1
400	100	432.4	614.5	800	-250	702.8	795.1
400	150	441.1	663.7	800	-200	722.4	749.1
400	200	449.8	713.0	800	-150	741.9	703.0
				800	-100	761.5	657.0
500	-250	511.3	257.0	800	-50	781.0	611.0
500	-200	512.2	307.0	800	0	800.6	565.0
500	-150	513.2	357.0	800	50	820.2	519.0
500	-100	514.1	407.0	800	100	839.7	473.0
500	-50	515.1	457.0	800	150	859.3	427.0
500	0	516.0	507.0	800	200	878.8	380.9
500	50	516.9	557.0	800	250	898.4	334.9

A2.2.4 Measurement points in (x_j, y_j) and its corresponding points in (x, y) for $S = 5.06\%$, $Q = 31.2$ L/s, $z = 150$ mm

x_j (mm)	y_j (mm)	x (mm)	y (mm)	x_j (mm)	y_j (mm)	x (mm)	y (mm)
100	-200	36.4	451.9	500	100	517.9	607.0
100	-100	88.2	537.5	500	150	518.8	657.0
100	-50	114.1	580.2	500	200	519.8	707.0
100	0	140.0	623.0	500	250	520.7	757.0
100	50	165.9	665.8				
100	100	191.8	708.5	600	-250	581.4	759.7
				600	-200	588.1	710.2
200	-200	142.0	394.0	600	-150	594.9	660.6
200	-150	163.2	439.2	600	-100	601.6	611.1
200	-100	184.5	484.5	600	-50	608.3	561.5
200	-50	205.7	529.7	600	0	615.0	512.0
200	0	227.0	575.0	600	50	621.7	462.5
200	50	248.3	620.3	600	100	628.4	412.9
200	100	269.5	665.5	600	150	635.1	363.4
200	150	290.8	710.8	600	200	641.9	313.8
				600	250	648.6	264.3
300	-200	255.7	351.0				
300	-150	271.3	398.5	700	-300	629.9	820.3
300	-100	286.8	446.0	700	-250	643.7	772.2
300	-50	302.4	493.5	700	-200	657.6	724.2
300	0	318.0	541.0	700	-150	671.4	676.1
300	50	333.6	588.5	700	-100	685.3	628.1
300	100	349.2	636.0	700	-50	699.1	580.0
300	150	364.7	683.5	700	0	713.0	532.0
300	200	380.3	731.0	700	50	726.9	484.0
				700	100	740.7	435.9
400	-250	371.5	269.8	700	150	754.6	387.9
400	-200	380.2	319.0	700	200	768.4	339.8
400	-150	388.9	368.3	700	250	782.3	291.8
400	-100	397.6	417.5				
400	-50	406.3	466.8	800	-400	644.1	933.1
400	0	415.0	516.0	800	-350	663.7	887.1
400	50	423.7	565.2	800	-300	683.2	841.1
400	100	432.4	614.5	800	-250	702.8	795.1
400	150	441.1	663.7	800	-200	722.4	749.1
400	200	449.8	713.0	800	-150	741.9	703.0
				800	-100	761.5	657.0
500	-250	511.3	257.0	800	-50	781.0	611.0
500	-200	512.2	307.0	800	0	800.6	565.0
500	-150	513.2	357.0	800	50	820.2	519.0
500	-100	514.1	407.0	800	100	839.7	473.0
500	-50	515.1	457.0	800	150	859.3	427.0
500	0	516.0	507.0	800	200	878.8	380.9
500	50	516.9	557.0	800	250	898.4	334.9

A2.2.5 Measurement points in (x_j, y_j) and its corresponding points in (x, y) for $S = 10.52\%$, $Q = 31.2$ L/s, $z = 10$ mm

x_j (mm)	y_j (mm)	x (mm)	y (mm)	x_j (mm)	y_j (mm)	x (mm)	y (mm)
100	-70	74.4	574.0	500	-250	201.1	93.8
100	-40	48.4	559.0	500	-200	233.1	132.2
100	0	109.0	594.0	500	-150	265.1	170.7
100	50	152.3	619.0	500	-100	297.1	209.1
100	100	195.6	644.0	500	-50	329.0	247.6
100	150	238.9	669.0	500	0	361.0	286.0
100	200	282.2	694.0	500	50	393.0	324.4
100	250	325.5	719.0	500	100	424.9	362.9
100	300	368.8	744.0	500	150	456.9	401.3
				500	200	488.9	439.8
200	-140	45.9	431.8	500	250	520.9	478.2
200	-100	79.1	454.1	500	300	552.8	516.7
200	-50	120.5	482.1	500	350	584.8	555.1
200	0	162.0	510.0				
200	50	203.5	537.9	600	-200	329.7	58.6
200	100	244.9	565.9	600	-150	357.3	100.4
200	150	286.4	593.8	600	-100	384.9	142.1
200	200	327.9	621.8	600	-50	412.4	183.8
200	250	369.3	649.7	600	0	440.0	225.5
200	300	410.8	677.6	600	50	467.6	267.2
200	350	452.3	705.6	600	100	495.1	308.9
				600	150	522.7	350.6
300	-200	68.4	304.4	600	200	550.3	392.4
300	-150	107.3	335.8	600	250	577.8	434.1
300	-100	146.2	367.2	600	300	605.4	475.8
300	-50	185.1	398.6				
300	0	224.0	430.0	700	-140	467.7	51.1
300	50	262.9	461.4	700	-100	485.8	86.8
300	100	301.8	492.8	700	-50	508.4	131.4
300	150	340.7	524.2	700	0	531.0	176.0
300	200	379.6	555.6	700	50	553.6	220.6
300	250	418.5	587.0	700	100	576.2	265.2
300	300	457.5	618.4	700	150	598.8	309.8
300	350	496.4	649.8	700	200	621.5	354.4
				700	250	644.1	399.0
400	-190	154.2	221.2	700	300	666.7	443.6
400	-150	182.8	249.1				
400	-100	218.5	284.1	800	-90	589.4	51.1
400	-50	254.3	319.0	800	-50	603.9	88.4
400	0	290.0	354.0	800	0	622.0	135.0
400	50	325.7	389.0	800	50	640.1	181.6
400	100	361.5	423.9	800	100	658.3	228.2
400	150	397.2	458.9	800	150	676.4	274.8
400	200	433.0	493.8	800	200	694.5	321.4
400	250	468.7	528.8	800	250	712.7	368.0
400	300	504.5	563.8	800	300	730.8	414.6
400	350	540.2	598.7				

A2.2.6 Measurement points in (x_j, y_j) and its corresponding points in (x, y) for $S = 10.52\%$, $Q = 31.2$ L/s, $z = 70$ mm

x_j (mm)	y_j (mm)	x (mm)	y (mm)	x_j (mm)	y_j (mm)	x (mm)	y (mm)
100	-100	40.9	537.9	500	-290	167.8	113.7
100	-50	78.0	571.4	500	-250	197.5	140.5
100	0	115.1	604.9	500	-200	234.6	174.0
100	50	152.3	638.4	500	-150	271.7	207.5
100	100	189.4	671.9	500	-100	308.8	240.9
100	150	226.5	705.4	500	-50	346.0	274.4
100	200	263.6	738.9	500	0	383.1	307.9
100	250	300.8	772.4	500	50	420.2	341.4
100	300	337.9	805.9	500	100	457.3	374.9
				500	150	494.5	408.4
200	-150	70.8	430.2	500	200	531.6	441.9
200	-100	107.9	463.7	500	250	568.7	475.4
200	-50	145.0	497.2	500	300	605.8	508.9
200	0	182.1	530.7	500	350	643.0	542.4
200	50	219.2	564.2	500	400	680.1	575.9
200	100	256.4	597.7				
200	150	293.5	631.2	600	-250	264.5	66.2
200	200	330.6	664.6	600	-200	301.6	99.7
200	250	367.7	698.1	600	-150	338.7	133.2
200	300	404.9	731.6	600	-100	375.8	166.7
200	350	442.0	765.1	600	-50	413.0	200.2
				600	0	450.1	233.7
300	-250	63.5	289.0	600	50	487.2	267.2
300	-200	100.6	322.5	600	100	524.3	300.7
300	-150	137.7	355.9	600	150	561.4	334.2
300	-100	174.9	389.4	600	200	598.6	367.7
300	-50	212.0	422.9	600	250	635.7	401.2
300	0	249.1	456.4	600	300	672.8	434.6
300	50	286.2	489.9				
300	100	323.4	523.4	700	-150	405.7	59.0
300	150	360.5	556.9	700	-100	442.8	92.5
300	200	397.6	590.4	700	-50	479.9	125.9
300	250	434.7	623.9	700	0	517.1	159.4
300	300	471.9	657.4	700	50	554.2	192.9
300	350	509.0	690.9	700	100	591.3	226.4
				700	150	628.4	259.9
400	-200	167.6	248.2	700	200	665.6	293.4
400	-150	204.7	281.7	700	250	702.7	326.9
400	-100	241.9	315.2	700	300	739.8	360.4
400	-50	279.0	348.7				
400	0	316.1	382.2	800	-50	621.2	118.7
400	50	353.2	415.7	800	0	584.1	85.2
400	100	390.3	449.2	800	50	621.2	118.7
400	150	427.5	482.7	800	100	658.3	152.2
400	200	464.6	516.2	800	150	695.4	185.7
400	250	501.7	549.6	800	200	732.5	219.2
400	300	538.8	583.1	800	250	769.7	252.7
400	350	576.0	616.6	800	300	806.8	286.2
				800	350	843.9	319.6

A2.2.7 Processed mean velocity and turbulence data in jet flow for $S = 5.06\%$,

$Q = 31.2$ L/s, $z = 10$ mm

x_j (mm)	y_j (mm)	u (m/s)	v (m/s)	w (m/s)	$\sqrt{u'^2}$ (m/s)	$\sqrt{v'^2}$ (m/s)	$\sqrt{w'^2}$ (m/s)	$-\overline{u'v'}$ (m ² /s ²)	$-\overline{u'w'}$ (m ² /s ²)	$-\overline{v'w'}$ (m ² /s ²)
100	-130	-0.055	0.114	-0.0003	0.081	0.092	0.034	0.001926	0.000527	0.000348
100	-100	-0.012	0.103	0.0126	0.089	0.099	0.037	0.001581	0.000235	-0.000039
100	-50	0.421	-0.065	-0.0104	0.325	0.224	0.069	0.044630	-0.006564	0.004078
100	0	0.975	-0.234	-0.0057	0.153	0.311	0.116	-0.013291	-0.001777	-0.006073
100	50	0.495	-0.030	-0.0582	0.302	0.161	0.086	-0.023120	0.008214	0.002238
100	100	0.181	-0.011	-0.0068	0.099	0.081	0.039	-0.001195	0.000289	0.000205
100	150	0.183	0.025	0.0011	0.095	0.082	0.034	-0.002683	0.000161	0.000246
100	200	0.160	0.026	0.0080	0.106	0.100	0.034	-0.005451	-0.000129	-0.000036
200	-200	-0.018	0.130	0.0032	0.118	0.107	0.037	-0.001494	-0.000051	-0.000023
200	-150	0.010	0.092	0.0066	0.123	0.124	0.040	0.001628	-0.000405	-0.000008
200	-100	0.248	-0.027	0.0158	0.232	0.206	0.047	0.027276	-0.000837	0.000588
200	-50	0.629	-0.137	-0.0013	0.275	0.228	0.083	0.031364	-0.004500	0.002967
200	0	0.804	-0.130	-0.0126	0.268	0.202	0.094	-0.007429	-0.001113	-0.002274
200	50	0.597	0.020	-0.0504	0.294	0.181	0.095	-0.022607	0.005621	0.000316
200	100	0.243	0.039	-0.0055	0.167	0.144	0.048	-0.010602	0.000669	0.000522
200	150	0.133	-0.003	0.0183	0.120	0.114	0.038	-0.004082	-0.000848	-0.000578
200	200	0.095	-0.055	0.0120	0.123	0.124	0.035	-0.006636	-0.000700	-0.000821
200	250	0.048	-0.092	0.0086	0.123	0.125	0.038	-0.007481	-0.000650	-0.000665
200	300	-0.040	-0.140	0.0044	0.133	0.134	0.039	-0.009104	-0.000203	-0.000203
300	-250	-0.032	0.100	-0.0017	0.137	0.106	0.038	-0.001332	-0.000411	0.000070
300	-200	0.050	0.057	0.0043	0.156	0.154	0.045	0.005983	-0.000753	0.000190
300	-150	0.171	-0.008	0.0063	0.199	0.195	0.046	0.018523	-0.000809	0.000387
300	-100	0.407	-0.107	0.0059	0.255	0.219	0.066	0.028675	-0.001871	0.000865
300	-50	0.609	-0.121	-0.0030	0.241	0.205	0.088	0.018165	-0.002941	0.001651
300	0	0.724	-0.094	-0.0148	0.241	0.183	0.085	0.001103	-0.000362	-0.000167
300	50	0.664	0.041	-0.0369	0.271	0.171	0.081	-0.013353	0.002927	0.000171
300	100	0.457	0.109	-0.0293	0.242	0.181	0.079	-0.020882	0.001993	0.000795
300	150	0.194	0.031	0.0042	0.142	0.154	0.047	-0.007790	-0.000177	0.000305
300	200	0.102	-0.056	0.0100	0.130	0.156	0.044	-0.006619	-0.000245	-0.000347
300	250	0.029	-0.118	0.0036	0.133	0.146	0.040	-0.006653	-0.000089	-0.000261
300	300	-0.072	-0.158	0.0021	0.135	0.140	0.042	-0.008070	0.000056	0.000116
400	-300	-0.073	0.044	0.0026	0.183	0.124	0.043	0.003917	-0.000465	0.000253
400	-250	0.021	0.033	0.0016	0.172	0.144	0.046	0.007572	-0.000717	0.000509
400	-200	0.140	-0.001	0.0021	0.188	0.178	0.050	0.014760	-0.000872	0.000804
400	-150	0.297	-0.052	0.0037	0.213	0.201	0.055	0.021365	-0.001432	0.000868
400	-100	0.449	-0.097	0.0048	0.226	0.201	0.066	0.021455	-0.001862	0.001150
400	-50	0.613	-0.104	-0.0045	0.215	0.191	0.076	0.014826	-0.001922	0.001100

**A2.2.7 Processed mean velocity and turbulence data in jet flow for $S = 5.06\%$,
 $Q = 31.2$ L/s, $z = 10$ mm (cont'd)**

x_j (mm)	y_j (mm)	u (m/s)	v (m/s)	w (m/s)	$\sqrt{u'^2}$ (m/s)	$\sqrt{v'^2}$ (m/s)	$\sqrt{w'^2}$ (m/s)	$-\overline{u'v'}$ (m ² /s ²)	$-\overline{u'w'}$ (m ² /s ²)	$-\overline{v'w'}$ (m ² /s ²)
400	0	0.701	-0.037	-0.0142	0.225	0.169	0.076	0.004065	-0.000852	0.000524
400	50	0.679	0.040	-0.0221	0.238	0.167	0.075	-0.004587	0.000321	-0.000012
400	100	0.553	0.122	-0.0181	0.230	0.177	0.069	-0.013668	0.000352	-0.000011
400	150	0.348	0.090	-0.0005	0.189	0.189	0.060	-0.016473	-0.000245	0.000262
400	200	0.180	-0.003	0.0090	0.163	0.188	0.052	-0.012853	-0.000877	-0.000469
400	250	0.006	-0.097	0.0027	0.169	0.170	0.049	-0.012831	-0.000145	-0.000202
400	300	-0.098	-0.136	0.0016	0.164	0.167	0.049	-0.012543	0.000346	0.000072
500	-300	-0.078	-0.027	0.0070	0.219	0.157	0.052	0.013744	-0.000594	0.000879
500	-250	0.048	-0.037	0.0041	0.218	0.177	0.053	0.017553	-0.000734	0.001069
500	-200	0.182	-0.058	0.0062	0.194	0.184	0.056	0.016869	-0.001687	0.001702
500	-150	0.352	-0.115	0.0094	0.207	0.202	0.059	0.020930	-0.001070	0.001276
500	-100	0.444	-0.117	0.0037	0.213	0.199	0.063	0.018617	-0.001113	0.001323
500	-50	0.592	-0.124	-0.0013	0.193	0.188	0.071	0.012510	-0.000366	0.001232
500	0	0.696	-0.093	-0.0093	0.201	0.178	0.069	0.007942	0.000293	0.000860
500	50	0.668	-0.025	-0.0126	0.211	0.164	0.068	0.000612	0.000987	0.000070
500	100	0.598	0.031	-0.0101	0.243	0.168	0.059	-0.007912	0.001334	0.000045
500	150	0.448	0.053	-0.0024	0.223	0.180	0.060	-0.017925	0.000745	0.000476
500	200	0.230	-0.005	0.0061	0.221	0.187	0.054	-0.020986	0.000228	0.000326
500	250	0.002	-0.081	0.0062	0.203	0.168	0.050	-0.013641	0.000095	0.000371
500	300	-0.143	-0.107	0.0049	0.193	0.165	0.049	-0.013052	0.000610	0.000544
600	-350	-0.117	-0.036	0.0082	0.210	0.164	0.052	0.014173	-0.000063	0.000663
600	-300	0.054	-0.060	0.0088	0.221	0.178	0.056	0.017610	-0.000916	0.000819
600	-250	0.214	-0.087	0.0081	0.225	0.184	0.058	0.017438	-0.000524	0.001262
600	-200	0.321	-0.095	0.0049	0.195	0.181	0.061	0.015046	-0.000750	0.001300
600	-150	0.459	-0.116	0.0016	0.200	0.195	0.065	0.017230	-0.000476	0.001283
600	-100	0.573	-0.108	-0.0022	0.182	0.183	0.067	0.012747	0.000196	0.000839
600	-50	0.658	-0.074	-0.0057	0.193	0.180	0.063	0.011261	0.000416	0.000275
600	0	0.666	-0.031	-0.0062	0.192	0.173	0.061	0.003361	0.000725	0.000284
600	50	0.643	0.010	-0.0039	0.211	0.170	0.058	-0.005018	0.000607	-0.000164
600	100	0.500	0.031	0.0016	0.223	0.175	0.061	-0.012072	0.000610	0.000090
600	150	0.273	-0.003	0.0068	0.244	0.183	0.057	-0.021160	0.000029	0.000219
600	200	0.045	-0.043	0.0060	0.236	0.173	0.055	-0.016164	-0.000904	-0.000043
700	-300	-0.016	-0.056	0.0146	0.224	0.160	0.057	0.011750	0.000389	0.000698
700	-250	0.152	-0.060	0.0089	0.211	0.176	0.058	0.014701	-0.000167	0.000963
700	-200	0.274	-0.055	0.0066	0.212	0.195	0.065	0.017546	-0.000410	0.001426
700	-150	0.398	-0.091	0.0072	0.191	0.187	0.065	0.016297	-0.000406	0.001435
700	-100	0.510	-0.081	0.0008	0.187	0.188	0.063	0.014647	0.000282	0.001058

**A2.2.7 Processed mean velocity and turbulence data in jet flow for $S = 5.06\%$,
 $Q = 31.2$ L/s, $z = 10$ mm (cont'd)**

x_j (mm)	y_j (mm)	u (m/s)	v (m/s)	w (m/s)	$\sqrt{u'^2}$ (m/s)	$\sqrt{v'^2}$ (m/s)	$\sqrt{w'^2}$ (m/s)	$-\overline{u'v'}$ (m ² /s ²)	$-\overline{u'w'}$ (m ² /s ²)	$-\overline{v'w'}$ (m ² /s ²)
700	-50	0.610	-0.060	0.0003	0.192	0.193	0.059	0.013238	0.000737	0.000460
700	0	0.636	-0.026	-0.0003	0.197	0.182	0.054	0.006384	0.000709	-0.000190
700	50	0.578	-0.013	0.0043	0.217	0.176	0.052	-0.002020	0.000549	0.000082
700	100	0.442	-0.008	0.0085	0.234	0.164	0.055	-0.009392	0.000190	-0.000065
700	150	0.188	-0.003	0.0106	0.261	0.171	0.056	-0.010572	-0.000862	-0.000070
700	200	0.009	-0.018	0.0065	0.261	0.154	0.055	-0.013390	-0.000698	-0.000101
700	250	-0.177	-0.002	0.0056	0.221	0.155	0.054	-0.010794	0.000336	0.000263
800	-250	-0.036	-0.024	0.0171	0.264	0.172	0.063	0.019346	0.002901	0.000442
800	-200	0.174	-0.042	0.0138	0.256	0.183	0.066	0.023879	0.001761	0.000705
800	-150	0.324	-0.047	0.0090	0.220	0.196	0.063	0.020717	0.000139	0.001073
800	-100	0.441	-0.013	0.0060	0.198	0.201	0.061	0.018714	0.000650	0.000583
800	-50	0.573	-0.023	0.0063	0.187	0.191	0.058	0.011711	0.000756	0.000237
800	0	0.579	0.014	0.0076	0.181	0.193	0.051	0.008664	0.000341	-0.000422
800	50	0.549	0.010	0.0069	0.206	0.184	0.052	0.003861	-0.000059	-0.000297
800	100	0.381	0.032	0.0111	0.247	0.189	0.049	-0.001759	-0.000228	-0.000558
800	150	0.168	0.028	0.0097	0.250	0.172	0.055	-0.006385	-0.001165	-0.000163
800	200	-0.039	0.067	0.0067	0.247	0.180	0.056	-0.007583	-0.000278	-0.000387
900	-150	-0.044	0.076	-0.0055	0.296	0.224	0.077	0.040202	-0.003621	0.003085
900	-100	0.348	0.106	0.0122	0.242	0.227	0.069	0.026358	0.002037	0.000192
900	-50	0.475	0.113	0.0123	0.210	0.213	0.060	0.020311	0.000985	0.000164
900	0	0.535	0.060	0.0123	0.182	0.194	0.050	0.010400	0.000318	-0.000293
900	50	0.486	0.074	0.0143	0.188	0.186	0.048	0.002316	-0.000230	-0.000637
900	100	0.316	0.080	0.0148	0.215	0.182	0.050	-0.003601	-0.001243	-0.000691
900	150	0.119	0.090	0.0071	0.230	0.160	0.059	-0.006465	-0.001579	-0.000864
900	200	-0.087	0.119	0.0115	0.238	0.162	0.060	-0.006593	-0.000093	-0.000376

**A2.2.8 Processed mean velocity and turbulence data in jet flow for $S = 5.06\%$,
 $Q = 31.2$ L/s, $z = 100$ mm**

x_j (mm)	y_j (mm)	u (m/s)	v (m/s)	w (m/s)	$\sqrt{u'^2}$ (m/s)	$\sqrt{v'^2}$ (m/s)	$\sqrt{w'^2}$ (m/s)	$-\overline{u'v'}$ (m ² /s ²)	$-\overline{u'w'}$ (m ² /s ²)	$-\overline{v'w'}$ (m ² /s ²)
100	-200	-0.1049	0.1454	-0.0068	0.0737	0.0798	0.0746	0.000078	0.001331	0.000297
100	-100	0.0353	0.1092	0.0042	0.1083	0.0921	0.0705	0.001544	0.000136	0.000220
100	-50	0.9022	0.0734	0.0330	0.2997	0.2251	0.1767	0.027105	-0.003055	-0.001225
100	0	1.1661	0.1866	-0.0022	0.1673	0.2247	0.1680	-0.011907	-0.004115	-0.002636
100	50	0.1389	-0.0594	-0.0711	0.1849	0.1279	0.0990	-0.009203	0.002048	0.001750
100	100	-0.0234	-0.1170	-0.0153	0.0919	0.1036	0.1013	-0.001050	0.000565	0.002138
200	-200	-0.0778	0.1185	-0.0164	0.1199	0.1004	0.0932	0.000123	-0.001058	-0.000168
200	-150	0.0169	0.1179	-0.0135	0.1405	0.1177	0.1081	0.003875	-0.000392	0.000006
200	-100	0.2284	0.1189	-0.0082	0.2351	0.1558	0.1223	0.015450	-0.001978	0.000778
200	-50	0.7423	0.0937	-0.0105	0.3299	0.1962	0.1637	0.031562	-0.003464	0.000710
200	0	1.0437	0.1848	-0.0185	0.2571	0.1925	0.1430	-0.004332	-0.003414	-0.001458
200	50	0.5799	0.1017	-0.0662	0.3280	0.2115	0.1571	-0.044906	0.003214	0.002633
200	100	0.0847	-0.0900	-0.0021	0.1264	0.1459	0.1158	-0.005046	0.001564	0.004527
200	150	0.0147	-0.1311	0.0392	0.1016	0.1188	0.1085	-0.000987	-0.000733	0.001205
300	-200	-0.0040	0.1157	-0.0179	0.1527	0.1241	0.1162	0.003927	-0.001551	-0.000130
300	-150	0.1185	0.1185	-0.0166	0.1734	0.1401	0.1259	0.007497	-0.001676	-0.000335
300	-100	0.3081	0.1172	-0.0283	0.2500	0.1770	0.1403	0.020112	-0.000517	-0.000168
300	-50	0.6513	0.0470	-0.0273	0.3190	0.2231	0.1626	0.030595	-0.001991	0.001334
300	0	0.9125	0.1002	-0.0245	0.2880	0.2042	0.1481	0.007811	-0.002485	-0.001785
300	50	0.7037	0.0881	-0.0562	0.3191	0.2086	0.1508	-0.035909	0.000376	0.000427
300	100	0.2812	-0.0095	-0.0146	0.2128	0.1812	0.1268	-0.021124	0.005559	0.004929
300	150	0.0644	-0.1160	0.0227	0.1274	0.1407	0.1199	-0.004620	0.000008	0.002070
300	200	-0.0127	-0.1588	0.0164	0.1262	0.1316	0.1111	-0.004831	-0.001376	0.000602
400	-250	-0.0258	0.0726	-0.0066	0.1792	0.1456	0.1291	0.007176	-0.000868	0.000695
400	-200	0.0840	0.0824	-0.0104	0.2037	0.1574	0.1420	0.011934	-0.001386	0.000101
400	-150	0.1789	0.1169	-0.0297	0.2013	0.1474	0.1432	0.011729	-0.001352	0.000102
400	-100	0.4004	0.0408	-0.0356	0.2652	0.2207	0.1494	0.027208	-0.001737	0.001313
400	-50	0.5552	0.0788	-0.0280	0.2844	0.2199	0.1533	0.026295	0.000378	0.001245
400	0	0.7686	0.0458	-0.0287	0.2960	0.2169	0.1455	0.010389	-0.000980	-0.000541
400	50	0.6947	0.0433	-0.0387	0.2838	0.2055	0.1480	-0.022126	0.002200	0.000919
400	100	0.4185	-0.0016	0.0001	0.2535	0.1899	0.1330	-0.026428	0.004619	0.002980
400	150	0.1397	-0.0961	0.0249	0.1642	0.1521	0.1259	-0.008663	0.000662	0.001380
400	200	0.0173	-0.1301	0.0166	0.1586	0.1472	0.1274	-0.007382	0.000093	0.001045
500	-250	-0.0091	0.0477	0.0091	0.1972	0.1660	0.1435	0.011880	-0.001493	-0.000298
500	-200	0.1224	0.0422	-0.0038	0.2154	0.1874	0.1548	0.016099	-0.003751	-0.000516
500	-150	0.2472	0.0567	-0.0266	0.2212	0.1811	0.1593	0.015651	-0.001123	-0.000261
500	-100	0.4295	0.0230	-0.0242	0.2470	0.2062	0.1549	0.021840	-0.000858	0.000389
500	-50	0.6031	0.0223	-0.0225	0.2642	0.2223	0.1541	0.027027	-0.001154	0.001996
500	0	0.7458	0.0282	-0.0135	0.2577	0.2149	0.1405	0.013918	0.000424	0.000064
500	50	0.7236	0.0263	-0.0086	0.2704	0.1961	0.1334	-0.008893	0.001634	-0.000437

**A2.2.8 Processed mean velocity and turbulence data in jet flow for $S = 5.06\%$,
 $Q = 31.2$ L/s, $z = 100$ mm (cont'd)**

x_j (mm)	y_j (mm)	u (m/s)	v (m/s)	w (m/s)	$\sqrt{u'^2}$ (m/s)	$\sqrt{v'^2}$ (m/s)	$\sqrt{w'^2}$ (m/s)	$-\overline{u'v'}$ (m ² /s ²)	$-\overline{u'w'}$ (m ² /s ²)	$-\overline{v'w'}$ (m ² /s ²)
500	100	0.4680	-0.0128	0.0041	0.2570	0.1800	0.1304	-0.020613	0.002438	0.001380
500	150	0.2265	-0.0703	0.0191	0.2031	0.1637	0.1343	-0.014513	0.000646	0.001721
500	200	0.0159	-0.1074	0.0135	0.1711	0.1437	0.1361	-0.006465	-0.000241	0.000651
500	250	-0.1104	-0.1090	-0.0181	0.1639	0.1356	0.1335	-0.005446	-0.001533	0.000568
600	-300	-0.0605	0.0118	0.0346	0.2167	0.1699	0.1524	0.010672	-0.002635	0.001509
600	-250	0.0464	0.0199	0.0172	0.2094	0.1738	0.1610	0.011346	-0.002546	0.000597
600	-200	0.1670	0.0149	0.0036	0.2057	0.1891	0.1677	0.013070	-0.002348	-0.000006
600	-150	0.3006	0.0106	-0.0031	0.2405	0.1957	0.1654	0.019880	-0.000322	-0.000074
600	-100	0.4381	0.0241	-0.0176	0.2452	0.2064	0.1638	0.021098	0.001659	0.001031
600	-50	0.5996	0.0191	-0.0145	0.2500	0.2136	0.1459	0.021477	0.000224	0.001157
600	0	0.6923	0.0182	-0.0112	0.2389	0.2007	0.1352	0.008693	0.000790	0.000501
600	50	0.6347	0.0137	0.0057	0.2580	0.1935	0.1272	-0.000800	0.002573	0.000675
600	100	0.4645	-0.0112	0.0218	0.2430	0.1826	0.1291	-0.014848	0.002326	0.000973
600	150	0.2136	-0.0269	0.0205	0.2167	0.1681	0.1366	-0.007029	-0.001348	0.001056
600	200	0.0568	-0.0423	0.0157	0.1881	0.1581	0.1470	-0.007069	-0.001165	0.000409
600	250	-0.1311	-0.0529	-0.0133	0.1808	0.1405	0.1489	-0.004078	-0.001484	0.000309
700	-300	-0.0100	-0.0306	0.0768	0.1836	0.1770	0.1524	0.006843	0.001205	0.002538
700	-250	0.0956	-0.0297	0.0563	0.2085	0.1836	0.1734	0.008524	0.001482	0.000877
700	-200	0.2058	-0.0155	0.0423	0.2354	0.1953	0.1804	0.014735	0.001065	0.001392
700	-150	0.3084	0.0090	0.0201	0.2233	0.1929	0.1742	0.014788	0.001178	-0.001003
700	-100	0.4396	0.0202	0.0165	0.2332	0.1977	0.1669	0.018587	0.001040	0.000021
700	-50	0.5611	0.0322	0.0072	0.2385	0.2033	0.1528	0.019575	0.000769	0.000726
700	0	0.6478	0.0355	0.0083	0.2188	0.2020	0.1327	0.011887	0.000559	0.000546
700	50	0.5822	0.0530	0.0204	0.2318	0.2028	0.1279	0.004736	0.001663	-0.000163
700	100	0.3973	0.0496	0.0288	0.2465	0.1953	0.1364	-0.002085	0.000102	-0.000616
700	150	0.1969	0.0382	0.0212	0.2142	0.1850	0.1411	-0.004197	-0.003167	0.001151
700	200	-0.0045	0.0987	-0.0030	0.1829	0.1923	0.1478	-0.001358	-0.001453	-0.001853
700	250	-0.1508	0.0576	-0.0188	0.1807	0.1631	0.1458	-0.005764	-0.002051	-0.001201
800	-350	-0.0188	-0.0606	0.0161	0.1591	0.1793	0.1333	0.001894	-0.000967	0.004710
800	-300	0.0320	-0.0382	0.0344	0.1804	0.2050	0.1510	0.004401	0.000542	0.003473
800	-250	0.1231	-0.0353	0.0453	0.2032	0.2089	0.1696	0.012534	-0.001117	0.005301
800	-200	0.1953	-0.0303	0.0512	0.2150	0.2075	0.1763	0.014799	-0.002450	0.003878
800	-150	0.3026	0.0060	0.0653	0.2246	0.2163	0.1839	0.015331	-0.000794	-0.001420
800	-100	0.4087	0.0370	0.0417	0.2226	0.2088	0.1698	0.016337	-0.000153	-0.002207
800	-50	0.5258	0.0501	0.0453	0.2182	0.1985	0.1587	0.015410	0.003067	-0.002530
800	0	0.5905	0.0649	0.0370	0.2007	0.2009	0.1365	0.010652	0.000359	-0.001220
800	50	0.5593	0.0685	0.0265	0.1913	0.1883	0.1239	0.004415	-0.000664	0.000343
800	100	0.3955	0.0772	0.0294	0.2017	0.1877	0.1321	-0.000254	-0.002628	0.000629
800	150	0.2200	0.0786	0.0138	0.1999	0.1726	0.1418	-0.005185	-0.003553	0.000652
800	200	0.0379	0.1017	0.0000	0.1914	0.1627	0.1467	-0.004895	-0.003259	-0.000220
800	250	-0.1291	0.1408	-0.0085	0.1905	0.1587	0.1486	-0.004819	-0.005143	-0.000582

A2.2.9 Processed mean velocity and turbulence data in jet flow for $S = 5.06\%$,

$Q = 31.2$ L/s, $z = 150$ mm

x_j (mm)	y_j (mm)	u (m/s)	v (m/s)	w (m/s)	$\sqrt{u'^2}$ (m/s)	$\sqrt{v'^2}$ (m/s)	$\sqrt{w'^2}$ (m/s)	$-\overline{u'v'}$ (m ² /s ²)	$-\overline{u'w'}$ (m ² /s ²)	$-\overline{v'w'}$ (m ² /s ²)
100	-200	-0.0999	0.1359	0.0079	0.0711	0.0792	0.0786	0.000577	-0.000265	0.000471
100	-100	0.0709	0.0953	0.0040	0.1074	0.0903	0.0789	0.001949	0.000100	0.000293
100	-50	0.9898	0.0554	0.0139	0.2576	0.1835	0.1666	0.017792	0.002061	-0.000445
100	0	1.1671	0.1830	0.0216	0.1641	0.2055	0.1523	-0.010407	-0.003591	-0.001892
100	50	0.1580	-0.0499	-0.0592	0.1951	0.1469	0.1256	-0.011023	0.000333	0.000558
100	100	-0.0441	-0.1454	-0.0230	0.1057	0.0984	0.1064	-0.001305	-0.001065	0.000385
200	-200	-0.0623	0.1045	-0.0272	0.1071	0.1052	0.0926	0.001255	-0.000151	-0.000041
200	-150	0.0474	0.1002	-0.0461	0.1347	0.1139	0.1074	0.003709	0.001863	-0.000209
200	-100	0.2788	0.1014	-0.0155	0.2433	0.1510	0.1277	0.015920	0.001693	0.000254
200	-50	0.8213	0.0647	0.0199	0.3232	0.1931	0.1599	0.029027	0.003305	-0.000433
200	0	1.0585	0.1396	0.0205	0.2669	0.1938	0.1436	-0.015411	-0.004881	-0.001994
200	50	0.5448	0.0687	-0.0509	0.3186	0.2077	0.1694	-0.042267	0.001337	0.000609
200	100	0.0938	-0.1025	-0.0060	0.1283	0.1359	0.1260	-0.005022	0.000108	0.002091
200	150	-0.0013	-0.1501	0.0227	0.1139	0.1230	0.1167	-0.001864	-0.001071	0.000730
300	-200	-0.0401	0.1139	-0.0286	0.1244	0.1176	0.1153	0.002434	-0.000579	-0.000174
300	-150	0.1196	0.1151	-0.0371	0.1925	0.1431	0.1305	0.010174	0.002516	-0.000532
300	-100	0.4114	0.0688	-0.0179	0.3053	0.2164	0.1501	0.036315	0.002214	0.001147
300	-50	0.7493	-0.0066	0.0063	0.3143	0.2262	0.1583	0.028045	0.001070	-0.000199
300	0	0.9590	0.0588	0.0120	0.2810	0.1964	0.1521	-0.001778	-0.003835	-0.002613
300	50	0.6674	0.0375	-0.0400	0.3093	0.1763	0.1614	-0.031763	0.002502	-0.000323
300	100	0.2731	-0.0522	-0.0077	0.2059	0.1721	0.1349	-0.018480	0.002921	0.001879
300	150	0.0537	-0.1242	0.0211	0.1331	0.1403	0.1312	-0.004697	-0.002495	-0.000183
300	200	-0.0311	-0.1618	0.0140	0.1238	0.1320	0.1170	-0.003633	-0.002398	0.000031
400	-250	-0.0992	0.1007	-0.0170	0.1532	0.1285	0.1238	0.004181	-0.000251	-0.000068
400	-200	0.0100	0.1001	-0.0280	0.1753	0.1381	0.1358	0.007383	-0.001056	-0.001600
400	-150	0.1766	0.1142	-0.0386	0.2262	0.1671	0.1425	0.017169	0.001177	-0.000827
400	-100	0.4689	0.0027	-0.0181	0.2859	0.2217	0.1452	0.029361	-0.000982	0.002055
400	-50	0.7054	-0.0007	0.0013	0.3078	0.2221	0.1490	0.028833	0.002166	-0.000199
400	0	0.8448	0.0133	0.0065	0.2831	0.2069	0.1495	0.004494	-0.000375	-0.002360
400	50	0.6980	0.0066	-0.0029	0.3076	0.1917	0.1521	-0.027717	0.000338	-0.001507
400	100	0.3679	-0.0470	0.0134	0.2388	0.1766	0.1416	-0.022967	0.002399	0.001295
400	150	0.1344	-0.1030	0.0203	0.1615	0.1523	0.1371	-0.008473	-0.003670	-0.000608
400	200	-0.0140	-0.1394	0.0115	0.1424	0.1429	0.1351	-0.004410	-0.002246	0.000162
500	-250	-0.0908	0.0801	-0.0027	0.1735	0.1523	0.1361	0.007200	-0.002364	-0.000596
500	-200	0.0670	0.0693	-0.0350	0.2210	0.1869	0.1657	0.017540	-0.000237	-0.000606
500	-150	0.2405	0.0556	-0.0329	0.2490	0.1996	0.1576	0.025000	0.001345	0.000160
500	-100	0.4914	-0.0040	-0.0250	0.2707	0.2306	0.1602	0.032755	0.002180	0.000806
500	-50	0.6632	-0.0097	0.0060	0.2833	0.2268	0.1500	0.028512	0.000391	0.000256
500	0	0.7966	-0.0231	0.0014	0.2557	0.2010	0.1388	0.006081	-0.000578	-0.001756
500	50	0.6742	-0.0165	0.0132	0.2862	0.1847	0.1365	-0.012232	0.000242	-0.001350

**A2.2.9 Processed mean velocity and turbulence data in jet flow for $S = 5.06\%$,
 $Q = 31.2$ L/s, $z = 150$ mm (cont'd)**

x_j (mm)	y_j (mm)	u (m/s)	v (m/s)	w (m/s)	$\sqrt{u'^2}$ (m/s)	$\sqrt{v'^2}$ (m/s)	$\sqrt{w'^2}$ (m/s)	$-\overline{u'v'}$ (m ² /s ²)	$-\overline{u'w'}$ (m ² /s ²)	$-\overline{v'w'}$ (m ² /s ²)
500	100	0.4489	-0.0336	0.0224	0.2511	0.1741	0.1458	-0.019384	-0.002005	-0.001200
500	150	0.1745	-0.0659	0.0213	0.1842	0.1579	0.1450	-0.010074	-0.003226	0.000210
500	200	-0.0109	-0.0973	-0.0007	0.1531	0.1459	0.1489	-0.004960	-0.003632	-0.000069
500	250	-0.1549	-0.0829	-0.0204	0.1527	0.1465	0.1368	-0.002954	-0.002564	-0.000397
600	-250	-0.0316	0.0372	0.0145	0.1876	0.1749	0.1655	0.010598	0.001892	0.000135
600	-200	0.1007	0.0404	-0.0155	0.2176	0.1953	0.1680	0.018152	0.002220	-0.001099
600	-150	0.3305	-0.0088	-0.0074	0.2704	0.2166	0.1760	0.030487	0.004043	-0.000806
600	-100	0.4809	-0.0052	0.0045	0.2675	0.2226	0.1673	0.028176	0.004257	0.000581
600	-50	0.6357	-0.0171	0.0128	0.2563	0.2251	0.1520	0.022139	0.002578	0.001031
600	0	0.7276	-0.0107	0.0202	0.2531	0.2105	0.1361	0.013584	0.001544	-0.001274
600	50	0.6576	-0.0217	0.0295	0.2523	0.1870	0.1342	-0.005552	-0.000466	-0.001321
600	100	0.4557	-0.0129	0.0313	0.2317	0.1687	0.1394	-0.009987	-0.001772	0.000669
600	150	0.2066	-0.0337	0.0173	0.1892	0.1537	0.1495	-0.008334	-0.003543	0.000163
600	200	0.0140	-0.0292	-0.0037	0.1722	0.1634	0.1495	-0.003049	-0.003102	0.000824
600	250	-0.1579	-0.0302	-0.0260	0.1636	0.1441	0.1462	-0.002662	-0.002162	-0.000262
700	-300	0.0042	0.0042	0.0594	0.1853	0.1790	0.1715	0.007075	0.001930	0.000664
700	-250	0.0874	0.0011	0.0561	0.2011	0.1850	0.1805	0.008287	0.001635	-0.000517
700	-200	0.2022	-0.0005	0.0246	0.2260	0.2016	0.1865	0.015838	0.005607	-0.001347
700	-150	0.3116	-0.0004	0.0170	0.2472	0.2046	0.1829	0.022041	0.005338	-0.001401
700	-100	0.4590	0.0047	0.0195	0.2552	0.2076	0.1650	0.021877	0.002968	0.000294
700	-50	0.6087	-0.0041	0.0263	0.2419	0.2094	0.1466	0.019006	0.002874	0.000063
700	0	0.6625	0.0181	0.0293	0.2280	0.2006	0.1348	0.010756	0.000945	-0.000850
700	50	0.5585	0.0463	0.0343	0.2303	0.1902	0.1330	0.003692	-0.002003	-0.001034
700	100	0.4061	0.0495	0.0320	0.2133	0.1813	0.1399	-0.000815	-0.002254	0.000140
700	150	0.2185	0.0404	0.0084	0.1944	0.1681	0.1522	-0.006722	-0.004537	-0.000956
700	200	0.0075	0.0536	-0.0119	0.1615	0.1642	0.1539	-0.004823	-0.001365	0.000275
700	250	-0.1816	0.0493	-0.0378	0.1664	0.1439	0.1530	-0.004201	-0.003884	0.000515
800	-400	0.0172	-0.0187	-0.0158	0.1605	0.1723	0.1318	-0.006913	0.000359	0.001347
800	-350	0.0490	-0.0494	0.0130	0.1644	0.1814	0.1572	-0.000790	-0.001022	0.001532
800	-300	0.0777	-0.0769	0.0235	0.1863	0.1780	0.1645	0.002546	0.000781	0.000080
800	-250	0.1424	-0.0482	0.0342	0.1984	0.1935	0.1682	0.006013	0.000547	0.000487
800	-200	0.2145	-0.0434	0.0402	0.2237	0.1964	0.1913	0.010983	0.001924	-0.001263
800	-150	0.2874	-0.0393	0.0372	0.2259	0.1903	0.1749	0.013260	0.002550	-0.002072
800	-100	0.4117	0.0091	0.0275	0.2389	0.1995	0.1611	0.016982	0.002701	-0.000833
800	-50	0.5311	0.0439	0.0352	0.2285	0.2083	0.1507	0.016881	0.001192	-0.000488
800	0	0.5963	0.0468	0.0306	0.2107	0.2015	0.1380	0.011871	0.000450	-0.000477
800	50	0.5436	0.0544	0.0408	0.2046	0.1883	0.1367	0.005134	-0.000985	-0.000234
800	100	0.3995	0.0657	0.0275	0.1932	0.1703	0.1382	-0.001922	-0.002945	0.000225
800	150	0.1995	0.0861	0.0066	0.1782	0.1576	0.1501	-0.005018	-0.002737	-0.000037
800	200	0.0060	0.1168	-0.0244	0.1817	0.1539	0.1520	-0.004896	-0.002959	0.000247
800	250	-0.1803	0.1282	-0.0361	0.1802	0.1404	0.1527	-0.003410	-0.003165	-0.000037

A2.2.10 Processed mean velocity in jet flow for $S=10.52\%$, $Q=31.2\text{L/s}$, $z=10\text{mm}$

x_j (mm)	y_j (mm)	u (m/s)	v (m/s)	w (m/s)	x_j (mm)	y_j (mm)	u (m/s)	v (m/s)	w (m/s)
100	-70	0.5765	-0.0882	0.0609	500	-250	0.3653	-0.2889	0.0632
100	-40	1.3796	-0.1444	0.0245	500	-200	0.5951	-0.3885	0.0397
100	0	1.3167	0.0429	-0.1051	500	-150	0.7388	-0.3419	0.0191
100	50	0.3309	0.0327	-0.0315	500	-100	0.8691	-0.2506	0.0127
100	100	0.2379	0.0096	0.0053	500	-50	0.9014	-0.1154	0.0105
100	150	0.2083	-0.0517	0.0046	500	0	0.9268	-0.0103	0.0054
100	200	0.0996	-0.0791	-0.0027	500	50	0.8559	0.0821	0.0008
100	250	0.0368	-0.1326	-0.0020	500	100	0.6279	0.1014	-0.0016
100	300	-0.0057	-0.1696	0.0009	500	150	0.4203	0.0844	0.0037
					500	200	0.2897	0.0615	0.0066
200	-140	0.2583	-0.0895	-0.0435	500	250	0.1792	0.0410	0.0075
200	-100	0.4479	-0.1128	0.0053	500	300	0.0654	0.0507	0.0093
200	-50	1.0702	-0.2191	0.0186	500	350	-0.0747	0.0628	0.0089
200	0	1.1485	0.0356	-0.0534					
200	50	0.6357	0.1086	-0.0303	600	-200	0.2998	-0.1247	0.0923
200	100	0.3090	0.0421	0.0012	600	-150	0.5750	-0.2458	0.0622
200	150	0.2227	0.0080	0.0023	600	-100	0.8248	-0.2539	0.0320
200	200	0.1594	-0.0356	-0.0032	600	-50	0.8584	-0.1619	0.0161
200	250	0.0799	-0.0763	-0.0083	600	0	0.8909	-0.0687	0.0096
200	300	0.0301	-0.1211	-0.0023	600	50	0.8138	0.0335	0.0031
200	350	-0.0517	-0.1288	-0.0034	600	100	0.6393	0.0681	0.0024
					600	150	0.4485	0.0731	0.0047
300	-200	0.5356	-0.3862	0.0181	600	200	0.2938	0.0707	0.0067
300	-150	0.5775	-0.2482	-0.0073	600	250	0.1297	0.0650	0.0081
300	-100	0.7244	-0.1544	-0.0016	600	300	-0.0004	0.0973	0.0104
300	-50	1.0025	-0.1063	-0.0065					
300	0	1.1853	0.0638	-0.0272	700	-140	0.3809	0.0829	0.0855
300	50	0.7998	0.1513	-0.0209	700	-100	0.6297	-0.0701	0.0678
300	100	0.4420	0.0905	-0.0039	700	-50	0.8384	-0.0995	0.0340
300	150	0.2746	0.0456	0.0033	700	0	0.8045	-0.0410	0.0130
300	200	0.2022	0.0018	-0.0034	700	50	0.8188	0.0370	0.0082
300	250	0.1407	-0.0268	-0.0043	700	100	0.6154	0.0861	0.0025
300	300	0.0698	-0.0347	-0.0037	700	150	0.4410	0.1051	0.0042
300	350	-0.0273	-0.0440	0.0001	700	200	0.2503	0.1101	0.0054
					700	250	0.0798	0.1315	0.0051
400	-190	0.6383	-0.3721	0.0166	700	300	-0.0724	0.1609	0.0032
400	-150	0.7373	-0.3136	0.0126					
400	-100	0.8606	-0.2011	0.0050	800	-90	0.5039	0.1654	0.0757
400	-50	1.0553	-0.1050	-0.0006	800	-50	0.6696	0.0140	0.0554
400	0	1.0129	0.0288	-0.0060	800	0	0.7898	-0.0118	0.0286
400	50	0.8678	0.1125	-0.0132	800	50	0.6861	0.0192	0.0126
400	100	0.5785	0.1099	-0.0074	800	100	0.5720	0.0805	0.0052
400	150	0.3561	0.0673	0.0004	800	150	0.3857	0.1228	0.0015
400	200	0.2378	0.0274	-0.0027	800	200	0.2089	0.1595	0.0009
400	250	0.1903	0.0151	-0.0019	800	250	0.0334	0.1853	-0.0042
400	300	0.0765	0.0071	0.0008	800	300	-0.1181	0.2255	-0.0085
400	350	-0.0309	0.0079	0.0050					

A2.2.11 Processed mean velocity in jet flow for $S=10.52\%$, $Q=31.2\text{L/s}$, $z=70\text{mm}$

x_j (mm)	y_j (mm)	u (m/s)	v (m/s)	w (m/s)	x_j (mm)	y_j (mm)	u (m/s)	v (m/s)	w (m/s)
100	-100	0.2472	-0.1627	-0.0663	500	-290	0.3016	-0.0760	0.1945
100	-50	1.0016	-0.1699	-0.0636	500	-250	0.3099	-0.1064	0.0695
100	0	1.4632	-0.0047	-0.0926	500	-200	0.3472	-0.1253	-0.0250
100	50	0.2747	-0.1033	-0.0578	500	-150	0.4498	-0.1033	-0.0618
100	100	0.2047	-0.1140	-0.0116	500	-100	0.6465	-0.0646	-0.0627
100	150	0.1371	-0.1171	0.0054	500	-50	0.8659	0.0111	-0.0539
100	200	0.0728	-0.1073	0.0049	500	0	0.9430	0.0929	-0.0435
100	250	-0.0202	-0.1345	0.0103	500	50	0.7557	0.1166	-0.0365
100	300	-0.1075	-0.1530	0.0190	500	100	0.4627	0.0731	-0.0226
					500	150	0.3050	0.0646	-0.0072
200	-150	0.2542	-0.1112	-0.1576	500	200	0.1893	0.0651	0.0106
200	-100	0.7555	-0.2084	-0.2003	500	250	0.0799	0.0778	0.0208
200	-50	1.1914	-0.0915	-0.1570	500	300	-0.0393	0.1090	0.0289
200	0	1.1775	0.0368	-0.0872	500	350	-0.1800	0.1317	0.0107
200	50	0.4423	-0.0597	-0.0493	500	400	-0.2995	0.1811	-0.0075
200	100	0.2642	-0.0580	-0.0214					
200	150	0.1909	-0.0576	-0.0097	600	-250	0.3711	-0.1059	0.2948
200	200	0.1060	-0.0721	-0.0108	600	-200	0.4170	-0.1177	0.1530
200	250	0.0183	-0.1031	-0.0065	600	-150	0.5031	-0.1179	0.0339
200	300	-0.0610	-0.1339	-0.0024	600	-100	0.6056	-0.0594	-0.0343
200	350	-0.1561	-0.1472	0.0090	600	-50	0.7390	0.0454	-0.0480
					600	0	0.8352	0.1569	-0.0395
300	-250	0.1629	-0.1233	0.0039	600	50	0.7355	0.2174	-0.0293
300	-200	0.2069	-0.1246	-0.0343	600	100	0.5461	0.2102	-0.0184
300	-150	0.4663	-0.1350	-0.0818	600	150	0.3627	0.1860	-0.0079
300	-100	0.7598	-0.0693	-0.1127	600	200	0.1916	0.1753	-0.0017
300	-50	1.1419	-0.0251	-0.0960	600	250	0.0467	0.1823	0.0018
300	0	1.0717	0.0337	-0.0579	600	300	-0.1034	0.1975	-0.0103
300	50	0.6014	-0.0040	-0.0490					
300	100	0.3178	-0.0313	-0.0187	700	-150	0.4813	0.0086	0.3231
300	150	0.2227	-0.0386	-0.0123	700	-100	0.6081	0.0040	0.1846
300	200	0.1654	-0.0646	-0.0212	700	-50	0.6747	0.0508	0.0599
300	250	0.0881	-0.0881	-0.0278	700	0	0.7150	0.1494	-0.0010
300	300	-0.0160	-0.0977	-0.0206	700	50	0.6943	0.2409	-0.0248
300	350	-0.1186	-0.1068	-0.0109	700	100	0.5942	0.2896	-0.0250
					700	150	0.4235	0.3007	-0.0251
400	-200	0.2697	-0.1348	-0.0300	700	200	0.2570	0.2841	-0.0274
400	-150	0.4341	-0.1134	-0.0458	700	250	0.0845	0.2819	-0.0358
400	-100	0.6918	-0.0669	-0.0592	700	300	-0.0736	0.2582	-0.0493
400	-50	1.0053	-0.0035	-0.0611					
400	0	1.0410	0.0577	-0.0460	800	-50	0.6241	0.2437	0.2758
400	50	0.6845	0.0400	-0.0416	800	0	0.6725	0.2002	0.1735
400	100	0.3737	0.0047	-0.0196	800	50	0.6475	0.2261	0.0823
400	150	0.2591	-0.0048	-0.0090	800	100	0.5883	0.2669	0.0252
400	200	0.1916	-0.0024	-0.0034	800	150	0.4767	0.2845	-0.0036
400	250	0.1062	-0.0048	-0.0011	800	200	0.3277	0.2764	-0.0263
400	300	0.0006	0.0080	0.0126	800	250	0.1926	0.2585	-0.0389
400	350	-0.1213	0.0287	0.0197	800	300	0.0527	0.2214	-0.0422
					800	350	-0.0880	0.1574	-0.0362

A2.2.12 Processed turbulence data in jet flow for $S=10.52\%$, $Q=31.2L/s$, $z=10mm$

x_j (mm)	y_j (mm)	$\sqrt{u'^2}$ (m/s)	$\sqrt{v'^2}$ (m/s)	$\sqrt{w'^2}$ (m/s)	$-\overline{u'v'}$ (m ² /s ²)	$-\overline{u'w'}$ (m ² /s ²)	$-\overline{v'w'}$ (m ² /s ²)	ε (m ² /s ³)	λ_g (mm)	η (mm)
100	-70	0.535	0.267	0.111	0.09076	-0.00645	0.00358	0.485	2.261	0.04
100	-40	0.178	0.299	0.100	0.01778	-0.00475	0.00168	0.024	6.059	0.09
100	0	0.164	0.233	0.116	-0.00950	0.00132	-0.00705	0.024	5.168	0.09
100	50	0.125	0.112	0.035	-0.00578	0.00092	0.00107	0.027	2.712	0.09
100	100	0.085	0.120	0.040	-0.00268	-0.00037	0.00005	0.009	4.117	0.11
100	150	0.101	0.135	0.039	-0.00385	-0.00045	-0.00038	0.009	4.692	0.11
100	200	0.102	0.128	0.044	-0.00055	0.00007	0.00018	0.018	3.244	0.09
100	250	0.120	0.138	0.045	0.00243	0.00001	0.00059	0.087	1.662	0.06
100	300	0.129	0.151	0.047	0.00434	-0.00035	0.00081	0.806	0.589	0.04
200	-140	0.240	0.235	0.116	0.00583	0.00016	-0.00017	0.453	1.368	0.04
200	-100	0.384	0.297	0.138	0.05730	-0.00811	0.00287	0.709	1.551	0.04
200	-50	0.333	0.214	0.101	0.03355	-0.00175	-0.00214	0.159	2.654	0.05
200	0	0.243	0.178	0.083	-0.01692	0.00055	-0.00179	0.081	2.831	0.06
200	50	0.298	0.185	0.056	-0.03790	0.00263	0.00134	0.142	2.443	0.06
200	100	0.110	0.126	0.036	-0.00533	-0.00008	0.00023	0.009	4.683	0.11
200	150	0.097	0.126	0.039	-0.00342	-0.00009	-0.00024	0.012	3.820	0.10
200	200	0.103	0.124	0.042	-0.00138	-0.00005	-0.00002	0.016	3.432	0.10
200	250	0.114	0.137	0.049	-0.00076	-0.00021	0.00040	0.033	2.648	0.08
200	300	0.139	0.163	0.047	0.00120	-0.00038	0.00082	0.088	1.922	0.06
200	350	0.145	0.150	0.052	0.00112	-0.00010	0.00062	0.086	1.888	0.06
300	-200	0.251	0.223	0.097	0.01355	-0.00207	-0.00076	0.241	1.843	0.05
300	-150	0.231	0.218	0.097	0.01684	-0.00161	-0.00104	0.220	1.830	0.05
300	-100	0.296	0.226	0.099	0.03140	-0.00402	0.00158	0.280	1.884	0.05
300	-50	0.296	0.187	0.086	0.02009	-0.00041	-0.00085	0.145	2.452	0.06
300	0	0.292	0.172	0.080	-0.01290	0.00177	-0.00088	0.132	2.476	0.06
300	50	0.319	0.193	0.064	-0.04062	0.00120	0.00036	0.127	2.754	0.06
300	100	0.201	0.151	0.040	-0.01829	0.00067	0.00037	0.040	3.296	0.08
300	150	0.119	0.135	0.037	-0.00687	0.00015	-0.00015	0.014	4.053	0.10
300	200	0.101	0.120	0.046	-0.00323	0.00000	-0.00022	0.010	4.199	0.11
300	250	0.127	0.135	0.048	-0.00395	-0.00007	0.00016	0.012	4.532	0.10
300	300	0.126	0.128	0.048	-0.00426	-0.00007	0.00013	0.029	2.818	0.08
300	350	0.168	0.143	0.049	-0.00634	0.00021	0.00027	0.119	1.696	0.06
400	-190	0.243	0.219	0.086	0.01773	-0.00342	0.00052	0.124	2.487	0.06
400	-150	0.262	0.222	0.090	0.02164	-0.00371	0.00116	0.134	2.511	0.06
400	-100	0.271	0.202	0.079	0.02080	-0.00240	0.00129	0.140	2.398	0.06
400	-50	0.291	0.199	0.070	0.01935	-0.00077	0.00056	0.153	2.379	0.06
400	0	0.279	0.169	0.067	-0.00250	-0.00007	-0.00053	0.138	2.327	0.06
400	50	0.291	0.148	0.065	-0.02205	-0.00019	-0.00053	0.057	3.594	0.07
400	100	0.260	0.157	0.050	-0.02477	0.00029	-0.00012	0.046	3.692	0.07
400	150	0.160	0.134	0.038	-0.01140	0.00016	-0.00006	0.019	3.970	0.09
400	200	0.112	0.110	0.040	-0.00376	-0.00029	-0.00045	0.010	4.276	0.11
400	250	0.126	0.115	0.043	-0.00489	-0.00024	-0.00023	0.008	5.202	0.12
400	300	0.139	0.111	0.044	-0.00444	0.00018	0.00010	0.022	3.194	0.09
400	350	0.181	0.120	0.047	-0.00621	0.00039	0.00001	0.081	2.025	0.06

A2.2.12 Processed turbulence data in jet flow for $S = 10.52\%$, $Q = 31.2$ L/s, $z = 10$ mm (cont'd)

x_j (mm)	y_j (mm)	$\sqrt{u'^2}$ (m/s)	$\sqrt{v'^2}$ (m/s)	$\sqrt{w'^2}$ (m/s)	$-\overline{u'v'}$ (m ² /s ²)	$-\overline{u'w'}$ (m ² /s ²)	$-\overline{v'w'}$ (m ² /s ²)	ε (m ² /s ³)	λ_g (mm)	η (mm)
500	-250	0.225	0.202	0.072	0.01727	-0.00389	0.00234	0.153	2.054	0.06
500	-200	0.257	0.202	0.084	0.01884	-0.00436	0.00134	0.154	2.228	0.06
500	-150	0.261	0.204	0.084	0.01865	-0.00385	0.00154	0.133	2.422	0.06
500	-100	0.262	0.202	0.082	0.01928	-0.00216	0.00178	0.106	2.712	0.06
500	-50	0.256	0.186	0.059	0.01343	0.00012	0.00116	0.115	2.458	0.06
500	0	0.271	0.182	0.059	0.00197	0.00081	0.00016	0.114	2.540	0.06
500	50	0.272	0.176	0.056	-0.01030	-0.00008	-0.00099	0.051	3.765	0.07
500	100	0.270	0.156	0.046	-0.01910	0.00005	-0.00054	0.050	3.646	0.07
500	150	0.195	0.140	0.037	-0.01359	-0.00008	-0.00028	0.019	4.582	0.09
500	200	0.155	0.125	0.035	-0.00866	-0.00011	-0.00013	0.009	5.623	0.11
500	250	0.142	0.117	0.037	-0.00569	-0.00013	-0.00009	0.007	5.753	0.12
500	300	0.179	0.114	0.040	-0.00637	-0.00004	0.00009	0.022	3.734	0.09
500	350	0.198	0.111	0.042	-0.00559	0.00074	0.00025	0.045	2.806	0.08
600	-200	0.242	0.197	0.083	0.01895	-0.00389	0.00285	0.185	1.944	0.05
600	-150	0.234	0.181	0.081	0.01606	-0.00413	0.00146	0.116	2.324	0.06
600	-100	0.263	0.214	0.069	0.02145	-0.00226	0.00139	0.108	2.727	0.06
600	-50	0.248	0.183	0.061	0.01467	-0.00057	0.00134	0.099	2.589	0.06
600	0	0.219	0.189	0.061	0.00766	-0.00021	0.00075	0.027	4.627	0.09
600	50	0.251	0.179	0.058	-0.00028	-0.00047	-0.00053	0.036	4.299	0.08
600	100	0.272	0.148	0.049	-0.00903	-0.00033	-0.00064	0.057	3.407	0.07
600	150	0.227	0.132	0.042	-0.01134	-0.00041	-0.00026	0.026	4.263	0.09
600	200	0.183	0.122	0.035	-0.00872	-0.00024	0.00001	0.021	4.002	0.09
600	250	0.170	0.104	0.041	-0.00486	0.00014	0.00002	0.017	3.997	0.10
600	300	0.208	0.114	0.045	-0.00540	0.00070	0.00013	0.040	3.128	0.077
700	-140	0.231	0.200	0.083	0.01149	-0.00140	0.00045	0.114	2.427	0.06
700	-100	0.234	0.182	0.068	0.01508	-0.00322	0.00149	0.075	2.861	0.07
700	-50	0.247	0.208	0.062	0.01662	-0.00150	0.00116	0.077	3.071	0.07
700	0	0.214	0.179	0.058	0.00882	-0.00079	0.00065	0.030	4.261	0.08
700	50	0.272	0.193	0.059	0.00644	-0.00106	0.00032	0.050	3.935	0.07
700	100	0.270	0.161	0.054	-0.00436	-0.00080	-0.00029	0.062	3.309	0.07
700	150	0.247	0.142	0.051	-0.00702	-0.00043	-0.00035	0.039	3.770	0.08
700	200	0.222	0.128	0.047	-0.00702	-0.00016	-0.00013	0.036	3.546	0.08
700	250	0.214	0.119	0.050	-0.00558	0.00078	0.00001	0.069	2.458	0.07
700	300	0.211	0.117	0.054	-0.00531	0.00085	0.00014	0.095	2.084	0.06
800	-90	0.214	0.208	0.076	0.00829	-0.00095	-0.00052	0.088	2.693	0.06
800	-50	0.218	0.200	0.060	0.01308	-0.00194	0.00104	0.084	2.687	0.06
800	0	0.243	0.208	0.058	0.01470	-0.00127	0.00081	0.069	3.196	0.07
800	50	0.241	0.173	0.054	0.00580	-0.00084	0.00005	0.068	2.999	0.07
800	100	0.250	0.164	0.056	0.00157	-0.00105	0.00011	0.059	3.243	0.07
800	150	0.250	0.151	0.060	-0.00366	-0.00130	-0.00019	0.042	3.787	0.08
800	200	0.244	0.144	0.059	-0.00693	-0.00043	-0.00016	0.073	2.764	0.07
800	250	0.237	0.132	0.065	-0.00608	-0.00041	-0.00011	0.366	1.196	0.04
800	300	0.233	0.125	0.068	-0.00688	0.00055	0.00023	0.115	2.083	0.06

A2.2.13 Processed turbulence data in jet flow for $S=10.52\%$, $Q=31.2\text{L/s}$, $z=70\text{mm}$

x_j (mm)	y_j (mm)	$\sqrt{u'^2}$ (m/s)	$\sqrt{v'^2}$ (m/s)	$\sqrt{w'^2}$ (m/s)	$-\overline{u'v'}$ (m^2/s^2)	$-\overline{u'w'}$ (m^2/s^2)	$-\overline{v'w'}$ (m^2/s^2)	ε (m^2/s^3)	λ_g (mm)	η (mm)
100	-100	0.285	0.270	0.135	0.018990	0.004286	-0.004129	0.950	1.102	0.04
100	-50	0.429	0.241	0.163	0.009105	-0.000984	-0.002749	0.353	2.260	0.04
100	0	0.162	0.226	0.169	-0.010141	-0.002045	0.000389	0.020	6.002	0.09
100	50	0.105	0.086	0.085	-0.002113	0.000487	0.000879	0.015	3.426	0.10
100	100	0.088	0.092	0.083	-0.001116	0.000829	0.002079	0.010	3.858	0.11
100	150	0.103	0.100	0.089	-0.002285	0.000877	0.001577	0.020	3.095	0.09
100	200	0.100	0.108	0.085	-0.002131	0.000982	0.001682	0.031	2.512	0.08
100	250	0.105	0.120	0.091	-0.002138	0.001206	0.001651	0.134	1.298	0.06
100	300	0.111	0.120	0.097	-0.002105	0.001526	0.001603	0.038	2.524	0.08
200	-150	0.346	0.339	0.142	0.033377	0.005171	-0.002951	2.227	0.875	0.03
200	-100	0.392	0.309	0.176	0.035265	0.011567	-0.003272	0.579	1.801	0.04
200	-50	0.298	0.241	0.170	-0.002124	0.007481	0.003304	0.130	3.017	0.06
200	0	0.348	0.218	0.159	-0.038872	0.002924	0.001917	0.200	2.548	0.05
200	50	0.204	0.111	0.087	-0.011096	0.000977	0.000633	0.042	3.140	0.08
200	100	0.095	0.091	0.082	-0.001550	0.000585	0.001214	0.011	3.840	0.11
200	150	0.100	0.106	0.084	-0.002011	0.000885	0.000397	0.012	3.931	0.10
200	200	0.105	0.124	0.090	-0.001267	0.000765	0.000512	0.019	3.520	0.09
200	250	0.116	0.136	0.101	-0.000756	0.000253	0.000830	0.180	1.252	0.05
200	300	0.118	0.141	0.111	-0.000583	0.000275	0.001107	0.069	2.128	0.07
200	350	0.132	0.132	0.115	-0.000722	0.002108	0.001154	0.031	3.251	0.08
300	-250	0.265	0.239	0.168	0.009013	-0.012208	0.003753	0.814	1.131	0.04
300	-200	0.320	0.264	0.170	0.021514	-0.012049	0.003355	1.105	1.105	0.03
300	-150	0.358	0.260	0.166	0.029506	-0.006958	0.002291	0.808	1.360	0.04
300	-100	0.384	0.259	0.158	0.026756	-0.005202	0.002558	0.693	1.521	0.04
300	-50	0.303	0.206	0.148	0.004434	-0.004767	0.002468	0.189	2.356	0.05
300	0	0.322	0.193	0.146	-0.030364	0.000221	0.000706	0.151	2.687	0.06
300	50	0.278	0.142	0.108	-0.021405	0.001959	0.000753	0.080	3.032	0.07
300	100	0.131	0.098	0.079	-0.003379	0.001194	0.000503	0.017	3.635	0.10
300	150	0.108	0.108	0.082	-0.001550	-0.000111	-0.000753	0.010	4.397	0.11
300	200	0.112	0.119	0.094	-0.001441	0.000787	-0.000697	0.015	3.967	0.10
300	250	0.119	0.119	0.102	-0.001394	0.000267	-0.000105	0.032	2.874	0.08
300	300	0.132	0.128	0.116	-0.001066	0.001193	0.000025	0.183	1.317	0.05
300	350	0.151	0.125	0.125	-0.000015	0.003172	0.000151	0.032	3.345	0.08
400	-200	0.323	0.241	0.186	0.017472	-0.021281	0.004739	0.798	1.286	0.04
400	-150	0.346	0.231	0.175	0.022561	-0.018104	0.003813	0.356	1.960	0.04
400	-100	0.391	0.210	0.161	0.021069	-0.014444	0.003095	0.379	1.985	0.04
400	-50	0.328	0.195	0.138	0.004305	-0.007754	0.001643	0.248	2.106	0.05
400	0	0.294	0.190	0.133	-0.021609	-0.002753	-0.000185	0.133	2.659	0.06
400	50	0.309	0.152	0.107	-0.026546	0.000392	-0.000149	0.080	3.290	0.07
400	100	0.154	0.105	0.077	-0.005971	0.000759	0.000087	0.019	3.839	0.09
400	150	0.115	0.099	0.084	-0.002512	0.000272	-0.000214	0.012	4.116	0.10
400	200	0.112	0.108	0.092	-0.002589	0.000082	-0.000533	0.012	4.239	0.10
400	250	0.117	0.108	0.096	-0.002210	0.000843	-0.000983	0.017	3.699	0.10
400	300	0.136	0.106	0.107	-0.002746	0.001141	-0.000070	0.040	2.625	0.077
400	350	0.159	0.110	0.112	-0.003417	0.002444	-0.000373	0.024	3.725	0.09

A2.2.13 Processed turbulence data in jet flow for $S = 10.52\%$, $Q = 31.2$ L/s, $z = 70$ mm (cont'd)

x_j (mm)	y_j (mm)	$\sqrt{u'^2}$ (m/s)	$\sqrt{v'^2}$ (m/s)	$\sqrt{w'^2}$ (m/s)	$-\overline{u'v'}$ (m ² /s ²)	$-\overline{u'w'}$ (m ² /s ²)	$-\overline{v'w'}$ (m ² /s ²)	ε (m ² /s ³)	λ_g (mm)	η (mm)
500	-290	0.233	0.223	0.178	0.008375	-0.010120	0.002240	0.250	1.906	0.05
500	-250	0.250	0.225	0.176	0.008891	-0.013034	0.002208	0.297	1.805	0.05
500	-200	0.290	0.219	0.179	0.013143	-0.015692	0.003419	0.338	1.806	0.05
500	-150	0.340	0.212	0.184	0.012809	-0.018232	0.002637	0.404	1.793	0.04
500	-100	0.386	0.211	0.169	0.017042	-0.018549	0.002329	0.366	2.017	0.04
500	-50	0.356	0.199	0.150	0.006068	-0.013991	0.001603	0.302	2.049	0.05
500	0	0.285	0.188	0.130	-0.011144	-0.005791	0.000078	0.135	2.576	0.06
500	50	0.296	0.171	0.118	-0.022570	-0.002222	-0.000435	0.082	3.266	0.06
500	100	0.211	0.127	0.092	-0.011977	0.000818	0.000328	0.036	3.613	0.08
500	150	0.132	0.107	0.087	-0.004344	0.000649	0.000492	0.014	4.237	0.10
500	200	0.112	0.098	0.087	-0.002110	-0.000174	0.000531	0.014	3.790	0.10
500	250	0.122	0.097	0.095	-0.002355	0.000404	0.000462	0.026	2.939	0.09
500	300	0.142	0.111	0.105	-0.002736	0.000509	0.001498	0.080	1.908	0.07
500	350	0.165	0.118	0.115	-0.005133	0.000549	0.001102	0.034	3.269	0.08
500	400	0.177	0.120	0.118	-0.006364	-0.000115	0.001734	0.032	3.532	0.08
600	-250	0.242	0.206	0.175	0.008623	-0.010196	0.000095	0.187	2.172	0.05
600	-200	0.272	0.195	0.176	0.009923	-0.011659	0.000130	0.260	1.920	0.05
600	-150	0.315	0.200	0.172	0.009451	-0.013626	0.001718	0.298	1.949	0.05
600	-100	0.329	0.193	0.170	0.005873	-0.014647	0.001679	0.238	2.214	0.05
600	-50	0.336	0.201	0.163	0.001403	-0.013566	0.001174	0.236	2.260	0.05
600	0	0.290	0.198	0.143	-0.004130	-0.008257	0.000913	0.165	2.416	0.05
600	50	0.272	0.194	0.124	-0.010096	-0.005163	0.000308	0.084	3.174	0.06
600	100	0.251	0.180	0.115	-0.016728	-0.001894	0.001013	0.068	3.273	0.07
600	150	0.195	0.155	0.108	-0.009828	-0.000924	0.001340	0.045	3.301	0.08
600	200	0.156	0.125	0.109	-0.003128	-0.000565	0.002644	0.041	2.908	0.08
600	250	0.149	0.121	0.112	-0.003389	-0.000433	0.002772	0.128	1.606	0.06
600	300	0.164	0.125	0.117	-0.004581	-0.000330	0.002292	0.083	2.126	0.06
700	-150	0.210	0.177	0.170	-0.001923	-0.008038	-0.003029	0.053	3.616	0.07
700	-100	0.285	0.188	0.170	-0.002559	-0.011821	-0.002283	0.175	2.363	0.05
700	-50	0.300	0.194	0.168	-0.004341	-0.014187	-0.000688	0.206	2.250	0.05
700	0	0.286	0.193	0.153	-0.004690	-0.011315	0.000105	0.176	2.329	0.05
700	50	0.263	0.198	0.146	-0.005454	-0.008870	0.000489	0.130	2.581	0.06
700	100	0.246	0.196	0.134	-0.008486	-0.006742	0.000913	0.102	2.765	0.06
700	150	0.221	0.182	0.132	-0.009115	-0.004385	0.001273	0.078	2.924	0.07
700	200	0.198	0.170	0.130	-0.008274	-0.003556	0.002340	0.095	2.449	0.06
700	250	0.180	0.162	0.134	-0.006304	-0.003008	0.001927	0.208	1.567	0.05
700	300	0.167	0.160	0.138	-0.006388	-0.002451	0.001647	0.186	1.614	0.05
800	-50	0.244	0.195	0.167	-0.011705	-0.008748	-0.003033	0.124	2.608	0.06
800	0	0.254	0.193	0.156	-0.007844	-0.010766	-0.003072	0.124	2.610	0.06
800	50	0.238	0.195	0.151	-0.007939	-0.008638	-0.002694	0.105	2.738	0.06
800	100	0.233	0.190	0.141	-0.008169	-0.007835	-0.000551	0.100	2.719	0.06
800	150	0.226	0.193	0.136	-0.010514	-0.007326	-0.000447	0.098	2.711	0.06
800	200	0.210	0.193	0.135	-0.012051	-0.006333	-0.000149	0.101	2.573	0.06
800	250	0.195	0.195	0.138	-0.012040	-0.006345	-0.000509	0.120	2.307	0.06
800	300	0.180	0.193	0.146	-0.011247	-0.005222	-0.000409	0.347	1.326	0.05
800	350	0.167	0.203	0.153	-0.011583	-0.004960	0.000196	0.145	2.068	0.06